COMBUSTION
AND
FLAME

QUARTERLY JOURNAL OF THE COMBUSTION INSTITUTE

VOLUME IV

Editors

F. H. GARNER BERNARD LEWIS (U.S.A.)

Editorial Board

L. Deffet (BELGIUM)
W. Jost (GERMANY)
P. Laffitte (FRANCE)
J. W. Linnett (U.K.)
P. Lloyd (U.K.)
J. P. Longwell (U.S.A.)
F. E. Marble (U.S.A.)
W. T. Olson (U.S.A.)
D. T. A. Townend (U.K.)
S. Yagi (JAPAN)
E. F. M. van der Held (NETHERLANDS)

LONDON
BUTTERWORTHS SCIENTIFIC PUBLICATIONS
1960

A C

THER
resea
latio
are
stabi
of m
(i.e.
of a
solu
time
istics
radia
categ
natu
cylin
gatio
Th
been
and
the c
equa
cold
flow
diffe
with
achi
foun
the p

---

*Exte
versi
Jet

A Contribution to the Theory of Laminar Flames with Radial Symmetry[*]

J. MENKES

Jet Propulsion Laboratory, California Institute of Technology, Pasadena, California

(Received December 1958)

The differential equations of motion of a flame with radial symmetry are transformed into an integral equation. The integral equation is solved numerically by a method of successive approximations. The dependence of the mass flow per unit area on the flame thickness and flame radius as well as on the temperature of the unreacted gas is investigated. It is demonstrated that the rate of change of the mass flow is determined by any two of the three parameters. The results of the calculations are presented graphically. The implications of the findings for the stability of combustion waves is discussed.

Introduction

THERE are two areas in the field of combustion research where the need for exploratory calculations is probably the greatest. Those areas are *non*-one-dimensional flames and flame stability. The difficulty of solving the equations of motion of any other but the one-dimensional (i.e. plane) flame leads one to consider problems of a more artificial nature, which might be soluble with comparative ease while at the same time retaining some of the dynamic characteristics of the physical system. Flames with radial symmetry seem to fall neatly into this category. The spherical flame is of course the natural model for a burning droplet. The cylindrical flame might be of use in investigations of flame stability.

The burning of a monopropellant droplet has been investigated by J. LORELL and H. WISE[1] and by F. A. WILLIAMS[2]. Lorell and Wise solve the equations of motion by 'brute force'; i.e. the equations are integrated numerically from the cold boundary for assumed values of the mass flow (which is an eigenvalue of the system of differential equations) till satisfactory agreement with the hot boundary conditions at $r = +\infty$ is achieved. Williams used the approach that was found so successful in the analytical treatment of the plane flame by S. F. BOYS and J. CORNER[3], and by T. VON KÁRMÁN and G. MILLAN[4]. While the problem is similar to the premixed laminar flame propagation problem it differs in one important aspect: the distance variable cannot be eliminated from the equations of motion. Its effect, however, can be concentrated in one unknown function for which one tries to make a shrewd guess. Shrewd guessing is a time-honoured custom in engineering analysis and its success depends largely on the physical insight of the person making the guess.

The cylindrical flame is solved not for its intrinsic value since there are hardly any flames resembling a cylinder, but for its implications on stability analysis. G. MARKSTEIN[5] has demonstrated that the stability of a laminar flame depends critically on the dependence of the flame speed on the mean flame radius of curvature. J. FABRI[6] gave an expression for the dependence of the flame speed on the radius of curvature. His analysis which makes no pretence at being rigorous predicts the increase of flame speed with decrease in the radius of curvature. Markstein and Fabri assume that the flame thickness is very small and they deduce the dependence of the flame speed on the radius of curvature by a perturbation about the flat flame value. It should be noted at this point that there is an essential difference between a slightly wrinkled flat flame and a cylindrical flame. For the flat flame the mass

---

[*] External Publication No. 536. This paper represents a condensed version of the results set forth in *Progress Report No. 20–361*, Jet Propulsion Laboratory, California Institute of Technology.

04901

flow per unit area, ρu, is a constant. For the cylindrical flame, however, it is the source strength $\rho v r$ which is a constant of the system. It is clear from this difference that if one assumes, as Markstein and Fabri have done, that $\rho v \simeq$ constant and that r can be replaced by the mean radius of the flame R in the expression for grad T one will find that in order to satisfy the equation of continuity ρv would have to be inversely proportional to R.

In the present analysis an attempt was made to include for the first time the effects of curvature on the internal structure of the flame. It is demonstrated that the problem can be reduced to an equivalent flat flame problem with a reaction rate function that is weighted by a function of r. The equations of motion were solved numerically by an adaptation of the method due to G. Klein[7]. By transforming the differential equation into an integral equation and by lumping the effect of the curvature into one unknown function it was possible to develop an algorism that not only provided a first guess at the unknown function, and usually a good one, but it also permitted one to improve this guess by subsequent iterations. This method does not depend for its success on a particularly clever first guess and is thus practically foolproof.

Analysis

The governing equations for a laminar steady flame are the equations of continuity, conservation of species, and the conservation of energy. A detailed derivation of the one-dimensional conservation laws can be found, for example, in the paper by J. O. Hirschfelder and C. F. Curtiss[8]. The transformation to polar coordinates can be carried out by any convenient method. The momentum equation can usually be neglected when the Mach number with which the flame is propagated is sufficiently small. The latter restriction applies to practically all laminar hydrocarbon–air flames. It is usually necessary to make some further assumption as to the nature of the reaction that is taking place. T. von Kármán and S. S. Penner[9] have demonstrated that quite complicated reactions can be adequately described by one global reaction. In the present analysis we take the simplest possible reaction of the type $A \longrightarrow B$. Such a flame is properly represented by a first order reaction rate. To simplify the mathematical details and particularly the computational work the Lewis number was taken to be unity. In addition λ, c_p and the chemical time τ were assumed to be constant values suitably averaged over the temperature interval.

By combining the three conservation laws and utilizing the equation of state of a perfect gas which reduces here to the statement that ρ is proportional to $1/T$, one obtains a single equation

$$x^2\frac{d^2\theta}{dx^2}+(1-\alpha)x\frac{d\theta}{dx}=-x^2\left(\frac{c_p\rho_b\theta_a}{\lambda\tau}\right)\frac{1-\theta}{\theta}\exp\left(-\frac{\theta_a}{\theta}\right) \quad \ldots .[1]$$

where x denotes the space variable in the radial direction (r is used in the Introduction in conformity with the notation of the authors that were discussed), $\theta = T/T_f$, $\theta_a = A/RT_f$ is a non-dimensional activation temperature, and $\alpha = x\rho U c_p/\lambda$ is an eigenvalue of the problem homologous to the mass flow parameter in the one-dimensional case. The boundary conditions are as follows:

$$\text{at } x=0, \qquad \theta=\theta_0 \text{ and } d\theta/dx=0$$
$$\text{at } x=+\infty, \quad \theta=1 \text{ and } d\theta/dx=0$$

Equation 1 is a second-order differential equation with two singular points at $x=0$, and $x=\infty$. The need to impose four boundary conditions on a second order equation with one free parameter (i.e. α) introduces an overdeterminancy. The overdeterminancy can be handled by introducing the temperature as the independent variable and the temperature gradient as the dependent variable which depresses the order of the equation by one. In the flat flame this transformation leads to a determinate differential equation because the distance x does not enter explicitly into the equation. The central problem of the radially symmetric case is the treatment of this difficulty. It is clear that the distance coordinate cannot be eliminated.

Derivation of the integral equation

Starting with equation 1 one first sets $x/x_f = \sigma$, and normalizes the RHS by dividing through by

$$\frac{c_p\rho_0\theta_0}{\lambda\tau}\int_{\theta_0}^{1}\sigma^2\frac{(1-\theta)}{\theta}\exp\left(-\frac{\theta_a}{\theta}\right)\mathrm{d}\theta$$

x_0 is a characteristic length that denotes the physical size of the flame, $(c_p\rho_0\theta_0/\lambda\tau)^{-\frac{1}{2}}$ denotes a length, say, L. The value of the definite integral may be denoted by $I(\theta_0)$ to indicate its dependence on the cold temperature. The normalized reaction rate function is denoted by $\phi(\theta)$ where

$$\phi(\theta)=\frac{\frac{(1-\theta)}{\theta}\exp\left(-\frac{\theta_a}{\theta}\right)}{I(\theta_0)} \quad \ldots . [2]$$

A non-dimensional independent variable is introduced by the transformation

$$x/L\{I(\theta_0)\}^{\frac{1}{2}}=\xi \quad \ldots . [3]$$

thus equation 1 is cast into what may be called its standard form

$$\xi^2\frac{\mathrm{d}^2\theta}{\mathrm{d}\xi^2}+(1-\alpha)\xi\frac{\mathrm{d}\theta}{\mathrm{d}\xi}=-\xi^2\phi(\theta) \quad \ldots . [4]$$

The form of equation 4 suggests the introduction of a new dependent variable defined by

$$y=(\xi/\xi_f)\mathrm{d}\theta/\mathrm{d}\xi \quad \ldots . [5]$$

The variable y is the cylindrical equivalent of the temperature gradient introduced in the one-dimensional case. By straightforward differentiation and substitution into equation 4 one obtains

$$y\left(\frac{\mathrm{d}y}{\mathrm{d}\theta}-\mu\right)=-\sigma^2\phi(\theta) \quad \ldots . [6]$$

where $\mu=\alpha/\xi_f$ and $\sigma=\xi/\xi_f$. The associated boundary conditions are:

$$\text{at } \theta=\theta_0, \quad y=0$$
$$\text{at } \theta=1, \quad y=0^*$$

The flat flame equation can be recovered from equation 6 by setting $\sigma\equiv1$, and noting that as the curvature goes to zero the source strength becomes infinite, while μ which is proportional to the mass flow per unit of flame area remains finite. The integral equation is obtained from equation 6 by simply multiplying it by $\mathrm{d}\theta$ and integrating it formally from θ to 1, setting $y(1)=0$.

$$\tfrac{1}{2}y^2(\theta)=\int_{\theta}^{1}\sigma^2\phi\,\mathrm{d}\theta-\mu\int_{\theta}^{1}y\,\mathrm{d}\theta \quad \ldots . [7]$$

A *sufficient* condition for $y(\theta_0)=0$ is given by

$$\mu=\int_{\theta_0}^{1}\sigma^2\phi\,\mathrm{d}\theta\Big/\int_{\theta_0}^{1}y\,\mathrm{d}\theta \quad \ldots . [8]$$

One substitutes now equation 8 into equation 7

$$\tfrac{1}{2}y^2=\int_{\theta}^{1}\sigma^2\phi\,\mathrm{d}\theta-\int_{\theta}^{1}y\,\mathrm{d}\theta\Big/\int_{\theta_0}^{1}y\,\mathrm{d}\theta \quad \ldots . [9]$$

where use was made that by definition

$$\int_{\theta_0}^{1}\sigma^2\phi\,\mathrm{d}\theta\equiv1$$

The only explicit indication that we are not dealing with a flat flame in equation 9 is the presence of $\sigma(\theta)$. From the definition of σ and of y, σ may be recovered as a function of θ by a single quadrature, giving

$$\sigma(\theta;\,\xi_f)=\exp\left(-\frac{1}{\xi_f}\int_{\theta}^{1}\frac{\mathrm{d}\theta}{y}\right) \quad \ldots . [10]$$

The expression for σ may now be substituted into equation 9 to yield an integral equation for y. An alternative procedure is to select a reasonable function $\sigma(\theta;\,\xi_f)$ and substitute it directly into equation 9. Assuming, for the present, that a suitable approximation to σ can be found, one proceeds with the solution to equation 9 as follows: one selects as the zero'th approximation to y a function that satisfies the boundary conditions but not necessarily the integral equation. Call this function y_0. One substitutes y_0 into the RHS of equation 9 and performs the indicated quadratures. This operation provides one with a new, and possibly improved, approximation to the solution of the equation; this new function may be called y_1. The procedure of integration and re-substitution

---

*Equation 6 illustrates an interesting feature common to flames with radial symmetry. The flat flame differential equation can be written in the form (see, e.g., D. B. SPALDING[15])

$$\mathrm{d}g/\mathrm{d}\theta=\lambda\Phi(\theta)/\theta-g$$

where $g\equiv\theta-\mathrm{d}\theta/\mathrm{d}x$. The cold boundary condition can be satisfied only if $\Phi(\theta_0)=0$. While this requirement is fulfilled *approximately* by all reaction rate functions of physical interest, it is not satisfied exactly for any temperature above absolute zero. Inspection of equation 6 reveals that the cold boundary condition can be satisfied *exactly* in the radially symmetric case because $\sigma(\theta_0)$ vanishes *a fortiori*.

is repeated as often as is necessary to obtain satisfactory convergence. The νth approximation that differs a prescribed amount or less from the $(\nu-1)$th approximation for all values of θ is denoted by $y^{(1)}$. This function is now introduced into equation **10** and the indicated quadrature is performed to obtain an improved choice for σ, which is called $\sigma_1(\theta;\,\xi_f)$. Utilizing this improved function $\sigma(\theta)$ one repeats the procedure outlined above. There would be little to be gained if the convergence with respect to σ were poor. The calculations, however, showed that for a particular choice of σ_0 the calculated values of $y^{(1)}$ and $\mu^{(1)}$ differed from $y^{(2)}$ and $\mu^{(2)}$ by at worst five per cent. σ_0 was chosen to be a constant. The value of the constant is calculated in Appendix B. With this simplification $y^{(1)}$ can be obtained from equation **9** with no greater difficulty than in the flat flame case. Knowing $y^{(1)}$ permits one to calculate $\sigma_1(\theta)$ which is to be substituted into equation **9** for the calculation of $y^{(2)}$, etc.

The recurrence relations between successive approximations can now be developed. One observes that

$$\int_\theta^1 \sigma^2\varphi\,\mathrm{d}\theta=\left(\frac{1}{I_0}\right)\left\{\sigma^2(\theta^*)\int_\theta^1\frac{1-\theta}{\theta}\exp\left(-\frac{\theta_0}{\theta}\right)\mathrm{d}\theta\right\} \qquad \ldots\ldots [11]$$

For conciseness one sets

$$\int_\theta^1\frac{1-\theta}{\theta}\exp\left(-\frac{\theta_0}{\theta}\right)\mathrm{d}\theta\equiv\Phi(\theta)$$

and

$$\int_\theta^1 y\,\mathrm{d}\theta\equiv Y(\theta)$$

Equations **8** and **9** assume then the symmetric form:

$$\tfrac{1}{2}y^2_{\nu+1}=\frac{\Phi(\theta)}{\Phi(\theta_0)}-\frac{Y_\nu(\theta)}{Y_\nu(\theta_0)}\;;\quad \mu_{\nu+1}=\frac{1}{Y_\nu(\theta_0)}$$

from which $\sigma(\theta)$ has disappeared. The solution to the last equations has been given by Klein. It may be well to point out that the actual computation time on the computer† took no more than a few minutes. As a final remark one might point out that in view of the fact that σ_0 was taken to be a constant the remarks concerning the satisfaction of the cold boundary condition in the flat flame case made above are to be applied here.

Discussion

In all the calculations, q, the total heat release per unit mass due to chemical reaction was kept constant. For a constant pressure deflagration this implies that the temperature difference between the initial and the final temperature is fixed, since $q=c_p(T_f-T_0)$. Two characteristic length scales enter into the problem, one is the flame thickness and the other is the flame radius. Both of these quantities are, mathematically speaking, infinite because the final temperature is reached only asymptotically. Hence the flame thickness was defined as the rectilinear distance travelled by a particle while its temperature is raised from 0·5 T_f to 0·99 T_f. At the lower temperature the reaction rate is negligibly small and at the higher temperature the reaction is practically completed. Analogously the flame radius is defined as the distance from the source point to the point where the temperature has reached 0·99 T_f. The quantity G, which is presented in *Figure 1*, is the dimensionless mass flow per unit area through a cylindrical control

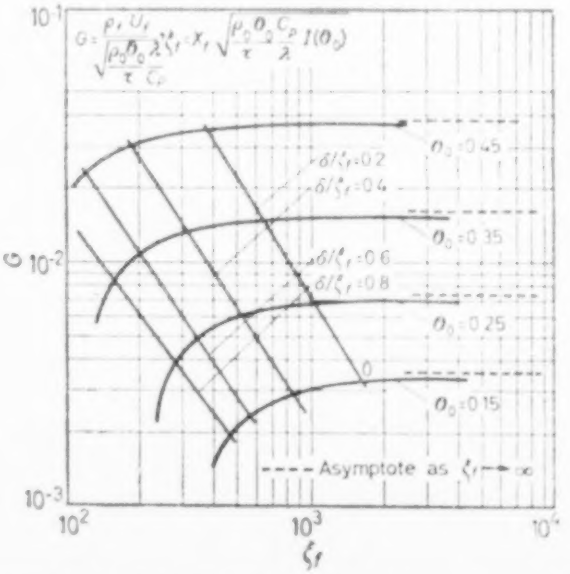

Figure 1. Mass flow per unit area versus flame radius

surface at the flame radius. It should also be borne in mind that the ratio of the *dimensional* inlet temperatures is not the same as the ratio of the non-dimensional inlet temperatures, i.e. $T_{01}/T_{02} \neq \theta_{01}/\theta_{02}$. The reason for this is that the difference between initial and final temperatures has been assumed to be the same for all cases considered, consequently to each θ_{0} corresponds a different T_{0}.

---

†The computations were carried out on a digital computer built by ElectroData, Pasadena, California, Datatron 201.

The particular fashion in which the curves were plotted in *Figure 1* permits one to examine the interplay of the three quantities θ_0, ξ_f, δ/ξ_f that govern the phenomenon. Going along a line of constant flame thickness shows that as the inlet temperature goes up the flame radius decreases, and the specific mass flow increases quite rapidly. This result appears to be in agreement with the approximate treatment of Markstein and Fabri. For a fixed inlet temperature, however, the flame thickness increases so fast while the radius is decreased that the mass flow actually drops. The interpretation of this behaviour is facilitated by considering the problem from a slightly different point of view. The result of the analysis provided us with $\sigma(\theta; \xi_f, \delta/\xi_f, \theta_0)$. Only two of the three parameters are independent. Since θ_0 has been assumed to be constant it follows that to each ξ_f corresponds a unique value of δ/ξ_f. Fixing our attention on equation 6 we notice that knowing σ permits us to replace the reaction rate by an *effective* reaction rate, say, ϕ_e which is defined by $\phi_e = \sigma^2\phi$. In this notation equation 6 is identical to the flat flame equation. The function σ^2 which appears as a weighting function on the reaction rate represents the effect of the curvature on the *internal* structure of the flame. ϕ_e depends *explicitly* only on θ; *implicitly*, however, it depends on a geometrical parameter. For a given temperature interval the mass flow is roughly proportional to the integral $\int \phi_e \mathrm{d}\theta$. *Figure 2* illustrates the effect of the flame thickness on ϕ_e. As δ/ξ_f increases, the area under ϕ_e decreases and the mass flow consequently drops.

Let us now apply the above considerations to the stability of a plane flame. We assume that the flame has been perturbed by an external agent and has suddenly developed a bulge. This wrinkle is assumed to be approximately cylindrical and for definiteness we assume that it is concave with respect to the unburnt gas. The presence of the wrinkle will cause the flame speed to increase at first because θ_0 increases.

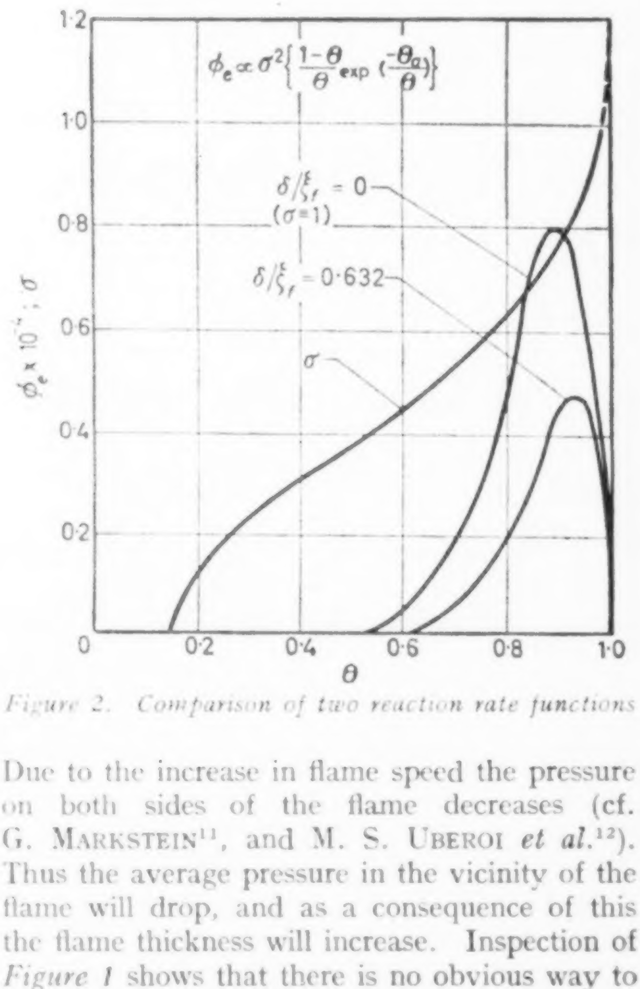

Figure 2. Comparison of two reaction rate functions

Due to the increase in flame speed the pressure on both sides of the flame decreases (cf. G. MARKSTEIN[11], and M. S. UBEROI *et al.*[12]). Thus the average pressure in the vicinity of the flame will drop, and as a consequence of this the flame thickness will increase. Inspection of *Figure 1* shows that there is no obvious way to predict the direction of change in either θ_0 or the mass flow as the flame thickness increases. It seems clear, however, that there is no justification to state categorically that the effect of curvature is always stabilizing and that the change in the mass flow is always inversely proportional to the change in the flame radius. In closing it might be of interest to point out that the stability analysis of G. I. BARENBLATT and Y. B. ZELDOVICH[13], and of J. MENKES[14] who take proper cognizance of the internal structure of the flame, do indeed predict the flame to be stable in contrast to the findings of Markstein.

The author wishes to express his thanks to Professor Frank E. Marble who suggested the problem and to Dr F. Hamilton Wright for his helpful criticism. The help of Mr J. Robert Mueller who carried out the numerical computations is gratefully acknowledged.

This paper presents the results of one phase of research carried out at the Jet Propulsion Laboratory, California Institute of Technology, under Contract No. DA-04-495-Ord 18, sponsored by the Department of the Army, Ordnance Corps.

Appendix A

Derivation of the integral equation for a spherical flame

The combined equations of energy, continuity and conservation of species give

$$\frac{d^2\theta}{dr^2}+\frac{2}{r}\frac{d\theta}{dr}-\frac{c_p}{\lambda}\rho u\frac{d\theta}{dr}=-\frac{c_F\rho_a\theta_a}{\lambda\tau}\frac{(1-\theta)}{\theta}\exp\left(-\frac{\theta_a}{\theta}\right) \quad \ldots . [12]$$

substituting for $\rho ur^2=m=\text{constant}$

$$\frac{d^2\theta}{dr^2}+\frac{2}{r}\frac{d\theta}{dr}-\frac{c_p m\,d\theta}{\lambda r^2 dr}=-\frac{1}{L^2}\frac{(1-\theta)}{\theta}\exp\left(-\frac{\theta_a}{\theta}\right) \quad \ldots . [13]$$

or

$$\frac{1}{L^2}\frac{d}{dr}\left(r^2\frac{d\theta}{dr}\right)-\frac{M}{r^2}\frac{d\theta}{dr}=-\Psi(\theta) \quad \ldots [14]$$

where

$$M=c_p m/\lambda$$

and

$$\Psi(\theta)=\frac{1}{L^2}\frac{(1-\theta)}{\theta}\exp\left(-\frac{\theta_a}{\theta}\right)$$

The new dependent variable P defined as $P=r^2(d\theta/dr)$ is now introduced; as the independent variable, θ is taken again. With this notation equation 14 is transformed into

$$P\,dP/d\theta-MP=-r^4\Psi(\theta) \quad \ldots . [15]$$

or

$$P(dP/d\theta-M)=r^4\Psi(\theta) \quad \ldots . [16]$$

Now divide both sides by r_f^4, where r_f is a scaling parameter; setting $r/r_f=\Sigma$, $P/r_f^2=\pi$ and $M/r_f^2=\mu_s$, yields the fundamental differential equation

$$\pi(d\pi/d\theta-\mu_s)=-\Sigma^4\Psi(\theta) \quad \ldots . [17]$$

and by integrating once, the integral equation

$$\frac{\pi^2}{2}=\int_{\theta}^{1}\Sigma^4\Psi\,d\theta-\mu_s\int_{\theta}^{1}\pi\,d\theta \quad \ldots . [18]$$

where the eigenvalue μ_s is defined by

$$\mu_s=\int_{\theta_0}^{1}\Sigma^4\Psi\,d\theta\bigg/\int_{\theta_0}^{1}\pi\,d\theta \quad \ldots . [19]$$

From this point on the numerical procedure follows along the lines indicated for the cylindrical flame.

Appendix B

The zero'th approximation to σ will be obtained from the asymptotic evaluation of the integral $I(\theta_a)$ by a special form of the *method of steepest descent* (cf. A. ERDELYI[13]). The integral is repeated here for convenience

$$I(\theta_a)=\int_{\theta_0}^{1}\Sigma^2\left(\frac{1-\theta}{\theta}\right)\exp\left(-\frac{\theta_a}{\theta}\right)d\theta \quad . . [20]$$

One now makes a trivial change of variable

$$1/\theta-1=x \quad \ldots . [21]$$

The use of x as a variable of integration should cause no confusion with the distance coordinate. The transformed integral with interchanged limits is

$$I=\exp(-\theta_a)\int_{0}^{\frac{1}{\theta_0}-1}\frac{\Sigma^2(x)}{(x+1)^2}\exp\theta_a\left\{\frac{\ln x}{\theta_a}-x\right\}dx \quad \ldots . [22]$$

The integrand is now of the general form $\chi(x)\exp\{\theta_a h(x)\}$ where θ_a is a large positive constant, and $\chi(x)$ is a monotonic function. The asymptotic value of an integral of this type is given by

$$\lim_{\theta_a\to\infty}\int_{a}^{b}\chi(x)\exp\{\theta_a h(x)\}\,dx$$

$$\sim\chi(\xi)\exp(\{\theta_a h(\xi)\}\left\{\frac{-2\pi}{\theta_a h''(\xi)}\right\}^{\frac{1}{2}}$$

where $a \leqslant \xi \leqslant b$ is the point at which $h(x)$ has a maximum. In the present case $h(x)$ is $h(x) = (1/\theta_a) \ln x - x$. It has an *extremum* at $x = 1/\theta_a$; that this stationary point is a maximum is ascertained by the fact that the second derivative at this point is negative, i.e.

$$h''(1/\theta_a) = -\theta_a \quad \ldots . [23]$$

Finally, the value of I as $\theta_a \longrightarrow \infty$ is given by I_a

$$I_a = \frac{\Sigma^2(\xi)}{(\xi+1)^2} \exp(-\theta_a) \cdot \exp \theta_a \left\{ \frac{\ln \frac{1}{\theta_a}}{\theta_a} - \frac{1}{\theta_a} \right\} \cdot \frac{(2\pi)^{\frac{1}{2}}}{\theta_a} \quad \ldots . [24]$$

setting

$$\theta_a / (1 + \theta_a) = \theta_1^* \quad \ldots . [25]$$

which has the limiting value of unity, gives

$$I_a = (2\pi)^{\frac{1}{2}} \left\{ \frac{\sigma(\theta_1^*)}{\theta_a / \theta_1^*} \right\}^2 \exp\left(-\frac{\theta_a}{\theta_1^*} \right) \quad . . [26]$$

If we set $\sigma = 1$, then the accuracy of the formula can be estimated. For $\theta_a = 8$, the exact value of the integral is $3{\cdot}54 \times 10^{-6}$ and the approximate value is $3{\cdot}82 \times 10^{-6}$; the relative error is 8 per cent.

Since σ is a positive and continuous function and since $\Phi(\theta)$ is integrable, the mean value theorem of the integral calculus may be employed to evaluate the first integral in equation 9 (cf. R. COURANT[16])

$$I(\theta) = \sigma^2(\theta_2^*) \int_\theta^1 \frac{1-\theta}{\theta} \exp\left(-\frac{\theta_a}{\theta} \right) d\theta \quad . . [27]$$

where $\theta \leqslant \theta_2^* \leqslant 1$. From equations 27 and 20 it follows that if in particular $\theta = \theta_0$, and $I(\theta_0) \simeq I_a(\theta_0)$ within the accepted approximation we may set $\theta_1^* = \theta_2^* = \theta^*$. It is now proposed to neglect the dependence of θ^* on θ (i.e. the lower limit of the integral) and set $\sigma(\theta) = \sigma(\theta^*) =$ constant. With this simplification the integral becomes

$$\int_\theta^1 \exp\left\{ -\frac{2}{\xi_f} \int_z^1 \frac{d\zeta}{y(\zeta)} \right\} \phi \, dz = \sigma(\theta^*) \int_\theta^1 \phi \, dz. \quad [28]$$

which is independent of y, and the iteration can now take its course in exactly the same fashion as for the flat flame.

References

[1] LORELL, J. and WISE, H. *J. chem. Phys.* 1955, **23,** 1928–1932

[2] WILLIAMS, F. A. Daniel and Florence Guggenheim Jet Propulsion Center, California Institute of Technology, *Tech. Rep. No. 21,* February 1958

[3] BOYS, S. F. and CORNER, J. *Proc. Roy. Soc.* 1949, **197,** 90–106

[4] VON KÁRMÁN, T. and MILLAN, G. *Biezano Anniversary Volume on Applied Mechanics,* pp 59–69. Stam: Haarlem, Antwerp, Djakarta, 1953

[5] MARKSTEIN, G. *J. aero. Sci.* 1951, **18,** No. 3, 199–209

[6] FABRI, J. *Selected Combustion Problems,* Vol. I, pp 42–58. Butterworths: London, 1954

[7] KLEIN, G. *Phil. Trans.* 1957, **249,** 389–415

[8] HIRSCHFELDER, J. O. and CURTISS, C. F. *J. chem. Phys.* 1949, **17,** 1076–1081

[9] VON KÁRMÁN, T. and PENNER, S. S. *Selected Combustion Problems,* Vol. I, pp 5–41. Butterworths: London, 1954

[10] SPALDING, D. B. *Combustion & Flame,* 1957, **1,** 296–307

[11] MARKSTEIN, G. *Fourth Symposium (International) on Combustion,* pp 51–55. Williams and Wilkins: Baltimore, 1953

[12] UBEROI, M. S., KUETHE, A. M. and MENKES, H. R. *Physics of Fluids,* 1958, **1,** 150–158

[13] BARENBLATT, G. I. and ZELDOVICH, Y. B. *Prikl. Mat. Mekh.* (*Appl. Math. Mech., Leningr.*), 1957, **21,** No. 6 (available in translation from Morris D. Friedman, Inc., Foreign Technical Translations, 67 Reservoir Street, Needham Heights 94, Massachusetts)

[14] MENKES, J. *Proc. Roy. Soc.* 1959, **253,** 380–389

[15] ERDÉLYI, A. *Asymptotic Expansions.* Dover: New York, 1956

[16] COURANT, R. *Differential and Integral Calculus,* Vol. I, pp 126–128. Interscience: New York, 1949

Is
wa
fla
vat
an
late
dec
rate
tha
hal
of t

T
dec
kin
dec
whe
trat
con
by
and
vati
it w

---

*Pres
vers

The Effect of Pressure on the Mechanism and Speed of the Hydrazine Decomposition Flame

G. K. ADAMS and G. B. COOK*

Explosives Research and Development Establishment, Waltham Abbey, Essex
and
**Armament Research and Development Establishment, Fort Halstead, Sevenoaks, Kent*

(Received January 1959)

The hydrazine decomposition flame reaction is approximated by a simple one-centre chain reaction with the termination step second order in radical concentration. The differential equations of flame propagation for this reaction scheme are solved by an unsteady state method programmed for a high speed digital computer. The results presented are the radical concentration/temperature distributions and space integral reaction rates (proportional to flame speed) for a range of final flame temperatures and pressures. These show that with the values of the reaction rate constants proposed, the radical concentration is significantly different from that given by the radical stationary state approximation at all total pressures below 100 atmospheres, although, if the termination reaction is assumed to be third order in total pressure, this approximation is valid in the limit of high pressure. The temperature coefficient of flame speed is shown to be relatively insensitive to variation in pressure or in termination rate constant whereas the pressure exponent is sensitive to the mechanism assumed. When the total order of the terminating reaction is greater than that of the propagating reaction the pressure exponent passes through a minimum value as the pressure increases before reaching the constant value corresponding to the stationary state radical distribution.

IN AN earlier paper[1] a radical chain mechanism was proposed for the hydrazine decomposition flame. This proposal was based upon the observations that the experimental flame speed was an order of magnitude greater than that calculated on the assumption that the overall rate of decomposition of hydrazine was equal to the rate of decomposition into NH_2 radicals and that the temperature coefficient was about one half of that calculated from the activation energy of this reaction.

The probable reaction steps in the chain decomposition scheme were discussed and kinetic expressions derived for the rate of decomposition of hydrazine under conditions where a stationary state for the radical concentrations could be assumed. That is, under conditions where the concentration is determined by equilibrium between the rates of generation and destruction. This led to an overall activation energy of the required order. However, it was pointed out that in the reaction zone of the decomposition flame the radical concentration would be influenced by diffusion and convection as well as by the rates of generation and destruction and that the stationary state approximation was not necessarily valid. Since the detailed formulation of the chain reaction involved reaction steps for which there were no reaction rate data available, it was proposed that the behaviour of a much simplified model should be examined by numerical integration of the differential equations of continuity for the flame problem.

The simplified reaction scheme proposed consisted of three steps:

Chain initiating	$a \longrightarrow 2\,b$
Chain propagating	$b+a \longrightarrow 2\,c+b$
Chain terminating	$b+b \longrightarrow 2\,c$

The hydrazine molecule is supposed to decompose into two radicals through a unimolecular reaction with a large activation energy. These radicals react with another hydrazine molecule to give two molecules of stable product, but reproducing the radical in a bimolecular reaction of low activation energy. Radicals are destroyed in a zero activation energy process, second order in radical concentration but probably third order with respect to total pressure, to give stable products.

---

*Present address: Electronic Computing Laboratory, The University, Leeds 2.

The dissimilarities in the activation energies and reaction orders of the individual reaction rate terms in the continuity equation preclude the solution of the differential equations by approximate analytical methods of the Boys–Corner type. Attempts to integrate the steady state equations numerically from the hot boundary by step-by-step methods have failed to give convergent solutions for the radical concentration.

In 1956 D. B. **Spalding**[2] examined this reaction scheme using a graphical method of solution for the unsteady flow problem. He was able to show that, for atmospheric pressure conditions, the radical destruction term was comparatively unimportant except in the vicinity of the hot boundary, and that the radical concentration distribution in the important part of the reaction zone was far removed from that required by the stationary state approximation. He evaluated the flame speed at two values of the flame temperature and obtained values in good agreement with the experimentally observed speeds. It appeared that the reaction scheme and the numerical values of the reaction rate constants proposed gave the required temperature coefficient even though the stationary state approximation was inapplicable.

G. **Millan** and I. **Sanz**[3] have since used an analytical, successive approximation treatment, the results of which appear to indicate that the numerical values of the flame speed and its temperature coefficient, obtained by neglecting radical recombination on the one hand or by assuming a stationary radical concentration on the other, give values for the flame speed and temperature coefficient which are almost identical. Although it is clear that, with the numerical values used for the reaction rate constants, the stationary state assumption does not give a true representation of the reaction under flame conditions at atmospheric pressure, it appears that it gives approximately the correct order of magnitude of flame speed and temperature coefficient.

It would also be possible to choose yet another set of reaction rate parameters which would allow the steady state assumption to be valid and would satisfy the experimental results for flame speed and temperature coefficient. This is a consequence of the fact that the solution depends upon three reaction rate constants and that the temperature coefficient is mainly determined by that of the initiating reaction. It is evident that the prediction of flame speed and temperature coefficient is not sufficient to verify either the mechanism or the method of solution.

Another property of the flame which any proposed reaction scheme must satisfy and which can be used as a check on mechanism, is the variation of flame speed with pressure. Since the individual reaction rate terms in the simplified scheme have different pressure dependences it is not possible to calculate the overall pressure dependence of flame speed by approximate methods or to determine it by dimensional analysis. We have therefore solved the flame equations for a range of flame temperatures and pressures using the reaction rate data employed by Spalding and by Millan and Sanz, but taking account of the radical destruction term. We also consider the effect of varying the order of the initiating and terminating reactions.

Formulation and Solution of the Flame Equations

For complex reaction schemes, the numerical approach proposed by Spalding, of solving the time-dependent equations, has much to recommend it. It is shown below that the problem is essentially the solution of a set of coupled parabolic partial differential equations under certain initial and boundary conditions. With the aid of a high-speed automatic computer, it is possible to integrate these equations by standard finite difference techniues to give temperature and reactant concentration as numerical functions of space and time. The integration can be continued until these variables and a certain integral of one of the reaction rates have tended sufficiently closely to their steady state values.

The method is free from the computational problems which appear to beset step-by-step integration from the boundaries in the steady state problem and is simpler in formulation than G. KLEIN's method[4] of successive approximations to the solution of integral equations which is difficult to apply when the radical concentration distribution is very different from the stationary state distribution. The unsteady state method has the additional advantage of giving a more comprehensible view of flame propagation and of being able to provide information on ignition and stability properties.

The energy equation

Consider a gaseous system consisting of a number of species a, b, . . ., j, . . . and let $\alpha, \beta, \ldots, \chi, \ldots$ denote the mass fraction concentration of these species respectively so that, if ρ denotes the density and m_j and n_j denote the molecular weight and mole concentration of species j respectively, $\alpha = m_a n_a / \rho$, $\beta = m_b n_b / \rho$ and, in general, $\chi = m_j n_j / \rho$.

Further, for species j, let q_j and w_j denote the heat of reaction per unit mass and reaction rate (mass per unit volume and time) respectively. Then, if T denotes the absolute temperature, λ the thermal conductivity and v the convectional velocity, the energy equation may be written

$$\rho \frac{\partial (cT)}{\partial t} = \frac{\partial (\lambda \partial T / \partial x)}{\partial x} - \rho v \frac{\partial (cT)}{\partial x} + \sum_j q_j w_j \quad . \, [1]$$

where kinetic energy and pressure terms have been neglected and, in the last term, the summation extends over all reactions of all species a, b, c, . . ., j, . . . In equation 1, t and x denote the time and the distance from a certain origin respectively. The time $t = 0$ and the origin $x = 0$ are identified essentially in the statement of the initial conditions of the problem given below. Assuming that c and $\lambda\rho$ are independent of temperature, the first-order space derivative in equation 1 can be eliminated[2] by means of the transformation

$$\mathrm{d}y = \frac{\rho \mathrm{d}x}{\rho_1} \quad . \; . \; . \; . \, [2]$$

and by use of the continuity equation

$$\frac{\partial \rho}{\partial t} = -\frac{\partial}{\partial x}(\rho v) \quad . \; . \; . \; . \, [3]$$

The suffix 1 denotes values for the state of complete reaction. The resulting equation may be further simplified by introducing the dimensionless variables ψ and θ defined by:

$$\psi = \left(\frac{kc\rho_1^2}{\lambda\rho} \right)^{\frac{1}{2}} y$$

$$\theta = kt$$

where k is an arbitrary scaling constant having dimensions sec^{-1}. These transformations give

$$\frac{\partial T}{\partial \theta} = \frac{\partial^2 T}{\partial \psi^2} + \frac{1}{\rho c k} \sum_j q_j w_j \quad . \; . \; . \; . \, [4]$$

The diffusion equations

The exact forms of the diffusion equations as given by J. O. HIRSCHFELDER *et al.*[3] for multicomponent mixtures are too unwieldy to be transformed into the simple form of equation 4.

However, if we use the form applicable to binary mixtures, the conservation of species equations can be written in terms of the mass fraction concentrations. Thus for 'a' and for each other species

$$\rho \frac{\partial \alpha}{\partial t} = \frac{\partial (D\rho \partial \alpha / \partial x)}{\partial x} - \rho v \frac{\partial \alpha}{\partial x} + w_a \quad . \; . \, [5]$$

where $D\rho$ is independent of composition and of the species 'a'. The last term in equation 5, w_a, is the net rate of production of species 'a'. (Since $\sum_j \chi = 1$, the number of equations required is one less than the total number of components and in this instance we require only two equations, one for species 'a' and one for 'b'.)

We make the further assumption that $D\rho c / \lambda = 1$. We can then, using the same transformations as for the energy equation, write the continuity equations for each of the reacting species a, b . . . in the form

$$\frac{\partial \alpha}{\partial \theta}=\frac{\partial^2 \alpha}{\partial \psi^2}+\frac{1}{\rho k}w_a \text{ etc.} \qquad \ldots . [6]$$

Kinetic model of the hydrazine flame

In the general formulation of the energy and diffusion equations given in the two previous sections, we now identify species 'a' with hydrazine and species 'b' with the radical intermediate in the decomposition to form a stable product 'c'. The net rate of disappearance of 'a' is the sum of the rates of decomposition into radicals and the rate of reaction with radicals to form stable product

$$\text{a} \longrightarrow 2\text{b} - 66 \text{ kcal/mol}$$

$$\text{a}+\text{b} \longrightarrow 2\text{c}+\text{b}+33 \text{ kcal/mole of hydrazine}$$

The heats of reaction are taken with a small adjustment from ref. 1. The rate of the first reaction is assumed to be proportional to the hydrazine mol-concentration and the second to the product of this concentration and that of the radical. The rate constants were assumed to be of a simple Arrhenius type, the parameters were given nominal values on the basis of the reaction rate data quoted in ref. 1 and are identical with those used by Spalding[2]. Then, in terms of the mass fraction concentrations α and β, local temperature T°K, density ρ in g/cm^3, and radical molecular weight m_b,

$$-w_a/\rho=10^{13}\alpha \exp(-33\,000/T)$$
$$+10^{13}\frac{\rho\alpha\beta}{m_b}\exp(-3\,500/T) \quad \ldots [7]$$

Similarly, the net rate of production of radicals is the sum of the rate of formation from hydrazine and the rate of recombination in a reaction to form stable products: 2b ⟶ 2c + 99 kcal/mole of hydrazine. This last reaction is assumed to have zero temperature dependence and its rate proportional to the square of the concentration of radicals times the total concentration of all species.

Then

$$w_b/\rho=10^{13}\alpha \exp(-33\,000/T)-10^{16}\frac{\rho^2\beta^2}{m_b\overline{m}} \qquad \ldots . [8]$$

where the mean molecular weight $\overline{m}$ is calculated from

$$1/\overline{m}=\alpha/m_a+(1-\alpha)/m_b \qquad \ldots . [9]$$

and where

$$m_a=2m_b=32$$

The density ρ is given in terms of the mean molecular weight $\overline{m}$ and the pressure P in atmospheres by

$$\rho=P\overline{m}/82{\cdot}063\,T \qquad \ldots . [10]$$

The net rate of heat production $\sum_j q_j w_j$ in equation 1 is given by the sum of the products of the reaction rates and the heats of reaction and is equal to

$$\sum_j q_j w_j=\frac{10^3\rho}{m_a}\Big\{-66\times 10^{13}\alpha \exp(-33\,000/T)+$$
$$33\times 10^{13}\frac{\rho\alpha\beta}{m_b}\exp(-3\,500/T)+99\times 10^{16}\frac{\rho^2\beta^2}{\overline{m}m_b}\Big\} \qquad \ldots . [11]$$

or, as can easily be verified,

$$\sum_j q_j w_j=\overline{q}\,(w_a+3w_b) \qquad \ldots . [12]$$

where $\overline{q}$ is the heat of reaction per gramme of hydrazine decomposing to stable products

$$\overline{q}=33\times 10^3/32 \quad \text{cal/g}$$

Initial and boundary conditions

The initial conditions were formulated so as to make the total enthalpy constant on both sides of the ignition boundary. At $\theta=0$, the region $\psi>0$ was assumed to contain reactant 'a' at constant temperature T_0 and fractional mass concentration α_0 (the other component being product 'c'), while the region $\psi<0$ was assumed to contain only product 'c' at constant temperature T_1. We therefore have the following relation

$$T_1=T_0+\overline{q}\alpha_0/c \qquad \ldots . [13]$$

where c is the heat capacity. The boundary conditions for $\theta > 0$ to be satisfied are the following:

$$\psi \longrightarrow -\infty, \quad T \longrightarrow T_0, \quad \alpha \longrightarrow \alpha_0, \quad \beta \longrightarrow 0$$

$$\psi \longrightarrow +\infty, \quad T \longrightarrow T_1, \quad \alpha \longrightarrow 0\,, \quad \beta \longrightarrow 0$$

On account of the assumption of equal mass and thermal diffusivities ($D\rho c = \lambda$) and the initial boundary conditions, it may be verified easily that from equations 4, 6 and 12

$$T_1 - T = (\bar{q}/c)\,(\alpha + 3\beta) \qquad \ldots . [14]$$

a relation valid for all ψ and θ. Therefore, only two of α, β and T are independent and only two of the three equations need be integrated, the third dependent variable being obtained from equation 14.

Method of integration

The problem is essentially the numerical integration of equations 4 and 6 under the given initial and boundary conditions. The ψ/θ plane is replaced by a rectangular mesh with intervals $\Delta\psi$ and $\Delta\theta$ and a step-by-step integration in θ is carried out. If $T_{n,j}$ denotes the value of T at the mesh point with coordinates $n(\Delta\psi)$, $j(\Delta\theta)$, we have, replacing the space derivative by a central difference and the θ derivative by a forward difference, for equation 4

$$T_{n,j+1} = T_{n,j} + \sigma\,(T_{n+1,j} + T_{n-1,j} - 2T_{n,j})$$

$$+ \bar{q}2T\frac{\Delta\theta}{\rho c k}(w_a + 3w_b)_{n,j} \qquad \ldots . [15]$$

where $(w_a + 3w_b)_{n,j}$ means the quantity in brackets is evaluated at $n(\Delta\psi)$, $j(\Delta\theta)$. The parameter $\sigma = \Delta\theta/(\Delta\psi)^2$ was taken to be 1/6 since, for the simple heat conduction equation without sources, the truncation error for the particular type of replacement used is a minimum. The computation was programmed for a Ferranti Mark I* computer in a general form which would be suitable for the integration of up to four coupled equations.

The value of k was chosen for computational convenience and in most cases for which results are quoted below, the value used was $10^{13}\ e^{-12\cdot 8}\ \text{sec}^{-1}$.

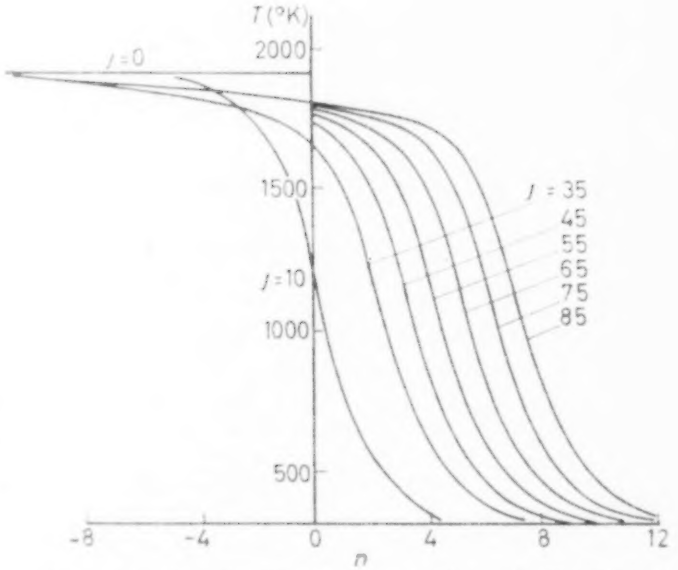

Figure 1. Temperature/space profile as a function of time, $\psi = n\,(\Delta\psi)$, $\theta = j\,(\Delta\theta)$ [$\Delta\theta = 8$, $\sigma = 1/16$, $k = 10^{13}$ $e^{-12\cdot 8}$ sec^{-1}, one atmosphere pressure, $T_1 = 1900°K$, $T_0 = 300°K$]

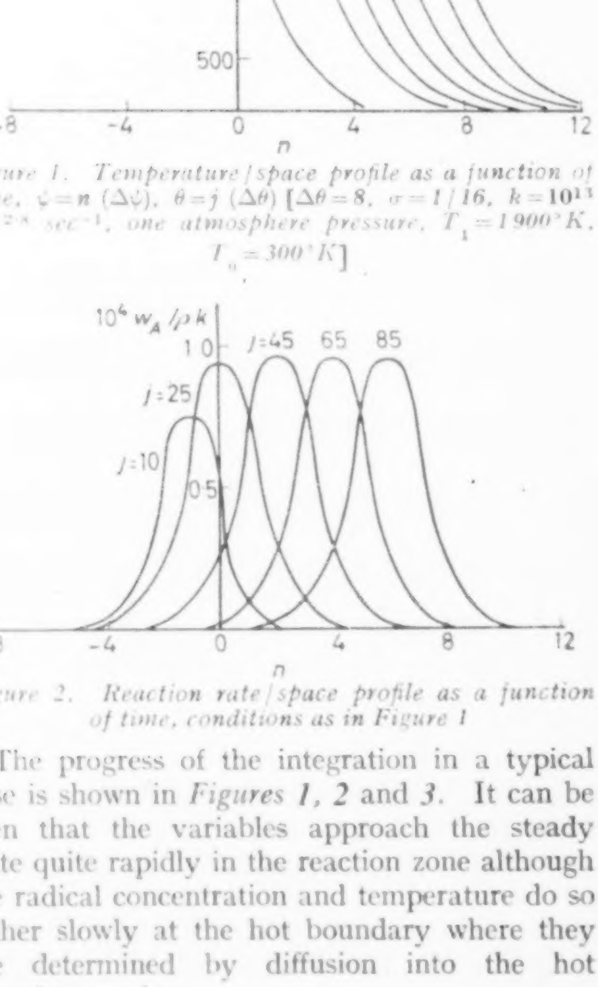

Figure 2. Reaction rate/space profile as a function of time, conditions as in Figure 1

The progress of the integration in a typical case is shown in *Figures 1, 2* and *3*. It can be seen that the variables approach the steady state quite rapidly in the reaction zone although the radical concentration and temperature do so rather slowly at the hot boundary where they are determined by diffusion into the hot boundary region.

The flame propagates into the unreacted gas, after a short delay, with a speed which has very rapidly assumed its steady state value. The latter can best be evaluated from the space integral reaction rate which, from *Figure 4*, also rapidly approaches a constant value. This is related to the flame speed, v, by the equation

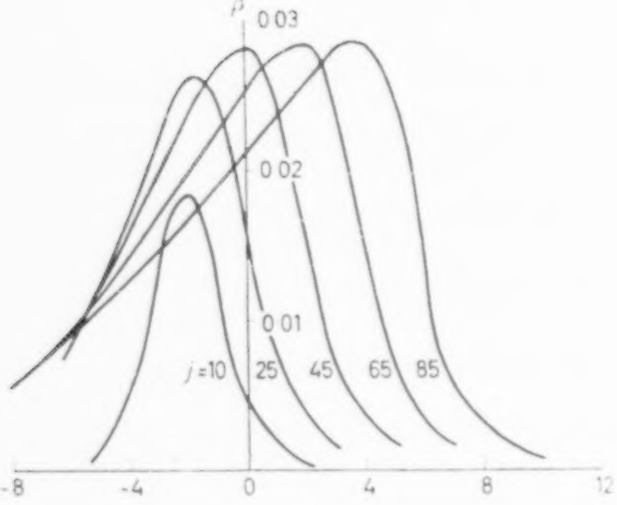

Figure 3. Radical concentration/space profile as a function of time, conditions as in Figure 1

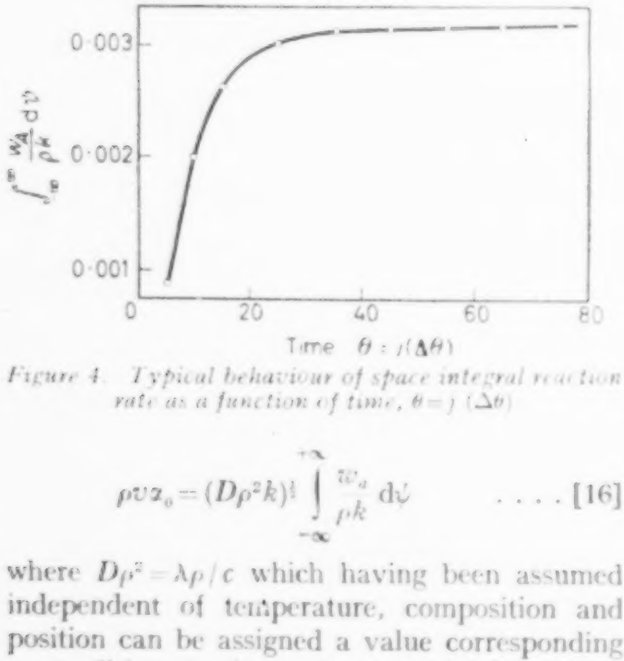

Figure 4. Typical behaviour of space integral reaction rate as a function of time, θ = j (Δθ)

$$\rho v \alpha_0 = (D\rho^2 k)^{\frac{1}{2}} \int_{-\infty}^{+\infty} \frac{w_a}{\rho k} \, d\psi \quad \ldots . [16]$$

where $D\rho^2 = \lambda\rho/c$ which having been assumed independent of temperature, composition and position can be assigned a value corresponding to conditions in the products at the final flame temperature.

The Pressure Dependence of the Hydrazine Flame Model

The stationary state approximation applied to reaction in a flame amounts to the assumption that the diffusion and convection terms in the conservation of species equation for the radical are small compared to the chemical reaction rate terms. Then the radical concentration in the flame can be evaluated by equating the RHS of equation 8 to zero, obtaining

$$\beta^2 = 10^{-3} \frac{\alpha m \overline{m}}{\rho^2} \exp - \left(\frac{33\,000}{T} \right) \quad \ldots . [17]$$

This expression for β can be inserted into the reaction rate equation 7 for hydrazine, to obtain the approximation

$$-w_a/\rho = 10^{11.5} \left(\frac{\overline{m}}{m_h} \right)^{\frac{1}{2}} \alpha^{3/2} \exp - \left(\frac{20\,000}{T} \right) \quad [18]$$

To obtain a knowledge of the conditions under which this approximation is valid we may follow J. O. HIRSCHFELDER and J. C. GIDDINGS[4] in requiring that the chemical lifetime of the radical must be shorter than that of the reactant. Since

$$1/t_r \sim 10^{14} \rho^2 \beta / m_r \overline{m}$$

and

$$1/t_a \sim 10^{12} (\rho\beta/m_h) \exp(-3\,500/T)$$

the condition is that

$$\rho > 10^{-3} \overline{m} \exp(-3\,500/T) \quad \ldots . [19]$$

or

$$P > 8{\cdot}2 \times 10^{-2} T \exp(-3\,500/T)$$

Thus for any given temperature level in the flame the stationary state radical concentration approximation will be valid above some critical pressure. We may regard equation 18 for the rate of decomposition of hydrazine as being valid throughout the flame reaction zone in the limit of high pressures. This equation is first-order with respect to total pressure although of 3/2 order with respect to hydrazine. It is therefore convenient to express the results of flame speed calculations over a range of pressures and flame temperatures in terms of the dimensionless first-order reaction time τ or the first-order reaction rate $1/\tau$ where, from equation 16,

$$1/\tau = (\rho v)^2/(D\rho^2 k)_1 = \left[\int \frac{w_a}{\rho k_1} d\psi \right]^2 \alpha_0^{-2} \quad \ldots [20]$$

Here D and ρ are assigned values corresponding to complete reaction at the hot boundary and

k_1 is made equal to the high pressure specific rate constant at the hot boundary obtained from equation **18**

$$k_1 = 10^{11 \cdot 5} \exp(-20\,000/T_1)$$

At any fixed flame temperature $1/\tau$ should tend to a limiting value at high pressures which, from elementary flame theory, should be about equal to the quantity $2(T_1/20\,000)^{2 \cdot 5}$ in magnitude.

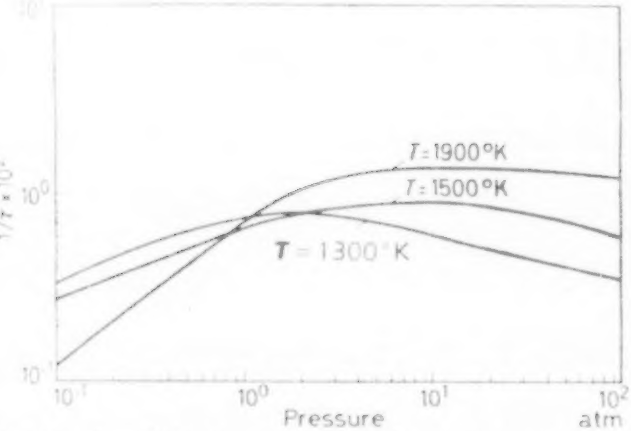

Figure 5. Effective dimensionless rate constant defined by $1/\tau = (\rho v)^2/(D\rho^2 k)_1$ *as a function of pressure, where* $k_1 = 10^{11 \cdot 5} \exp(-20\,000/T)$ *sec*$^{-1}$

Table 1. Calculated results for Figure 5
$k_1 = 10^{11 \cdot 5} \exp(-20000/T_1)$ sec^{-1}

Flame temperature T_1 *°K*	*Initial concentration* α_0	*Pressure atm*	$1/\tau = \frac{(\rho v)^2}{(D\rho^2 k)_1} \times 10^3$
1 900	1	0·1	1·26
1 900	1	0·5	4·19
1 900	1	1·0	6·83
1 900	1	10·0	13·8
1 900	1	100·0	12·3
1 700	$\frac{7}{8}$	0·1	1·78
1 700	$\frac{7}{8}$	1·0	7·28
1 500	$\frac{3}{4}$	0·1	2·81
1 500	$\frac{3}{4}$	1·0	6·51
1 500	$\frac{3}{4}$	10·0	9·27
1 500	$\frac{3}{4}$	100·0	6·05
1 300	$\frac{5}{8}$	0·1	3·47
1 300	$\frac{5}{8}$	1·0	7·30
1 300	$\frac{5}{8}$	10·0	6·13
1 300	$\frac{5}{8}$	100·0	3·55

In *Figure 5* we have plotted on a log/log scale the values obtained for $1/\tau$ as a function of pressure from 0·1 to 100 atmospheres and flame temperatures from 1 300° to 1 900°K (*Table 1*). To ensure consistency with equation **14** the appropriate values of α_0 used at the cold boundary and in the calculation of $1/\tau$ from equation **20** were computed from equation **14** assuming $\bar{q}/c = 1\,600$°K.

The variation in the $1/\tau$ values as the pressure is varied represents the deviation of the overall reaction rate from a first-order pressure dependence. For a first-order reaction the log $1/\tau$ curves would be horizontal lines. If their slope is z at any pressure the overall reaction order with respect to pressure is $1+z$. At high pressures the stationary state radical concentration approximation will tend to hold throughout the flame and the curves are asymptotic to the $1/\tau$ values for this condition. As the pressure decreases the value of $1/\tau$ is seen to increase and to pass through a maximum. In the region in which it increases with decreasing pressure, z is negative and the apparent reaction order less than one. This effect is most marked at the lower flame temperatures: at $T_1 = 1\,300$°K the apparent order appears to be about 2/3 in the region 10 to 50 atmospheres, although the calculated points are not sufficiently numerous to allow an accurate estimate.

Below the pressure at which $1/\tau$ has its maximum value the slope of the curves is positive and the overall order greater than one. In this region $1/\tau$ decreases with increasing flame temperature indicating that the overall activation energy is less than the 40 kcal/mol. assumed in the arbitrary scaling constant. This behaviour is a consequence of the decreasing importance of the third-order radical destruction rate term with decreasing pressure. Spalding[2] has made a dimensional analysis of the system, neglecting the radical destruction term, which indicates that at low pressures the order with respect to pressure should tend to 3/2 and the overall activation energy to the mean of those of the initiating and propagating reactions, i.e. 36·5 kcal/mol. Our results, which allow for the effect of radical concentration on the temperature within the flame profile, indicate that at the higher flame temperatures (>1 500°K), where the radical term in equation **14** is large near the hot boundary, the apparent order may be nearer two and the apparent activation energy a little less than 36·5 kcal/mol. The radical destruction is so slow compared with the propagating reaction at low pressures that the effective flame temperature is reduced by the persistence of radicals. Since the fractional radical concentration increases with decreasing pressure when the initiating reaction is first order, this effect increases with decreasing pressure.

The surprising feature of the $1/\tau$ against pressure curve is the existence of a maximum and therefore of a region in which the apparent order is less than one. The cause of this behaviour can be seen if the radical concentration/temperature curves at various pressures are compared with the stationary state curves representing the limiting behaviour at high pressures, as in *Figures* 6 and 7. Since the activation energy of the propagating reaction is low the rate of decomposition of hydrazine is, in the region which contributes the major portion of the total decomposition rate, more a function of the radical concentration than of the temperature or of the hydrazine concentration.

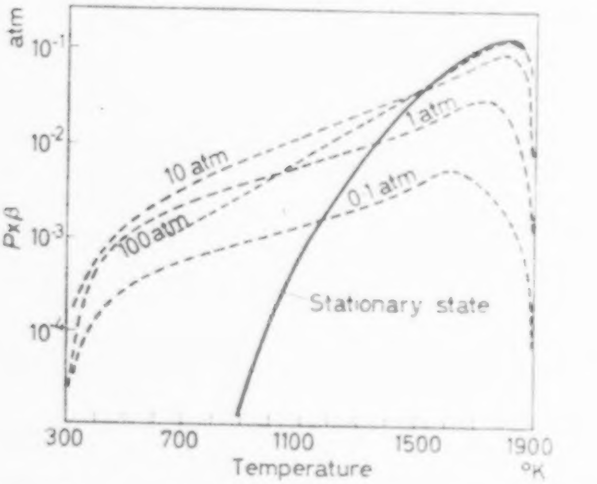

Figure 6. Mass fractional radical concentration times pressure as a function of local temperature at $T_1 = 1\,900°K$

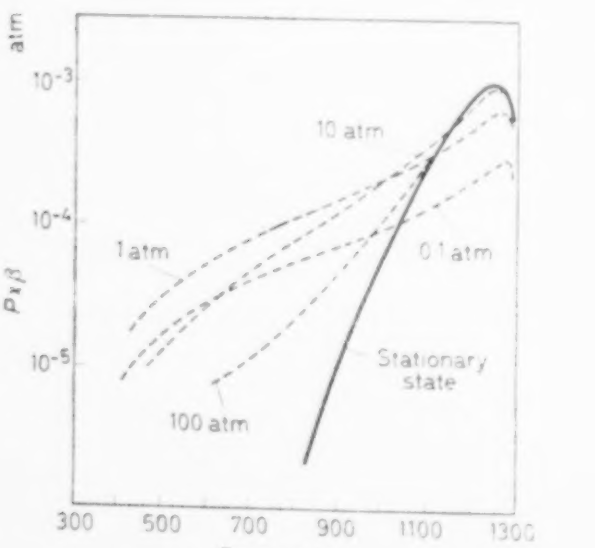

Figure 7. Mass fractional radical concentration times pressure as a function of local temperature at $T_1 = 1\,300°K$

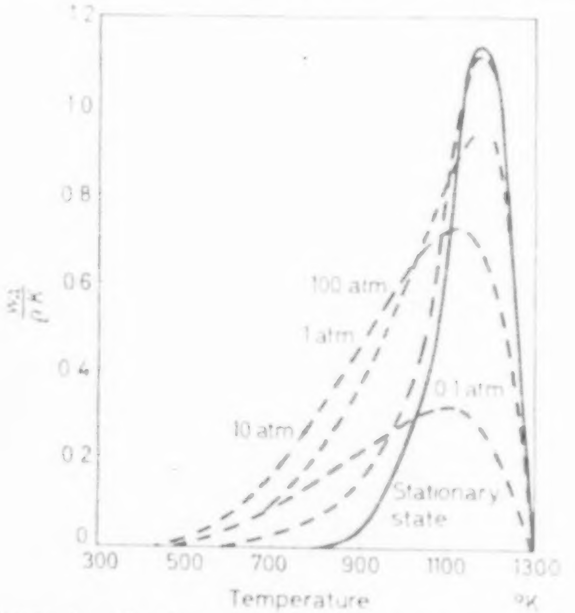

Figure 8. Reaction rate $w_a/\rho k$ *as a function of local temperature at* $T_1 = 1\,300°K$ [$k = 10^{13} e^{-12\cdot 8}$ sec^{-1}, *one ordinate unit equals* 10^{-2}]

This can be seen by comparing *Figure 8* where the hydrazine decomposition rate is plotted against temperature on a linear scale for a flame temperature of 1 300°K, with *Figure 7*.

As the pressure is decreased from 100 to 10 atmospheres the radical concentration in the hotter regions falls but that in the cooler regions increases, a consequence of the increasing importance of radical diffusion. The decrease in the space integral of the hydrazine reaction rate in the hotter regions is less than the increase at lower temperatures and the mean first-order rate increases. At some pressure below 10 atmospheres the radical concentration starts to fall over the whole temperature range and the mean first-order rate falls with decreasing pressure. The deviation from the steady state concentration distribution becomes significant at higher pressures as the flame temperature is increased.

Comparisons with Experimental Results

Although the kinetic scheme and the numerical values of the rate constants with which these calculations were made were suggested by data obtained in classical, isothermal studies of chemical kinetics, they are representative rather than exact formulations of reactions likely to occur in hydrazine decomposition flames. We should not expect to be able to calculate the absolute speeds of flame propagation from these calculations or indeed from the data at present available. The close agreement found by other authors using the same data[2, 3] between calculated and experimental flame speeds in hydrazine is fortuitous, although it can be said that the prediction of the correct order of magnitude of flame speed lends support to the relevance of the particular scheme which has been chosen.

Our results confirm the deduction which can be made from the approximate calculations, to the effect that the temperature coefficient of flame speed is insensitive to the assumptions made regarding the importance of the chain terminating reaction. However, this is a consequence of the fact that, for the scheme assumed, the rate of termination is small compared with the rate of the chain propagating reaction and that the activation energies of both are small compared to that of the chain initiating reaction. The result cannot be applied regardless of these conditions, to other chain reactions in flames.

The experimental results of P. Gray and J. C. Lee[7] on the effect of dilution with inert gases has now confirmed the deduction made[1] from those of R. C. Murray and A. R. Hall[8] with water vapour, that the temperature coefficient corresponds to an overall activation energy of little more than half that of the decomposition of hydrazine into NH_2 radicals. The assumption of low activation energies for the propagation and termination steps is therefore consistent with the experimental results.

In order to determine the influence of radical destruction in the hydrazine flame we should examine the experimental pressure dependence of flame speed. Before discussing this problem we must consider the assumptions made in the model concerning the pressure dependence of the rates of the individual reaction terms. We have assumed a termination reaction second order in radical concentration but third order with respect to total pressure. The first is necessary to obtain the required overall activation energy and is consistent with the chemistry of the radicals likely to be involved, the second follows from what we know of the behaviour of simple radicals, although the reaction might be second order at very high pressures. The propagation reaction is almost certainly second order at all pressures. We have assumed the chain initiating reaction to be first order. This was convenient since the case of three reactions of different order is the most difficult to treat by approximate methods, but is certain to be invalid at some low pressure where the rate of collisional activation becomes inadequate to maintain the concentration of activated molecules. The experimental data on hydrazine decomposition provide little information on this point* but we are able to make an estimate of the pressure range in which the unimolecular rate constant should become second order by comparison with other molecules of a similar molecular complexity. Although we have no such information for a comparable region of temperature we follow A. F. Trotman-Dickenson[9] in assuming that the relevant parameter is the value of E/RT. There is a little information on the kinetics of decomposition of dinitrogen tetroxide, N_2O_4, at values of $E/RT=23$ which suggest by analogy that the decomposition of hydrazine into radicals will be second order with respect to pressure above about 1 400°K for pressures about 10 atmospheres. The kinetic order will depend upon both pressure and temperature (for any given reaction an approximate condition for similarity is given[9] as $PT^{-n/2}=$constant, where

---

*Since the completion of this paper the data on hydrazine decomposition in a flow system have been examined by M. Gilbert (*Combustion and Flame*, 1958, **2**, 149) who concludes that it is consistent with a pseudo unimolecular second-order reaction law for the decomposition at about 0·1 atmosphere and 1 000°K.

n depends upon the complexity of the molecule but might be as large as ten for hydrazine) and an attempt to make an exact allowance for this effect is not possible at present. However, it is reasonably certain that at one atmosphere and below, the chain initiating reaction assumed for the hotter hydrazine vapour flames must be second order with respect to pressure. Since we know that the third-order radical destruction reaction is unimportant under these conditions the overall reaction can easily be shown to be exactly second order (the effect of radical concentration on flame temperature is independent of pressure in this case).

The experimental data on the effect of pressure on flame speed in nearly pure hydrazine vapour[7-10] indicate that at a flame temperature of about 1 900°K the overall reaction is second order with respect to pressure at and below atmospheric pressure. This is in agreement with our conclusion above based upon the probable second-order behaviour of the chain initiation reaction at high temperature and low pressure although it does not exclude the possibility that at atmospheric pressure it is in part a consequence of the effect of radical concentration on flame temperature for a reaction of order less than two. This question might be resolved by measuring the flame temperature profile at several pressures.

At lower flame temperatures and at pressures above one atmosphere the model chosen for numerical study can be expected to apply. It predicts the rather unusual result of a pressure dependence less than that of a simple first-order reaction. The calculated reaction order for a flame temperature of 1 300°K varies from a value of 1·4 a little below atmospheric pressure, through 1·0 at about two atmospheres and down to about 0·7 at about fifteen atmospheres. Above this latter pressure it increases and will become first order again above 100 atmospheres (if at higher pressures the termination reaction becomes second order with respect to total pressure then, since the stationary state approximation applies in this range, it can be shown that the overall order would increase still further to a value of 1·5).

A detailed knowledge of the experimental pressure dependence of the hydrazine decomposition flame at low flame temperatures and at pressures higher than atmospheric would therefore test the proposed reaction scheme.

However, such experimental data must be derived from measurements on flames on the surface of liquid hydrazine and those available have been obtained by one particular technique, the measurement of rate of consumption of liquid burning in glass tubes[1-7]. Although the existence of a liquid phase at the cold boundary does not raise any major theoretical problems since, to a first approximation, the flame speed is not sensitive to the cold boundary conditions, there are uncertainties in the deduction of the pressure exponent of flame speed from measurements of the exponent of consumption rate which prevent exact comparisons with theory. Qualitatively, the pressure exponent of mass consumption rate with respect to liquid hydrazine falls below 0·5 in the region of 20 to 30 atmospheres[1] which would correspond to a reaction order of less than one. This behaviour does not appear likely to be the result of the particular experimental technique in that it has not appeared in the behaviour of a variety of other self-combustible liquids studied by the same method and is independent of tube diameter.

References

[1] ADAMS, G. K. and STOCKS, G. W. *Fourth Symposium (International) on Combustion*, p 239. Williams and Wilkins: Baltimore, 1953
[2] SPALDING, D. B. *Phil. Trans.* 1956, **249**, 1
[3] MILLAN, G. and SANZ, I. *Report* on contract No. AF 61 (514 734c), ARDC European Office, 1956
[4] KLEIN, G. *Phil. Trans.* 1957, **249**, 389
[5] HIRSCHFELDER, J. O., CURTISS, C. F. and BIRD, R. *Molecular Theory of Gases and Liquids*. Chapman and Hall: London, 1954
[6] HIRSCHFELDER, J. O. and GIDDINGS, J. C. *Sixth Symposium (International) on Combustion*, p 207. Reinhold: New York, 1957
[7] GRAY, P. and LEE, J. C. *Sixth Symposium (International) on Combustion*, p 255. Reinhold: New York, 1957
[8] MURRAY, R. C. and HALL, A. R. *Trans. Faraday Soc.* 1951, **47**, 743
[9] TROTMAN-DICKENSON, A. F. *Gas Kinetics*, p 79. Butterworth: London, 1955
[10] HALL, A. R. and WOLFHARD, H. G. *Trans. Faraday Soc.* 1956, **52**, 1520

The Use of Reversed Diffusion Flames for the Production of Acetylene and Ethylene from Paraffin Hydrocarbons

J. R. Arthur and D. H. Napier

The British Coal Utilisation Research Association, Randalls Road, Leatherhead, Surrey

(Received February 1959)

The advantages of reversed flames for the preparation of unsaturated hydrocarbons from paraffins are that (a) the products from the flames pass into a cold, non-oxidizing gas and (b) geometrical arrangement of fuel and oxygen favours incompletely burnt products. The influence of the paraffin used, preheat of the gases fed to the burner, ratio of linear velocity of fuel and oxygen, oxygen enrichment, use of steam as diluent and other variables on the yield of acetylene and ethylene were examined. Carbon monoxide and hydrogen were also formed in considerable quantity. From a propane flame, products containing up to 7·0 per cent acetylene and 14·5 per cent ethylene were obtained. The main factors determining the quantities of unsaturated hydrocarbons sampled are discussed.

During an investigation into the mechanism of carbon formation in hydrocarbon diffusion flames, considerable use was made of the transposition of the fuel-air or oxygen supplies supporting the flames since this appeared to increase the ease of producing intermediates participating in the carbon-forming process[1]. Owing to the relative positions of fuel and oxidant in such a reversed flame, the gaseous products are necessarily incompletely burnt; and moreover, under such conditions it is to be expected, on thermodynamic grounds, that some acetylene will be formed. It may also be expected that some acetylene will survive outside the flame where the atmosphere is at a relatively low temperature and non-oxidizing. When preliminary experiments had actually established the presence of small amounts of acetylene in the products from a reversed flame of methane, systematic experiments were undertaken to examine the effect of variables in the system, and to increase these yields. Ethylene, carbon monoxide and hydrogen are also produced, and all four of these compounds are of interest from the aspect of organic chemical synthesis.

The general implications of flame reversal and some of the general properties of reversed flames (temperature, stability, structure etc.) have been given in our earlier paper[1].

Experimental

The apparatus was arranged as shown in *Figure 1*. Air or oxygen-enriched air was fed into the port A and hydrocarbon was introduced at four inlets placed symmetrically around A in the base of the flame tube D. The gases were ignited to form a reversed flame by electrically heating the platinum spiral E, which was subsequently withdrawn from the flame. Excess hydrocarbon and flame products passed out of the flame tube at F where they were burnt. A sampling point was provided at G as shown, and samples of the products leaving the flame tube were withdrawn at low rates into gas sample tubes.

In *Figure 1* the diameters of the flame tube and port are shown as $2R$ and $2r$ respectively. Let the volume flow rates of hydrocarbon and air be V and v respectively. Terms used in this paper may then be defined as follows:

$$\text{Velocity ratio} = \frac{\text{Linear velocity of 'air'}}{\text{Linear velocity of hydrocarbon}} = \frac{v(R^2 - r^2)}{Vr^2}$$

$$\frac{\text{Annulus}}{\text{Jet}}\ \text{ratio} = \frac{\text{Area of annulus}}{\text{Area of port}} = \frac{R^2 - r^2}{r^2}$$

As the wall thickness of the port was small it has been ignored in these definitions and in the work reported below. The diluent ratio of the 'air' stream is defined as the ratio of the volume of diluent to that of the oxygen introduced simultaneously.

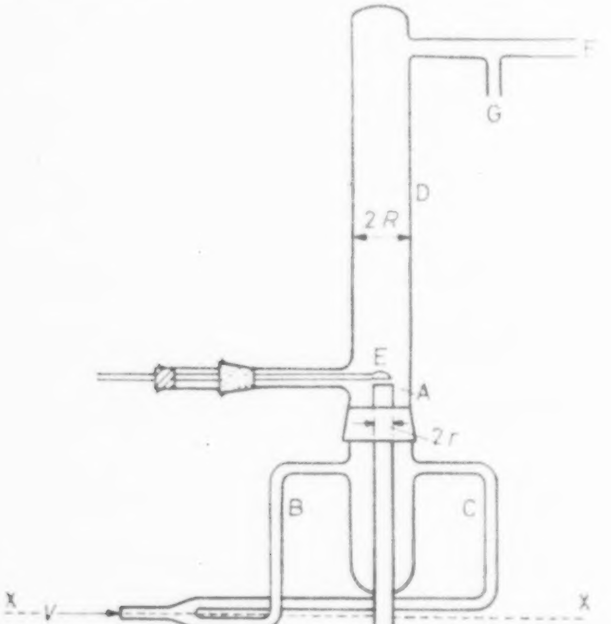

Figure 1. Reversed flame apparatus

When studying the effects of these variables, the results may be expressed in several ways: e.g. as the percentage of acetylene (or other constituent) in the cold, raw gas or as a percentage conversion to acetylene of the hydrocarbon introduced. The latter is calculated from the analysis of the cold product gas as the ratio of the volume of reactant hydrocarbon equivalent to the acetylene (or other constituent) formed to that of the equivalent methane reacted.

The gases produced were analysed in a Bone and Wheeler apparatus. Alkaline mercuric cyanide and activated sulphuric acid were employed as reagents for acetylene and ethylene respectively. For the former determination, a 1·5 ml portion of a 20 per cent solution of mercuric cyanide in 2M potassium hydroxide solution was agitated with the gas for 3 min. A small error occurred owing to the dissolution of acetylene in the potassium hydroxide used to absorb the carbon dioxide in the mixture, but this was negligible for low concentrations of acetylene.

Other gases were determined by conventional methods. Hydrogen and carbon monoxide were oxidized at low temperature over copper oxide, and paraffins were oxidized over an Arnil catalyst. In the latter determination a value for n in C_nH_{2n+2} may be calculated. The paraffin content was then expressed as a mixture of methane and either ethane or, if a propane flame was used, as propane.

As indicated in *Figure 1*, the flame tube D was based on a standard cone and socket assembly for which the relevant dimensions are given in *Table 1*.

Table 1. Dimensions of apparatus

Apparatus	*Int. diameter cm*	*Annulus/jet ratio*
B40	4·0	76·0
B24	2·35	23·9
B19	1·8	12·7
B14	1·7	6·5

Results

(i) *Initial experiments with various hydrocarbons*

Early work showed that greater quantities of acetylene were formed from olefins than from paraffins and from higher paraffins as compared with lower ones. Examples are given in *Table 2*.

It will be noted that appreciable quantities of olefins are formed from ethane and propane. Subsequent work was devoted entirely to the examination of reversed diffusion flames of paraffins.

(ii) *Effect of velocity ratio on conversion to acetylene*

The influence of velocity ratio on conversion

Table 2. *Gaseous products from 'reversed' flames of various hydrocarbons*

Hydrocarbon	*'Air' stream*	CO_2	C_2H_2	C_2H_4	O_2	H_2	CO	C_2H_6	C_3H_8	CH_4	N_2
Methane	O_2 + *Air*	7·8	0·5	0·3	0·1	3·9	4·7	0·9		16·6	65·2
Ethane	*Air*	5·9	2·3	2·9	0·2	7·0	6·0	7·6		1·0	67·1
Propane	*Air*	5·6	2·3	4·1	0·3	5·7	5·6		2·3	12·3	61·8
Ethylene	*Air*	5·5	4·0	17·3	0·2	6·0	7·9	0·2		0·6	58·3
Benzene	O_2 + *Air*	10·0	1·2	1·4	0·1	4·8	11·1	0·6			70·8

was studied at the four annulus/jet ratios shown in *Table 1*, and the results are given in *Figure 2*, which shows that there is an optimum value of velocity ratio for each arrangement of flame tube: for lower values of the annulus/jet ratio the maximum became very sharp, probably owing to the fact that for higher velocity ratios the flame increased in width and came into contact with the walls of the flame tube. In these cases, most of the hydrocarbon introduced passed through the flame front, so that the composition of the reaction products was closer to that obtained from a normal rather than from a reversed flame. *Figure 2* shows that as the annulus/jet ratio decreases, the maximum yields occur at higher percentage conversions and lower velocity ratios. Clearly, no reversed flame will be possible if the annulus/jet ratio becomes too small, and even at a value of 6·5 control becomes difficult.

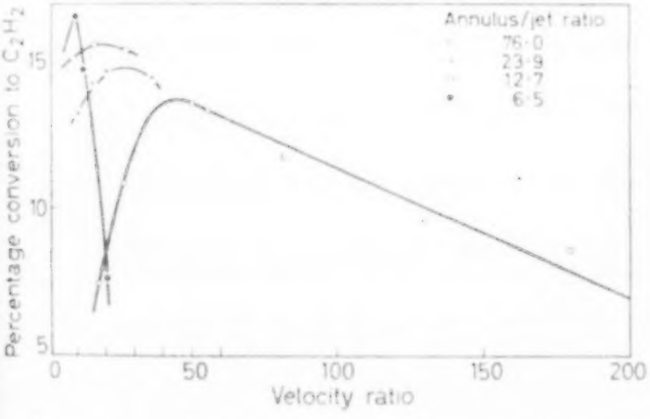

Figure 2. *Variation of percentage conversion to acetylene in reversed methane flames, with velocity ratio, for four annulus/jet ratios*

(iii) *Effect of diluent ratio on conversion to acetylene*

This variable was investigated at an annulus/jet ratio of 12·7 and at a velocity ratio of 16·2; its relation to conversion is shown in *Figure 3*. This shows that over a wide range of composition, as indicated by N_2/O_2 ratio, the conversion is not strongly dependent on that ratio. *Table 3* gives two complete analyses of gas samples corresponding to the above values of annulus/jet ratio and velocity ratio for two different N_2/O_2 ratios.

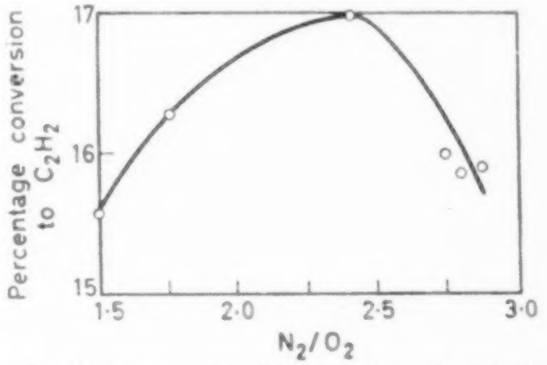

Figure 3. *Variation with diluent ratio, of percentage conversion to acetylene for reversed methane flames*

It should be noted that although the conditions were correct in the first sample for a maximum percentage conversion, the acetylene content may be increased beyond this (see second analysis) although the percentage conversion is reduced. This illustrates the difference in the two methods of expressing the results.

(iv) *Influence of linear velocity of air stream*

This variable governs the size of a reversed flame and hence the throughput with a given flame tube. It has been found that once a reversed flame has been stabilized, the composition of the gaseous products is independent of the flame height and hence of the linear velocity of the air (varied in the range 50 to 100 cm/s). None of the experiments was carried out in the region where turbulent combustion occurs.

Table 3. Influence of diluent ratio on gas composition for reversed methane flames

N_2/O_2	CO_2	C_2H_2	C_2H_4	O_2	H_2	CO	C_2H_6	CH_4	N_2	% *conversion to* C_2H_2
2·3	4·4	1·6	0·8	0·2	12·8	9·3	0·7	26·0	44·2	16·1
1·5	4·7	2·0	0·8	0·3	20·2	14·3	0·5	19·2	38·0	15·6

(v) *Products from reversed propane flames*

The variation of the percentage conversion and of the percentage C_2H_2 in the raw gas with diluent ratio is shown in *Figures 4* and *5*. The annulus/jet ratio was 12·7 and the velocity ratio about 22. The maximum in *Figure 4* occurs at the same diluent ratio as for methane. In *Table 4*, analyses are given of samples of the gases corresponding approximately to the maxima of the curves of *Figures 4* and *5*, together with the analysis of the gas obtained by supporting a flame with pure oxygen.

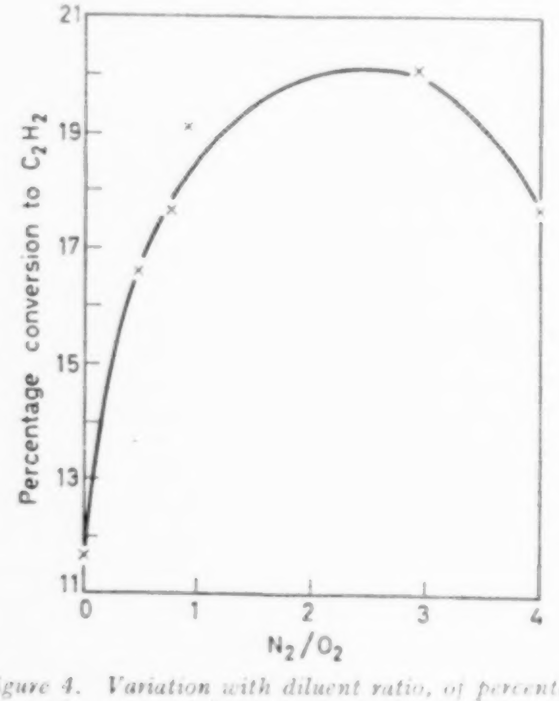

Figure 4. Variation with diluent ratio, of percentage conversion to acetylene for reversed propane flames

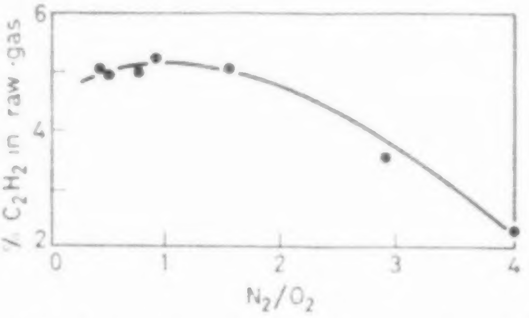

Figure 5. Variation with diluent ratio, of acetylene content in cold products for reversed propane flames

The diluent ratio is not very critical as regards the acetylene content of the raw gas, as was also true for methane flames. However, the percentage conversion falls off rapidly as the N_2/O_2 ratio falls. In the case of the flame supported by pure oxygen, the carbon dioxide content of the products, and hence the flame temperature, is much higher. Extensive carbonaceous deposits are also formed. The high ethylene content of the product gases supports the view that this gas is formed partly in the propane constituting the quenching medium around the flame, since this process would occur more extensively at the higher flame temperature. Two further observations support this mode of ethylene formation: first, when the amount of propane fed to the flame is reduced, the acetylene content of the product gases rises

Table 4. Analyses of samples from reversed propane flames

N_2/O_2	CO_2	C_2H_2	C_2H_4	O_2	H_2	CO	C_3H_8	CH_4	N_2	% *conversion to* C_2H_2
2·93	5·1	3·6	5·2	0·2	10·8	9·1	12·4	4·1	49·5	20·0
0·9	4·8	5·2	5·4	0·1	26·4	22·7	5·5	6·1	23·8	19·1
0·0	19·1	4·6	7·6	0·1	23·9	29·1	7·9	6·7	1·0	11·6

slightly and the ethylene content falls sharply. Secondly, when the propane stream is preheated to a temperature just below that at which appreciable cracking occurs, the acetylene content remains about the same but the ethylene production rises sharply.

(vi) *Attempted additional quenching of flame products*

Two methods were tried: the first involved the introduction of a fine water spray into the hydrocarbon feed and in the second the flame was surrounded with a water-cooled jacket just out of contact with the flame. No improvement resulted from either method: in the first case, the reversed flame became unstable, and the second method probably failed because the cooling surface was not applied in exactly the right region.

Table 5. Analyses of products from reversed methane flames fed by preheated gases

CO_2	C_2H_2	C_2H_4	O_2	H_2	CO	C_2H_6	CH_4	N_2	% *conv. to* C_2H_2	*Preheat temp. °C*	
										CH_4	*Air*
4·6	1·7	0·6	0·1	13·1	9·7	0·5	22·5	47·2	17·6	—	—
4·7	1·8	0·7	0·1	14·9	10·8	0·4	19·9	46·7	16·9	—	280
4·6	1·9	0·6	0·1	15·3	10·7	0·1	17·0	49·7	18·5	566	—
4·4	2·2	0·7	0·1	15·5	11·1	0·1	16·0	49·9	20·5	616	285
3·8	2·3	0·7	0·1	17·8	11·1	0·1	17·1	47·0	21·8	658	540
3·8	2·4	0·8	0·1	18·1	11·1	0·1	16·6	47·0	22·3	674	658

(vii) *Influence of preheat of feed gases on composition of flame products*

The influence of preheat upon reversed methane–'air' flames is shown by the analyses given in *Table 5*.

There is a measurable increase in acetylene content with preheat: a similar trend was established with propane flames, results for which are given in *Table 6*. If too much preheat is applied, cracking occurs with carbon deposition and production of olefins, and the nature of the feedstock is therefore altered. Such systems are not directly comparable.

(viii) *Use of steam rather than nitrogen as a flame diluent*

A diluent that could be readily removed or that could be removed by cooling (e.g. steam) would be a potential means of increasing the acetylene content of the product gases. It seemed likely, however, that the two obvious diluents, steam or carbon dioxide, would interfere in the flame reactions and not act as diluents only.

Some of the results obtained with steam as a diluent are given in *Table 7*. For comparative purposes, this table also contains details of samples having the highest acetylene content (Nos. 88 and 122) and those having the highest percentage conversion (Nos. 86 and 121) all of which were prepared using cold feed gases. Those in which preheated gases were used (Nos. 131 and 135) are also given. The results are expressed on a nitrogen-free basis and also on a nitrogen-free, excess-hydrocarbon-free basis. Results expressed in this manner show the acetylene content to be expected when an easily removable, non-reacting diluent is used. Such values may be compared directly with those obtained from experiments in which oxygen/steam mixtures were used, and with

Table 6. Analyses of products from reversed propane flames fed by preheated gases

CO_2	C_2H_2	C_2H_4	O_2	H_2	CO	C_3H_8	CH_4	N_2	% *conv. to* C_2H_2	*Preheat temp. °C*	
										C_3H_8	*Air*
4·8	5·2	5·4	0·1	26·4	22·7	5·5	6·1	23·8	19·1	—	—
4·6	5·4	6·0	0·1	26·8	22·4	5·8	5·3	23·6	19·6	451	188
3·4	6·1	6·1	0·1	31·9	22·4	0·7	7·4	21·9	21·2	634	202

Table 7. Analyses of samples from reversed methane and propane flames showing a comparison between yields produced using oxygen: nitrogen mixtures (expressed on a diluent-free basis) and oxygen: steam mixtures (removable diluent)

Hydrocarbon	*Volume composition of O_2-cont. stream*	*Sample*	CO_2	C_2H_2	C_2H_4	O_2	H_2	CO	C_3H_6	C_2H_6	CH_4	N_2
CH_4	$1O_2 : 2{\cdot}3N_2$	*131*	3·8	2·4	0·8	0·1	18·1	11·1		0·1	16·6	47·0
C_3H_8	$1O_2 : 0{\cdot}9N_2$	*135*	3·4	6·1	6·1	0·1	31·9	22·4	0·7		7·4	21·9
CH_4	$1O_2 : 2{\cdot}2N_2$	*86*	4·4	1·6	0·8	0·2	12·8	9·3		0·7	26·0	44·2
CH_4	$1O_2 : 1{\cdot}5N_2$	*88*	4·7	2·0	0·8	0·3	20·2	14·3		0·5	19·2	38·0
C_3H_8	$1O_2 : 2{\cdot}9N_2$	*121*	5·1	3·6	5·2	0·2	10·8	9·1	12·4		4·1	49·5
C_3H_8	$1O_2 : 0{\cdot}9N_2$	*122*	4·8	5·2	5·4	0·1	26·4	22·7	5·5		6·1	23·8
CH_4	$1O_2 : 2{\cdot}7H_2O$	*116*	17·2	2·6	0·6	<0·1	39·7	21·3		<0·1	14·8	3·7
C_3H_8	$1O_2 : 0{\cdot}9H_2O$	*141*	14·4	7·0	8·1	<0·1	35·6	21·5	3·4		9·4	0·5
C_3H_8	$1O_2 : 2{\cdot}3H_2O$	*155*	10·4	5·8	14·5	0·2	27·7	13·3	16·4		11·0	0·7
CH_4	$1O_2 : 1{\cdot}6H_2O$	*120*	12·7	2·5	0·8	0·2	36·9	19·1		0·3	23·4	4·1
C_3H_8	$1O_2 : 0{\cdot}7H_2O$	*142*	12·0	6·5	7·3	<0·1	37·0	24·3	3·6		8·6	0·6

	N_2-free basis					*N_2-free, fuel-free basis*					
Hydrocarbon	CO_2	C_2H_2	C_2H_4	H_2	CO	CO_2	C_2H_2	C_2H_4	H_2	CO	*% conv. to* C_2H_2
CH_4	7·2	4·5	1·5	34·1	20·9	10·4	6·6	2·2	49·7	30·5	21·8
C_3H_8	4·3	7·9	7·9	40·4	28·5	4·3	7·9	7·9	41·2	28·9	21·2
CH_4	7·9	2·9	1·4	22·9	16·7	14·8	5·4	2·7	42·9	31·3	16·2
CH_4	7·5	3·2	1·3	32·5	23·1	11·0	4·7	1·9	47·2	33·4	15·6
C_3H_8	10·1	7·1	10·3	21·4	18·0	13·4	9·4	13·6	28·3	23·8	20·0
C_3H_8	6·3	4·8	7·1	34·6	29·8	6·7	7·3	7·6	37·3	32·1	19·1
CH_4						21·1	3·2	0·7	48·7	26·1	
C_3H_8						15·0	7·3	8·4	37·0	22·3	
C_3H_8						12·5	7·0	17·5	33·4	16·0	
CH_4						17·5	3·4	1·1	50·9	26·3	12·8
C_3H_8						12·5	6·8	7·6	38·6	25·3	19·7

these results expressed on a fuel-free basis. Simple calculation shows that when steam is used, the acetylene content of the product gases should be up to about **4·5** per cent for methane and for propane up to nearly **8** per cent. The actual contents obtained (see *Table 7*) are lower than these: samples **116** and **141** are examples of high acetylene contents from methane and propane flames respectively, and samples **120** and **142** represent high conversions for methane and propane flames. For sample **155**, considerable preheat was used.

The use of steam as a diluent has the following effects:

(*i*) carbon dioxide is increased

(*ii*) acetylene is increased but not to the extent expected if the steam was acting only as a diluent which was subsequently removed from the products by condensation

(*iii*) ethylene is not much changed for methane flames but is increased for propane flames. Again, the increase is not as high as expected

(*iv*) hydrogen increases above that expected from calculation

(*v*) carbon monoxide is higher for methane flames, but for propane flames no definite trend arises.

Discussion

Figure 6 shows the free energy of formation of some simple hydrocarbons as a function of temperature. The increasing stability of acety-

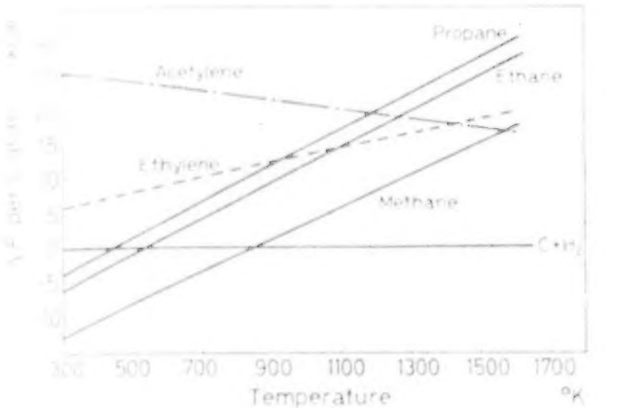

Figure 6. Diagram showing the variation of free energy of formation of some simple hydrocarbons with temperature

Relations used:

Methane	$\Delta F = -19\,450 + 23{\cdot}0T$ cal
Ethane	$\Delta F = -26\,700 + 51{\cdot}0T$ cal
Propane	$\Delta F = -32\,700 + 76{\cdot}0T$ cal
Ethylene	$\Delta F = 5\,700 + 21{\cdot}1T$ cal
Acetylene	$\Delta F = 54\,900 - 13{\cdot}6T$ cal

lene with increasing temperature differentiates this hydrocarbon from the remainder. Acetylene is never stable with respect to its elements because hydrogen is completely dissociated before ΔF, the free energy of formation, reaches zero, and the equilibrium

$$2C\,(\text{graphite}) + 2H \rightleftharpoons C_2H_2$$

is displaced to the LHS by increasing temperature. It is clear that high yields of acetylene are favoured by a high temperature and by rapid quenching, and it was explained qualitatively at the outset how this is attained in reversed flame systems.

The simplest assumption one could make would be that there are two independent reaction processes, viz. combustion and pyrolysis occurring independently side by side, the heat of the former being partly absorbed by the endothermic reactions occurring in the latter. In attempting to decide how far this is an over-simplification, much will depend on the exact location of the reactions: if the reactions occur very close together it can hardly be expected that they will really be independent, especially since the same intermediate species (e.g. hydrogen atoms and methyl radicals) are involved in both.

The results from reversed methane flames have been considered in an attempt to assess how far combustion and pyrolysis are independent. Although the precise mechanism of the pyrolysis of methane is uncertain, the path through stable products is known to be

$$2CH_4 \longrightarrow C_2H_6(+H_2) \underset{\text{REACTION 1}}{\longrightarrow} C_2H_4(+H_2)$$

$$\underset{\text{REACTION 2}}{\longrightarrow} C_2H_2(+H_2) \underset{\text{REACTION 3}}{\longrightarrow} 2C + H_2$$

If fractions of the stable products decomposing in reactions 1, 2 and 3 are calculated from the analyses of the cold gaseous products, account being taken of the reacted methane only, impossible values are usually obtained, i.e. either greater than unity or negative. The stage in most doubt is the third, in that previous work on carbon formation has indicated that the mechanism is more complex than this. If reaction 3 is neglected (carbon formation was almost negligible from most of the reversed flame experiments reported here), values for the fractions decomposing in reactions 1 and 2 may be calculated, and a prediction of the hydrogen produced may be made. This prediction is invariably much lower than that obtained in practice. A mechanism postulating that pyrolytic and combustion reactions occur simultaneously in the flame and are related only by the thermal dependence of the former on the latter is thus shown to be inadequate and it is indicated that a more intimate relationship exists between the two reactions.

A particularly direct example of the interaction of the combustion and pyrolytic reactions is provided by the equilibria which can be set up between products from the two processes, viz. the homogeneous water-gas reaction involving carbon monoxide, carbon dioxide, steam and hydrogen, where hydrogen is favoured at low temperatures and carbon monoxide at higher temperatures. This equilibrium will be considerably affected by the use of steam as a diluent of the oxygen feed, and it is possible that the difference between predicted and practical acetylene contents when changing from nitrogen to steam as diluent may be explained on this basis. It was investigated quantitatively with reversed ethylene–oxygen-enriched air flames, the water formed being estimated by chilling the product gases and weighing them. Nitrogen was used as the unchanged reference gas connecting input quantities to percentage composition of the product gases. The values of the equilibrium constants obtained corresponded well to values expected for the experimental temperatures for these flames reported in our previous paper. Details of two of these experiments are given in *Table 8*.

Table 8. Equilibrium constants (K) for water-gas reaction in reversed ethylene flames

Gas rates ml/min						
C_2H_4	N_2	O_2	$\frac{N_2}{O_2}$	*K*	°C	C_2H_2 %
252	170	105	1·6	3·1	1337	5·7
365	138	131	1·05	3·5	1447	6·1

The experiment with the highest oxygen rate gave the higher temperature and the higher acetylene content in the product gases.

Other equilibria which may be involved in the flames include the following:

$$C_2H_4 \rightleftharpoons C_2H_2+H_2 \quad \ldots\ldots [4]$$

$$C_2H_6 \rightleftharpoons C_2H_4+H_2 \quad \ldots\ldots [5]$$

$$CO_2+CH_4 \rightleftharpoons 2CO+2H_2 \quad \ldots\ldots [6]$$

$$C+CO_2 \rightleftharpoons 2CO \quad \ldots\ldots [7]$$

For reaction **4**, the constant calculated from the gas compositions from both methane and propane flames corresponds to temperatures in the range **1 200°** to **1 600°C**. For reaction **5**, the value of the equilibrium constant obtained corresponds to a temperature range of **900°** to **1300°C**, while that for reaction **7** corresponds to a temperature range of **820°** to **900°C**. The reason for the pronounced reduction in the values of the latter range is not known, but both may correspond to a reaction shift during cooling from the peak temperature.

The value of the equilibrium constant for reaction **6** corresponds to a temperature range of **650°** to **850°C** for reversed methane flames and to **850°** to **1050°C** for reversed propane flames. In the first case, equilibrium is attained outside the flame envelope with the relatively high concentration of methane occurring there, while in the second case methane only occurs in low concentration as one of the stable products of decomposition formed at elevated temperatures.

In the case of propane, there are two main primary pyrolytic reactions:

$$C_3H_8 \rightleftharpoons C_2H_4+CH_4 \quad \ldots\ldots [8]$$

$$C_3H_8 \rightleftharpoons C_3H_6+H_2 \quad \ldots\ldots [9]$$

If mechanism 9 were important, some C_3 hydrocarbons (propylene and methyl acetylene) might be expected in the reaction products. In fact, a complete analysis of a gas sample from a reversed propane–steam and oxygen flame was made and the small quantity of both C_3 hydrocarbons indicates that only a small quantity of propane is decomposed by reaction 9 (see *Table 9*).

Table 9. Analysis of a gas sample from a reversed propane–steam + oxygen flame

H_2	37·7	CH_4	9·1	C_3H_4	0·3
CO	23·4	C_2H_6	7·1	C_3H_6	0·6
CO_2	11·7	C_2H_4	5·7	C_3H_8	1·5
N_2	2·6			C_4	0·3

It seems likely therefore that so far as the purely pyrolytic reactions are concerned, reaction 8 will be the main primary process, to be followed by the appropriate reactions occurring in methane and ethylene pyrolysis. For both methane and propane reversed flames, unburnt hydrocarbons close to the flame front absorb heat not only by virtue of their own thermal capacity but also by undergoing endothermic decomposition. The endothermic decomposition is particularly important for propane which undergoes pyrolysis at relatively low temperatures, and it is obvious that controlled preheat of the propane will enhance the effect.

One of the most obvious differences between the reversed diffusion flames used here and premixed flame systems is the large difference in the thicknesses of the reaction zones and hence of the residence times at high temperatures. In the present experiments, this time was of the order 10^{-2} sec compared with 10^{-4} to 10^{-3} sec in premixed flames. The comparative yields of unsaturated hydrocarbons suggest that it is unnecessary to resort to the premixed flame system in order to produce acetylene and ethylene.

The discussion so far has centred on the chemical aspects of the reactions giving rise to the product gases. The physical arrangement (geometry) of the apparatus obviously has a large effect in determining the quality of the gases evolved. The primary variable is obviously the annulus/jet ratio which partly controls the quantity of hydrocarbon passing around the flame. The disadvantage of a very large annulus is to give a highly diluted product. If the annulus is too small, a reversed flame can no longer be stabilized, a flame front being established in the form of an inverted cone stretching from the port to the flame tube wall; all the hydrocarbon passes through this flame front.

Whilst, generally speaking, the size of the flame is controlled by the linear velocity of the air, it is to a small extent affected by the velocity ratio. There are several effects of this variable. If the value is decreased too far there will be an excessive quantity of hydrocarbon passing the flame. Such an excess will have the advantage of carrying the flame products away rapidly but it will also dilute them excessively. If the value becomes too high, the flame alters in shape so that, as described in connection with annulus/jet ratio, a reversed flame is no longer obtained.

The other important variable is the diluent ratio in the 'air' stream. As this ratio is reduced the flame temperature will increase, which is favourable to acetylene formation. This, however, increases the quenching problem and will give more time (at higher temperatures) for the acetylene formed to decompose or react. This is illustrated by the fact that a plot of acetylene content or of percentage conversion against diluent ratio has a maximum which does not occur at zero. Thus while when pure oxygen is used the product gases are not diluted and the flame temperature is higher, the loss of acetylene originally formed must also be greater. The curves given in *Figures 4* and *5* illustrate this point.

The effect of velocity ratio and annulus/jet ratio is apparent from *Figure 2* as already mentioned. It should be emphasized that conversions are considered here and that it is this expression of acetylene content (i.e. independent of diluent) that rises as annulus/jet ratio decreases. The maxima in the curves indicate the balance necessary, between dilution and speed of removal from close proximity to the flame.

Values of these variables affect the production of ethylene, carbon monoxide and hydrogen, but the exact mechanism of the effects is somewhat doubtful. The concentrations of oxides of carbon in the products will depend largely on combustion reactions, and they will also depend upon the rate of cooling of the gases, i.e. upon the extent to which equilibrium is established in the homogeneous water-gas reaction at successively lower temperatures. The ethylene and ethane contents have been shown, for reversed methane flames, to depend upon the equilibrium

$$C_2H_6 \rightleftharpoons C_2H_4 + H_2$$

at the highest temperatures in the flame. For propane flames, the ethylene content will tend to be increased above this equilibrium value due to ethylene formed outside the flame. This will depend on flame temperature (i.e. diluent ratio) and the final content will be linked to the rate of cooling as governed by velocity ratio and annulus/jet ratio.

Conclusion

The intrinsic value of the results reported above lies in the fact that they show that the reversed flames of paraffin hydrocarbons can be controlled to allow the isolation of appreciable quantities of unsaturated hydrocarbons. From the examination of these results inferences may be drawn as discussed above.

Owing to the complexity of the reaction system it is not possible to formulate a complete reaction mechanism for the processes occurring in reversed flames. However, it has been shown that pyrolysis and combustion become intimately linked in this process of partial combustion and cannot be separated into heat-producing and heat-absorbing systems.

This conclusion is similar to that reached by the authors concerning carbon formation in flames when stress was laid on the role of oxygen and the presence of oxygenated intermediates. The composition of the gas mixtures obtained cannot be related to that predicted by a simple pyrolytic reaction scheme[2] involving acetylene as intermediate and carbon as end-product. This is not unexpected, since in a diffusion flame combustion reactions dependent upon a large oxygen supply occur simultaneously with carbon formation.

The permission of the British Coal Utilisation Research Association to publish this paper is gratefully acknowledged.

The authors acknowledge the invaluable help of J. M. Horspool of the B.C.U.R.A. who tested methods for analysing the gas mixtures and carried out the analysis.

The authors wish to express their thanks to D. Harvey, I.C.I. Ltd, Billingham, who obtained the results upon which Table 9 *is based.*

References

[1] ARTHUR, J. R. and NAPIER, D. H. *Fifth Symposium (International) on Combustion*, pp 303–315. Reinhold: New York, 1955

[2] PORTER, G. *Fourth Symposium (International) on Combustion*, pp 248–252. Williams and Wilkins: Baltimore, 1953

The Effects of Certain Additives on Two-stage Cool Flames Stabilized in a Flat–flame Burner

W. G. AGNEW

Research Laboratories, General Motors Corpn, General Motors Technical Center, 12 Mile and Mound Roads, Warren, Michigan

(Received February 1959)

As a contribution to our knowledge of the manner in which additives affect the self-ignition of fuel–air mixtures and, in particular, anti-knock action, observations have been made of the effects of nine compounds added to the central portion of a rich, two-stage, diethyl ether–air cool flame. Photographs illustrate the additive action in terms of retardation or acceleration of the separate reaction stages. With qualifications and some exceptions the additives acted about as would be expected from their known engine anti-knock or pro-knock effects. Visible emission spectra of the affected regions of the flame provide evidence for additive reactions which is discussed in the light of various theories for anti-knock action. Although the results with tetraethyl lead tend to favour the Erhard–Norrish theory, there is insufficient evidence to reach definite conclusions about any of the specific reaction mechanisms involved.

PREVIOUS spectroscopic studies[1] have indicated a similarity between the cool flame reactions stabilized in a flat-flame burner and the preflame reactions associated with knocking combustion in a spark-ignition engine. In view of this fact, it appeared of interest to examine the effects exhibited on the burner cool flames of certain chemical additives known from prior engine work to be anti-knock or pro-knock agents. Stabilization of the reactions in this way permits leisurely observation and study with a variety of analytical tools.

Equipment

Burner

A diagram of the modified flat-flame burner is shown in *Figure 1*. The copper burner tube had an inside diameter of 2 in., and the 30 mesh stabilizing screen was 1·5 in. above the burner port. The burner matrices were made by winding alternate strips of flat and corrugated Inconel in a spiral. The additive tube was made from 0·25 in. copper tubing, and the outlet was tapered to a knife-edge. The additive tube reached to the underside of the top matrix 1 in. below the burner port. This made it possible to 'dope' the centre portion of the flame with different concentrations of additive without appreciably affecting the flow distribution across the burner port.

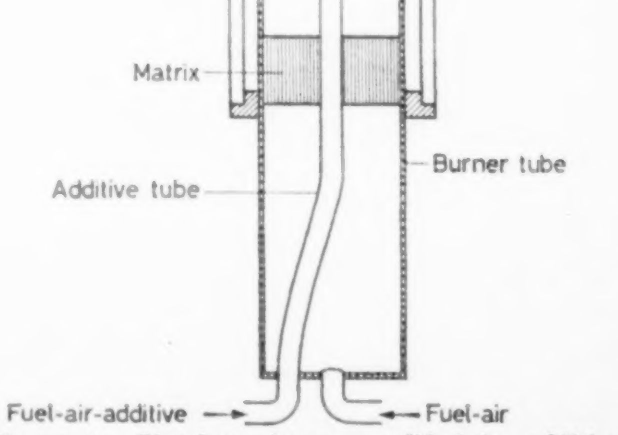

Figure 1. Flat-flame burner modified for additive studies

Fuel–air supply

The fuel and air supply systems are represented in *Figure 2*. The fuel, diethyl ether, was evaporated in a 2 litre closed steel tank immersed in a hot water bath. The bath was maintained at 130° F (55° C) by a temperature-controlled steam coil. The fuel tank operating pressure was around 12 to 15 lb/in² gauge. Fuel vapour tapped from the top of the tank passed through a needle valve and a hot water-jacketed rotameter to its junction with the air stream.

Air was supplied from the building compressed air lines through a needle valve to a rotameter. The air was then mixed with the fuel vapour, and the mixture was then divided into two streams. The main mixture was fed to the usual burner inlet, while the secondary mixture stream was fed through a needle valve to a 250 ml flask, where it passed over the surface of the liquid additive, and from there to the additive tube in the burner.

For adding nitric oxide to the flame a line was run from a high pressure gas cylinder through a needle valve and rotameter to the flask in the additive line.

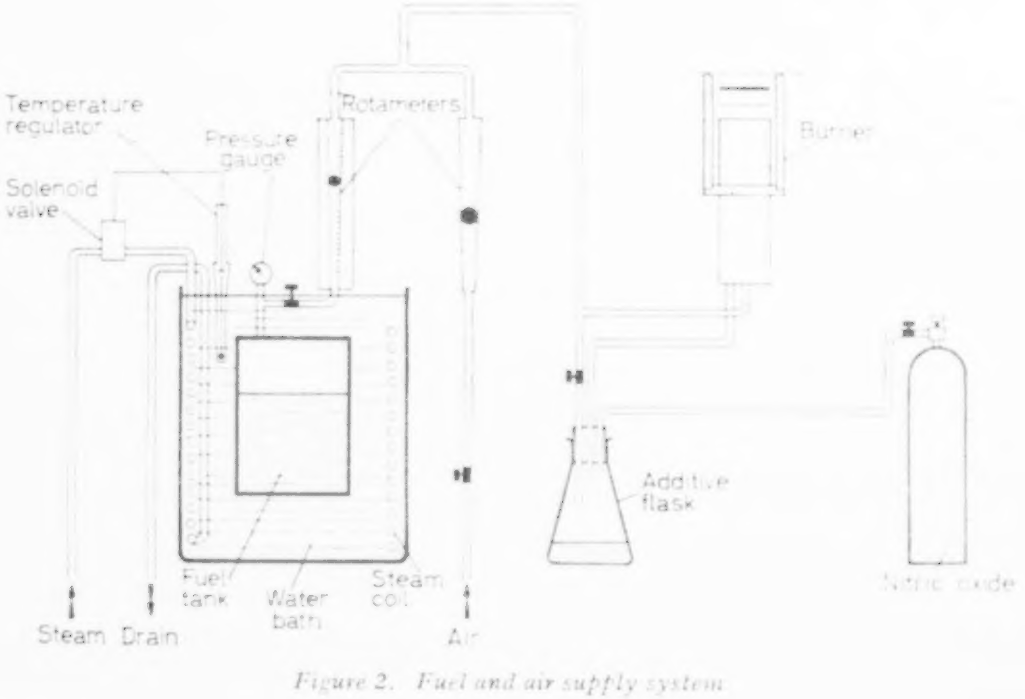

Figure 2. Fuel and air supply system

The entire apparatus was mounted in a ventilated hood, and the burner itself was supported by a micromanipulator for spectral studies.

Optical system

For spectral studies an 80 mm diameter spherical mirror (r = 294 mm) was arranged to focus an image of the centre of the flames on the spectrometer entrance slit. An image rotator made from two flat mirrors served to rotate the flame image 90° so that the horizontal flame fronts were aligned vertically on the vertical spectrometer slit. A magnification of about three occurred in this arrangement, so that the 12 mm long spectrometer slit received radiation from a 4 mm wide 'slice' of the flame. The 'slice' of flame in view had a double-wedge shape, 1 mm high in the centre of the flame and about 10 mm high at the edges of the flame. In this wedge the gases at the central focal plane made the greatest contribution to the radiation signal.

Spectrometer

A Perkin–Elmer Model 99 monochromator was used with a lithium fluoride prism and an RCA 1P21 photomultiplier detector. No corrections were made for the wavelength sensitivity variation of the detector.

Camera

For photographing the flames a 4 × 5 graphic view camera with an *f*4·5, 152 mm lens was used. The image of the flame on the film was about one-half actual size. Colour photographs were made with Kodak Ektacolor Type S film and 10 minute exposures. Black and white photographs were made with Kodak Tri X film and 30 second exposures.

Procedure

Two-stage cool flames were established at total flow rates in the range of 1·3 to 1·8 lb of mixture per hour, which resulted in a very smooth laminar flow. Except when the mixture ratio was purposely varied, the weight percentage of ether in the mixture was 28·3, or about three times richer than stoichiometric. Rich mixtures of diethyl ether were used in this initial work, since they were most convenient to study, and a large amount of information had already been collected on this system.

The two stages of the reaction at these fuel–air ratios are about 0·5 in. apart. Although flat, disc-shaped flame fronts can be obtained, greater stability results when the first-stage flame is allowed to 'cup' over the burner port, and the edges of the second-stage flame are allowed to curl upward as shown in the photograph, see *Figure 3*. This was the condition used for most of the studies and represents the reaction with no additive. A more complete description of this two-stage flame is contained in a previous paper[2]. For the normal case of *Figure 3*, both flame fronts and the faint column of luminosity between them appeared blue to the eye. Over-exposure of the photographic print to bring out some of the weaker details caused some loss of definition in the second-stage flame, which appeared to the eye to have a sharply defined thickness about twice that of the first stage.

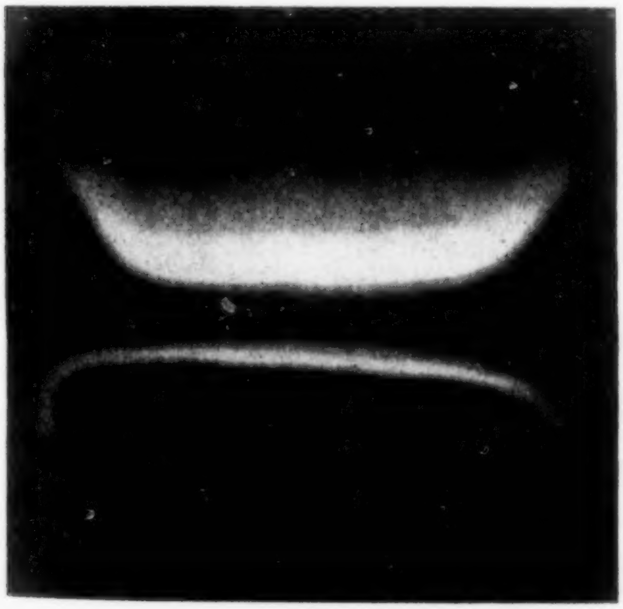

Figure 3. Two-stage flame with no additive

The standard two-stage flame was always established prior to introduction of an additive. Liquid additives were then introduced by shutting off the ether–air flow to the additive flask (which, incidentally, had no visible effect on the two-stage flame, the flow merely being diverted to the main stream), pouring 10 ml or so of the additive into the flask, and opening the additive flow line once more to the desired flow rate. The volatile liquid additives produced a vapour pressure in the additive flask sufficient to carry an appreciable concentration of the additive into the additive line. For less volatile additives the additive flask was placed in the 130°F (55°C) water bath to increase the vapour pressure. The concentration of additive in the central portion of the flame could be controlled to some extent by the flow rate through the additive line because of the diffusion which occurred between the 'doped' additive line flow and the undoped main-stream mixture. Increasing the additive line flow increased the concentration of additive in the central portion of the flame.

Concentrations of tetraethyl lead in the region of the burner where reaction occurred were estimated by probe sampling of the cold flow (flame extinguished). Analysis of the condensed ether–tetraethyl lead mixture sample gave tetraethyl lead concentrations in ml per gallon of ether in the zone of reaction. No attempt was made to measure concentrations for any additive other than tetraethyl lead.

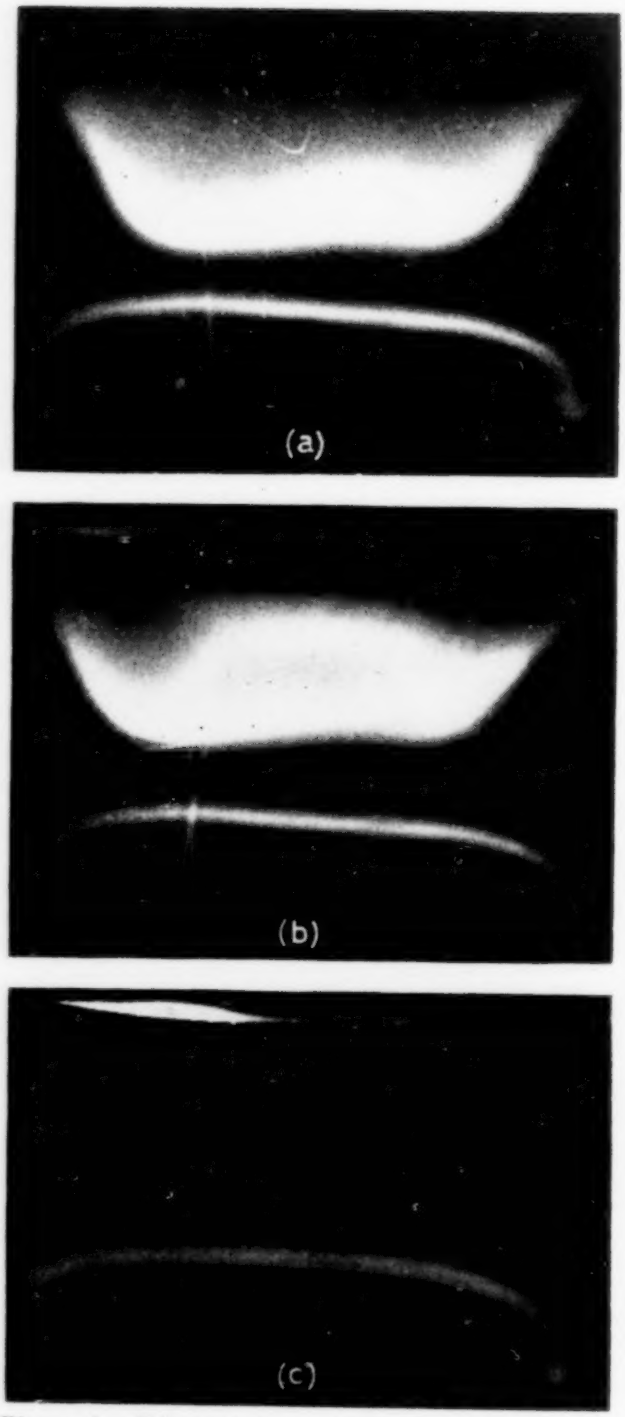

Figure 4. Effect of increasing tetraethyl lead concentration on two-stage flame spectrum

Results

Tetraethyl lead

Figure 4 indicates the effects of tetraethyl lead additions. The three flame photographs represent increasing concentrations of tetraethyl lead in the range between 1·0 and 16 ml per gallon of diethyl ether.

There appeared to be no effect, for any concentration tried, on the first-stage cool flame.

As the tetraethyl lead was first introduced in small concentration, a bump appeared in the centre of the second-stage flame, indicating some retardation of the second-stage reaction. The bump initially showed little colour change from the normal blue reaction zone, but slightly more tetraethyl lead made the bump paler, approaching a whitish-grey. This is the condition shown in *Figure 4*(a).

Increasing tetraethyl lead increased the size of the bump, both in height and diameter, and the top became flat as it approached the stabilizing screen. The flat portion of the bump turned distinctly white and increased in brightness [*Figure 4*(b)].

Still more tetraethyl lead caused the entire second-stage flame to back up to (or through) the stabilizing screen and become extinguished. In this condition there was no visible gas emission other than that from the still unaffected first-stage flame [*Figure 4*(c)].

It might be mentioned that the horizontal streak of light noted in *Figure 4* above the second-stage flame emission is from the hot stabilizing screen and carbon deposited on it. The vertical and curled streaks are from loose carbon particles falling through the flame or being swept to one side by the flow during the photographic exposure. There was a somewhat greater tendency for carbon to deposit and precipitate with tetraethyl lead added than without.

Visible emission spectra illustrating the effects of tetraethyl lead are shown in *Figures 5* and *6*. *Figure 5* shows spectra of the second stage for a flame with 28·5 per cent ether and 1·5 lb of mixture flow per hour. (The first-stage flame spectra showed no effect of the additive.) Spectra 5(a) to 5(f) inclusive show the effects of increasing the additive concentration. In 5(a) the additive line valve was wide open and the gas flow in the line was at the maximum, but the additive flask had no tetraethyl lead in it; from 5(b) to 5(f) there was tetraethyl lead at

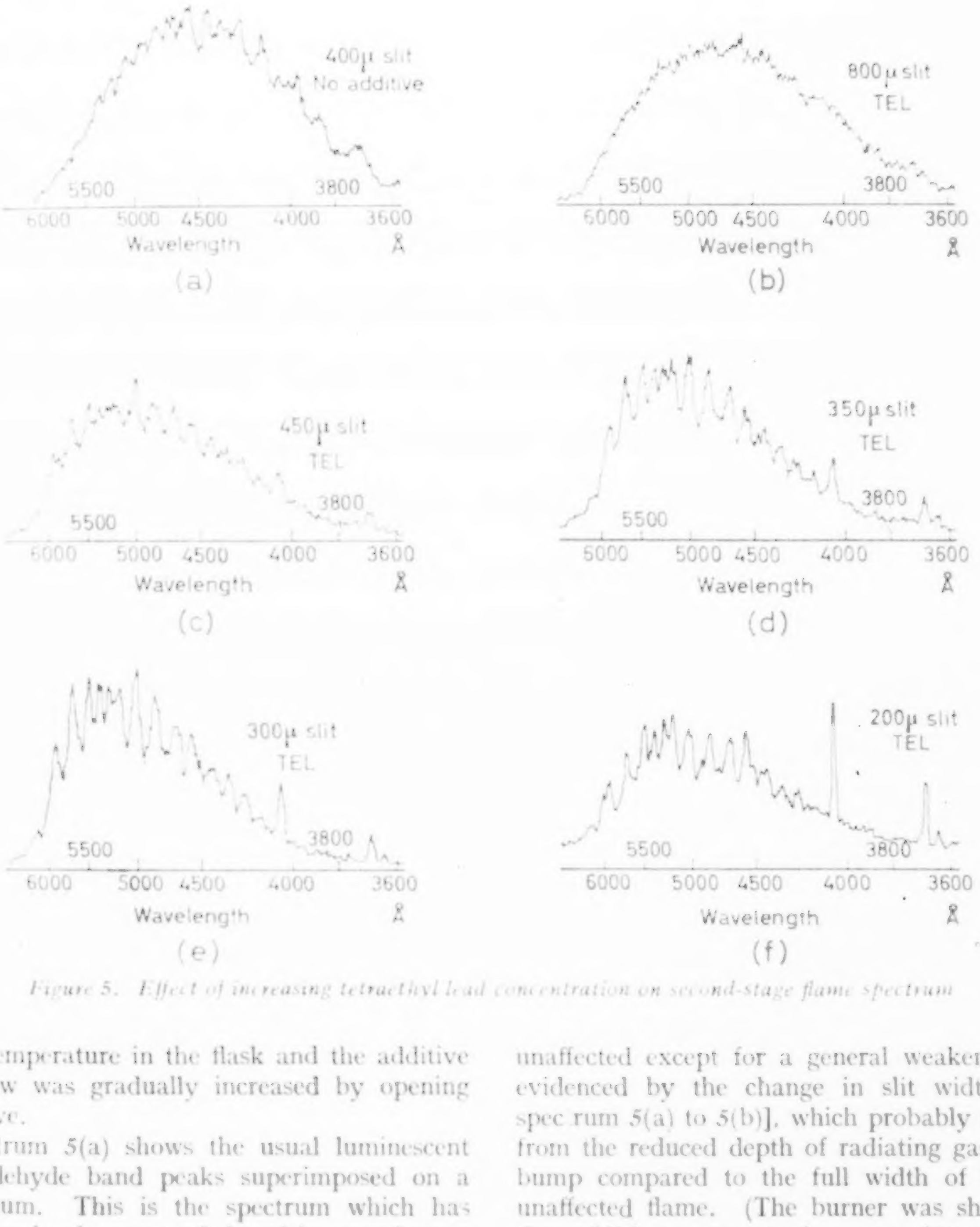

Figure 5. Effect of increasing tetraethyl lead concentration on second-stage flame spectrum

room temperature in the flask and the additive line flow was gradually increased by opening the valve.

Spectrum 5(a) shows the usual luminescent formaldehyde band peaks superimposed on a continuum. This is the spectrum which has been previously reported for rich second-stage flames[2].

Spectrum 5(b) corresponds to the condition mentioned earlier at about 1 or 2 ml tetraethyl lead per gallon of ether in which a bump appeared in the second-stage flame, but there was little colour change. It can be seen that the formaldehyde band peaks were essentially wiped out. The continuous emission seemed unaffected except for a general weakening [as evidenced by the change in slit width from spectrum 5(a) to 5(b)], which probably resulted from the reduced depth of radiating gas in the bump compared to the full width of the flat unaffected flame. (The burner was shifted as the additive concentration was increased in order to keep the affected portion of the reaction zone focused on the spectrometer slit.)

In spectrum 5(c) the bump in the second-stage flame was a grey-white, and lead oxide bands became prominent in the spectrum between 4 100 and 6 000 Å. Atomic lead emission lines at 3 640, 3 683 and 4 058 Å appeared weakly.

In spectra 5(d) and 5(e) both the lead oxide bands and the lead lines grew stronger, as evidenced by the reduction in slit width required to obtain the spectra.

Spectrum 5(f) corresponds about to the condition illustrated in *Figure 4*(b) in which the tetraethyl lead concentration was in the range of **10** to **15** ml per gallon of ether. In this case the lead lines seemed to be considerably stronger relative to the lead oxide bands.

Figure 6 shows the progressive change in the second-stage flame spectrum, with **10 to 15** ml of tetraethyl lead per gallon of ether added, as the fuel–air mixture was gradually leaned from **28·5** per cent ether to **19·1** per cent ether. The atomic lead emission lines grew progressively stronger relative to the lead oxide bands as the mixture became leaner, and at the leanest condition CH radical emission appeared. Also at this condition relatively strong continuous emission appeared in the range from **5 000** to **6 000** A. The CH and continuous emission are characteristic of the leaner flame with no additive (the continuum is from the yellow column normally appearing behind the leaner second-stage flame)².

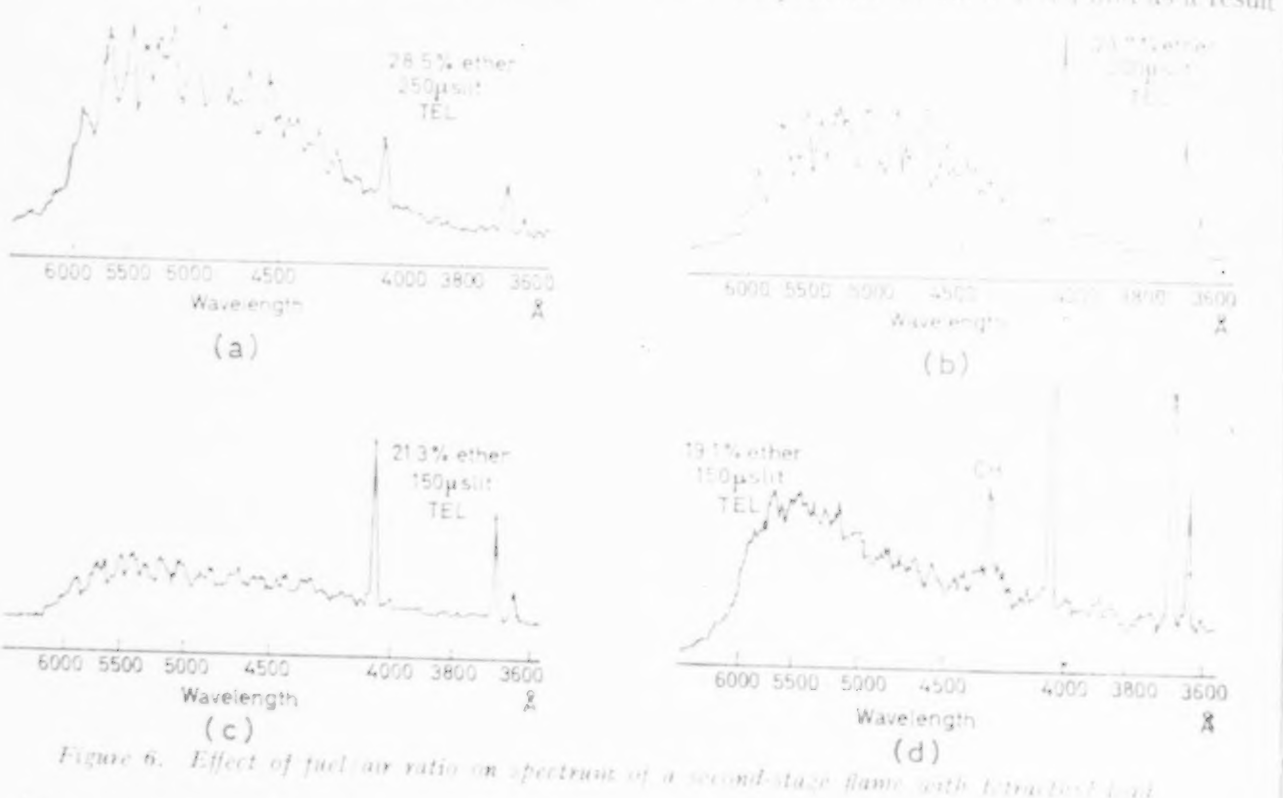

Figure 6. Effect of fuel/air ratio on spectrum of a second-stage flame with tetraethyl lead

Tetramethyl lead

Figure 7 shows photographs of flames with tetramethyl lead added. The additive concentration was progressively increased from (a) to (d) by gradually increasing the flow rate through the additive line. The additive flask was kept at room temperature for these tests, and as a result of the high volatility of tetramethyl lead, only relatively small flow rates were required to give appreciable effects. Some of the effects were similar to those with tetraethyl lead. In no case was there evidence of an effect on the first-stage flame. At the lowest concentration, *Figure 7*(a), a definite retardation of the second-stage flame occurred, but there was little colour change. A slightly higher concentration turned the flame a grey-white [*Figure 7*(b)], and at a still higher concentration of tetramethyl lead a distinct brilliant white spot suddenly appeared in the centre of the grey-white zone [*Figure 7*(c)]. This spot grew in size with increased concentration and eventually extended downward below the normal position of the second-stage flame, as shown in *Figure 7*(d). Thus, with tetramethyl lead there was an indication of

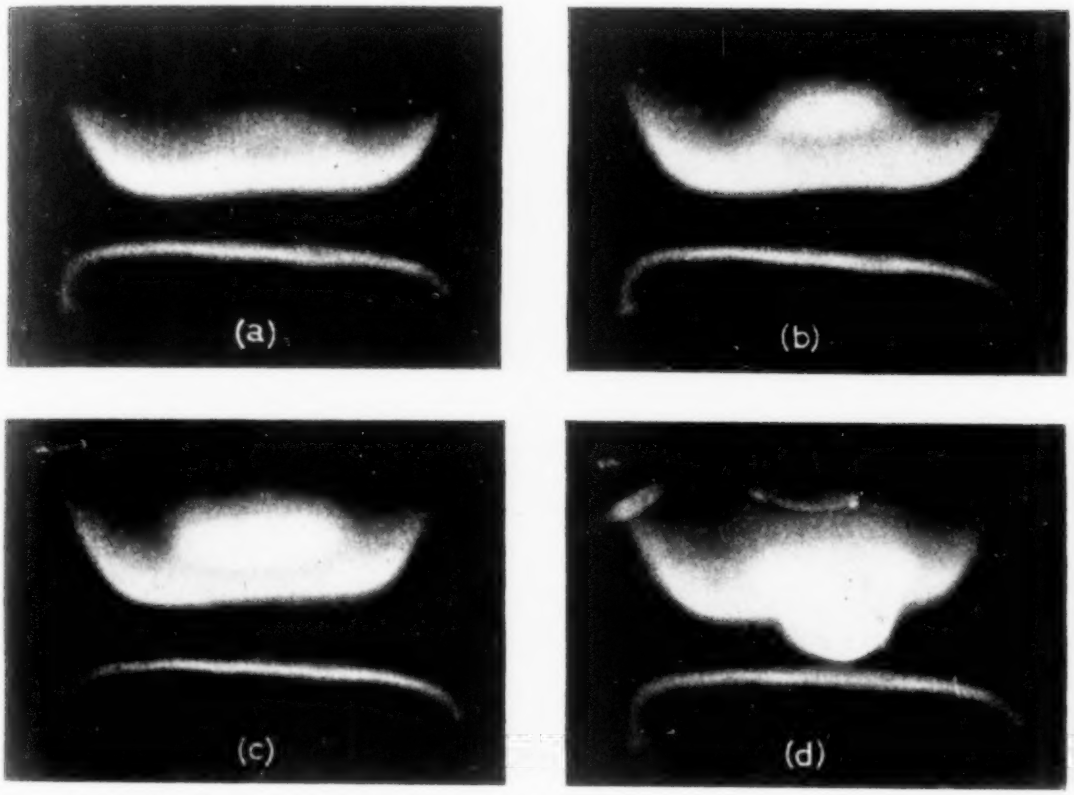

Figure 7. Effect of increasing tetramethyl lead concentration on two-stage flame

acceleration of the second-stage reaction at high concentrations, in contrast to tetraethyl lead which extinguished the second-stage flame at high concentrations.

Spectra of the flames with tetramethyl lead were very similar to those with tetraethyl lead, and in this case the appearance of atomic lead lines definitely correlated with the sudden appearance of the brilliant white spot in the centre of the grey-white lead oxide zone.

Iron carbonyl

Figure 8 shows the effects of two concentrations of iron carbonyl added to the normal rich two-

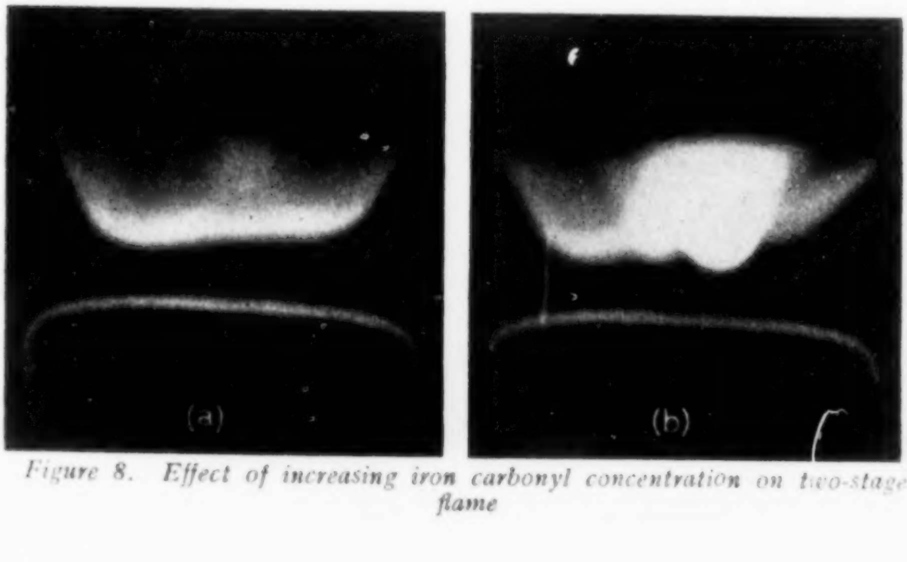

Figure 8. Effect of increasing iron carbonyl concentration on two-stage flame

stage flame. In each case the additive flask was at room temperature. The lower concentration [*Figure 8*(a)] produced a small bump in the second-stage flame, indicating some retardation of that reaction, and a narrow orange-red column behind the bump, extending up to the stabilizing screen. With increased concentration the orange-red column increased in intensity, becoming somewhat more yellow, and eventually extended downward through the normal position of the second-stage flame [*Figure 8*(b)] in a manner similar to tetramethyl lead. [*Figure 8*(b) shows a double image due to reflection of the brilliant yellow zone by the glass enclosing tube around the burner.] No effect of iron carbonyl on the first-stage flame was noted at any concentration.

A second-stage visible emission spectrum corresponding to the condition of *Figure 8*(b) is given in *Figure 9*. The spectrum for the lower concentration was essentially the same. It appears that the addition of iron carbonyl eliminated the normal second-stage flame spectrum, and substituted for it a continuum which peaks sharply near 5 870 A. (This peak location is governed largely by the sensitivity of the 1P21 photomultiplier detector, which reaches a maximum at about 4 000 A and is negligible above 6 500 A.) No iron emission lines or iron oxide emission bands were identified in the spectrum.

Additional spectra were recorded of the orange-red zone of the iron carbonyl-doped flame using a cadmium selenide detector for the 6 000 to 11 000 A region, a lead sulphide detector for the 1·0 to 2·8 micron region and a thermocouple for the 3·0 to 12 micron region of the spectrum. These spectra also showed strong continuous emission as if from a black body.

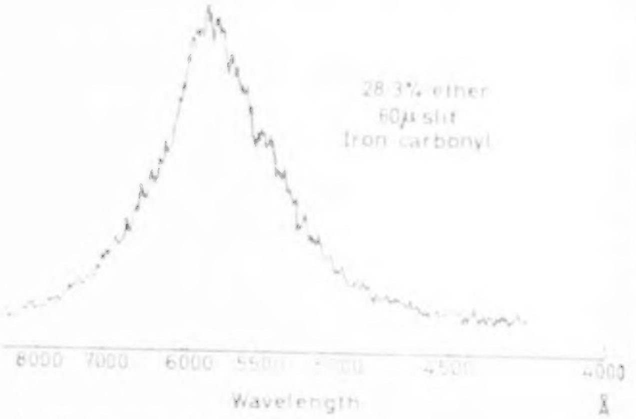

Figure 9. Effect of iron carbonyl on second-stage flame spectrum

Ethyl nitrate

Figure 10 shows two photographs of rich two-stage flames with ethyl nitrate added. In both cases the additive flask was at room temperature. *Figure 10*(a) shows a low concentration of the additive, in which case the first-stage flame was accelerated to such an extent that it seated itself on the burner matrix. The second-stage flame was slightly deflected upward over about two thirds of its diameter, but it is

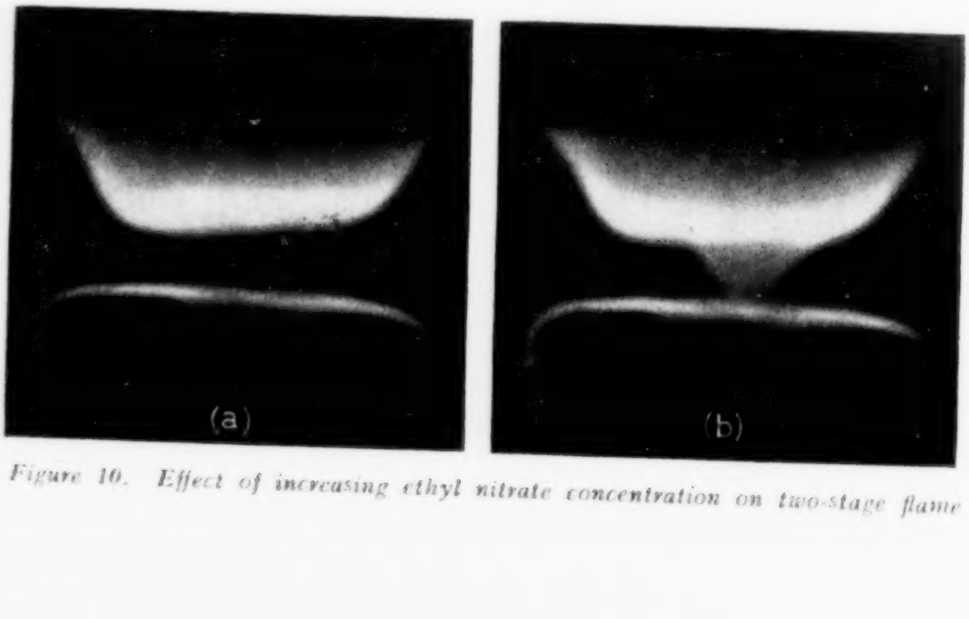

Figure 10. Effect of increasing ethyl nitrate concentration on two-stage flame

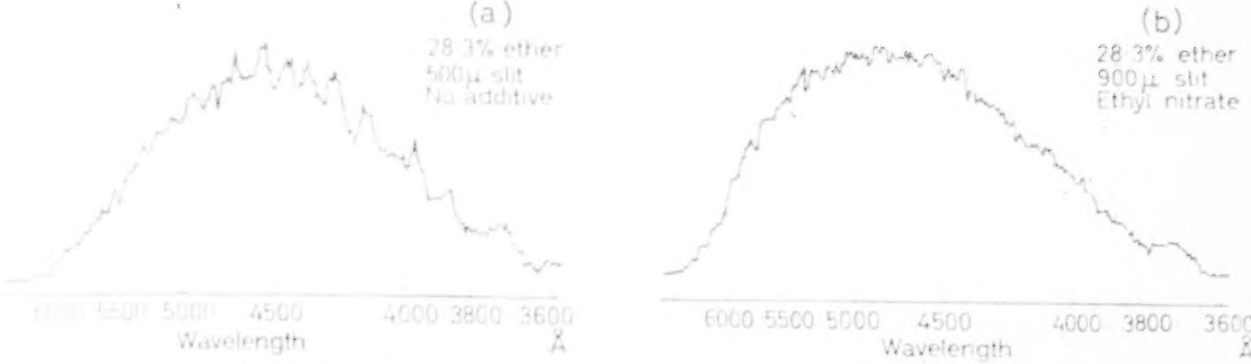

Figure 11. Effect of ethyl nitrate on second-stage flame spectrum

believed that this is an aerodynamic effect rather than a chemical retardation of the reaction. The attachment of the centre portion of the first-stage flame to the burner grid apparently alters the velocity profile across the burner in such a way that the centre portion of the stream is accelerated, driving the second-stage upward in this region. The effect had been noted previously when the first-stage flame occasionally became attached to a carbon particle lying on the burner matrix. In such cases a slight hump in the second-stage flame always appeared directly over the dip in the first stage.

In the very centre of the second-stage flame of *Figure 10*(a), the colour photograph showed a small nodule protruding downward and coloured a faint pink. This apparently represented a chemical acceleration of the second-stage reaction, for with an increase in concentration the protrusion increased greatly in size and became distinctly rose-coloured [*Figure 10*(b)].

Second-stage spectra recorded with and without ethyl nitrate are shown in *Figures 11*(a) and *11*(b) respectively. Spectrum *11*(b) corresponds to the condition pictured in *Figure 10*(b). With the spectrometer sighted on the rosy nodule, the radiation was less intense than when sighted on the unaffected flame since the depth of radiating gas was less. Thus, spectrum *11*(b) required a wider slit width than *11*(a).

The only changes noted in the spectrum were the disappearance of the formaldehyde band peaks and an increase in the intensity of the long wavelength (red) end of the continuous background. The increased long wavelength radiation probably accounts for the rose tint of the ethyl nitrate nodule.

Ethyl nitrite

This compound was available in a solution containing 8 to 15 per cent ethyl alcohol, and as a result of its very high vapour pressure at room temperature, no satisfactory spectra or colour photographs of its effects were obtained (the ethyl nitrite all passed out of solution and left only the alcohol effect within the 10-minute exposure period). However, the short exposure black-and-white photograph, *Figure 12*, shows that this compound had only a very slight

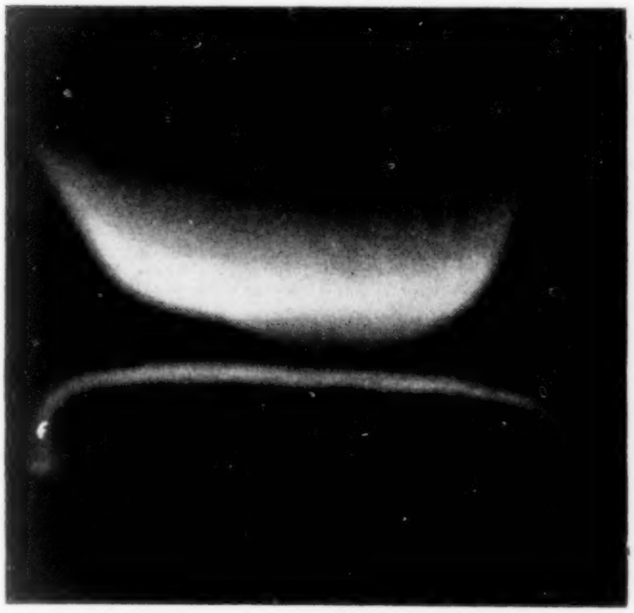

Figure 12. Effect of ethyl nitrite on two-stage flame

accelerating effect on the first-stage flame, but produced a rosy nodule extending downward from the second-stage flame in a manner similar to ethyl nitrate. The nodule in this case was somewhat broader and more diffuse than with the nitrate, a fact which might be explained by a higher diffusion rate for the lighter nitrite molecule.

Alcohols
Photographs of flames with added methanol and ethanol are shown respectively in *Figures 13*(a) and *13*(b). Both additives were maintained at room temperature in the additive flask. Both of these materials retarded the first-stage flame and at the same time accelerated the second-stage flame, so that the two flame fronts tended to approach each other and actually coalesced with high concentrations. No changes in colour were noted, and the spectra with and without the additives appeared identical.

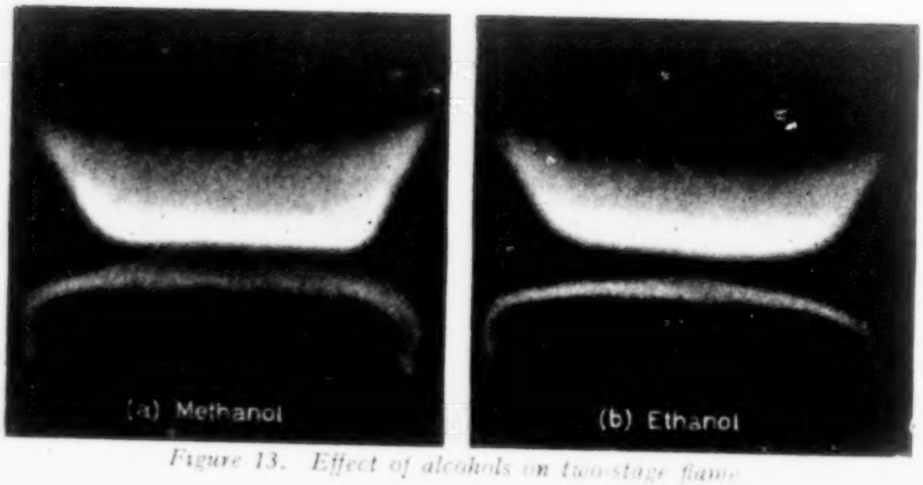

Figure 13. Effect of alcohols on two-stage flame

Di-t-butyl peroxide
Figure 14 shows the result of adding di-*t*-butyl peroxide at room temperature in the additive flask. The first-stage flame was accelerated and seated on the burner matrix, and the second-stage flame was retarded in a large hump. It is possible that part of the hump in the second-stage flame was due to aerodynamic effects resulting from the first-stage flame seating on the burner matrix as in the case with small concentrations of ethyl nitrate. However, the hump appears too large to be entirely explained in this manner, and it is suspected that a real chemical retardation also occurred. The central part of the second-stage hump turned from blue to grey-yellow.

Figure 15 shows the visible spectral changes which occurred when di-*t*-butyl peroxide was added. Spectrum *15*(a) represents no additive, and spectrum *15*(b) corresponds to the condition pictured in *Figure 14*. It is seen that the formaldehyde luminescence bands were made less prominent and a new radiation peak appeared near 5 500 A. It is not clear that the

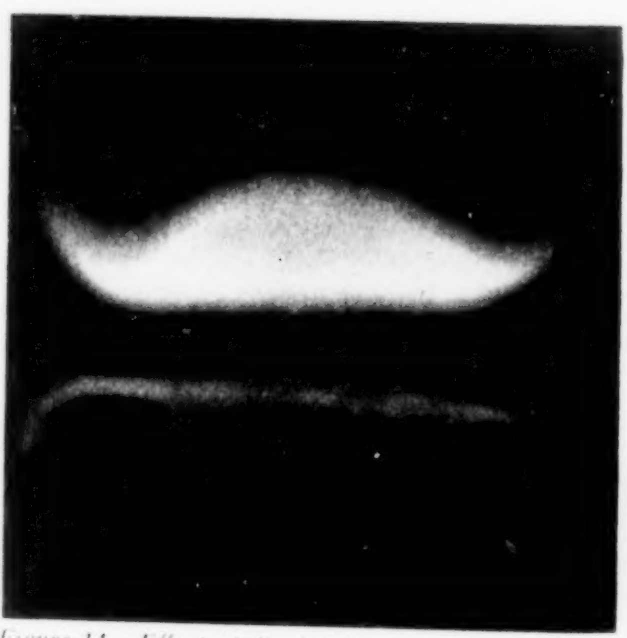

Figure 14. Effect of di-t-butyl peroxide on two-stage flame

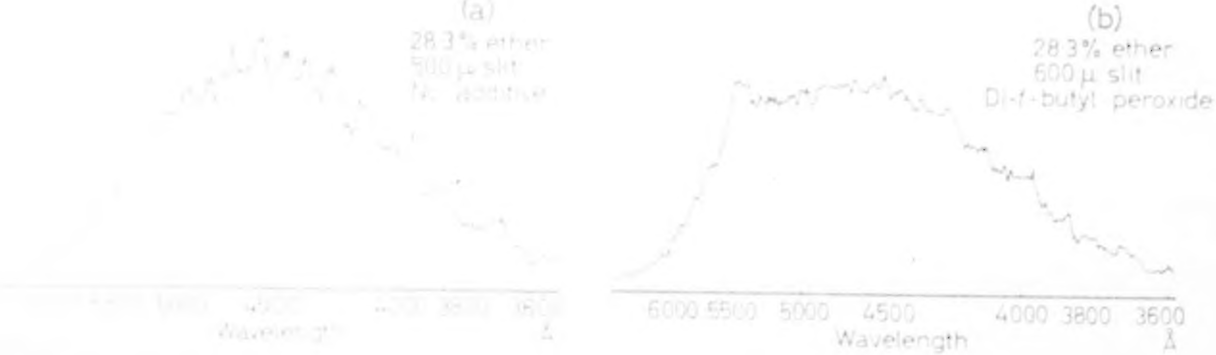

Figure 15. Effect of di-t-butyl peroxide on second-stage flame spectrum

[illegible] actually represents an emission [illegible] at 5 500 Å. [illegible] at 5 500 Å [illegible] more green than yellow, and [illegible] colour change was to a dirty [illegible] perhaps a greenish yellow would also [illegible] it is indicated that the radiation in [illegible] range from 5 500 Å to, say, 6 000 Å [illegible] increased in intensity. The rapidly [illegible] photomultiplier sensitivity from 5 500 to 6 000 Å might well combine with this [illegible] increase in intensity to give the result in spectrum 15(b).

Nitric oxide

Figure 16 shows the effect of adding nitric oxide to the additive flask at a rate of 0·0051 lb/h (0·39 mol per cent of the total mixture flow or 2·99 per cent of the fuel concentration). Smaller concentrations of nitric oxide appeared to give no effect on the flames, and slightly greater concentrations extinguished both flames.

Although *Figure 16* does not show it clearly, the nitric oxide appeared to extinguish entirely the first-stage flame over the entire area of the burner port, leaving only the scalloped 'skirt' of flame around the burner edge which is evident in the photograph.

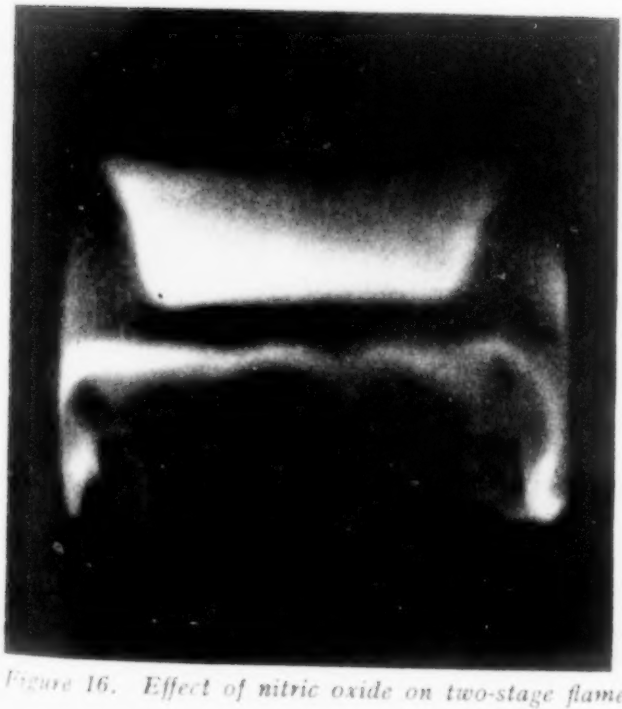

Figure 16. Effect of nitric oxide on two-stage flame

The second-stage flame was retarded slightly over its entire diameter, although it retained its original shape, and the flat portion was all coloured a faint pink. The widespread effect of nitric oxide would seem to result from its high diffusion rate as compared to the liquid additives. *Figure 17* shows a spectrum of the second-stage flame doped with nitric oxide, and it is seen that the additive produced an effect similar to ethyl nitrate and di-*t*-butyl peroxide. That is, the formaldehyde peaks were attenuated, and the red end of the background

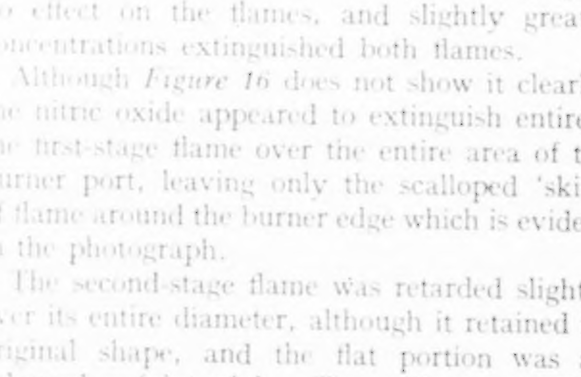

Figure 17. Spectrum of second-stage flame with nitric oxide

continuum was increased in intensity. The excess radiation at the red end of the spectrum with nitric oxide has a different intensity distribution from that given by either ethyl nitrate or di-*t*-butyl peroxide, but again there was no apparent band structure to help identify the emitter.

The rather large noise level exhibited in the trace of *Figure 17* resulted from a fluttering of the flame front, which was made quite unstable by the nitric oxide addition.

Discussion

It has obviously been the intention of this work to contribute to our knowledge of the manner in which additives affect the self-ignition of fuel–air mixtures, and in particular, anti-knock action in spark-ignition engines. In this regard, it is tempting to draw conclusions from the burner work which may be directly applied by analogy to engine operation. This dangerous practice must be avoided, and the line of attack should rather be to attempt an understanding of the burner phenomenon immediately at hand, with the hope that some aspects of this mechanism may be of a general enough nature eventually to aid in understanding the engine situation. On the other hand, since the burner study has not yet progressed to the point where much independent interpretation of the observations is possible, it does no harm to compare these burner experiments with similar experiments performed under other circumstances in different systems. The comparisons may, in fact, prove useful in suggesting possible interpretations to be proved later.

With some qualification and a few exceptions, the nine additives reacted in the burner two-stage flames about as one would expect from their known engine anti-knock or pro-knock effects.

Tetraethyl lead, tetramethyl lead and iron carbonyl

Tetraethyl lead has been shown to affect the later stages of preflame reactions in an engine and have little effect on the early stages[3–7]. These effects are entirely analogous to the burner performance of tetraethyl lead.

Tetraethyl lead has been shown to produce absorption lines of atomic lead in the unburnt gases in an engine at the time it is exerting its anti-knock effect, although no lead oxide bands were evident[8]. This effect is unlike the rich mixture burner performance, in which both lead oxide bands and lead lines appeared. However, at leaner mixtures in the burner (more nearly like the engine condition) the lead oxide bands were much less prominent than the lead lines in spite of the more oxidizing atmosphere, and perhaps this situation bears some similarity to the engine case. The increased relative intensity of lead emission lines with leaner mixtures in the burner might also simply result from the higher flame temperature which would tend to dissociate more lead oxide while at the same time exciting more atomic lead to radiating energy levels.

In normal hot flames, both in bunsen burners and engines, added tetraethyl lead has been shown to produce both lead oxide bands and atomic lead lines[9, 10]. In the bunsen burner experiments many lines appeared in the inner cone, but they decreased in intensity in the outer enevelope where the lead oxide bands were more prominent. In the engine experiments, the spectra were more like those found with the two-stage flame; only three strong lead lines and the lead oxide bands appeared, with roughly equal intensity in the flame fronts and the afterglow.

In recent flash photolysis studies of acetylene–oxygen explosions sensitized with amyl nitrate, K. H. L. Erhard and R. G. W. Norrish[11] found that tetraethyl lead increased the induction period, and that during the induction period lead oxide bands were visible in absorption. At the onset of the delayed ignition the lead oxide absorption bands were replaced by lead lines. It was concluded that tetraethyl lead itself reacted with the oxygenated intermediates formed in the cool flames to form lead oxide and delay ignition; the lead oxide was then reduced to atomic lead by reaction with free radicals. The latter process, by destroying radicals, thus served as a second means of delaying ignition. This theory differs fundamentally from those of G. H. N. Chamberlain and A. D. WALSH[12], of D. E. HOARE and A. D. WALSH[13], and of E. B. RIFKIN[14] who proposed an anti-knock action on the surface of lead oxide smoke particles, and also differs from the theory of L. L. WITHROW and G. M. RASSWEILER[7] who originally suggested only the latter part of the Erhard and Norrish theory, that lead oxide vapour acted as an anti-knock while being reduced to lead.

If the present flat-flame burner work has any relationship at all to those other systems, then one might say it tends to support the first part of the Erhard–Norrish theory as opposed to the other theories. Although it is entirely possible that a small amount of solid lead oxide may exist in equilibrium with the gaseous oxide detected, there is no evidence of the continuous emission which would be expected from appreciable quantities of solid lead oxide in the reaction zone (solid lead oxide did deposit on the burner stabilizing screen, and a small amount of smoke was occasionally noted above the screen). There was definite evidence for gaseous lead oxide formed just where Erhard and Norrish might predict, behind the first-stage cool flame where the oxygenated intermediates are in maximum concentration[15], where initial decomposition of the tetraethyl lead probably occurs, and where the inhibiting action is actually evident. The flame inhibition occurs with the very first traces of tetraethyl lead addition, when lead oxide bands appear strongly and the lead lines are quite weak. It is only at the higher concentrations of tetraethyl lead that the lead lines increase in intensity relative to the lead oxide, and thus it seems unlikely that reduction of lead oxide to lead is involved in the inhibition. However, this does not rule out the possibility that lead oxide might exert an additional effect by destroying radicals in the final fast auto-ignition which constitutes engine knock, as suggested by Erhard and Norrish. Such a process is not simulated in the flat-flame burner.

It may be that the ineffectiveness of tetraethyl lead, tetramethyl lead and iron carbonyl in altering the first-stage reaction results from the failure of the additives to decompose (or react with the oxygenated intermediates) at such low temperatures (about 800°F in the first stage, compared to 1 300°F for the second stage[15]). Rifkin[14] gives the percentages of additive decomposed per millisecond at 800°F as 1·5, 5·5 and 35 for tetramethyl lead, tetraethyl lead, and iron carbonyl respectively. With a flow velocity of about 10 to 15 cm/s in the first-stage flame front, the gases travel about one or two millimetres in 10 milliseconds, after which about 13·9, 42·2 or 97 per cent of the three additives respectively would be decomposed.

It has been reported[16] that in at least one fuel, sufficiently large concentrations of tetraethyl lead (greater than 1 per cent of the fuel) cause a reversal of the anti-knock effect, and tetraethyl lead actually acts as a knock inducer. It has been suggested that this might result from a large number of free ethyl radicals released in the tetraethyl lead decomposition. No corresponding effect was noted in the burner studies with tetraethyl lead. However, tetramethyl lead and iron carbonyl (for which high-concentration engine data are not available) both appeared to reverse their inhibitory effects on the second-stage flame at high concentrations. There appears to be no analogy in other systems for the differences in action of tetraethyl and tetramethyl lead at high concentrations in the burner. Decomposition rates help little in the explanation, since tetraethyl lead decomposes more readily than tetramethyl lead[14].

It has also been reported[17, 18] that in certain fuels, in particular *cyclo*pentadiene, both tetraethyl lead and iron carbonyl act as pro-knocks at all concentrations. No data are available regarding the engine effectiveness of tetraethyl lead or iron carbonyl in diethyl ether, since diethyl ether will not run in an engine under ordinary conditions.

Experimental evidence has been cited that nickel carbonyl[19] may induce ignition of hydrocarbons by its own spontaneous ignition if the carbonyl concentration is high enough. This perhaps corresponds again to the promoting effect indicated in the burner for high concentrations of iron carbonyl.

Previous spectral studies[9, 20] have shown that iron carbonyl added either to bunsen burner flames or to engine flames produces a spectrum of iron lines (strongest in the range 3 400 to 3 900 Å) and iron oxide bands (in the range 5 400 to 6 500 Å). The diffusion flame of iron carbonyl also shows a continuous spectrum[20]. Iron carbonyl in a low pressure oxy–acetylene flame shows a continuum in the yellow to blue-green region in a fore-zone ahead of the main reaction zone[21]. This continuum was presumed to be associated with the decomposition of the iron carbonyl.

In the flat-flame burner studies the strong emission recorded by the photomultiplier at 5 870 Å for iron carbonyl-doped flames might be mistaken for unresolved iron oxide bands normally occurring in this region. However, the fact that continuous emission occurred from 4 800 Å in the visible region all the way through the cadmium selenide and lead sulphide detector ranges and out to 12 microns in the infra-red leaves little doubt that a solid emitter is involved. Whether this emitter is the same one noted previously in the fore-zone of a low pressure oxy–acetylene flame is unknown. Perhaps solid particles of iron or iron oxide are involved, since some smoke was observed above the burner and reddish deposits collected on the stabilizing screen.

It is interesting to note that evidence for solid particles, which might be involved in anti-knock action, turns up with iron carbonyl and not with tetraethyl lead for which Walsh *et al.*[12, 13] originally proposed such a mechanism.

Although the noise level is rather large in the spectrum of *Figure 9*, it might be imagined that there actually is some band structure superimposed on the continuous emission between 5 400 and 6 500 Å. If so, this might be interpreted as superimposed iron oxide bands.

Ethyl nitrate

Ethyl nitrate is a known engine pro-knock[22] and it accelerated both stages of the flat-flame burner reaction. The rosy tint of the ethyl nitrate-doped flame was apparently accounted for by an increased intensity of the continuous emission in the red region of the spectrum. The red CN bands might be suggested here, except that no band structure was resolved and there was no trace of the CN violet system. The decomposition flame of ethyl nitrate has shown[23] a two-stage reaction in which the first zone emits the usual formaldehyde cool flame spectrum, and the second zone emits a continuum in the red and green regions which was unidentified. This continuum may be what was observed in the present study. Perhaps NO + O association is a possible source of this continuum.

Alcohols

Neither methanol nor ethanol are normally classed as anti-knock compounds, although they are fairly knock-resistant fuels. Their octane numbers (Motor Method) have been reported to be 98 and 99·5 respectively[24]. The indications here are that they do not undergo two-stage preflame reaction, but react with one preflame stage only.

Di-t-butyl peroxide

The remarkable result with di-*t*-butyl peroxide —acceleration of the first stage and retardation of the second stage—seems to indicate that no explanation of additive effects on preflame reactions is likely to be simple. This material is a distinct pro-knock in engines[3] in spite of the fact that it apparently retards the completion of the two-stage reaction in the burner. It has been proposed by some[7, 22] that the first-stage cool flame results when a critical concentration of organic peroxides is built up and the peroxides start to decompose. In such a case it would be quite conceivable that added peroxide would tend to make the first-stage cool flame appear earlier, as it did in the flat-flame burner. However, there is no immediate explanation for retardation of the second-stage flame, or for the sharp increase in yellow radiation in the second-stage flame.

Nitric oxide

Nitric oxide presented an interesting case, and it is useful to compare the retarding effect of nitric oxide in the flat-flame burner with other experiments in which oxides of nitrogen have been used as additives in combustion systems.

First, tests performed in conjunction with the present study consisted of adding nitric oxide in various concentrations to the intake manifold immediately ahead of the intake valve of a single-cylinder engine. The fuel was *iso*octane, the compression ratio 8·5, and knocking tendency was measured by the knock-limited spark advance. As shown in *Figure 18*, nitric oxide exhibited an anti-knock effect at all concentrations below about 9 mol per cent of the total mixture with the maximum anti-knock effect at about 1·8 mol per cent. Above 9 per cent the effect was pro-knock. The burner result is in general accord with this result, although concentrations are difficult to compare.

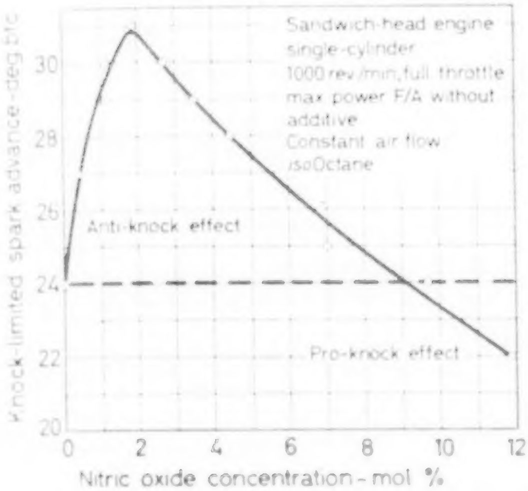

Figure 18. Effect of nitric oxide on knocking tendency of a single-cylinder engine

Second, tests by Z. G. Szabó and D. Gál[25] indicated that additions of nitric oxide to a slowly reacting ethane–oxygen–nitrogen system in concentrations below 0·1 mol per cent of the total mixture (0·13 per cent of the fuel concentration) gave inhibition, and in the range 0·1 to 2·0 mol per cent gave acceleration of the reaction. The burner result agrees qualitatively with this result, but again the different chemical systems make the comparison of concentrations uncertain.

Third, G. R. Freeman, C. J. Danby and C. N. Hinshelwood[26] found that concentrations of nitric oxide in the range of about 0·5 to 10 mol per cent reduced the rate of decomposition of diethyl ether to about one quarter of its uninhibited rate. Nitric oxide concentrations of 28 to 65 per cent (depending on pressure) gave decomposition rates exceeding that with no nitric oxide. These results also agree in general with the burner experiments.

Fourth, Aivazov, Neumann and Kane (see ref. 27) have shown that low concentrations of nitrogen dioxide added to reaction vessels in which cool flames are made to occur shortens the induction period to the cool flame and also decreases the critical pressure limit for cool flames. With larger concentrations (of the order of 0·3 mol per cent nitrogen dioxide) cool flames are suppressed. These results are opposite to those found in the burner and those listed above for nitric oxide.

Fifth, Downs, Walsh and Wheeler[22] indicated that nitrogen dioxide added to the air entering a single-cylinder test engine in a concentration corresponding to 3·2 mol per cent of the fuel (about 0·2 mol per cent in the system) had only a very slight pro-knock effect. However, when added to and mixed with the fuel before test, it had a 'profound' pro-knock effect for the first 0·2 to 0·4 mol per cent added (about 0·02 per cent in the system); subsequent addition had a negligible effect. This result too is opposite to the burner effect and contrary to the engine effect noted above.

Estimates of the amount of nitrogen dioxide formed from nitric oxide prior to passage through the flame were calculated for the burner and engine experiments. It was concluded that the additive in the engine experiment was essentially all nitric oxide, but in the burner flame a large portion of the additive was actually nitrogen dioxide.

It is not surprising that the engine experiment agreed more closely with the prior nitric oxide tests than with the nitrogen dioxide tests, but the fact that the burner experiment also showed inhibition at low additive concentrations is unexpected from the prior tests with nitrogen dioxide.

Again there is no explanation of the increased continuous radiation at the red end of the visible spectrum for the nitric oxide-doped second-stage burner flame. Freeman, Danby and Hinshelwood[26] found HCN and CH_3CN formed in the nitric oxide-induced decomposition of diethyl ether. HCN has an absorption band system around 7 900 to 8 600 Å, and CN has a red emission spectrum from 4 400 to 9 400 Å. These cyanides might contribute the red emission, or perhaps some association reaction such as NO + O accounts for it.

It may also be mentioned that recent studies[25] have shown no acceleration or inhibition by nitric oxide of the propagation of normal hot flames in a bunsen burner.

Conclusion

Perhaps the most noteworthy feature of the present study is the fact that additives in the diethyl ether cool flames produce results much like those occurring in gasoline-fuelled engines. Only the most obvious effects have been noted so far, and it is expected that continued studies with other fuel–air and additive systems and probe sampling will soon permit more definite conclusions about the mechanism by which additives affect preflame reactions.

Engine knock, however, has a many-sided character. While cool flame reactions seem important with hydrocarbon fuels, the knocking of hydrogen and moist carbon monoxide in engines[7] apparently takes place with no such cool flames. The fact that tetraethyl lead affects the preflame reactions of hydrocarbons (and diethyl ether), and also acts as an anti-knock with hydrogen and moist carbon monoxide[7], indicates that there is also more than one side to the anti-knock question. Any complete explanation of the knock reaction and the action of anti-knock agents must cover all of these observations. In this regard, the suggestion of Erhard and Norrish that tetraethyl lead has a double-barrelled punch, one at oxygenated intermediates in the preflame reactions and one at radicals in the rapid auto-ignition, appears to be a reasonable approach. However, a great deal more verification is required before any such theory may be accepted. It is hoped that continued efforts along the line of the present study will help supply the much-needed verification.

References

[1] Agnew, J. T., Agnew, W. G. and Wark, K., Jr. *Sixth Symposium (International) on Combustion*, pp 894–902. Reinhold: New York, 1957

[2] Agnew, W. G. and Agnew, J. T. *Industr. Engng Chem. (Industr.)*, 1956, **48**, 2224

[3] Cornelius, W. and Caplan, J. D. *S.A.E. Quart. Trans.* 1952, **6**, 488

[4] Downs, D., Street, J. C. and Wheeler, R. W. *Fuel, Lond.* 1953, **32**, 279

[5] Melby, A. O. *J. Inst. Petrol.* 1952, **38**, 965

[6] Pastell, D. L. *S.A.E. Quart. Trans.* 1950, **4**, 571

[7] Sturgis, B. M. *Trans. Soc. automot. Engrs, N.Y.* 1955, **63**, 253

[8] Withrow, L. L. and Rassweiler, G. M. *Industr. Engng Chem. (Industr.)*, 1935, **27**, 872

[9] Rassweiler, G. M. and Withrow, L. L. *Industr. Engng Chem. (Industr.)*, 1931, **24**, 528

[10] Withrow, L. L. and Rassweiler, G. M. *Industr. Engng Chem. (Industr.)*, 1931, **23**, 769

[11] Erhard, K. H. L. and Norrish, R. G. W. *Proc. Roy. Soc.* 1956, **243**, 178

[12] Chamberlain, G. H. N. and Walsh, A. D. *Proc. Roy. Soc.* 1952, **215**, 175

[13] Hoare, D. E. and Walsh, A. D. *Proc. Roy. Soc.* 1952, **215**, 454

[14] Rifkin, E. B. Paper presented at 23rd Mid-Year Meeting of American Petroleum Institute, Los Angeles, May 1958

[15] Donovan, R. E. and Agnew, W. G. *J. chem. Phys.* 1955, **23**, 1592

[16] Campbell, J. M. Private communication

[17] Campbell, J. M., Signaigo, F. K., Lovell, W. G. and Boyd, T. A. *Industr. Engng Chem. (Industr.)*, 1935, **27**, 593

[18] Cramer, P. L. and Campbell, J. M. *Industr. Engng Chem. (Industr.)*, 1949, **41**, 893

[19] Badin, E. J., Hunter, P. C. and Pease, R. N. *J. Amer. chem. Soc.* 1948, **70**, 2055

[20] Gaydon, A. G. *The Spectroscopy of Flames*, pp 223–224. Wiley: New York, 1957

[21] Gaydon, A. G. and Wolfhard, H. G. *Proc. Roy. Soc.* 1948, **194**, 169

[22] Downs, D., Walsh, A. D. and Wheeler, R. G. *Phil. Trans. A*, 1951, **243**, 463

[23] Wolfhard, H. G. *Fuel, Lond.* 1955, **34**, 60

[24] Egloff, G. J. *J. Instn Petrol. Tech.* 1937, **23**, 645

[25] Szabó, Z. G. and Gál, D. *Combustion & Flame*, 1957, **1**, 404

[26] Freeman, G. R., Danby, C. J. and Hinshelwood, C. N. *Proc. Roy. Soc.* 1958, **245**, 28

[27] Lewis, B. and von Elbe, G. *Combustion, Flames and Explosions of Gases*, p 159. Academic Press: New York, 1951

[28] Rosser, W. A., Jr. and Wise, H. *Final Rep. Phase I* Stanford Research Institute Project No. SU-1715, May 15, 1957

Carbon Formation in Premixed Flames

P. H. DANIELS

'Shell' Research Ltd, Thornton Research Centre, P.O. Box 1, Chester

(Received March 1959)

Examination of the work of J. C. Street and A. Thomas on the suppression of carbon in premixed flames has shown that there is a simple connection between the behaviour of individual members within either the n*-paraffin or olefin series and between the two series as a whole. The behaviour of acetylene is related in a simple manner to that of ethylene and ethane, and a connection is apparent between the behaviour of benzene and that of* n*-paraffins and olefins. The relationships do not extend to alkyl substituents in benzene, which have a disproportionately large effect in increasing the carbon-forming tendency of the flames.*

THE suppression of carbon formation in flames of hydrocarbons by premixed air has been studied in some detail by J. C. STREET and A. THOMAS[1] using a bunsen type burner from which secondary air was excluded.

The results were expressed either as critical air/fuel ratios at which carbon formation was suppressed or as fractions of the stoichiometric amount of air required to suppress carbon formation. Expression of the results in these ways allowed general conclusions to be drawn regarding different classes of hydrocarbons and showed an effect of molecular weight but failed to indicate a number of interesting conclusions which can be drawn from the work. The purpose of this paper is, essentially, to draw attention to these.

Expression of Results

The method of expressing results adopted by Street and Thomas has advantages where it is intended to use the results in the practical applications of petroleum products. However, a more fundamental method of expressing them is on the basis of number of oxygen atoms required by each hydrocarbon molecule for carbon to be suppressed in the premixed flame.

Table 1 shows results obtained by Street and Thomas, together with results expressed in this manner. Examination of these values shows that carbon suppression occurs in a much more systematic manner than the paper of Street and Thomas would indicate.

The Flames of Ethane, Ethylene and Acetylene

Concerning the amount of premixed air to suppress carbon formation Street and Thomas state that 'acetylene needs only 0·484 times

Table 1

Hydrocarbon	*Air to suppress carbon formation as a fraction of stoichiometric*	*Stoichiometric number of oxygen atoms per molecule of hydrocarbon*	*No. of oxygen atoms per molecule of hydrocarbon to suppress carbon (OASC)*
Ethane	0·60	7	4·2
Propane	0·64	10	6·4
Butages (mainly butane)	0·67	13	8·7
n-*Pentane*	0·68	16	10·9
iso*Pentane*	0·67	16	10·7
n-*Hexane*	0·69	19	13·1
iso*Hexane*	0·69	19	13·1
n-*Octane*	0·72	25	18·0
iso*Octane*	0·69	25	17·3
iso*Dodecane*	0·71	37	26·3
n-*Cetane*	0·74	49	36·3
Acetylene	0·484	5	2·42
Ethylene	0·55	6	3·3
Propylene	0·60	9	5·4
Butylene	0·64	12	7·7
Amylene	0·65	15	9·8
cyclo*Hexane*	0·66	18	11·9
n-*Heptene*	0·69	21	14·5
Benzene	0·70	15	10·5
Toluene	0·75	18	13·5
Xylene	0·79	21	16·6
Cumene	0·78	24	18·7
Tetralin	0·95	26	24·7
Decalin	0·79	29	22·9
1-Methyl naphthalene	0·97	27	26·2

stoichiometric (0·484λ) to suppress carbon formation whereas ethylene needs 0·55λ and ethane 0·61λ. Carbon can thus be formed from ethane under conditions which prohibit its formation from ethylene and acetylene; this makes it somewhat unlikely that the latter are intermediates'.

However, comparison of the number of oxygen atoms per molecule of hydrocarbon necessary to suppress carbon formation (OASC) in flames of ethane, ethylene and acetylene (*Table 1*), shows that ethylene requires 0·9 more than acetylene, and ethane requires 0·9 more than ethylene. There are two hydrogen atoms difference in each case, and the differences in OASC values are nearly unity, and equivalent to the hydrogen.

Thus, the indications would be the reverse of those suggested by Street and Thomas, and their results would suggest that ethylene and acetylene could well be intermediates in carbon formation in an ethane flame, and that acetylene could be an intermediate in an ethylene flame.

The paraffin and olefin series

The relationship between OASC values for ethane and ethylene holds for other normal paraffins and olefins. Each normal paraffin requires one more atom of oxygen than the corresponding olefin (*Table 1*).

The effect of increase in carbon number of normal paraffins and olefins on OASC is linear (*Figure 1*) and almost completely without deviations. Gradients are almost identical, every additional CH_2 in the chain requiring 2·27 atoms of oxygen in the case of normal paraffins, and 2·24 atoms in the case of olefins.

Thus there is a well defined relationship between the normal paraffin and olefin series and between members of the same series.

As pointed out by Street and Thomas *iso*-paraffins need less oxygen to suppress carbon formation than do normal paraffins, and *cyclo*hexane fits the olefin series closely. The limited amount of data suggests that the *iso*paraffins also show a linear relationship between carbon number and OASC.

The difference between OASC values for normal hexane and *cyclo*hexane can be largely accounted for by the difference of two hydrogen atoms. However, *cyclo*hexane shows a slight deviation from the olefin series but whether this is a structural effect or due to experimental error in the determination is not known.

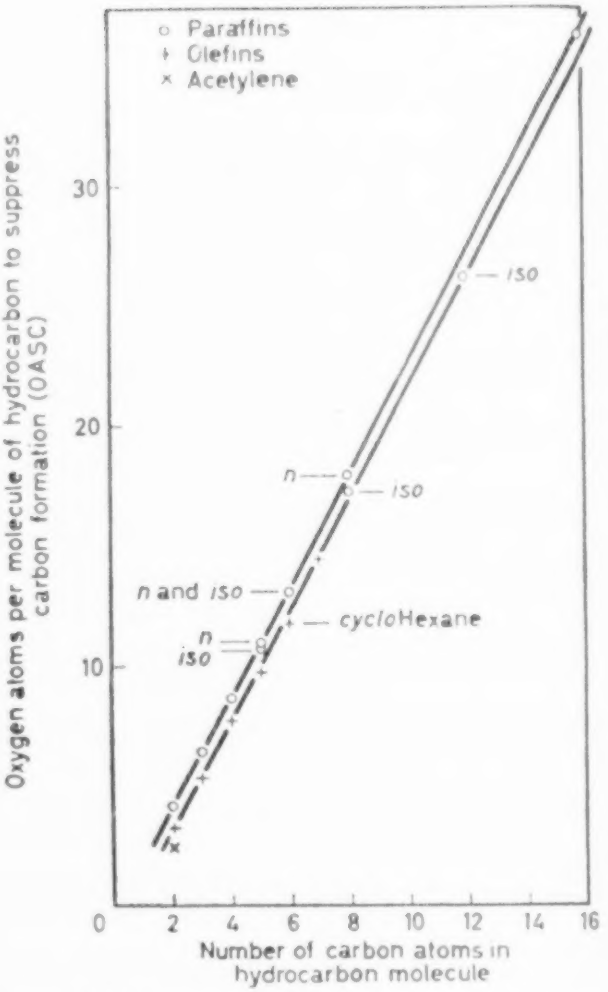

Figure 1. Suppression of carbon in flames of paraffins, olefins and acetylene

Aromatic hydrocarbons

The OASC of benzene cannot be related directly to those of the paraffins, olefins and acetylene, but a relationship is apparent if it is assumed that fractional values of OASC can be compared.

Since the OASC for acetylene is 2·42 and the molecule contains two CH units then the OASC for CH in acetylene is $\frac{1}{2}(2{\cdot}42) = 1{\cdot}21$.

The plots of OASC for paraffins and olefins against carbon number (*Figure 1*) show that each additional CH_2 increases OASC by 2·27 for paraffins, and 2·24 for olefins.

A value for CH can then be derived from these data for CH_2 by subtracting 0·5 in each case, giving the following values:

For normal paraffins

$$\text{OASC per CH} = 2{\cdot}27 - 0{\cdot}5 = 1{\cdot}77$$

For olefins

$$\text{OASC per CH} = 2{\cdot}24 - 0{\cdot}5 = 1{\cdot}74$$

Benzene contains six CH units and has an OASC value of 10·5. For benzene the OASC of CH is, therefore,

$$\tfrac{1}{6}(10{\cdot}5) = 1{\cdot}75$$

On this basis, therefore, OASC for CH in benzene is much higher than for acetylene but is the same as for CH units within the chain of normal paraffins and olefins.

No such relationship can be seen with aromatics with condensed rings. Street and Thomas showed that in the case of 1-methyl naphthalene carbon could only be suppressed by adding nearly the stoichiometric amount of air. A value for OASC for CH in 1-methyl naphthalene cannot be determined as for benzene but the approximate value of 2·4 (i.e. 26·2/11) compared with 1·75 for benzene shows the extremely marked effect of a fused aromatic ring on benzene.

Methyl substitution in benzene has a very marked effect on OASC, which is much greater than the increase which occurs when the chain length in the olefin or paraffin series is increased by one carbon atom. Thus, in passing from benzene to toluene the difference in OASC is 3·0 as against about 2·25 for CH_2 in ascending the paraffin and olefin series. A second methyl group (in xylene) causes a further increase of 3·1 in OASC value (*Table 1*).

The same kind of enhancement is apparent in the case of cumene but the effect of the *iso*propyl group is less, in proportion to its size, than that of methyl substitution.

Naphthenic hydrocarbons

*cyclo*Hexane can be more readily related to the olefins and normal paraffins than to benzene. It has an OASC of 11·9 and an attempt to relate it to benzene by subtracting 3 (equal to six hydrogen atoms) would give a result of 8·9, whereas 10·5 was found for benzene by experiment.

In the same way decalin appears to be unrelated to naphthalene, although a direct comparison cannot be made since naphthalene itself was not tested. However, an approximate indirect comparison can be made. Assuming that the methyl group has the same effect on naphthalene as it has on benzene, then since the OASC value of 1-methyl naphthalene is 26·2 the OASC value of naphthalene would be $26{\cdot}2 - 3{\cdot}0 = 23$ approximately. The OASC value of decalin is 22·9, but subtraction of 5 (equal to ten hydrogen atoms) from this would give a value for naphthalene of only 17·9 instead of 23.

On the other hand, tetralin appears to have some relationship with naphthalene since subtraction of 2 (equal to four hydrogen atoms) from it gives 22·7, which is not far removed from the approximate value of 23 calculated for naphthalene.

The difference between tetralin and decalin is very marked. Although decalin has six more atoms of hydrogen than tetralin it has a lower OASC.

Thus, the purely naphthenic hydrocarbons *cyclo*hexane and decalin are very different in properties from the corresponding aromatics, but the naphthenic aromatic tetralin appears to behave in a similar way to aromatics, so far as suppression of carbon in its flame is concerned.

Suppression of carbon formation

In a flame of a hydrocarbon containing premixed air suppression of carbon formation can only be brought about by an oxidation process acting in competition with processes of polymerization which would ultimately lead to carbon formation.

Street and Thomas interpreted their results on normal paraffins and olefins on the basis of a more rapid oxidation of olefins in the premixed flame, and a consequent reduction of the extent to which carbon-forming reactions could proceed in the flames of olefins. However, as has been shown, the difference between an olefin and the corresponding normal paraffin can be explained simply by the difference in hydrogen content.

At flame temperatures it would appear, therefore, that differences between the general oxidation stabilities of olefins and corresponding normal paraffins disappear, or that oxidation of the fuel molecule itself is not the first stage in suppression of carbon formation.

In the particular case of ethane and ethylene the OASC values correspond with a loss of hydrogen to give acetylene, but whether carbon suppression is due to direct oxidation of acetylene itself is not indicated, although it seems highly probable.

The OASC value for CH in ethane, ethylene and acetylene is less than that of the additional CH in propane or propylene. This difference may perhaps be attributed to the formation of allyl radicals as intermediates in the pre-flame oxidation of C_3 hydrocarbons. These resonance-stabilized radicals might tend to persist in a flame and require larger amounts of premixed air to eliminate them.

K. RUMMEL and P. O. VEH[2] postulated that polynuclear aromatic hydrocarbons are intermediates in carbon formation, and there is recent work which would support this[3]. If benzene is one of the earlier precursors of carbon in flames of paraffins and olefins it is not surprising that the CH in benzene has the same OASC value as that of CH units within the chains of normal paraffins and olefins.

Alkyl substitution in benzene has an unduly marked effect in increasing the OASC. This may perhaps be due to the ability of such groups to participate in ring closures to give polynuclear aromatic precursors of carbon during pyrolysis in the flame. This has been observed in the case of toluene which, on pyrolysis in the vapour phase in a heated tube, can give anthracene in appreciable yield. The extreme carbon-forming tendency of aromatics with fused rings is well known, and was clearly shown quantitatively by Street and Thomas in the case of 1-methyl naphthalene.

Thus, the work of Street and Thomas would in general conform to a mechanism of carbon formation in which polynuclear aromatics are formed from fuels in flames, and are then converted to carbon by dehyrogenative polymerization.

A ring structure does not, necessarily, cause unusually high OASC values, and as has been shown for *cyclo*hexane and decalin there is no direct connection with the corresponding aromatic on the basis of difference in hydrogen content. Suppression of carbon in their flames would therefore appear to follow some route other than via initial dehydrogenation to aromatics. It seems likely that ring opening occurs initially followed by mechanisms of carbon suppression similar to those which occur with paraffins and olefins.

However, in the case of the naphthenic aromatic, tetralin, the OASC would appear to indicate that dehydrogenation to naphthalene is in the main the first stage in the combustion, and that the condensed ring structure has a very pronounced effect on the overall carbon-forming properties of this hydrocarbon in a premixed flame.

Conclusions

The examination of the data obtained by Street and Thomas has allowed a number of conclusions to be reached which were not drawn originally by these workers. These conclusions are summarized as follows.

There is a linear relationship between the number of carbon atoms in normal paraffins and olefins and the number of oxygen atoms per molecule of hydrocarbon necessary to suppress carbon formation in the premixed flames of the hydrocarbons. From the limited amount of data available, a similar relationship appears to hold for *iso*paraffins.

Normal paraffins require one oxygen atom more per molecule for carbon suppression in their flames than do corresponding olefins. Acetylene requires an oxygen atom less per molecule than does ethylene.

In normal paraffins and olefins above ethane and ethylene in the homologous series, each additional CH requires the same number of atoms of oxygen for carbon suppression as does the CH in benzene.

Alkyl groups attached to benzene increase the oxygen needed to suppress carbon in the flame of the hydrocarbon by an amount greatly in excess of that calculated from the requirements of CH in normal paraffins, olefins or benzene itself. This may be due to participation of side chains in ring closures yielding polynuclear aromatics in the flame, thus giving compounds from which it is difficult to suppress carbon formation.

The naphthenes *cyclo*hexane and decalin cannot be related to the corresponding aromatics on the basis of difference in hydrogen content. In the suppression of carbon from the flames of naphthenes it seems unlikely, therefore, that simple dehydrogenation to an aromatic occurs as a first stage. However, in the case of the naphthenic aromatic, tetralin, this may be the main reaction occurring initially.

The permission of the Directors of 'Shell' Research Limited to publish this work is gratefully acknowledged.

References

[1] STREET, J. C. and THOMAS, A. *Fuel, Lond.* 1955, **34**, 4

[2] RUMMEL, K. and VEH, P. O. *Arch. Eisenhüttenw.* 1941, **14**, 489

[3] ARTHUR, J. R., COMMINS, B. T., GILBERT, J. A. S., LINDSEY, A. J. and NAPIER, D. H. *Combustion & Flame*, 1958, **2**, 267

Th
Tr
fla
the
wh
tha
wo
is

ma
so
in
an
pr
th
an
su
sy
re

pr
fla
fo
fo
w
be
m

T
If
pa

The Theory of Steady Laminar Spherical Flame Propagation: Equations and Numerical Solution

D. B. SPALDING

Imperial College of Science and Technology, London, S.W.7

(*Received May 1959*)

A combustible gas is supposed to emerge steadily from a point source immersed in an atmosphere of adiabatic combustion products. The differential energy equation is solved numerically, and it is shown that the effective radius of the spherical flame is larger than that predicted from the assumptions that the flame is very thin and that it has the same burning rate per unit area as a plane flame. The error increases as the rate of injection and the laminar flame speed of the mixture decrease. The thermal conductivity of the gas is assumed constant in the numerical analysis, but it is shown how the resulting data can be used in cases for which conductivity depends upon temperature.

1. Introduction

The problem

THE theory of the propagation of laminar plane flames has been extensively developed. This theory can be applied to curved flames only when the radius of curvature is much larger than the flame thickness. In the present paper we consider the case arising when this condition is not satisfied.

We suppose that combustible gas flows uniformly and steadily outward from a point source [*Figure 1*]. The surrounding gas is infinite in extent and is identical in composition and temperature with the adiabatic combustion products of the injected gas. A flame surrounds the injection point. Because buoyancy forces and non-radial mass motion of the gas are supposed absent, the flame is spherically symmetrical about the injection point in all respects.

The gas can be injected at any rate. The problem is to determine the position of the flame, and the temperature distribution in it, for a given injection rate. The problem therefore differs from that of plane flame propagation, where only one mass flow rate is possible, this being the flame speed which has to be determined.

The thin-flame approximation

If the flame can be assumed very thin compared with its radius of curvature, the mass rate of burning per unit area can be taken as equal to that in a plane flame. If the latter quantity is $\dot{m}_f''$ [say, in g/cm^{2}s], the flame radius r_f is obviously related to the mass injection rate $\dot{m}$ by

$$\dot{m} = 4\pi r_f^2 \dot{m}_f'' \qquad \ldots . [1]$$

The temperature distribution within the flame

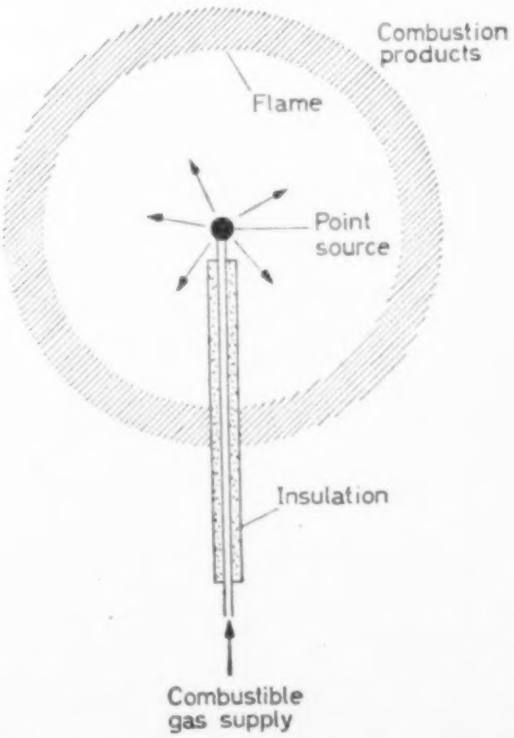

Figure 1. *Sketch of spherical steady flame symmetrically surrounding a point source*

shell is then easily determined from considerations of thermal conduction and mass flow. It is this temperature distribution which is needed if the theory is to be used; for example, to lead to a prediction of the burning time of monopropellant droplets.

When the flame thickness is not small, however, the terms 'flame radius' and 'mass flow rate per unit flame area' cease to have any precise meaning; the temperature distribution near the origin cannot now be determined simply. *Figure 2* illustrates the temperature distribution in the gas (a) when the flame is thin, (b) when it is not.

Method
To determine the influence of flame curvature, the differential energy equation is considered anew. Solutions are obtained numerically for a single shape of reaction-rate curve over a wide range of the thickness/curvature parameter. To ease the solution, the thermal conductivity has been taken as uniform and the diffusion coefficients as normal [Lewis number, unity].

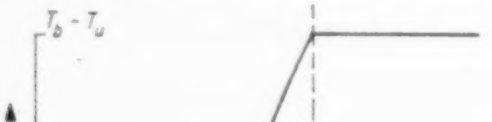

(a) Thin flame

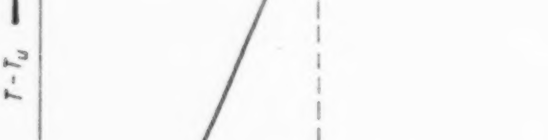

(b) Thick flame

Figure 2. Temperature distributions near point source

Summary of main results of analysis
It is convenient to discuss the results in terms of an 'effective thin-flame radius', r^* [*Figure 2*(b)]. This is the radius obtained by extrapolating, through the region where reaction is taking place, the temperature curve valid for the region upstream of the reaction zone; r^* is the radius at which this curve reaches the temperature of the combustion products.

For a thin flame, r^* is identical with r_f, calculated from equation 1. The analysis below shows that, for thick flames, the ratio r^*/r_f is a function of the dimensionless parameter $\dot{m}\dot{m}_f''c^2/4\pi k^2$, where r_f is now defined by equation 1, c is the gas specific heat and k is the thermal conductivity. *Figure 7* shows how r^*/r_f rises from unity to infinity as $\dot{m}\dot{m}_f''c^2/4\pi k^2$ tends to zero. So the thin-flame equation 1 is asymptotically correct for large injection rates and highly reactive gases, but otherwise underestimates the effective flame thickness.

2. Equations

Notation

c	Specific heat of gases at constant pressure, assumed constant (cal/gs)
k	Thermal conductivity of gases (cal/cm s °C)
k_b	Thermal conductivity of adiabatic combustion products (cal/cm s °C)
$\dot{m}$	Strength of point source of combustible gas (g/s)
$\dot{m}_f''$	Mass burning rate in a plane laminar flame propagating through the injected gas (g/cm² s)
$\dot{q}'''$	Volumetric reaction rate in flame (cal/cm³ s)
$\overline{\dot{q}'''}$	$\int_{T_u}^{T_b} \dot{q}''' \mathrm{d}T/(T_b - T_u)$ (cal/cm³ s)
r	Radius (cm)
r_f	$(\dot{m}/4\pi\dot{m}_f'')^{\frac{1}{2}}$. Equals flame radius when flame is thin (equation 1)
r^*	Radius of effective thin flame (cm)
T	Gas temperature (°C)

T_b Temperature of adiabatic combustion products (°C)
T_u Temperature of unburnt combustible (°C)
n $k/c\dot{m}''_u$, thickness of plane flame (cm)
λ $\overline{\dot{q}'''}k(4\pi r^{*2})^2/\dot{m}^2c^2(T_b-T_u)$ (—)
ξ $\exp\{-\dot{m}c/4\pi kr\}$, dimensionless radius (—)
ξ^* $\exp\{-\dot{m}c/4\pi kr^*\}$, dimensionless effective thin-flame radius (—)
$\Delta\xi$ Interval of ξ in numerical integration (—)
τ $(T-T_u)/(T_b-T_u)$, reactedness (—)
ϕ $\dot{q}'''/\overline{\dot{q}'''}$, dimensionless reaction rate (—)

Steady-flow energy equation

We consider for simplicity the case of a combustible gas for which the volumetric reaction rate is 'temperature-explicit' in the sense of ref. 1. The First Law of Thermodynamics for our spherically symmetrical system can then be written

$$\frac{1}{r^2}\frac{\mathrm{d}}{\mathrm{d}r}\left(kr^2\frac{\mathrm{d}T}{\mathrm{d}r}\right)-\frac{\dot{m}c}{4\pi r^2}\frac{\mathrm{d}T}{\mathrm{d}r}+\dot{q}'''=0 \quad . [2]$$

where r denotes radius from the point of gas injection [cm], k is gas conductivity [cal/cm s °C], T is gas temperature [°C], $\dot{q}'''$ is volumetric reaction rate [cal/cm^{3}s] and other symbols are as above.

The specific heat at constant pressure has been assumed independent of temperature, while $\dot{q}'''$ is a known function of temperature, usually of the general shape indicated in *Figure 3*. In particular, $\dot{q}'''$ is equal to zero at the temperature of the injected gas, T_u, and at that of the adiabatic combustion products T_b. The latter is of course the temperature prevailing in the gas reservoir [$r \longrightarrow \infty$], while the former prevails at the point of injection [$r=0$].

Equation 2 contains the continuity equation implicitly, in the form of the coefficient of the temperature gradient $\mathrm{d}T/\mathrm{d}r$. This expresses the fact that the mass flow rate per unit area is inversely proportional to radius.

Boundary conditions

These are, as just foreshadowed:

$$r=0 \;:\; T=T_u \quad \ldots . [3]$$

$$r=\infty \;:\; T=T_b \quad \ldots . [4]$$

These two conditions will just suffice to define the solution when the mass injection rate $\dot{m}$ is prescribed. This is therefore not an eigenvalue problem.

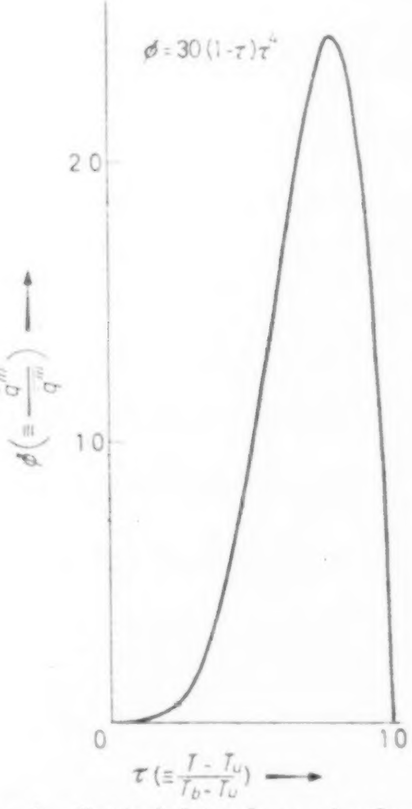

Figure 3. Typical dependence of volumetric reaction rate on temperature

Dimensionless form

For simplicity, it will be supposed that the conductivity k is independent of T; although large conductivity variations may arise in practice, there is no reason to suppose that they have particular relevance to the curvature effect which is at present under discussion.

We then render equation 2 dimensionless, remove the first-order differential coefficient, and make the range of integration finite, by means of the following transformations:

$$\tau \equiv (T-T_u)/(T_b-T_u) \quad \ldots . [5]$$

$$\xi \equiv \exp\{-\dot{m}c/4\pi kr\} \quad \ldots . [6]$$

$$\xi^* \equiv \exp\{-\dot{m}c/4\pi kr^*\} \quad \ldots . [7]$$

$$\lambda \equiv \frac{\overline{\dot{q}'''}k(4\pi r^{*2})^2}{\dot{m}^2c^2(T_b-T_u)} \quad \ldots . [8]$$

$$\overline{\dot{q}'''} \equiv \int_{T_u}^{T_b} \dot{q}''' \, \mathrm{d}T / (T_b - T_u) \quad \ldots . [9]$$

$$\phi \equiv \dot{q}''' / \overline{\dot{q}'''} \quad \ldots . [10]$$

There results

$$\frac{\mathrm{d}^2\tau}{\mathrm{d}\xi^2} = -\frac{\lambda}{\xi^2}\left[\frac{\ln \xi^*}{\ln \xi}\right]^4 \times \phi \quad \ldots . [11]$$

with the boundary conditions:

$$\xi = 0 \ : \ \tau = 0 \quad \ldots . [12]$$

$$\xi = 1 \ : \ \tau = 1 \quad \ldots . [13]$$

Remarks on equation 11

Equation 11 is rendered non-linear by the fact that ϕ is a non-linear function of τ, its shape corresponding to *Figure 3*. The equation is similar, except for the term $[\ln \xi^* / \ln \xi]^4$, to the equation for an adiabatic plane flame in the form used in ref. 2. A similar transformation of the space variable for a plane flame has also been made by G. ROSEN[3].

ξ^* is defined, through equation 7, in terms of r^*, of which only a non-mathematical definition has so far been given. We now make the definition precise by noting that, at temperatures too low for an appreciable rate of reaction, equation 11 can be reduced to

$$\mathrm{d}^2\tau / \mathrm{d}\xi^2 = 0 \quad \ldots . [14]$$

the solution of which is a straight line passing through the point $\xi = 0$, $\tau = 0$ [see *Figure 4*]. According to the definition of r^* therefore, ξ^* is the value of ξ at which this straight line intersects the line $\tau = 1$. So ξ^* is related to the temperature gradient at the origin by

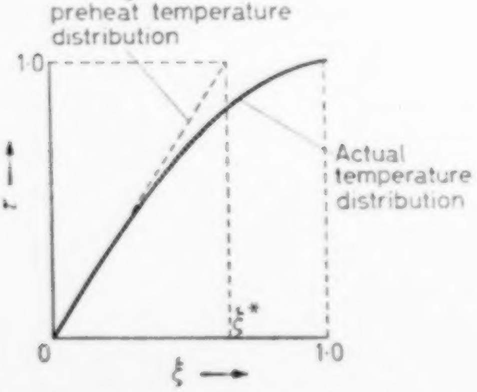

Figure 4. A solution to equation 11

$$\left(\frac{\mathrm{d}\tau}{\mathrm{d}\xi}\right)_{\xi=0} = \frac{1}{\xi^*} \quad \ldots . [15]$$

which may be taken as the mathematical definition of ξ^*.

In the plane-flame problem, the additional boundary condition $(\mathrm{d}\tau/\mathrm{d}\xi) = 0$ at $\xi = 1$ is given [ref. 2]; λ then must be determined as an eigenvalue. The present problem permits a range of values for λ; equation 11, together with its boundary conditions 12 and 13, may be regarded as defining a relation between λ and ξ^*. This relation is the main objective of the mathematical analysis.

3. Solution of the Energy Equation

Reaction-rate expression

In the present paper it has been assumed that the relation between the volumetric reaction rate and the temperature is given by

$$\phi = 30(1 - \tau)\tau^4 \quad \ldots . [16]$$

This relation, which is plotted in *Figure 3*, has a shape which is fairly representative of flame reactions; it is also one member of a family of reaction-rate expressions which was investigated in ref. 1 in connection with plane flames.

It is intended to study other reaction-rate expressions in later papers.

Method of solution

Equation 11 is conveniently solved by numerical stepwise integration from the cold boundary $[\xi = 0]$. For a given $(\mathrm{d}\tau/\mathrm{d}\xi)_0$, i.e. for a given ξ^*, curves of τ versus ξ are plotted by means of the integration formula, which represents equation 11 in finite-difference form,

$$\tau_{n+1} = 2\tau_n - \tau_{n-1} - \Delta\xi^2 \times \frac{\lambda}{(\xi_n)^2}\left(\frac{\ln \xi^*}{\ln \xi}\right)^4 \times \phi(\tau_n) \quad \ldots . [17]$$

where $\Delta\xi$ is the interval between successive calculated points, and the subscripts $(n-1)$, n, $(n+1)$ denote evaluation at successive points in the direction of increasing ξ.

Figure 5 shows, as an example, a set of curves obtained, for various values of λ, with $\xi^*=0{\cdot}1$. Large values of λ cause the curves to curl downward; small values of λ allow the curves to intersect the line $\tau=1$. The required value of λ is that which causes the curve to pass through the point ($\xi=1$, $\tau=1$). In the example of *Figure 5*, this value is clearly between **0·4335** and 0·435; the limits can be narrowed as closely as desired. In the example of *Figure 5*, $\lambda=0{\cdot}434$ was accepted as the required value, accurate to three decimal places.

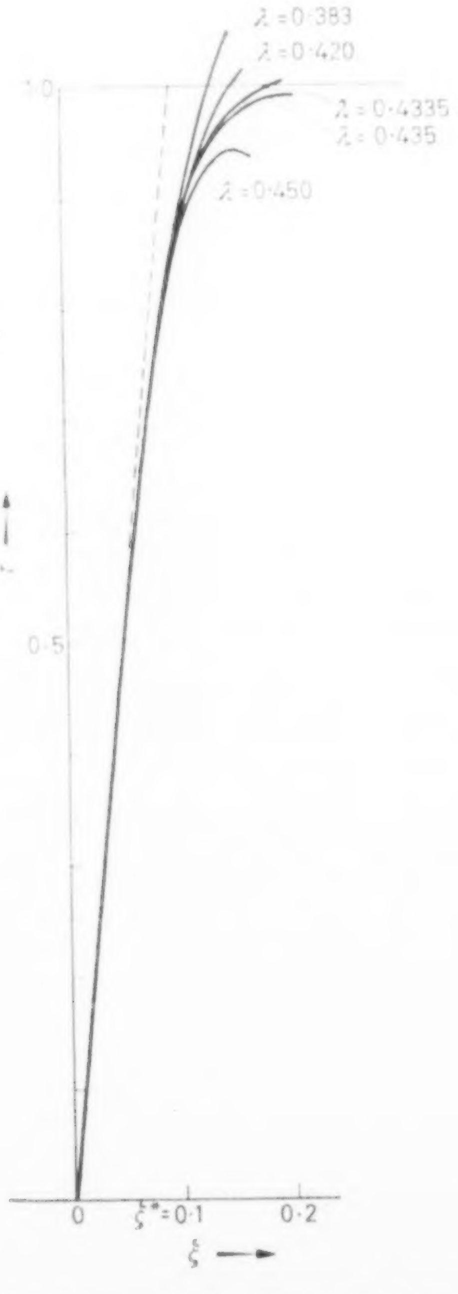

Figure 5. Curves plotted in obtaining λ for ξ = 0·1*

This process was carried out for various values of ξ^*, the integration interval $\Delta\xi$ being reduced until no change occurred in the third decimal place.

For very small values of ξ^*, the ratio $[\ln \xi^*/\ln \xi]^{\frac{1}{2}}$ tends to depart less and less from unity within the reaction zone, as may easily be proved. The case of $\xi^*=0$ was therefore solved by putting this ratio equal to unity. This was done merely as a check on the procedure, for this case is identical with that of the plane flame for which λ is known from ref. 1. The two methods gave the same value of λ for the reaction-rate curve in question, namely **0·277**.

Results

The results of the numerical integrations are contained in *Table 1*, and are also plotted in *Figure 6*.

Table 1

ξ^*	0	0·0001	0·0002	0·01	0·025	0·05
λ	0·277	0·310	0·317	0·352	0·372	0·396
ξ^*	0·10	0·20	0·30	0·40	0·50	
λ	0·434	0·510	0·597	0·714	0·880	

4. Discussion

Comparison with thin-flame theory

If we denote by λ_0 the value of λ at which $\xi^*=0$, the burning rate in a plane flame is given by

$$\dot{m}_f''=\left[\frac{k\overline{\dot{q}'''}}{\lambda_0 c^2 (T_b-T_u)}\right]^{\frac{1}{2}} \quad \ldots\ldots [18]$$

where $\lambda_0=0{\cdot}277$ for reaction-rate curves of the form 16, as already stated.

Equation 18 can be used, together with the definition (equation 8) of λ, to relate the effective 'thin-flame' radius, r^*, to r_f, which is now taken as *defined* by equation 1. We obtain:

$$\frac{r^*}{r_f}=r^*\left[\frac{4\pi\dot{m}_f''}{\dot{m}}\right]^{\frac{1}{2}}=\left(\frac{\lambda}{\lambda_0}\right)^{\frac{1}{2}} \quad \ldots\ldots [19]$$

This quantity can be evaluated by means of the contents of *Table 1* as a function of ξ^*. Now ξ^* is related to physical quantities by

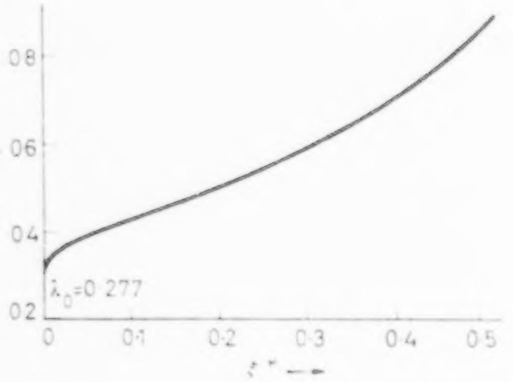

Figure 6. Variation of λ with ξ for* $\phi=30\,(1-\tau)\,\tau^3$

equation 7. This expression also contains r^*; a more convenient quantity against which to plot r^*/r_f is $\dot{m}\dot{m}_f''c^2/4\pi k^2$, which is related to ξ^*, via equations 1, 7 and 19 by

$$\frac{\dot{m}\dot{m}_f''c^2}{4\pi k^2}=\left(\frac{\lambda}{\lambda_0}\right)^{\frac{1}{2}}\left(\ln\frac{1}{\xi^*}\right)^2 \quad \ldots\ldots [20]$$

Figure 7 contains a plot of r^*/r_f versus $\dot{m}\dot{m}_f''c^2/4\pi k^2$, derived from the contents of *Table 1*. It is evident that, for large values of the latter quantity, r^*/r_f is close to unity; this means that the thin-flame assumption predicts the temperature distribution upstream of the flame with good accuracy. Only when the quantity $\dot{m}\dot{m}_f''c^2/4\pi k^2$ is below 10·7 is r^* 10 per cent greater than r_f.

Figure 7 shows in particular that r^*/r_f *is* always greater than unity. It follows that the thin-flame approximation always over-estimates the steepness of the temperature gradient upstream of the flame. This may be interpreted as signifying that the effect of flame curvature is to reduce the effective burning velocity, if the latter is defined as the mass rate of burning divided by the surface area of a sphere of radius r^*.

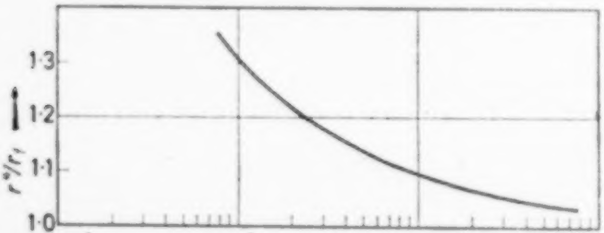

Figure 7. *Comparison of effective thin-flame radius,* r^*, *with that predicted by the thin-flame assumption,* r_f

The quantity $\dot{m}\dot{m}_f''c^2/4\pi k^2$ can be interpreted geometrically. If we define a 'flame thickness' δ by

$$\delta=k/c\dot{m}_f'' \quad \ldots\ldots [21]$$

it is easy to show that

$$\frac{\dot{m}\dot{m}_f''c^2}{4\pi k^2}=\frac{r_f^2}{\delta^2} \quad \ldots\ldots [22]$$

So the abscissa of *Figure 7* is proportional to the square of the ratio of flame radius to flame thickness.

Relevance to the burning rate of monopropellant droplets

Ref. 4 demonstrates how the thin-flame assumption can be used to calculate the burning rate and time of liquid monopropellant droplets. We now see that the effective flame radius is larger than would be expected from the thin-flame theory, so the burning rates predicted in ref. 4 will be over-estimates.

The implications of spherical-flame theory for droplet combustion will be examined more fully in a later paper. However, already it is possible to predict that the over-estimates of ref. 4 will not be very large. The reason is that at small values of $\dot{m}\dot{m}_f''c^2/4\pi k^2$, where the curvature effects are large, the vaporization rate of the droplet is not usually much influenced by the chemical reaction rate, but is close to that valid for vaporization in the absence of combustion. At the other end of the scale, the thin-flame analysis is satisfactory.

Temperature distribution upstream of the flame

In the region where τ is small and the reaction rate ϕ is negligible, the solution is

$$\tau=\xi/\xi^* \quad \ldots\ldots [23]$$

In terms of physical quantities, this equation becomes

$$\tau=\frac{\exp\{-\dot{m}c/4\pi kr\}}{\exp\{-\dot{m}c/4\pi kr^*\}} \quad \ldots\ldots [24]$$

In *Figure 8*, τ is plotted against the dimensionless radius, $4\pi kr/\dot{m}c$, for various values of the dimensionless effective flame radius, $4\pi kr^*/\dot{m}c$, in accordance with equation 24. Although drawn stretching above the $\tau=1$ line, the curves of course only represent actual temperature distributions for values of τ well below unity.

Only one of the curves satisfies the boundary conditions at $r=\infty$; this is the one for $4\pi kr^*/\dot{m}c=\infty$. This curve represents the temperature distribution which would prevail if the injected gas were entirely inert.

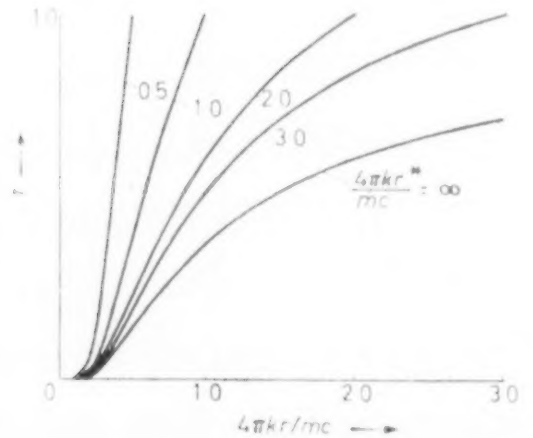

Figure 8. Temperature distributions upstream of flame for various values of $4\pi kr^*/\dot{m}c$

Summing up the relations between the flame region and the upstream region, one may say that the rate of chemical reaction, measured by $\dot{m}\dot{m}_r''c^2/4\pi k^2$, settles what the value of $4\pi kr^*/\dot{m}c$ will be; the internal temperature distribution then adjusts itself correspondingly. It will be noted that

$$\frac{4\pi kr^*}{\dot{m}c}=\frac{r^*}{r_t}\left[\frac{k^2}{\dot{m}\dot{m}_r''c^2}\right]^{\frac{1}{2}} \quad \ldots . [25]$$

which is easily evaluated. *Figure 9* contains a plot of the term $4\pi kr^*/\dot{m}c$ versus $\dot{m}\dot{m}_r''c^2/4\pi k^2$ valid for the reaction-rate relation 16.

Effect of temperature-dependent conductivity

The least satisfactory feature of the present analysis is the assumption that the thermal conductivity of the gas is a constant. This assumption could be dropped by re-defining ξ as

$$\xi\equiv\exp\{\int_r^{\infty}(\dot{m}c/4\pi kr^2)\mathrm{d}r\} \quad \ldots . [26]$$

in which the integral has to be evaluated taking cognizance of the dependence of k, through τ, on r. Then the term $[\ln\xi^*/\ln\xi]^4$ in equation 17 could be replaced by $[r/r^*]^4$, r being evaluated by way of equation 26.

Since the variation of τ with ξ is not known initially, the ξ/r relation has first to be guessed. Trial-and-error is necessary, and the solution procedure becomes rather tedious.

In the absence of exact analysis of the temperature dependence along the above lines, the following approximate procedure appears most suitable:

(*i*) Insert k_b in $\dot{m}\dot{m}_r''c^2/4\pi k^2$ when evaluating r^*/r_t, etc., where k_b is k at T_b. This is advisable because the whole reaction region is near the burnt gas temperature, and because the range of integration in equation 26 is from r to ∞, i.e. the hot region.

(*ii*) When calculating the temperature distribution upstream of the flame, replace equation 24 by

$$\int_r^1\frac{k\,\mathrm{d}\tau}{k_b\tau}=\frac{\dot{m}c}{4\pi k_b r}-\frac{\dot{m}c}{4\pi k_b r^*} \quad \ldots . [27]$$

Equation 27 has been derived by integrating equation 2 with $\dot{q}'''$ put equal to zero.

The procedure just outlined takes full account of the temperature dependence of conductivity only for reaction-rate functions which are very steeply temperature-dependent; for there the temperature of the reaction zone is very close

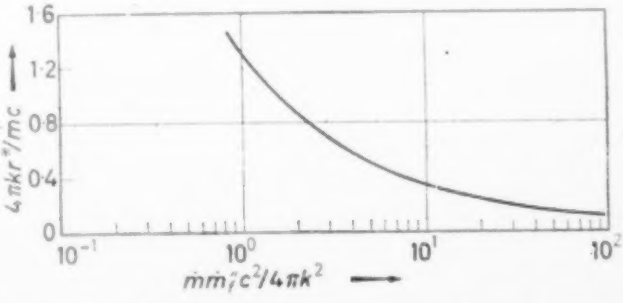

Figure 9. Dimensionless effective thin flame position for $\phi=30\ (1-\tau)\ \tau^4$

to that of the combustion products. The procedure will, however, probably be sufficiently accurate for practical cases even when the activation energy is less great.

Directions of further work
The results of the present paper are only valid for combustible mixtures for which the volumetric reaction rate depends on temperature in accordance with equation 16. Other temperature-explicit reaction-rate expressions are currently being studied by analytical and analogue-computer methods. This work will be reported elsewhere.

5. Conclusions

(*a*) The 'thin-flame' theory over-estimates the steepness of the temperature gradients upstream of the reaction zone of a spherical flame.

(*b*) The over-estimate, in terms of r^*/r_f, is less than 10 per cent if the parameter $\dot{m}\dot{m}''c^2/4\pi k^2$ exceeds about 10. This parameter has the significance of the square of 'flame radius/flame thickness'.

(*c*) In the absence of exact analysis of the case of varying k, the thermal conductivity to be inserted in $\dot{m}\dot{m}''c^2/4\pi k^2$ and similar quantities is that of the adiabatic combustion products.

The author's thanks are due to Miss M. P. Steele who carried out the numerical computations described above.

References

[1] SPALING, D. B. *Combustion & Flame*, 1957, **1**, 287 and 296

[2] SPALDING, D. B. *Proc. Roy. Soc. A*, 1957, **240**, 83

[3] ROSEN, G. *Seventh Symposium (International) on Combustion*, p 339. Butterworths: London, 1959

[4] SPALDING, D. B. and JAIN, V. K. *Aeronaut. Res. Coun. Paper No. 20, 176* (C.F. 441, R. 436), May 1958

The Theory of Burning of Solid and Liquid Propellants

D. B. SPALDING

Imperial College of Science and Technology, London, S.W.7

(Received June 1959)

The Centroid Rule of laminar gas-flame is applied to a simple model of condensed-phase propellant combustion; the propellant is supposed to undergo successively a phase-changing reaction and a gaseous combustion reaction. Curves are presented enabling the rate of burning in the gaseous flame to be calculated as a function of the propellant surface temperature and the centroid of the reaction-rate function. These curves, combined with information about the process of phase change, enable surface temperature and burning rate to be determined. Normal diffusion is assumed in the gas phase. The effect of heat loss from the propellant surface is considered. It is shown that this can lead, under some circumstances, to the existence of both lower and upper limits to the pressure under which stable burning is possible.

1. Introduction

1.1. *The problem*

DOUBLE-BASE propellants, and liquids such as ethyl nitrate or hydrazine, often burn in practice in a steady one-dimensional manner; that is to say that the flame and the propellant surface are substantially plane, and that variations in temperature and composition occur only in the direction normal to these planes. Even composite propellants can be expected to burn more or less in this manner when the particle size is sufficiently small compared with the flame thickness.

For this reason, theoretical studies have been made by several authors of a plane, one-dimensional, propellant model capable of two consecutive reactions, the first producing a change of phase and the second producing exothermic combustion. The present paper also discusses such a model. The problem considered is that of relating the burning rate to the physical and chemical properties of the model propellant, and of determining, in particular, the effect of pressure.

1.2. *Outline of existing theories*

The two pioneer papers in this field, first presented in 1947, are those of O. K. RICE and R. GINELL[1] and of R. G. PARR and B. L. CRAWFORD[2]. Their work has been reviewed by R. D. GECKLER[3], who with R. W. LAWRENCE[4], has extended the theory, and by G. K. ADAMS and L. A. WISEMAN[5]. The theories have in common the assumption that the decomposition of the solid phase, occurring either at a surface as suggested by R. E. WILFONG *et al.*[6], or in a foam region as postulated in ref. 2, can be spatially separated from the region of gas-phase reaction. Heat transfer occurs between the two regions. The theories chiefly differ in the methods used for obtaining approximate solutions of the differential equations, in the detailed assumptions regarding chemical reaction, and in the extent to which diffusion of the reactants is considered.

The theory of laminar flame propagation in gases, which presents simpler problems than does solid propellant combustion, has undergone considerable development in the last decade. In particular, the calculation of the burning velocity in gases can now often be carried out with adequate accuracy without the necessity to solve non-linear differential equations. These recent developments do not, however, appear to have been applied to solid propellant theory.

1.3. *Outline of present theory*

In this paper, the attempt is made to carry one stage further the line of thought initiated by Rice and Ginell, and by Parr and Crawford. On the one hand, some of the mathematical approximations which beset their theories have been removed, while the physical approximations have been clarified. On the other hand, calculations of burning rate, surface temperature, etc., are presented for a sufficient number of examples, and with sufficient accuracy, for the process to be understood qualitatively and for quantitative trends to be perceived. These improvements have been made possible by the use of techniques developed in connection with gaseous flames.

As in earlier theories, spatial separation is assumed between the regions in which the phase-changing reaction and the combustion reaction occur. However, the calculations are carried out in a general way, so that it has not been necessary to accept a particular postulate for the former reaction; indeed a simple vaporization process also fits into the theoretical framework. Two families of gas-phase reaction-rate functions have been considered; the relevant computations for these functions are presented graphically, in dimensionless form. It is hoped that the reaction-rate functions, and the corresponding graphs, are sufficiently general and accurate to make further computations of this type unnecessary.

In addition to providing a means of computing the burning velocity of an adiabatic propellant, the effect is considered of thermal radiation from the propellant surface to cold surroundings. As is to be expected, in view of experience with other combustion systems[8, 9], it is shown that the radiative heat loss can produce combustion instability; for example, it may make combustion impossible below, or above, a critical pressure. Such pressure limits are of course known to exist.

2. Thermodynamic Analysis

2.1. *The model propellant*

The assumed reactions—We suppose that before combustion the propellant exists in the condensed phase (solid or liquid) as a single chemical compound A.

Substance A is supposed to be capable of being transformed physically or chemically into the gaseous substance B. The transition may simply involve vaporization or sublimation without chemical change; or it may involve a chemical re-arrangement or decomposition. The 'reaction' may be either endothermic or exothermic.

Substance B, which is also supposed to be, or behave like, a single chemical compound, is capable of a further chemical transformation to form the gaseous substance C. We call this the combustion reaction; it is invariably exothermic. Our assumptions can be represented symbolically by:

$$A \xrightarrow[\text{phase change}]{} B \xrightarrow[\text{combustion}]{} C$$

The enthalpy/temperature relations—*Figures 1*(a) and *1*(b) give two examples of how the enthalpies of the substances A, B and C may depend on temperature at the pressure in question. The lines are slightly curved upwards, indicating that the specific heat of each pure compound varies with temperature; the specific heats of the compounds are not supposed equal.

The vertical distance between two curves measures the heat of reaction at the temperature in question. Therefore, *Figure 1*(a), which has the B line below the A line, is valid for an exothermic A ⟶ B reaction. *Figure 1*(b), which shows B to have a higher enthalpy than A at any given temperature, corresponds to an endothermic A ⟶ B reaction. *Figure 1*(b) would be valid for a liquid propellant which changed phase by simple vaporization.

Insolubility of gases in the condensed phase—It is assumed that the gas B and the combustion product C do not dissolve appreciably in the condensed phase A. So the condensed phase is pure A, while the gas phase consists only of B and C.

It is this assumption which ensures spatial separation of the A ⟶ B and B ⟶ C reactions. It would not be valid if the propellant were a fluid at a pressure above the critical.

Diffusion—No question of diffusion arises in the condensed phase. In the gaseous phase the substances B and C will be supposed to diffuse in accordance with Fick's law. If either B or C really consists of several chemical compounds, or both do, these will all be supposed to have equal diffusion coefficients.

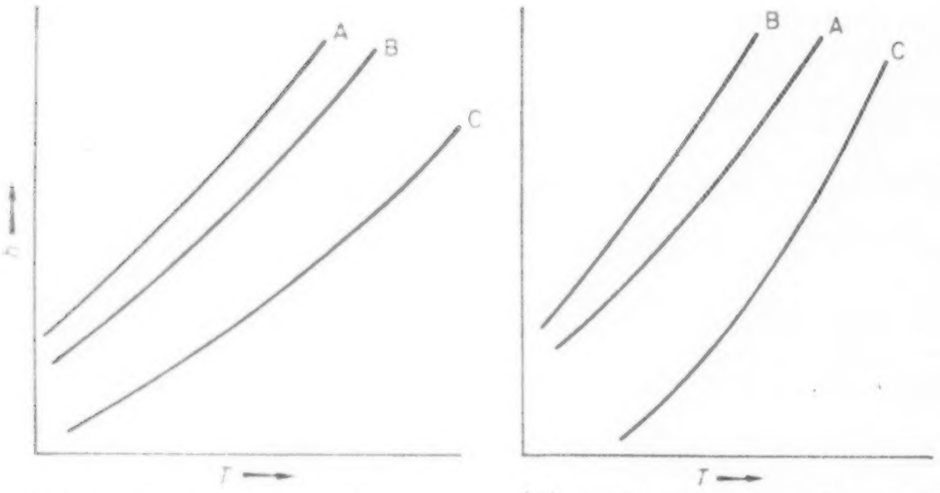

(a) Exothermic A → B reaction (b) Endothermic A → B reaction

Figure 1. Enthalpy/temperature curves for the substances A, B and C

2.2. Qualitative description of reaction region

Figure 2 illustrates the temperature and composition distributions which may prevail near the propellant surface; the latter is supposed to be at rest, the unburnt propellant being supplied steadily from the left, while the combustion products stream away to the right.

Temperature distribution—In the example shown, the temperature gradient exhibits a discontinuity at the phase boundary. The direction of the change implies (assuming that the gas conductivity is not greater than that of the condensed phase, and for the moment neglecting radiative loss) that the reaction occurring at the surface is exothermic. If this reaction occurred in a 'foam' region of finite thickness, as postulated by Parr and Crawford, the temperature gradient would change continuously rather than abruptly†.

The temperature curve is concave upwards in the gaseous flame region also, as a consequence of the exothermic reaction occurring there. Although, in *Figure 2*, there is a gap between the gaseous flame and the propellant surface, this will not always exist, and is not a general feature of the present theory.

Far to the left of the surface, the propellant has the initial temperature T_u: far to the right of the surface the gas temperature is uniform at T_b. The surface temperature is T_s; the determination of this temperature is an important intermediate objective in the theory to be presented.

Composition distribution—The local concentration of component j is measured by m_j, defined as the mass of j present in unit mass of local mixture. It follows that $m_A = 1$ to the left of the propellant surface (unless a foam region is considered), and zero elsewhere. The concentration of B, m_B, attains a finite value discontinuously as the surface is crossed, and thereafter decreases to zero; m_C correspondingly rises, for in the gas phase we have

$$m_B + m_C = 1 \qquad \ldots . [1]$$

The gradients of the m_B and m_C curves ensure that diffusion fluxes of B and C are superimposed on the convective flux: B diffuses downstream, towards the reaction zone; C diffuses in an upstream direction.

2.3. *Flame conditions represented on the enthalpy/temperature diagram*

Notation—

- *b* Exponent in liquid–vapour equilibrium law, equation 39
- *c* Specific heat of combustion products at constant pressure and at temperature $T_{b,\mathrm{ad}}$.

---

†For this statement to have meaning, the bubble diameter of the foam must be small compared with $(T_b - T_u)/(\mathrm{d}T/\mathrm{d}x)$.

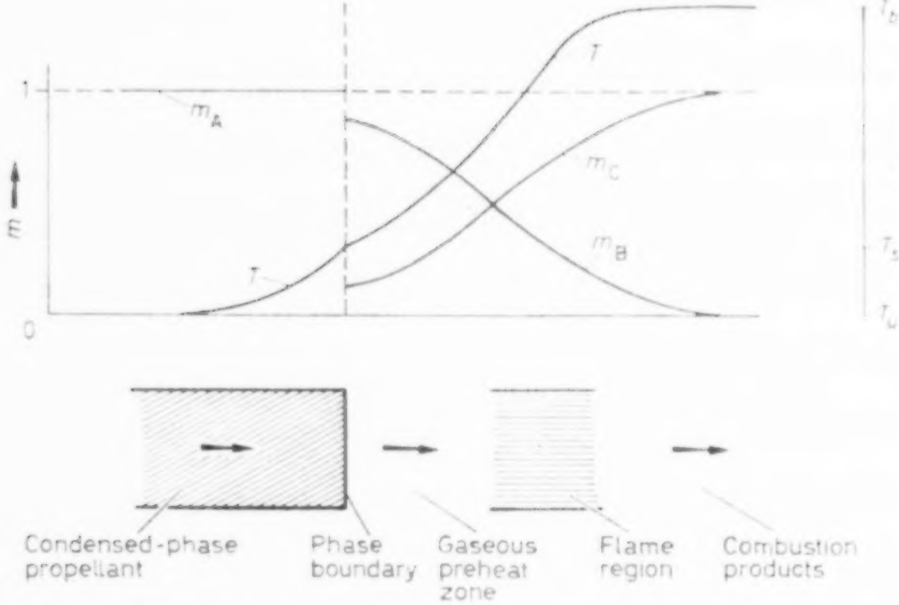

Figure 2. Illustrating conditions in gaseous and condensed phases near the propellant surface

c_m	Local mixture specific heat at constant pressure
D	Diffusion coefficient
d	Temperature exponent of decomposition reaction
G	Mass decomposition and burning rate
h	Enthalpy of gas mixture, or suffix component
K	Thermal conductivity of gas mixture
k	Pressure exponent of volumetric reaction rate
m	Mass of suffix component per unit mass of local mixture
$\dot{m}_C'''$	Rate of generation of C by chemical reaction per unit volume
n	Exponent of τ in chemical reaction-rate laws, equations 37 and 38
N	Exponent of temperature rise in gas-phase burning rate law, equation 44
p	Dimensionless temperature gradient, $d\tau/dy$
P	Pressure
Q	Dimensionless heat loss parameter, equation 46
$\dot{q}''$	Heat loss rate by radiation per unit propellant surface area
R	See equation 18
$\overline{R}$	See equation 19
$\mathscr{R}$	Universal gas constant
T	Absolute gas temperature
x	Distance normal to propellant surface
y	Dimensionless distance, equation 17
ε	Surface emissivity of propellant
θ	Dimensionless temperature, equation 43
λ	Eigenvalue of gaseous flame equation, equation 21
ρ	Density
σ	Stefan–Boltzmann constant
τ	Reactedness or concentration of C, equation 16
ϕ	Dimensionless reaction-rate function, equation 20

Subscripts—

ad.	Adiabatic, i.e. no radiation from propellant surface
A	Condensed-phase propellant
b	Fully burnt, downstream condition
B	Gaseous-phase unburnt propellant
c	Centroid
C	Gaseous-phase fully burnt propellant
d	Reference state
s	In gas-phase at propellant surface.
u	Unburnt condensed-phase propellant, far upstream
0	When $\tau_s = 0$
min.	Minimum. So $T_{s,\mathrm{min.}} \equiv$ lowest possible value of the surface temperature for given burnt gas temperature T_b.

The uniform-enthalpy condition—Until §5, we consider the case in which radiative heat transfer at the propellant surface can be neglected. Then the First Law of Thermodynamics ensures that the enthalpies of the unburnt propellant and of the combustion products are equal. The points representing these states on an h/T diagram, u and b respectively on *Figure 3*, lie on the same horizontal line. *Figure 3* happens to be drawn for an exothermic A ⟶ B reaction, but the following discussion applies to the endothermic case also.

Let the surface temperature be T_s. Consider any temperature, T_g, between T_s and the burnt-gas temperature T_b: this represents a temperature prevailing somewhere in the gas-phase region, as a glance at *Figure 2* will show. Let the corresponding values of the enthalpies of B and C, assuming the Gibbs–Dalton laws of gaseous mixtures to prevail, be h_B and h_C (*Figure 3*). If the enthalpy of the mixture is h, then

$$h = m_B h_B + m_C h_C \qquad \ldots . [2]$$

$$= (1 - m_C) h_B + m_C h_C \qquad \ldots . [3]$$

by consideration of condition 1.

Now it is a well-known result of laminar-flame theory that, if the diffusion coefficients equal the thermal diffusivity (Lewis number, unity; normal diffusion), the enthalpy is uniform in the gas phase. This result applies here also, as is proved below. We may therefore write, for the gas phase:

$$(1 - m_C) h_B + m_C h_C = h = h_b = h_u \quad \ldots . [4]$$

Since h_B and h_C are known functions of temperature, equation 4 links m_C and T uniquely. Representing the gas states on *Figure 3*, we see that they all lie on the horizontal line sb, and that m_C can be represented for ideal mixtures by a ratio of vertical lengths, viz.

$$m_C = gg_B / g_C g_B \qquad \ldots . [5]$$

Condensed-phase conditions—To the left of the propellant surface in *Figure 2*, and of any foam region which may be present, the temperature is non-uniform; on the other hand, because diffusion cannot take place, the composition is uniform. Here the uniform-enthalpy result cannot prevail; the conditions represented on *Figure 2* are instead to be found on the line A, of *Figure 3*.

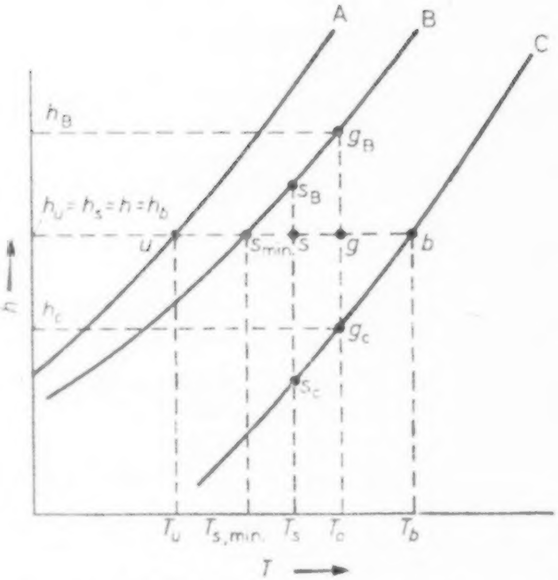

Figure 3. Propellant and gas conditions in flame represented on enthalpy/temperature diagram. Exothermic A → B reaction

Limits to T_s—Although the surface temperature cannot be determined in general from thermodynamic considerations alone, it is possible to set upper and lower limits to it.

First, T_s cannot exceed T_b if the B ⟶ C reaction is exothermic as postulated; for, if it did, equation **5** shows that m_C would exceed unity, which is physically impossible.

Secondly, T_s cannot be lower than $T_{s,\mathrm{min}}$ (*Figure 3*) which corresponds to $h_B = h_u$; for if it were lower, equations **4** or **5** indicate that m_C would be negative, which is also impossible.

If the A ⟶ B reaction is endothermic so that $T_{s,\mathrm{min}}$ is less than T_u, as illustrated in *Figure 4*, the same results are valid. Usually, however, the surface temperature will exceed that of the unburnt propellant.

2.4. *Conditions determining T_s*

As has been demonstrated above, m_C and T are linked in the gas phase. *Figures 5*(a) and *5*(b) illustrate the nature of the linkage respectively for exothermic and endothermic A ⟶ B reactions. The portions of the curves for $T < T_s$ do not correspond to real conditions in a given flame; they are drawn dotted.

Vaporization—*Figure 5* permits the factors determining T_s to be clearly represented in one case, namely that where the A ⟶ B reaction is a simple vaporization which takes place sufficiently rapidly for thermodynamic equilibrium to prevail at the phase boundary. This condition implies that, at a prescribed pressure, there is a fixed relation between the surface temperature, T_s, and the surface concentration of vapour, $m_{B,s}$. But

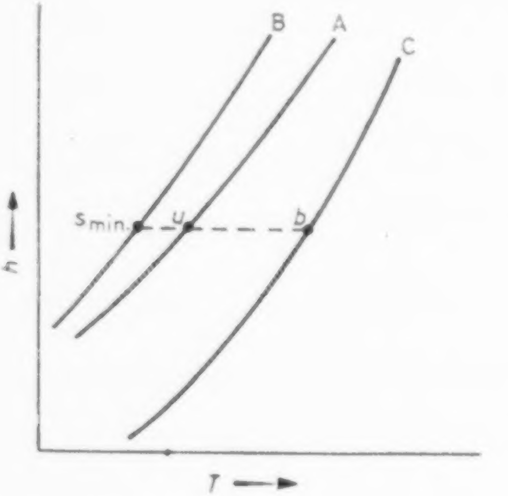

Figure 4. Unburnt propellant, burnt gas, and minimum temperature surface states for endothermic A → B reaction

$$m_{B,s} = 1 - m_{C,s} \quad \ldots . [6]$$

so the equilibrium requirement implies a curve on an m_C/T diagram.

A typical curve of this nature is sketched in *Figure* 5(b). It falls steeply downward, intersecting the line $m_C = 0$ ($m_B = 1$) at $T = T_{B.P.}$, the boiling-point of the propellant at the prevailing pressure. The intersection of the curve with the m_C/T line for the propellant gases defines the state of the propellant surface; T_s will therefore always be slightly below $T_{B.P.}$, and will rise as the pressure rises.

Chemical reaction—When the A ⟶ B reaction involves a chemical transformation, T_s cannot be determined so simply; now, the influence of this reaction is embodied in a relation between the surface temperature and the rate at which the reaction takes place. To make use of such information, it is necessary to obtain a simultaneous relation between the same quantities from consideration of the rate-processes in the gas phase. It is to this problem that attention is now turned.

3. Theory of Burning Rate in the Gas Phase

3.1. *Outline*

In this section we demonstrate that, although the upstream boundary conditions are somewhat different, the gaseous reaction zone of a propellant flame can be handled by the techniques developed for laminar flame propagation in gases.

First the differential equations of mass and energy conservation are written down, and it is demonstrated that uniform gas-phase enthalpy still results from the assumption of normal

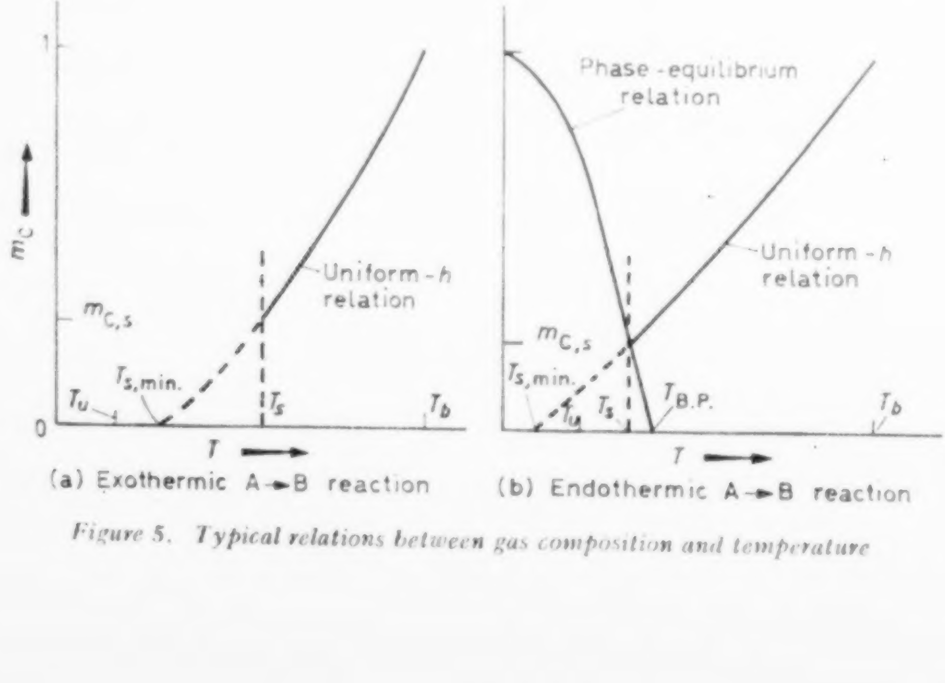

(a) Exothermic A → B reaction (b) Endothermic A → B reaction

Figure 5. Typical relations between gas composition and temperature

diffusion in the new situation. The opportunity is taken to show that the common assumption of constancy of specific heats is not a necessity; the slight unfamiliarity of some of the initial steps in the derivation is solely due to this, and not to any radical novelty.

Thereafter approximate solutions of the equations are obtained, and evaluated for two families of reaction-rate functions. These solutions yield the desired relation between the gas-phase burning rate and the propellant surface temperature, T_s. It is found that, as might be expected, an increase in T_s for constant T_b decreases the burning rate; this occurs chiefly because the area under the curve of reaction rate versus temperature becomes reduced.

3.2. *Differential equations of conservation*

Conservation of C—Considering a control volume of infinitesimal length in the x direction (*Figure 2*), and employing Fick's diffusion law, we have

$$\frac{\mathrm{d}}{\mathrm{d}x}\left(D_c\rho\frac{\mathrm{d}m_c}{\mathrm{d}x}\right)-G\frac{\mathrm{d}m_c}{\mathrm{d}x}+\dot{m}_c'''=0 \quad .\ [7]$$

The first term represents the net influx of C into the control volume as a result of diffusion. $D_c\rho$ represents the proportionality constant between the concentration gradient and the net flux of m_c by diffusion. D_c is the diffusion coefficient of C, ρ the local mixture density.

The second term represents the convective flux of C, G being the net mass flux per unit area (burning rate).

The third term, $\dot{m}_c'''$, represents the rate of generation of the chemical species C, per unit volume, as a result of chemical reaction. It can depend only on the local state of the mixture and so is a function of m_c, T and the pressure.

Steady-flow energy equation—Application of the First Law of Thermodynamics to the same control volume, with the restriction that the only boundary fluxes are those associated with the flow of the substances B and C by convection and diffusion, leads to

$$\frac{\mathrm{d}}{\mathrm{d}x}\left\{D_{\rm B}\rho h_{\rm B}\frac{\mathrm{d}m_{\rm B}}{\mathrm{d}x}+D_c\rho h_c\frac{\mathrm{d}m_c}{\mathrm{d}x}+K\frac{\mathrm{d}T}{\mathrm{d}x}\right\}-G\frac{\mathrm{d}}{\mathrm{d}x}(m_{\rm B}h_{\rm B}+m_ch_c)=0 \quad \ldots .\ [8]$$

where K is the thermal conductivity of the mixture.

Conservation of mass—Since only the two compounds, B and C, are present, the conservation-of-mass principle leads to

$$\frac{\mathrm{d}}{\mathrm{d}x}\left(D_{\rm B}\rho\frac{\mathrm{d}m_{\rm B}}{\mathrm{d}x}\right)+\frac{\mathrm{d}}{\mathrm{d}x}\left(D_c\rho\frac{\mathrm{d}m_c}{\mathrm{d}x}\right)-G\frac{\mathrm{d}m_{\rm B}}{\mathrm{d}x}-G\frac{\mathrm{d}m_c}{\mathrm{d}x}=0 \quad \ldots .\ [9]$$

On introduction of equation 6, equation 9 is quickly seen to imply:

$$D_{\rm B}=D_c\equiv D,\ \text{say} \quad \ldots .\ [10]$$

as a necessary consequence of mass conservation, not as an assumption.

Simplification of the energy equation—We now assume a relation between the thermal conductivity and the diffusion coefficient, namely

$$D\rho=Kc_m \quad \ldots .\ [10a]$$

where c_m is the local mixture specific heat at constant pressure. This is the 'normal diffusion' or 'Lewis number unity' assumption, which is fairly closely satisfied by many gas mixtures.

Substituting equations 10 and 10a in 8, and introducing h from equation 2, we obtain the energy equation in the form

$$\frac{\mathrm{d}}{\mathrm{d}x}\left(D\rho\frac{\mathrm{d}h}{\mathrm{d}x}\right)-G\frac{\mathrm{d}h}{\mathrm{d}x}=0 \quad \ldots .\ [11]$$

3.3. *Demonstration that h is uniform in the gas phase*

Equation 11 can be integrated to give:

$$D\rho\frac{\mathrm{d}h}{\mathrm{d}x}-Gh=\text{const.}=-Gh_b \quad \ldots .\ [13]$$

the constant being evaluated from the consideration that $\mathrm{d}h/\mathrm{d}x=0$ far downstream of the flame.

Integrating once more, we obtain

$$h-h_b=A\exp\left[+\int_0^x\frac{G}{D\rho}\,\mathrm{d}x\right] \quad ..\ [14]$$

which would contravene the requirement $h=h_b$ at $x=\infty$ unless the arbitrary constant A were equal to zero.

We have therefore proved that, in the gas phase,

$$h = h_b - h_u \qquad \ldots . [15]$$

which is the familiar result of laminar flame theory that was used above.

It should be noted that, in proving this result, the specific heats have not been assumed constant or equal, and that, since only two components are supposed to be present, the equality of the diffusion coefficients has been proved, not assumed.

3.4. *The mathematical problem*

Dimensionless form of the C-conservation equation—Equation 7 is the one to be solved. To simplify it, we introduce the following substitutions, in a manner similar to that of ref. 7:

$$m_c \equiv \tau \qquad \ldots . [16]$$

$$\mathrm{d}y \equiv (G/D\rho)\,\mathrm{d}x \qquad \ldots . [17]$$

$$R \equiv \{D\rho/(D\rho)_b\}\,\dot{m}_c''' \qquad \ldots . [18]$$

$$\bar{R} \equiv \int_0^1 R\,\mathrm{d}\tau \qquad \ldots . [19]$$

$$\phi \equiv R/\bar{R} \qquad \ldots . [20]$$

$$\lambda \equiv (D\rho)_b \bar{R}/G^2 \qquad \ldots . [21]$$

Here it needs to be pointed out that $\dot{m}_c'''$ depends only on the local composition and local temperature, which are linked via equation 3. So $\dot{m}_C'''$, and therefore R, can be expressed as functions of τ alone, their nature depending on the activation energy of the reaction, the specific-heat variation of the gas, the temperature-dependence of the diffusion coefficient, etc. This fact means that ϕ is a function of τ (assumed known).

Equation 7 now takes the well-known form

$$\frac{\mathrm{d}^2\tau}{\mathrm{d}y^2} - \frac{\mathrm{d}\tau}{\mathrm{d}y} = -\lambda\phi(\tau) \qquad \ldots . [22]$$

Boundary conditions—The gas-phase region stretches from the propellant surface to downstream-infinity. At the surface, recognition that the net transfer of C is zero (since only B emerges from the surface) leads to

$$\left(D\rho\frac{\mathrm{d}m_C}{\mathrm{d}x}\right)_s - G\left(\frac{\mathrm{d}m_c}{\mathrm{d}x}\right)_s = 0 \quad . . [23]$$

At downstream-infinity combustion is complete; therefore m_c equals unity there.

The corresponding boundary conditions are:

$$y = y_s \;:\; \mathrm{d}\tau/\mathrm{d}y = \tau \qquad \ldots . [24]$$

$$y = \infty \;:\; \tau = 1 \qquad \ldots . [25]$$

First-order form—Still following ref. 7, we note that y appears only in the differential form in equations 22, 24 and 25, so that the equation can be reduced in order. Putting

$$p \equiv \mathrm{d}\tau/\mathrm{d}y \qquad \ldots . [26]$$

we obtain, as the equation to be solved,

$$p\,\mathrm{d}p/\mathrm{d}\tau - p = -\lambda\phi \qquad \ldots . [27]$$

with the boundary conditions:

$$\tau = \tau_s \;:\; p = \tau \qquad \ldots . [28]$$

$$\tau = 1 \;:\; p = 0 \qquad \ldots . [29]$$

λ is an eigenvalue to be determined.

Preliminary discussion of the solution—Equations 27 and 29 are identical with those for temperature-explicit chemical reaction in a gas mixture. The difference between the two problems lies in the upstream boundary condition 28: in the usual problem of laminar flame theory, this is replaced by $p = \tau = 0$.

Figure 6(a) shows a curve of ϕ versus τ which typifies, in its main features, those expected to represent actual propellants. *Figure* 6(b) illustrates a p/τ relation which satisfies the equation and boundary conditions.

Now examination of equations 27 and 28 shows that, if $\phi = 0$ in a range of τ values adjacent to $\tau = \tau_s$, we have, in that range

$$p = \tau \qquad \ldots . [30]$$

which passes through the point $\tau = 0$, $p = 0$; but the latter represents the upstream boundary condition for flame propagation through gases as just stated. The solution to equations 27, 28 and 29 therefore includes, and has the same λ as, the solution to equations 27 and 29 with the boundary condition $p = 0$ at $\tau = 0$, provided that $\phi(\tau)$ is put equal to zero for $\tau < \tau_s$.

Expressing the same conclusion in physical terms, we may say that the burning rate in the gaseous flame downstream of a condensed-phase propellant surface is equal to that of an all-gaseous flame in which the reaction rate is zero at temperatures below the temperature of the phase boundary; the reaction-rate curve of *Figure 6*(a) has to be cut off on the left in the manner indicated by the broken line.

3.5. *Some solutions for the burning velocity*

The Centroid Rule—Having thus reduced the problem to that of flame propagation through gases, we now need to choose a method of solving the latter problem. A convenient one is the Centroid Rule method of ref. 7 which usually gives one per cent accuracy.

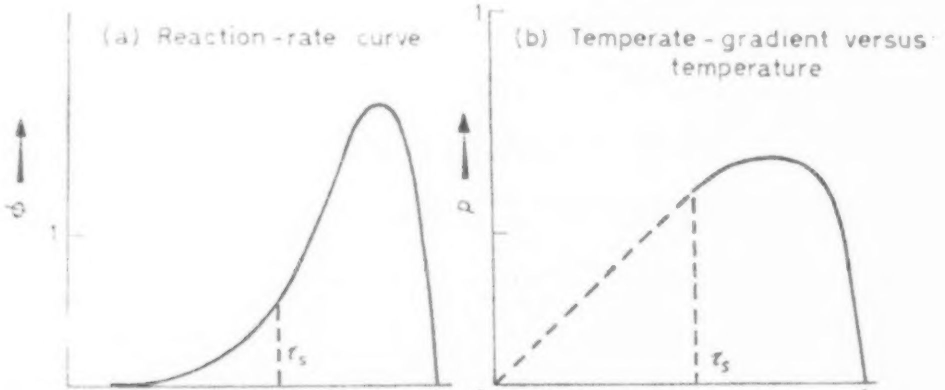

Figure 6. Typical curves occurring in the solution of the gaseous flame problem

The case of propagation through gases can be identified by putting $\tau_s = 0$. If the corresponding burning rate is G_0, the Centroid Rule states that:

$$G_0 = [(1/\lambda_0)\,(D\rho)_b \bar{R}]^{\frac{1}{2}} \quad \ldots . [31]$$

$$\lambda_0 = 0{\cdot}5 - 0{\cdot}6604\,(1-\tau_{c,0}) - 0{\cdot}4283\,(1-\tau_{c,0})^2 \quad \ldots . [32]$$

$$\tau_{c,0} = \int_0^1 \tau R\,\mathrm{d}\tau / \bar{R} = \int_0^1 \tau\phi\,\mathrm{d}\tau \quad \ldots . [33]$$

Knowing $R(\tau)$, G_0 can then be evaluated.

Application to condensed-phase combustion—When the surface temperature, T_s, exceeds T_u, i.e. when $\tau_s > 0$, the argument of §3.4 shows that the Centroid Rule must be modified to:

$$G = [(1/\lambda)\,(D\rho)_b \bar{R} \int_{\tau_s}^1 \phi\,\mathrm{d}\tau]^{\frac{1}{2}}$$

$$= G_0[(\lambda_0/\lambda) \int_{\tau_s}^1 \phi\,\mathrm{d}\tau]^{\frac{1}{2}} \quad \ldots . [34]$$

$$\lambda = 0{\cdot}5 - 0{\cdot}6604\,(1-\tau_c) - 0{\cdot}4283\,(1-\tau_c)^2 \quad \ldots . [35]$$

and

$$\tau_c = \int_{\tau_s}^1 \tau\phi\,\mathrm{d}\tau \Big/ \int_{\tau_s}^1 \phi\,\mathrm{d}\tau \quad \ldots . [36]$$

Examples—Equations 34, 35 and 36 have been evaluated for two of the families of reaction-rate functions which were studied in ref. 7. Although they do not represent any chemical reactions in particular, it will usually be possible to find a member of one or other of the families which will fit a prescribed reaction-rate function fairly well.

The families are:

$$(i)\quad \phi = (n+1)\,(n+2)\,(1-\tau)\,\tau^n \quad \ldots . [37]$$

and

$$(ii)\quad \phi = \tfrac{1}{2}(n+1)\,(n+2)\,(n+3)\,(1-\tau)^2\,\tau^n \quad \ldots . [38]$$

The parameter n, which may be regarded as representing activation energy (G. ROSEN[10] has worked out the connection explicitly), has been given values ranging from 2 to 15.

Figures 7(a) and 7(b) contain the results in the form of plots of G/G_0 versus τ_s for each reaction-rate family. Marked against each curve are the appropriate values of n. The graphs demonstrate that as τ_s rises to unity G falls, after an initial horizontal region, to zero. This fall begins earlier, the lower is the activation energy of the reaction.

'Universal' curves—The Centroid Rule gives a good approximation to the flame speed of gases because the detailed shape of the reaction-

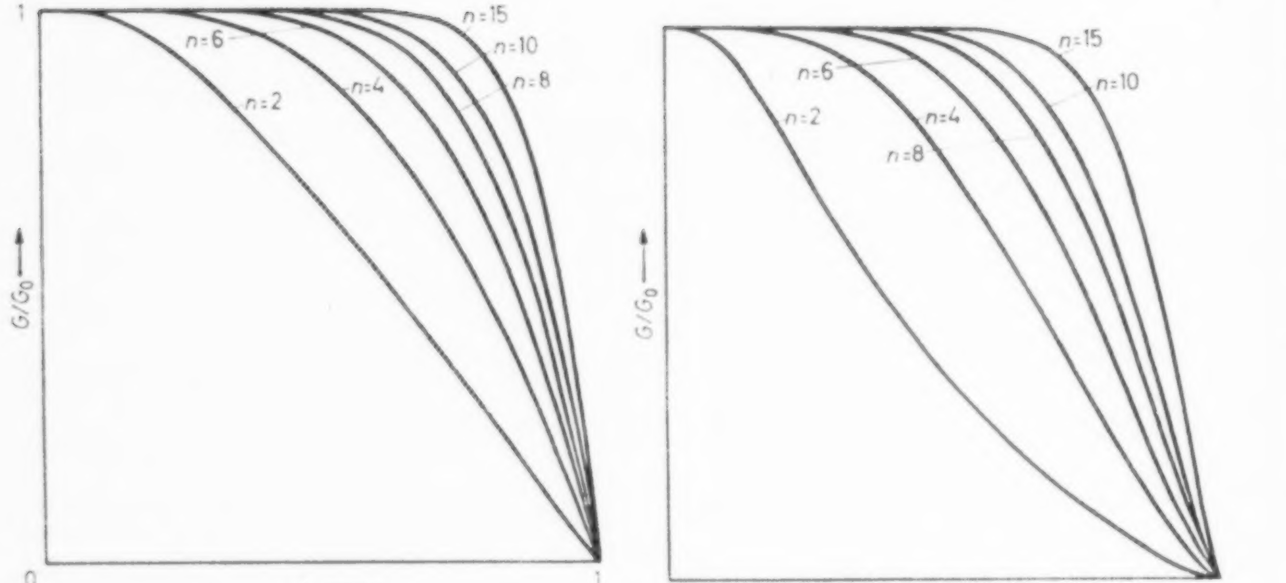

(a) Reaction-rate family (i): $\phi=(n+1)(n+2)(1-\tau)\tau^n$ (b) Reaction-rate family (ii) $\phi=\frac{1}{2}(n+1)(n+2)(n+3)(1-\tau)^2\tau^n$

Figure 7. Curves showing influence of surface temperature on burning rate in gaseous flame

rate curve is not important; it suffices to take account of the centroid reactedness. We now examine whether this is true of condensed-phase propellants also.

Figure 8 shows G/G_0 plotted versus $\tau_{c,0}$ for various values of τ_s. The curves have been obtained by interpolation and cross-plotting of the data of *Figures* 7(a) and 7(b). The relations between $\tau_{c,0}$ and n are:

For equation 37

$$\tau_{c,0}=(n+1)/(n+3) \quad \ldots \text{[37a]}$$

For equation 38

$$\tau_{c,0}=(n+1)/(n+4) \quad \ldots \text{[38a]}$$

Inspection of *Figure 8* shows that the two reaction-rate families give roughly the same values of G/G_0 for the same τ_s and $\tau_{c,0}$, although the agreement between the two sets of curves is not as good as that for flames in gases (ref. 7). It may be concluded that, at least so long as τ_s does not exceed $\tau_{c,0}$, the shape of the reaction-rate function is of small importance.

Figure 9 has been constructed from *Figure 8* by plotting the arithmetic mean of the G/G_0 values of the two reaction-rate families for a given τ_s and $\tau_{c,0}$. The curves of *Figure 9* may be used for calculating the effect of the propellant surface temperature on the burning rate in the gas phase when only the centroid position of the (complete) reaction-rate function is known.

4. Discussion

In this section we discuss the implications of *Figure 9*, with particular reference to the dependence of burning rate G upon the ambient pressure. Three cases can be distinguished:

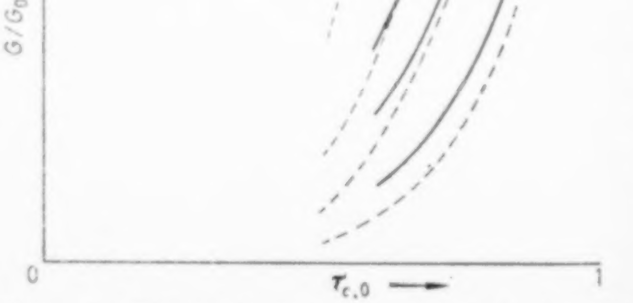

Figure 8. Plot to determine whether G/G_0 depends on $\tau_{c,0}$ alone, for given τ_s

the vaporizing liquid, the propellant decomposing at a surface, and the foam reaction. Finally, certain transient effects are pointed out, of relevance to the unstable burning of solid propellants.

First, however, we note that, if the reaction rate, as measured by R, is proportional to pressure to the power k, equation 31 shows that G_0 is proportional to pressure to the power $k/2$. This result is well known.

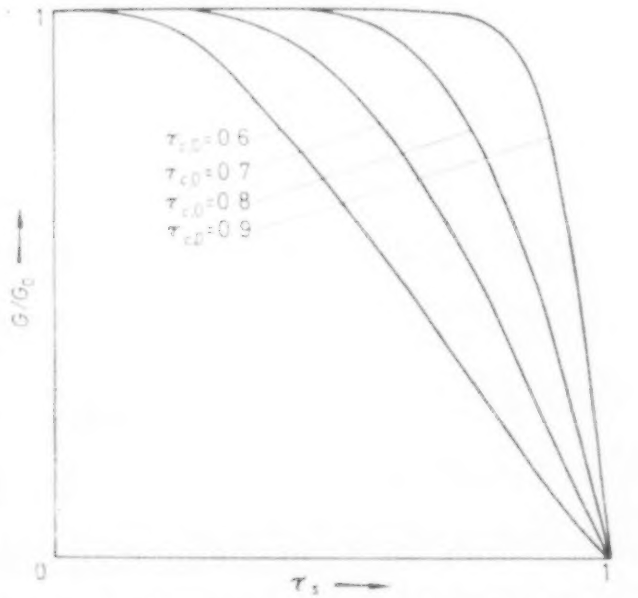

Figure 9. Plots of G/G_0 versus τ_s; curves recommended for general use

4.1. *The vaporizing liquid*

In this case, as discussed in §2.4, the requirement of equilibrium between the vapour B and the liquid A fixes the surface temperature uniquely in terms of pressure, regardless of the chemical reaction rate in the gas. As the pressure P rises, so does τ_s. *Figure 9* shows that, for a given $\tau_{c,0}$, G/G_0 at first equals unity; so G rises in proportion to $P^{k/2}$. At higher values of P and τ_s, however, G/G_0 falls below unity; so the increase of G with pressure is less rapid. Eventually, when the boiling point of the liquid approaches the adiabatic combustion temperature of the propellant, G begins to fall with rising pressure and eventually becomes equal to zero.

Because the variation of G with pressure depends on $\tau_{c,0}$, on k and on the τ_s/P relation, it is impracticable to plot general curves. Instead a single example is considered, in which $\tau_{c,0}$ has the common value of 0·8, $k=2$ (second-order reaction) and τ_s depends on P in accordance with

$$\tau_s=(P/P^*)^b \qquad \ldots\ldots [39]$$

where b will in general be a number very much less than unity, and P^* is the pressure at which the boiling point equals the adiabatic combustion temperature.

Figure 10 shows a plot of G/G_0^* versus P/P^* for various values of b. G_0^* is the value which G would have at the pressure P^* were τ_s equal to zero. It is seen that all the curves show the qualitative behaviour just described, and that deviations from the linear burning-rate law occur at pressures considerably lower than P^*.

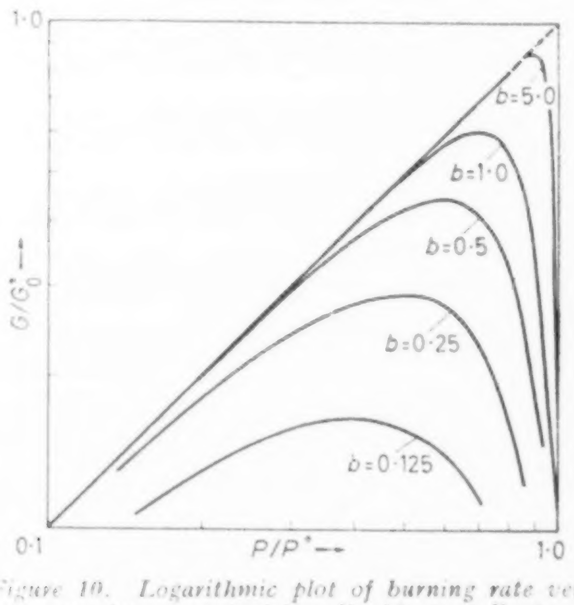

Figure 10. Logarithmic plot of burning rate versus pressure for a vaporizing liquid propellant with various pressure exponents of boiling point ($k=2$; $\tau_{c,0}=0{\cdot}8$)

The author does not know of experimental data on liquids which exhibit the predicted reduction of burning rate as pressure rises; nor are sufficient data available on the relation between propellant temperature and vapour pressure. It does, however, seem certain that behaviour such as is predicted must appear in practice, provided that the critical pressure is not exceeded and that no possibility of a direct A ⟶ C reaction exists.

4.2. *The surface decomposition*

A number of propellant chemicals appear to change phase as a result of a surface decomposition reaction, the rate of which depends only on the surface temperature and not on the pressure. Experimental methods and data have been reported by R. D. SCHULTZ and A. O. DEKKER[11], by W. H. ANDERSON *et al.*[12] and by R. D. SCHULTZ, L. GREEN and S. S. PENNER[13]. For example, Anderson *et al.* state that in the range of surface temperatures from 180° to 300°C, the decomposition of ammonium nitrate can be represented to good accuracy by the equation

$$G/\rho_u = 120 \exp(-7\,100/\mathscr{R}T_s)\ \text{cm/s} \quad \ldots [40]$$

where ρ_u is the unburnt propellant density, $\mathscr{R}$ is the universal gas constant = 1·985 cal/g mole °C and T_s is in °K.

Determining the surface temperature—The rate of decomposition at the phase boundary must be identical with the rate of combustion in the gaseous flame. We therefore determine the burning rate from the intersection of the two curves of G versus τ_s, representing respectively the A ⟶ B and the B ⟶ C reactions.

Figure 11 illustrates this. The drooping curves represent combustion rates in the gaseous reaction zone at various pressures plotted in accordance with *Figure 9*; the rising curve represents a relation of the type of equation 40 for the surface decomposition. The intersections give the burning rates and surface temperatures as a function of pressure; the higher the pressure, the hotter the propellant surface.

Once again it is impracticable to plot general curves because of the large number of parameters. Instead, a few examples are considered. We suppose that the combustion reaction obeys the law

$$G_0/G_d = (P/P_d)^{k/2} \quad \ldots . [41]$$

Further, the dependence of the decomposition reaction on temperature is supposed to obey the relation

$$G/G_d = \tau_s^d \quad \ldots . [42]$$

where G_d is the decomposition rate at $T = T_b$, and d is a constant. We consider a gas-phase reaction-rate function having $\tau_{e,u} = 0{\cdot}8$.

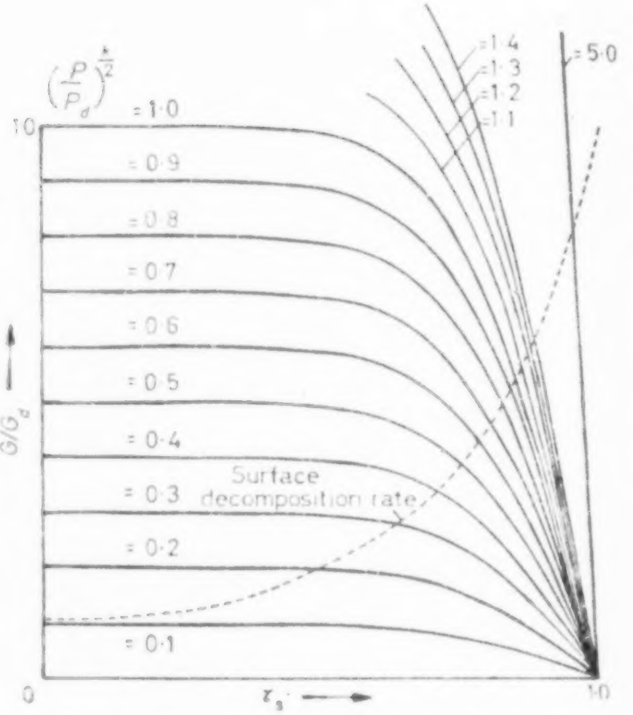

Figure 11. Determination of surface temperature and burning rate: influence of pressure on point of intersection of gaseous-flame curves and surface-decomposition curve

It is now an easy matter to use these data, in combination with *Figure 9*, for the evaluation of the burning rate as a function of pressure. *Figure 12* shows the result, in the form of a plot of G/G_d versus (P/P_d) for $k = 2$ and for various values of d. The graph shows how at low pressures the burning rate follows the line of equation 41 indicating that the gas-phase reaction is controlling; at high pressures the curve flattens out so that the maximum value of G is G_d. It will be noted that the decomposition reactions with steepest temperature-dependence have the lowest burning rates at any pressure.

Discussion of Figure 12—Experimental burning-rate data for many propellants show a similar tendency to the curves of *Figure 12*: the so-called 'platonized propellants', for example, have curves with substantial horizontal sections. However, these horizontal regions are often followed, at still higher pressures, by regions in which the burning rate again rises with pressure.

The present model of a burning solid propellant cannot explain this subsequent behaviour. It is therefore interesting to speculate as to why the model is inadequate. One shortcoming of the model is that it involves a sharp division between the gaseous and non-gaseous phases. In practice, however, this division ceases to exist as the critical pressure is exceeded; even before this, there must be an appreciable penetration of component C into component A.

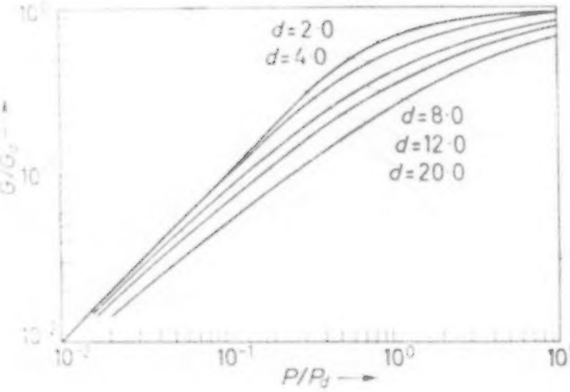

Figure 12. Influence of temperature dependence of surface decomposition rate on burning rate law ($k=2$; $\tau_{c,0}=0{\cdot}8$)

One aspect of the blurring of the distinction between gas and non-gas is that a direct reaction path from A to C may come into being. Indeed, at very high pressures, the actual processes may be more realistically described by the simple A → C model than by the A → B → C model of the present paper. The burning rate will then again increase with pressure in the same way as at low pressures. This is in full qualitative accord with experimental work.

The study of a model permitting simultaneous A → B → C and A → C reaction paths remains as a task for the future; so far almost no theoretical work has been done on flames involving parallel reaction paths.

Exothermic decomposition reactions at low pressures—The use of equation 42 implies that the propellant does not decompose at a finite rate when $T_s = T_{s,\text{min.}}$. Often, however, the decomposition reaction is exothermic to a sufficient extent to make $T_{s,\text{min.}}$ quite large; then the decomposition rate can be quite appreciable when $T_s = T_{s,\text{min.}}$, which implies that there is no heat transfer from the gaseous flame to the surface.

This situation is illustrated in the lower left-hand corner of *Figure 11* where the decomposition line has a finite ordinate at $\tau_s = 0$.

A consequence is that, if the pressure is sufficiently low, the maximum possible burning rate in the gaseous flame, G_0, is less than the rate of the decomposition reaction. When this occurs, there can be no intersection between the combustion and decomposition lines in *Figure 11*, and no steady state in which the gaseous flame maintains a constant distance from the surface. The flame is swept downstream and can only be stabilized by some departure from the one-dimensional conditions postulated here.

4.3. *The foam reaction*

If the A → B reaction occurs in depth, in a foam region, rather than at the propellant surface, only slight modifications of the above procedure are necessary. It can be assumed that this decomposition still proceeds at a rate which is a function of the surface temperature alone at any fixed pressure. The techniques of flame theory could be applied to relate this rate to the rate constants of the foam reaction; since, however, knowledge of these seems to be even scantier than for the gaseous reaction, we shall here merely regard the G versus T_s relation as one which has to be determined experimentally, for example by the technique of ref. 11.

Parr and Crawford[2] postulate that the foam reaction is first-order. This means that the rate of decomposition, G, is proportional to pressure to the power $\frac{1}{2}$, for the same reasons that operate in gaseous flames. Whatever the actual pressure dependence, *Figure 11* must be modified by having, in general, a different decomposition line for each pressure; surface temperatures are then determined from the intersections of corresponding pairs of decomposition and combustion curves.

It should be obvious that, if the foam reaction has a lower pressure exponent than the combustion reaction, the former will control the burning-rate law at high pressures while the latter does so at low pressures. Since in other respects the foam reaction enters the calculations in the same way as does the surface decomposition, it will not be further discussed.

4.4. *Transient effects*

Whatever the nature of the A ⟶ B reaction, it seems certain that surface temperature, T_s, almost always rises with increasing pressure, and brings about a subsequent increase in burning rate. However, a sudden pressure increase cannot bring about an equally sudden surface temperature rise; for there must first be a finite heat transfer to the propellant from the flame, which takes a finite time.

This transient process appears to be difficult to analyse quantitatively, since the effective adiabatic combustion temperature of the gaseous flame is reduced during the supply of this additional heat; this has an effect on the rate of the combustion reaction.

Nevertheless, it seems quite clear that a finite time lag must exist between the application of a pressure increase and the attainment of the corresponding increase in burning rate. Theories of oscillatory combustion indicate that, were it not for this time lag, 'screaming' of solid propellant motors would be the rule rather than the exception[14].

It may be of interest to point out that dimensional analysis, and acquaintance with the theory of unsteady heat flow, readily show that the time-lag is of the order of $k\rho/cG^2$, where k, ρ and c refer to the condensed phase. So propellants with high burning rates will have the smallest time-lags and so be most unstable. This will be the subject of a later paper.

5. Influence of Radiative Heat Loss from the Surface

5.1. *The problem*

Most solid propellants will only burn if the pressure exceeds a critical value; this behaviour cannot be explained in terms of the foregoing theory. The consideration of heat loss by radiation has led to explanations of inflammability limits in gases[8] and of the stability of other reacting systems[9]; we now consider whether the low-pressure limits of solid propellants can be explained in a similar way.

Although gas radiation is quite appreciable at rocket pressures, it will here be neglected; only radiation from the propellant surface is considered, partly because this case is the simplest and partly because it lies at the other end of the scale from that of ref. 8, which involves gas radiation alone.

A cigarette-burning charge may be considered, in a motor of which the casing and nozzle are kept relatively cool. The burning propellant surface can therefore radiate freely to its surroundings and receive little radiation in return. A similar situation arises in laboratory equipment designed to measure the burning rate of the propellant.

Heat loss from the propellant surface causes the enthalpy of the whole gas phase, though it remains uniform, to have a value lower than that of the unburnt propellant. The G versus τ curve of the B ⟶ C reaction is thus lowered as compared with adiabatic combustion, and this can only lead to a lower equilibrium burning rate.

More interesting than this reduction in burning rate is the fact that, as will be proved, the radiative loss can lead to the existence of a minimum burning rate for a given propellant and, consequently, to the existence of a range of conditions under which reaction is impossible.

Below, these conditions are examined quantitatively. It will appear that the whole phenomenon has much in common with that which is familiar in gases. Qualitatively, the theory to be presented provides an explanation of the low-pressure combustion limit; a quantitative comparison of theory and experiment necessitates more data than are available to the author, and has not been made.

5.2. *Definitions and assumptions*

For a fixed pressure, let the burning rate for $\tau_s = 0$, and zero heat loss from the surface, be $G_{0,\text{ad}}$. Then G_0, the burning rate at the same pressure with a finite surface heat loss, will depend on the final combustion product temperature T_b. Let us suppose, for the sake of example, that the influence of T_b on G_0 can be expressed by the exponential relation

$$\frac{G_0}{G_{0,\mathrm{ad}}} = \left\{\frac{T_b - T_u}{T_{b,\mathrm{ad}} - T_u}\right\}^N \quad \ldots . [43]$$

where N is a constant.

Heat loss—A similar exponential law will be assumed, again for purposes of illustration only, for the heat loss $\dot{q}''$ from the surface; this is

$$\dot{q}'' = \sigma\varepsilon(T_s - T_u)^4 \quad \ldots . [44]$$

which approximately represents the Stefan-Boltzmann law if σ is Stefan's constant and ε is the surface emissivity. The surroundings which the surface 'sees' are supposed to be at the temperature of the unburnt propellant.

The following dimensionless measure of the heat loss intensity will be useful below

$$Q \equiv \sigma\varepsilon(T_{b,\mathrm{ad}} - T_u)^4 / cG_{0,\mathrm{ad}} \quad \ldots . [45]$$

where c is the mean specific heat at constant pressure of the combustion products c at temperatures close to $T_{b,\mathrm{ad}}$.

Heats of reaction—For simplicity, we shall suppose that the enthalpy change of the phase-changing reaction is negligible. Then, in the adiabatic case,

$$T_{s,\min} = T_u \quad \ldots . [46]$$

In addition, the specific heats of substances B and C will be supposed equal and independent of temperature. This permits us to write, by reason of the definition 16 of τ and the uniformity of gas-phase enthalpy

$$\tau_s = 1 - (T_b - T_s)/(T_{b,\mathrm{ad}} - T_u) \quad \ldots [47]$$

5.3. *Determination of G versus T_s*

First Law considerations—Applications of the Steady Flow Energy Equation to a control volume enclosing the whole pre-heat and reaction regions leads to

$$-\dot{q}'' = Gc(T_b - T_{b,\mathrm{ad}}) \quad \ldots . [48]$$

Combining this equation with **44** and **45**, we obtain

$$\frac{G}{G_{0,\mathrm{ad}}} = Q\left(\frac{T_s - T_u}{T_{b,\mathrm{ad}} - T_u}\right)^4 \Big/ \left(1 - \frac{T_b - T_u}{T_{b,\mathrm{ad}} - T_u}\right) \cdot [49]$$

Gas-phase reaction — A second relation between G, T_b and T_s is obtained by combining 43 with the appropriate relation of *Figure 9*. We obtain

$$\frac{G_{0,\mathrm{ad}}}{G} = \left(\frac{T_b - T_u}{T_{b,\mathrm{ad}} - T_u}\right)^N \mathrm{f}(\tau_s) \quad \ldots . [50]$$

where $\mathrm{f}(\tau_s)$ is the *Figure 9* expression just mentioned, and τ_s is obtained from equation **47**.

The G/T_s relation—Equations **49** and **50** enable T_b to be eliminated. There results a family of relations between $G/G_{0,\mathrm{ad}}$ and $(T_s - T_u)/(T_{b,\mathrm{ad}} - T_u)$ with Q as parameter.

Calculations have been carried out using the $\mathrm{f}(\tau_s)$ curve for $\tau_{c,0} = 0{\cdot}8$ and a value of N equal to 5. The resulting relations are shown in *Figure 13*. It is seen that each value of T_s gives rise, in general, to two possible burning velocities; but these are imaginary when T_s exceeds a critical value, which depends on Q.

There is nothing surprising in this result; it corresponds to the following easily understood experience. Suppose the cooled metal plate of a porous-plug burner is replaced by a refractory plug free to radiate heat to cool surroundings, and that the cooling water is shut off. Let the downstream surface temperature of this plug be measured. When the velocity of the gases through the plug is low, so is the surface temperature. Increasing the flow rate causes the temperature to increase at first; however, a maximum temperature is attained, whereafter a further flow increase lowers the surface temperature. By the time the flame is about to be blown off, the plug temperature is equal to that of the unburnt stream.

5.4. *Determination of burning rate*

Figure 13 contains the relations between G and T_s which correspond to the above case; further information is necessary before T_s can be fixed and G evaluated under given conditions. This information comes in statements about the phase-changing (A $\longrightarrow$ B) reaction. Two cases will be considered: surface decomposition, and vaporization without chemical reaction.

First, the curves of *Figure 13* are re-plotted so as to bring out the effect of pressure more clearly. *Figure 14* shows $cG/\sigma\varepsilon(T_{b,\mathrm{ad}} - T_u)^4$ plotted versus $(T_s - T_u)/(T_{b,\mathrm{ad}} - T_u)$ for various values of Q. The former quantity is of course merely the ordinate of *Figure 13* divided by Q.

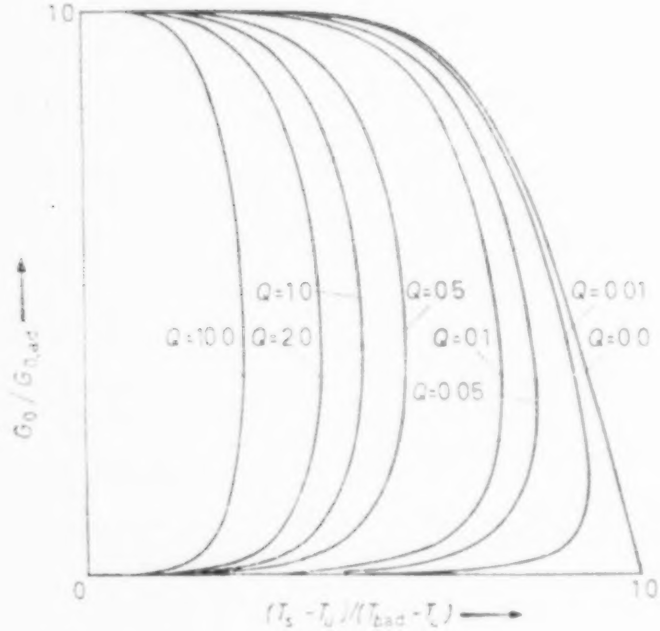

Figure 13. Gas-phase burning rate versus surface temperature for various values of surface heat-loss parameter Q ($\tau_{c,u}$=0·8; N=5)

but now contains no terms, apart from *G*, which are pressure-dependent.

If equation 41 is accepted for $G_{u,ad}$, then the parameter of the curve family in *Figure 14*, namely *Q*, can be regarded as indicative of pressure. For

$$Q=\frac{\sigma\varepsilon(T_{b,ad}-T_u)^4}{cG_d}\left(\frac{P_d}{P}\right)^{k/2} \qquad \dots [51]$$

G_d and P_d are of course constants of the propellant. So *Q* increases as *P* decreases.

The curves of *Figure 14* correspond to those of *Figure 11*, which are valid for the case of adiabatic reaction. The change wrought by the action of heat losses is very great.

Surface decomposition reaction—Suppose that the A ⟶ B reaction proceeds by way of a decomposition at the propellant surface. Then there is a unique relation between surface temperature and burning rate. The broken curve of *Figure 14* represents an example of such a relation.

The surface temperature and burning rate which must prevail in the steady state at any particular pressure are given by the intersection of the broken curve with the full curve valid for the appropriate value of *Q*. Inspection of *Figure 14* shows that, as in *Figure 11*, the intersections lie at high τ_s when the pressure is high (*Q* small) and move to the left as the pressure is reduced. Unlike *Figure 11*, however, which was for adiabatic reaction, *Figure 14* shows (*i*) that there are in general two or more intersections, (*ii*) that as *Q* increases the two intersections approach each other, and (*iii*) that when *Q* exceeds a critical value (0·3 in the example of *Figure 14*) no intersections exist at finite values of τ_s at all.

This situation has many parallels in other branches of chemical reaction theory (see e.g. ref. 9). It is easily shown that only the upper of the two intersections mentioned corresponds to a stable equilibrium; the lower one represents unstable equilibrium. The condition of coales-

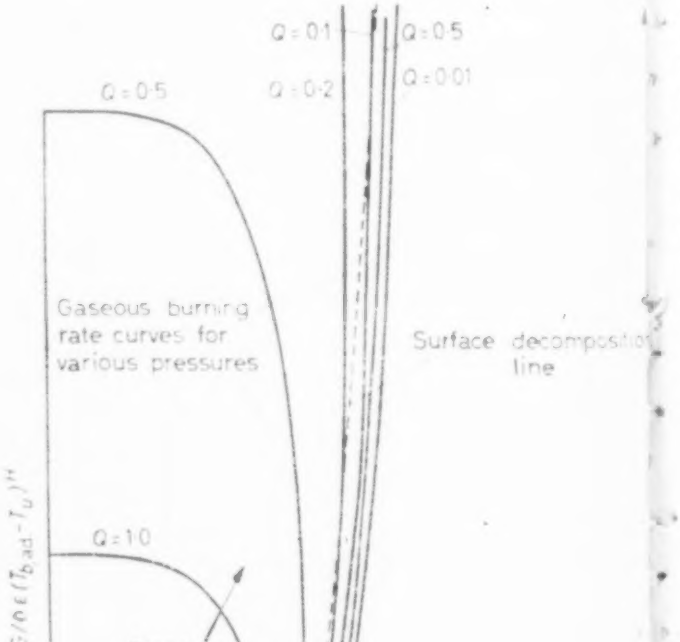

Figure 14. Dete mination of surfa temperature wh heat losses are pr sent (contrast wi ***Figure 11***)

ence of the two equilibria represents an inflammability limit: if the pressure of the chamber in which the propellant is burning is gradually lowered, extinction occurs when the critical pressure is reached. The actual value of this pressure is obtained by evaluating equation 51 for the value of Q which causes the decomposition and gas-reaction lines to touch.

It should be noted that in a rocket motor the tendency to flame extinction is even stronger than appears from the above discussion; for the flow characteristics of the outlet nozzle ensure that the chamber pressure is directly proportional to the burning rate. The reduction in burning rate consequent on heat losses therefore causes a fall in chamber pressure and so an increase in the heat-loss parameter Q.

We have thus found that the inclusion into the theoretical model of heat loss from the propellant surface provides an adequate qualitative explanation of the existence of a lower limiting pressure for steady combustion. Whether the theory is quantitatively satisfactory requires more data on propellant properties than are at present available to the author. However, it is easily verified that practical propellants radiating freely to cool surroundings might have values of Q as great as unity if they burned at atmospheric pressure; so radiation can certainly have an effect sufficient in magnitude to cause extinction.

Strongly exothermic surface decomposition—If the energy of decomposition is large, the A ⟶ B reaction can be sustained without any heat transfer from the gaseous flame. If in addition the decomposition rate is sufficiently large, the decomposition line can be so high that the extinction phenomenon is absent. This is shown by the chain-dotted line in *Figure 14*.

At sufficiently low pressures, the gaseous flame of such a propellant is blown right away from the surface, as discussed in §4.2. Then *Figure 14* becomes inappropriate for determining the surface condition. It is fairly easy to demonstrate that in this case the possibility of extinction as a result of heat loss still exists, provided that the decomposition rate depends more steeply on surface temperature than does the heat loss; the limiting condition is, however, independent of pressure for a zero-order reaction. The problem is so like those of ref. 9 that it will not be discussed further here.

Vaporization or sublimation—We now consider the case in which, as discussed in §§2.4 and 4.1, thermodynamic equilibrium exists between A (liquid or solid) and B (vapour) at the propellant surface. We may still take this to imply that T_s is only very slightly below boiling point of the propellant.

With τ_s thus given by specification of the pressure, the burning rate is found from the intersection of the corresponding vertical with the appropriate gas-reaction curve of *Figure 13* or *14*. In general there are, once again, two intersections, corresponding to stable and unstable burning (respectively the upper and lower intersections).

However, as P increases, T_s rises; provided that the critical pressure is not exceeded, it is possible eventually for the boiling point to exceed the adiabatic combustion temperature of the propellant. At some pressure below this, the two intersections must disappear.

This is best seen by plotting the abscissae $([T_s-T_u]/[T_{b,\mathrm{ad.}}-T_u])_{\mathrm{max.}}$ of the points of vertical tangent of the constant-Q curves of *Figure 14* against pressure which, for $k=2$, is proportional to $1/Q$; this is done in *Figure 15*. Also shown in *Figure 15* is a curve representing the rise of T_s with pressure as a consequence of the phase equilibrium requirement. Since the former curve cannot rise above $\tau_s=1$ whereas the latter is bound to, there must be a pressure at which the whole constant-Q curve of *Figure 14* is to the left of the appropriate vertical.

These considerations demonstrate that there ought to exist an upper limit to the pressure at which propellants of this kind can burn. Such upper pressure limits do exist, but it would be premature to conclude that they are caused by heat losses in the way described. However, the suggestion may prove worthy of investigation.

Whether a lower pressure limit exists for vaporizing propellants depends upon whether the two curves of *Figure 15* exhibit a second intersection at low P; it will be true for some propellants and not for others. When ε_s tends to zero, radiative heat loss from the surface may become unimportant compared with radiative heat loss from the gas. This, more complex, process is known to be capable of causing a lower pressure limit of its own accord[8].

6. Conclusions

6.1. *Adiabatic propellant*

(*a*) The Centroid Rule, valid for flame propagation through gases, may be used to predict the dependence on propellant-surface temperature of the rate of burning in the gaseous reaction zone of a condensed-phase propellant. Normal diffusion, laminar flow and a single gas-phase reaction are assumed.

(*b*) As the surface temperature rises, at fixed pressure, the burning rate in the gaseous reaction zone decreases [*Figures* 7(a), 7(b) and 9].

(*c*) A vaporizing or subliming solid propellant may be expected to exhibit a negative pressure exponent at high pressures (*Figure 10*).

(*d*) The surface temperature of a propellant changing phase by zero-order surface decomposition may be expected to exhibit a zero pressure exponent at high pressures (*Figure 12*).

(*e*) When the surface decomposition is highly exothermic, the gaseous flame is 'blown downstream' at low pressures. In this region also the pressure exponent will be zero.

(*f*) Decomposition via a foam reaction can be handled in much the same way as decomposition by a surface reaction.

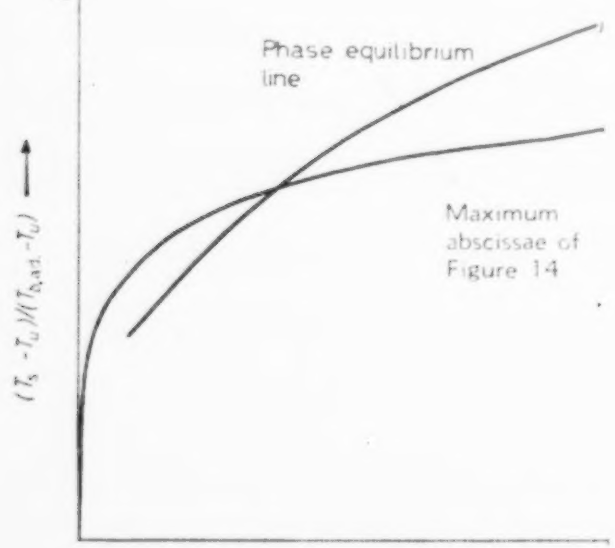

Figure 15. Showing that combustion is impossible at high pressures when heat loss occurs at the surface and the $A \rightarrow B$ reaction is a simple phase change

6.2. *Propellant with radiative heat loss from the surface*

(*a*) Heat loss from the propellant surface makes it possible for the gas-phase reaction zone of a given propellant to have two distinct burning rates for a given surface temperature (*Figure 13*).

(*b*) A consequence is that propellants decomposing endothermically will be unable to burn below a critical pressure, while propellants decomposing exothermically may or may not exhibit such a low-pressure limit (*Figure 14*).

(*c*) Propellants changing phase by vaporization or liquefaction may also exhibit extinction above an upper pressure limit (*Figure 15*).

The author gratefully acknowledges the assistance of Miss M. P. Steele, who carried out the above computations.

References

[1] RICE, O. K. and GINELL, R. *J. phys. Chem.* 1950, **54**, 885

[2] PARR, R. G. and CRAWFORD, B. L. *J. phys. Chem.*, 1950, **54**, 929

[3] GECKLER, R. D. *Selected Combustion Problems*. Butterworths: London, 1954

[4] LAWRENCE, R. W. and GECKLER, R. D. Unpublished calculations 1951. Mentioned in ref. 3

[5] ADAMS, G. K. and WISEMAN, L. A. *Selected Combustion Problems*. Butterworths: London, 1954

[6] WILFONG, R. E., PENNER, S. S. and DANIELS, F. *J. phys. Chem.* 1950, **54**, 863

[7] SPALDING, D. B. *Combustion & Flame*, 1957, **1**, 287 and 296

[8] SPALDING, D. B. *Proc. Roy. Soc. A*, 1957, **240**, 83

[9] SPALDING, D. B. *Chem. Engng Sci.* 1959, **11**, 55

[10] ROSEN, G. *Jet Propulsion*, 1958, **28**, 839

[11] SCHULTZ, R. D. and DEKKER, A. O. *Fifth Symposium (International) on Combustion*, p 260. Reinhold: New York, 1955

[12] ANDERSON, W. H., BILLS, K. W., DEKKER, A. O., MISHUCK, E., MOE, G. and SCHULTZ, R. D. *Jet Propulsion*, 1958, **28**, 831

[13] SCHULTZ, R. D., GREEN, L. and PENNER, S. S. *Combustion and Propulsion. Third AGARD Colloquium*, p 367. Pergamon: London, 1958

[14] GRAD, H. *Comm. pure appl. Math.* 1954, **2**, 79

Recent Developments and Notes

A New Ceramic

A new ceramic material with a unique combination of properties has been announced by Dr Guy Suits, vice-president and director of research for the General Electric Company. It is a polycrystalline material called Lucalox, which is made from powdered aluminium oxide, and in addition to transmitting light, it possesses the extremely high strength characteristic of alumina ceramics, can withstand much higher temperatures than most ceramics now in use, and can be pressed into any shape desired. No other material combines translucence with this degree of strength, heat resistance, and ease of fabrication. The unique characteristics of Lucalox result from the fact that the micropores that are normally found in ceramic materials have been entirely removed, a feat that had been previously considered impossible. It is stable at temperatures almost up to 1 980°C.

Lucalox was first made by Robert L. Coble, of the General Electric Research Laboratory. Following his first research, important contributions were made by P. D. S. St Pierre, Edward Stover and Arno Gatti.

Cupola Aerodynamics

The programme of research in the Coal Research Section, N.S.W., Australia, dealing with the development of techniques for making foundry coke with the appropriate physical properties, includes work concerning the combustion of coke under the conditions obtaining in an operating cupola. Preliminary studies have now been made with cold models, to determine the aerodynamic factors that are important in the operation of cupolas. This work has been described in a report by G. L. Shires (Commonwealth Scientific and Industrial Research Organization, Reference *T.C. 29*. March 1959). The particular objective in this part of the research programme was to study the effect of coke size and tuyère geometry on the flow pattern.

A two-dimensional cold-air model, 1 ft in diameter, made of Perspex, was used so that by means of flow visualization the airflow pattern could be studied directly through the side walls. A thin rectangular section 3 in. in thickness was chosen for observation with the object of eliminating velocity components perpendicular to the walls which would have distorted the two-dimensional picture of the flow. Pressure loss through the coke bed, velocity distribution above the bed, and flow patterns in the bed were investigated.

In general terms the results so far show that in the tuyère zone the penetration of air into the bed is influenced to a major degree by coke size, and the size required to achieve the maximum penetration corresponds approximately to the ratio of coke size to cupola diameter giving maximum metal temperature in practice. The aerodynamic effect of other factors such as tuyère size and angle was found to be consistent with recent results reported in the literature, thus confirming the validity of the cold-model technique. A number of other deductions from the experimental work are given in the report.

Liquid Fuel for Open-hearth Furnaces

At the 'Conference of Major Developments in Liquid Fuel Firing 1948-59' organized by The Institute of Fuel and held in Torquay, 11 to 14 May 1959, R. Mayorcas reviewed the developments during the past ten years in the use of liquid fuel in open-hearth furnaces.

In 1948 there were about 100 furnaces in the U.K. operated with fuel oil, mainly producer-gas furnaces converted to oil-firing on account of cheapness. At the present time there are about 240 basic furnaces fired by liquid fuels and 101 by producer gas. The respective outputs in 1957 from these furnaces were 15·1 and 3·0 × 10^6 tons. There are now 48 acid furnaces on producer gas as compared with 63 in 1952 and five on liquid fuel. Today most of the oil-fired furnaces have been designed to meet the special requirements of liquid-fuel burners. Jet burners and oxygen-atomized fuel burners are envisaged for the near future.

The considerable amount of research on the design of oil burners is reviewed, with the conclusion that for a given fuel rate the shortest flame, that is, the quickest combustion, is obtained when the maximum thrust is developed at the burner nozzle, not at the back end of the burner. The state of atomization of the fuel is of secondary importance.

The author is of the opinion that furnaces are becoming simpler in design although there have been many attempts to design a furnace aerodynamically round a small-scale model. Instrumentation is becoming very important with the advent of automatic controls. A programme of the furnace-firing schedule may be found desirable. In the light of developments in data processing a new approach to recording equipment is being made in the steel industry.

With regard to the problem of sulphur in fuel oil, progress has been made in many respects but as a reduction in the sulphur content of liquid fuels is not likely, there must be found either cheaper desulphurizing methods or ways of reducing the pick-up of sulphur.

Heat Transfer Conference

A notably successful international conference on heat transfer arranged jointly by the American Society of Mechanical Engineers and the Institution of Mechanical Engineers was held in London in September 1951 and repeated in Atlantic City in the same year. At the suggestion of the A.S.M.E., a meeting of its representatives with those of the I.M.E. was held some time ago to discuss whether another joint conference of the same kind might be justified in the light of developments in the field of heat transfer during the intervening decade.

It was agreed that a second conference should be held and arrangements are being made by two organizing committees, one under the chairmanship of A. C. Mueller in the U.S.A. and the other under Professor O. A. Saunders in the U.K. The second conference will take place in Boulder, Colorado, from 28 August to 1 September 1961, and is to be repeated in London from 8 to 12 January 1962. It is hoped that some 100 papers will be available for presentation. Further information may be obtained from The Secretary, the Institution of Mechanical Engineers, 1 Birdcage Walk, Westminster, London, S.W.1.

Automation in Boiler Operation

A conference on 'Fuel Economy through Automatic Operation' arranged by The Combustion Engineering Association was held in Scarborough on 3 and 4 November 1959, the chairman being S. P. Chambers, who is President of the Association and a deputy chairman of Imperial Chemical Industries Ltd.

The object of the conference was to examine and discuss the technical and economic aspects of the use of automatic controls on medium sized solid fuel fired boiler plant, and to consider the development and improvement of fully automatic coal-fired boiler plant. The main papers presented were: 'Why automatic operation?' by R. H. E. Thomas, The National Coal Board; 'What is needed to achieve automatic operation', by B. E. A. Vigers, Laporte Industries Ltd; 'Fuel and ash handling', by F. S. Stent, Babcock and Wilcox Ltd; 'Combustion and mechanical firing', by M. V. Murray, Wm Cory and Son Ltd; 'Automatic control equipment', by J. S. Hales, The British Coal Utilisation Research Association; 'Present day practice in automatic control', by L. W. Stevenson, Kelvin and Hughes Ltd.

The general thesis of the conference may be said to have been that automation is making coal as convenient as oil. This necessitates a fully automatic installation to feed the fuel into the boiler, control its combustion, separate the ash from the burning coal, and rapidly adjust itself to changes in factory load, for several days at a time. Evidence was adduced by the speakers to support the view that coal still offers a clean, flexible, easily handled and economical fuel not only for big industrial plants, but also for the smaller factories and for large residential buildings such as blocks of flats. Experience is now being obtained in the operation of the B.C.U.R.A. miniature chain grate unit installed in a $1{\cdot}5 \times 10^6$ B.t.u./h sectional boiler in a block of flats in London, automatic feeding of fuel from a bunker and extraction of ash into suitable containers being provided.

It was claimed that fully automatic methods not only give better and more efficient operation, because they eliminate the risk of human error, but they can also save up to 10 per cent of a factory's coal consumption. On a typical installation which by hand methods would need a team of three stokers and a trimmer, mechanical firing is said to reduce the requirement to a single stoker, a saving on the wage bill alone of about £2 000 a year.

In discussing the question as to whether there is a lower limit of size of steam-raising plant beyond which automation is no longer practical, it was stated that complete automation was unlikely to be economically justifiable below 10 000 lb/h evaporation, from 10 000 to 40 000 lb/h being a marginal zone, and above that it seemed that complete automation might always be justified. The future development of automatic ash removal and disposal on shell boilers was said to depend on cheaper equipment and this is now being investigated by the B.C.U.R.A.

The National Coal Board were said to be carrying out trials on blending back fines with small coal and fears were expressed that the quality of the fines might have different characteristics from the small coal itself and reference was also made to difficulties that have been caused by fluctuations in the fines content. The blending of fines which is contemplated is not more than that which may be necessary in central washeries which handle coal from several mines.

Coke Burning Appliances

In April last the Gas Council and the National Coal Board were invited to take over from the Ministry of Power the testing and approval of domestic solid fuel appliances. Following this arrangement the Domestic Solid Fuel Appliances Approval Council was formed. The results of appliance type-testing in the Coke Appliances Laboratories of the gas industry are now made available to the new organization to enable them to continue the publication of the list of names of *Approved Domestic Solid Fuel Appliances*.

The latest information on such appliances is given in the handbook on *Coke Burning Appliances*, the sixth edition of which has recently been published in loose-leaf form (The Gas Council, Coke Department, 1 Grosvenor Place, London, S.W.1, 558 pp, 35*s*, November 1959) This edition is considerably larger than the previous one in 1957 and its supplement in 1958 combined.

Details of over four hundred tested and approved solid fuel appliances are contained in the handbook, which is illustrated with photographs and diagrams. Full technical information on each appliance, including the heat service, is given on data sheets. The book is divided into sections for the various types of appliances, and each section is preceded by introductory notes of technical interest and value. Reference is made at the beginning to the conditions and procedure for approval of appliances and details on suitable sizing, densities and calorific values of coke are given.

A new British Standards Specification (*No. 3142*, 1959) has been published covering open fire cokes.

Turbo-charging of Diesel Engines

Several papers given to the Fifth International Congress on Internal Combustion Engines at Wiesbaden last June [*Engineer, Lond.* **1959, 208,** 119] dealt with turbo-charging of diesel engines. One paper, by E. KÜCHLER, of Daimler–Benz A. G., Stuttgart, was concerned with the marginal performance of turbo-super-charged precombustion-chamber engines. High-speed diesel engines with single-stage turbo-chargers are able to generate, at their maximum speed, charging pressures up to 3 atm abs. In the opinion of the author of this paper such engines may be operated safely at a b.m.e.p. up to about 18 kg/cm² without any excessive thermal stresses, but this value should not be exceeded as, with the present available materials and with peripheral speeds of 350 to 400 m/sec, turbine blades could not stand up to exhaust temperatures above 650° C. At such a temperature the engine itself is not yet thermally stressed to its limits, whereas the gas turbine is the weakest link in the chain of factors which limit output.

Explosibility of Mine Atmospheres

A recent publication by M. G. Zabetakis, R. W. Stahl and H. A. Watson, of the U.S. Bureau of Mines, presents a simplified graphic method for determining the explosibility of mine atmospheres under mine-fire conditions from mine-atmosphere composition data [U.S. Department of the Interior, Bureau of Mines, *Inform. Circ. No. 7901*, **1959**].

The method employs a series of diagrams that can be used to determine quickly whether an area that has been sealed in efforts to extinguish a coal-mine fire can be reopened safely. The atmosphere in such places frequently contains gas mixtures that are explosive or can become explosive when mixed with air. Hence, unsealing them may be hazardous. After the composition of the atmosphere has been determined by chemical analysis, the explosibility or potential explosibility of the atmosphere can be calculated very quickly from the diagrams.

The principle employed in this diagrammatic method is not new but was put forward 30 years ago by H. F. Coward in a detailed paper presented to the Midland Institute of Mining Engineers [*Trans. Instn Min. Engrs, Lond.* 1929, **77**, 94–108].

Flammability Regions of Hydrocarbons

The regions of flammability of gases at low pressures formed when plotting the limiting pressures at which mixtures containing different proportions of combustibles become flammable, depend upon various experimental conditions, such as the temperature, the direction of flame propagation, the nature of the experimental vessel, and the mode of ignition. In particular, it has been shown by R. Delbourgo and P. Laffitte [*C.R. Acad. Sci., Paris*, **1951**, 233, **958**] that when ignition is by a train of electric sparks instead of a single spark, the region of flammability is larger and is composed of two lobes or regions which have different flame characteristics; in the *first region* the flames fill the whole cross section of the tube, and in the *second region* the flames are axial. The *second region* has been observed for mixtures rich in butane or propane and for mixtures weak in methane. It has been suggested by G. Dalmai [*Rev. Inst. franç. Pétrole*, **1958**, **12**, **1683**] that the *second region* is due to the preferential diffusion during the passage of the train of sparks of the more mobile constituent present in defect.

A recent paper describing a continuation of the above investigations has been published by A. Azoulay, G. Dalmai and P. Laffitte, of the Laboratoire de Chimie Générale, Sorbonne, Paris [*Bull. Soc. chim. Fr.* **1959, 957**]. In this work the regions of flammability of methane-butane-air mixtures were examined and since methane is more mobile than oxygen which in turn is more mobile than butane, a continuous variation in the physical and chemical properties of the mixtures can be expected. The results obtained with these ternary mixtures confirm the previous ones with binary mixtures.

The explanation given is that the gas mixture concentrated in the electrode zone is modified by the train of sparks so that a mixture initially non-flammable becomes able to burn, having now a concentration within the limits of flammability due to the diffusion effect. There is thus formed an additional region of axial flame for mixtures in which the constituent in defect is the more mobile one. The flames of mixtures whose concentration is near the limit of the *first region* are easily disturbed. Probably flame vibrations, resulting in flame extinction, are responsible for the pronounced point of separation of the two regions.

Cyclonic Flame

W. F. Kenny and L. F. Albright have made a short communication on the stabilization of flames by cyclonic flow and their rate of release of energy [*Industr. Engng Chem.* (*Industr.*) **1959, 51, 227**]. This type of flow results in low static pressures along the flow axis of the duct which in turn causes a reverse flow that pilots fresh feed gases and stabilizes the flame.

The cylonic flow was obtained and studied in 2 in. ducts, 9·5, 19 and 28·5 in. long and combustion efficiencies of propane were determined with flows from 0·16 to 0·39 mole per hour. The gases enter a swirl chamber of the nozzle through eight curved vanes the tips of which could be controlled by means of a disc attached to the end of an $\frac{1}{8}$ in. pipe. This pipe of the cyclonic nozzle permitted introduction of the fuel gas into the swirl chamber where it was mixed with air introduced through the vanes. Adjustment of the above disc controlled the degree of cyclonic motion.

Cyclonic flame was obtained that had an energy release rate of $13{\cdot}4 \times 10^6$ B.t.u. per hour per cubic foot with a pressure drop of less than 4 in. of mercury. The highest rate of energy release for the flame with complete combustion was $11{\cdot}8 \times 10^6$ B.t.u. per hour per cubic foot. Stable cyclonic flames were, however, obtained at combustion efficiencies of appreciably less than 10 per cent and with very low rates of energy release. The combustion efficiency and rates of energy release were found to depend primarily on the air-to-fuel ratio, flow rates and degree of cyclonic flow.

Reaction Zone in Detonation of Knallgas

A few years ago some investigation by H. G. Wagner and his colleagues on the reaction zone in carbon monoxide–oxygen detonation systems at an initial pressure of 1 atm showed that the length of the zone was approximately 1 cm. The addition of hydrogen to these mixtures reduced the length and extrapolated results indicated that the reaction zone length in a pure stoichiometric mixture of hydrogen and oxygen might be from 0·1 to 1 mm. In order to obtain exact measurements in knallgas detonations a procedure different from that used in carbon monoxide–oxygen detonations was found to be necessary and an account of this work has now been published by T. Just and H. G. Wagner [*Z. phys. Chem.* **1959, 19, 250**]. The detonation tube of 8 cm i.d. was provided with two longitudinal quartz windows on opposite sides of the tube, and through these windows a narrow beam of light was passed so that measurements could be made of variations in intensity by absorption within the detonation zone and also of deflection of the beam by changes in the refractive index of the medium (schlieren effect). The measuring equipment included an oscillograph and a secondary electronic multiplier. The length of the reaction zone was measured by a combined schlieren–absorption method, the concentration of OH radicals by absorption at 3 100 Å, and the temperature within the reaction zone by the line reversal method.

The length of the reaction zone in knallgas detonations was deduced as approximately 1·4 mm at atmospheric pressure.

Spontaneous Ignition Reactions

A. Martinengo and H. G. Wagner have described an investigation on the spontaneous ignition reactions of hydrocarbon–air mixtures [*Z. phys. Chem.* **1959, 20, 206–218**]. The adiabatic compression method of ignition was used since by this means it is possible to investigate initial reactions lasting between 10^{-4} and 10^{-1} sec without the intervention of wall effects. The hydrocarbons used were *n*-decane, *n*-hexane, *n*-heptane, octane and *iso*octane. Records were obtained of pressure development, flame travel and some emission spectra. The induction period in the ignition process consists of two stages. The first of these stages, corresponding to incomplete reaction, is the period from the end of the compression up to a point of inflection in the pressure/time curve. This is followed by the second stage, in which the rate of development of pressure is much slower, and leads to the establishment of the explosion under conditions of temperature, pressure and composition of mixture different from the initial conditions. The ignition delay periods of the two reaction stages and the rate of reaction during the whole process of ignition were examined by the authors in relation to the temperature, pressure and mixture composition for the hydrocarbons used.

Sonic Mixing of Combustion Gases

In the use of solid propellant rockets it is highly desirable that some method of control during flight should be available other than simply an on-off device. A probable method of achieving this is now being studied by the American organization of Acoustica Associates, Long Island. This involves the use of high-intensity sound with a frequency greater than 10^4 c/s for mixing the combustion gases close to the burning surface of a solid-propellant rocket. In the system at present being investigated, a whistle or siren is used to send sound waves through the core of the solid propellant in the direction of travel taken by the combustion products. It is estimated that the burning rate could be increased 3 to 10 times by such sonic mixing [*Daily Telegraph*, 11 August 1959].

Radiant Heat Transfer in a Flowing Medium

The special feature in a treatment by V. N. ADRIANOV and S. N. SHORIN of radiant heat transfer in a flowing medium is the coupling of convective and radiative heat fluxes [*Izvest. Akad. Nauk S.S.S.R., Otdel tekh. Nauk*, **1958** (No. 5), 46]. The problem considered by the authors is a steady-state cooling of a radiating gas flowing in a circular pipe and between infinite parallel plates having a prescribed wall temperature. Convection and radiation are the two modes of heat transfer assumed to be present. The scattering of radiation is neglected and it is postulated that the radiant energy emitted by a unit volume of gas and absorbed by another unit volume is negligible compared with the radiant energy emitted by the gas and absorbed by the duct surfaces. The solution of a coupled system of equations of motion and the integro-differential equation of energy conservation is eliminated by assuming one-dimensional flow and various velocity profiles in the ducts. The energy equation is solved and temperature distributions are determined for certain velocity profiles.

Several new dimensionless numbers are introduced; in particular, use is made of a dimensionless parameter which governs the coupling between convective and radiative energy fluxes [R. VISKANTA, *Appl. mech. Rev.* **1959**, **12**, 647].

Flammability of Foams of Aviation Turbine Fuels

Under certain circumstances during the de-aeration of fuel in aircraft tanks at high altitudes air bubbles can be liberated so violently that thick foam may form on the surface of the fuel for a short time. The rising of air bubbles through the liquid can result in the accumulation of an electrical charge in the foam. Since air is present in the foam there arises the question as to the possibility of ignition and flammability of foams produced under these conditions. This problem has been studied by B. V. POULSON, of Shell International Petroleum Co. Ltd and A. THOMAS, of Shell Research Ltd who have recently published an account of their work [*J.R.aero.Soc.* **1959**, **63**, 581].

The authors consider the process of air release from the fuel and the composition of the liberated gas. They assessed the possibility of flammability of foams formed from kerosine corresponding to *D.Eng.R.D. 2482* specification and from gas oil, by a technique similar to that of determining the limits of flammability. The electrical behaviour was studied of foams produced under conditions simulating those at various altitudes up to 45 000 ft.

It is concluded that the process of liberation of dissolved air from kerosine at moderate altitudes and above can produce flammable foams. The condition of flammability in respect of composition of foam lasts, however, only for the duration of the degassing process, say 30 seconds for kerosine, but for a longer time with wide-cut fuel and over a very wide range of operating conditions. The absence of hazard during such periods depends on the absence of a source of ignition.

It is shown that there is an accumulation of electric charge in foam layers which can be increased by the presence of traces of electrically active materials such as corrosion inhibitors, by ice haze in the fuel when de-aeration occurs, and by de-aeration being delayed until altitudes of over 40 000 ft are reached.

In aviation turbine fuels at present in use the electrical charge is regarded as almost certainly insufficient for ignition to take place, but this may not obtain in future aircraft and operating conditions.

Thermal Radiation Detector

A thermal radiation detector has been described by R. V. JONES which depends on the linear expansion of a thin metallic strip a few millimetres long [*Proc. Roy. Soc. A*, 1959, **249** (1256), 100–113]. Expansions of the order of 10^{-7} to 10^{-10} cm are converted into rotations of 10^{-10} to 10^{-7} radians by means of a mechanical system using a galvanometer-type suspension strip as a flexure pivot. The rotations are measured with an optical lever and photoelectric amplifying system. Constantan 0·1 micron thick is employed as the expansion material, and the receiving area is about 1 mm^2.

The device was developed primarily to determine whether the thermal fluctuation limit of sensitivity could be more closely approached than with conventional detectors. Observations on several of the best of the expansion devices show that they come within a factor of between two and three of the best possible sensitivity for a receiving area of 1 mm^2, achieving a noise equivalent signal of less than $1{\cdot}5 \times 10^{-11}$ W for a band width of 1 c/s. In its present form the instrument is not very practical, but may possibly be improved [From author's summary by C. F. BONILLA, Puerto Rico, *Appl. mech. Rev.* 1959, **12**, 647].

New Antiknock Agent

A new antiknock agent was announced a few months ago by the Texas Co. It is tertiary butyl acetate; alone it has no beneficial effect on octane rating, but with 0·75 per cent by volume added to gasoline containing up to the legal maximum of tetraethyl lead, 3 ml/gal, there is an important gain in octane number for present day premium and higher grade motor fuels. Whether or not its use will be found by refineries to be economical will depend on future demands for higher octane ratings. The chemical is not at present commercially made, and the same is true of the new antiknock substance, AK–33X, containing manganese, announced by the Ethyl Corpn about eighteen months ago [see *Combustion and Flame*, 1958, **2**, 312].

Oxidation of Propane and Ethane

The rate constants of reactions in the low temperature oxidation of hydrocarbons have been investigated by J. H. KNOX, of the Department of Chemistry, University of Edinburgh, and his collaborators, R. F. SMITH and A. F. TROTMAN-DICKENSON [*Seventh Symposium (International) on Combustion, London and Oxford, 1958*; pp 623, 627: Butterworths; London, 1959; *Trans. Faraday Soc.* 1958, **54**, 1509; see also *Combustion and Flame*, 1959, **3**, 258]. In continuing this research into the nature of the basic chain-propagating steps and of the reactive intermediates responsible for the degenerative branching mechanism the oxidation of propane and ethane at 318°C has recently been studied, particularly the period of acceleration following that of induction τ, and the maximum rate of pressure rise $\rho_{\max.}$ [J. H. KNOX, *Trans. Faraday Soc.* 1959, **55**, 1362] He points out that dependence of the acceleration constant ϕ on reaction conditions has not been widely investigated, probably due to the belief that its dependence is similar to that of $\rho_{\max.}$. Since this is not strictly true differences in the behaviour of the two parameters ϕ and $\rho_{\max.}$ may give useful data about the reaction mechanism. The author considers that the most useful parameter for this purpose is ϕ. The interpretation of measurements of τ is shown to be extremely difficult and that of $\rho_{\max.}$ uncertain.

It was found that the oxidation of ethane and propane occurs in uniformity with theoretical relations for the dependence of ϕ on reactant concentrations. The lifetimes of the branching intermediates are approximately 2 and 1 min respectively. The results indicate that only very few molecules of these intermediates are formed by each complete reaction chain and the efficiency factor must therefore be quite small. This is at variance with most of the mechanisms previously proposed for which the efficiency factor has been assumed to be unity.

This conclusion is supported by the analytical data which show that the main chain reaction responsible for removing propane is similar to the high temperature one in which an HO_2 radical chain forms propylene as its major product. This reaction does not lead to the formation of any branching intermediate except indirectly through the oxidation of the propylene thereby formed.

Diffusional Flames

Some interesting results have been published by V. I. Blinov and G. N. Khudiakov as a result of their investigation into the diffusive burning of liquids [*Dokl. Akad. Nauk S.S.S.R.* (*N.S.*), 1957, **113** (5), 1094: Courtesy of *Fire Research Abstracts and Reviews*]. In their experimental work on the natural burning of different petroleum products, chiefly gasoline kerosine, diesel oil and solar oil, a very wide range of pan sizes was used, from 0·37 cm to 22·9 m in diameter and the relationships obtained may be regarded as being of considerable significance.

Visual and photographic observations of the flames were recorded and burning rates and flame heights were measured. It was found that as the pan diameter increases, the flame structure changes from a conical steady flame in 1·1 cm pans to a pulsating-tip flame of maximum frequency about 18–20 c/s in 3 cm pans. Further increase in pan diameter reduces the pulsations, but the unstable portion of the flame shifts downwards until, for a 15 cm pan, the entire flame is changing continuously in structure everywhere; and with 1·3 m pans the random turbulent motion is fully established.

The relation between burning velocity and pan diameter has the same general structure for all the oils. It first decreases with increasing pan diameter, with an almost constant product of the two. This is the laminar flow régime, with R, less than about 20, based on properties of the non-burning fuel vapour. With further increase in pan diameter the decrease in velocity becomes less, changes sign, rises rapidly in the range of R, from 20 to 200, and finally levels off again at a pan diameter about 1 m or R, about 500. Above that value the burning is turbulent and the burning velocity is substantially uninfluenced by pan diameter or fuel type.

A continuous decrease in the flame length δ/pan diameter d ratio persists into the turbulent régime where it becomes constant for gasoline, the one fuel adequately studied. In the laminar régime a constant negative slope corresponds to the relation $(\delta/d) \propto d^{-n}$. In the same régime the burning rate curves may be expressed by the relation $v \propto d^{-m}$. These relations may be combined to give

$$(v)(d/\delta) \propto d^{n-m}$$

or

$$vd^2/\delta \propto d^{n+1-m}$$

In the turbulent régime the flame length/pan diameter ratio is constant at high Reynolds numbers. This is analogous to findings from studies of turbulent flames of fuel jets, where the flame length/diameter ratio is found to be independent of Reynolds number. The result is a consequence of air–fuel mixing by turbulent rather than by molecular transport.

The burning rate keeps pace with the fuel vaporization rate, which is controlled by heat transfer. The rate of heating q is the sum of q_1, q_2, q_3, representing the transfer rates from the pan rim, by convection, and by flame radiation, respectively. The authors call attention to the fact that in large reservoirs q_1 and q_2 are smaller than q_3 and that in consequence the constancy of burning velocity v for turbulent combustion indicates that the irradiation rate per unit of the liquid surface is independent of reservoir diameter.

In reviewing this work H. C. Hottel puts forward a partial quantitative analysis of the rates of heat transfer from the pan rim, by convection and by flame radiation [*Appl. Mech. Rev.* 1959, **12**, 876]. For gasoline the results indicate that on the basis of U, the convection coefficient, $=1$ (English units), F, the geometrical view-factor that the liquid has of the flame, $=\frac{1}{4}$, and d, the pan diameter, large enough to make the flame opaque, the burning rate corresponds to radiation and convection from a flame at about 870°C.

Detonation of Methane–Air Mixtures

The detonation limits of some hydrocarbon–air mixtures have been investigated by S. M. Kogarko who has reported, in particular, that methane–air mixtures are capable of being detonated in tubes of very large diameter, about 30 cm, within a wide range of methane concentrations in the mixture [*Soviet Phys.-Tech. Phys.* Apr 1959, 3 (9), 1904: translation of *Zh. tekh. Fiz., Mosk.*, Sep 1958, **28** (9), 2072 by American Institute of Physics, Inc., New York].

In a tube of small diameter, 2 cm, methane–air mixtures with any content of methane within the ignition limits could not be detonated even when a very powerful shock wave, such as arises from exploding a powerful detonator, was used for initiation. It is concluded from the experimental results that the detonation limits and possibility of detonation in gaseous mixtures with relatively long periods of chemical reaction depend on the diameter of the tube. A theoretical explanation is put forward to account for this. It was also found that the detonation limits of benzene–air mixtures in a tube of large diameter were widened as compared with the limits in a tube of small diameter.

Wave Superheater

A recent device known as the *wave superheater*, designed for use in hypersonic research, appears to have possible applications in studies of gaseous combustion and heat transfer. The fundamental principles of its design and operation have been described in two reports, the first by W. E. SMITH and R. C. WEATHERSTON [AFOSR *TN 58–158* (Cornell Aeronautical Lab., Inc., *Rep. HF–1056–A–1*; ASTIA *AD 207 244*), 115 pp, Dec 1958], the second by R. C. WEATHERSTON, A. L. RUSSO, W. E. SMITH and P. V. MARRONE [AFOSR *TN 59–107* (Cornell Aeronautical Lab., Inc., *Rep. AD–1118–A–1*; ASTIA *AD 210 223*), xiii + 133 pp, Feb 1959].

The wave superheater is capable of producing continuously a supersonic flow of uncontaminated air or other gases at temperatures and pressures needed for realistic hypersonic testing in the laboratory. A prototype has been built and operated successfully at its designed conditions of 3 000°R in air and 5 500°R in argon, starting from room temperature. The superheater consists essentially of a large number of shock tubes mounted on a rotating drum and fired cyclically in a manner to produce an uninterrupted jet of gas that is collected and expanded through a nozzle and test section. High jet power and a large mass flow of test gas are thus produced during the blowdown of the stored driver gas. In this way the unique flow conditions, characterized by homogeneity, purity, high temperature, pressure and velocity that are generated in hypersonic shock tubes and shock tunnels for short periods can be sustained for many seconds in a wave superheater.

A version of the superheater described in the second report is designed to generate a temperature of 9 000°R in air. It uses preheated helium as the driver gas and preheated test gases and can superheat 4·3 lb air/sec at 200 atm stagnation pressure. It is said that argon can be superheated to 17 000°R at the rate of 12 lb/sec.

Drakelow C Power Station

The Central Electricity Generating Board has commissioned The English Electric Company Ltd to start work on the two largest single-shaft steam turbo-alternators yet to be built in Europe. The sets are to be installed in the Board's new Drakelow C Power Station near Burton-on-Trent and the East Midlands coalfield, which is a major source of the low-grade coals used in the production of electricity. The cost will be nearly £5 million and will include two 350 MW steam turbo-alternators with their feed heating and evaporating plants. Ultimately the total installed capacity of the station will be 1 400 to 1 500 MW. The site of this station is at a focal point of the 275 kV Supergrid system, and the output of the station can be fed into the system without the construction of additional overhead transmission lines.

The design of the 350 MW steam turbo-alternator is significant as it represents an outstanding stage in the English Electric Co.'s policy to continue the development of the large single-shaft, single alternating unit. This will result in increased economy in fuel consumption, in unit cost, in space and in operating staff and it enables the C.E.G.B. to implement its own policy of using large units sited in the coalfields to help to keep down the price paid for electrical energy.

The 350 MW unit includes a three-cylinder, 3 000 rev/min reheat turbine with quadruple exhaust arranged as a tandem compound unit coupled to a hydrogen/water cooled alternator of the direct-cooled type and fed by a John Thompson water-tube boiler capable of evaporating nearly 1 100 tons of water per hour to give 2 400 lb/in^2 gauge steam at 1 055°F. In the turbo-alternator, solid couplings are employed between cylinders and each shaft is mounted on two main bearings so that the assembly and maintenance of the machine are kept as simple as possible.

In line with modern developments the turbine operates with steam at 2 300 lb/in^2 gauge, 1 050°F at the turbine stop valve, with reheat steam returning from the boiler to the intermediate pressure cylinder at 1 050°F. The vacuum at maximum and economic rating is 28·7 in. of mercury.

To meet the specified high pressure and temperature requirements, the high pressure cylinder has a double casing arrangement over the outside of the inner casing to pass through the remaining stages. These combined features enable the pressure differences and operating temperatures in the metal to be reduced, compared with those applied to a single-casing design.

New High Temperature Material for Gas Turbines

A new composition based on silicon nitride which is considered to be an important addition to the range of high temperature ceramics has been developed by the Admiralty Materials Laboratory at Holton Heath. The properties of the material, its method of production, and some applications and field trials in experimental gas turbines are described in a paper by D. M. Rae, of the Admiralty Materials Laboratory [*NRDC Bull., No. 15*, Oct 1959, 4], which is based on a report by N. L. Parr, G. F. Martin and E. R. W. May [*A.M.L. Rep. No. A/75(S)*].

Of the four intrinsic properties required in an engineering component to withstand high temperature, ceramics normally possess good resistance to oxidation, structural stability and creep strength, but good resistance to thermal shock is more difficult to provide. The factors required for this are low coefficient of thermal expansion and Young's modulus, high strength and thermal conductivity, the first mentioned being the most important. A fifth property which is necessary, that of resistance to mechanical shock, can be provided to some extent by appropriate design.

As a result of a search for stator blade materials for use in gas turbines at 1 200°C, silicon nitride, Si_3N_4, was eventually selected for investigation. It has high resistance to oxidation at this temperature, adequate creep strength and excellent resistance to thermal shock. A technique was developed for using this substance stiffened with 5 to 10 per cent of a fine dispersion of silicon carbide to produce the compound in the required form.

Another possible use for this ceramic is in the manufacture of electrical insulators subjected to violent temperature changes such as are experienced on rocket launching platforms. It may also be found of use as a support for high temperature catalysts, in thermocouple sheaths and for furnace chamber linings.

Combustion in Supersonic Flow

The first prize in the Waverley Gold Medal Essay Competition for 1959, sponsored by *Research*, was awarded to R. A. Gross, who is a National Science Foundation Senior Post-Doctoral Fellow in the Department of Physics, University of California. He was formerly Chief Research Engineer at the Fairchild Engine Division of Fairchild Engine and Airplane Corporation. He is the first United States citizen to have won the Waverley Gold Medal.

The subject of his paper is a study of combustion in supersonic flow [*Research, Lond.* 1959, 12, 381]. The primary objective of the experimental work was to stabilize a detonation wave and study the phenomena associated with it. For this purpose a Mach 3 tunnel was built to run steadily at inlet stagnation temperatures up to about 1 950°C. The test section flow area of the rectangular tunnel is 3 in. by 6 in. and is arranged so that a Mach reflected shock can be generated, behind which ignition takes place.

In studying plane detonation waves in hydrogen–air mixtures which were ignited by bringing the tunnel inlet stagnation conditions to 760° C and 110 lb/in^2 absolute, a new pattern of waves was observed for a variety of fuel–air conditions. These waves were steady, stable and remarkably plane and the author considers that they could not be the classical Chapman–Jouguet waves since there is only one fuel–air ratio that produces such waves at a given Mach number.

A new ignition 'hysteresis' effect was observed. Once the burning wave was established by ignition conditions as above, the inlet temperature could be greatly reduced and ignition and combustion continued under conditions such that in the entire flow field there was no region of sufficient temperature to ignite the mixture thermally. This effect is regarded as implying that transport mechanisms within the wave itself are important once the combustion process has been initiated. Whilst this is not in accord with the von Neumann–Zeldovich analysis of detonation phenomena it is said to support the recent theoretical work of J. O. HIRSCHFELDER *et al.*, in which it is claimed that transport properties within a detonation wave are important [*J. chem. Phys.* 1958, **28**, 1130, 1147].

It is said that this is the first time stabilized plane and oblique detonations have been produced in the laboratory. Some applications of these phenomena and the theoretical implications involved are discussed, such as in new chemical production methods, hypersonic air-breathing propulsion systems, and the study of chemical kinetics.

Operation School Burning

In December 1958 a fire at Our Lady of the Angels School, Chicago, caused the deaths of 95 pupils and teachers. As a result of this intensive inspections of schools in Los Angeles were carried out and arrangements were made for extensive fire tests to be undertaken in a 90 ft three-storey section of the Robert Louis Stevenson Junior High School in the city, which was scheduled for demolition. The tests were carried out by the Los Angeles Fire Department over a period of about ten weeks, and an official report of far-reaching significance has now been published under the title *Operation School Burning* [National Fire Protection Association, 60 Batterymarch Street, Boston 10, Mass., 269 pp, 1959; $4.75].

The particular purpose of the tests was to investigate methods of protecting occupants of multistorey, open-stairway school buildings from fire and smoke. It is pointed out in the report that the enclosure of stairways in buildings has long been a recognized means of protection by minimizing the spread of fire and smoke. Fire protection authorities, however, are continually confronted with the problem of having doors blocked open at stairway openings, as in schools this facilitates the passage of scholars between classes.

Full instrumentation was used and the fire protection equipment investigated included automatic sprinklers, forced and natural draught vents, draught or fire curtains, fusible links, door closers, automatic fire detection equipment, smoke detection equipment and aspirators for improving venting facilities. The test fires were in wood pallets, 4 ft by 5 ft. The majority of the fires involved 1 400 lb of pallets. The limitations of the tests are carefully noted. Very detailed results are given of the individual tests.

In the summary of results there is a general observation that with the test fires used and no fuel added to the fire due to the construction of the building, smoke was the principal life safety hazard, specifically as it pertains to visibility and irritant effects. Untenable smoke conditions preceded untenable temperature conditions in nearly every test.

Industrial Use of Gas in Europe

The second Dempster Travelling Fellowship was awarded by The Institution of Gas Engineers to T. WARD who made a study in the winter of 1957–58 in Belgium, France, Germany, Holland and Italy, of recent technical developments in the use of gas in industry [The Institution of Gas Engineers, *Publication No. 561*; 1959]. Some of the more interesting observations are given here.

In Germany, and also in Belgium and Italy where low-price methane is available, gas is used in the steel-melting shops in Siemens-Martin furnaces mainly because the use of gas-and-oil combination burners gives increased refractory life. With a 50 : 50 gas–oil mixture the number of melts is about 500 before large-scale repairs are necessary as compared with 250 melts using oil alone.

Gas is also economical under some conditions for billet-heating processes, billets up to 2½ tons in weight being heated by gas prior to rolling. The largest continuous furnace seen in operation was 250 ft long and of the pusher hearth type. It had a construction which is said to be unique, being divided into sections of about 2 m in length. Each section was again divided into an upper and lower section, which could easily be removed for re-bricking. In one factory where tinplate was produced it was claimed that the high quality attained was due to the use of coal gas prior to all rolling stages for 1 ton billets and downwards, on account of the ease of proportioning air and gas supplies. No instances were found of large billet-heating furnaces or open-hearth furnaces operating on gas.

Increase in gas prices in Europe has resulted in competition arising from the oil industry in forging. There has consequently been considerable improvement in the design of forge furnaces. An example is given of a furnace in Germany, 40 ft long and 6 ft wide, capable of continuously heating 100 lb billets up to 1 200°C. Oil is not completely satisfactory as a fuel in the forging industry, due to its long carbon-bearing flame. Investigations in the Gaswärme Institut in Essen have shown that a combination of oil and gas is very satisfactory, so that carbon and scale production are kept to a minimum and greater heat transfer achieved than with either fuel separately.

An impressive use of gas in the ferrous metal industries is that of oxy-coal gas hardening. Automatic application of the flame rapidly raises the skin of suitable materials to hardening temperature, and this is followed by rapid water or oil quenching. The burners used are simple in construction, being made in two halves from copper. Oxygen and coal gas are mixed in an inspirator and supplied to the burner at a pressure of 300 mm w.g. A distribution plate within the burner housing ensures even discharge of the mixture, which burns at the slot-type exit, 2 litres of gas and 1·2 litres of oxygen are normally discharged from 1 mm of slot per minute. Some 1 000 of these machines are in use in Germany, 360 in Canada, and 20 or so in Britain.

Preference for gas-fired furnaces appeared general in the copper industry for smelting and billet heating. In the motor car industry gas is used for many purposes; the bulk of the annealing and heat-treatment furnaces being gas-fired, but the mode of firing varies in different countries. Nozzle-mixing burners are preferred in Germany and Holland, whereas pre-mixed zero-governed burners took preference in France, Belgium and Italy. The outstanding impression of the visit was the use of waste-heat recovery plant, especially with nozzle-mixing burners. It is considered that in Germany, this difference in basic approach to the burning of gas, superior proportioning, instrumentation and pre-heating of air for combustion, gives industrial applications of gas a firm superiority over oil and other competitive fuels.

High-temperature Gas-fired Furnace

E. A. K. Patrick and R. D. Hastie, of the Industrial Laboratory, Watson House, London Research Station, The Gas Council, presented a paper to the autumn research meeting of The Institution of Gas Engineers, in November last, describing a recuperative town gas-fired furnace which they have constructed, suitable for working at temperatures up to 2 000°C. [The Gas Council, *Res. Commun. No. GC 62*; The Gas Council: London, 1959]. An oven-type furnace with a hearth about 1 ft square was decided on as it was felt desirable that the furnace should be large enough to be of commercial use. For a furnace of such a size oxygen enrichment would not be economic and consequently recuperation or regeneration would be required for the provision of preheated air. An air temperature of about 1 000°C was contemplated for which conventional reversing regenerators might seem to be appropriate. This approach to the problem was rejected on account of the fluctuations in working conditions produced by regenerators. It was eventually decided to attempt the construction of a high-temperature recuperator at the hot end of which refractory tubes would be used.

Magnesia bricks were used for the furnace lining and powdered magnesia for the high-temperature insulating material. The recuperator was built on a separate base from the furnace, so that either unit could be built independently. At a later stage in the work it was found necessary to add some cold air to the hot flue gases when the furnace temperature exceeded 1 800°C in order to prevent damage to the recuperator; this imposed an upper temperature limit of 1 200°C for the preheated air. The recuperator has given good service over a long period. The burning out of the hottest part of the steel tubes after nine months use is not regarded as being a serious detriment, and since reconstruction of the recuperator it has given no trouble. The use of two inwardly directed jets of preheated air in association with a refractory Hypact burner proved a satisfactory means of attaining temperatures up to 2 000°C. The problem of temperature measurement was overcome by the temporary expedient of applying an extra filter to a standard optical pyrometer.

Western States Section of The Combustion Institute

We are advised by the Secretary, G. S. Bahn, of the Western States Section of The Combustion Institute, 16902 Bollinger Drive, Pacific Palisades, Calif., that Preprints of Papers read at the 1958 Summer Meeting at the University of California are still available at $3.00. Readers interested in the papers or the associated panel discussion can obtain further information from the Secretary. The titles of papers and their respective authors are given here for convenience.

The prediction of the transport property coefficients. C. W. Baulknight

On the existence of steady-state flames. A. L. Berlad and C. H. Yang

A thermal layer mechanism of combustion of solid-composite propellants. R. F. Chaiken

Extinction of laminar flames. A. L. Berlad and C. H. Yang

Metal alkyls as hypergolic fuels. D. J. Simkin and C. J. O'Brien

Heterogeneous combustion of multicomponent fuels. B. J. Wood, H. Wise and S. H. Inami

Heterogeneous combustion in high turbulence flow fields. F. B. Cramer and W. T. Webber

Use of fine thermocouples in combustion studies. M. H. Hunt

Results of a screech investigation program with a two dimensional model ramjet combustor. I. Elias

1959 Fall Meeting of Western States Section of The Combustion Institute

A Conference on Equilibria and the Performance of High Temperature Systems, sponsored by the Marquardt Corpn and the Rocketdyne Division of North American Aviation, Inc., took place during 2 to 5 November 1959 at Los Angeles (this Journal, 1959, pp 270 and 415). The *Proceedings* of this Conference will be published this summer by Butterworths Scientific Publications in book form and it is expected that the following papers will be among those included in the volume:

Chemical species in high temperature systems. R. S. Scheffee and C. B. Henderson

Estimation of the heats of formation of gaseous combustion product molecules. C. J. O'Brien, J. R. Perrin and J. Perrine

Some provisional tables of species thermodynamic properties. R. R. Koppang, C. M. Sherwood and G. S. Bahn

Automatic computation of ideal-gas thermodynamic functions for diatomic molecules. J. S. Gordon and R. Robinson

On the apparent divergence of the thermodynamic properties of dilute gases at high temperatures; thermodynamic functions for diatomic molecules. L. Haar

Approximations to high-temperature thermodynamics of air in closed form. A. R. Hochstim

The thermodynamic properties of the products of H_2–O_2 combustion at elevated temperatures. W. C. Moffat, F. D. Skinner and R. J. Zaworski

Equilibria at high temperatures for the formation of the molecular species C_2, C_3, Cu_2 and Si_2. S. Zaff, L. E. Ashley and C. M. Cobb

Calculation of the thermodynamic properties of multicomponent systems and evaluation of propellant performance parameters. S. R. Brinkley, Jr

Propellant thermodynamic performance calculations for rocket engines. Propellant systems containing aluminium, ammonium perchlorate and a polyurethane–nitrocellulose–nitroglycerine binder. P. G. Baer, R. Greene, H. Smith and J. Wortman

Machine computation of chemical equilibria in reacting systems. D. G. McMahon and R. Roback

Programme for computing equilibrium temperature and composition of chemical reactions. R. M. Mentz

A note on the linearization method for computing chemical equilibrium in complex systems. R. L. Wilkins

Performance calculations using an IBM 650 computer. J. D. Breazeale

Hand calculation of equilibrium compositions as a learned habit, and speed-up effected with the IBM 610 computer. G. S. Bahn

Computation of complicated combustion equilibria on a high speed digital computer. D. S. Villars

A practical approach to computer programming for specific impulse calculations. L. J. Gordon and H. Boeklin

Calculation of thermodynamic properties of combustion gases with a small punch-card electronic computer. R. W. Smith, Jr and E. Cook

Extension to multiphase systems of the Rand method for determining equilibrium compositions. B. R. Kubert and S. E. Stephanou

The computation of high temperature engine performance. H. E. Brandmaier and J. J. Harnett

Complex chemical equilibria by minimizing free energy. L. M. Naphtali

Perturbation technique for fitting jet engine performance parameters. W. E. Simon

Evaporation and break-up of fuel droplets in one-dimensional gas flow in a combustion chamber. L. M. Naphtali and S. Z. Burstein

An analysis of rocket engine performance with nearly constant temperature burning in the combustion chamber and exhaust nozzle. P. L. Blackshear, Jr

Studies of chemical non-equilibrium in hypersonic nozzle flows. J. G. Hall and A. L. Russo

Criteria for design and development of automatic, self-linearizing self-editing electronically calibrated transducers. G. Birkel, Jr

The expansion parameter as a tool in first-cut comparisons of exotic ramjet fuel formulations. G. S. Bahn and R. R. Koppang

Thermodynamics of high temperature gas mixtures; propellants containing boron. J. S. Gordon, W. Mitchell, D. Goland and Maryianne P. Stoltenberg

W. A. Kirkby

Publications

ROCKET PROPELLANTS

F. A. WARREN. New York: Reinhold; London: Chapman and Hall, 1958. *viii*+218 *pp.* 52*s*.

Although a number of books have been published on rockets and rocket propulsion there are none up till now which deal exclusively with rocket propellants. There is undoubtedly a need for such books both for those working in the field and for the intelligent layman. The same treatment of the subject will not suit both and WARREN's book is written for the layman and the semi-technical reader. Such readers will not look for comprehensive physicochemical data or accurate performance figures and will not regret the absence of up-to-date information on solid propellants caused by antiquated security restrictions. This book contains selected facts on composition, manufacturing methods, performance, combustion, ignition, safety and evaluation of propellants. The author assumes no previous knowledge by the reader and moves rapidly over the wide range of his subject achieving a reasonably balanced picture with a little bias in favour of solid propellants which have been his own professional interest. The chapter on 'Safety', although very brief, serves to warn the would-be amateur practitioner that propellants, like fire, are good servants but bad masters. Now that the use of rockets for the exploration of space is making greater demands on the rocket engine, the limitations of chemical fuels are of interest and in his last chapter WARREN discusses this and mentions possible alternative methods of achieving higher performance.

W. G. PARKER

VISTAS IN FREE RADICAL CHEMISTRY

Edited by W. A. WATERS, F.R.S. London: Pergamon, 1959. *ix*+251 *pp.* 75*s*

THIS volume has been published by a group of collaborators, friends and students of the late Dr MORRIS S. KHARASCH. The idea of a memorial volume originated with Sir ROBERT ROBINSON, on behalf of the organizers of *Tetrahedron*, and it has the intention of assessing the importance of the researches performed by KHARASCH, and his influence on the development of modern organic chemistry. The volume contains a complete list of the research papers of KHARASCH and his collaborators, dating back to 1920 ('Aromatic mercury–organic derivatives', by KHARASCH and PICCARD). This valuable compilation follows a discussion by WATERS and MAYO of the significance of the work of KHARASCH in the field of free radical chemistry. The main portion of the volume contains a number of papers which have been selected, by WATERS and MAYO, in order to emphasize the main steps in the elucidation of the mechanisms with which KHARASCH is now so closely associated. This has been done very well, and the section serves, in fact, as a history of a major branch of chemistry during the last 35 years. There follows a series of invited articles in which other colleagues review the present position, and the future trends, in several homolytic reaction systems.

Readers of *Combustion and Flame* will be particularly interested in the survey by KUTCHKE and STEACIE on the 'Chemistry of free radicals in the gas phase'. In this article a number of aspects of gas phase free radical reactions are considered according to type, and the present generally accepted interpretations are summarized in each case without the confusing quantity of detail which is present in so many reviews. This article, therefore, has particular value for the gas kineticist.

The aim of the editors of the volume has been well achieved. The volume will be useful for a long time, both as an important monograph in its own right, and as a worthy memorial of the great man whom it commemorates. It is clear that KHARASCH not only had an instinct for the subject but that he was fortunate with timing and with location. In fact . . . . 'with his wide knowledge of industrial chemical processes, with the industrial support, with the high industrial and academic interest in aliphatic chemistry and polymerization in the United States, and with a large group of students and post graduates to draw from, KHARASCH had unusual opportunity; it is obvious that he made the most of it. His success can be cited to justify the American academic system of encouraging large graduate schools and post graduate research' (p 4). Clearly, the lack of such facilities in the United Kingdom, except for a few institutions, does not assist the growth of our chemical industry.

G. J. MINKOFF

JETS AND ROCKETS

A. BARKER, T. R. F. NONWEILER and R. SMELT. London: Chapman and Hall, 1959. *xiv*+268 *pp.* 35*s*

THIS book was apparently projected in 1945. Had it been published shortly after that time, when few connected accounts of jet propulsion were available, it might have served a useful purpose. In 1959 it is hard to see to what class of readers it can be recommended.

The book is written in a jaunty style which would make it suitable for the semi-technical reader who wants to know what is going on in engine development but will not need to apply his knowledge professionally. Such a reader will, however, no longer be interested in yet another account of German wartime rocket motors and early British gas-turbine development. Too many of the facts are out-of-date, and some positively wrong, for example the statement: 'It is safe to say that reliability of operation has not yet been achieved with hydrocarbon fuel regeneratively cooled (rocket) motors'.

Of course, the fundamental theory does not date. Unfortunately this is presented, in the reviewer's opinion, in too slapdash and imprecise a fashion for it to be recommended to any student. For example, equilibrium constants are tabulated without an indication of the units in which the partial pressures are to be measured. On the other hand the molecular weight of oxygen is quoted as 32 *grams*! The authors do not appear to have had a clear idea of their readership; engineering graduates will already know more of the fundamentals than the book presents; undergraduates will need a sounder and more extended treatment; the layman will find the book too mathematical.

The proof-reading has been carelessly carried out, e.g. *flourine* for *fluorine*, *Holsworth* for *Holzwarth*, *Just* for *Jost*. The references are equally haphazard. Several are unpublished (and so unobtainable) M.O.S. reports; no reference is given at all to a paper by Lutz on dissociation, which the reader is enjoined to study. The cited papers and books are not referred to by number or arranged in any order that the reviewer could discover.

D. B. Spalding

ANNUAL REPORTS ON THE PROGRESS OF CHEMISTRY, VOLUME 55, 1958

London: The Chemical Society, 1959.
xv+527 *pp.* 40*s*.

The *Reports* have been sub-divided under the headings General and Physical Chemistry, Inorganic Chemistry, Organic Chemistry, Biological Chemistry, Analytical Chemistry and Crystallography. The balance is not entirely satisfactory, for twice as much space is devoted to Organic Chemistry as to General and Physical Chemistry; an additional section on Theoretical Chemistry would be helpful and might do something to redress the inequality of balance. Subjects such as Quantum Organic Chemistry and Theoretical Organic Chemistry, at present included under Organic Chemistry, could then be included in a separate section.

The General and Physical Chemistry section is a collection of reports on separate and limited topics rather than one of general reports, the intention being to give complete coverage of interesting physicochemical subjects over a period of two to three years. This would seem to be the only method of avoiding too much generalization if the *Annual Reports* are to retain their present format.

A feature of the *Reports* is the increasing use of physicochemical techniques in all branches of Chemistry. Spectrophotometry, for instance, is used in the determination of acidity constants, in following polymerization reactions, in the analysis of rare earth mixtures, the determination of sulphur in steel, in the determination of unsaturation in organic compounds and in many other varied applications.

Free radical properties and reaction mechanisms are discussed in several sections; some overlap is unavoidable and probably necessary, taking into account the related interests of physical and organic chemists. The sub-section entitled 'Kinetics of chemical change' is rather misleading, as the author restricts himself to free radical and ion-molecule reactions. However, the treatment of this diverse and intricate subject taken in conjunction with the sub-sections on 'Radical polymerization' and 'Energy transfer in liquids and gases' gives an interesting account of progress in the fields of Excited States and Radical Reactions.

The increasing interest in Inorganic Chemistry is reflected in the increased number of publications in this field.

Work on Analytical Chemistry is not confined to the section under this title. Trotman-Dickenson, reiterating the late Sir Alfred Egerton's editorial in *Combustion and Flame* a year ago, draws attention to the powerful combination of Gas Chromatography and Mass Spectrometry as analytical techniques in the study of reaction kinetics and mechanisms. The rapid increase in the use of gas–liquid and gas–solid chromatographic methods has necessitated some standardization of units and methods of recording data and this is emphasized in the sub-section on Chromatography.

The section under the heading Analytical Chemistry draws together many of the techniques described in earlier sections. The present trend towards automation of analytical techniques is discussed and methods of continuous analytical control and monitoring are described; for example, a modification of Winkler's method for the determination of dissolved oxygen in water is given; the method is automatic and continuously records dissolved oxygen in the range 0 to 15 p.p.m. by weight of oxygen. It is interesting to observe that many of the latest analytical techniques are derived from the solution of problems in applied chemistry.

There is a good deal of direct interest for those working in the field of Combustion. Relaxation data obtained under conditions which occur in shock waves and chemical reactions are discussed in some detail. The vibrational levels of the OH radical in hydrogen flames, the lifetime of the HO_2 radical, details of increase of flame temperature above the reaction zone, and the modification of the Lindemann mechanism for first order reactions, are some other topics mentioned.

The task of compiling the *Annual Reports on the Progress of Chemistry* becomes more formidable every year. The volume of work produced in this field is prodigious and the Chemical Society is to be congratulated on its remarkable feat of condensation and on the continuing high standard of its publication.

I. Fells

Letters to the Editors

Letters to the Editors on points of scientific interest related to combustion and flames are invited. The Editors do not hold themselves responsible for opinions expressed in correspondence. Anonymous contributions cannot be accepted.

Extinction of a One-dimensional Laminar Flame between Cooled Porous Plugs

REFERENCE 1 reports that, if a one-dimensional laminar flame is stabilized between two porous plates, flame extinction occurs when the separation distance is reduced to a critical value; for slightly larger distances, two flame speeds may be exhibited by a mixture of fixed initial enthalpy (mixture ratio and Q). The purpose of the present letter is to show that this result is qualitatively in accordance with the theory reported in ref. 2; a more quantitative comparison will be made at a later date.

Ref. 2 shows that the influence of downstream cooling makes itself felt by way of the dimensionless quantity E. It is necessary to relate E to the plate separation of the burner of ref. 1. This may be done by solving the equation for enthalpy diffusion and convection for the space between the plates. The result is

$$E = \frac{-(1-\tau_2)}{\tau_1}\exp\left\{\frac{-cG(x_2-x_1)}{k}\right\} \quad \ldots [1]$$

where τ_1 and τ_2 are the dimensionless temperatures of the cooled plates (1 upstream, 2 downstream), c is the specific heat of the gas at constant pressure, G is the mass rate of burning per unit area, $x_2 - x_1$ is the plate separation, and $\bar{k}$ is an average thermal conductivity defined as equal to $1 / \int_{x_1}^{x_2} (1/k)\mathrm{d}x$.

The plate temperatures, τ_1 and τ_2, are fixed by the experimenter; the ratio $(1-\tau_2)/\tau_1$ will often exceed unity. When this ratio is known, equation 1 can be evaluated as a relation between (G/G_0) and E, with $cG_0(x_2-x_1)/\bar{k}$ as a parameter.

Figure 1 shows curves plotted in this manner for $(1-\tau_2)/\tau_1 = 2$; the graph also shows one curve (valid for $n = 6$) obtained from ref. 2 and expressive of the reaction-kinetic conditions which the flame must satisfy in addition to the purely physical ones of equation 1.

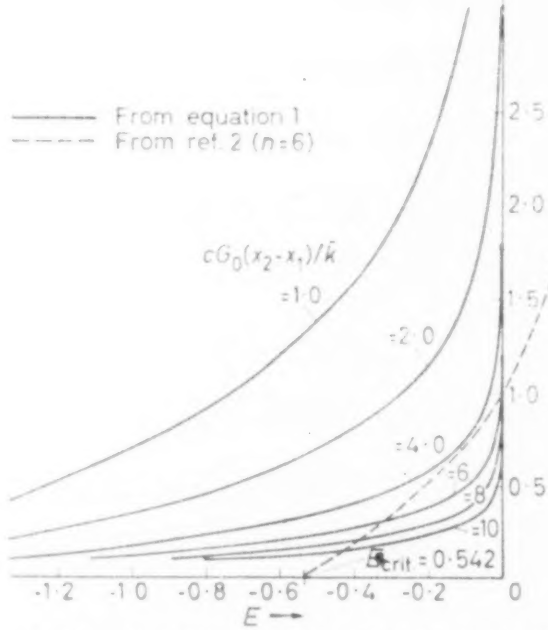

Figure 1. Graphical solution of the simultaneous relations from ref. 2 and equation 1

Inspection of *Figure 1* shows that there are in general two intersections between a curve according to equation 1 and the curve from ref. 2. When the dimensionless quantity $cG_0(x_2-x_1)/\bar{k}$ becomes too small, however, these intersections are imaginary.

The physical implications of the deductions are obvious. When $cG_0(x_2-x_1)/\bar{k}$ is large (high adiabatic flame speed, large plate separation), two flame speeds are possible; one is very close to the adiabatic speed, the other very much lower. When $cG_0(x_2-x_1)/\bar{k}$ is reduced, for example by pushing the plates nearer together, the two flame speeds approach each other; at a critical value of the (dimensionless) separation, the two values coincide. No real flame is possible for smaller values of the plate separation; when the separation is less than the critical, the flame is extinguished. In the example shown, the critical value of $cG_u(x_2-x_1)/\bar{k}$ is somewhat more than 2·0; this means that the critical separation is equal to a few flame thicknesses.

It should be clear that these predicted phenomena are in qualitative agreement with the results reported in ref. 1. More experimental and theoretical results are needed for a full quantitative comparison.

D. B. Spalding

Imperial College of Science and Technology,
South Kensington, London, S.W.7

(*Received November 1959*)

References

[1] Spalding, D. B. and Yumlu, V. S. *Combustion & Flame*, 1959, **3**, 553

[2] Spalding, D. B. and Adler, J. *Combustion & Flame*, 1960, **4**, 94

One-dimensional Laminar Flame Propagation with an Enthalpy Gradient

Most analyses of laminar flame propagation postulate equality of gas enthalpy upstream and downstream of the flame zone. Important practical cases in which this condition is not fulfilled include: flames with appreciable radiative or conductive heat loss from the combustion products[1]; flames upstream of a cooled plate[2]; flames upstream of a heated porous plate[3]; the gaseous decomposition flame of a solid or liquid propellant immersed in a gaseous atmosphere with which the decomposition products can react chemically.

We have made a theoretical analysis of this problem for flames embodying the class of first-order chemical reactions analysed in ref. 4, with normal diffusion (Lewis number, unity). The purpose of the present letter is to present the main results briefly; they will be reported in full later.

The dimensionless criterion expressing the magnitude of the enthalpy gradient proves to be the ratio of the gradient of enthalpy to the specific heat times the gradient of the gas temperature upstream of the reaction zone. If this ratio is given the symbol E, then

$$E \equiv 1 + \left(\frac{\mathrm{d}z}{\mathrm{d}y}\right)_{\infty} \Big/ \left(\frac{\mathrm{d}\tau}{\mathrm{d}y}\right)_{-\infty}$$

in the notation of ref. 4, where z represents the (dimensionless) concentration of combustible, while τ represents the (dimensionless) concentration of temperature. In the normal-diffusion flames analysed in ref. 4, E is zero; in a flame in a gas flowing into a hot plug or a reactive atmosphere, E is positive; in a flame with downstream heat loss (cold plug or radiative loss), E is negative.

Figure 1 shows the result of the calculation, which was obtained by numerical solution of the differential equation on a digital computer. The abscissa is the quantity E just referred to; the ordinate is the ratio of the mass burning

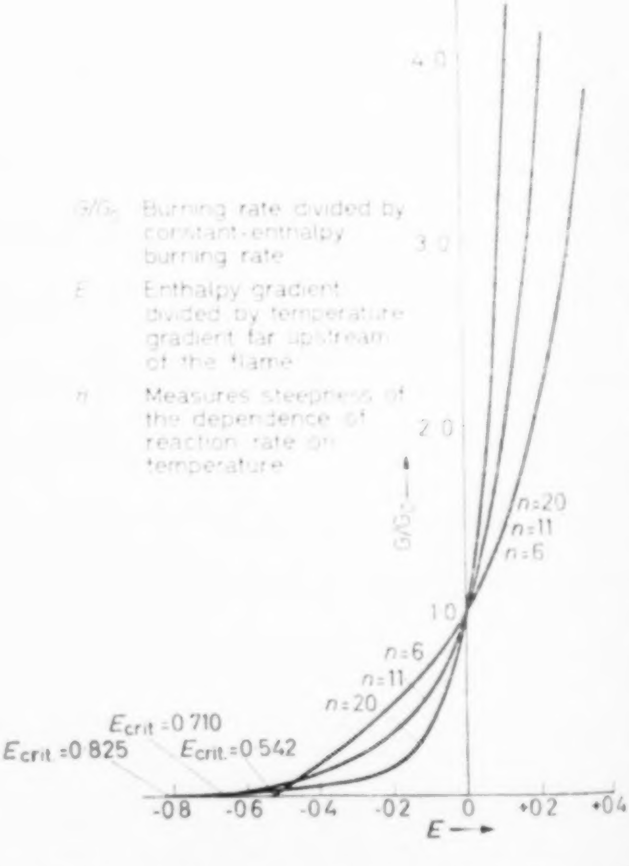

Figure 1. Influence of enthalpy gradient on burning rate for activation energies

rate G to the mass burning rate G_u which prevails when the enthalpy gradient is absent ($h = 0$). The parameter is n, the temperature exponent of reaction used in ref. 4.

Examination of *Figure 1* leads to the following conclusions:

(i) As E increases from zero, so does the flame speed. The effect is greatest for reactions of large activation energy (large n).

(ii) As E decreases from zero, so does the flame speed. Once again the effect increases with the value of n.

(iii) When E falls to a critical negative value, E_{crit}, the flame speed falls to zero. E_{crit} is greater, the larger is the activation energy.

Temperature and composition profiles have also been calculated. A feature of the solutions is that, as E approaches E_{crit}, a finite proportion of combustible always passes through the flame without burning; this does not occur for positive values of E, however.

The solutions enable quantitative analyses to be made of flames of the type listed above. In particular the solutions may be employed to interpret the results of experiments of the type reported in refs. 2 and 3 to get quantitative information about the reaction constants.

D. B. SPALDING
J. ADLER

Imperial College of Science and Technology, South Kensington, London, S.W.7

(*Received November 1959*)

References

[1] SPALDING, D. B. *Proc. Roy. Soc. A*. 1957, **240**, 83–100

[2] SPALDING, D. B. and YUMLU, V. S. *Combustion & Flame*, 1959, **3**, 553

[3] DIXON-LEWIS, G. and ISLES, G. L. *Seventh Symposium (International) on Combustion*, p. 475. Butterworths: London, 1959

[4] SPALDING, D. B. *Combustion & Flame*, 1957, **1**, 287–307

The Thermal Conductivity of Hydrazine Vapour

IN recent years, hydrazine flames have received considerable attention[1]. Their quantitative interpretation requires reliable thermal data in addition to kinetic data. Hitherto, estimates of specific heats[2] and thermal conductivities[3] have been based on analogy with other gases; in particular, with ethylene. Although calculated and experimental specific heats are now available[4] in the literature, values of the transport properties are still lacking. Accordingly, the thermal conductivity of hydrazine vapour has been measured in an apparatus[5] of the type described by A. B. CALLEAR and J. C. ROBB[6]. At 6 mm pressure and 25°C the thermal conductivity is

$$K_{(N_2H_4)} = (3{\cdot}49 \pm 0{\cdot}04) \times 10^{-5} \text{ cal (cm sec °C)}^{-1}$$

There is no detectable variation of thermal conductivity over the accessible pressure range which is, of course, limited by the low saturation vapour pressure of hydrazine (about 10 mm at 20°C). Measurements are made as rapidly as possible because after a time the thermal conductivity increases and a non-condensable gas is formed, presumably by decomposition of hydrazine on metal or metal oxide of the cell wires.

This value of $K_{(N_2H_4)} = 3{\cdot}49 \times 10^{-5}$ cal (cm sec °C)$^{-1}$ differs markedly from that for ethylene at the same temperature, $K_{(C_2H_4)} = 4{\cdot}76 \times 10^{-5}$ cal (cm sec °C)$^{-1}$. The discrepancy reflects the different molecular masses and structures: hydrazine (mol. wt, 32) is polar (dipole moment 1·8 D) and non-planar; ethylene (mol. wt, 28) is non-polar and planar.

A better analogy to hydrazine is provided by methanol. It has the same mass (mol. wt, 32), is polar (dipole moment 1·7 D) and non-planar. The thermal conductivity of methanol measured in the same apparatus at the same temperature and at low pressures is found to be only five per cent different from that of hydrazine

$$K_{(CH_3OH)} = (3{\cdot}67 \pm 0{\cdot}04) \times 10^{-5} \text{ cal (cm sec °C)}^{-1}$$

It would thus appear that, in calculations requiring the thermal conductivity of hydrazine at elevated temperatures, the best *a priori* assumption is that it is approximately equal to that of methanol. The thermal conductivities of alcohols have been investigated in some detail[7] and might be extrapolated to higher temperatures by analogy with the data[8] for steam. The values below have been derived in this way, and are presented as the most satisfactory interim values for hydrazine at elevated temperatures:

Temp., °C	0	25	100	200	500	1 000
Conductivity 10^{-5} *cal* *(cm sec °C)*$^{-1}$	3·1	3·49*	6·5	7·5	15	30

*experimental value

P. Gray
P. G. Wright†

School of Chemistry,
University of Leeds

(*Received December 1959*)

References

[1] See, e.g. Gray, P. and Lee, J. C. *Seventh Symposium (International) on Combustion*, p 61. Butterworths: London, 1959, and references cited therein

[2] Hall, A. R. and Murray, R. C. *Trans. Faraday Soc.* 1951, **47**, 743

[3] Gray, P. and Lee, J. C. *Trans. Faraday Soc.* 1954, **50**, 719

Lee, J. C. *Ph.D. Thesis*, University of Cambridge, 1955

[4] Audrieth, L. F. and Ogg, B.A. *The Chemistry of Hydrazine*, pp **70-72**. Wiley: New York, **1951**

[5] Gray, P. and Wright, P. G. (1958). To be published

[6] Callear, A. B. and Robb, J. C. *Trans. Faraday Soc.* 1955, **51**, 630

[7] Shushpanov, P. I. *Zh. eksp. teor. Fiz.* 1939, **9**, **875**; 1940, **10**, 674

Lambert, J. D., Staines, E. N. and Woods, S. D. *Proc. Roy. Soc. A*, 1950, **200**, 262

Vines, R. G. and Bennett, L. A. *J. chem. Phys.* 1954, **22**, 360

[8] Dorsey, N. E. *Properties of Ordinary Water Substance*. Reinhold: New York, 1940

---

†Present address: Chemistry Department, Queens College, Dundee

Obituary

Sir Alfred Egerton, F.R.S. (1886-1959)

FOR many years before he died Sir ALFRED EGERTON had been the acknowledged leader in Britain of those scientists engaged in research in the field of Combustion, Explosions and Flame. So it was most natural that he should become the first Chairman of the British Section of the Combustion Institute when it was formed a few years ago. He was also the first Editor-in-Chief of *Combustion and Flame*, the official Journal of the Institute. To both of these offices he brought his wisdom, long experience and high sense of duty and, as a result, the Institute can now be proud of a lively and growing journal and of the very successful Symposium that was held in London and Oxford in 1958. This was the first of the International Symposia on Combustion to be held outside the United States of America, and for many years Sir ALFRED had hoped and planned for one to be held in England. He spent a great deal of time and effort to ensure the success of the Symposium in all its aspects. At the first session at the Royal Institution, he gave one of the opening addresses describing the beautiful experiments of Sir HUMPHREY DAVY on flames. He showed how DAVY had initiated work on many of the aspects of combustion which engaged the interests of the scientists attending the Symposium. It was apparent throughout that Sir ALFRED derived great joy from talking in the Royal Institution itself of the work of Sir HUMPHREY DAVY, and the lecture, to which much careful thought had been devoted, was not only instructive and informative but also wholly delightful. This lecture and the excellent speech that he gave at the dinner at Guildhall later on the same day were further examples of the time and trouble Sir ALFRED was willing to take in the affairs of the Combustion Institute and of the Seventh Symposium.

Unfortunately I only knew Sir ALFRED during the last dozen years of his life. For half of these he had already retired from his Professorship at the Imperial College of Science and Technology and had become an Emeritus Professor. Nevertheless during all the time I knew him, his interest in Combustion was most vital and he retained until his death the ability to experience the thrill of new ideas and new experiments. Moreover, after the 1939–45 war, when he was about sixty years of age, he devised with one of his students the Egerton–Powling flat-flame burner, which has proved such a boon to those desiring to make measurements on flames under ideal conditions. However, a most important quality he possessed as Head of the Chemical Engineering Department at the Imperial College was an intense interest in and concern for the practical applications of science. It was his grasp of both the fundamentals and their applications that enabled him to make important contributions to our understanding of the chemistry of the internal combustion engine.

Sir ALFRED's interest and zeal for science date back to his boyhood when he founded the Eton College Scientific Society. After being a student in London, he worked with Sir WILLIAM RAMSAY there and then with Professor NERNST in Berlin. In 1919 he moved to Oxford where he was Reader in Thermodynamics till he went to the Imperial College in 1936. He commenced work on combustion in Oxford, but before that, among other experiments, he made some very skilful measurements of low vapour pressures by an effusion method. These formed a model for those who adopted the method later. Before, during and after the 1939–45 war Sir ALFRED gave unstintingly of his time to the work of scientific societies, government committees, science in India, and many other important scientific activities of public importance.

Sir ALFRED was an extremely kind and generous person. He showed a deep and fatherly interest in the younger people who were associated with him in his Department, and was always ready to promote their interests and to help them in any way he could. He had a great love for his Department at the Imperial College which he retained during the years following his retirement. Though Sir ALFRED had the kindly and gentle good manners of an older generation he was prepared to fight resolutely against what he thought was wrong. He did this reluctantly and with distaste but nevertheless without shirking.

For a long time to come, I and many others will remember Sir ALFRED EGERTON for his unassuming kindnesses and for his youthful zest for things scientific, and we will continue to profit from our recollections of his simple generosity and of his scholarly work.

J. W. LINNETT

Burning Rates and Ignition Temperatures of Hydrogen Peroxide Solutions

C. N. SATTERFIELD, E. KEHAT and MARIA A. T. MENDES

Department of Chemical Engineering, Massachusetts Institute of Technology, Cambridge, Massachusetts, U.S.A.

(Received January 1959)

The hydrogen peroxide decomposition flame above concentrated liquid solutions has been studied at atmospheric pressure. Mass burning rates were found to agree closely with the flame velocities as measured for the vapour by the bunsen burner method, when compared at equal adiabatic decomposition temperatures. The limiting combinations of solution concentration and temperature for ignition of flames above hydrogen peroxide solutions are reported to help establish the regions of hazard in handling this material.

IF A concentrated aqueous hydrogen peroxide solution is heated to a temperature in the region of 100° C, it is possible to ignite a continuously propagating 'flame' above the liquid surface that consists of the decomposition reaction alone. Such flames, which were first reported by A. B. HART[1], are invisible under ordinary conditions but can be observed by optical methods such as shadow photography. The purpose of the present work was to determine the limiting conditions under which such flames can be ignited and to establish some of the characteristics of such flames, particularly the rate of burning. Such studies are of concern in establishing safety limits for storage, handling and manufacture of hydrogen peroxide and are also of interest in conjunction with the use of concentrated hydrogen peroxide as a compact source of energy.

Experimental

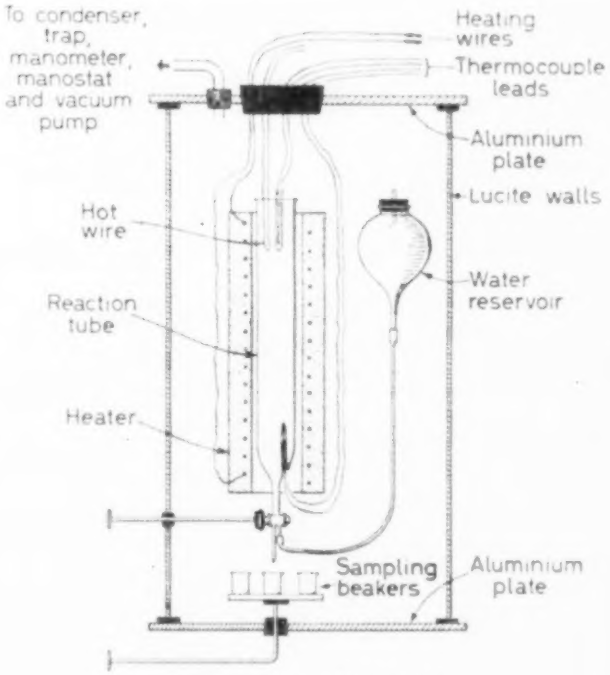

Figure 1. Apparatus

Burning rate data were obtained by following the rate at which the liquid level dropped in a heated tube 15 mm in inside diameter and 30 cm long (see *Figure 1*). The heater itself consisted of two concentric Pyrex tubes. On the inner tube, and insulated from both tubes by strips of asbestos tape, Chromel A resistance wire was wound. Uniformity of temperature in a vertical direction was obtained by winding the resistance wire more closely at the bottom than at the top which thus increased convection currents in the liquid. A three way stopcock connected to the bottom of the tube made it possible to take samples of the solution or to inject water at the end of a run to flood the tube contents and thereby extinguish the flame.

The temperature of the liquid was measured by two iron–constantan thermocouples, one in a Pyrex insert at the bottom of the reaction tube and the other in a Pyrex well at the open end of the reaction tube. The liquid was ignited with a heated platinum wire and a cathetometer was used to measure the rate of drop of liquid level. In order to make studies at subatmospheric pressures, the whole assembly was enclosed in a vessel consisting essentially of a Lucite tube 7 in. in diameter with top and bottom plates of aluminium. As a protective measure the whole apparatus was built behind a steel-walled cell containing a safety glass window for observations.

The reaction tube was cleaned by immersion for twelve hours in a hot mixture of concentrated sulphuric and nitric acids (3 : 1), washed with distilled water and then filled with hydrogen peroxide and placed in the heater. After steady state conditions were reached, a sample was withdrawn, the liquid was ignited and readings were taken of the time required for the liquid level to drop one centimetre. After fifteen readings had been obtained another sample was withdrawn and the flame extinguished. The standard method of analysis of hydrogen peroxide with permanganate solution[7] was followed.

In runs where the liquid concentration change during the run was less than 0·4 mole per cent, the burning rate was essentially constant (within ±5 per cent) throughout the run and results for the entire run were averaged. In runs where the liquid concentration changed one per cent or more, point conditions, at the beginning and end of the run, of concentration and of the rate of level drop were used and are designated as *a* and *b*, respectively, in *Table 1*. The liquid densities for each liquid concentration and temperature were calculated from data available on specific volumes of hydrogen peroxide solutions[2]. The adiabatic flame temperature for each run was calculated in the usual way from appropriate thermodynamic data[2] assuming that the hydrogen peroxide was completely decomposed.

Minimum ignition temperatures above liquid hydrogen peroxide were determined for most studies in test tubes having an inside diameter of 16 mm and length of 14 cm with a thermocouple well through the bottom. Each tube was deactivated by immersion in a hot mixture of sulphuric and nitric acids for 24 hours or more, washed, annealed for 3 hours at 470° to

Table 1. Hydrogen peroxide burning rates (one atmosphere pressure)

Run	*Liquid conc. mole %*	*Liquid temp. °C*	*Liquid density g/cm^3*	*Adiabatic decomp'n temp., °C*	*Burning rate mg sol'n/(sec)(cm^2)*
7	95·0	119	1·32	1044	26
11	95·0	122	1·31	1050	29
12	95·8	120	1·32	1047	24
13	95·8	117	1·32	1042	29
14	96·0	118	1·33	1045	25
15	87·0	115	1·30	920	16
17	85·5	115	1·30	907	16
18	83·0	117	1·28	854	14
19*a*	72·8	132	1·23	740	9
20*a*	74·0	132	1·25	824	10
21	93·8	125	1·35	1044	34
23*a*	94·6	139	1·29	1074	43
23*b*	92·8	139	1·29	1054	32
24*a*	95·0	126	1·31	1052	33
24*b*	96·8	126	1·32	1054	33
25*a*	95·0	123	1·35	1051	38
25*b*	92·7	123	1·31	1019	37
26*a*	70·8	130	1·24	732	13
26*b*	69·8	130	1·23	697	13
27*a*	75·6	127	1·25	782	13
27*b*	72·8	127	1·24	740	13
28	97·0	114	1·32	1053	19
29*a*	81·0	121	1·28	855	15
29*b*	71·2	132	1·23	717	11

For Runs 26 and 27 the reaction tube was wrapped in aluminium foil. Runs 28 and 29 were carried out in a reaction tube 3 cm in diameter.

190 C, cooled gradually and placed in a vertical tubular heater of the type used in the burning rate studies. The tube was filled up to 1 to 2 cm from its top with hydrogen peroxide solution of suitable composition. The hot wire and shielded vapour thermocouple were adjusted to a position about 5 mm above the surface and the tube was then heated at a rate of 1 to 2°C per minute. Above some temperature estimated from experience ignition was attempted (1·1 ohm, 5·5 A, wire heated for 10 sec) every minute until ignition was obtained. The temperature of the solution at this point was taken as the ignition temperature for the run. In the spark ignition runs the liquid level was up to the top of the tube and ignition was obtained with a pair of aluminium electrodes 3 to 4 mm apart fed by a Ford coil. The electrodes were lowered to touch the surface each time ignition was attempted. Energy consumption was 3 to 4 W for 2 to 3 sec compared with 30 W for 10 sec for the hot wire.

The establishment of a flame is characterized by one or more of the following phenomena:

(*1*) Increase of vapour temperature

(*2*) Calming of the surface of the liquid and disappearance of any bubbles on the surface

(*3*) Crackling sound of the flame

(*4*) Red glow of the hot wire after ignition is stopped (with hot wire ignition)

(*5*) Disappearance of condensate from electrodes (with spark ignition).

Probing the liquid with a thermocouple showed that the surface temperature of the liquid at all temperatures and concentrations studied was about 2·5°C below the bottom thermocouple temperature. All ignition temperature data quoted are for the surface temperature and contain this small correction. Measurements of the reaction gas temperature by probing with a thermocouple showed that the maximum temperature occurred at a point less than 1 mm above the liquid surface. The flame is not luminous and attempts to obtain a shadowgram of the flame failed because apparently, like the hydrazine flame[3], this flame front follows the contour of the liquid surface and is very close above it.

Discussion

Burning rates

In *Figure 2* are plotted the burning rates as obtained here together with some measurements of the flame velocity in hydrogen peroxide vapours obtained by W. CECKLER[1] (see *Table 2*) using the bunsen burner technique, his data being converted here to a mass basis. *Table 1* gives the liquid concentration and temperature for each run, plus the basic data from which *Figure 2* was calculated. It is significant that the burning rates as obtained by the two quite different methods agree closely when correlated on the basis of the adiabatic flame temperature. For example, an adiabatic flame temperature of 1 050°C results from burning slightly super-

Table 2. Flame velocities in hydrogen peroxide vapour by bunsen burner method

Run	*Mole fraction H_2O_2 in vapour*	*Temp. of vapour before reaction °K*	*Density of vapour before reaction mg/cm³*	*Adiabatic flame temp. °C*	*Flame velocity ft/sec*	*Equivalent burning rate mg/(cm²)(sec)*
3	0·403	415	0·715	1062	1·79	39
4	0·394	416	0·712	1048	1·43	31
8	0·414	425	0·707	1090	1·66	36
10	0·363	444	0·654	1017	1·23	24
11	0·385	449	0·655	1056	1·87	37
12	0·399	419	0·711	1058	1·48	32
13	0·404	418	0·711	1066	1·46	32
14	0·407	412	0·724	1065	1·41	31
15	0·405	414	0·719	1064	1·13	25
18	0·386	439	0·668	1053	1·30	26
19	0·450	423	0·725	1148	2·85	63
20	0·479	427	0·733	1198	3·04	68

Data from W. CECKLER[1].

heated hydrogen peroxide vapour of about 40 mole per cent (the remainder being water vapour) or liquid hydrogen peroxide of about 92 mole per cent at its boiling point. More recent data by Ceckler, as yet unpublished, further confirm the correlation shown in *Figure 2*.

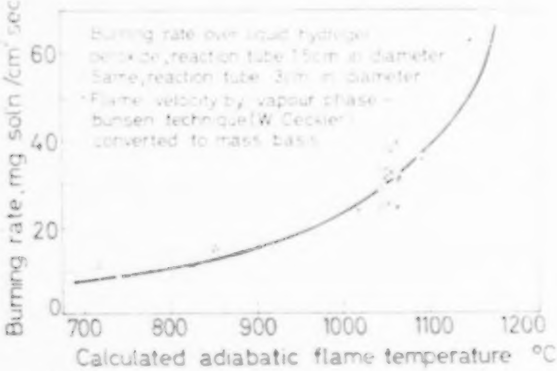

Figure 2. Effect of adiabatic flame temperature on burning rate

The fact that the liquid being burned here is a two-component system that can easily vary in composition with time introduces a barely predictable source of variation in burning rates that does not occur in most other monopropellant flames, such as those of hydrazine or alkyl nitrates. The scatter of data in the liquid phase studies seemed to be associated with variations in the circulation pattern of the liquid hydrogen peroxide solution, and this in turn seemed to depend substantially on the extent to which the liquid was below the boiling point of the solution. For runs at liquid temperatures the furthest below the boiling point, a sharp interface was observed about 3 mm below the surface while the flame burned. This top layer presumably consisted of less dense solution at a higher temperature than the bulk solution temperature, and possibly also of slightly lower concentration. For these particular runs, the measured liquid concentration was constant during the run, whereas in runs in which the liquid was near the boiling point there was usually a gradual drop in concentration with time, indicating some recirculation of decomposed liquid immediately beneath the flame back into the bulk solution.

Some studies were also made at sub-atmospheric pressures, although the lower the total pressure, the smaller the range of liquid concentration and temperature that will support a flame, until at 110 mm of mercury, for example, only hydrogen peroxide solutions very near to the boiling point and almost 100 per cent in concentration could be ignited in our apparatus. Some fragmentary data that were obtained indicated that the burning rate does not appreciably change with a drop of pressure from 760 to 400 mm of mercury but decreases somewhat with further drop in pressure to 200 mm of mercury. Runs 26 and 27 were conducted with the reaction tube wrapped in aluminium foil in order to observe the effect of heat reflected back to the flame front. As expected, the measured velocities were higher. The flame temperature was measured for run 26 and found to be within 10 °C of the calculated adiabatic flame temperature. Runs 28 and 29 were conducted with a 30 mm internal diameter Pyrex reaction tube. Comparison with runs made with the regular 15 mm reaction tube (*Figure 2*) shows negligible effect of the twofold increase in tube diameter. This agrees with similar conclusions obtained for the hydrazine decomposition flame[9].

Composition of the products—Calculations of the adiabatic flame temperature assumed that no undecomposed hydrogen peroxide passed through the flame. This assumption was checked by condensing and collecting in an acidified permanganate solution samples of the vapour above the flame. From the average liquid composition, the weight of condensed sample and the analysis of the hydrogen peroxide it contained, the degree of decomposition of hydrogen peroxide in the flame was found with an accuracy of about 5 to 10 per cent. At burning rates of about 15 mg solution/(cm²) (sec) or greater, substantially less than one per cent of the hydrogen peroxide passes through the flame undecomposed; at all rates above 30 mg/(cm²) (sec), the undecomposed hydrogen peroxide amounted to 0·1 to 0·2 per cent. Only at the lowest flame velocities, near the ignition limit, does an appreciable amount of hydrogen peroxide pass through the flame front undecomposed, possibly because the flame is not continuous over the liquid surface under these conditions. This would displace upward by a small amount the lowest part of the curve in *Figure 2*.

Ignition limits above concentrated hydrogen peroxide solutions

The ignition limits of hydrogen peroxide in vapour mixtures with inert gases at atmospheric and sub-atmospheric pressures have been published[1]. At one atmosphere, for example, the ignition limit is 26·0 mole per cent or 198 mm of mercury partial pressure and this limit is unaffected by moderate variations in the ratio of water to oxygen or water to nitrogen in the inert gas present. These vapour ignition limit data[1] and vapour-liquid equilibrium data[2] can be combined to calculate those combinations of hydrogen peroxide solution concentration and temperature at which the vapour in equilibrium with the liquid has a composition equal to that at the vapour ignition limit. This establishes what is termed here the 'vapour ignition curve'.

Any hydrogen peroxide solution whose composition and temperature locate it above this curve has a vapour in equilibrium above it that is ignitable by a spark, hot wire or catalytic impurity. Vapour ignition curves have been calculated for total pressures of 760, 400, 200 and 100 mm of mercury and are shown in *Figure 3*. It is seen that the hazardous region for ignition of vapour above the liquid decreases with decreasing pressure.

A significant question is whether or not a flame can be established atop the liquid whenever the vapour composition exceeds the vapour ignition curve. *Figures 4* and *5* show, for 760 and 400 mm of mercury total pressure, respectively, the vapour ignition curve and the actual minimum conditions under which it was found possible to ignite flames above the liquid, in tubes 16 mm in diameter. It is evident that the minimum conditions for establishment of flames differ significantly from the minimum conditions under which the vapour itself can be ignited. At lower concentrations, the minimum liquid temperature at which a flame could be established at one atmosphere pressure corresponds to a hydrogen peroxide partial pressure appreciably higher than 198 mm of mercury, but at very high concentrations the reverse was true. At the lower concentrations, the flame temperature is apparently insufficient to cause propagation of the flame over the liquid even when the vapour itself is above the vapour ignition limit. On the other hand, at the highest concentrations, a spark or hot wire if held close to the liquid surface can presumably heat the liquid locally to a temperature producing ignitable vapour and the higher flame temperature can cause continual propagation.

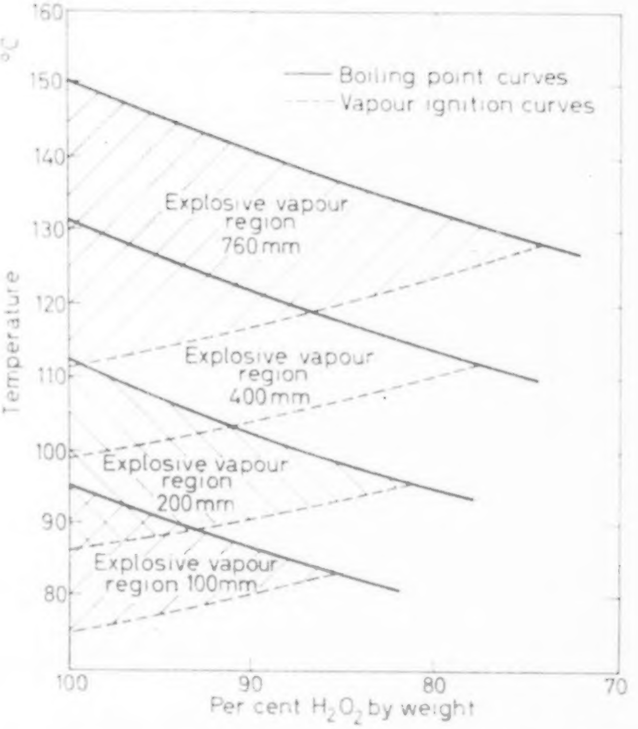

Figure 3. Combinations of temperature and liquid composition producing equilibrium vapours of explosive composition

The large scatter in the ignition data seemed to be caused principally by the considerable variation in the rates of decomposition of the hydrogen peroxide solutions from run to run. In small test tubes, higher rates of decomposition increased the minimum ignition temperature, presumably by diluting the vapour. However, when beakers were used the reverse effect was observed. This can be attributed to the difference in the convection patterns and mechanism of heat transfer in the two cases.

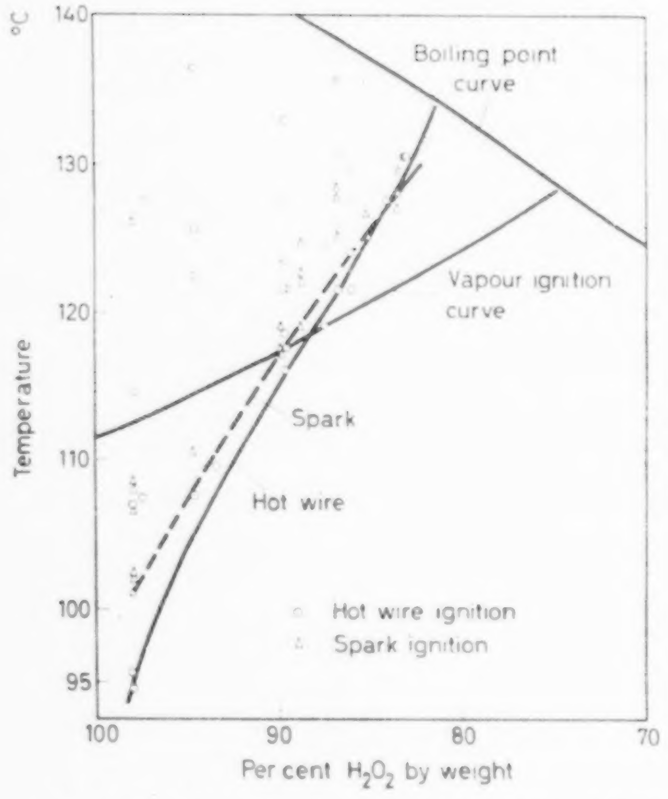

Figure 4. Flame ignition limits at surface of liquid hydrogen peroxide at one atmosphere pressure

In the tubes heat is transferred from the hot wire to the surface of the liquid mainly by radiation, whereas in beakers, the convection currents set up by decomposition apparently more than offset the adverse effect of diluting the gas phase. Observations showed the appearance of spiralling white vapours as the temperature went up increasing in intensity to a maximum at the ignition temperature. The whole surface of the liquid in the beakers seems to become ignited at the same time, similar to a small pool of gasoline into which a lighted match is thrown.

The effect of a fivefold variation of ignition vessel diameter was studied with one liquid composition, 89·6% wt, using a variety of tubes and beakers of internal diameters varying from 16 mm to 74 mm. Over this range, effect of diameter is negligible, in any event being overshadowed by slight variations from run to run caused by varying degrees of decomposition and differences in the distance of the hot wire from the liquid surface.

Self-extinction of hydrogen peroxide flames

The limiting conditions for ignition of flames and the burning rates themselves are, of course, dependent upon the extent to which the environment removes heat and possibly also free radicals from the reaction zone. For example, attempts to propagate a flame when the tube containing the hydrogen peroxide solution was surrounded by an oil bath, which is a more effective heat sink than our usual apparatus, failed even at concentrations of 93% wt hydrogen peroxide and at temperatures near boiling. Similarly, P. GRAY and J. C. LEE[6] reported that when a hydrazine flame was propagating inside a tube, the outer surface of the tube was about 100° C, but when they immersed the tube in a thermostat and progressively lowered the temperature the flame velocity decreased and at 80° it stopped propagating. In our apparatus if the heating of an ignition tube were discontinued the rate of burning decreased as the tube cooled slowly. Solutions of concentrations above 90% wt burned until

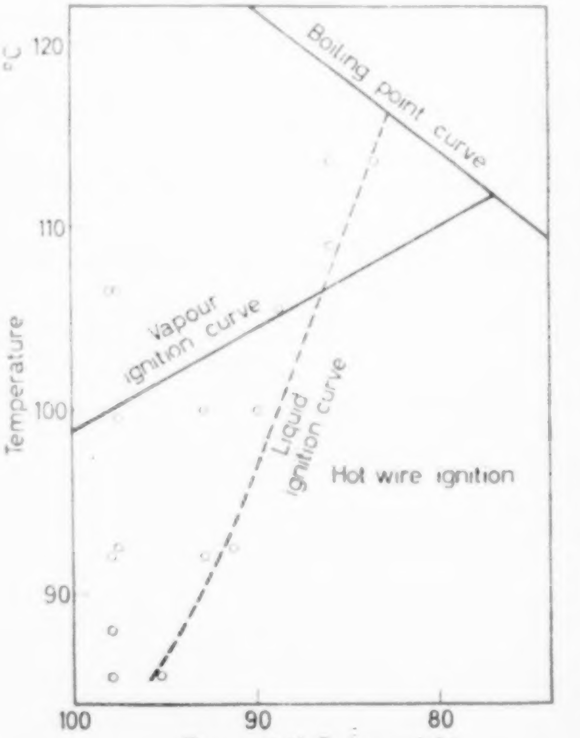

Figure 5. Flame ignition limits at surface of liquid hydrogen peroxide at 400 mm of mercury pressure

all liquid was consumed. In solutions of lower concentration the flame went out at a bulk liquid temperature appreciably lower than the ignition temperature for the same initial solution concentration. The burning rate near this extinction point is very slow. This phenomenon was investigated systematically by recording the liquid and vapour temperatures at small time intervals as burning progressed. The instant of cessation of flame is indicated by the change in appearance of the surface and cessation of flame noise. At the same time, the vapour temperature drops rapidly to that of the liquid. This temperature at which the two temperatures become equal was taken as the extinction temperature. A plot of extinction temperature versus residual concentration for three initial concentrations is presented in *Figure 6*. The result shows great sensitivity to the final concentrations and the extinction temperatures are lower by 15° to 20°C than the ignition temperatures. The level at which the flame stopped was different for different runs. Since there is a slight temperature gradient through the liquid, this might account for some of the scatter in the data.

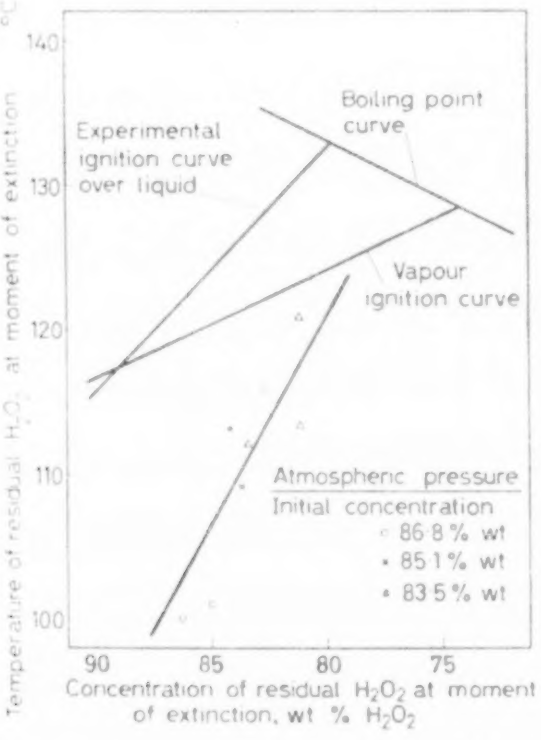

Figure 6. Experimental conditions under which hydrogen peroxide flame extinguished itself

The probable explanation for the substantial difference between ignition and extinction temperatures is that the rate of heat transferred back to the liquid surface when a flame is burning is much greater than the rate of transfer to the surface from the hot wire under ignition conditions. Therefore, propagation of a flame is possible at lower bulk temperatures than ignition temperature.

The authors wish to acknowledge the financial support of the U.S. Office of Naval Research, under contract Nonr 1841 (11), NR–092–008. Reproduction in full or in part is permitted for any purpose by the United States Government.

References

[1] HART, A. B. *Nature, Lond.* 1949, **163**, 876

[2] SCHUMB, W. C., SATTERFIELD, C. N. and WENTWORTH, R. L. 'Hydrogen peroxide'. *Amer. chem. Soc. Monogr. No. 128*. Reinhold: New York, 1955

[3] ADAMS, G. K. and STOCKS, G. W. *Fourth Symposium (International) on Combustion*, p 239. Williams and Wilkins: Baltimore, 1953

[4] CECKLER, W. Unpublished experimental work, Massachusetts Institute of Technology, 1955

[5] SATTERFIELD, C. N., KAVANAGH, G. M. and RESNICK, H. *Industr. Engng Chem.* (*Industr.*), 1951, **43**, 2507

[6] GRAY, P. and LEE, J. C. *Sixth Symposium (International) on Combustion*, p 255. Reinhold: New York, 1957

Some Properties of Carbonaceous Deposits Accumulated in Internal Combustion Engines

J. L. LAUER and P. J. FRIEL

Basic Research Division, Research and Development Department, Sun Oil Co.,
Marcus Hook, Pennsylvania, U.S.A.

(*Received January 1959*)

Although generally less than 20 per cent of the total deposit from fuel containing 3 ml of tetraethyl-lead per gallon is carbonaceous, the carbonaceous portion of the deposit significantly influences engine performance. Engine 'carbon' contains 20 to 30 per cent oxygen, most of which is bound in acid and ester carbonyl groups. Fuel and lubricant carbon look similar under the electron microscope; in one instance, they could be separated by ultrasonic dispersion. In an engine, fuels and oils yield deposits of varying oxygen content, depending on the constitution of the fuel and/or oil. In the laboratory, similar results can be obtained through a bench test using periodic ignition and extinction. Carbonaceous engine deposits most likely originate in an oxidative pyrolysis of fuel and lubricant.

DEPOSITS collected on combustion chamber walls of internal combustion engines are of importance to fuel manufacturers and engine designers because of their marked influence on performance. As deposits accumulate, fuels of increasingly higher octane quality become necessary for knock-free operation.

Therefore, a systematic study of the formation and properties of engine deposits was undertaken. Since the work of several investigators[1, 2] has shown that the carbonaceous portion of the lead-containing fuel deposits forms the binder holding them to the combustion chamber surfaces and that exposed carbon particles can ignite the charge in the combustion chamber by their own spontaneous ignition, most of our work concerned the organic part of the deposits. Clearly the importance of the carbonaceous portion of the deposit to the engine deposit problem is far greater than the relative weight would indicate, only 20 per cent or less of the total deposit from fuel containing 3 ml of tetraethyl-lead (TEL) per gallon being organic. Our results should be helpful in closing gaps still existing in our understanding of engine deposit formation and of the effect of engine deposits on octane requirement increase.

Changes in Properties of Combustion Chamber Deposits with Engine Operating Time

The octane requirement (minimum octane number of fuel required for knock-free operation) of most automotive engines increases during the break-in period and then remains relatively constant. This behaviour is paralleled by changes in amount and composition of engine deposits. In order to study the trend of these changes, the following experiment was carried out.

A single-cylinder, L-head Lauson engine was operated at 7 : 1 compression ratio on a commercial motor fuel containing 2·7 ml of TEL per gallon and a multigrade lubricating oil for 15, 35, 65 and 89 h. (Equilibrium conditions were reached after about 89 h.) After every run the head was removed and the deposit scraped and collected separately from valve and piston areas of the head and from the piston surface. *Table 1* shows the observed trends. As expected, carbon contents decreased and lead contents increased with time. Initially more carbon must have been laid down than lead salt, for the percentage of carbon decreased after 15 hours while the lead content steadily increased. Bulk density (weight of 1 ml of

Table 1. Data obtained on Lauson engine deposits for operations of varying time
(Commercial fuel containing 2·7 ml TEL/gal, multigrade commercial oil, compression ratio 7:1)

Area from which deposit was scraped	*Run time* h	*Deposit weight* g	*Bulk density* g/ml	*Elemental analysis* % C	% H	% Pb	*Solubility (wt %) in* *Benzene*	*Pyridine*
Valve area (head)	15	1·01	0·70	32·1	1·3	40·6	2·2	68·0
	35	2·06	0·87	18·0	1·0	46·4	0·9	63·9
	65	2·96	1·10	14·8	0·7	48·1	1·4	71·8
	89	3·50	1·15	13·2	0·8	69·3	0·8	68·9
Piston area (head)	15	0·49	0·74	25·6	1·3	24·9	3·5	51·3
	35	0·91	1·00	23·6	1·7	44·1	2·0	47·8
	65	0·77	0·92	21·6	1·4	47·5	1·9	54·7
	89	0·92	0·95	20·4	1·4	52·1	1·9	50·9
Piston	15	0·66	0·83	26·5	1·8	18·5	3·9	38·4
	35	0·65	1·09	25·4	2·1	26·3	3·1	45·5
	65	0·97	1·06	22·3	1·6	41·7	1·5	48·2
	89	0·79	1·16	18·5	1·3	55·6	1·0	47·8

scraped deposit, mixed, ground and sifted to about 100 mesh size) reached constancy much sooner than elemental composition. Porosity and homogeneity changes of deposit particles were probably responsible for this behaviour. It is noteworthy that the deposit from the valve (presumably the hottest) area of the head showed the greatest lead and lowest carbon content at all times.

Physical Properties of Deposits from Lead-free Fuels

Since it is difficult to separate organic and inorganic deposit portions, much work was done with unleaded (clear) fuels and with lubricating oils containing no metallic additives. Combinations of (*a*) *iso*octane fuel with hydrocarbon lubes and (*b*) toluene fuel with synthetic (polyether) lubes resulted in approximately equal deposit weights. Since (because of known combustion characteristics) the deposit from combination (*a*) was almost entirely lube carbon and from combination (*b*) almost entirely fuel carbon, it was deduced that both fuel and lubricating oil contributed to engine deposits[3].

Because of their usual inhomogeneity, many deposits had to be examined on their original support. Parts of the wall of the combustion chamber head of a Lauson single-cylinder engine were cut out and replaced by removable and interchangeable plugs. These plugs with the deposit formed on their front surface during engine operation became our samples for thickness measurements.

Deposit thickness was measured by viewing the plugs edgewise with a measuring microscope after removing slices of deposits along the edges. The thicknesses shown in *Table 2* represent averages of many readings which were taken on each plug deposit. Because of the roughness of some deposit surfaces, only averages of thicknesses at a great many spots are suitable for comparisons.

Total weights and bulk densities are also included in *Table 2*. Toluene and paraffinic lube oil gave heavier but more porous (lower bulk density) deposits than *iso*octane and the naphthenic lube oil. These fuels and lubricating oils were chosen as examples because they represent extremes of most commercial compositions.

Electron microscope studies of fine dispersions of engine deposits from (*a*) a toluene–synthetic oil combination, (*b*) an *iso*octane–paraffinic oil combination, and (*c*) a toluene–paraffinic oil combination, carried out by Professor S. Mrozowski at the University of Buffalo, showed that these deposits, whether from fuel or oil, were all essentially similar carbons. They all seemed to consist of agglomerates of small spheres of varying density and packing. Spheres are generally characteristic of carbon blacks, i.e. carbon formed in the gas phase from diffusion flames. The cokes formed by heating liquid and solid organic materials in containers in the presence or absence of oxygen usually have rectangular edges when viewed in dispersion under the electron microscope. The samples

Table 2. *Weights, thicknesses and bulk densities of some engine deposits*
(Lauson engine operated 100 h, compression ratio 7 : 1)

	Paraffinic			Naphthenic		
Fuel/Oil	*Wt* g	*Thickness* mm	*Density* g/ml	*Wt* g	*Thickness* mm	*Density* g/ml
iso-Octane	0·4	0·07	0·63	0·4	0·09	0·65
Toluene	1·2	0·25	0·23	0·9	0·24	0·58
Commercial fuel (clear)	1·1	0·11	0·63	0·6	0·15	0·67

examined represent extremes of a great many fuel and oil combinations. Samples (*b*) and (*c*) consisted of denser agglomerates of particles than sample (*a*) and could not be distinguished from each other. This result can be explained by assuming the formation of denser deposits from oil carbons and indeed this assumption is in agreement with bulk density measurements (*Table 2*). Since mixtures of light and dense particles appear dense under the microscope, the similarity of (*b*) and (*c*) is not surprising. *Figure 1* shows the electron photomicrograph corresponding to sample (*a*) and *Figure 2* shows that corresponding to sample (*b*) [or (*c*)]. Further confirmation of our explanation came from the appearance of electron photomicrographs of ultrasonically dispersed deposits. Suspensions of samples (*a*) and (*b*) in a liquid medium could not be further dispersed by ultrasonic irradiation under conditions causing a similar suspension of sample (*c*) to disintegrate into particles resembling those found in samples (*a*) and (*b*). *Figure 3* is the electron photomicrograph of an ultrasonically dispersed sample

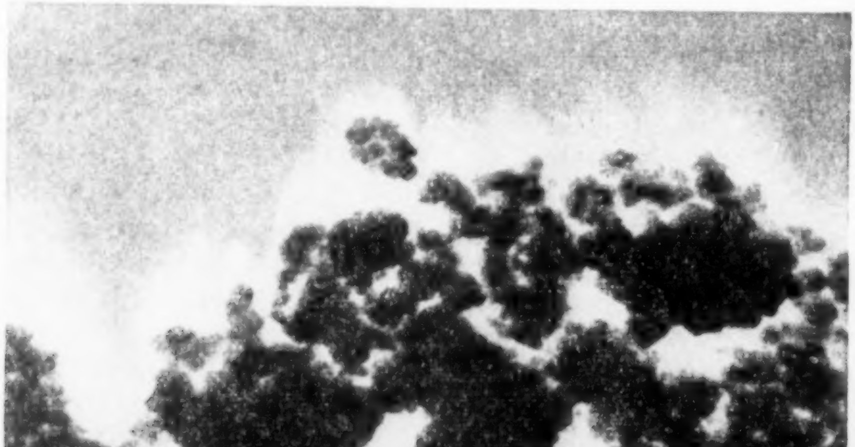

Figure 1. Electron photomicrograph of deposit from a toluene–synthetic oil combination. Magnification: 18 000×; reduced ½ on reproduction

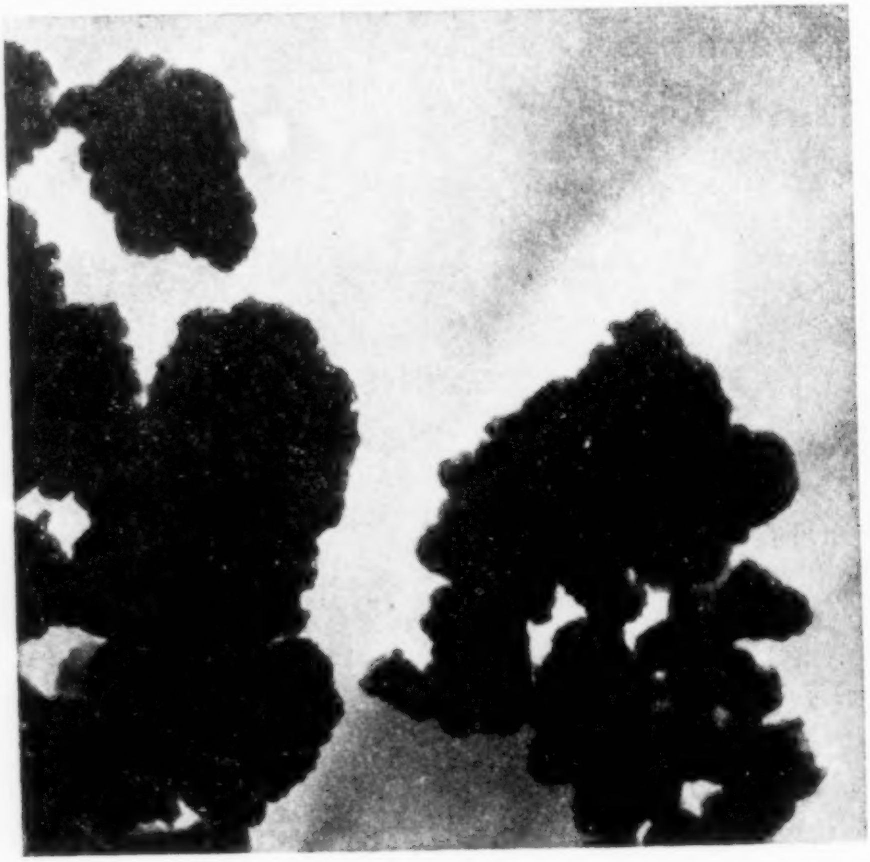

Figure 2. Electron photomicrograph of deposit from an isooctane paraffinic oil combination. Magnification: 18000×; reduced ½ in reproduction

(*c*), showing groups of dense and light particles. The electron photomicrographs of the ultrasonic dispersions of the other two samples were essentially identical with *Figures 1* and *2*, i.e. the electron photomicrographs of the deposits before ultrasonic dispersion. These results indicate that fuel and oil carbon have similar particle structure; oil carbon being denser, however.

Chemical Properties of Deposits from Lead-free Fuels

Representative elemental analyses are shown in *Table 3*. Toluene produced deposits of high carbon content and higher C/H ratio than isooctane. The naphthenic lubricating oils gave rise to higher oxygen and lower carbon contents than the paraffinic oils. The high C/H ratio for toluene deposits could be regarded as an

Table 3. Elemental analyses and solubilities of some engine deposits
(Lauson engine operated 100 h, compression ratio 7 : 1)

Fuel/Oil	*Paraffinic*					*Naphthenic*				
	Solubility (wt %) in					*Solubility (wt %) in*				
	Benzene	*Pyridine*	*% C*	*% O*	*C/H**	*Benzene*	*Pyridine*	*% C*	*% O*	*C/H**
iso*Octane*	4	15	65	25	1·3	5	40	57	36	1·2
Toluene (clear)	6	14	72	20	1·8	2	27	60	28	1·8
Commercial fuel	4	27	66	27	1·1	3	34	64	29	1·8

**Atom ratio*

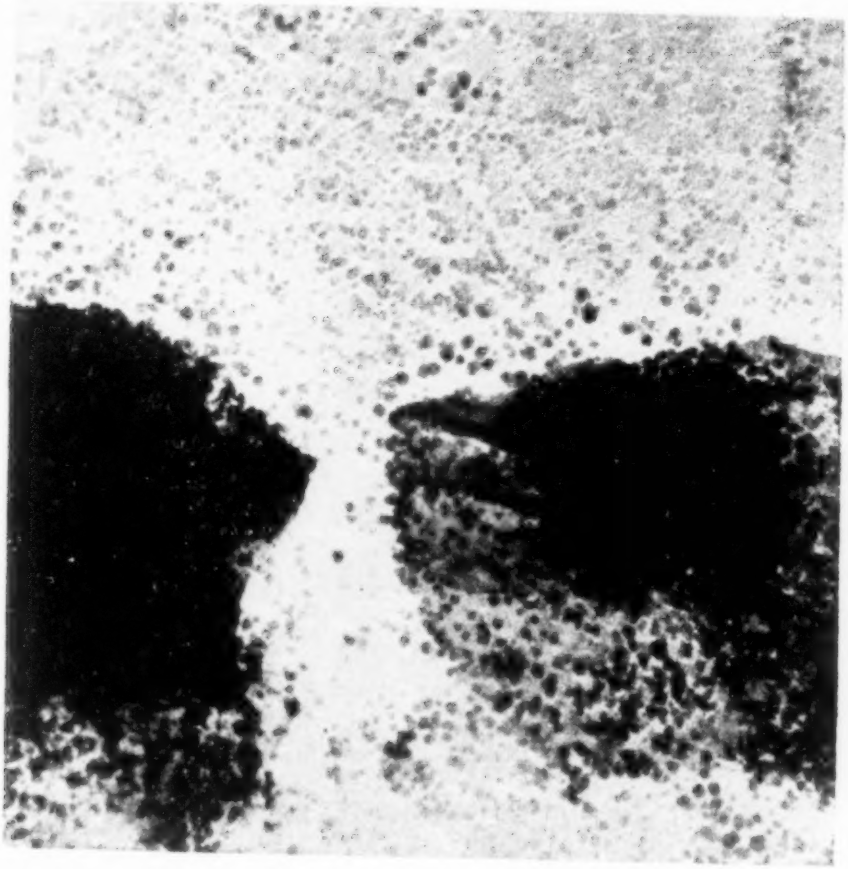

Figure 3. Electron photomicrograph of deposit from a toluene-paraffinic oil combination. Magnification: 10000×; reduced ½ on reproduction; ultrasonically dispersed

indication of aromatic content. However, no ultra-violet absorptions to substantiate this hypothesis could be obtained, although a small amount of fluorescence was noted under ultra-violet excitation.

Solubilities in benzene and pyridine were determined as measures of low molecular weight hydrocarbon and polar material content, respectively. The following procedure was used. The deposits were first washed with *iso*octane to remove oil condensed on them when the engine was shut off at the conclusion of an experiment. They were then dried and extracted with benzene from an alundum thimble in a Soxhlet apparatus. The residue after this extraction was also extracted with pyridine. Solubilities were calculated from weight changes after drying. The data of *Table 3* show parallelism between oxygen content and pyridine solubility. Infra-red spectrograms are in agreement with the assumption that acidic functional groups (e.g. carboxyl) are mainly responsible for pyridine solubility (see below). Crude pH measurements on water slurries of deposits showed some measure of correspondence between low pH and high pyridine solubility, thus giving additional support to the carboxyl group assumption. Further support came from saponification and acid numbers. Nevertheless, all the oxygen could not be contained in such groups for, while oxygen content and pyridine solubility run parallel to each other, they are not proportional to each other.

Infra-red absorption spectra were obtained on the benzene and pyridine solutions and on the residues after benzene and pyridine extractions (using the potassium bromide disc technique).

The most significant region of all these spectra was that between 5 and 8 microns (*Figure 4*). The other regions, in general, showed only broad absorption bands which could not be associated with any particular type of structure other than that of complex high molecular weight material. Bands due to carbon–hydrogen groups and carbonyl groups could be definitely identified. The band at 5·8 microns is attributed to the carbonyl group, mostly in saturated monobasic carboxylic acids and partly in aldehydes, ketones, esters or anhydrides. The band resolved at about 6·3 microns in the spectra of the residues remaining after extraction is attributed to ionized salts of carboxylic acids. There was no spectral evidence for the presence of nitro groups as was found by R. S. Spindt and co-workers[4].

Typical examples of infra-red spectra are shown in *Figure 4*. Benzene extracts always contained appreciable amounts of C—H groups as denoted by the bands at 6·85 and 7·25 microns. Carbonyl groups are responsible for the absorption at 5·8 microns. Pyridine extracts contained quite a lot of oxygenated materials in the form of C=O, but the C—H portion of the sample was considerably less. The final residues had little hydrocarbon structure, also less C=O, but considerably higher COO— (i.e. 6·3 micron band) concentration.

Since these results pointed to the presence of carboxyl groups in engine carbon, a few experiments were performed to determine the loss in weight at elevated temperatures and the nature of the evolved gases. The procedure used was this. Small amounts of *iso*octane-washed engine deposits were heated for two hours under nitrogen in a closed container at a number of temperatures between 200° and 610°C. The gas above the samples was flushed through solid caustic soda absorbent and partly identified as carbon dioxide. The gain in weight of the absorbent paralleled the weight loss of the deposit. This loss increased sharply at about 325°C and again at 510°C for almost all deposits studied in the Lauson engine (*Figure 5*). The temperature of 325°C can, therefore, be regarded as an upper limit for the effective deposit temperature during engine operation. Decarboxylation seemed to account for most of the weight loss.

Very significantly, we think, the weight loss curve of *Figure 5* is quite analogous to those shown by F. H. Winslow and co-workers[5] for the temperature dependence of the gas evolution from pyrolysed polytrivinylbenzene. The infra-

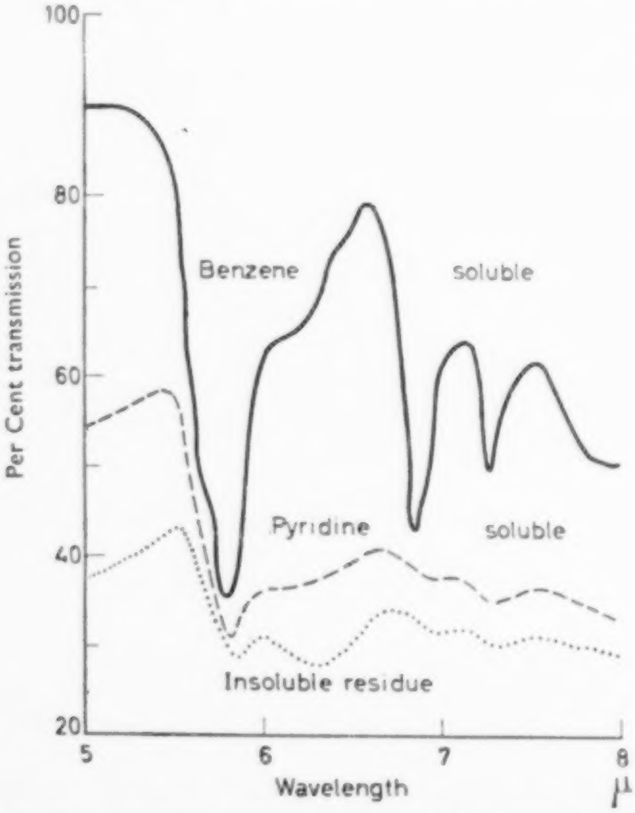

Figure 4. Infra-red spectra of engine deposit from an isooctane–paraffinic oil combination

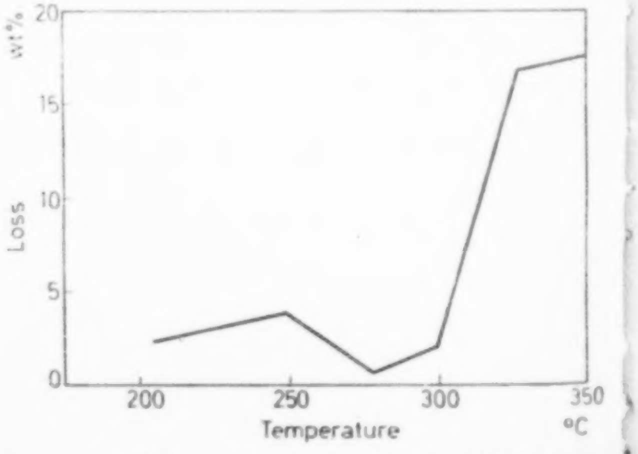

Figure 5. Weight loss on heating a deposit from a toluene–paraffinic oil combination

red spectrum published by these authors for divinyl/ethylvinylbenzene copolymer pyrolysed in air in very thin sheets, shows rather close resemblance to our deposit spectra.

It is quite probable that the acid or anhydride groups present in carbonaceous engine deposits are at least partly responsible for their adhesion to combustion chamber walls.

Relation Between Deposit Density and Octane Requirement

L. F. DUMONT[1] postulated three mechanisms by which combustion chamber deposits might cause octane requirement increase (the difference in fuel knock resistance demanded by an engine with deposits and a clean engine). They were: (*a*) reduction of combustion chamber volume (effectively increasing compression ratio), (*b*) smaller cooling efficiency because of the insulating layer provided by deposits, and (*c*) a possible unexplained catalytic effect. J. J. MIKITA and B. M. STURGIS[2] have shown that effects (*a*) and (*b*), and especially the latter, are of the greatest importance. The bulk density of deposits from clear fuels and metal-free lubricating oils should be a measure of both of these effects. The higher the bulk density, the more thermally insulating the deposit layer and—total deposit weights being equal—the more the effective compression ratio of the engine will have increased because of reduction in actual combustion chamber volume. Although engine deposits are not homogeneous, the bulk density of the total deposits from all combustion chamber surfaces still met this expectation. At least the general trend, viz. low density corresponding to large octane requirement increase, is clearly recognized from the data shown in *Figure 6*.

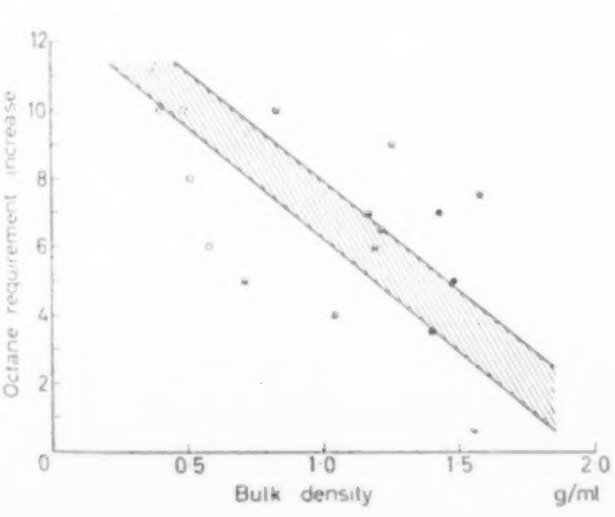

Figure 6. Relation of octane requirement increase to bulk density of deposit

Since it is well known that octane requirement increase drops with higher compression ratio, higher deposit densities are expected for higher compression ratios. The data of *Table 4* agree with this reasoning.

Table 4. Effect of compression ratio on deposit density

(Fuel: isooctane, oil: multigrade, operating time: 100 h)

Engine	*Compression ratio*	*Bulk density g/ml*
Lauson	7:1	0·55
COT	8·5:1	0·69
COT	11:1	1·04

Laboratory Bench Methods of Producing Carbonaceous Residues Resembling Fuel and Engine Carbon

In order to gain additional information on the mechanism by which combustion chamber deposits are produced, bench methods were devised to simulate some of the apparently essential conditions prevailing in an engine. Clearly, only another engine could simulate all the conditions. In the course of this work we became aware of the importance played by the periodic ignition and extinction of fuel and oil and the effect of a large excess of air. Carbonaceous residues produced by heating oils in shallow dishes never contained more than two per cent of oxygen even when exposed to an air flow while, as shown above, oil or fuel deposits from engine combustion chambers contained over 20 per cent of oxygen (*Table 3*). Similarly, carbon deposits from fuels burnt in diffusion flames contained very little oxygen. Therefore, ordinary thermal cracking and coking is not the mechanism by which engine deposits are produced.

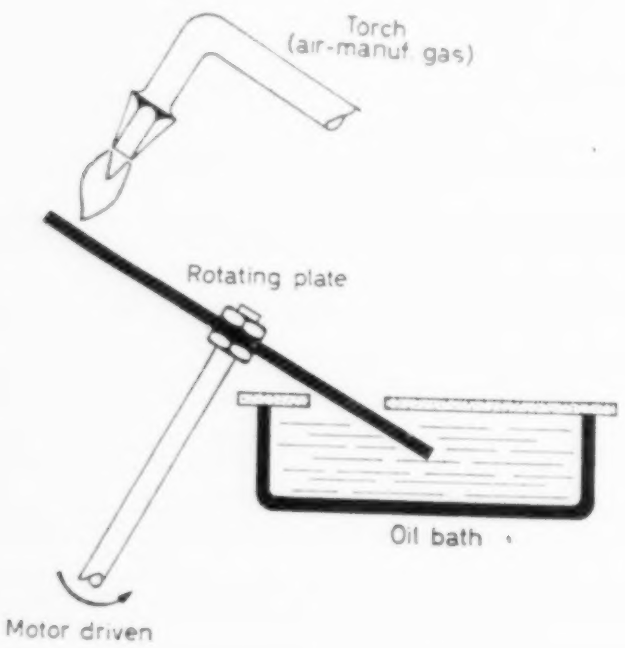
Torch
(air-manuf. gas)
Rotating plate
Oil bath
Motor driven

Figure 7. 'Burning disc' apparatus

Table 5. Elemental analysis and solubility of residues produced by 'burning disc' method compared to corresponding engine deposits

Oil	% C	% H	% O	*Pyridine Solubility* (*wt* %)
A. *Simulated deposits*				
Paraffinic	71·5	8·8	14·5	11·7
Naphthenic	70·0	3·0	24·3	30·0
B. *Engine deposits**				
Paraffinic	65	4·2	25	15
Naphthenic	57	3·9	36	40

**Table 3*, Row 1.

The 'burning disc' apparatus illustrated in *Figure 7* provided us with residues which had the same relative oxygen content and pyridine solubility as the corresponding engine deposits (*Table 5*). Actual values were somewhat lower for the burning disc residues than for the engine deposits, but exact agreement cannot really be expected. The burning disc is merely a round sheet of metal, partly exposed to a colourless gas flame and partly dipping into an oil reservoir. Rotation of the disc about an axis through its centre and perpendicular to its plane brings new films of oil on to the surface which are periodically ignited and extinguished. 100 mg of deposit was usually accumulated in four hours when the oil clinging to the disc was ignited about twice a second.

The 'oscillating Smithells flame' (*Figure 8*) achieved analogous (though not as strikingly similar) results with fuels. Fuel is aspirated by air in a Beckman oxyhydrogen flame photometer burner. It is mixed with oxygen at the burner tip and above the tip in a resistance wire heated tube leading to the inner tube of a water-cooled condenser. This condenser constitutes the Smithells tube proper. Under equilibrium conditions a premixed flame is formed within it and a diffusion flame on its upper end. However, the oxygen flow rate was so adjusted as to periodically form and extinguish the inner and upper flames alternately. *Table 6* gives a comparison of properties of burner deposits to those from an engine operated on a corresponding fuel. The same trends appear although the actual values differ considerably.

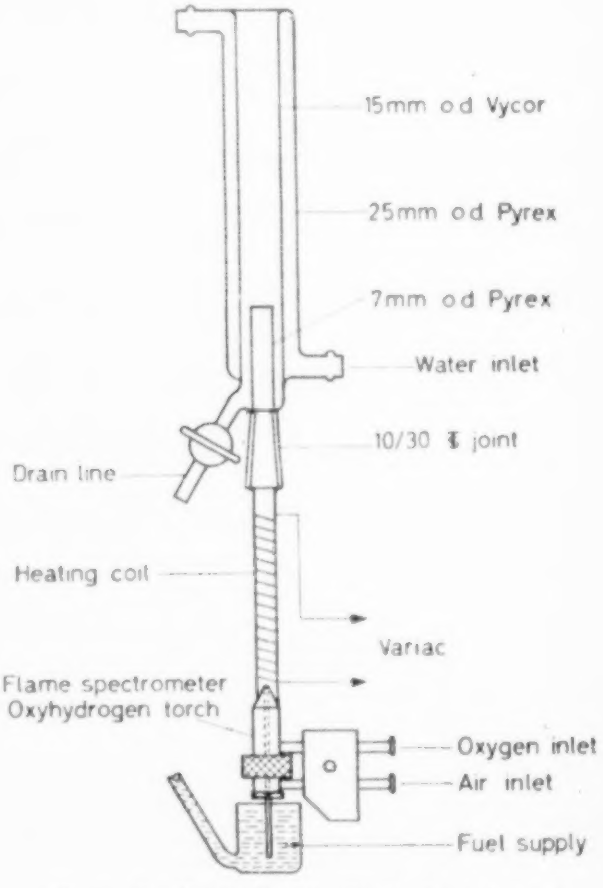
15mm o.d. Vycor
25mm o.d. Pyrex
7mm o.d. Pyrex
Water inlet
10/30 ₮ joint
Drain line
Heating coil
Variac
Flame spectrometer
Oxyhydrogen torch
Oxygen inlet
Air inlet
Fuel supply

Figure 8. Oscillating Smithells flame burner

Table 6. Comparison of properties of residues produced in the 'oscillating Smithells burner' to those of engine deposits

Fuel	*% O*	*Bulk density g/ml*	*Pyridine solubility wt %*
A. *Simulated deposits*			
Commercial clear	12·1	0·4	10
Benzene	4·5	0·3	5
B. *Engine deposits**			
Commercial clear	27	0·6	27
Toluene	20	0·2	14

*Paraffinic lube oil was used.

Concluding Remarks

Perhaps the most significant result of this (continuing) study is the similarity of the deposits formed from various starting materials. Engine deposits are definitely not just pyrolysed oils or fuels. A mechanism of 'oxidative pyrolysis' seems to underly deposit formation.

We thank Professor S. Mrozowski and his students at the University of Buffalo for the electron photomicrographs shown here. The staff of our Automotive Laboratory under Mr E. F. Marshall provided the engine data. Mrs A. R. Donnell of our Analytical Division made the spectroscopic analyses. Mr Paul Antal performed most of the experimental work. Their help is gratefully acknowledged.

References

[1] DUMONT, L. F. 'Possible mechanisms by which combustion-chamber deposits accumulate and influence knock'. *Trans. Soc. automot. Engrs, N.Y.* 1951, **5**, 565

[2] MIKITA, J. J. and STURGIS, B. M. 'Chemistry of combustion chamber deposits'. *Proceedings of the Fourth World Petroleum Congress* Section VI/F, pp 357–80. Rome, 1956

[3] BARTLESON, J. D. and HUGHES, E. C. 'Combustion chamber deposits as related to carbon-forming properties of motor oils. *Industr. Engng Chem.* (*Industr.*) 1953, **45**, 1501

[4] SPINDT, R. S., WOLFE, C. L. and STEVENS, D. R. 'Nitrogen oxides, combustion, and engine deposits'. S.A.E. Golden Anniversary Fuels and Lubricants Meeting, Philadelphia, 1955 (*Preprint No. 638*)

[5] WINSLOW, F. H., BAKER, W. O., PAPE, N. R. and MATREYEK, W. 'Formation and properties of polymer carbon'. *J. Polymer Sci.* 1955, **16**, 101

Studies of Combustion Processes Leading to Ignition in Hydrocarbons

K. C. SALOOJA

'Shell' Research Ltd, Thornton Research Centre, P.O. Box 1, Chester

(Received March 1959)

The extents of overall reaction at various temperatures preceding ignition and also the ignition temperature/concomitant lag relationships of a number of C_6–C_8 hydrocarbons have been studied in a quartz reaction chamber at atmospheric pressure. The hydrocarbons studied include n*-heptane, methylcyclohexane, isooctane, diisobutylene, benzene, toluene,* m*-xylene and ethylbenzene. Marked differences exist between hydrocarbons with regard to their extents of pre-flame reactions and ignition characteristics, and also with regard to the effect of fuel–air composition on these properties. As regards the pre-flame reactions the temperature at which a hydrocarbon first starts to react, the extent of reaction that it undergoes at different stages before ignition and the development of cool flames, if any, are characteristic features of each hydrocarbon. Studies of ignition characteristics reveal marked differences in the autogenous ignition tendencies of different fuels. The results which give a comprehensive account of the combustion characteristics help to coordinate a considerable amount of the existing diverse information on them.*

CONSIDERABLE work has already been done by various investigators on the oxidation of hydrocarbons in the pre-flame stages and on the measurement of minimum autogenous ignition temperatures. However, collation of the experimental evidence is difficult and the associated theoretical discussions are rather confusing. The reason is largely that different hydrocarbons have been studied by different workers under conditions that are not easily comparable.

For the measurement of the autogenous ignition temperature alone, the conditions adopted by various investigators during the last decade have been widely different[1–8]. The same is true of the larger volume of work on the pre-flame oxidation of various hydrocarbons. In both cases, different investigators have often obtained markedly different results for the same hydrocarbon.

Very little attention has been paid in most of the early work to the significance of the relationship between the autogenous ignition temperature of a hydrocarbon and the reactions that lead up to the stage at which ignition occurs. D. E. SWARTS and M. ORCHIN[9] have recently attempted to examine this relationship. But their results on pre-flame reactions were obtained under experimental conditions that bore no resemblance to those used for the determination of ignition temperatures; some of their pre-flame studies were carried out at higher temperatures than the autogenous ignition temperatures measured in a different apparatus.

To get a truer picture of how the pre-flame oxidation reactions lead up to ignition, it is desirable that such reactions should be studied in the same equipment and under similar conditions to those used for the measurement of ignition temperatures. With this objective in mind, equipment has been designed with which studies can be made of both the pre-flame reactions and the ignition phenomenon, and the effects of various factors influencing these processes can be examined.

The apparatus consists of a flow system in which a fuel–air mixture of desired composition is passed through a reaction chamber held at a uniform temperature inside a furnace. The temperature of the furnace is raised gradually and the onset of 'cool flame' and normal ignition phenomena observed visually through windows in the side of the furnace. The product gases,

Co
va
ca
mo
ter
mo
the
Th
ha
con

I
ign
ado
las
san
the
In
obt
san

V
of
rela
tem
that
occu
rece

Studies of Combustion Processes Leading to Ignition in Hydrocarbons

K. C. SALOOJA

'Shell' Research Ltd, Thornton Research Centre, P.O. Box 1, Chester

(Received March 1959)

The extents of overall reaction at various temperatures preceding ignition and also the ignition temperature/concomitant lag relationships of a number of C_6–C_8 *hydrocarbons have been studied in a quartz reaction chamber at atmospheric pressure. The hydrocarbons studied include* n*-heptane, methylcyclohexane, isooctane, diisobutylene, benzene, toluene,* m*-xylene and ethylbenzene. Marked differences exist between hydrocarbons with regard to their extents of pre-flame reactions and ignition characteristics, and also with regard to the effect of fuel–air composition on these properties. As regards the pre-flame reactions the temperature at which a hydrocarbon first starts to react, the extent of reaction that it undergoes at different stages before ignition and the development of cool flames, if any, are characteristic features of each hydrocarbon. Studies of ignition characteristics reveal marked differences in the autogenous ignition tendencies of different fuels. The results which give a comprehensive account of the combustion characteristics help to coordinate a considerable amount of the existing diverse information on them.*

CONSIDERABLE work has already been done by various investigators on the oxidation of hydrocarbons in the pre-flame stages and on the measurement of minimum autogenous ignition temperatures. However, collation of the experimental evidence is difficult and the associated theoretical discussions are rather confusing. The reason is largely that different hydrocarbons have been studied by different workers under conditions that are not easily comparable.

For the measurement of the autogenous ignition temperature alone, the conditions adopted by various investigators during the last decade have been widely different[1–8]. The same is true of the larger volume of work on the pre-flame oxidation of various hydrocarbons. In both cases, different investigators have often obtained markedly different results for the same hydrocarbon.

Very little attention has been paid in most of the early work to the significance of the relationship between the autogenous ignition temperature of a hydrocarbon and the reactions that lead up to the stage at which ignition occurs. D. E. SWARTS and M. ORCHIN[9] have recently attempted to examine this relationship. But their results on pre-flame reactions were obtained under experimental conditions that bore no resemblance to those used for the determination of ignition temperatures; some of their pre-flame studies were carried out at higher temperatures than the autogenous ignition temperatures measured in a different apparatus.

To get a truer picture of how the pre-flame oxidation reactions lead up to ignition, it is desirable that such reactions should be studied in the same equipment and under similar conditions to those used for the measurement of ignition temperatures. With this objective in mind, equipment has been designed with which studies can be made of both the pre-flame reactions and the ignition phenomenon, and the effects of various factors influencing these processes can be examined.

The apparatus consists of a flow system in which a fuel–air mixture of desired composition is passed through a reaction chamber held at a uniform temperature inside a furnace. The temperature of the furnace is raised gradually and the onset of 'cool flame' and normal ignition phenomena observed visually through windows in the side of the furnace. The product gases, after removal of condensable materials, are passed through infra-red carbon dioxide and carbon monoxide analysers. For all hydrocarbons, these oxides of carbon (mainly the monoxide) are the major products formed in the pre-ignition stages, and so measurements of their concentration at various temperatures provides an indication of the rate at which the hydrocarbon structure breaks down at various stages preceding ignition. The condensable products isolated in the cold traps can also be subjected to detailed analysis of the various intermediate products.

At the temperature at which ignition takes place, the value of the concomitant lag can be calculated from the residence time of the fuel–air mixture in the reaction chamber. Measurements of the minimum ignition temperature at different residence times provide information on the relationship between ignition temperature and the concomitant ignition lag.

The results described in this paper relate to the following eight typical C_6–C_8 hydrocarbons: *n*-heptane, methyl*cyclo*hexane, *iso*octane, di*iso*butylene, benzene, toluene, *m*-xylene and ethylbenzene. The purity of all these hydrocarbons was ascertained to be greater than 99 per cent by means of gas–liquid chromatographic and infra-red analysis. The present studies were carried out at atmospheric pressure and the data on the extent of pre-flame reactions are presented only in terms of the oxides of carbon formed. Work on detailed analysis of the various intermediate products, which is in hand, will be reported later.

Experimental

Reaction chamber

The reaction chamber was made of fused silica. It was of a conical shape with a re-entrant cone inside it (*Figure 1*). To maintain uniform temperature over the entire surface of the reaction chamber, two channels allowed the forced draught of hot air inside the furnace to flow along the surface of the inner cone as well. The volume of the reaction chamber was approximately 43 cm³ and its surface to volume ratio, about 3·3 cm⁻¹.

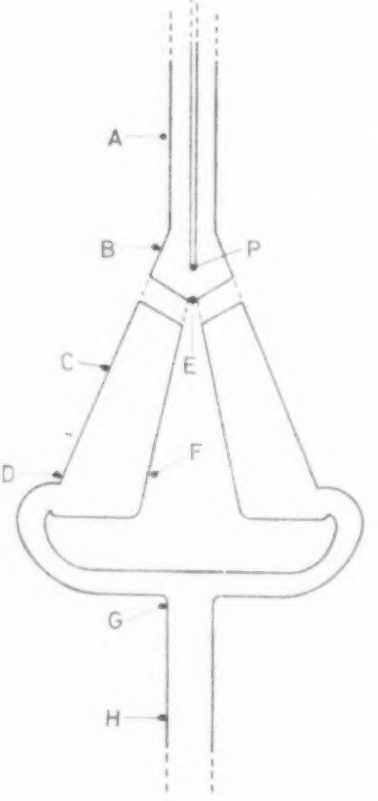

Figure 1. Reaction chamber and arrangement of thermocouples on it

Furnace

The design of the furnace used in these investigations is shown diagrammatically in *Figure 2*. The furnace provided a zone of uniform temperature around the reaction chamber and its temperature could be varied at a steady rate up to 800°C.

For the measurement of temperature, eight chromel/constantan thermocouples, A to H, arranged as shown in *Figure 1*, were attached to the reaction chamber. A platinum/platinum–rhodium thermocouple (P) in a narrow thin-walled silica sheath measured the temperature inside the reaction chamber.

Fuel and air supply

Fuel was injected into a stream of pre-heated air at a uniform rate by means of a mechanically operated syringe which was capable of providing flow rates ranging from about 0·001 cm³/sec to 0·010 cm³/sec.

An air flow rate of 20 cm³/sec at room

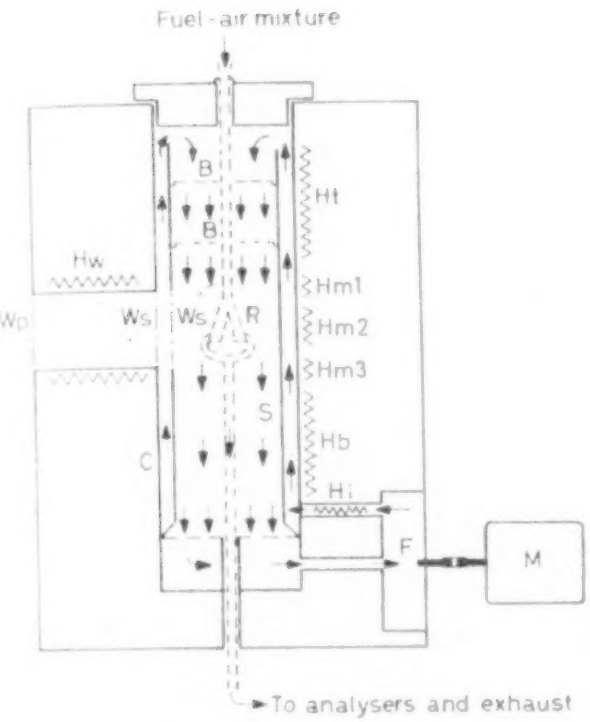

Figure 2. Diagram of furnace

C	*main furnace tube*	Ht	*top heater*
S	*stainless steel sleeve*	Hm 1, 2, 3	*middle heaters*
B	*baffle plates*	Hb	*bottom heater*
F	*impeller fan*	Hi	*Inconel heater in air stream*
M	*fan motor*		
Ws	*silica window*	Hw	*Window heater*
Wp	*Pyrex window*	R	*Reaction chamber*

temperature was selected for the present flow system studies as this was the most appropriate one for the eventual passage of the gases through the infra-red carbon monoxide and carbon dioxide analysers.

The air–fuel vapour mixture, before entering the reaction chamber, was passed through a mixing section maintained at a temperature a few degrees above the boiling point of the fuel.

Treatment of outgoing gases

The gases leaving the reaction chamber were passed through traps cooled by solid carbon dioxide in methylethylketone to condense out unconsumed hydrocarbon and condensable reaction products. The gases then passed through the carbon dioxide analyser and were subsequently freed of their carbon dioxide content by passing them through a tube packed with soda asbestos. The gases finally passed through the carbon monoxide analyser.

Results

Experiments were carried out with a number of different fuel–air mixtures with fuel concentration varying over the range 1·0 × stoichiometric to about 3·0 × stoichiometric. The overall pattern of the extent of reaction in terms of carbon monoxide and carbon dioxide was similar for all hydrocarbons; however, carbon dioxide was formed in much smaller amounts than carbon monoxide. Therefore, the results of the studies with different fuel–air mixtures have been presented mainly in terms of carbon monoxide formed. To indicate the relative amounts of carbon monoxide and carbon dioxide formed, the results in terms of carbon dioxide as well are presented for only one of the fuel–air mixtures studied, namely the 2·0 × stoichiometric mixture.

n-*Heptane*

The results on the overall extent of reaction at different temperatures up to the ignition point are shown in *Figures 3* and *4*. From the temperature of commencement of reaction (about 280°C) to about 420°C, reactions were accompanied by the appearance of cool flames. These could be visually detected in the richer fuel mixtures (>2·0 × stoichiometric). In the weaker mixtures cool flames were not easily visible but their presence could be inferred from the sudden rise in temperature on the thermocouple inside the reaction chamber over that on the surface of the chamber. This temperature difference gradually decreased at higher reaction chamber temperatures and nearly disappeared at about 450°C. Thereafter the temperature of the gas inside the chamber stayed close to the temperature of the surface of the chamber till very nearly the ignition temperature was reached.

At the start of the reaction, just before vigorous formation of the oxides of carbon set in, a drop in temperature of about 5° to 10°C was observed to take place in the gas phase. Soon after the appearance of oxides of carbon, however, the temperature began to rise and when cool flame appearance became prominent, a sharp rise in temperature occurred. The drop in the temperature in the gas phase at the

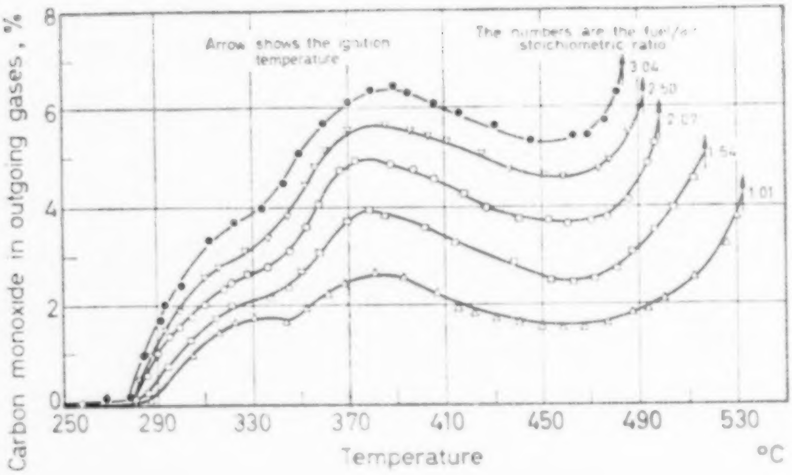

Figure 3. n-*Heptane pre-ignition reactions. Effect of temperature at various fuel concentrations on carbon monoxide production up to ignition point*

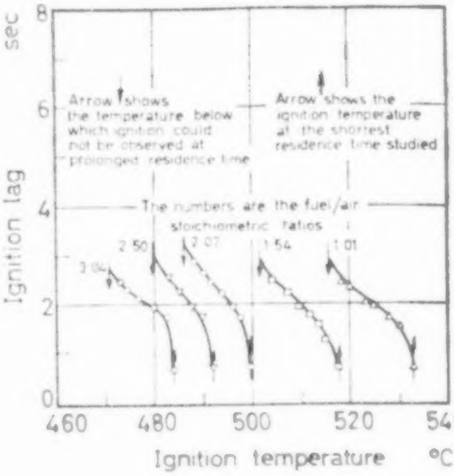

Figure 5. n-*Heptane. Ignition lag/temperature relationship for different concentrations of fuel in air*

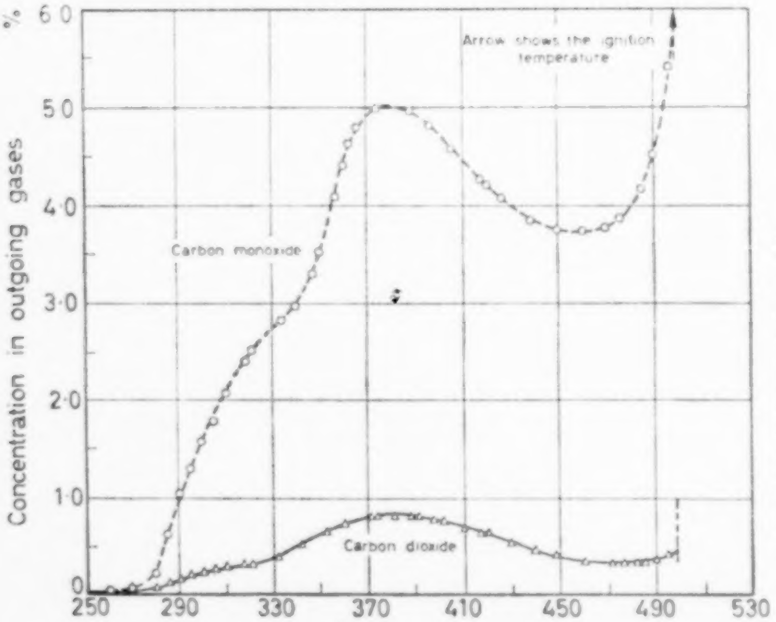

Figure 4. n-*Heptane–air mixture, 2 × stoichiometric, pre-ignition reactions. Relative concentrations of carbon dioxide and carbon monoxide formed at various temperatures up to the ignition point*

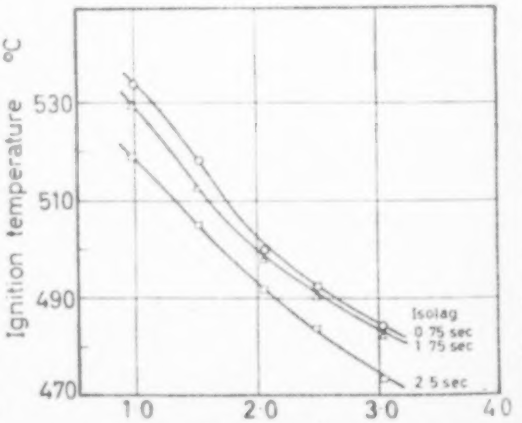

Figure 6. n-*Heptane. Effect of fuel concentration on ignition temperature under various isolag conditions*

commencement of the reaction provides evidence of the endothermic nature of the initial stage of oxidation[10].

The results obtained on the overall extent of oxidation of *n*-heptane at various temperatures preceding ignition agree well with the observations of H. A. BEATTY and G. EDGAR (in terms of oxygen consumed)[11] and of F. H. GARNER and D. S. PETTY (in terms of *n*-heptane consumed)[12] even though the experimental conditions and the method of investigation used by these investigators were widely different from the present ones.

The results on the variation of ignition lag with temperature for the different *n*-heptane–air mixtures are shown in *Figure 5*. The flames were pale blue in colour and were of feeble intensity, particularly with the weaker mixtures. The low intensity of the light emitted by the flames further diminished at lower temperatures, rendering it still more difficult to observe the onset of ignition, if any, near the minimum ignition temperature. Experiments were repeated a number of times and no ignition appeared to occur below the minimum ignition point indicated by arrows pointing downwards in *Figure 5*.

From the data in *Figure 5*, the variation of the ignition temperature with fuel concentration, for different sets of constant ignition lag, has been plotted in *Figure 6*. These results clearly show that increases in fuel concentration cause a marked reduction in the ignition temperature at different isolag conditions.

The values of the minimum ignition temperature obtained for various *n*-heptane–air mixtures, while they agree well with those reported by Beatty and Edgar, are very much higher than those determined by the other investigators in stainless steel crucibles or in glass vessels under static conditions. Most of the reported values lie around 250°C, a temperature which is nearly 25°C below the start of the 'cool flame' reaction region under the present conditions of experiment. The time of residence of the fuel–air mixture in the reaction chamber, under the present experimental conditions, at temperatures between 270° and 290°C is only about 0·9 sec, whereas the ignition at the reported temperatures of 250°C is accompanied by a delay of about 30 sec. This could partly account for the observed lower ignition temperatures and the reactions that precede such ignitions. Furthermore, from the reported fact that the minimum ignition temperatures in these cases were noted at the first sign of illumination in the fuel–air mixture and that the experiments were carried out in a dark room, it seems that the low values of minimum ignition temperature, reported earlier, correspond to that of the onset of the cool flame.

Methylcyclohexane

The results are presented in *Figures 7* to *10*. The general pattern of the overall extent of pre-flame reactions is similar to that of *n*-heptane. However, the initiation of the reaction in the cool flame zone occurred at a temperature about 30°C higher than with *n*-heptane, and there was a very much greater reduction in the rate of reaction in the subsequent region. As observed with *n*-heptane, there was a drop in temperature by 4° or 5°C in the gas phase over that on the surface of the chamber just before the vigorous reactions in the 'low temperature region' set in at about 310°C. This was followed by a sudden rise in temperature. The temperature difference between the body of the gas and the surface, however, diminished almost to nil when the temperature of the vessel went beyond 430°C.

The flames of different methyl*cyclo*hexane–air mixtures were brighter than those of the corresponding mixtures of *n*-heptane, and the ignition lag/temperature relationship for various mixtures of methyl*cyclo*hexane was found to extend over a wider range than with *n*-heptane. However, as in the case of *n*-heptane, increasing fuel concentration sharply lowered the ignition temperature.

The values of minimum ignition temperature for methyl*cyclo*hexane reported in the literature differ considerably. D. E. SWARTS and M. ORCHIN[9], and C. W. SORTMAN, H. A. BEATTY and S. D. HERON[13] measured the ignition temperatures in a 43 cm^3 stainless steel cup with pre-heated air flowing through it at the rate of 125 cm^3/min. Their values are 323° and

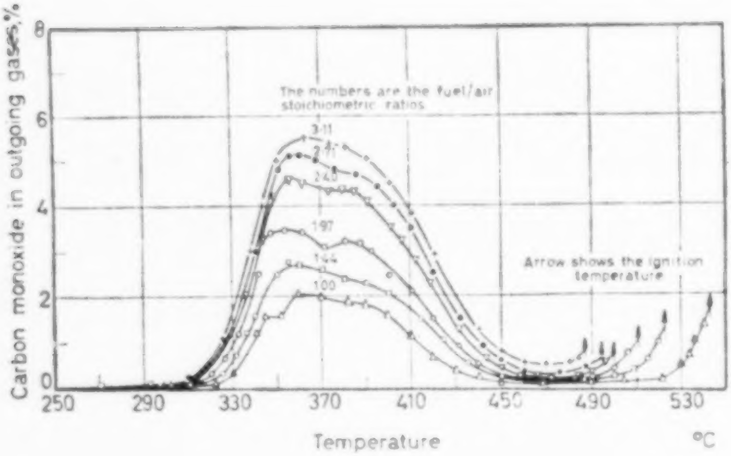

Figure 7. Methylcyclohexane pre-ignition reactions. Effect of temperature at various fuel concentrations on carbon monoxide production up to ignition point

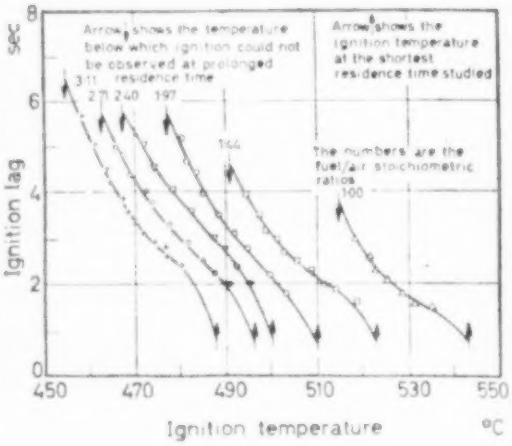

Figure 9. Methylcyclohexane. Ignition lag/temperature relationship for different concentrations of fuel in air

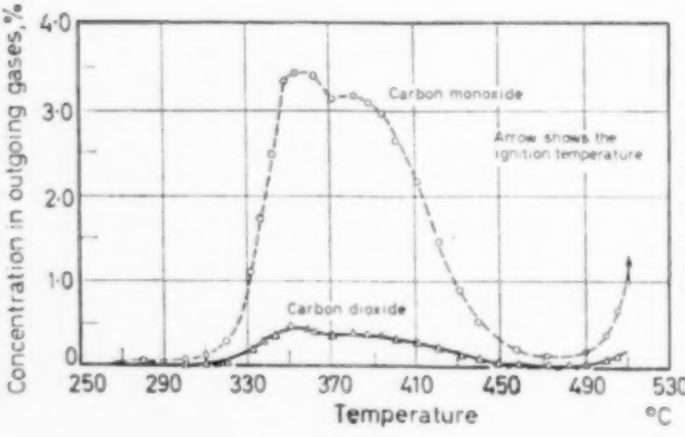

Figure 8. Methylcyclohexane–air mixture, 2 × stoichiometric, pre-ignition reactions. Relative concentrations of carbon dioxide and carbon monoxide formed at various temperatures up to ignition point

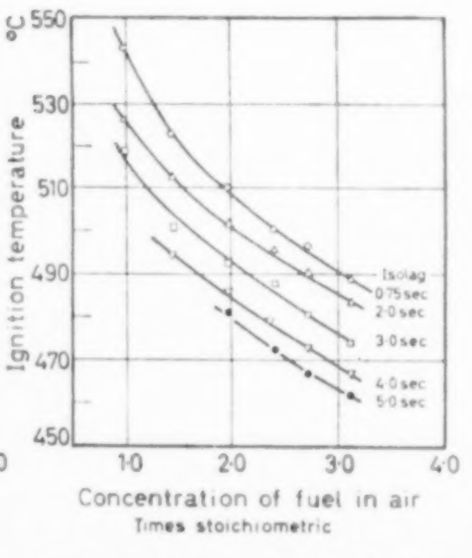

Figure 10. Methylcyclohexane. Effect of fuel concentration on ignition tempreature under various isolag conditions

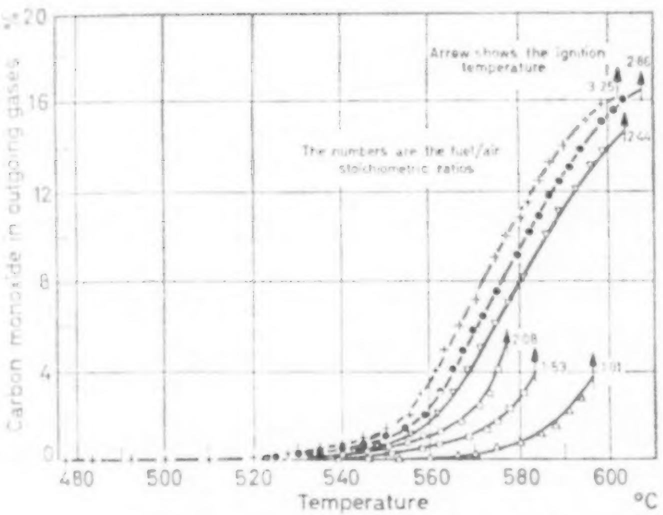

Figure 11. iso*Octane pre-ignition reactions. Effect of temperature at various fuel concentrations on carbon monoxide production up to ignition point*

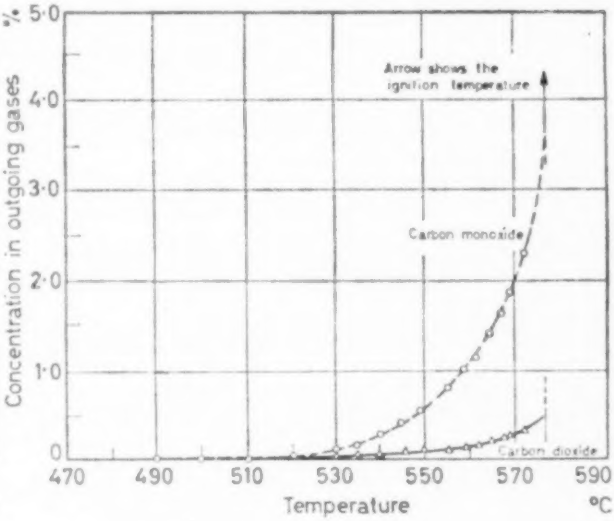

Figure 12. iso*Octane–air mixture, twice stoichiometric, pre-ignition reactions. Relative concentrations of carbon dioxide and carbon monoxide formed at various temperatures up to ignition point*

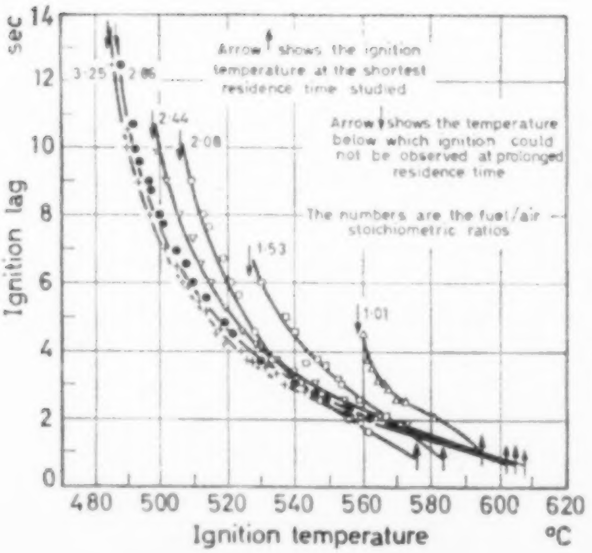

Figure 13. iso*Octane. Ignition lag/temperature relationship for different concentrations of fuel in air*

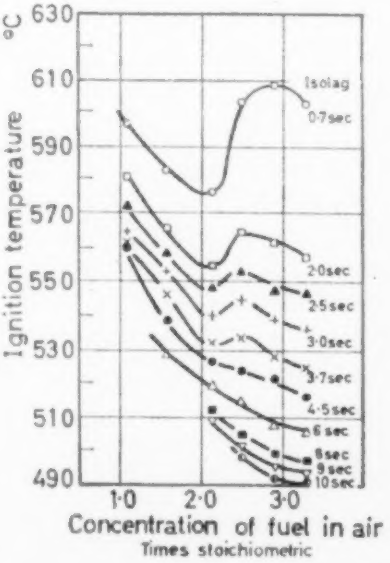

Figure 14. iso*Octane. Effect of fuel concentration on ignition temperature under various isolag conditions*

393·3°C respectively. J. L. JACKSON[6] reported a value of 265°C with an accompanying ignition lag of 108 sec from his experiments in a 125 cm^3 conical flask. All these values, as in the case of *n*-heptane, are much lower than those found in the present experiments and most probably, again, pertain to the appearance of cool flames.

The extent of overall reaction at different temperatures in the pre-flame stage as measured under the present conditions in terms of carbon monoxide and carbon dioxide produced, compares well with the observations of Garner and Petty[12] in terms of methyl*cyclo*hexane and oxygen consumed even though their experiments were carried out under different conditions.

iso*Octane*

The results are shown in *Figures 11* to *14*. Unlike *n*-heptane and methyl*cyclo*hexane, there was no reaction whatsoever in the cool flame region between 300° and 420°C and the temperature of the gases inside the reaction chamber stayed very nearly at the same level as that on the surface of the chamber.

The ignition temperature dropped as the fuel concentration was increased from 1·0 to 2·0 × stoichiometric. On further increasing the fuel concentration, however, the ignition was found to be strongly retarded even though the extent of reaction, as indicated by formation of the oxides of carbon, gradually increased (*Figure 11*).

The effect of fuel concentration on ignition temperature showed marked changes with variation in isolag conditions (*Figure 14*). The tendency for the ignition temperature to rise sharply between 2·0 and 2·5 × stoichiometric concentration at short residence times decreased at longer residence times. At ignition lags of approximately 4·5 sec and longer, the ignition temperature continued to fall even in mixtures richer than 2·0 × stoichiometric. The lowest ignition temperature observed under the present experimental conditions was 486°C with a concomitant lag of 12·5 sec for a 3·25 × stoichiometric mixture (*Figure 13*).

The reported values of the minimum ignition temperature for *iso*octane vary considerably. These have been recorded in *Table 1* along with a brief description of the experimental conditions used for their determinations.

The variation in the values of ignition temperature is particularly large in those cases where they have not been obtained under similar experimental conditions. This variation, as has already been pointed out by Swarts and Orchin, is largely attributable to the differences in the ratio of surface to volume of the reaction chambers used.

No direct information seems to be available in the literature on the extent of overall oxidation reaction at various temperatures up to ignition. The earlier work[14, 15] refers mainly to the attempts made to identify the various reactive intermediates formed in the slow combustion region under particular experimental conditions. Frank and Blackham, however, have shown that, in the 'low temperature reaction zone' wherein *n*-heptane undergoes a considerable amount of oxidation, there is hardly any reaction detectable with *iso*octane.

Di*isobutylene*

The results are presented in *Figures 15* to *18*. Like *iso*octane, di*iso*butylene showed no trace of cool flame activity. However, in contrast with *iso*octane, the di*iso*butylene–air mixtures ignited at lower temperatures, the richer mixtures ignited more readily than the weaker ones, increase in residence time had considerably less effect on the ignition temperature, and the extent of reaction preceding ignition was markedly smaller.

The present observation that di*iso*butylene–air mixtures ignite at lower temperatures than the corresponding *iso*octane–air mixtures is in line with the reported[2] values of ignition temperature, viz. 470°C for di*iso*butylene as against 518°C for *iso*octane.

F. H. GARNER, R. LONG and G. A. WEBSTER[16], who have studied the vapour phase oxidation of di*iso*butylene and *n*-heptane in a stainless steel reaction tube (1¼ in. diameter, 10 in. long) by following the concentration of peroxides, carbonyls and acids formed at various temperatures, have shown that compared with *n*-heptane, di*iso*butylene does not give rise to a zone of vigorous reaction in the 'low tempera-

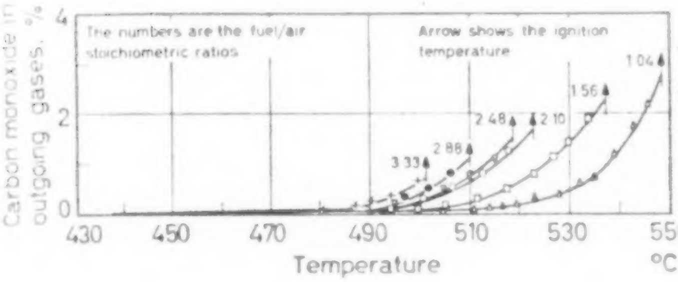

Figure 15. Diisobutylene pre-ignition reactions. Effect of temperature at various fuel concentrations on carbon monoxide production up to ignition point

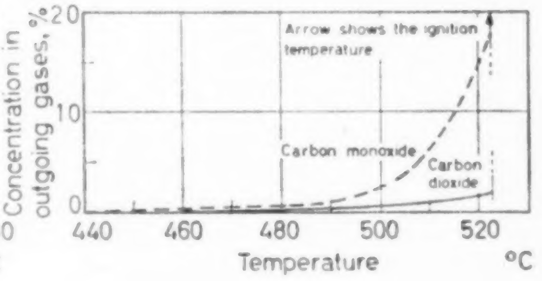

Figure 16. Diisobutylene–air mixture, twice stoichiometric, pre-ignition reactions. Relative concentrations of carbon dioxide and carbon monoxide formed at various temperatures up to ignition point

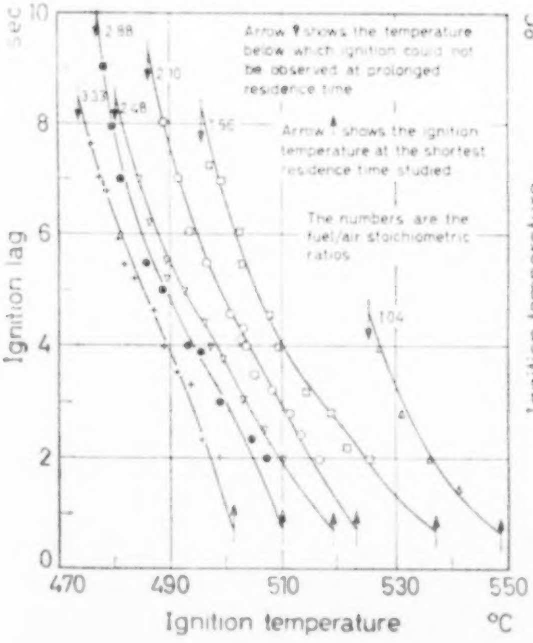

Figure 17. Diisobutylene ignition lag/temperature relationship for different concentrations of fuel in air

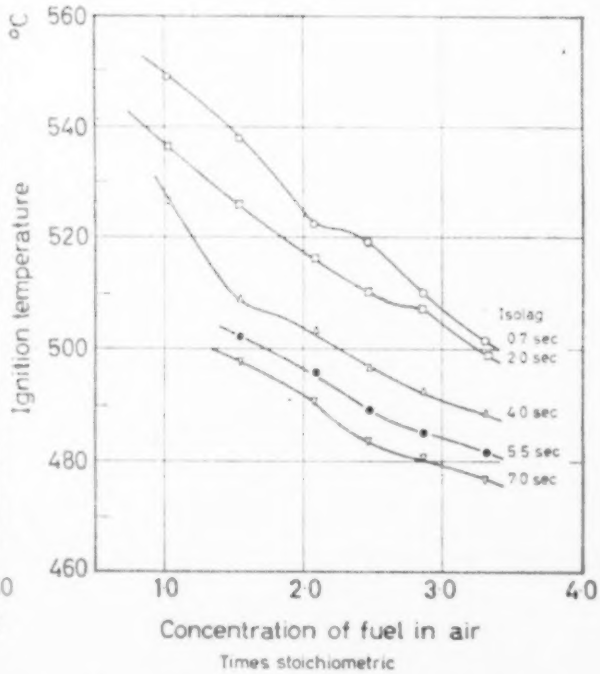

Figure 18. Diisobutylene. Effect of fuel concentration on ignition temperature under various isolag conditions

Table 1. Reported determinations of minimum autogenous ignition temperature of isooctane

Reference	*Reaction vessel*				*Air flow* cm^3/min	*Minimum autogenous ignition temp.* °*C*	*Time lag before ignition sec*
	Size cm^3	*Shape*	*Surface/Volume* cm^{-1}	*Material*			
Sortman, Beatty and Heron[13]	43	*Cylinder*	1·55	*Stainless steel*	125	529·4	—
Swarts and Orchin[9]	43	*Cylinder*	1·55		125	515	—
Frank, Blackham and Swarts[2]	43	*Cylinder*	1·55		125	518	—
Frank and Blackham[1]	43	*Cylinder*	1·55		125	515	—
					25	502	—
Scott, Jones and Scott[5]	125	*Erlenmeyer flask*	1·14	*Borosilicate glass*	*Nil*	434	20
Jackson[6]	125	*Erlenmeyer flask*	1·14	*Borosilicate glass*	*Nil*	447	12
Zabetakis, Furno and Jones[7]	200	*Erlenmeyer flask*	0·98	*Quartz*	*Nil*	418	27

ture region' and that the concentration of oxidation products remains very small up to a temperature of about 450°C.

That di*iso*butylene undergoes less reaction in the pre-flame stage than *iso*octane and that both these hydrocarbons suffer much less reaction than *n*-heptane even under the complex conditions existing in an internal combustion engine has been clearly shown by the work of A. J. PAHNKE, P. M. COHEN and B. M. STURGIS[17]. They studied the pre-flame oxidation reactions of these hydrocarbons in a motored engine by following the concentrations of intermediate products formed—peroxides, carbonyls and unsaturates—as a function of the peak-cycle temperatures. Their results, which were presented separately for each hydrocarbon, have been replotted on the same graph in *Figure 19*, and exhibit a marked similarity to those for the extent of pre-flame reactions observed under the present conditions.

Benzene

The results are shown in *Figures 20* to *23*. The ignition temperatures were well above those for *n*-heptane, methyl*cyclo*hexane, di*iso*butylene and *iso*octane. No carbon monoxide could be detected in the outgoing gases till the temperature was about 600°C and its concentration even for the richest mixture studied did not exceed 0·1 per cent till the temperature was well over 650°C.

The values of ignition temperature of benzene reported by earlier workers vary a good deal amongst themselves. These values, along with the details of experimental conditions under which they were obtained, have been tabulated in *Table 2*. The variation in the values of ignition temperatures, as pointed out by Setchkin, and by Swarts and Orchin, can be attributed largely to the changes in the surface/volume ratio of the reaction chamber used.

Toluene

The results are presented in *Figures 24* to *27*. As with benzene, there was no sign of a reaction in the cool flame region and the concentration of carbon monoxide, even for the richest mixture studied, remained below 0·1 per cent up to 630°C. The ignition characteristics of toluene

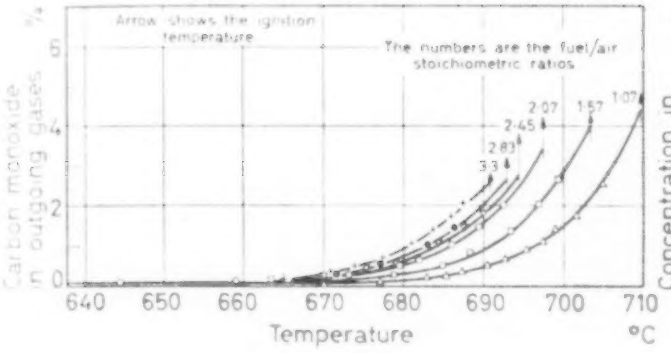

Figure 20. Benzene pre-ignition reactions. Effect of temperature at various fuel concentrations on carbon monoxide production up to ignition point

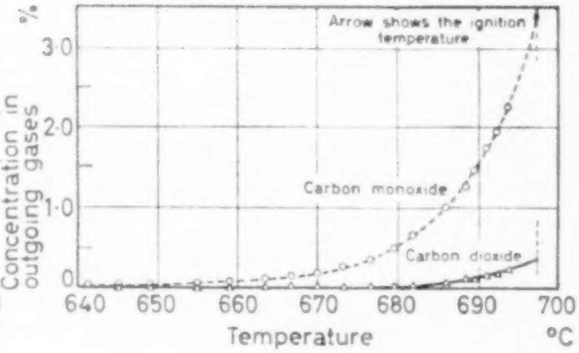

Figure 21. Benzene–air mixture, twice stoichiometric, pre-ignition reactions. Relative concentrations of carbon dioxide and carbon monoxide formed at various temperatures up to ignition point

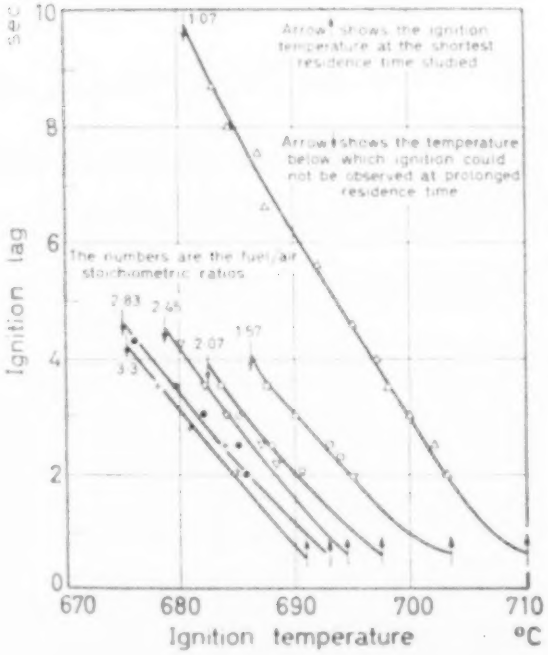

Figure 22. Benzene. Ignition lag/temperature relationship for different concentrations of fuel in air

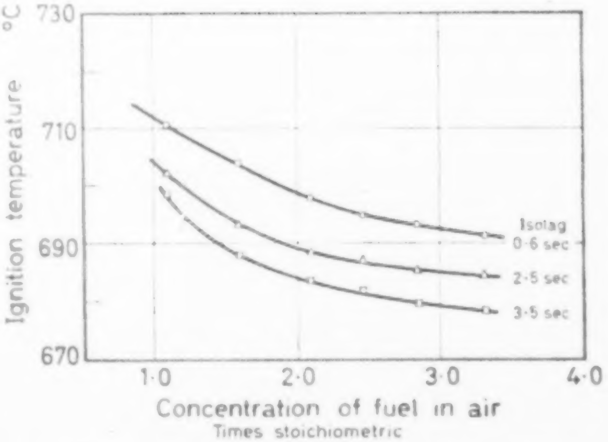

Figure 23. Benzene. Effect of fuel concentration on ignition temperature under various isolag conditions

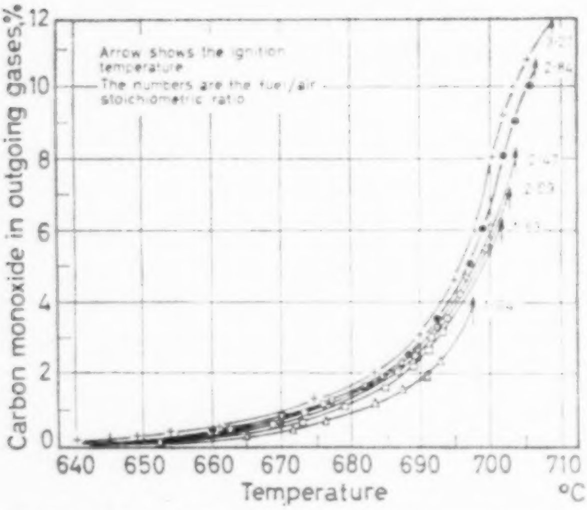

Figure 24. Toluene pre-ignition reactions. Effect of temperature at various fuel concentrations on carbon monoxide production up to ignition point

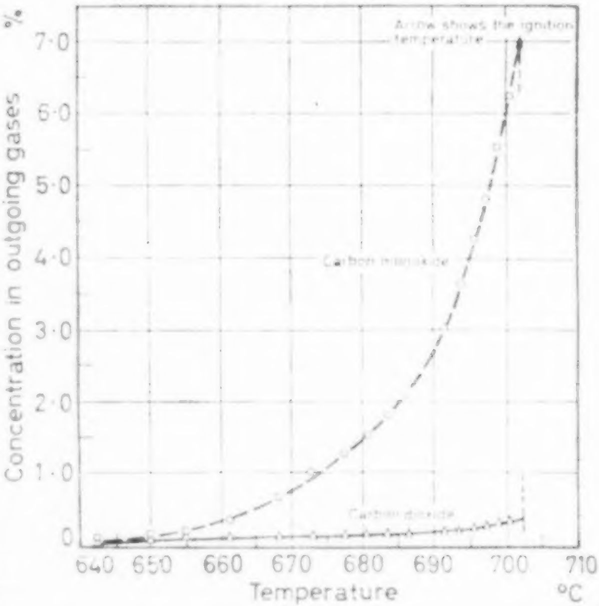

Figure 25. Toluene–air mixture, twice stoichiometric, pre-ignition reactions. Relative concentrations of carbon dioxide and carbon monoxide formed at various temperatures up to ignition point

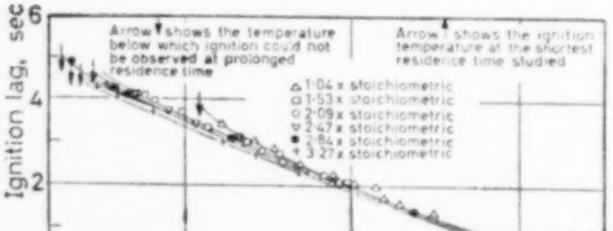

Figure 26. Toluene. Ignition lag/temperature relationship for different concentrations of fuel in air

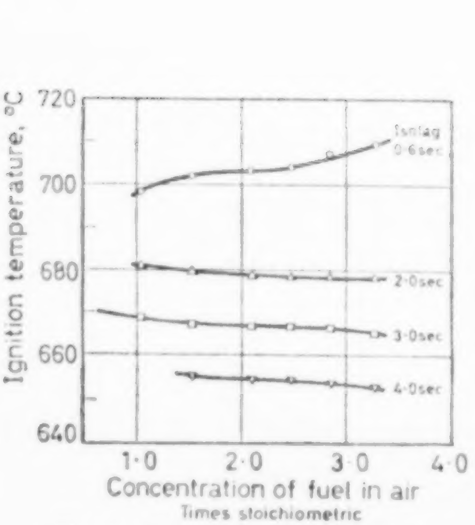

Figure 27. Toluene. Effect of fuel concentration on ignition temperature under various isolag conditions

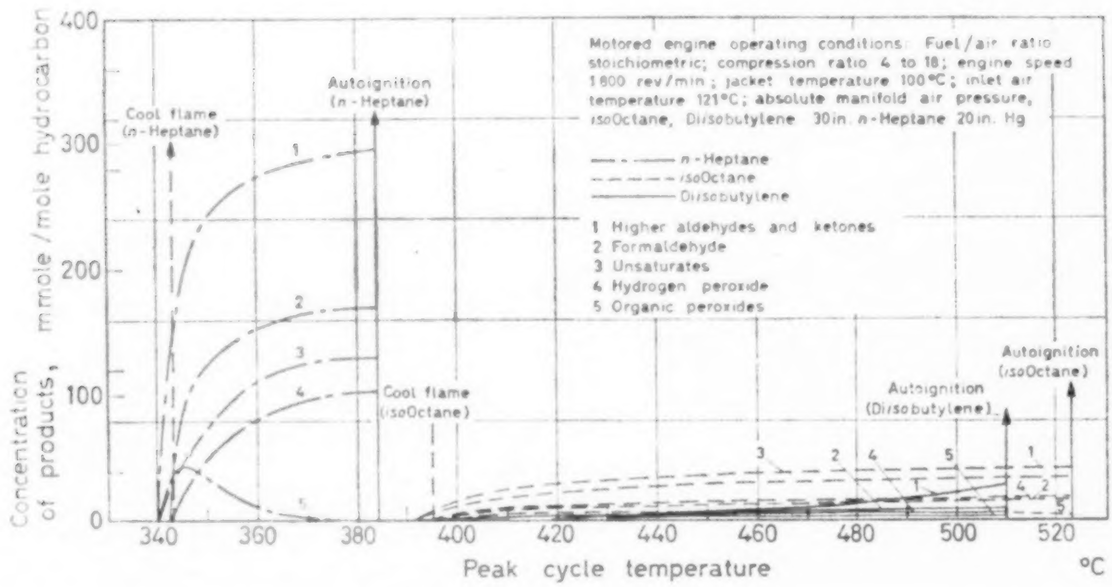

Figure 19. Pre-flame oxidation of n*-heptane,* isooctane *and* diisobutylene *in a motored engine* (*after* A. J. Pahnke, P. M. Cohen *and* B. M. Sturgis[17])

differ markedly from those of benzene. The ignition temperature for toluene–air mixtures at short residence times rises steadily with fuel concentration. This occurs in spite of the fact that the richer mixtures are undergoing far more reaction than the weaker ones. At higher residence times, this tendency for the ignition temperature to rise with increasing fuel concentration diminishes gradually and eventually at residence times greater than about two seconds the ignition temperature begins to fall with increasing fuel concentration. For any given fuel–air mixture, the fall in ignition temperature with increasing residence time is greater in the case of toluene than for benzene and at longer residence times toluene–air mixtures ignite at much lower temperatures than the corresponding benzene–air mixtures. The earlier investigators, who determined the lowest ignition temperatures with the longest possible lags (*Table 2*), observed that toluene ignited at lower temperatures than benzene.

m-*Xylene*

The results are presented in *Figures 28* to *31*. As with benzene and toluene, there was no indication of cool flame reactions with *m*-xylene. The ignition characteristics resembled those of toluene, however; the effect of fuel concentration, in particular, was more pronounced.

Widely varying values of minimum ignition temperature have been reported in the literature (*Table 2*). Those investigators[1, 13] whose equipment necessitated the determination of ignition temperatures at higher temperature levels and hence presumably, at correspondingly lower ignition lags, have found *m*-xylene to ignite at higher temperatures than toluene and benzene; on the other hand, those[6, 7] who carried out the estimation in a lower temperature range, and at consequently longer ignition lags, found *m*-xylene to have a minimum ignition temperature lower than those for toluene and benzene. The reason for such diversity of observations of earlier investigators can be easily understood in the light of the present data.

Ethylbenzene

The results are shown in *Figures 32* to *35*. An interesting feature of the results with ethylbenzene is that it ignites at much lower temperatures than the other aromatics studied. However, as with the other aromatics, there is no indication of cool flame reactions.

Increasing fuel concentration causes marked lowering of ignition temperature at all values

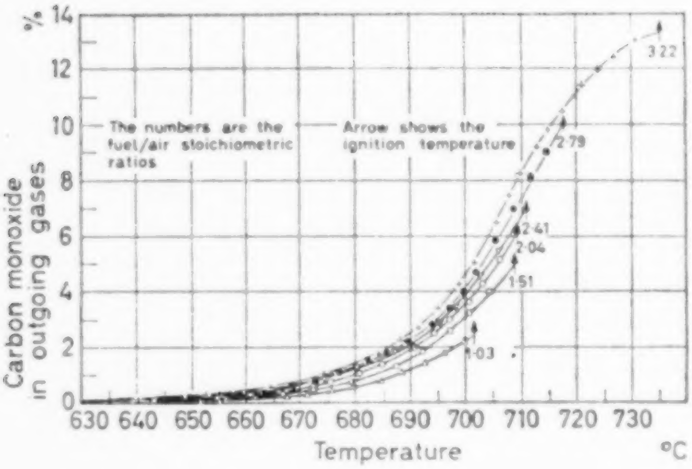

Figure 28. m-*Xylene pre-ignition reactions. Effect of temperature at various fuel concentrations on carbon monoxide production up to ignition point*

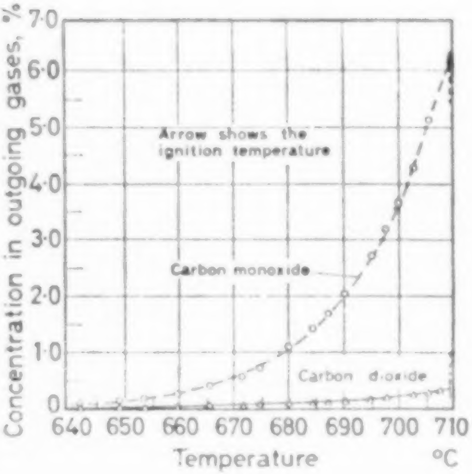

Figure 29. m-*Xylene–air mixture, twice stoichiometric, pre-ignition reactions. Relative concentrations of carbon dioxide and carbon monoxide formed at various temperatures up to ignition point*

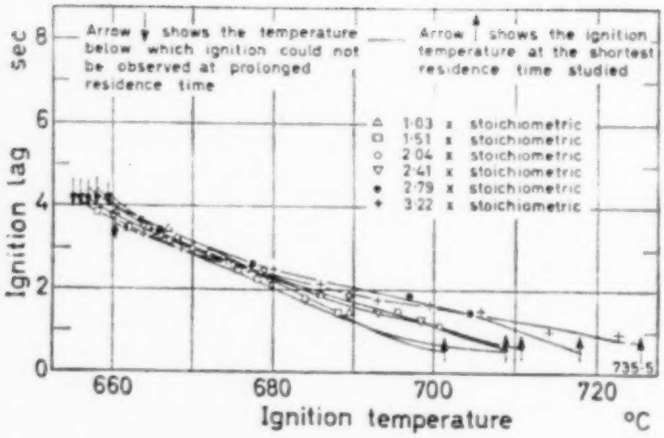

Figure 30. m-*Xylene. Ignition lag/temperature relationship for different concentrations of fuel in air*

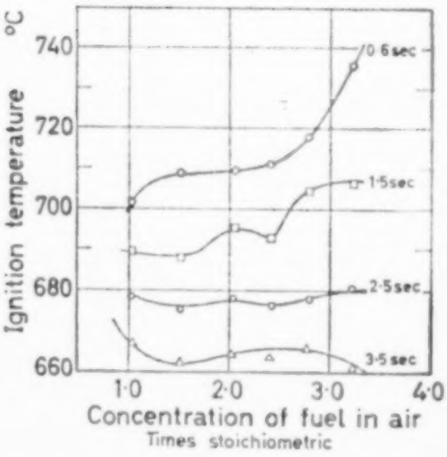

Figure 31. m-*Xylene. Effect of fuel concentration on ignition temperature under various isolag conditions*

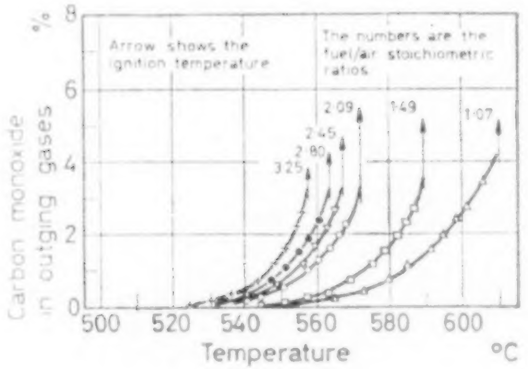

Figure 32. Ethylbenzene pre-ignition reactions. Effect of temperature at various fuel concentrations on carbon monoxide production up to ignition point

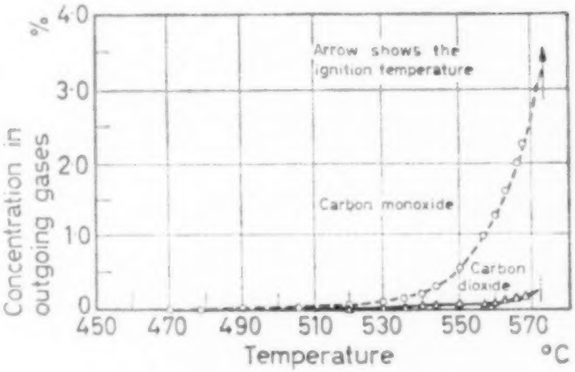

Figure 33. Ethylbenzene–air mixture, twice stoichiometric, pre-ignition reactions. Relative concentrations of carbon dioxide and carbon monoxide formed at various temperatures up to ignition point

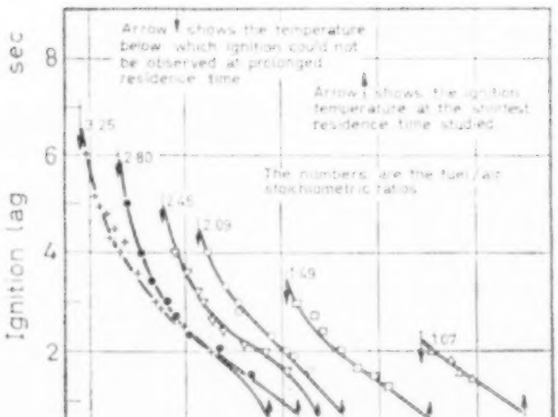

Figure 34. Ethylbenzene. Ignition lag/temperature relationship for different concentrations of fuel in air

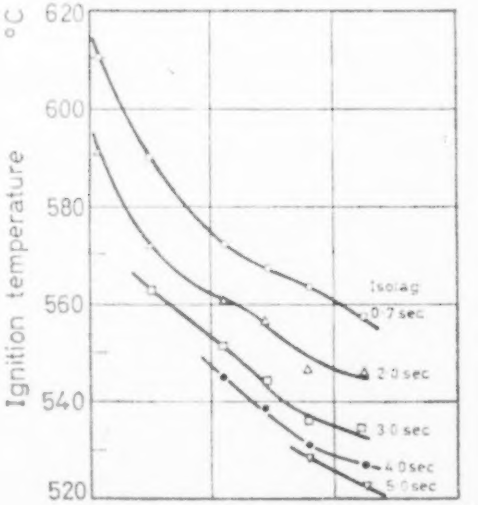

Figure 35. Ethylbenzene. Effect of fuel concentration on ignition temperature under various isolag conditions

Table 2. Reported determinations of minimum autogenous ignition temperatures of benzene, toluene, m-*xylene and ethylbenzene*

Reference	Reaction vessel				Air flow cm³/min	Benzene		Toluene		m-Xylene		Ethylbenzene	
	Size cm³	Shape	Surface/Volume cm⁻¹	Material		Ignition temp. °C	Ignition lag sec	Ignition temp. °C	Ignition lag sec	Ignition temp. °C	Ignition lag sec	Ignition temp. °C	Ignition lag sec.
Sortman, Beatty and Heron[13]	43	*Cylinder*	1·55	*Stainless steel*	125	651·7	—	629·4	—	688·9	—	—	—
Sullivan, Wolfe and Zisman[18]	43	*Cylinder*	1·55		125	701·7	—	—	—	—	—	—	—
Frank and Blackham[1]	43	*Cylinder*	1·55		125 25	645 639	— —	635 630	— —	652 645	— —	— —	— —
Jackson[6]	125	*Erlenmeyer flask*	1·14	*Borosilicate glass*	*Nil*	592	42	568	48	563	54	460	18
Thompson[19]	125	*Round flask*	0·97	*Pyrex*	*Nil*	580	—	—	—	—	—	—	—
	150	*Erlenmeyer flask*	1·08	*Pyrex*	*Nil*	582	—	552	—	—	—	—	—
	150	*Round flask*	0·91	*Pyrex*	*Nil*	580	—	553	—	—	—	—	—
Zabetakis, Furno and Jones[7]	200	*Erlenmeyer flask*	0·98	*Quartz*	*Nil*	562	32	536	72	528	61	432	18
Setchkin[8]	8	*Round flask*	2·42	*Quartz*	*Nil*	668	—	649	—	—	—	—	—
	35	*Round flask*	1·47	*Quartz*	*Nil*	619	—	584	—	—	—	—	—
	200	*Round flask*	0·83	*Quartz*	*Nil*	579	65	538	45	—	—	—	—
	1 000	*Round flask*	0·48	*Quartz*	*Nil*	559	48	519	55	—	—	—	—
	12 000	*Round flask*	0·21	*Quartz*	*Nil*	—	—	482	220	—	—	—	—

of isolags studied and this effect is even more marked than that in the case of benzene.

That ethylbenzene ignites at much lower temperatures than *m*-xylene, toluene or benzene, has been observed by the earlier workers (*Table 2*).

The present work on benzene and its alkyl derivatives (toluene, *m*-xylene and ethylbenzene) enables these hydrocarbons to be compared directly amongst themselves and with other hydrocarbons studied, in regard to their ignition temperatures and the extent of overall reaction that they undergo at various stages in the pre-flame region, under similar experimental conditions. The work of other investigators on aromatic hydrocarbons points to similar conclusions, although an exact comparison is not possible since the experimental conditions used by others have been so widely different. Thus, for instance, in their recent (1956) work R. G. W. NORRISH and G. W. TAYLOR[20, 21] have studied the combustion of benzene in a flow system at atmospheric pressure in a 23 cm long and 2 cm diameter quartz vessel and that of toluene and ethylbenzene in a static system in a 700 ml capacity quartz spherical vessel. J. H. BURGOYNE[22], and J. H. BURGOYNE, T. L. TANG and D. M. NEWITT[23] determined the pressure/temperature ignition curves for benzene, toluene and ethylbenzene at sub-atmospheric pressures in a 500 ml capacity quartz spherical vessel and found the relative order of reactivity towards oxidation and ignition to be ethylbenzene > toluene > benzene. No information, however, was given on the combustion of *m*-xylene under these conditions. Experiments on *m*-xylene were carried out in a 500 ml stainless steel bomb at higher than atmospheric pressures, ranging from 3 to 13 atmospheres, under which conditions it was found to be more reactive than the other hydrocarbons.

Discussion

The present investigations encompassing a study of pre-flame reactions as well as ignition characteristics under similar experimental conditions in the same apparatus have thrown light on various aspects of the combustion phenomenon.

In most of the earlier work on the measurement of ignition temperatures, fuel–air mixtures were neither uniform nor of a known overall composition. That the variation in fuel–air composition has a great influence on the ignition temperatures, and that the exact relationship is indeed a characteristic one for each hydrocarbon, has become evident from the present studies.

In some of the earlier work, ignition temperatures for hydrocarbons have been reported without mention of the concomitant ignition lags. It is clear that, for any fuel–air mixture, the ignition temperature and the concomitant lag have to be considered together. Any change in one affects the other. The ignition temperature alone, without reference to its concomitant lag, is therefore almost meaningless.

In the present work, results have been obtained on the relationship between ignition temperature and the ignition lag for a number of hydrocarbons at different fuel/air concentrations. These results have shown that the exact nature of this relationship is characteristic for each hydrocarbon.

The most marked feature of each hydrocarbon with respect to its ignition temperature/lag relationship, however, is the effect of the variation of the fuel concentration. For any hydrocarbon, not only does the ignition temperature vary as the fuel concentration is changed at any one particular lag, but also the effect is quite different at different lags. At sufficiently long ignition lags (residence time in the reaction chamber) all hydrocarbons tend to ignite at lower temperatures as their concentration in air is increased. At shorter residence times in the reaction chamber, however, marked differences in the behaviour of the individual hydrocarbons begin to appear, as the concentration of the fuel in air is varied over the same range as before.

For benzene, ethylbenzene, di*iso*butylene, methyl*cyclo*hexane and *n*-heptane, the effect of increasing fuel concentration at short reaction times is to lower the ignition temperature, although the steepness of the drop in ignition temperature with rising concentration is different in each case.

On the other hand, with toluene and *m*-xylene, the ignition temperature is raised as the fuel concentration is increased, whereas with *iso*octane the increase in ignition temperature sets in only when the fuel concentration is increased beyond twice stoichiometric. This tendency of the richer mixtures to ignite at higher temperatures than the weaker ones at short lag conditions becomes progressively less pronounced with longer time lags, until eventually the effect involves a reduction in the ignition temperature with increasing fuel concentration (within the limits investigated).

The concept of the relative resistance of pre-flame reactions to self-ignition

The results on the ignition temperature/concomitant lag relationship and the way in which changes in the fuel concentration affect this relationship for different hydrocarbons, lead one to consider the relative resistances of the pre-flame reactions of different hydrocarbons to self-ignition. The characteristics which reflect these resistances are:

(*1*) the slope of the ignition temperature versus lag curves, and

(*2*) the effect of fuel concentration on ignition temperature at different reaction times.

For instance, comparison of the ignition temperature/lag relationships for *iso*octane, ethylbenzene and di*iso*butylene shows that the resistance of the pre-flame reactions towards ignition must be highest for *iso*octane. To reduce the ignition lag of *iso*octane from four to two seconds, the temperature has to be raised by 28° at about 520°C, whereas, for a similar reduction in ignition lag of ethylbenzene, the temperature needs to be raised by only 13° at 525°C and with di*iso*butylene by only 11° and that moreover at a much lower temperature level, about 490°C.

Examination of the effect of varying fuel concentration on the ignition temperature of these hydrocarbons at different isolag conditions again leads to the conclusion that the resistance of the pre-flame reactions towards ignition must be highest for *iso*octane. At relatively short ignition lags, increase in fuel concentration above twice stoichiometric causes a marked increase in the ignition temperature of *iso*octane, whereas with ethylbenzene and di*iso*butylene it leads to a significant lowering of the ignition temperature.

The increase in ignition temperature with *iso*octane occurs in spite of the relatively much greater extent of overall pre-flame reaction that it undergoes in comparison with the other two hydrocarbons. Thus, it is the relative stability of the pre-flame reactions towards ignition, rather than the resistance of the basic structure of the fuel to chemical attack, that influences the proneness of a hydrocarbon to self-ignition.

Under the conditions of shortest residence time, the increase in the ignition temperature of *iso*octane is the highest observed, but this increase diminishes as the residence time is gradually increased. Eventually, when sufficiently long residence time has been allowed, there is no longer an increase in ignition temperature but only a continuous fall. Interpreting these data in terms of the relative stability of the pre-flame reactions, it appears that when the reaction time allowed is short in comparison with the life period of the intermediate reaction stage, the temperature required to bring about ignition has to be raised. When the time allowed for reaction is longer, ignition takes place more readily, that is at lower temperatures.

Amongst benzene, toluene and *m*-xylene, the last two have a much wider range of ignition temperature than benzene within the same ignition lag limits. Increasing the fuel concentration, particularly at shorter reaction times, causes an increase in the ignition temperature of toluene and even more so in that of *m*-xylene, whereas that of benzene is lowered appreciably. As longer reaction times are allowed, the ignition temperatures of the richer mixtures of toluene and *m*-xylene rise less steeply with increasing fuel concentration until eventually, at sufficiently long reaction times, they tend to fall. From these observations it is concluded that the relative resistances of the pre-flame reactions for these hydrocarbons are in the following decreasing order: *m*-xylene > toluene > benzene.

Of these, benzene, which has the lowest

stability in its pre-flame reaction stage towards ignition, has the highest stability of its parent structure. The first sign of a reaction between benzene and air appears at a higher temperature than it does with toluene or *m*-xylene. That the stability of the parent molecule does not directly reflect the stability of the pre-flame reactions towards ignition has been observed before while considering the behaviour of *iso*-octane. Furthermore, it is obvious that a simple comparison of the minimum autogenous ignition temperatures of hydrocarbons does not by itself give an indication of this important hydrocarbon characteristic. The relative resistance of the pre-flame reactions to ignition is indeed an independent characteristic of each hydrocarbon, and a knowledge of this is essential for judging the relative ignition qualities of different hydrocarbons.

Ignition characteristics and pre-flame reactions

In order to understand the fundamental factors responsible for ignition which result in such wide differences in the ignition characteristics of different hydrocarbons, it is necessary to know the chemical processes that take place in fuel–air mixtures at various stages preceding ignition. The investigations carried out so far on the overall extent of reactions at various pre-flame stages have already shown that vast differences do exist between hydrocarbons. Some hydrocarbons start reacting vigorously—giving rise to cool flames—well below their normal ignition temperatures, while others react only a little before igniting. The temperature at which a hydrocarbon first starts to react, and the extent of reaction that it undergoes before ignition, are as much a characteristic feature of each hydrocarbon as the ignition temperature and other ignition properties.

Swarts and Orchin have generalized that the greater the extent of pre-flame reaction, the greater is the ease with which a hydrocarbon ignites. This generalization can only hold on a very broad basis. For instance, normal ignition in the case of methyl*cylco*hexane takes place in the same temperature range as that of di*iso*butylene, yet the extent of the overall pre-flame reactions in the two cases is vastly different. Again, the richer fuel–air mixtures in all hydrocarbons examined undergo a greater amount of pre-flame reaction than the weaker ones, yet the ignition temperatures, while they are lowered in some cases, are raised markedly in others in spite of the higher rates of reaction.

Further work on the extent of overall pre-flame reactions and the ignition characteristics of different hydrocarbons is in hand. A more detailed analysis of the reaction products formed at various stages preceding ignition is also being attempted. These results and the bearing they have on the possible mechanism of combustion of the hydrocarbons will be reported in a later paper.

The author wishes to thank the Directors of 'Shell' Research Ltd for permission to publish this work, and to record his indebtedness to the members of the staff of Thornton Research Centre, particularly Mr M. Smith, for assistance during the course of the work.

References

[1] Frank, C. E. and Blackham, A. U. *Industr. Engng Chem. (Industr.)*, 1952, **44,** 862

[2] Frank, C. E., Blackham, A. U. and Swarts, D. E. *Industr. Engng Chem. (Industr.)*, 1953, **45,** 1753

[3] Johnson, J. E., Crellin, J. W. and Carhart, H. W. *Industr. Engng Chem. (Industr.)*, 1954, **46,** 1512

[4] A.S.T.M. Specification (Designation *D 286–30*)

[5] Scott, G. S., Jones, G. W. and Scott, F. E. *Analyt. Chem.* 1948, **20,** 238

[6] Jackson, J. L. *Industr. Engng Chem. (Industr.)*, 1951, **43,** 2869

[7] Zabetakis, M. G., Furno, A. L. and Jones, G. W. *Industr. Engng Chem. (Industr.)*, 1954, **46,** 2173

[8] Setchkin, N. P. *J. Res. nat. Bur. Stand.* 1954, **53,** 49

[9] Swarts, D. E. and Orchin, M. *Tech. Note Nat. Adv. Comm. Aero., Wash., No. 3579* (1955); *Industr. Engng Chem. (Industr.)*, 1957, **49,** 432

[10] Salooja, K. C. *Nature, Lond.* 1959, **183,** 602

[11] Beatty, H. A. and Edgar, G. *J. Amer. chem. Soc.* 1934, **56,** 107

[12] Garner, F. H. and Petty, D. S. *Trans. Faraday Soc.* 1951, **47,** 889

[13] Sortman, C. W., Beatty, H. A. and Heron, S. D. *Industr. Engng Chem. (Industr.)*, 1941, **33,** 357

[14] Frank, C. E. and Blackham, A. U. *Industr. Engng Chem. (Industr.)*, 1954, **46,** 212

[15] Rust, F. F. and Collamer, D. O. *J. Amer. chem. Soc.* 1954 **76,** 1055

[16] Garner, F. H., Long, R. and Webster, G. A. *Fifth Symposium (International) on Combustion*, p 541. Reinhold: New York, 1955

[17] PAHNKE, A. J., COHEN, P. M. and STURGIS, B. M. *Industr. Engng Chem.* (*Industr.*), 1954, **46**, 1024
[18] SULLIVAN, M. V., WOLFE, J. K. and ZISMAN, W. A. *Industr. Engng Chem.* (*Industr.*), 1947, **39**, 1607
[19] THOMPSON, N. J. *Industr. Engng Chem.* (*Industr.*), 1929, **21**, 134
[20] NORRISH, R. G. W. and TAYLOR, G. W. *Proc. Roy. Soc. A*, 1956, **234**, 160
[21] NORRISH, R. G. W. and TAYLOR, G. W. *Proc. Roy. Soc. A*, 1956, **238**, 143
[22] BURGOYNE, J. H. *Proc. Roy. Soc. A*, 1940, **174**, 394
[23] BURGOYNE, J. H., TANG, T. L. and NEWITT, D. M. *Proc. Roy. Soc. A*, 1940, **174**, 379

Theoretical Calculations in Gaseous Detonation[*]

C. L. EISEN, R. A. GROSS and T. J. RIVLIN

Research Group, Fairchild Engine Division, Deer Park, N.Y.

(Received March 1959)

Extensive Chapman–Jouguet, strong and weak detonation properties have been obtained for a five atom (C, H, O, N, A) system. A digital computer programme has been developed which determines detonation properties in steady one-dimensional equilibrium flow. The equations and method of solution are set forth. Equilibrium and frozen sound speeds are calculated for the hot product mixtures. The effect of initial conditions and comparisons with experiment are given.

A FUNDAMENTAL physical problem in combustion is the determination of the rate of propagation of combustion and the attendant change in the properties of the gases involved. The theoretical calculation of subsonic flame speed has proved to be quite difficult, while the calculation of the supersonic detonation speed is somewhat simpler. Subsonic flame speed appears to be determined by a complex interaction between heat transfer, diffusion and high temperature kinetics. However, in supersonic flow the propagation rate appears to be governed mainly by considerations of fluid mechanics and thermodynamics. Since about 1880 investigators in this field have been able to predict detonation velocities with some precision.

We have made extensive numerical computations of the combustion properties of a five-atom system (C, H, O, N, A) in one-dimensional steady flow—in the Mach number range from 0 to 10—where the products of combustion are in thermodynamic equilibrium. We wish to describe these computations here, present a representative sampling of these results, discuss them and compare them with the work of others. Similar studies are to be found in the literature, but most of them are concerned with only a two-atom system, for example, hydrogen–oxygen. Our computations were done on an automatic digital computer (IBM 650). The results are believed to be the most extensive ever obtained. It is hoped that they may serve as the basis for experimental comparison and a standard reference for others engaged in allied research. A report which describes more completely the details and results is available[1].

1. Fundamental Equations

Consider the one-dimensional steady flow of a gas. *Figure 1* shows the arrangement and 1 and 2 refer to entrance and exit conditions, respectively. A homogeneous gaseous mixture flows steadily across plane 1. The gas is a chemically metastable mixture (fuel and air). All the thermodynamic and physical properties of the flow in this plane are considered as known and are indicated by subscript 1. The inlet flow is characterized by the pressure, temperature, velocity and chemical composition.

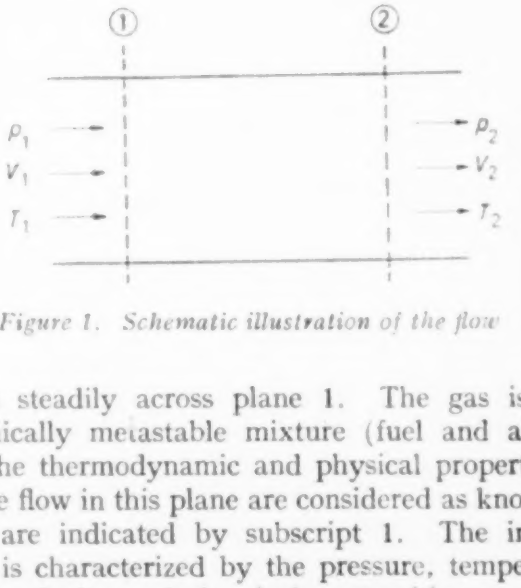

Figure 1. Schematic illustration of the flow

Solutions to the hydrodynamic equations of steady flow are sought to determine conditions at plane 2 after combustion has taken place. In addition, the exit flow is considered to be in chemical equilibrium. Conservation of mass,

---

[*] This work was carried out under support of the Air Force Office of Scientific Research, Contract No. AF49(638)-15.

momentum and energy together with the requirement of chemical equilibrium determine the solution. These equations are well known and may be found in various forms, together with some particular solutions[2, 3].

Notation

a_i	Moles of *i*th reactant
b_i	Moles of *i*th product
c	Sound speed
c_p	Constant pressure molar specific heat
c_{1-7}	Constants
F	Gibbs free energy
h	Specific enthalpy
ΔH_0	Heat of reaction
ΔH_i	Heat of formation of *i*th species
K_i	Equilibrium constant of *i*th species
m	Average molecular weight
M	Mach number
p	Static pressure
R	Universal gas constant
S	Entropy
T	Absolute temperature
V	Velocity
w	Molecular weight
x	Number of carbon atoms
x_i	Logarithm of mole fraction of *i*th product
y	Number of hydrogen atoms
y_i	Mole fraction of *i*th product
γ	Specific heat ratio
μ	Chemical potential
ν	Stoichiometric coefficient
ρ	Density

Subscripts

e	Equilibrium
f	Frozen
1	Initial condition
2	Final condition

(a) *Class of reactions*

We consider the reactants to be a homogeneous mixture of an arbitrary hydrocarbon, C_xH_y, oxygen, nitrogen and argon. The gas is assumed to obey the Perfect Gas Law throughout. The class of reactions considered is:

$$\begin{aligned} &a_0C_xH_y + a_1O_2 + a_2N_2 + a_3A \\ &\qquad \longrightarrow b_1CO_2 + b_2H_2O + b_3N_2 + b_4O_2 + b_5CO \\ &+ b_6OH + b_7N + b_8O + b_9H + b_{10}NO \\ &+ b_{11}H_2 + b_{12}A \qquad \ldots\ldots [1.1] \end{aligned}$$

where a_i is the number of moles of the *i*th reactant and b_i is the number of moles of the *i*th product. a_0 is chosen to be 1. For the temperature range investigated (400°R to 10000°R) all other product species are present only in negligible amounts. Four other product species of interest, O_3, NO_2, C and NO^+, although rare, are included in later calculations as a perturbation to the major constituents shown in equation 1.1.

(b) *Fundamental equations*

The fact that the total number of atoms of each atomic species remains constant is expressed by the following set of five equations:

$$\left.\begin{aligned} x &= b_1 + b_5 \\ y &= 2b_2 + b_6 + b_9 + 2b_{11} \\ a_1 &= b_1 + \tfrac{1}{2}b_2 + b_4 + \tfrac{1}{2}b_5 + \tfrac{1}{2}b_6 + \tfrac{1}{2}b_8 + \tfrac{1}{2}b_{10} \\ a_2 &= b_3 + \tfrac{1}{2}b_7 + \tfrac{1}{2}b_{10} \\ a_3 &= b_{12} \end{aligned}\right\} \quad [1.2]$$

The equations expressing conservation of momentum and mass, respectively, can be written as:

$$\frac{p_1}{p_2} = \frac{1+\gamma_2 M_2^2}{1+\gamma_1 M_1^2} \qquad \ldots\ldots [1.3]$$

and

$$\frac{V_2}{V_1} = \frac{m_1}{m_2} \cdot \frac{p_1}{p_2} \cdot \frac{T_2}{T_1} \qquad \ldots\ldots [1.4]$$

where p is the static pressure, V the velocity, M the Mach number $[=V(\gamma RT/m)^{-\frac{1}{2}}$ here], m the average molecular weight of the mixture, T the absolute temperature and γ the ratio of specific heats.

For one-dimensional steady flow of a homogeneous mixture of gases conservation of energy is expressed by

$$\begin{aligned} &\left(\tfrac{1}{2}\sum_{i=0}^{3} a_i w_i\right) V_1^2 + \sum_{i=0}^{3} a_i h_i(T_1) \\ &\qquad = \left(\tfrac{1}{2}\sum_{i=1}^{12} b_i w_i\right) V_2^2 + \sum_{i=1}^{12} b_i h_i(T_2) \end{aligned}$$

where h_i is the specific enthalpy of the *i*th species and w_i the molecular weight of the *i*th species. We introduce the heat of reaction of the hydrocarbon, ΔH_0 defined by

$$\begin{aligned} \Delta H_0 &= \Delta H_{C_xH_y} \\ &= h_{C_xH_y} + (x + \tfrac{1}{4}y)\, h_{O_2} - x h_{CO_2} - \tfrac{1}{2}y\, h_{H_2O} \end{aligned}$$

where $\Delta H_0 > 0$ for exothermic reactions. The heat of formation of the ith product, ΔH_i, $i=1, \ldots, 12$ is defined typically for $i=11$, say, by

$$\Delta H_{11} = h_{H_2} - 2h_H$$

Using these definitions we can obtain the energy equation in the following useful form

$$\left.\begin{aligned}
&\tfrac{1}{2}[V_1^2 \Sigma a_i w_i - V_2^2 \Sigma b_i w_i] \\
&\qquad - b_1 \Delta h_{CO_2} - b_2 \Delta h_{H_2} \\
&- b_3 \Delta h_{N_2} - b_4 \Delta h_{O_2} - b_5 \Delta h_{CO} \\
&\qquad - b_6 \Delta h_{OH} - b_7 \Delta h_N - b_8 \Delta h_O \\
&- b_9 \Delta h_H - b_{10} \Delta h_{NO} - b_{11} \Delta h_{H_2} \\
&\qquad - b_{12} \Delta h_A + (a_2 - b_3) \Delta H_{N_2}(T_1) \\
&- b_{10} \Delta H_{NO}(T_1) + \Delta H_{C_xH_y}(T_1) \\
&\qquad + (\tfrac{1}{2}y - b_2) \Delta H_{H_2O}(T_1) \\
&- b_6 \Delta H_{OH}(T_1) - b_{11} \Delta H_{H_2}(T_1) \\
&\qquad + (x - b_1) \Delta H_{CO_2}(T_1) \\
&- b_5 \Delta H_{CO}(T_1) \\
&\quad + (a_1 - b_4 - x - \tfrac{1}{4}y) \Delta H_{O_2}(T_1) = 0
\end{aligned}\right\} \quad \ldots [1.5]$$

where Δh_i is $h_i(T_2) - h_i(T_1)$.

A mixture of gases is in chemical equilibrium when the Gibbs function for the mixture is a minimum. For the reactions expressed by equation 1.1, chemical equilibrium of the products requires that the following set of equations be satisfied:

$$\left.\begin{aligned}
K_{N_2}(T_2) &= \frac{b_3 \Sigma b_i}{b_7^2 p_2} && N_2 \rightleftarrows 2N \\
K_{H_2O}(T_2) &= \frac{b_2 (\Sigma b_i)^2}{b_9^2 b_8 p_2^2} && H_2O \rightleftarrows 2H + O \\
K_{O_2}(T_2) &= \frac{b_4 \Sigma b_i}{b_8^2 p_2} && O_2 \rightleftarrows 2O \\
K_{OH}(T_2) &= \frac{b_6 \Sigma b_i}{b_8 b_9 p_2} && OH \rightleftarrows O + H \\
K_{H_2}(T_2) &= \frac{b_{11} \Sigma b_i}{b_9^2 p_2} && H_2 \rightleftarrows 2H \\
K_{NO}(T_2) &= \frac{b_{10} \Sigma b_i}{b_7 b_8 p_2} && NO \rightleftarrows N + O \\
K_{CO_2}(T_2) &= \frac{b_1^2 \Sigma b_i}{b_5^2 b_4 p_2} && 2CO_2 \rightleftarrows 2CO + O_2
\end{aligned}\right\} \quad \ldots\ldots [1.6]$$

where K the equilibrium constant is a known function of temperature.

The conditions at plane 1 are known. We seek the values at plane 2 of p_2, T_2, V_2, $b_1 - b_{12}$. These constitute 15 unknowns. Equations 1.2 to 1.6 are a system of 15 independent equations in these unknowns. In these computations the thermodynamic data given by the National Bureau of Standards, Washington, and others[4-7] were used. These data were made available to the machine in the form of least square polynomial curve fits valid over the temperature range from 18°R to 12000°R.

2. Solution of the Equations

To solve the equations 1.2 to 1.6 by means of an automatic digital computer an iterative procedure is suggested. To this end it is useful to have preliminary estimates of the solution. These can be derived by considering the simpler problem in which dissociation is absent.

(a) *The non-dissociative case*

The absence of dissociation means that equations 1.6 are deleted and $b_6 = b_7 = b_8 = \ldots = b_{11} = 0$. Also, depending on the fuel to oxygen ratio either $b_4 = 0$—richer than stoichiometric—or $b_5 = 0$—leaner than stoichiometric—or $b_4 = b_5 = 0$, the stoichiometric case is at hand. Thus, we need to solve the eight equations 1.2 to 1.5 for eight unknowns. However, the equations 1.2 are linear and can be solved readily for b_{12}, b_1, b_2, b_3 and b_4 or b_5, as the case may be. There remain three equations 1.3, 1.4 and 1.5 in the unknowns V_2, T_2, p_2. Eliminating p_2 between 1.3 and 1.4 we obtain two equations in two unknowns, V_2, T_2, which we solve by the Newton-Raphson method.

These equations were solved for a wide variety of initial conditions and hydrocarbon fuels. The solutions not only provide us with a guide to the solution of the full set of equations, but serve as a comparison with the dissociative solution in providing information about the effect of dissociation. The results in the non-dissociative case are discussed in §3.

(b) *The dissociative case*

With our solutions of the non-dissociative case as a guide we turn next to the solution of equations 1.2 to 1.6. It seems preferable to attempt to reduce the number of equations and variables by preliminary algebraic manipulations at the expense of complicating the resulting equations. In order to facilitate the elimination of unknowns and the reduction of the number of variables we replace the variables $b_1, \ldots, b_{11}$ (the trivial equation $b_{12}=a_3$ is deleted and we put $b_{12}=a_3$ everywhere in the other equations) by new variables $x_1, \ldots, x_{11}$ where

$$x_i=\log y_i=\log b_i / \sum_{j=1}^{12} b_j$$

The x_i are the logarithms of the mole fractions. When these new variables are introduced into equations 1.6 and the logarithms of both sides are taken, these seven equations become linear in $x_5, \ldots, x_{11}$, and we solve easily for $x_5, \ldots, x_{11}$ in terms of the remaining variables x_1, x_2, x_3, x_4, T_2 and p_2. These substitutions are now made in the remaining seven equations 1.2, 1.3, 1.4 and 1.5 thus producing seven equations in the seven unknowns $x_1, \ldots, x_4, T_2, p_2, V_2$. It is advantageous to have $x_1, \ldots, x_4$ as independent variables since we can use the results of the non-dissociative solutions as a guide to initial guesses for these variables in the dissociative case.

A final reduction is now made by solving 1.4 for V_2 and substituting the results in 1.3 and 1.5. The resulting set of six equations in the six unknowns x_1, x_2, x_3, x_4, T_2, p_2 is as follows:

$$\left.\begin{aligned}
&c_1(y_1+y_5)-(2y_2+y_6+y_9+2y_{11})=0\\
&c_2(y_1+y_5)-(y_1+\tfrac{1}{2}y_2+y_4+\tfrac{1}{2}y_5\\
&\qquad\qquad+\tfrac{1}{2}y_6+\tfrac{1}{2}y_8+\tfrac{1}{2}y_{10})=0\\
&c_3(y_1+y_5)-(y_3+\tfrac{1}{2}y_7+\tfrac{1}{2}y_{10})=0\\
&\sum_{i=1}^{11} y_i-1+(a_3/x)\,(y_1+y_5)=0\\
&(c_4-p_2)p_2(y_1+y_5)-c_5T_2=0\\
&c_6(y_1+y_5)-c_7T_2^2/\{p_2^2(y_1+y_5)\}\\
&\qquad\qquad\qquad-\sum_{i=1}^{11} y_i\Delta h_i\\
&-\sum_{\substack{i=1\\ i\neq 7,8,9}}^{11} y_i\Delta H_i-(a_3/x)\,(y_1+y_5)\Delta h_{12}=0
\end{aligned}\right\} \quad [2.1]$$

where $y_i=e^{x_i}$, $i=1, \ldots, 11$ and $x_5, x_6, \ldots, x_{11}$ are expressed in terms of x_1, x_2, x_3, x_4, T_2 and p_2 as mentioned above. Also the constants (depending only on initial conditions) are:

$c_1=y/x$

$c_2=a_1/x$

$c_3=a_2/x$

$c_4=p_1(1+m_1V_1^2/RT_1)$

$c_5=V_1^2m_1^2p_1^2x/RT_1^2\Sigma a_iw_i$

$c_6=\frac{1}{2}V_1^2\Sigma a_iw_i/x+(1/x)\,[\Delta H_0+a_2\Delta H_3$
$\qquad+\frac{1}{2}y\Delta H_2+x\Delta H_1+(a_1-x-\frac{1}{4}y)\Delta H_4]$

$c_7=\frac{1}{2}V_1^2m_1^2p_1^2x/T_1^2\Sigma a_iw_i$

We solve the set of equations 2.1 by the Newton–Raphson method with truncation error less than 0·1 per cent. A selection of these results is given in the tables and graphs and will be discussed below.

(c) *Rare species and ionization*

A good estimate can be made of the concentration of some interesting, but rare, species present in the product flow. The concentration of C, O_3, NO_2, and NO^+ is about 10^{-4} times those of the major constituents of the product flow. This permits these rarer species to be treated as a perturbation to the main problem. Their concentrations can be determined with good accuracy from the following equilibrium equations:

$$\left.\begin{aligned}
b_C&=\frac{b_5\Sigma b_i}{b_8p_2K_C(T_2)} && CO \rightleftarrows C+O\\
b_{O_3}&=\frac{b_8^3p_2^2K_{O_3}(T_2)}{(\Sigma b_i)^2} && O_3 \rightleftarrows 3O\\
b_{NO_2}&=\left(\frac{b_3b_4^2p_2K_{NO_2}(T_2)}{\Sigma b_i}\right)^{\frac{1}{2}} && 2NO_2 \rightleftarrows N_2+2O_2\\
b_{NO^+}&=\left(\frac{b_{10}\Sigma b_i}{p_2K_{NO^+}(T_2)}\right)^{\frac{1}{2}} && NO \rightleftarrows NO^+ + e^-
\end{aligned}\right| \quad \ldots\ldots [2.2]$$

where b_i and T_2 are known from the solution of the main problem. Gaseous ionization is usually small below 10000°R. The only ionized gas considered in the products is NO^+ which has a low ionization potential (9·5V) and is treated by the last of equations 2.2. Any impurities with low ionization potentials, such as the alkali metals, would significantly change the electron concentration in the product flow.

3. Discussion of Results

(a) *Chapman–Jouguet conditions*

Once our computer programme for solving equations 2.1 was functioning satisfactorily, it was possible to obtain many results. To a given set of initial data (data at plane 1) the equations generally provided two solutions, corresponding to weak and strong detonations, respectively, in the supersonic case. For fixed p_1, T_1 and a_0, a_1, a_2, a_3, there is a value of V_1 (and hence of M_1) for which the two detonation solutions coalesce into one. This is the Chapman–Jouguet velocity which experiment has indicated to be very close to the detonation velocity occurring in nature.

We find the Chapman–Jouguet velocity by repeatedly solving the equations for decreasing V_1 until the two solutions coalesce. In *Table 1* we give detailed information about the results at the Chapman–Jouguet point for 15 stoichiometric fuel–oxidant mixtures at initial conditions at room temperature and atmospheric pressure.

(b) *Speed of sound*

Theory dictates that at the Chapman–Jouguet point $M_2=1$. This then provides an excellent check on the accuracy of the computations. Great care must be taken, however, in computing M_2. M_2 is defined here as V_2/c_2 where c_2 is the speed of propagation of small disturbances in the gas at state 2. However, in high temperature gas mixtures when dissociation is significant, prediction of the speed of propagation of small disturbances becomes complex because of the influence of chemical reactions. Chemical reactions may result from the change in pressure and temperature in the sound wave itself. In such cases one must distinguish between the equilibrium sound speed, c_e (velocity of sound at zero frequency or infinite chemical reaction rates), and the velocity of sound at any other frequency, c, which may depend upon relaxation times, chemical reaction rates and other rate phenomena.

When the sound speed is based upon a mixture of fixed chemical composition it is referred to as a 'frozen' sound speed, c_f. This case would be expected for very high frequencies or very slow chemical reaction rates*. It is the equilibrium sound speed c_e which must be used for c_2 to compute M_2 so that at the Chapman–Jouguet (singular) point $M_2=1$†. We compute the equilibrium sound speed as follows.

Consider a gas whose equation of state is

$$p=p(\rho_1,\ S,\ b_1,\ \ldots,\ b_n)$$

where p is the pressure, ρ the density, S the entropy and b_i the number of moles of the ith chemical constituent of the mixture. The equilibrium speed of sound c_e is defined by

$$\begin{aligned} c_e^2 &= \left(\frac{\partial p}{\partial \rho}\right)_{S,\,\Delta F=0} \\ &= \left(\frac{\partial p}{\partial \rho}\right)_{S,\,b_i} + \sum_{i=1}^{n}\left(\frac{\partial p}{\partial b_i}\right)_{\rho,\,S,\,\Delta F=0}\cdot\left(\frac{\partial b_i}{\partial \rho}\right)_{S,\,\Delta F=0} \end{aligned} \quad \ldots\ldots [3.1]$$

where $\Delta F=\sum_{i=1}^{n}\nu_i^{(\alpha)}\mu_i$ is the Gibbs free energy, μ_i is the chemical potential of substance i and $\nu_i^{(\alpha)}$ is the stoichiometric coefficient of the ith substance in the αth chemical reaction. The term $(\partial p/\partial \rho)_{S,\,b_i}$ is the frozen speed of sound. This is the familiar sound speed of low temperature, low speed aerodynamics. The summation in equation 3.1 corresponds to the contribution to the sound speed by changes in the composition produced by the slight change in pressure and temperature in the sound wave itself. For a fixed chemical composition the sound speed of an ideal gas is given by

$$c_f^2=\left(\frac{\partial p}{\partial \rho}\right)_{S,\,b_i}=\frac{\gamma RT}{m}$$

where T is the temperature, γ the ratio of specific heats, R the universal gas constant and m the average molecular weight of the gas mixture.

The particular gas medium with which we are concerned here is composed of those species given on the RHS of 1.1 in amounts determined by b_1, . . ., b_{12}. We wish to calculate c_e taking into account change in composition across the small disturbance, as well as the changes in the

---

*The question of the appropriate sound speed in high temperature detonative gas was raised by S. R. BRINKLEY, Jr and J. M. RICHARDSON⁸ and the present status of this question was recently summarized by W. W. WOOD and J. G. KIRKWOOD⁹.

†Professor Howard Emmons first called this to our attention.

Table 1. Chapman–Jouguet conditi

Reaction equation: $a_0C_xH_y + a_1O_2 + a_2N_2 + a_3A \rightarrow b_1CO_2 + b_2H_2O + b_3N_2 + b_4O_2 + b_5CO$

Initial conditions: $T_1 = 537°R$; $p_1 = 1$ atm.

Fuel		H_2	H_2	CH_4	C_2H_6	C_3H_8	C_4H_{10}	C_6H_1
C_{p_0}	*(BTU/mole °R)*	6·887	6·887	8·536	$1·258 \times 10^{1}$	$1·756 \times 10^{1}$	$2·329 \times 10^{1}$	3·420 ×
ΔH_0	*(BTU/mole)*	$1·040 \times 10^{5}$	$1·040 \times 10^{5}$	$3·449 \times 10^{5}$	$6·139 \times 10^{5}$	$8·787 \times 10^{5}$	$1·142 \times 10^{6}$	1·671 ×
a_1	*(moles* O_2*)*	$5·000 \times 10^{-1}$	$5·000 \times 10^{-1}$	2·000	3·500	5·000	6·500	9·500
a_2	*(moles* N_2*)*	—	1·864	7·458	$1·305 \times 10^{1}$	$1·864 \times 10^{1}$	$2·424 \times 10^{1}$	3·542 ×
a_3	*(moles A)*	—	$2·220 \times 10^{-2}$	$8·878 \times 10^{-2}$	$1·554 \times 10^{-1}$	$2·220 \times 10^{-1}$	$2·885 \times 10^{-1}$	4·217 ×
y_1	(CO_2)	—	—	$6·967 \times 10^{-2}$	$7·928 \times 10^{-2}$	$8·354 \times 10^{-2}$	$8·596 \times 10^{-2}$	8·838 ×
y_2	(H_2O)	$5·310 \times 10^{-1}$	$2·939 \times 10^{-1}$	$1·718 \times 10^{-1}$	$1·478 \times 10^{-1}$	$1·383 \times 10^{-1}$	$1·332 \times 10^{-1}$	1·278 ×
y_3	(N_2)	—	$6·250 \times 10^{-1}$	$6·891 \times 10^{-1}$	$6·965 \times 10^{-1}$	$6·999 \times 10^{-1}$	$7·018 \times 10^{-1}$	7·036 ×
y_4	(O_2)	$5·438 \times 10^{-2}$	$8·508 \times 10^{-3}$	$1·006 \times 10^{-2}$	$1·143 \times 10^{-2}$	$1·185 \times 10^{-2}$	$1·205 \times 10^{-2}$	1·231 ×
y_5	(CO)	—	—	$2·324 \times 10^{-2}$	$2·812 \times 10^{-2}$	$2·977 \times 10^{-2}$	$3·057 \times 10^{-2}$	3·157 ×
y_6	(OH)	$1·230 \times 10^{-1}$	$1·594 \times 10^{-2}$	$8·307 \times 10^{-3}$	$8·601 \times 10^{-3}$	$8·522 \times 10^{-3}$	$8·433 \times 10^{-3}$	8·386 ×
y_7	(N)	—	$1·964 \times 10^{-6}$	$6·093 \times 10^{-7}$	$7·773 \times 10^{-7}$	$8·167 \times 10^{-7}$	$8·288 \times 10^{-7}$	8·559 ×
y_8	(O)	$4·019 \times 10^{-2}$	$2·257 \times 10^{-3}$	$1·263 \times 10^{-3}$	$1·510 \times 10^{-3}$	$1·570 \times 10^{-3}$	$1·592 \times 10^{-3}$	1·632 ×
y_9	(H)	$8·184 \times 10^{-2}$	$6·171 \times 10^{-3}$	$1·773 \times 10^{-3}$	$1·867 \times 10^{-3}$	$1·842 \times 10^{-3}$	$1·813 \times 10^{-3}$	1·800 ×
y_{10}	(NO)	—	$8·276 \times 10^{-3}$	$7·528 \times 10^{-3}$	$8·487 \times 10^{-3}$	$8·756 \times 10^{-3}$	$8·871 \times 10^{-3}$	9·041 ×
y_{11}	(H_2)	$1·695 \times 10_{-}^{1}$	$3·243 \times 10^{-2}$	$8·936 \times 10^{-3}$	$8·095 \times 10^{-3}$	$7·598 \times 10^{-3}$	$7·299 \times 10^{-3}$	7·024 ×
y_{12}	(A)	—	$7·489 \times 10^{-3}$	$8·248 \times 10^{-3}$	$8·345 \times 10^{-3}$	$8·383 \times 10^{-3}$	$8·405 \times 10^{-3}$	8·431 ×
y_{13}	(C)	—	—	$7·651 \times 10^{-14}$	$1·334 \times 10^{-13}$	$1·516 \times 10^{-13}$	$1·583 \times 10^{-13}$	1·714 ×
y_{14}	(O_3)	$1·455 \times 10^{-7}$	$2·746 \times 10^{-9}$	$2·647 \times 10^{-9}$	$3·532 \times 10^{-9}$	$3·820 \times 10^{-9}$	$3·950 \times 10^{-9}$	4·143 ×
y_{15}	(NO_2)	—	$3·952 \times 10^{-6}$	$4·685 \times 10^{-6}$	$5·587 \times 10^{-6}$	$5·881 \times 10^{-6}$	$6·017 \times 10^{-6}$	6·205 ×
y_{16}	(NO^+)	—	$2·308 \times 10^{-9}$	$6·670 \times 10^{-10}$	$8·932 \times 10^{-10}$	$9·499 \times 10^{-10}$	$9·685 \times 10^{-10}$	1·008 ×
m_1	*(lb/mole)*	$1·201 \times 10^{1}$	$2·101 \times 10^{1}$	$2·774 \times 10^{1}$	$2·902 \times 10^{1}$	$2·957 \times 10^{1}$	$2·987 \times 10^{1}$	3·020 ×
m_2	*(lb/mole)*	$1·447 \times 10^{1}$	$2·400 \times 10^{1}$	$2·718 \times 10^{1}$	$2·759 \times 10^{1}$	$2·777 \times 10^{1}$	$2·787 \times 10^{1}$	2·798 ×
γ_1		1·395	1·402	1·389	1·377	1·369	1·364	1·358
γ_{2f}		1·217	1·245	1·249	1·250	1·251	1·251	1·251
γ_{2e}		1·128	1·163	1·169	1·167	1·166	1·166	1·166
c_1	*(ft/s)*	$1·761 \times 10^{3}$	$1·335 \times 10^{3}$	$1·156 \times 10^{3}$	$1·125 \times 10^{3}$	$1·112 \times 10^{3}$	$1·104 \times 10^{3}$	1·096
c_{2f}	*(ft/s)*	$5·260 \times 10^{3}$	$3·699 \times 10^{3}$	$3·384 \times 10^{3}$	$3·381 \times 10^{3}$	$3·375 \times 10^{3}$	$3·371 \times 10^{3}$	3·368
v_1	*(ft/s)*	$9·314 \times 10^{3}$	$6·454 \times 10^{3}$	$5·911 \times 10^{3}$	$5·909 \times 10^{3}$	$5·901 \times 10^{3}$	$5·894 \times 10^{3}$	5·889
$v_2 = c_{2_e}$	*(ft/s)*	$5·063 \times 10^{3}$	$3·577 \times 10^{3}$	$3·273 \times 10^{3}$	$3·264 \times 10^{3}$	$3·258 \times 10^{3}$	$3·253 \times 10^{3}$	3·249
M_1		5·289	4·834	5·112	5·251	5·307	5·339	5·374
M_{2_f}		$9·626 \times 10^{-1}$	$9·668 \times 10^{-1}$	$9·671 \times 10^{-1}$	$9·655 \times 10^{-1}$	$9·654 \times 10^{-1}$	$9·651 \times 10^{-1}$	9·647
T_2	*(°R)*	$6·616 \times 10^{3}$	$5·309 \times 10^{3}$	$5·011 \times 10^{3}$	$5·075 \times 10^{3}$	$5·088 \times 10^{3}$	$5·092 \times 10^{3}$	5·101
$v_2/v_1 = \rho_1/\rho_2$		$5·436 \times 10^{-1}$	$5·540 \times 10^{-1}$	$5·535 \times 10^{-1}$	$5·524 \times 10^{-1}$	$5·521 \times 10^{-1}$	$5·519 \times 10^{-1}$	5·516
p_2/p_1		$1·882 \times 10^{1}$	$1·562 \times 10^{1}$	$1·721 \times 10^{1}$	$1·799 \times 10^{1}$	$1·828 \times 10^{1}$	$1·842 \times 10^{1}$	1·859
T_2/T_1		$1·232 \times 10^{1}$	9·886	9·332	9·450	9·475	9·483	9·499

conditi stoichiometric fuel–oxidant mixtures

$+b_5\mathrm{CO} + b_8\mathrm{O} + b_9\mathrm{H} + b_{10}\mathrm{NO} + b_{11}\mathrm{H}_2 + b_{12}\mathrm{A} + b_{13}\mathrm{C} + b_{14}\mathrm{O}_3 + b_{15}\mathrm{NO}_2 + b_{16}(\mathrm{NO}^+ + e^-)$

where $y_i = b_i / \Sigma b_i$ are the mole fractions.

C_6H_1	H_{18}	$C_{10}H_{22}$	$C_{12}H_{26}$	C_2H_4	C_3H_6	C_2H_2	C_2H_2	C_6H_6
$3{\cdot}420 \times$	$\times 10^{1}$	$5{\cdot}607 \times 10^{1}$	$6{\cdot}700 \times 10^{1}$	$1{\cdot}041 \times 10^{1}$	$1{\cdot}527 \times 10^{1}$	$1{\cdot}050 \times 10^{1}$	$1{\cdot}050 \times 10^{1}$	$1{\cdot}952 \times 10^{1}$
$1{\cdot}671 \times$	9×10^{6}	$2{\cdot}728 \times 10^{6}$	$3{\cdot}257 \times 10^{6}$	$5{\cdot}688 \times 10^{5}$	$8{\cdot}282 \times 10^{5}$	$5{\cdot}398 \times 10^{5}$	$5{\cdot}398 \times 10^{5}$	$1{\cdot}363 \times 10^{6}$
$9{\cdot}500$	0×10^{1}	$1{\cdot}550 \times 10^{1}$	$1{\cdot}850 \times 10^{1}$	$3{\cdot}000$	$4{\cdot}500$	$2{\cdot}500$	$2{\cdot}500$	$7{\cdot}500$
$3{\cdot}542 \times$	1×10^{1}	$5{\cdot}780 \times 10^{1}$	$6{\cdot}898 \times 10^{1}$	$1{\cdot}119 \times 10^{1}$	$1{\cdot}678 \times 10^{1}$	—	$9{\cdot}322$	$2{\cdot}797 \times 10^{1}$
$4{\cdot}217 \times$	9×10^{-1}	$6{\cdot}880 \times 10^{-1}$	$8{\cdot}212 \times 10^{-1}$	$1{\cdot}332 \times 10^{-1}$	$1{\cdot}998 \times 10^{-1}$	—	$1{\cdot}110 \times 10^{-1}$	$3{\cdot}329 \times 10^{-1}$
$8{\cdot}838 \times$	9×10^{-2}	$9{\cdot}046 \times 10^{-2}$	$9{\cdot}099 \times 10^{-2}$	$8{\cdot}608 \times 10^{-2}$	$8{\cdot}924 \times 10^{-2}$	$9{\cdot}480 \times 10^{-2}$	$8{\cdot}807 \times 10^{-2}$	$1{\cdot}112 \times 10^{-1}$
$1{\cdot}278 \times$	0×10^{-1}	$1{\cdot}233 \times 10^{-1}$	$1{\cdot}221 \times 10^{-1}$	$1{\cdot}121 \times 10^{-1}$	$1{\cdot}138 \times 10^{-1}$	$8{\cdot}725 \times 10^{-2}$	$6{\cdot}174 \times 10^{-2}$	$6{\cdot}911 \times 10^{-2}$
$7{\cdot}036 \times$	6×10^{-1}	$7{\cdot}053 \times 10^{-1}$	$7{\cdot}056 \times 10^{-1}$	$7{\cdot}026 \times 10^{-1}$	$7{\cdot}047 \times 10^{-1}$	—	$7{\cdot}071 \times 10^{-1}$	$7{\cdot}223 \times 10^{-1}$
$1{\cdot}231 \times$	8×10^{-2}	$1{\cdot}251 \times 10^{-2}$	$1{\cdot}257 \times 10^{-2}$	$1{\cdot}525 \times 10^{-2}$	$1{\cdot}428 \times 10^{-2}$	$1{\cdot}220 \times 10^{-1}$	$2{\cdot}234 \times 10^{-2}$	$1{\cdot}619 \times 10^{-2}$
$3{\cdot}157 \times$	3×10^{-2}	$3{\cdot}235 \times 10^{-2}$	$3{\cdot}257 \times 10^{-2}$	$4{\cdot}051 \times 10^{-2}$	$3{\cdot}769 \times 10^{-2}$	$3{\cdot}442 \times 10^{-1}$	$6{\cdot}552 \times 10^{-2}$	$4{\cdot}500 \times 10^{-2}$
$8{\cdot}386 \times$	7×10^{-3}	$8{\cdot}318 \times 10^{-3}$	$8{\cdot}306 \times 10^{-3}$	$1{\cdot}044 \times 10^{-2}$	$9{\cdot}505 \times 10^{-3}$	$1{\cdot}043 \times 10^{-1}$	$1{\cdot}266 \times 10^{-2}$	$7{\cdot}735 \times 10^{-3}$
$8{\cdot}559 \times$	5×10^{-7}	$8{\cdot}732 \times 10^{-7}$	$8{\cdot}793 \times 10^{-7}$	$1{\cdot}678 \times 10^{-6}$	$1{\cdot}312 \times 10^{-6}$	—	$5{\cdot}410 \times 10^{-6}$	$1{\cdot}374 \times 10^{-6}$
$1{\cdot}632 \times$	6×10^{-3}	$1{\cdot}659 \times 10^{-3}$	$1{\cdot}668 \times 10^{-3}$	$2{\cdot}896 \times 10^{-3}$	$2{\cdot}202 \times 10^{-3}$	$1{\cdot}283 \times 10^{-1}$	$5{\cdot}744 \times 10^{-3}$	$2{\cdot}389 \times 10^{-3}$
$1{\cdot}800 \times$	8×10^{-3}	$1{\cdot}781 \times 10^{-3}$	$1{\cdot}777 \times 10^{-3}$	$2{\cdot}640 \times 10^{-3}$	$2{\cdot}246 \times 10^{-3}$	$7{\cdot}814 \times 10^{-2}$	$4{\cdot}157 \times 10^{-3}$	$1{\cdot}743 \times 10^{-3}$
$9{\cdot}041 \times$	1×10^{-3}	$9{\cdot}165 \times 10^{-3}$	$9{\cdot}203 \times 10^{-3}$	$1{\cdot}145 \times 10^{-2}$	$1{\cdot}058 \times 10^{-2}$	—	$1{\cdot}748 \times 10^{-2}$	$1{\cdot}147 \times 10^{-2}$
$7{\cdot}024 \times$	5×10^{-3}	$6{\cdot}776 \times 10^{-3}$	$6{\cdot}716 \times 10^{-3}$	$7{\cdot}933 \times 10^{-3}$	$7{\cdot}285 \times 10^{-3}$	$4{\cdot}103 \times 10^{-2}$	$6{\cdot}647 \times 10^{-3}$	$4{\cdot}236 \times 10^{-3}$
$8{\cdot}431 \times$	3×10^{-3}	$8{\cdot}449 \times 10^{-3}$	$8{\cdot}455 \times 10^{-3}$	$8{\cdot}431 \times 10^{-3}$	$8{\cdot}454 \times 10^{-3}$	—	$8{\cdot}524 \times 10^{-3}$	$8{\cdot}665 \times 10^{-3}$
$1{\cdot}714 \times$	2×10^{-13}	$1{\cdot}804 \times 10^{-13}$	$1{\cdot}834 \times 10^{-13}$	$6{\cdot}356 \times 10^{-13}$	$3{\cdot}979 \times 10^{-13}$	$5{\cdot}376 \times 10^{-8}$	$6{\cdot}575 \times 10^{-12}$	$4{\cdot}726 \times 10^{-13}$
$4{\cdot}143 \times$	4×10^{-9}	$4{\cdot}286 \times 10^{-9}$	$4{\cdot}330 \times 10^{-9}$	$6{\cdot}876 \times 10^{-9}$	$5{\cdot}830 \times 10^{-9}$	$1{\cdot}130 \times 10^{-6}$	$1{\cdot}744 \times 10^{-8}$	$7{\cdot}081 \times 10^{-9}$
$6{\cdot}205 \times$	7×10^{-6}	$6{\cdot}347 \times 10^{-6}$	$6{\cdot}389 \times 10^{-6}$	$8{\cdot}058 \times 10^{-6}$	$7{\cdot}435 \times 10^{-6}$	—	$1{\cdot}328 \times 10^{-5}$	$8{\cdot}531 \times 10^{-6}$
$1{\cdot}008 \times$	$\times 10^{-9}$	$1{\cdot}033 \times 10^{-9}$	$1{\cdot}042 \times 10^{-9}$	$2{\cdot}192 \times 10^{-9}$	$1{\cdot}654 \times 10^{-9}$	—	$8{\cdot}507 \times 10^{-9}$	$1{\cdot}780 \times 10^{-9}$
$3{\cdot}020 \times$	7×10^{1}	$3{\cdot}047 \times 10^{1}$	$3{\cdot}054 \times 10^{1}$	$2{\cdot}890 \times 10^{1}$	$2{\cdot}955 \times 10^{1}$	$3{\cdot}030 \times 10^{1}$	$2{\cdot}874 \times 10^{1}$	$3{\cdot}030 \times 10^{1}$
$2{\cdot}798 \times$	$\times 10^{1}$	$2{\cdot}806 \times 10^{1}$	$2{\cdot}809 \times 10^{1}$	$2{\cdot}803 \times 10^{1}$	$2{\cdot}810 \times 10^{1}$	$2{\cdot}328 \times 10^{1}$	$2{\cdot}854 \times 10^{1}$	$2{\cdot}902 \times 10^{1}$
$1{\cdot}358$		$1{\cdot}354$	$1{\cdot}353$	$1{\cdot}384$	$1{\cdot}373$	$1{\cdot}321$	$1{\cdot}380$	$1{\cdot}375$
$1{\cdot}251$		$1{\cdot}251$	$1{\cdot}251$	$1{\cdot}253$	$1{\cdot}252$	$1{\cdot}269$	$1{\cdot}259$	$1{\cdot}254$
$1{\cdot}166$		$1{\cdot}165$	$1{\cdot}165$	$1{\cdot}161$	$1{\cdot}163$	$1{\cdot}152$	$1{\cdot}157$	$1{\cdot}162$
$1{\cdot}096$	2×10^{3}	$1{\cdot}089 \times 10^{3}$	$1{\cdot}088 \times 10^{3}$	$1{\cdot}131 \times 10^{3}$	$1{\cdot}114 \times 10^{3}$	$1{\cdot}079 \times 10^{3}$	$1{\cdot}132 \times 10^{3}$	$1{\cdot}101 \times 10^{3}$
$3{\cdot}368$	$\times 10^{3}$	$3{\cdot}365 \times 10^{3}$	$3{\cdot}364 \times 10^{3}$	$3{\cdot}423 \times 10^{3}$	$3{\cdot}397 \times 10^{3}$	$4{\cdot}532 \times 10^{3}$	$3{\cdot}507 \times 10^{3}$	$3{\cdot}348 \times 10^{3}$
$5{\cdot}889$	5×10^{3}	$5{\cdot}884 \times 10^{3}$	$5{\cdot}884 \times 10^{3}$	$5{\cdot}979 \times 10^{3}$	$5{\cdot}936 \times 10^{3}$	$7{\cdot}955 \times 10^{3}$	$6{\cdot}116 \times 10^{3}$	$5{\cdot}845 \times 10^{3}$
$3{\cdot}249$	$\times 10^{3}$	$3{\cdot}247 \times 10^{3}$	$3{\cdot}246 \times 10^{3}$	$3{\cdot}294 \times 10^{3}$	$3{\cdot}272 \times 10^{3}$	$4{\cdot}320 \times 10^{3}$	$3{\cdot}362 \times 10^{3}$	$3{\cdot}221 \times 10^{3}$
$5{\cdot}374$	1	$5{\cdot}402$	$5{\cdot}410$	$5{\cdot}289$	$5{\cdot}329$	$7{\cdot}374$	$5{\cdot}402$	$5{\cdot}309$
$9{\cdot}647$	5×10^{-1}	$9{\cdot}649 \times 10^{-1}$	$9{\cdot}650 \times 10^{-1}$	$9{\cdot}623 \times 10^{-1}$	$9{\cdot}632 \times 10^{-1}$	$9{\cdot}532 \times 10^{-1}$	$9{\cdot}587 \times 10^{-1}$	$9{\cdot}621 \times 10^{-1}$
$5{\cdot}101$	$\times 10^{3}$	$5{\cdot}107 \times 10^{3}$	$5{\cdot}109 \times 10^{3}$	$5{\cdot}273 \times 10^{3}$	$5{\cdot}209 \times 10^{3}$	$7{\cdot}576 \times 10^{3}$	$5{\cdot}608 \times 10^{3}$	$5{\cdot}217 \times 10^{3}$
$5{\cdot}516$	5×10^{-1}	$5{\cdot}517 \times 10^{-1}$	$5{\cdot}517 \times 10^{-1}$	$5{\cdot}509 \times 10^{-1}$	$5{\cdot}512 \times 10^{-1}$	$5{\cdot}430 \times 10^{-1}$	$5{\cdot}497 \times 10^{-1}$	$5{\cdot}510 \times 10^{-1}$
$1{\cdot}859$	$\times 10^{1}$	$1{\cdot}872 \times 10^{1}$	$1{\cdot}876 \times 10^{1}$	$1{\cdot}838 \times 10^{1}$	$1{\cdot}850 \times 10^{1}$	$3{\cdot}381 \times 10^{1}$	$1{\cdot}913 \times 10^{1}$	$1{\cdot}841 \times 10^{1}$
$9{\cdot}499$	5	$9{\cdot}510$	$9{\cdot}513$	$9{\cdot}819$	$9{\cdot}700$	$1{\cdot}411 \times 10^{1}$	$1{\cdot}044 \times 10^{1}$	$9{\cdot}715$

other thermodynamic properties in the medium. We seek, therefore, a set of equations satisfied by all the changes, together with the conditions that the entropy remain constant, and that the composition be in equilibrium. This set of equations is provided by the atom balance equations, the ideal gas law, the equations for chemical equilibrium, and the equation for the entropy change.

The reaction equation we are dealing with is

$$\begin{aligned} & b_1CO_2 + b_2H_2O + b_3N_2 + b_4O_2 \\ & \qquad + b_5CO + b_6OH + b_7N + b_8O + b_9H \\ & + b_{10}NO + b_{11}H_2 + b_{12}A \\ & \qquad \longrightarrow (b_1 + \delta b_1)CO_2 + (b_2 + \delta b_2)H_2O \\ & + (b_3 + \delta b_3)N_2 + (b_4 + \delta b_4)O_2 \\ & \qquad + (b_5 + \delta b_5)CO + (b_6 + \delta b_6)OH \\ & + (b_7 + \delta b_7)N + (b_8 + \delta b_8)O \\ & \qquad + (b_9 + \delta b_9)H + (b_{10} + \delta b_{10})NO \\ & + (b_{11} + \delta b_{11})H_2 + (b_{12} + \delta b_{12})A \end{aligned}$$

where δ denotes a small change in the quantity following it.

Now, atom balance requires

$$\left.\begin{aligned} & \delta b_1 + \delta b_5 = 0 \\ & 2\delta b_2 + \delta b_6 + \delta b_9 + 2\delta b_{11} = 0 \\ & \delta b_1 + \tfrac{1}{2}\delta b_2 + \delta b_4 + \tfrac{1}{2}\delta b_5 \\ & \qquad + \tfrac{1}{2}\delta b_6 + \tfrac{1}{2}\delta b_8 + \tfrac{1}{2}\delta b_{10} = 0 \\ & \delta b_3 + \tfrac{1}{2}\delta b_7 + \tfrac{1}{2}\delta b_{10} = 0 \end{aligned}\right\} \quad \ldots [3.2]$$

while the ideal gas law yields

$$\frac{RT}{mp}\delta\rho + \frac{1}{T}\delta T - \frac{1}{p}\delta p - \frac{1}{m}\delta m = 0 \qquad \ldots . [3.3]$$

where $m = m_2$ and all the thermodynamic quantities take their values at station 2 throughout this discussion, so that we drop the subscript 2.

The change δm satisfies

$$\left(\sum_{k=1}^{12} b_k\right)\delta m + \sum_{k=1}^{11} (m - w_k)\delta b_k = 0 \qquad \ldots . [3.4]$$

by definition.

Differentiating the equilibrium equations 1.6 and applying the van't Hoff isobar,

$$\frac{\mathrm{d} \log k_j}{\mathrm{d}T} = \frac{\Delta H_j}{RT^2}$$

yields

$$\left.\begin{aligned} & \frac{1}{b_3}\delta b_3 + \frac{1}{\Sigma b_k}\Sigma\delta b_i - \frac{2}{b_7}\delta b_7 - \frac{1}{p}\delta p \\ & \qquad - \frac{\Delta H_3}{RT^2}\delta T = 0 \\ & \frac{1}{b_2}\delta b_2 + \frac{2}{\Sigma b_k}\Sigma\delta b_i - \frac{2}{b_9}\delta b_9 - \frac{1}{b_8}\delta b_8 \\ & \qquad - \frac{2}{p}\delta p - \frac{\Delta H_2}{RT^2}\delta T = 0 \\ & \frac{1}{b_4}\delta b_4 + \frac{1}{\Sigma b_k}\Sigma\delta b_i - \frac{2}{b_8}\delta b_8 - \frac{1}{p}\delta p \\ & \qquad - \frac{\Delta H_4}{RT^2}\delta T = 0 \\ & \frac{1}{b_6}\delta b_6 + \frac{1}{\Sigma b_k}\Sigma\delta b_i - \frac{1}{b_8}\delta b_8 - \frac{1}{b_9}\delta b_9 \\ & \qquad - \frac{1}{p}\delta p - \frac{\Delta H_6}{RT^2}\delta T = 0 \\ & \frac{1}{b_{11}}\delta b_{11} + \frac{1}{\Sigma b_k}\Sigma\delta b_i - \frac{2}{b_9} - \frac{1}{p}\delta p \\ & \qquad - \frac{\Delta H_{11}}{RT^2}\delta T = 0 \\ & \frac{1}{b_{10}}\delta b_{10} + \frac{1}{\Sigma b_k}\Sigma\delta b_i - \frac{1}{b_7}\delta b_7 - \frac{1}{b_8}\delta b_8 \\ & \qquad - \frac{1}{p}\delta p - \frac{\Delta H_{10}}{RT^2}\delta T = 0 \\ & \frac{2}{b_1}\delta b_1 + \frac{1}{\Sigma b_k}\Sigma\delta b_i - \frac{2}{b_5}\delta b_5 - \frac{1}{b_4}\delta b_4 \\ & \qquad - \frac{1}{p}\delta p - \frac{2\Delta H_1}{RT^2}\delta T = 0 \end{aligned}\right\} \quad \ldots [3.5]$$

where summation on i runs from 1 to 11, on k from 1 to 12.

Finally, entropy change is set equal to zero giving

$$\begin{aligned} & (\Delta H_1 + \tfrac{1}{2}\Delta H_4)\delta b_1 + \sum_{\substack{j=2 \\ j \neq 5,7,8,9}}^{11} \Delta H_j \delta b_j \\ & \qquad + \left(\sum_{j=1}^{12} b_j c_{pj}\right)\delta T - \frac{RT}{p}\left(\sum_{k=1}^{12} b_k\right)\delta p = 0 \quad \ldots . [3.6] \end{aligned}$$

If we now give $\delta\rho$ an arbitrary value, equations 3.2 to 3.6 are (14) linear equations in 14 unknowns δT, δp, δm, δb_i, $i=1, \ldots, 11$. The ratios $\delta T/\delta\rho$, $\delta p/\delta\rho$, $\delta m/\delta\rho$ and $\delta b_i/\delta\rho$ are uniquely determined by solving these equations, and are independent of $\delta\rho$. Hence, in particular, for any choice of $\delta\rho$

$$\frac{\delta p}{\delta\rho} = \lim_{\delta\rho\to 0}\frac{\delta p}{\delta\rho} = \left(\frac{\partial p}{\partial\rho}\right)_{S,\,\Delta F=0}$$

In this fashion we compute δp by solving a set of 14 linear equations. The resulting c_e are given in *Table 1* (as are the c_f and M_{2_f} for comparison). They yield $M_2=1{\cdot}000$ for Chapman–Jouguet conditions, thus lending considerable credibility to the entire computation.

(c) *Results*

The programme used to solve the basic equations 2.1 is quite general and capable of producing a vast collection of results. We present some of these results for hydrogen burning in air, a case which has been widely studied.

Table 2 gives the Chapman–Jouguet Mach number M_1 for differing values of the initial temperature, $p_1=1$ atmosphere, for stoichiometric hydrogen–air. *Table 3* gives M_1 for differing initial pressures, at room temperature (537°R) for stoichiometric hydrogen–air. Both non-dissociative and dissociative data are given for comparison.

Figure 2 gives M_1 as a function of fuel/air ratio for hydrogen–air. It can be seen that below a fuel/air ratio of about 0·15 there are no appreciable dissociative effects. *Figure 3* shows velocity ratio as a function of initial Mach number for stoichiometric hydrogen–air at standard conditions. *Figures 4* and *5* give the same information for static pressure ratio and temperature ratio, respectively.

Table 2. Initial temperature dependence of Chapman–Jouguet detonation
(Initial conditions: stoichiometric hydrogen–air; $p_1=1$ atm)

T_1 °R	Dissociative case M_1	V_1 ft/s	T_2 °R	p_2 atm	Non-dissociative case M_1	V_1 ft/s	T_2 °R	p_2 atm
400	5·612	6498	5310	21·05	5·932	6870	6017	22·73
600	4·566	6433	5309	13·97	4·868	6861	6120	15·26
800	3·933	6374	5317	10·41	4·236	6855	6232	11·54
1000	3·498	6317	5333	8·296	3·795	6854	6350	9·324
1200	3·175	6263	5353	6·885	3·475	6855	6475	7·846
1400	2·922	6209	5376	5·883	3·229	6860	6607	6·803

4 Comparison of the Results with the Work of Others

We wish now to compare the results of our computations with the experimental and computational results already in the literature. Unfortunately, most published results contain insufficient data for a complete check, for the composition of the products along with the thermodynamic data is required for a true comparison. Moreover, some other computations have used the condition $M_2=1$ based on the frozen sound speed (see the preceding section) to find conditions at the Chapman–Jouguet point. This theoretical error leads to

Table 3. Initial pressure dependence of Chapman–Jouguet detonation
(Initial conditions: stoichiometric hydrogen–air; $T_1=537$°R)

p_1 atm	Dissociative case M_1	V_1 ft/s	T_2 °R	p_2 atm	Non-dissociative case M_1	V_1 ft/s	T_2 °R	p_2 atm
10^{-6}	3·957	5283	3441	$1{\cdot}103\times10^{-5}$	5·141	6871	6078	$1{\cdot}697\times10^{-5}$
10^{-3}	4·401	5876	4308	$1{\cdot}334\times10^{-2}$	5·141	6871	6078	$1{\cdot}697\times10^{-2}$
1	4·834	6454	5309	15·62	5·141	6871	6078	16·97
10	4·939	6594	5573	161·4	5·141	6871	6078	169·7

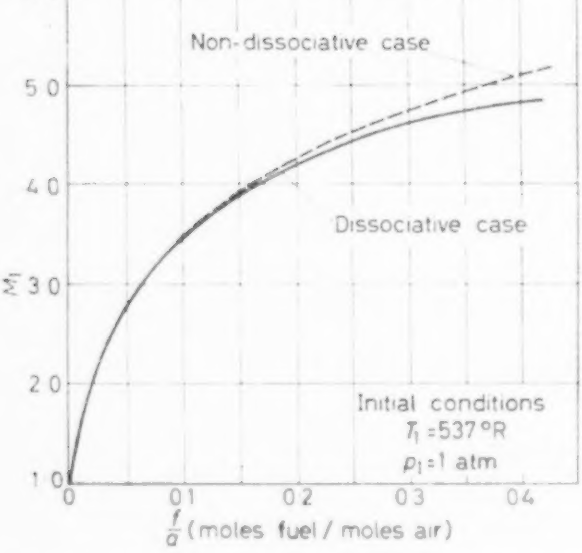

Figure 2. Chapman-Jouguet detonation Mach number as a function of fuel–air ratio for hydrogen–air

small discrepancies in the detonation velocity. In *Table 4* we compare our computations with those of others. We give our computations based on the frozen sound speed as well as on the equilibrium sound speed. Because of our use of a high speed electronic digital computer it was possible to hold the numerical accuracy

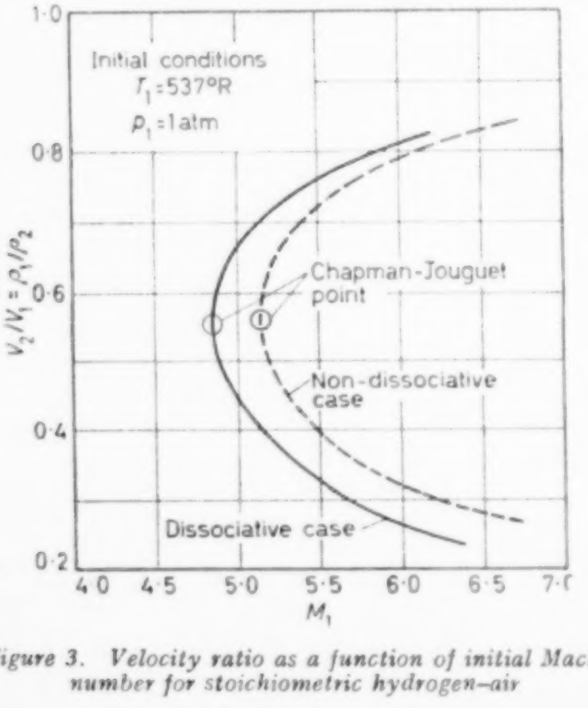

Figure 3. Velocity ratio as a function of initial Mach number for stoichiometric hydrogen–air

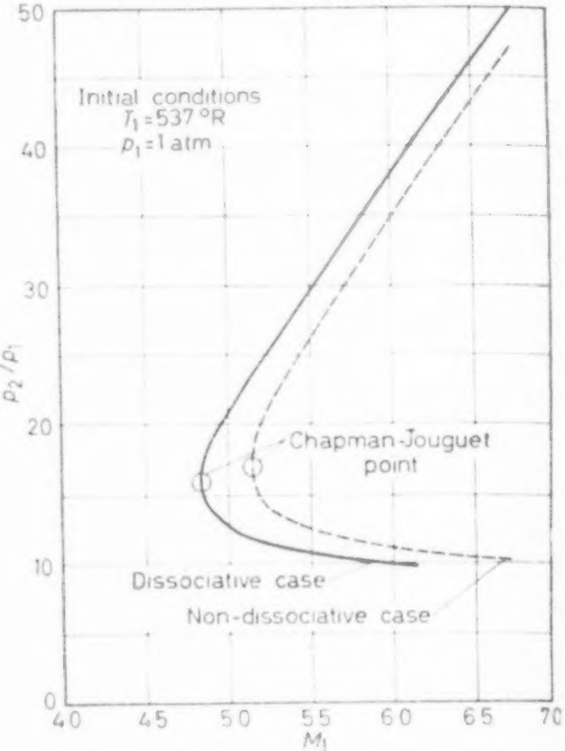

Figure 4. Static pressure ratio as a function of initial Mach number for stoichiometric hydrogen–air

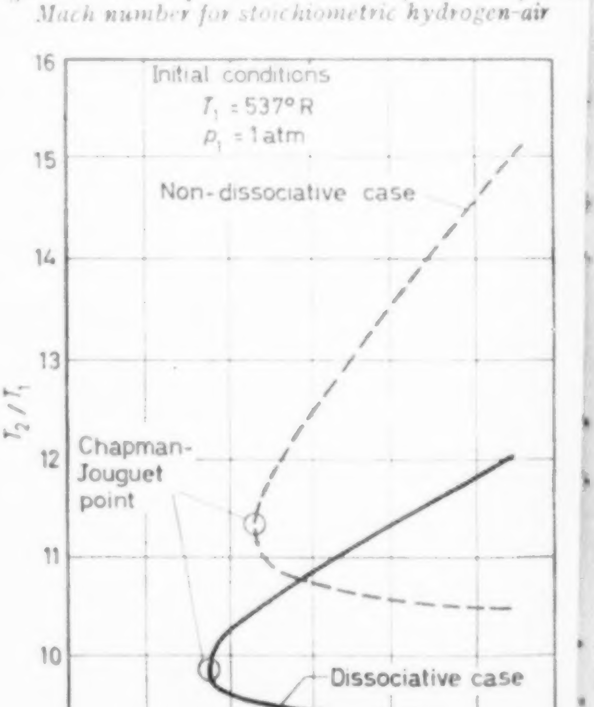

Figure 5. Temperature ratio as a function of ini Mach number for stoichiometric hydrogen–air

to a closer tolerance than is believed practicable by hand methods.

In addition, it was possible to explore numerically the sensitivity of the results; i.e. the influence of a small change in one variable and how it interacts with the other variables. In particular, very small changes in velocity in the vicinity of the Chapman–Jouguet point results in sizable perturbations in the product temperature and pressure.

Table 4. Stoichiometric hydrogen–oxygen detonation

[$p_1 = 1{\cdot}0$ atm, T_1 = room temperature (70°F); $2H_2 + O_2 \rightarrow$ dissociated products]

Source	*Measured velocity (ft/s)*	*Calculated*		
		V_1 (ft/s)	*p_2 (atm)*	*T_2 (°R)*
Berets, Greene and Kistiakowksy[10, *]	9268	9357	18·06	6620
Dunn and Wolfson[11, *]	9100	8961	17·22	6368
Lewis and Friauf[12, *]	9249	9206	18·05	6449
*Eisen, Gross and Rivlin**	—	9323	18·10	6595
Eisen, Gross and Rivlin	—	9314	18·82	6616
Moyle[13]	9072	—	—	—
Morrison[14]	8800	—	—	—

*These data are based on the frozen speed of sound.

It is interesting to compare briefly some experimental results with the well explored hydrogen–oxygen detonation calculations. Some data are presented in *Table 4*.

It can be seen that the experimental results appear to cluster about the computed values. In general, the newer calculations are slightly higher than the experimental results. Dissipative effects and two-dimensional effects, not included in the calculation, such as heat transfer and friction, would be expected to lower the experimental results below those obtained by theory. Unfortunately, there is such scatter and lack of detail in both the experimental and theoretical results previously published that it is impossible to state here whether the small difference between theory and experiment is significant.

References

[1] EISEN, C. L., GROSS, R. A. and RIVLIN, T. J. AFOSR, *TN 58–326*, ASTIA No. AD **154230**, **1958**

Some of the thermodynamic data used in ref. 1 are outdated. Consequently, the calculation was redone, using the latest thermodynamic information available, for the present paper.

[2] HIRSCHFELDER, J. O., CURTISS, C. F. and BIRD, R. B. *Molecular Theory of Gases and Liquids*. Wiley: New York, **1954**

[3] LEWIS, B. and FRIAUF, J. *J. Amer. chem. Soc.* **1930**, **52**, **3905**

[4] HILSENRATH, J. *et al. Tables of Thermal Properties of Gases*. [*Circ. U.S. Bur. Stand. No.* **564**.] Washington, **1955**

[5] HUFF, V. N., GORDON, S. and MORRELL, V. E. *Nat. Adv. Comm. Aero., Wash., Rep. No. 1037*, **1950**

[6] GILMORE, F. R. Project Rand *RM–1543* (**1955**)

[7] ROSSINI, F. D. *et al. Selected Values of Physical and Thermodynamic Properties of Hydrocarbons and Related Compounds*. Carnegie Press: Pittsburgh, Pa, **1953**

[8] BRINKLEY, S. R., Jr and RICHARDSON, J. M. *Fourth Symposium (International) on Combustion*, pp **450-457**. Williams and Wilkins: Baltimore, **1953**

[9] WOOD, W. W. and KIRKWOOD, J. G. *J. chem. Phys.* **1958**, **29**, **957**

[10] BERETS, D. J., GREENE, E. F. and KISTIAKOWSKY, G. B. *J. Amer. chem. Soc.* **1950**, **72**, **1080**

[11] DUNN, R. and WOLFSON, B. T. *W.A.D.C. tech. Note No. 54–13*, **1956**

[12] cf. ref. 3

[13] MOYLE, M. P. *Univ. Mich. Rep. No. IP–195*, **1956**

[14] MORRISON, R. B. *Univ. Mich. Rep. No. UMM–97*, **1952**

Tr
ex
cy
fo
pr
ha
ne
pa
wi
th
m
ga
to
ur
pr
in
ha
fla
of
in

ch
T

The Passage of Explosions through Narrow Cylindrical Channels

H. G. WOLFHARD* and A. E. BRUSZAK†

Division of Explosives Technology, Bureau of Mines, 4800 Forbes Avenue, Pittsburgh 13, Pa

(Received March 1959)

The transmission of explosions through narrow channels is investigated in this paper. The channels connect two explosion chambers. Ignition in the outer chamber following firing of an explosive mixture in the inner chamber depends on the geometry of the channel. It has been found that a propagating methane–air flame does not travel through channels of less than about 3mm diameter, although ignition may still occur in the outer chamber. The hot burnt gases from the inner chamber issue into the outer chamber and may lead to ignition which originates in the hot eddies of the turbulent jet. Ignition or non-ignition depends mainly on the gas dynamic properties of the jet, which in turn depend on the channel geometry. This mode of ignition is confirmed by theoretical considerations, as well as by the nature of the experimental results showing, for example, that very short channels are more efficient in preventing outside ignition than channels of about 10 mm length. Schlieren pictures of the outside ignition process also confirm the proposed mechanism.

Introduction

THIS paper deals with the mechanism by which explosions are transmitted through narrow cylindrical channels. This process is important for understanding flame traps and the flameproofing of electrical equipment in mines. It has been found that flameproofed equipment need not be completely enclosed but that narrow passages are permissible. Explosions initiated within the enclosure may eject visible 'flame' through these passages into the outside explosive mixture without igniting it. These ejected flame gases are obviously very hot, and their failure to ignite an explosive mixture is difficult to understand. Previous investigations of this problem have been confined largely to measuring the permissible width of such passages and have shown that a 1 mm gap between ½ in. long flanges provides protection against transmission of a methane–air explosion within the enclosure into an outside methane–air atmosphere[1,2].

In the present investigation, cylindrical channels were used for reasons of simplicity. The purpose was not to measure any 'safe' distances or diameters, but to study those parameters which would help to reveal the mechanism of the transmission of explosions. Some results of this investigation have already been published[3].

Experimental Arrangement

The 'inner' explosion chamber (*Figure 1*) was 8·7 cm in height and had a diameter of 3·4 cm. Gas could be circulated in this chamber and usually consisted of a stoichiometric methane–oxygen–nitrogen mixture. The oxygen index of the gas (OI = oxygen/oxygen plus nitrogen) determined the strength of the explosion and the temperature of the burnt gases. The top of the inner chamber was equipped with an interchangeable cap which contained the channel through which the inner explosion was transmitted into the 'outer' chamber. Channel diameters measured from 0·6 to 3·0 mm and occasionally up to 8 mm. The length of the channel ranged from 0·5 to 50 mm. Electrodes for sparking the inner mixture were close to the channel entry.

The outer chamber partly enclosed the inner chamber (*Figure 1*). It had its separate fuel–air supply which escaped at the top of the

---

*Former Bureau of Mines research scientist. Present address: Reaction Motors Division, Thiokol Chemical Corp., Denville, N.J.

†Physical chemist, Explosives Research Laboratory, Bureau of Mines, U.S. Department of the Interior, Pittsburgh, Pa.

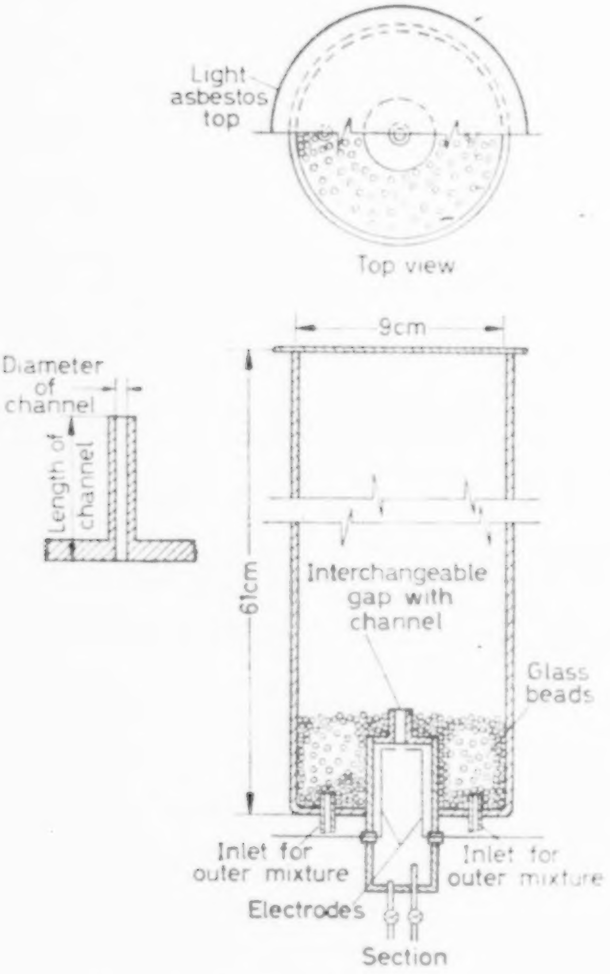

Figure 1. Experimental arrangement

chamber, where a light asbestos top prevented room air from vitiating the mixture in the outer chamber.

A second set of chambers was available with long optical windows in the outer chamber which permitted photography of the ignition process with a 35 mm Fastax camera. A standard schlieren arrangement was used. Critical ignition values in this second set of chambers were close to, but not identical with, those in the first set, as the two did not have the same dimensions.

The inner and outer chambers could be separated and 300 cm long copper tubes inserted between them, replacing the channels. One end of the tube was soldered to an interchangeable cap mounted on the inner chamber; the other end was inserted into the outer chamber through a rubber stopper.

Procedure and Accuracy of Results

20 cm^3/s of a stoichiometric methane–oxygen–nitrogen mixture having the required oxygen index (OI) was circulated through the inner chamber and 200 cm^3/s fuel–air mixture flowed through the outer chamber. By schlieren light it could be seen that a small amount of inner mixture escaped through the channel into the outer chamber. To allow this leakage gas to dissipate, the outer flow was interrupted about five seconds after the inner flow; the spark was then fired. If the explosion did not propagate into the outer chamber, only a mild report was audible. Ignition in the outside chamber caused a loud report; the asbestos lid blew off, and flames appeared above the outer chamber.

The OI of the inner mixture was a convenient measure for the ignitability of the outer mixture and the effectiveness of the channel geometry in suppressing the transmission of explosions. Accordingly, the OI was changed until the smallest OI was found for which three subsequent experiments led to three outer explosions. Then the highest OI was found for which no outer explosion occurred in three tries. The spread between the two OIs was usually 0·02, with slightly less accuracy if the OIs were above 0·50. The critical OIs as plotted in *Figures 2* to *6* are the average of these values as defined above.

It was important to determine whether the outer and inner mixtures interdiffused through the channel, thus influencing the results. A series of experiments was therefore run with long and short channels, with a cover over the top of the channel which was removed immediately prior to ignition. Critical OIs were the same, within experimental accuracy, whether a cover was employed or not. This held not only for long channels but also for short ones of large diameter.

Results

Figure 2 shows results of experiments for a 2·0 mm and 0·6 mm diameter channel, both 10 mm long. Methane–, ethane– and carbon monoxide–air mixtures were employed in the outer chamber; 10 per cent hydrogen was always mixed with the carbon monoxide to prevent side effects characteristic of pure carbon monoxide. The critical OI depends both on the type of fuel and on the strength of the outer mixture. The ignitability reaches a maximum (i.e. the plotted curve a minimum) at a mixture strength of 0·8 for methane–air, and of 0·9 for ethane–air. (The mixture strength is defined as the oxygen required for stoichiometric combustion divided by the oxygen present in mixture.) As carbon monoxide has no minimum, the stoichiometric point is therefore always taken to represent the ignitability of this fuel. Data as represented in *Figure 2* were taken for a great variety of channel diameters and lengths. The inner mixture was always methane–oxygen–nitrogen and its critical OI was determined for any given condition.

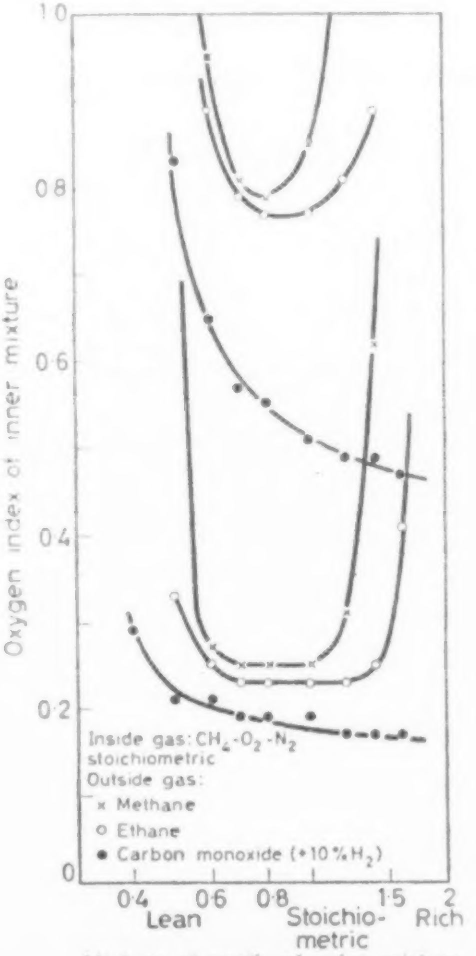

Figure 2. Influence of mixture strength on critical oxygen index of inner mixture for methane–, ethane–, and carbon monoxide–air. Channel: length 10 mm; diameter (3 upper curves) 0·6 mm and (3 lower curves) 2·0 mm

Figure 3 shows a cross-plot of critical OIs in which the channel length is constant at 10 mm but the channel diameter varies. Critical OIs vary only little between 1 and 3 mm channel diameter. Below 1 mm the slope changes drastically. Other channel lengths give similar shapes although the position of the curves is shifted on the ordinate. In all these plots methane, ethane and carbon monoxide are represented by mixture strengths of 0·8, 0·9 and 1·0, respectively.

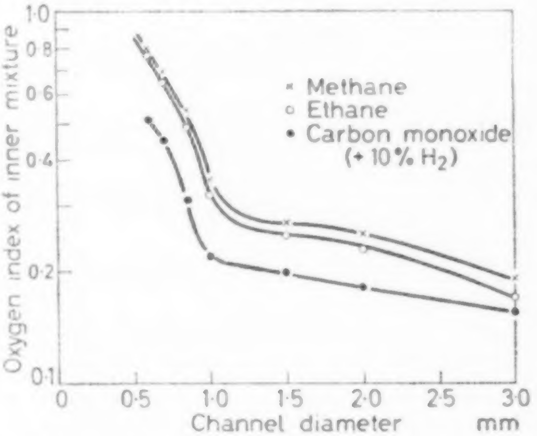

Figure 3. Cross-plot of critical oxygen indices against channel diameter for 10 mm long channel

In *Figures 4, 5* and *6* the channel diameter is held constant and the channel length is varied. It can be seen that for channel lengths of more than 10 mm, all curves tend to go to higher OIs. However, the curves also rise for very small channel lengths. Thus, all curves reach a minimum at channel lengths between 5 and 10 mm. Some points on the carbon monoxide curve could not be obtained as the critical OI dropped below 0·15, where the inner mixture failed to ignite.

The relative ignitability of a number of outside fuels was investigated for a channel of 1·2 mm diameter and 6·3 mm length, with ethane–oxygen–nitrogen mixtures inside. When the critical OI is plotted against mixture strength as in *Figure 2*, methane, ethane, propane, butane and propylene all have a minimum at about 0·23. The minima always occur between 0·8 and 1·0 of stoichiometric. *iso*Butylene has its minimum at 0·27, whereas that of ethylene is lower at 0·20. Carbon monoxide flattens out at 0·19, and the hydrogen curve is below 0·15. Methane mixtures inside caused the same relative ignitability of outside fuels.

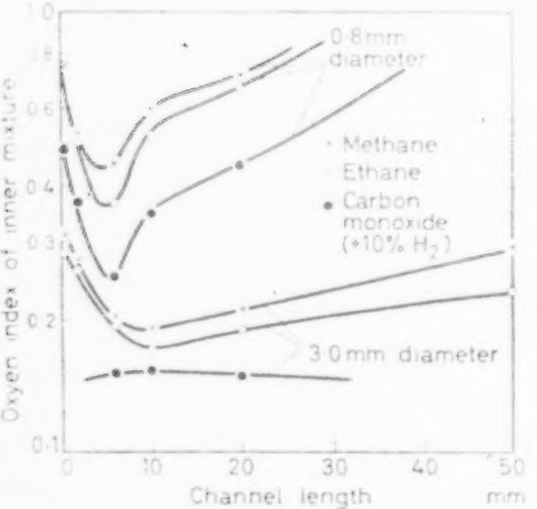

Figure 4. Cross-plot of critical oxygen indices against channel length for 3·0 and 0·8 mm channel diameters

In some experiments the inner methane mixtures were replaced by other gases having very different quenching diameters and flame temperatures. For example, stoichiometric hydrogen–air mixtures have a quenching diameter of only 0·9 mm compared with about 3·0 mm for methane–air. If the quenching diameter alone determined the passage of an explosion through a channel, hydrogen should be very superior to methane. Critical oxygen indices were therefore determined for stoichiometric hydrogen–oxygen–nitrogen inner mixtures. Typically, for a channel of 2 mm diameter and 50 mm length, methane–oxygen–nitrogen mixtures inside with methane–air outside have a critical OI of 0·48; hydrogen–oxygen–nitrogen inside with the same outer mixture have a critical OI of 0·37. This is a surprisingly small difference, and it so happens that methane at 0·48 and hydrogen at 0·37 have virtually the same flame temperature. With other channel dimensions, the differences again were small, although the flame temperatures at the critical OIs were not identical. Stoichiometric hydrogen–nitric oxide mixtures[4] are especially interesting as the quenching diameter is about 15 mm, a value far larger than for methane–air. From *Figure 3* it can be seen that a stoichiometric methane–air inner mixture requires a channel diameter of 2·75 mm at 10 mm length to transmit an explosion into an outer methane mixture. Hydrogen–nitric oxide required only 0·7 mm channel diameter to transmit an explosion. The quenching diameter of the inner mixture is therefore not of primary importance in determining outside ignition.

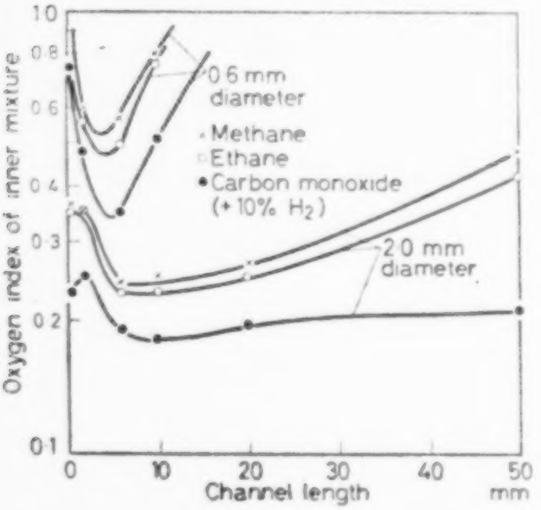

Figure 5. Cross-plot of critical oxygen indices against channel length for 2·0 and 0·6 mm channel diameters

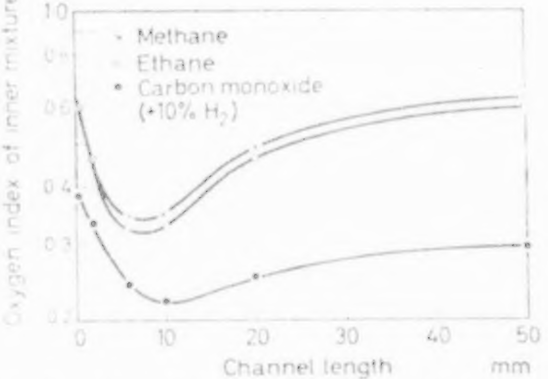

Figure 6. Cross-plot critical oxygen indices against channel length for 1·0 mm channel diameter

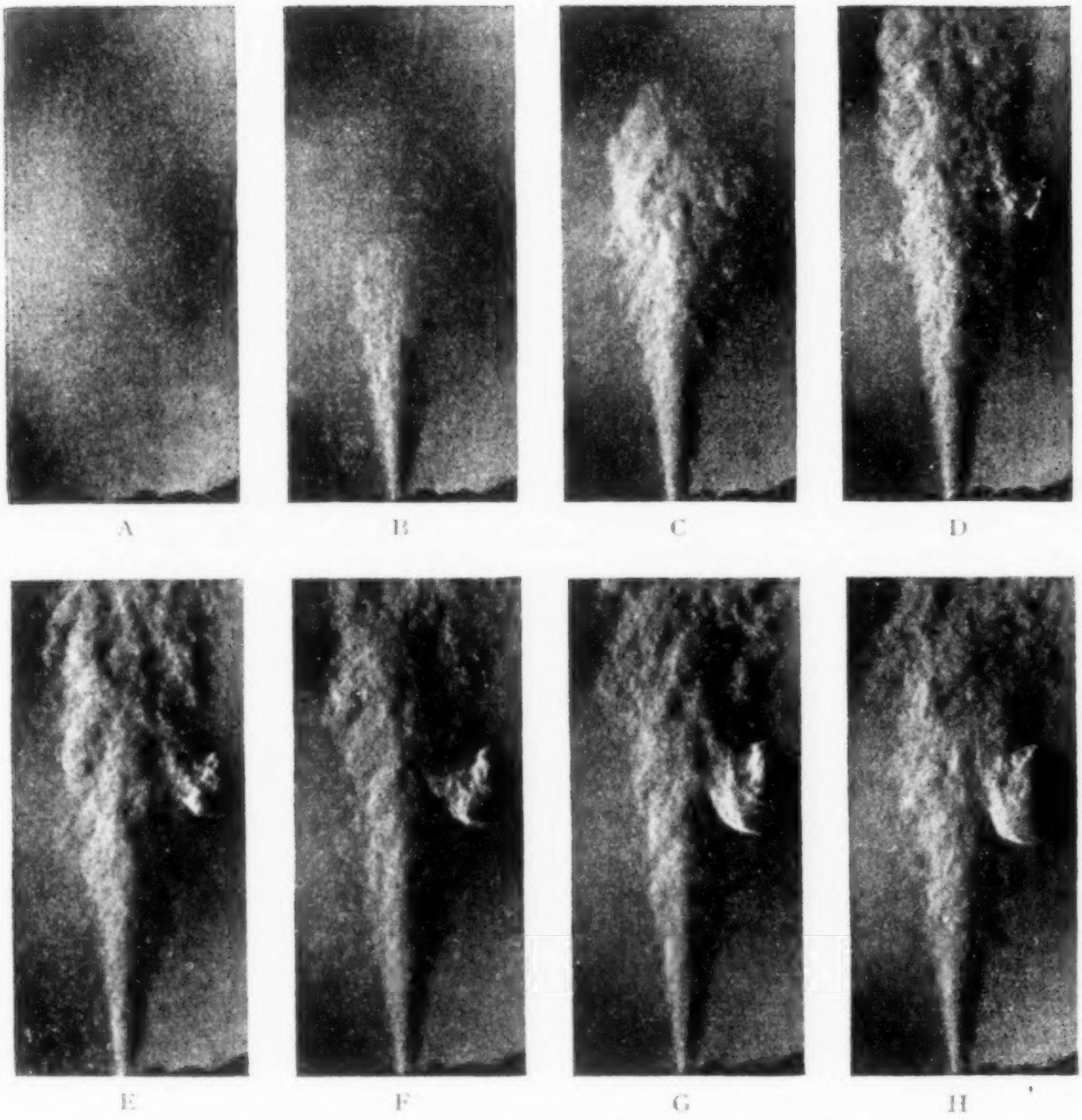

Figure 7. Jet emerging from a channel of 2 mm diameter and 50 mm length. Inner mixture: Stoichiometric H_2–O_2–N_2, *oxygen index 0·40. Outer mixture: Ethane–air. Knife-edge parallel to jet axis. Time interval between frames: 0·0005 sec. Field of view, in vertical direction, is 8 cm. Reduced 8/10 in reproduction*

Schlieren pictures of the ignition process were especially revealing. For 3 mm or narrower channels, a turbulent jet was visible above the channel exit that broadened out, so that its boundary resembled an inverted cone. The experimental cone angle is in full agreement with the theory of turbulent jets from small holes[5]. Eddies can be seen along the mantle. In *Figure 8* the first four frames are virtually the same whether ignition occurs or not. If no ignition occurs (i.e. if the OI is 0·50 instead of 0·52, see *Figure 8*) these eddies form and decay within less than a millisecond. On ignition a great number of these eddies grow and form the nucleus of separate flames. Many of these incipient flames decay again by being entrained into the jet especially at the base. In *Figure 7* conditions seem to be so critical that a single eddy leads to ignition, giving convincing proof that eddies are in fact the sources of ignition.

For channel diameters larger than 3 mm, eddies are no longer the only agents of ignition.

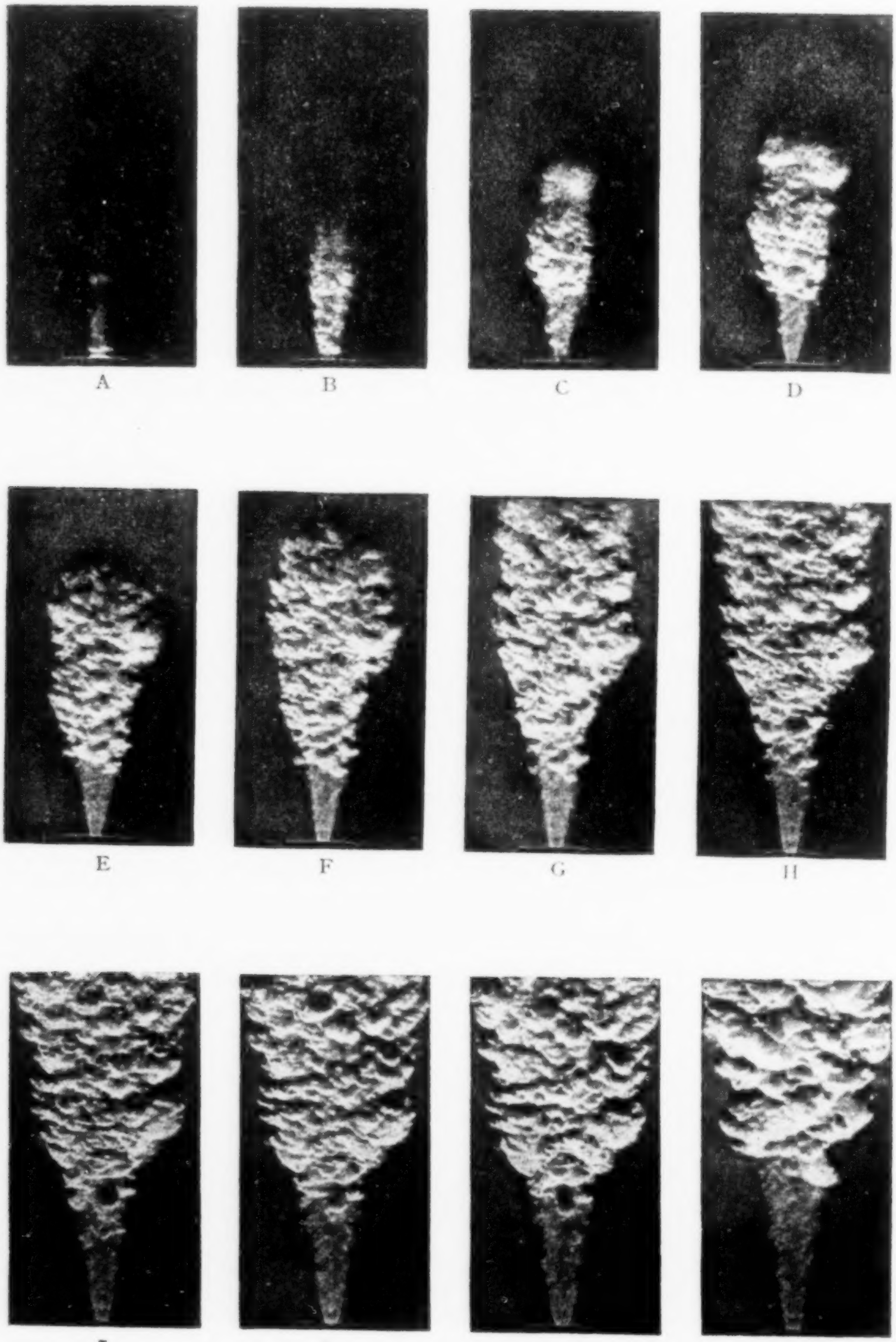

A B C D

E F G H

I J K L

Figure 9 (I to L) shows ignition from an 8 mm diameter channel 75 mm long. The inside methane oxygen–nitrogen mixture of OI = 0·15 leads to a very mild explosion with little pressure build-up. The outside mixture is stoichiometric methane–air. A laminar flame front is seen to emerge at the channel exit; however, the flame does not propagate smoothly into the outer gas, but is partly broken up by shear forces.

The experiments with 300 cm long tubes between the inner and outer chambers were done, as ignition could be produced in the outer chamber only by flames which travelled the entire length of the tubes. Hot gases from a flame extinguished in the tube would have cooled down too much to be considered as igniting agents. Because of the increased quenching diameter of turbulent flames, stoichiometric methane–air flames would not propagate through these tubes unless the diameter was at least 10 mm. *Figure 9* (E to H) shows an ignition in the outer chamber filled with methane–air, with the inner chamber and tube filled with ethylene–air. A fully turbulent flame is seen to enter the outer chamber at high speed, and turbulent flame propagation occurs throughout the vessel. The formation of mushrooms is very characteristic of this type of ignition. In *Figure 9* (B to D) the bottom of the inner chamber was removed directly prior to ignition. The flame therefore was not pushed violently through the tubes but propagated slowly in a laminar fashion with a slow spread of a laminar flame in the outer chamber. Under such conditions, flames of course could be made to propagate through tubes less than 10 mm in diameter.

Schlieren photography was also used to measure the total ejection time through channels. *Table 1* summarizes the results. The total ejection time depends therefore only little on the OI of the inner mixture. The decrease for an OI of 0·17 is probably due to large heat losses within the inner chamber, as the flame will propagate quite slowly. The ejection time did not depend on the channel length but strongly on channel diameter.

Table 1. Ejection time for a 2 mm diameter channel of 10 mm length into outer chamber filled with air

Oxygen index of stoichiometric CH_4–O_2–N_2 mixture	*Ejection time sec*
1·00	0·030
0·50	0·035
0·25	0·048
0·17	0·039

Discussion

For diameters below 3 mm, the channel is not an efficient pressure release and the explosion in the inner chamber will reach near theoretical pressures. The flow through the channel is therefore critical, i.e. the pressure in the channel itself is high and nearly the whole pressure drop occurs at the channel exit. Under such conditions standing shock waves are formed just above the exit. These shock waves showed up in all photographs of jets from narrow channels when the knife-edge of the schlieren set-up was normal to the jet axis (see *Figure 9A*). The measured ejection times agree fully with calculated values, assuming critical flow through an orifice.

The gas composition in the channel itself is important in considering the mechanism of flame transmission. Originally the channel contains the gas of the inner chamber. Interdiffusion of inner and outer gas during the interval between the closing of the gas supply and firing could alter this, especially for short channels. Experiments in which the channels were covered by a plate, however, suggest that this interdiffusion is not significant. Moreover the spark gap is several millimetres from the channel entry. Some inner gas will therefore

Figure 8. Jet emerging from channel of 2 mm diameter and 50 mm length. Inner mixture: Stoichiometric CH_4–O_2–N_2*, oxygen index 0·52. Outer mixture: Methane–air. Knife-edge normal to jet axis. Time interval between frames: 0·0002 sec, except between K and L: 0·0008 sec. Field of view, in vertical direction, is 8 cm. Reduced 8/10 in reproduction*

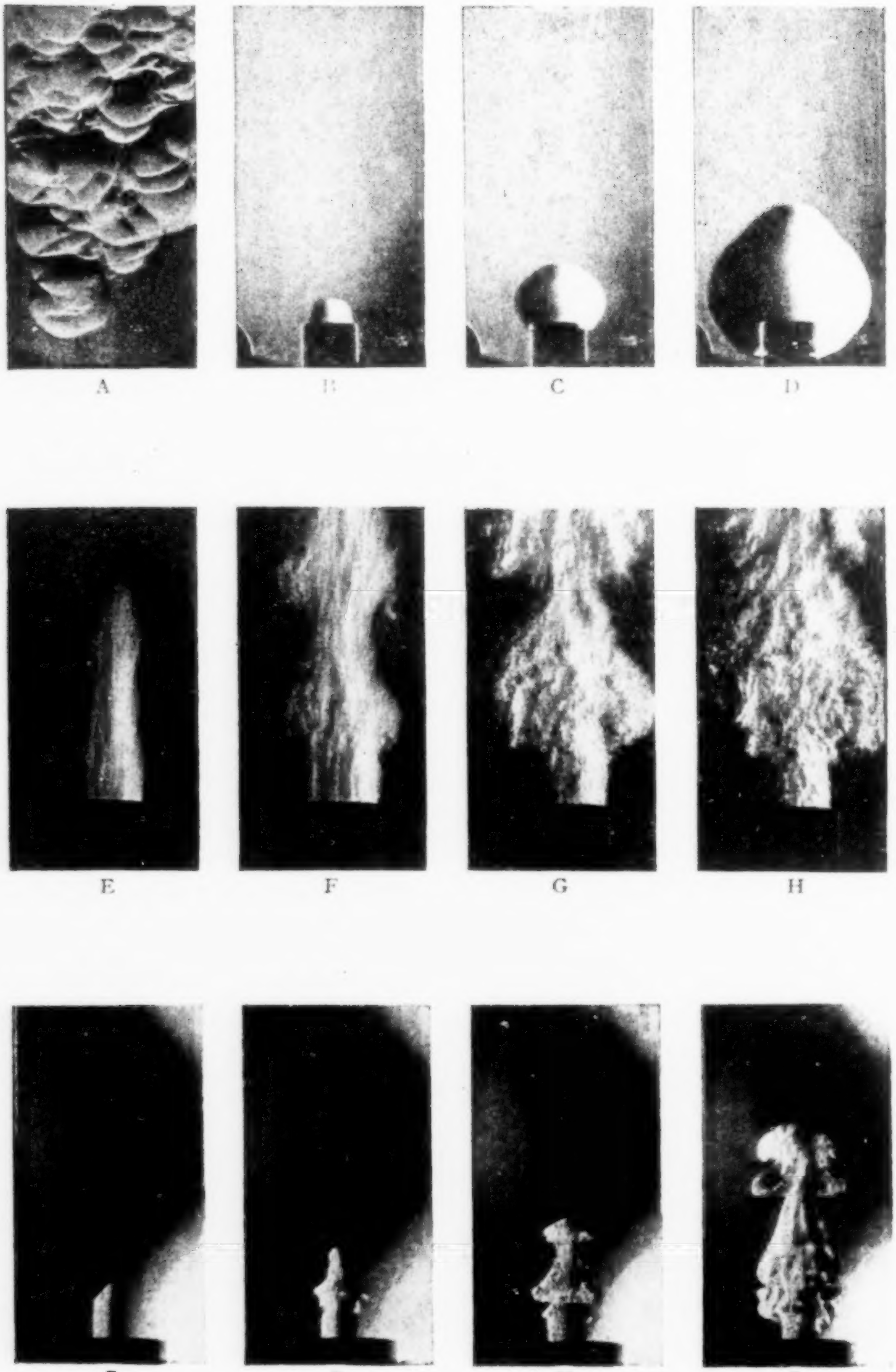
A
B
C
D
E
F
G
H
I
J
K
L

start flowing through the channel before the flame reaches the channel. Thus, the channel is self-purging. The great reproducibility of the results also could not be explained if flame transmission depended on the degree of intermixing within the channel. It is assumed therefore that flame transmission through the channel occurs in the presence of a gas mixture identical with that in the inner chamber.

Three mechanisms of flame transmission must be considered: (*A*) A laminar or turbulent flame is carried through the channel and propagates without discontinuity into the outer mixture. (*B*) The channel extinguishes the flame only gradually. A certain channel length is necessary to quench the flame completely. Critical OIs, as measured, would then just allow some elements of a flame front to reach the channel exit. (*C*) The flame front extinguishes virtually at the channel entry. Hot burnt gases from the inner mixture form a jet in the outer mixture and ignition of the outer mixture occurs in the boundary between hot burnt gas and cold explosive mixture. Flame propagation is therefore interrupted in the channel and re-ignition occurs outside.

Case A—A laminar or turbulent flame can only pass through a tube if the tube diameter is larger than the quenching diameter. A methane–oxygen–nitrogen inner mixture with an OI of 0·21 has a quenching diameter of about 3·0 mm. *Figure 3* shows that a channel diameter of 2·75 mm is necessary to get ignition of an outside methane mixture with an inside OI of 0·21. Thus the channel diameter is very close to the respective quenching distance. However, carbon monoxide ignites under such conditions with a channel diameter of only 1·2 mm. This still does not exclude flame propagation through the channel if it is remembered that the pressure in the channel can be close to the pressure in the inner chamber, as the quenching diameter is strongly pressure-dependent. However, the fact that carbon monoxide ignites better than methane would be rather difficult to interpret. Experiments with hydrogen–nitric oxide inner mixtures rule out normal quenching as the limiting factor of flame transmission in narrow channels. Even allowing for high pressure in the channel, such a flame cannot possibly pass a channel of only 0·7 mm diameter. B. KARLOVITZ *et al.*[6] have considered the extinction of flames by shear forces due to velocity gradients. In premixed flames burning on 3·16 cm diameter burners they found extinction at a Reynolds number of 100 000. In a 2 mm channel with near sonic flow at elevated pressure the Reynolds number is larger; shear forces are therefore much greater than in Karlovitz's case due to the smaller diameter. Therefore on the basis of theoretical considerations alone, we may assume that the flame is extinguished at the channel entry.

However, passage of a flame front will be operative on wide channels, especially if the velocities in the channel are small. In ***Figure 9*** (B to D) a laminar flame moves slowly through a long tube and a flame front propagates into the outer mixture without interruption. ***Figure 9*** (E to H) shows the same principle for a flame with a wider tube diameter and fast flow. In *Figure 9* (I to L) laminar flame emerges from an 8 mm diameter channel of 75 mm length; shear forces partly break up the flame front in

Figure 9. A. Frame from schlieren photograph showing standing shock pattern in jet underneath the developing flame. Knife-edge horizontal. 2 mm diameter channel, 50 mm long. Stoichiometric CH_4–O_2–N_2 *with oxygen index 0·28 inside;* CO–*air outside. B to D. Sequence of a laminar flame emerging from a 10 mm inner diameter, 300 cm long tube. B is 0·0025 sec, C is 0·0075 sec, and D is 0·0125 sec after the first emergence of the flame above the tube. Outer vessel:* CH_4*–air, stoichiometric. Mixture in inner vessel (open) and tube: Stoichiometric* C_2H_6*–air. E to H. Sequence of a turbulent flame emerging from a 20 mm inner diameter 300 cm long tube. Outer vessel:* CH_4*-air, stoichiometric. Mixture in inner vessel (closed) and tube: Stoichiometric* C_2H_4*–air. Time intervals between frames are 0·00025 sec. I to L. Laminar flame emerging from an 8 mm inner diameter, 7·5 cm long channel. Time interval between I and J, J and K, is 0·00026 sec. Time interval between K and L is 0·0013 sec. Stoichiometric* CH_4–O_2–N_2 *with oxygen index 0·15 inside. Stoichiometric* CH_4*–air outside. The field of view in a vertical direction in all frames is about 8 cm. Reduced 8/10 in reproduction*

the outer chamber but do not extinguish it.

Case B—This is an extension of Case A, where it is assumed that a flame is extinguished in channels smaller than quenching diameter, but that the quenching takes a short but finite time. Some elements of the flame front may therefore be carried a certain distance owing to the rapid flow in the channel and ignite outside if this distance is larger than the channel length. This assumption is in contradiction to the fact that very short channels inhibit flame transmission better than slightly longer ones. Accordingly, this mechanism is not applicable to narrow channels. In wide tubes the quenching of turbulent flames may well be a gradual process and it is known that long tubes transmit flames less readily than shorter ones. In the experiments with the 300 cm long tubes the flame often went out inside the tubes. The conditions under which fast turbulent flames extinguish in long tubes is little understood so far.

Case C—It has been shown that explosive mixtures can be ignited readily by jets of hot inert gases, previously heated in a furnace[7]. This makes it possible to get ignition in an outer mixture although flames cannot possibly pass through a narrow channel. *Figures 7* and *8* also prove this type of ignition beyond doubt. The experimental results of *Figures 2* to *6* will be discussed therefore under the assumption that ignition in the outside mixture occurs through contact between the hot burnt gases and the cold explosive mixture.

It was found that laminar jets of hot inert gases need a well-defined temperature to ignite surrounding fuel–air mixtures. For example, the ignition temperature of a hot nitrogen jet for methane–air was about 1 325°C whereas ethane needed only 915°C, while carbon monoxide and hydrogen were 700°C or lower[7]. The ignition process is governed by a competition between the heat lost by conduction and the rate of the chemical reaction between the fuel and the air diffusing into the jet.

In turbulent jets heat and mass transfer are vastly greater than in laminar jets. Turbulent jets therefore need higher initial temperature to ignite surrounding mixtures. Moreover, the temperature in the boundary of the jet is not uniform but varies with the scale of turbulence and the fluctuation velocity. This is the reason why ignition occurs in localized spots as observed. Turbulent jets seem to need such high temperatures for ignition that the gases leaving the channel are usually still quite luminous. This luminosity, however, is restricted to a thin pencil above the channel, i.e. it is in the core of the turbulent jet and far removed from the locus of ignition. There seems to be no relation between this luminosity and ignition except that the luminosity is a measure of the very high initial temperature of the jet.

The fact that luminous gases appear above the channel does not prove that a flame is present. It must be remembered that the delay between the consumption of inner gas close to the channel by a flame front and the appearance of the hot products outside is much less than a millisecond. The luminosity is therefore most probably due to an afterglow.

In long channels the jet loses some heat to the channel walls, and for this reason the critical OI increases with channel length. The increase in OI for very short channels is quite unexpected. However, it can be seen from schlieren photographs that the cone angle of the jet is wider for very short channels. This leads to increased mixing and heat loss. Channels between 5 and 10 mm long are therefore the most favourable to outside ignition.

The concept of hot-gas ignition makes it understandable that different gases in the outer mixture have different critical OIs of the inner mixture, the critical OI being a measure for the temperature of the ejected gas. It is fortunate that the OI otherwise does not change the flow characteristics of the jet very much as evidenced by the fact that the total ejection time is only moderately influenced by the OI. The fact that carbon monoxide ignites more readily than methane and ethane is in agreement with data from laminar hot jets. Even the shape of the carbon monoxide curve in *Figure 2* is paralleled by the ignition temperature versus mixture strength curve for laminar hot jets[7]. However, methane and ethane have very different ignition temperatures for laminar hot jets. (This difference is also noticeable in *Figures 2* to *6* but it is much smaller than expected, especially for small channel diameters.) In laminar hot jet ignition, a large volume heats up slowly by reaction until a flame front forms and begins to propagate into the outside mixture. The present turbulent hot jets are characterized by small volumes (eddies) which must ignite the outside mixture in less than a millisecond (lifetime of eddy). Although the basic principle of ignition seems to be the same in laminar and turbulent jets, time and space requirements are so different as to make the relative change in ignitability of methane and ethane plausible.

If the channel diameter is reduced, a higher OI is necessary to get ignition. This can be understood from the following principles: The jet issues gas into essentially the same volume, independent of channel diameter. This volume is determined by the constant angle of the inverted cone which is formed by the boundary layer. At a given distance from the channel exit the average gas temperature will therefore be lower for jets from narrow channels. Higher oxygen indices are therefore required to compensate for this temperature loss to get ignition.

It was observed from the schlieren records that ignition always occurred within about 1 millisecond after the hot jet appeared. Presumably this is due to the fact that the maximum pressure is not yet attained at this moment in the inner chamber. Turbulence and mixing of the jet may also differ somewhat in the period of initial jet growth from what they are when the final jet pattern has been established.

The picture emerging from the discussion is that the transmission of fuel–air explosions through channels smaller than about 3 mm in diameter is characterized by extinction of the flame front at the channel entry and formation of a new flame by a process of hot-gas ignition. This mechanism only holds if the inner chamber is closed, i.e. if large pressures and velocities develop, as occurs in many practical applications. Depending on the degree of confinement in the inner chamber, a different mechanism of transmission of explosion will take over for channel diameters of about 5 mm. This transition region needs further careful study.

References

[1] Smith, P. B. *Saf.-i.-Mines Res. Rep. No. 77*, 1953

[2] Titman, H. and Torry, R. *Saf.-i.-Mines Res. Rep. No. 123*, 1955

[3] Wolfhard, H. G. and Bruszak, A. E. 'Communication of flame through cylindrical channels'. *Rep. Invest. U.S. Bur. Min. No. 5457*, 1959; and 'Suppression and transmission of explosions by cylindrical channels'. *Rep. Invest. U.S. Bur. Min. No. 5945*, 1959

[4] Litchfield, E. L. and Blanc, M. V. Unpublished measurements at the Bureau of Mines

[5] Tollmien, W. *Z. angew. Math. Mech.* 1926, **6**, 468

[6] Karlovitz, B., Denniston, D. W., Jr. Knapschaefer, D. H. and Wells, F. E. *Fourth Symposium (International) on Combustion*, p 613. Williams and Wilkins: Baltimore, 1953

[7] Wolfhard, H. G. 'The ignition of combustible mixtures by hot gases'. *Jet Propulsion*, 1958, **28**, 798

Vanpée, M. and Wolfhard, H. G. 'Comparison between hot-gas ignition and limit flame temperatures'. *J. Amer. Rocket Soc.* 1959, **29**, 517

T
la
co
te
pr
ar
in
of
fa
o
ar
er
n
b
b
c
tl
g
d
c
n
s
f
a
t
t
a
f
t
c

The Theory of a Spherical Premixed Laminar Flame

A. A. Westenberg and S. Favin

Applied Physics Laboratory, Johns Hopkins University, Silver Spring, Md

(Received April 1959)

The general equations governing the behaviour of a low velocity, steady state, premixed, laminar flame are given for the case of spherical symmetry, and the differences from the plane flame pointed out. Numerical solutions obtained on the IBM-650 computer for the simple A → B *flame with Lewis number unity are discussed. Two innovations introduced to this type of calculation are :* (a) *the integrations were performed by starting at the cold instead of the hot boundary, which was simpler in this case, and* (b) *the flameholder temperature was regarded as the eigenvalue instead of the mass flow rate. The definition of burning velocity is discussed, and its dependence on radius of curvature is clearly shown by the results. The relation between flameholder heat loss and stability is examined in the light of a recent discovery by Hirschfelder and co-workers. The advantages of the spherical flame for flame structure studies are described.*

Introduction

THE experimental study of the structure of laminar flame fronts is now an active part of combustion science. Measurements of detailed temperature, composition and aerodynamic profiles have been reported by several groups[1-9], and refinements of the very difficult techniques involved are being worked on constantly. All of the results which have been obtained thus far were accomplished with laminar flame fronts of essentially plane geometry in one form or another. That is, the experimental flames were either flat flames stabilized on screens or porous metal flameholders of various kinds, or were bunsen flames of various shapes (conical, button, etc.) in which the useful flame region could be considered practically planar. One of the complications in studying flames of plane geometry is that they are not truly one-dimensional systems, a fact which has been clearly shown by particle-track aerodynamic measurements[4]. Instead, there is some expansion of the stream-tubes parallel to the flame front as the gas traverses the zone of reaction, and this can cause appreciable error in analysing the data if not taken into account. This stream-tube cross-sectional area expansion has been accounted for[6] by treating the experimental flame as a pseudo one-dimensional system in the sense that flow through a tube of varying cross section is so treated, i.e. flow in which the total mass flow continuity condition is fulfilled by recognizing that $\rho v a = \text{constant}$, where ρ is density, v is mass average velocity, and a is stream-tube cross-sectional area. At best, however, the fact of this area expansion adds to the complexity of the already exceedingly complicated experimental problem. The reason is that one is forced to make three different types of measurements through the flame zone; composition (always necessary) and two of the remaining three variables—temperature, velocity and stream-tube area. The fourth variable may then be obtained from the continuity relation. Furthermore, since one must always measure either velocity or area expansion, it is necessary to carry out particle-track studies, as this is the only technique available at present for measuring flame aerodynamics satisfactorily, and such studies are among the most difficult in flame structure work. If real plane flames were truly one-dimensional so that $\rho v = \text{constant}$, then one would only have to measure composition and temperature, which would be a great simplification. This would be especially desirable if, as seems likely, the sampling probe used to determine composition could be simultaneously used to measure temperature by employing it as a pneumatic probe.

A way out of this impasse presents itself in the form of a flame with spherical geometry. As R. M. FRISTROM has recently demonstrated[10], it is experimentally feasible to stabilize a premixed laminar flame on a spherical, porous flameholder, with the latter being supported by a fine tube which serves also to carry the incoming flow of combustible mixture to the centre of the hollow sphere. By working at quite low pressure and employing spheres of fine porosity the flames can be made thick enough and symmetrical enough for structural studies, although these have not yet been carried out. The great attraction offered by spherical flames, of course, is that perhaps they can be made practically one-dimensional and should have the advantages pointed out above.

In view of the probable usefulness of flames with spherical geometry, it was of interest to examine their characteristics theoretically. Considerable previous work has been done on spherical diffusion flames, presumably due to the technical importance of fuel droplet burning. The only theoretical consideration given to premixed spherical flames of which we are aware† is contained in some qualitative remarks in a review paper by J. W. Linnett[11]. The present paper summarizes the results of some calculations we have made on simple spherical flames. Also included are some general remarks on theoretical flame calculations which were occasioned by the experience gained during this work.

The Spherical Flame Equations

List of symbols

A	Reactant species
a	Stream-tube cross-sectional area
B	Product species
b	λ/T
C	Specific heat
D	Binary diffusion coefficient
D_{ij}	Multicomponent diffusion coefficient
E	Activation energy per mole
G_i	Fractional mass flow rate per unit area due to i
H_i	Specific enthalpy of i
K_i	Net chemical reaction rate of i per unit volume
k	Frequency factor of rate constant
M, M_i	Molecular weight, of species i
m_p	Mass flow rate per unit area
m_s	Total mass flow rate from spherical source
N	Total molar density
N_i	Molar density
q_f	Heat loss rate per unit area of flameholder
R	Molar gas constant
r	Radial distance coordinate
T	Absolute temperature
t	RT/E, dimensionless temperature
V_{ri}	Radial diffusion velocity of i
v	Mass average velocity
v_r	Radial mass average velocity
v_z	z-component of mass average velocity
X_i	Mole fractions
ρ	Density
λ	Thermal conductivity
σ	Stefan–Boltzmann constant

Subscripts

s	Pertains to spherical flame
p	Pertains to plane flame
r	Radial quantities
z	Cartesian z-component
i, j	Chemical species
∞	Refers to hot boundary
0	Refers to cold gas conditions upstream of flameholder
f	Refers to quantities at flameholder

Superscript

$*$	Refers to hot boundary with no heat loss from flameholder

The general equations

The general equations of change applying to laminar flame propagation have been formulated most conveniently and rigorously by J. O. Hirschfelder and his colleagues and are given in their recent treatise[12]. The usual assumptions introduced (which are well justified) are that the flame system is characterized by low velocity and negligible viscosity so that constant pressure exists throughout, and that no thermal diffusion or external forces need be considered. For the case of spherical symmetry the steady state equations then take the general form

Overall continuity:

$$m_s = 4\pi r^2 \rho v_r = \text{constant} \qquad \ldots . [1]$$

---

†During the preparation of this paper, a report by J. Menkes (California Institute of Technology Jet Propulsion Laboratory, *Progr. Rep. No. 20–361*, August 1958) came to our attention. This author has treated a simplified cylindrical flame using an integral equation technique, and points out how the method may be extended to the spherical case. The general approach is quite different from ours, however.

Species continuity:

$$\frac{\mathrm{d}G_i}{\mathrm{d}r}=\frac{4\pi r^2 M_i K_i}{m_s} \quad \ldots . [2]$$

Energy:

$$\frac{\mathrm{d}T}{\mathrm{d}r}=\frac{m_s}{4\pi\lambda r^2}\left[\sum_i H_i G_i-\left(\sum_i H_i G_i\right)_\infty\right] \quad \ldots . [3]$$

Diffusion:

$$V_i=\frac{N}{X_i\rho}\sum_j M_j D_{ij}\frac{\mathrm{d}X_j}{\mathrm{d}r} \quad \ldots . [4]$$

The function G_i is the fraction of the total mass rate of flow per unit area due to i, and is defined by the relation

$$G_i=\frac{N_i M_i(v_r+V_i)}{\rho v_r} \quad \ldots . [5]$$

The subscript ∞ refers to the place where a condition of thermodynamic equilibrium exists and is usually called the 'hot boundary' of the flame zone.

For the remainder of the discussion we shall consider only the simplest conceivable type of chemical reaction, namely the irreversible unimolecular reaction A ⟶ B for which $M_A=M_B=M$. For this case the expression for the reaction rate may be taken as

$$K_B=-K_A=k(1-X_B)N\mathrm{e}^{-E/RT} \quad \ldots [6]$$

Equation 4 for the diffusion velocity assumes the simple form for species B

$$V_B=-\frac{D}{X_B}\frac{\mathrm{d}X_B}{\mathrm{d}r} \quad \ldots . [7]$$

where D is the binary diffusion coefficient for A–B. Making the assumption of constant and equal specific heats (at constant pressure) C for both reactant and product, the specific enthalpies are

$$\left.\begin{aligned}H_A&=H_{A\infty}-C(T_\infty-T)\\H_B&=H_{B\infty}-C(T_\infty-T)\end{aligned}\right\} \quad \ldots . [8]$$

and the heat of reaction may be written as

$$H_{A\infty}-H_{B\infty}=C(T^*_\infty-T_0) \quad \ldots . [9]$$

The asterisk on the T^*_∞ indicates a hot boundary flame temperature with no heat loss from the flameholder as discussed later, and T_0 is the cold gas temperature upstream of the flameholder (see *Figure 1*).

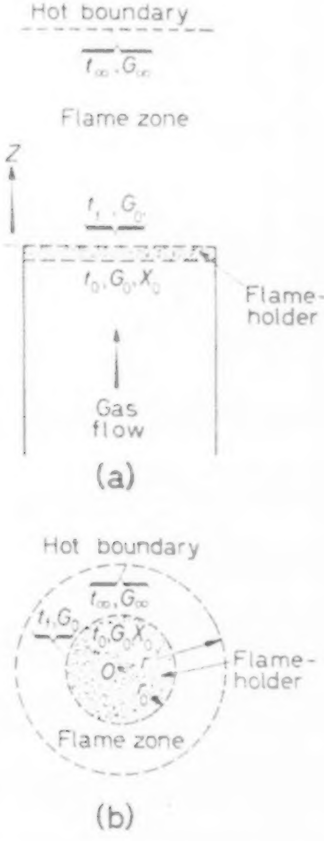

Figure 1. Schematic diagrams of (a) *plane flame, and* (b) *spherical flame*

If we note that $G_{B\infty}=1$, $G_{A\infty}=0$, equations 3, 8 and 9 may be combined to give

$$\frac{\mathrm{d}T}{\mathrm{d}r}=\frac{m_s C}{4\pi\lambda r^2}[(1-G_B)(T^*_\infty-T_0)-(T_\infty-T)] \quad \ldots . [10]$$

while making use of the fact that $\rho=NM$, with equations 2 and 6, gives

$$\frac{\mathrm{d}G_B}{\mathrm{d}r}=\frac{4\pi r^2 k\rho}{m_s}(1-X_B)\mathrm{e}^{-E/RT} \quad \ldots . [11]$$

From equations 5 and 7, we get

$$\frac{\mathrm{d}X_B}{\mathrm{d}r}=\frac{m_s}{4\pi r^2\rho D}(X_B-G_B) \quad \ldots . [12]$$

and the ideal gas equation of state yields

$$\rho/\rho_0=T_0/T \quad \ldots . [13]$$

The five equations 1, 10, 11, 12 and 13 form the set to be solved for the five dependent variables ρ, v_r, T, $G_{\rm B}$ and $X_{\rm B}$.

For our present purposes, another great simplification may be introduced without in any way restricting the general validity of the conclusions if we let the quantity $CD\rho/\lambda$ (the Lewis number) be constant and equal to unity. This is a common assumption in work of this kind, and is at least roughly correct for some gases in that simple kinetic theory predicts this quantity to be independent of temperature and pressure, and to have an absolute magnitude not far from unity. With this assumption it is easy to show by direct substitution that equations 10 and 12 are identical if $X_{\rm B}$ and T are related by

$$X_{\rm B}=1-\frac{T_\infty-T}{T^*_\infty-T_0} \quad \ldots . [14]$$

Thus, for this case, equation 12 and the variable $X_{\rm B}$ may be eliminated from the problem.

It is convenient to introduce a dimensionless temperature defined by

$$t=RT/E \quad \ldots . [15]$$

and an expression for the thermal conductivity

$$\lambda=bT=bEt/R \quad \ldots . [16]$$

although the temperature exponent in real gases is somewhat less than unity. (Note that in view of our requirement that the Lewis number be constant, this implies that $D \propto T^2$, since $\rho \propto T^{-1}$). Making use of equations 13 and 14, the working forms of the spherical flame equations 10 and 11 become

$$\frac{{\rm d}t}{{\rm d}r}=\frac{m_s CR}{4\pi bEr^2 t}[(1-G)(t^*_\infty-t_0)-(t_\infty-t)] \quad \ldots . [17]$$

$$\frac{{\rm d}G}{{\rm d}r}=\frac{4\pi k\rho_0 t_0 r^2(t_\infty-t){\rm e}^{-1/t}}{m_s(t^*_\infty-t_0)t} \quad \ldots . [18]$$

where the subscript B has been dropped for simplicity, i.e. $G \equiv G_{\rm B}$.

For later use, the corresponding equations for the one-dimensional plane flame may be written as

$$\frac{{\rm d}t}{{\rm d}z}=\frac{m_p CR}{bEt}[(1-G)(t^*_\infty-t)-(t_\infty-t)] \quad \ldots . [19]$$

$$\frac{{\rm d}G}{{\rm d}z}=\frac{k\rho_0 t_0(t_\infty-t){\rm e}^{-1/t}}{m_p(t^*_\infty-t_0)t} \quad \ldots . [20]$$

where the overall continuity condition is

$$m_p=\rho v_z=\text{constant} \quad \ldots . [21]$$

and G is given by

$$G=G_{\rm B}=\frac{X_{\rm B}M(v_z+V_{z{\rm B}})}{\rho v_z} \quad \ldots . [22]$$

The spatial coordinate z in the plane flame is taken as zero at the *flameholder surface*, while in the spherical flame the coordinate r is taken as zero at the *centre of the flameholder*. Note also that the function G has the same significance in both cases, namely, the fraction of the mass rate of flow *per unit area due* to component B.

Boundary Conditions and Method of Solution

The solution of the spherical A ⟶ B flame equations presents some interesting points of difference from the plane flame. In the latter case as solved previously[12], an obvious further simplification can be brought to equations 19 and 20 by dividing one by the other. Since the independent spatial variable z appears only in the derivatives, this division eliminates it altogether and the problem reduces to the solution of a single equation in G and t. More important, the problem extends over a finite range of values of the independent variable t, i.e. between the assumed values of initial and final temperature. It is then a relatively easy matter (in this simple case) to start at the hot boundary with an asymptotic solution and integrate numerically back to the cold boundary. The unique value of m_p which allows the satisfaction of the cold boundary conditions is the eigenvalue of the problem, and the corresponding value of v_z at the cold boundary is the laminar burning velocity, or flame speed. In the spherical flame, however, it is not possible to eliminate the spatial variable r in a similar way, as examination of equations 17 and 18 shows. This means that the range of the independent variable extends to infinity, which complicates matters somewhat. It is necessary to have an asymptotic solution valid near the hot boundary if the integration is to be started there, both because the problem is indeterminate at that point and because a practical, numerical computation cannot start at infinity. However, the authors were unable to find such an asymptotic solution to either the plane or spherical case when distance was not, or could not be, eliminated†. (It by no means follows, of course, that the solutions do not exist.)

In view of this, the situation at the cold boundary and the flameholder stabilization mechanism were examined more closely. One of the essential features of the flame theory developed by Hirschfelder and his colleagues is the introduction of a porous-plug flameholder [see *Figure 1*(a)] at the cold boundary which serves as a heat sink and also as a semi-permeable membrane preventing the diffusion of product molecules upstream. While the original reason for this was primarily a mathematical one, we are of the opinion that a flameholder with the heat sink property is an indispensable stabilizing influence for any physically realizable flame. The fact that product diffusion occurs right up to the flameholder means that the composition of the mixture may not be specified *a priori* at the cold boundary. This, in turn, means that it is not straightforward to integrate the flame equations from the cold to the hot boundary in the general case where the mole fractions are variables of the problem (see the Appendix for further comment on this point). However, in the special case being treated here where the Lewis number is unity in the A ⟶ B flame, the composition is not present as a variable, so that this cold boundary problem does not arise.

There remains the question of the heat loss to the flameholder and its significance. In Hirschfelder's treatment[12], a finite heat loss is included in the problem by assuming a cold boundary flameholder temperature [which we shall call t_f, see *Figure 1*(a)] somewhat higher than the actual initial gas temperature t_0 which is presumed to exist upstream of the flameholder. The equations are then integrated toward the boundary value t_f, and it is shown that the eigenvalue m_p is relatively insensitive to the choice of t_f within rather wide limits. For two reasons, we have chosen to handle the cold boundary heat loss problem in a somewhat different fashion. The first reason is that Hirschfelder *et al.* calculated the eigenvalue m_p as a function of t_f for the same fixed value of the final flame temperature t_∞. Since varying amounts of heat loss must be accounted for by energy conservation, a fixed value of t_∞ could only be attained by varying the initial temperature t_0, so that what was done, in effect, was to compare burning velocities of flames with both varying initial temperature and heat loss. If this point was realized, it has not been stated explicitly so far as we are aware‡. It seemed more realistic to us to keep the value of t_0 fixed and let varying flameholder heat loss show up as varying t_∞. This difference in approach is of little importance numerically, but is worth emphasizing from the point of view of principle.

The second reason for modifying the older heat loss treatment is a more 'operational' one. In previous theoretical work as mentioned, the method was to introduce the amount of heat loss (i.e. the temperature of the flameholder t_f) as one of the assumed parameters of the problem and then solve for the allowed eigenvalue m_p. This, of course, is not what is actually done in the laboratory. In reality, the parameter at one's disposal is the mass flow rate m_p (or m_s in the spherical case). The stable position of the flame zone and the heat loss from the flameholder are then determined by the value one has chosen for m_p, and not vice versa. Therefore, a more satisfying theoretical approach would seem to be to choose m_p (or m_s) and *solve for the boundary value t_f as an eigenvalue.* In this method (and in reality on flat flame burners) the 'burning velocity' is whatever value of gas velocity exists at the flameholder surface and is a function of the chosen mass flow rate[14]. The more familiar burning velocity which is considered a unique function of the initial gas mixture, temperature and pressure, is determined by the maximum stable value of m_p (very small heat loss). This point is discussed later.

---

†That is to say, a particular solution could not be found. The general solution is easy to obtain by the customary linearization procedure, but we were unable to evaluate an integration constant.

‡Since the present work was done, a recent report (see ref. 13) has reached us in which Hirschfelder and his group discuss the matter. They have performed some computations independently of us in which they allowed varying amounts of heat loss to be reflected in varying values of t_∞.

In order to carry out the above procedure, it is necessary to introduce an additional equation of constraint on the system. For the spherical A ⟶ B flame an enthalpy balance may be written as

$$m_s H_{A_0} - 4\pi r_0^2 q_f = m_s H_{B\infty} \quad \ldots . [23]$$

where q_f is the heat loss rate per unit area of flameholder. Using equations 8, 9 and 15 in 23 gives

$$q_f = \frac{m_s CE}{4\pi r_0^2 R}(t^*_\infty - t_\infty) \quad \ldots . [24]$$

We must now specify a heat loss mechanism. The particular mechanism chosen has no effect on the validity of the general method, but does affect the numerical results. It seems reasonable to assume that in a real flame the main heat loss is a result of radiation from the flameholder (unless cooled artificially in some way[14]). In our theoretical model, we have assumed a discontinuous jump in temperature from the upstream surface to the downstream surface of the flameholder, i.e. t_0 to t_f. If we now assume that the downstream surface radiates as a blackbody to cold surroundings at t_0, we may write

$$q_f = \sigma \left(\frac{E}{R}\right)^4 (t_f^4 - t_0^4) \quad \ldots . [25]$$

where σ is the Stefan–Boltzmann constant. Equating 24 and 25 gives finally

$$\frac{m_s C}{4\pi r_0^2}(t^*_\infty - t_\infty) = \sigma \left(\frac{E}{R}\right)^3 (t_f^4 - t_0^4) \quad \ldots [26]$$

The analogous equation for the plane flame is

$$m_p C(t^*_\infty - t_\infty) = \sigma \left(\frac{E}{R}\right)^3 (t_f^4 - t^4) \quad \ldots . [27]$$

The boundary conditions on G are

$$G_0 = G_f = 0; \qquad G_\infty = 1 \quad \ldots . [28]$$

for either plane or spherical geometry.

The general method of solution of the A ⟶ B spherical flame equations (with $CD\rho/\lambda = 1$) may therefore be summarized as follows:

(1) Choose a set of gas properties and initial conditions, i.e. C, b, E, ρ_0, k, t_0 and t^*_∞.

(2) Choose a flameholder radius r_0 and a mass flow rate m_s.

(3) Guess a value of t_f and solve equation 26 for the corresponding hot boundary temperature t_∞.

(4) Integrate equations 17 and 18 simultaneously by numerical means from the flameholder ($t = t_f$, $G = 0$) to the hot boundary ($t = t_\infty$, $G = 1$). In general, an incorrectly guessed t_f will not give a solution satisfying the hot boundary conditions.

(5) Repeat steps 3 and 4 until the unique value of t_f is found which gives a solution satisfying $t = t_\infty$ and $G = 1$ at the same value of the independent variable r. This value of t_f is the eigenvalue, and the corresponding solutions for G and t are the correct ones.

The plane flame solution procedure is identical except that there is no flameholder parameter corresponding to r_0 to be specified.

It is interesting to note that neither cold nor hot boundary temperature is known beforehand in this method. Specifying the mass flow rate and equation 26 takes the place of these two quantities. Also note that starting the integrations at the cold boundary in this case eliminates the need for an asymptotic solution in the starting region.

Numerical Results and Discussion

The constants for the actual examples of the A ⟶ B flame worked out were chosen to be the same as used previously[12] for the most part. They were as follows:

$t_0 = 0{\cdot}02$
$t^*_\infty = 0{\cdot}2$
$\rho_0 = 10^{-3}\,\mathrm{g\,cm^{-3}}$
$E = 3 \times 10^4\,\mathrm{cal\,mole^{-1}}$
$b = 10^{-7}\,\mathrm{cal\,sec^{-1}\,cm^{-1}\,deg^{-2}}$
$C = 0{\cdot}1885\,\mathrm{cal\,g^{-1}\,deg^{-1}}$
$k = 7{\cdot}162 \times 10^{10}\,\mathrm{sec^{-1}}$

The problem was programmed for the IBM-650 digital computer. For any given set of conditions, a convenient characteristic of the equations and the programme was used as the criterion for the 'correctness' of a solution. This is illustrated in *Figure 2* for the behaviour of the temperature variable t. When a guessed value of t_f was too small, the function t showed a maximum which was below the value of t_∞ calculated from equation 26. For a t_f which was too large, t gave a point of inflection above t_∞. The G function behaved exactly opposite to this. Thus it was possible to bracket the correct value of t_f and converge on it by iteration until the maximum value of t came as near to the calculated t_∞ as desired. In reality, of course, there should be no maximum in t or G at all. The fact that there were maxima in the numerical solutions was simply due to the 'sensitivity' chosen for the integrations. By going tó smaller intervals, the value of r at the maxima (and therefore the apparent flame 'thickness') could be made greater, and in the limit of an infinitesimal interval would approach infinity as it should. For practical calculations, a 'sensitivity' was chosen which gave a reasonable integration time on the machine, and the resulting maximum feature in t and G was made use of as a convenient way of defining the 'thickness' of the flame.

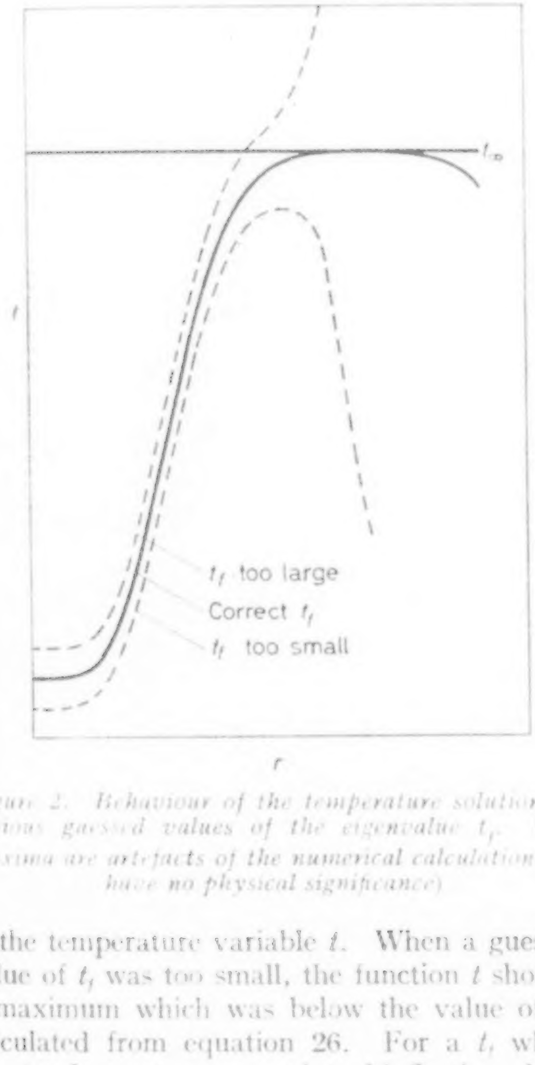

Figure 2. Behaviour of the temperature solution for various guessed values of the eigenvalue t_f. (The maxima are artefacts of the numerical calculation and have no physical significance)

In order to compare the spherical flame results with those for the plane flame, solutions were obtained for four different values of spherical flameholder radius r_0 as well as the plane flame —all at the same flameholder temperature. To do this, the procedure outlined in the preceding section was actually done in reverse, i.e. m_s (or m_p) was solved for as the eigenvalue after picking t_f, as in the older calculations. A value of $t_f = 0{\cdot}02001$ was chosen, and being so close to $t_0 = 0{\cdot}02$, the value of t_∞ calculated was essentially equal to $0{\cdot}2$. Thus for numerical purposes the amount of heat loss was negligible. The numbers obtained from these computations are given in *Table 1*, along with the values of the gas velocity at the flameholder, which are what one would commonly call the 'burning velocities'. The actual numerical values are of little importance in this simplified calculation, and trends and comparisons are what one seeks. Here it is to be noted that the calculated burning velocity clearly increases with decreasing radius of curvature of the flame front. This effect is as expected for a flame which is concave toward the cold gas, and has been predicted and commented on many times in the literature—the arguments having been qualitative and more or less intuitive. The correctness of the prediction had not been clearly shown either experimentally or theoretically, however, as far as we know. At the smallest radius examined,

Table 1. Eigenvalues and burning velocities for spherical and plane flames. $t_f = 0{\cdot}02001$, $t_\infty = 0{\cdot}2$

Configuration	m_s or m_p *g sec^{-1} or g cm^{-2} sec^{-1}*	v_{rf} or v_{zf} *cm sec^{-1}*
Spherical		
$r_0 = 1{\cdot}0$ *cm*	28·1955	2244·85
$r_0 = 0{\cdot}5$	7·06560	2250·17
$r_0 = 0{\cdot}1$	0·288045	2293·35
$r_0 = 0{\cdot}01$	0·00346060	2755·23
Plane	2·23837	2239·49

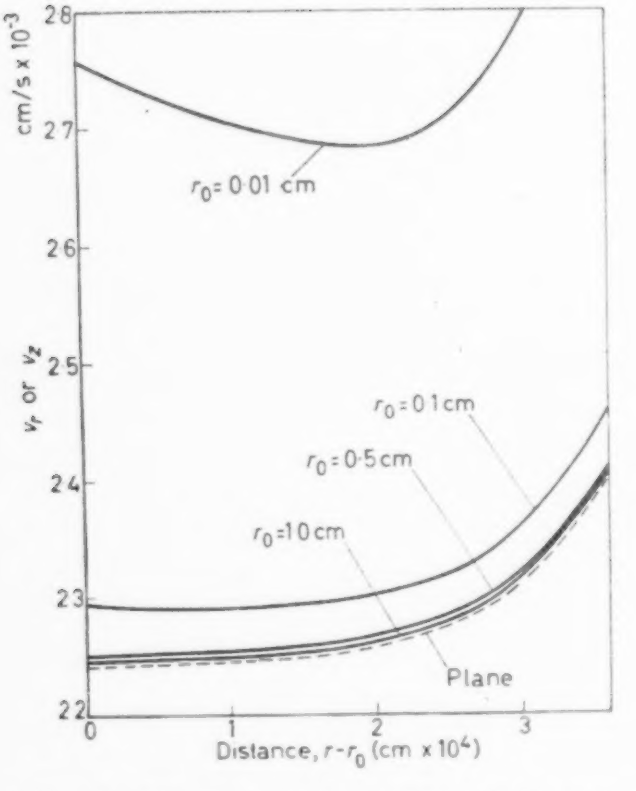

Figure 3. Solutions for the gas velocity in the region near the flameholder for various sized spherical flames and the plane flame. $t_f=0{\cdot}02001$, $t_\infty=0{\cdot}2$ *in all cases*

$r_0=0{\cdot}01$ cm (this is about five times the flame 'thickness'), the increase in burning velocity has already become quite pronounced. It may be worth emphasizing that this should not be confused with the increase in gas velocity at the surface of a sphere of decreasing radius which one would expect from simple continuity considerations, i.e. equation 1, when the total mass flow is kept fixed. In these calculations the mass flow was *not* fixed, of course, but was found in each case as a true eigenvalue characteristic of the conditions.

The effects of continuity may be seen, however, in the computed gas velocities just beyond the flameholder surface. *Figure 3* is an expanded plot of the gas velocities in a small region near the surface. Both the $r_0=0{\cdot}01$ and 0·1 cm spherical flames actually show a decrease in velocity before the density has decreased sufficiently so that acceleration overcomes the natural velocity decrease with increasing radius to be expected of a spherical gas flow. This initial drop in velocity only shows up for the smaller radius flames since for these a given increment in radius represents a larger fractional change.

For completeness, we have included the curves in *Figure 4*, which show the distributions in t, G, v, and X for the spherical flames with $r_0=0{\cdot}01$ and $r_0=1{\cdot}0$ cm. The plane flame solutions are superimposable on the latter on the scale shown. There is nothing unusual to comment on here.

We come now to the very interesting effects of flameholder heat loss and its relation to flame stability. All of the following calculations were carried out for the plane flame, but the same conclusions apply to the spherical flame. *Figure 5* shows the t and G profiles for three flames with different m_p values. The value of t_f was found as an eigenvalue in each case, by the procedure outlined in the preceding section. The results illustrate that the stable position of the flame zone moves closer to the flameholder with decreasing m_p. This raises the flameholder temperature t_f, which causes a greater heat loss rate and thus a lower hot boundary temperature t_∞. The changes produced in t_∞ are quite small compared with those in t_f, however.

The next question which naturally presents itself is what happens when the mass flow rate m_p is lowered indefinitely toward zero. In *Figure 6* t_f is plotted as a function of m_p. The interesting and surprising feature of this plot is the maximum shown by t_f. This type of behaviour, couched in somewhat different terms, was noted first by D. B. SPALDING[15] and later by J. O. HIRSCHFELDER and his colleagues[13]. As far as the mathematical solutions are concerned, there is nothing to distinguish between the regions on either side of the maximum. Physically, however, as has been previously pointed out[13, 15], the part of the curve to the left of the maximum is a region of instability. That is, any attempt to reduce the value of m_p below that at the maximum would move the flame closer to the flameholder, thus tending to raise t_f. But the solution for a lower m_p corresponds to a ***lower*** t_f, so the situation is an impossible one, and the value of m_p at the maximum

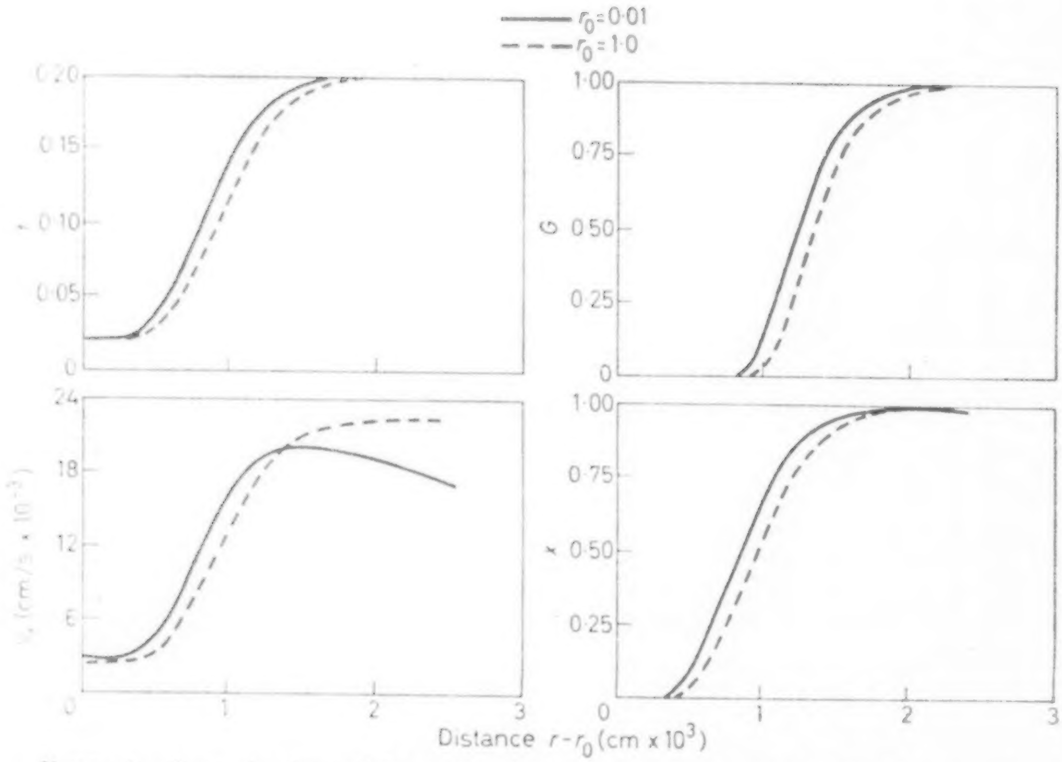

Figure 4. *Typical spherical flame distributions in temperature, fractional mass rate of flow, gas velocity and composition*

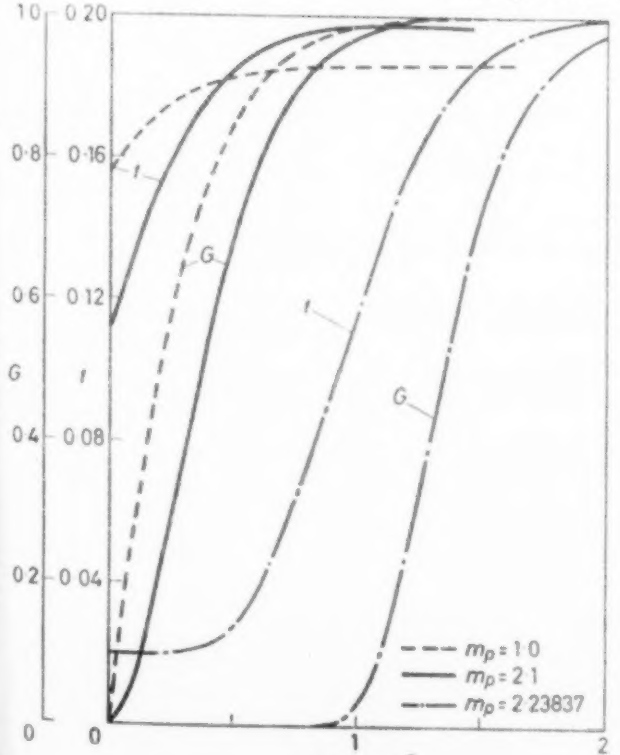

Figure 5. ***Dependence of t and G on m_p for the plane flame***

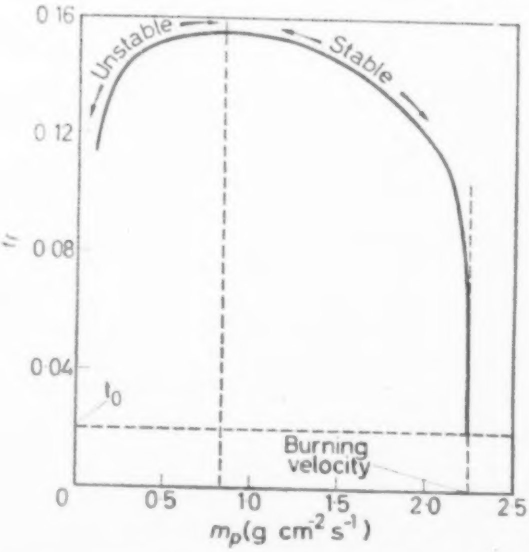

Figure 6. ***Dependence of the eigenvalue t_f (flame-holder temperature) on mass flow parameter m_p for the plane flame***

represents the minimum mass flow capable of sustaining a stable flame on the flameholder.

The right (stable) side of the curve in *Figure 6* is also interesting. It will be seen that t_f is a very sensitive function of m_p on the extreme right. A slight change in m_p causes a large change in flame position relative to the flameholder, and a resulting large change in t_f. Conversely, one might say that m_p is a very insensitive function of heat loss, or of t_f. It is this nearly constant region of m_p—or the extrapolated limit for zero heat loss—which is (or should be) referred to as *the* mass burning velocity for the particular mixture and cold gas conditions. An operational definition of this kind which directly involves the technique used for the measurement seems to be the only satisfactory one possible. It will be recognized that this is similar to the definition of burning velocity employed by J. P. BOTHA and D. B. SPALDING[14] in their flat flame burner. They used water-cooling of the flameholder as a heat loss device instead of the radiation mechanism postulated in this theoretical study, but this detail is irrelevant.

In the review paper[11] previously referred to, Linnett discusses at some length the difficulty of defining the term 'burning velocity' in a rigorous manner to fit any geometry. There certainly are difficulties in doing this with any generality. Furthermore, it is true that, as he points out, if one is using a common definition such as 'volumetric flow rate of unburnt gas divided by flame area', the velocity obtained depends on the area chosen in the spherical flame. However, if one is of the opinion, as are the writers, that it is impossible to realize a steady state flame of the type being considered without the use of a stabilizing flameholder, then there would seem to be no more difficulty in providing an operational definition of 'burning velocity' for a spherical flame than a plane flame. The fundamental definition of 'burning velocity' is *by way of a gas velocity*. For either flame, then, by 'burning velocity' we mean the gas velocity at the surface of the flameholder under conditions such that $t_\infty \simeq t_\infty^*$, i.e. essentially no heat loss. Linnett was saying practically the same thing in advocating use of a flame area 'as far on the unburnt side of the flame as possible'.

According to these results, it should be possible to stabilize a flame of a given combustible on either a flat or spherical flameholder only at a mass flow between two well-defined limits, as shown in *Figure 6*. How definite and reproducible these limits are in practice remains to be seen. It should be noted, finally, that Hirschfelder *et al.*[13] have examined the region at the extreme right side of curves like those in *Figure 6* in some detail. From a strictly mathematical point of view, it appears that, for extremely small heat losses, the values of m_p do not approach an asymptote as shown, but can take on very large values. Whether this behaviour has any real physical significance is not clear. It seems likely that this is an unstable (and therefore physically unobtainable) area also.

Appendix

It was mentioned in the main text that if the Lewis number is not taken as unity in the A ⟶ B flame, the composition variable $X_B(=X)$ and equation 12 cannot be eliminated from the problem. Since the value of X is not known at the cold boundary, this introduces a complication in integrating from the cold to the hot boundary. It is still possible to solve the problem, however. To demonstrate that this was so, the authors set up the same flame as used before except with $CD\rho/\lambda = 2$. With equation 12 included in the programme, the problem was regarded as having *two* eigenvalues —t_f and X_f. Iterative solutions were performed until the correct values of t_f and X_f were found which allowed the simultaneous satisfaction of all three hot boundary conditions, i.e. $t = t_\infty$, $G = X = 1$. The time required for such a double eigenvalue procedure was longer than the previous cases, of course, but was not excessive. However, for more complex flames involving more chemical species (and hence more X_i) the necessary labour would increase prohibitively. For these, spherical flame calculations would have to await satisfactory asymptotic solutions (if possible) so that the integrations could be started at the hot boundary.

This work was supported by Contract NOrd 7386 with the Bureau of Ordnance, U.S. Navy.

It is a pleasure to acknowledge the benefit we have derived from discussions with Dr R. M. Fristrom during this work, and the advice of Mr W. T. Remch in the machine computations.

References

[1] Fridman, R. and Burke, E. *J. chem. Phys.* 1954, **22,** 824

[2] Burgoyne, J. H. and Weinberg, F. J. *Proc. Roy. Soc. A*, 1954, **224,** 286

[3] Fridman, R. and Cyphers, J. A. *J. chem. Phys.* 1955, **23,** 1875

[4] Fristrom, R. M. *J. chem. Phys.* 1956, **24,** 888

[5] Fristrom, R. M., Prescott, R. and Grunfelder, C. *Combustion & Flame*, 1957, **1,** 102

[6] Fristrom, R. M. and Westenberg, A. A. *Combustion & Flame*, 1957, **1,** 217

[7] Fristrom, R. M., Avery, W. H. and Grunfelder, C. *Seventh Symposium (International) on Combustion*, p 304. Butterworths: London, 1959

[8] Breisacher, P., Dembrow, D. and Berl, W. G. *Seventh Symposium (International) on Combustion*, p 894. Butterworths: London, 1959

[9] Fridman, R. and Nugent, R. G. *Seventh Symposium (International) on Combustion*, p 311. Butterworths: London, 1959

[10] Fristrom, R. M. *Combustion & Flame*, 1958, **2,** 103

[11] Linnett, J. W. *Fourth Symposium (International) on Combustion*, p 20. Williams and Wilkins: Baltimore, 1953

[12] Hirschfelder, J. O., Curtiss, C. F. and Bird, R. B. *The Molecular Theory of Gases and Liquids*, Chap. 11. Wiley: New York, 1954

[13] Hirschfelder, J. O., McCone, A. and Odell, T. *Univ. Wis. Naval Res. Lab. Rep. No. CM-934*, August 1958

[14] Botha, J. P. and Spalding, D. B. *Proc. Roy. Soc.* 1954, **225,** 71

[15] Spalding, D. B. *Proc. Roy. Soc. A*, 1957, **240,** 83

I

fr

cl

th

p

ty

ti

d

te

of

a

P

H

a

ti

h

sl

e

w

s

la

re

o

An Approximate Solution of the Equation for Self-ignition

TOSIRO KINBARA

College of General Education, University of Tokyo, Komaba, Meguroku, Tokyo

and

KAZUO AKITA

Fire Research Institute of Japan, 700, Shinkawa, Mitaka, Tokyo

(Received May 1959)

A method is described for obtaining an approximate solution of the equation for self-ignition for the case when temperature increases with time. The method has been used in investigating the self-ignition of spherical sawdust heated in a uniform temperature field for several ambient temperatures and various radii. Good agreement is reported between theory and observation for the qualitative behaviour of temperature rise with time but results fell short of expectations with respect to the magnitude of the ignition time, which may be due to consumption of material by chemical reaction for which no allowance was made.

1. Introduction

IN THE theory of self-ignition which results from the slow accumulation of heat from chemical reaction in the material, and in the theory of explosion of combustibles, the heat production is assumed to be of the Arrhenius type, and the fundamental problem in these theories is to solve the equation of heat conduction having an Arrhenius heat generation term.

The equation, for the case of a steady state of temperature, has been studied by many authors including D. A. FRANK-KAMENETZKY[1], P. L. CHAMBRÉ[2], D. M. CLEMMOW and J. D. HUFFINGTON[3], S. M. GENENSKY[4], P. H. THOMAS[5] and others; and analytical or numerical solutions, when the temperature rise is not so large, have been given for materials in the form of slabs, cylinders or spheres. However, the equation for the case of temperature increasing with time has not yet been solved, although some numerical solutions obtained by calculations with high speed computers have been reported for the case of semi-infinite slabs[6,7].

In this paper there is described a method for obtaining an approximate solution of the equation for the case of temperature increasing with time. A certain special function was substituted for the Arrhenius heat generation term. When the equation, with this function, was solved for the steady state, the solution was very similar to the steady state solution for the equation containing the Arrhenius term obtained by D. A. FRANK-KAMENETZKY[1] and that found by P. L. CHAMBRÉ[2] using the table of S. CHANDRASEKHAR and G. W. WARES[8]. The differential equation in the case of a non-steady state was easily solved when this special function was also used for the heat generation term. Although there is a problem left open to discussion about the applicability of this function to the non-steady state, it can safely be said that the solution thus obtained is available for a small rise of temperature before ignition as in the case of self-ignition of fibre-materials.

2. Fundamental Equation

The equation for self-ignition containing a term of heat production of the unimolecular type is well known in the form

$$c\rho\partial T/\partial t = k\nabla^2 T + A\exp(-E/RT) \quad . . [1]$$

where c denotes specific heat, ρ is the density of materials, k is the thermal conductivity, T is the absolute temperature, A is the rate of heat production per unit volume when T is infinitely large, E is the activation energy, R is the gas constant, and the third term of equation 1 is the Arrhenius heat generation term.

We shall consider the case where a specimen of uniform material in the form of a slab, cylinder or sphere is placed in a field of temperature T_a. The temperature distribution within the object will be considered to be symmetrical about a maximum in the centre while the temperature rise is not large. For these conditions, equation 1 can be transformed into the following well known equation of dimensionless quantities.

$$\frac{\partial\theta}{\partial\tau}=\frac{\partial^2\theta}{\partial\xi^2}+\frac{m}{\xi}\,\frac{\partial\theta}{\partial\xi}+\delta e^{\theta} \qquad \ldots . [2]$$

Table 1. Relation between δ and θ_0 (for sphere)

Authors	$\delta=3{\cdot}32$	3·00	2·50	2·00	1·50	1·00
Chambré, Chandrasekhar	$\theta_0=1{\cdot}611$	0·954	0·649	0·455	0·310	0·189
Frank-Kamenetzky	$\theta_0=1{\cdot}610$	0·959	0·651	0·457	0·310	0·190
Kinbara and Akita	$\theta_0=1{\cdot}610$	0·951	0·647	0·458	0·311	0·190

where δe^6 corresponds to the heat generation term simplified following Frank-Kamenetzky, and δ stands for $(A/k)r^2(E/RT_a^2)\exp(-E/RT_a)$, θ is the reduced temperature $[(E/RT_a^2)\,(T-T_a)]$, ξ is the reduced distance $[x/r]$, τ is the reduced time $[(k/c\rho r^2)t]$, m is a constant depending on the shape of the body ($m=0$ for a slab, $m=1$ for a cylinder, and $m=2$ for a sphere), r is the radius or half thickness (in the case of a slab), and x is the distance from the centre measured perpendicularly to the surface.

Except where there is a possibility of confusing the reduced (dimensionless) with the dimensional variables we shall generally omit the word 'reduced' in the remainder of the paper.

3. Steady State with Constant Surface Temperature

Let us begin with the steady state of temperature and consider first the case in which surface temperature is kept equal to the ambient temperature. The equation is

$$\frac{d^2\theta}{d\xi^2}+\frac{m}{\xi}\,\frac{d\theta}{d\xi}+\delta e^{\theta}=0 \qquad \ldots . [3]$$

being subject to the boundary conditions

$$\text{(i)}\quad [\theta]_{\xi=1}=0, \qquad \text{(ii)}\quad \left[\frac{d\theta}{d\xi}\right]_{\xi=0}=0 \quad \ldots [4]$$

For $m=0$, Frank-Kamenetzky[1] solved this equation analytically; and for $m=1$ and $m=2$, he obtained the centre-temperature θ_0 for each value of δ by numerical calculation. Afterwards, Chambré[2] showed the analytical solution for $m=1$, and pointed out that the temperature distribution for $m=2$ can be estimated using the table of Chandrasekhar and Wares[8]. When δ is given, θ_0 can be estimated from this table. The result (for $m=2$) is shown in ***Table 1*** together with the one calculated numerically by Frank-Kamenetzky.

In all cases, δ has a critical value δ_c which depends on m. For $\delta>\delta_c$ no stationary θ_0 exists, the fact showing that the specimen in this case will finally run into self-ignition. The value of δ_c and the temperature θ_c corresponding to it for the three cases are as follows:

$$\left.\begin{aligned} m=0: &\quad \delta_c=0{\cdot}88, \quad \theta_c=1{\cdot}19 \\ m=1: &\quad \delta_c=2{\cdot}00, \quad \theta_c=1{\cdot}38 \\ m=2: &\quad \delta_c=3{\cdot}32, \quad \theta_c=1{\cdot}61 \end{aligned}\right\} \quad \ldots . [5]$$

4. New Method for Obtaining a Solution for the Steady State

Solutions which are very similar to those obtained by the above authors can be derived by an entirely different method.

Let us try to substitute a function $\delta(1+\beta\theta)$ for the heat generation term δe^{θ}, where β is assumed to be constant with respect to θ and ξ. Then, equation 3 can be transformed into

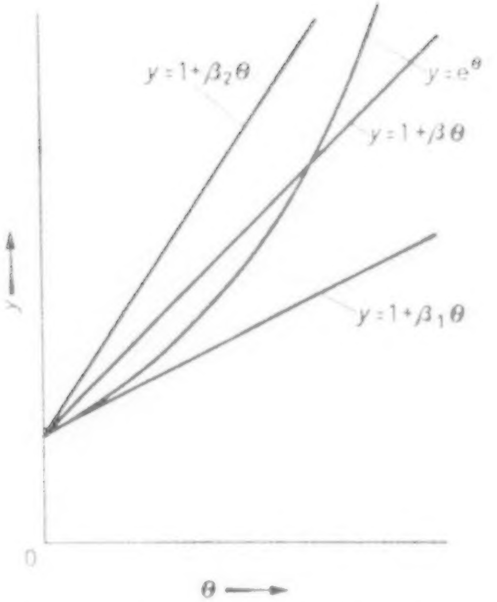

Figure 1. Comparison of e^{θ} with $(1+\beta\theta)$

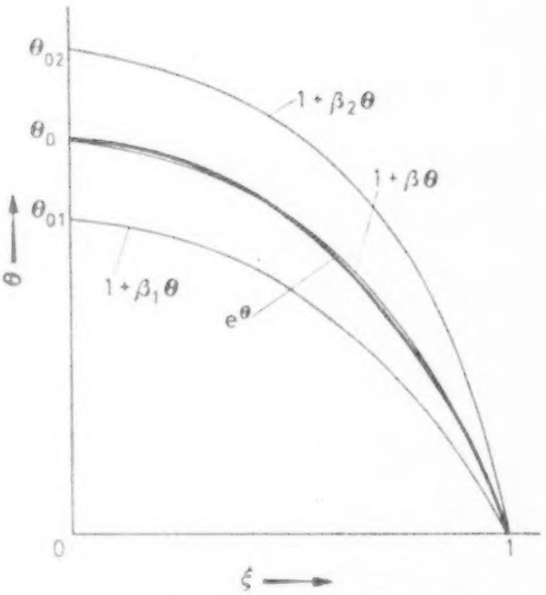

Figure 2. Supposed temperature distribution within a specimen

$$\frac{d^2\theta}{d\xi^2}+\frac{m}{\xi}\frac{d\theta}{d\xi}+\delta(1+\beta\theta)=0 \quad \ldots\ldots [6]$$

If β is as small as β_1, shown in *Figure 1*, the substituted function would give too small a heat generation for all θ. The calculated temperature distribution to be expected from equation 6 would be like $(1+\beta_1\theta)$ shown in *Figure 2* in comparison with the correct temperature distribution labelled e^{θ}. If $\beta=\beta_2$, the substituted function gives too high a value of heat generation for every θ and too high a temperature at every point as shown in *Figure 2*. There must be a certain value of β that will give a heat generation term which is too large for small θ and too small for large θ, and which gives the same temperature at the centre of the specimen as that obtained by the use of e^{θ}.

Now, the problem is how to determine this value of β. It is obvious that β cannot be an absolute constant, but depends on how we choose the region of θ. Since θ is highest at the centre and zero at the surface, the temperature range is θ_0 (centre temperature) to 0, and β will depend on θ_0. Large β corresponds to large θ_0, as can be expected from *Figure 1*.

In addition, β depends on the distribution of temperature within the specimen. For a given θ_0, β should be large if the greater part of the specimen is at a high temperature near θ_0, while it should be small if the greater part is at a low temperature. From this it also follows that β should be different according to whether the specimen is in the form of a slab, cylinder or sphere.

Thus, it is reasonable to assume that

$$\beta=1+a_1\theta_0+a_2\theta_0^2+a_3\theta_0^3+\ldots\ldots \quad [7]$$

where the a_ss are constants depending on the shape of the specimen.

Once β is given as a function of θ_0, it is easy to solve the equation. The method is almost the same for the three cases of slab, cylinder and sphere, so we shall confine the following discussion to a spherical body.

From equations 6 and 4 we get

$$\theta=\frac{1}{\beta}\left\{\frac{\sin q_0\xi}{\xi\sin q_0}-1\right\} \quad \ldots\ldots [8]$$

where

$$q_0^2=\beta\delta \quad \ldots\ldots [9]$$

and for $\xi=0$,

$$1+\beta\theta_0=q_0/\sin q_0 \quad \ldots\ldots [10]$$

It is required, in our method, to give suitable values to β in equation 7 so that θ_0 when calculated from equation 10 might just coincide with the value indicated in *Table 1*.

For the first step, it was assumed that

$$\beta = 1 + a_1\theta_0 + a_2\theta_0^2 \qquad \ldots . [11]$$

where θ_0 is not so large.

Suppose certain numerical values are given to a_1 and a_2, then $q_0/\sin q_0$ and $1+\beta\theta_0$ can be plotted against θ_0 as in *Figure 3*, where the solid line represents $y=1+\beta\theta_0$ and the dotted lines correspond to $y=q_0/\sin q_0$ for $\delta=\delta_1$, $\delta=\delta_c$ and $\delta=\delta_2$ respectively. When δ is as small as δ_1 in *Figure 3*, equation 10 will have a solution θ_1. But when δ is as large as δ_2 in *Figure 3*, the two curves will never intersect each other and equation 10 will have no solution. It means that the specimen finally runs into self-ignition.

Now, when δ is equal to δ_c, the curve $y=q_0/\sin q_0$ will just touch the curve $y=1+\beta\theta_0$, and θ_0 in this case will be θ_c. These δ_c and θ_c should be equal to the values given by relation 5. This is the criterion for determining two unknown quantities a_1 and a_2. Thus we can calculate a_1 and a_2 from

$$\delta_c = 3{\cdot}32, \quad \theta_c = 1{\cdot}61$$

$$\beta_c = 1 + a_1\theta_c + a_2\theta_c^2$$

$$1 + \beta_c\theta_c = (\beta_c\delta_c)^{\frac{1}{2}} / \sin\,(\beta_c\delta_c)^{\frac{1}{2}}$$

$$\left[\frac{\mathrm{d}}{\mathrm{d}\theta_0}(1+\beta\theta_0)\right]_c = \left[\frac{\mathrm{d}}{\mathrm{d}\theta_0}\frac{(\beta\delta_c)^{\frac{1}{2}}}{\sin\,(\beta\delta_c)^{\frac{1}{2}}}\right]_c$$

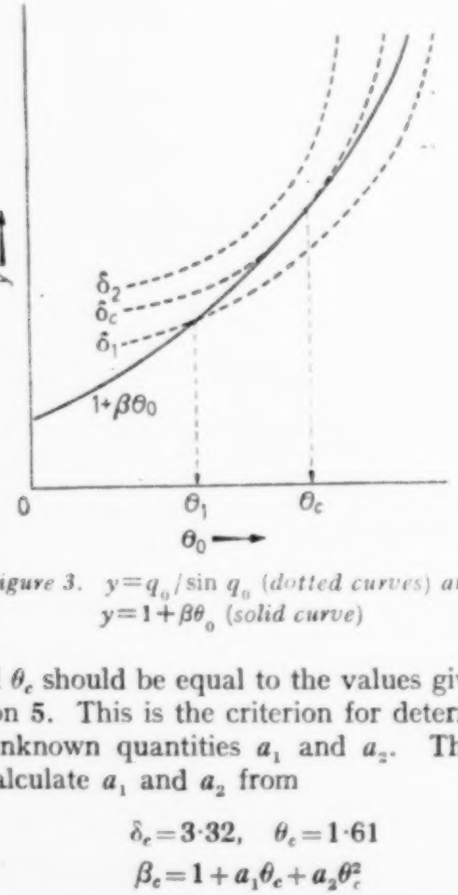

Figure 3. $y=q_0/\sin q_0$ *(dotted curves) and* $y=1+\beta\theta_0$ *(solid curve)*

and get the following relation

$$\beta_{(\mathrm{sphere})} = 1 + 0{\cdot}3691\,\theta_0 + 0{\cdot}0908\,\theta_0^2 \qquad \ldots . [12]$$

The third line in *Table 1* is θ_0 calculated from equations 10 and 12. It shows remarkably good agreement with the values given by Frank-Kamenetzky, by Chambré and by Chandrasekhar and Wares. This is because the assumption that β can be expressed by a quadratic function of θ_0 is quite adequate.

Now, once β is expressed as a function of θ_0, temperature distribution inside the spherical specimen can be given by equation 8. One can compare the distributions thus obtained with the one from the table of Chandrasekhar and Wares (*Figure 4*). The agreement is again satisfactory.

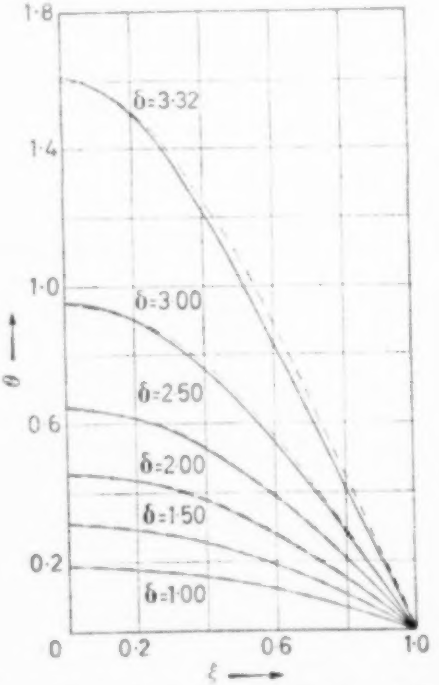

Figure 4. Comparison of temperature distribution. Solid curves: Chandrasekhar and Wares. Dotted curves: Kinbara and Akita

5. Steady State with Surface Cooling

The above-mentioned solutions are the ones subject to the boundary conditions 4. The solution when heat is transmitted from the surface of a specimen to the ambient region according to the law of cooling has been obtained by Thomas[5].

The boundary condition in this case is

$$\text{(i)}\ \left[\frac{d\theta}{d\xi}+\mu\theta\right]_{\xi=1}=0, \qquad \text{(ii)}\ \left[\frac{d\theta}{d\xi}\right]_{\xi=0}=0 \quad \ldots . [13]$$

where $\mu=(\alpha/k)r$, α being the heat transmission coefficient.

The surface temperature θ_s is, in general, different from 0, and β depends not only on θ_0 but also on θ_s. However, when μ is large and θ_s is nearly equal to zero, as in the case of a large size specimen, or of a specimen with very small conductivity k, we can assume relation 12 again as an approximation. Then, using condition 13 (ii), equations 8 and 10 can be transformed into

$$\theta=\frac{1}{\beta}\left[\frac{\mu}{q_0\cos q_0+(\mu-1)\sin q_0}\cdot\frac{\sin q_0\xi}{\xi}-1\right] \quad \ldots . [14]$$

and

$$1+\beta\theta_0=\frac{\mu q_0}{q_0\cos q_0+(\mu-1)\sin q_0} \quad . . [15]$$

It should be noted that δ again has a critical value δ_c and a specimen cannot remain in a steady state if $\delta>\delta_c$. These δ_cs and corresponding θ_cs for various values of μ are estimated graphically from equation 15 and are compared in *Table 2* with those obtained from Thomas's graph[5]. The surface temperature θ_s in the critical state is also set out in *Table 2*.

Table 2. Dependence of δ_c, θ_c and θ_s on μ

Authors	$\mu=5$	10	15	∞
Kinbara and Akita	$\delta_c=2{\cdot}30$	2·75	2·92	3·32
Thomas	2·31	2·74	2·94	3·32
Kinbara and Akita	$\theta_c=1{\cdot}55$	1·60	1·61	1·61
Thomas	1·5(6)	1·6(0)	1·6(0)	1·61
Kinbara and Akita	$\theta_s=0{\cdot}37$	0·21	0·14	0·00
Thomas	0·34	0·20	0·12	0·00

( ) means rough approximation.

In the case of sawdust, $\alpha\simeq 4{\cdot}4\times10^{-4}$ cal. cm^{-2}.s^{-1}.°C^{-1} and $k\simeq1{\cdot}4\times10^{-4}$ cal.cm^{-1}.s^{-1}.°C^{-1}, and so $\mu=5$ means that the radius is a few centimetres which is very small from a practical point of view.

6. Extension to the Non-Steady State

We shall now extend our method of replacing e^{θ} with $(1+\beta\theta)$ to the case where temperature varies with time. The applicability of equation 12 is in doubt. Correctly speaking, the temperature distribution at any instant in this non-steady state must be different from the one in the steady state even when the temperature at the centre is the same. Granted that this difference is negligible, it is not assured that equation 12 also holds in the present case, because a state having the centre-temperature θ_0 is attained through the preceding successive states of different centre-temperatures all of which are below θ_0. But, so far as θ_0 is small and β is assumed to be expressed by a quadratic function of θ_0, equation 12 should be considered to hold, because otherwise one would fail to deduce the relation that the specimen goes into self-ignition only when $\delta>3{\cdot}32$ and $\theta_0>1{\cdot}61$.

Thus we shall start from the equation

$$\frac{\partial\theta}{\partial\tau}=\frac{\partial^2\theta}{\partial\xi^2}+\frac{2}{\xi}\frac{\partial\theta}{\partial\xi}+\delta(1+\beta\theta) \quad \ldots [16]$$

Putting

$$\theta+1/\beta=\Theta=\exp w_n\tau\cdot u(\xi)$$

where $n=1, 2, 3, \ldots .$, and the w_ns are certain constants, this equation can be transformed into

$$\frac{d^2u}{d\xi^2}+\frac{2}{\xi}\frac{du}{d\xi}+(\beta\delta-w_n)u=0$$

and finally we get

$$\theta=-\frac{1}{\beta}+\sum_{n=0}^{\infty}C_n\exp w_n\tau\frac{\sin q_n\xi}{q_n}$$

where $q_0^2=\beta\delta$, $q_n^2=\beta\delta-w_n$ and the C_ns are arbitrary constants.

From the boundary condition 13 (i), C_0 and q_n are given as follows.

$$C_0=\frac{\mu}{\beta[q_0\cos q_0+(\mu-1)\sin q_0]} \quad \ldots [17]$$

$$\tan q_n=-\frac{q_n}{\mu-1}, \qquad n=1, 2, \ldots \quad . . [18]$$

Then the solution of equation 16 is

$$\theta=\frac{1}{\beta}\left[\frac{\mu\sin q_0\xi}{\xi[q_0\cos q_0+(\mu-1)\sin q_0]}-1\right]$$
$$+\sum_{n=1}^{\infty}C_n\exp\,(q_0^2-q_n^2)\,\frac{\sin q_n\xi}{\xi}\quad\ldots\;[19]$$

Next, let us consider the initial condition. If small fragments of specimens, laid separately in a room of temperature T_a, are brought together at $\tau=0$, then

$$[\theta]_{\tau=0}=0\qquad\ldots.\;[20]$$

Condition 20 also holds true when a sphere of low temperature is put in a room of high temperature T_a. According to the experiment carried out by one of the authors (K.A.), the rate of temperature rise near the surface which at first exceeds those of central parts, becomes inferior to them as the accumulation of heat due to the chemical reaction begins to take place, and all points in a sphere arrive at the room temperature T_a at nearly the same time. This instant can be assumed to be the origin of τ.

Assuming equation 20 for the initial condition, we get

$$\theta=\frac{1}{\beta}\left[\frac{\mu\sin q_0\xi}{\xi[q_0\cos q_0+(\mu-1)\sin q_0]}-1\right]-\frac{4\mu q_0^2}{\beta}$$
$$\sum_{n=1}^{\infty}\frac{\sin q_n\sin q_n\xi}{q_n(2q_n-\sin 2q_n)\,(q_n^2-q_0^2)\xi}\exp\,(q_0^2-q_n^2)\,\tau\quad\ldots.\;[21]$$

and, for the centre-temperature,

$$\theta_0=\frac{1}{\beta}\left[\frac{\mu q_0}{q_0\cos q_0+(\mu-1)\sin q_0}-1\right]-\frac{4\mu q_0^2}{\beta}$$
$$\sum_{n=1}^{\infty}\frac{\sin q_n}{(2q_n-\sin 2q_n)\,(q_n^2-q_0^2)}\exp\,(q_0^2-q_n^2)\,\tau\quad\ldots.\;[22]$$

Since q_n is nearly equal to $q_1+(n-1)\pi$, according to equation 18, the terms for $n>2$ in this series can be neglected except for the short period after the start. Then equation 22 can be transformed into

$$\tau=\frac{1}{q_1^2-q_0^2}\ln\left\{\frac{4q_0^2\mu\sin q_0}{(2q_1-\sin 2q_1)\,(q_1^2-q_0^2)}\right.$$
$$\left.\times\left[\frac{\mu q_0}{q_0\cos q_0+(\mu-1)\sin q_0}-(1+\beta\theta_0)\right]^{-1}\right\}\;[23]$$

This equation together with

$$q_0^2=\beta\delta$$
$$\beta=1+0{\cdot}3691\,\theta_0+0{\cdot}0908\,\theta_0^2$$

and

$$q_1=-(\mu-1)\tan q_1,\quad(q_1<\pi)$$

gives us τ corresponding to θ_0.

When $\mu=\infty$, we can put $q_1=\pi$, $\mu\sin q_1=\pi$; and the following simple expression for τ is deduced.

$$\tau=\frac{1}{\pi^2-q_0^2}\ln\frac{2q_0^2}{(\pi^2-q_0^2)\left\{\dfrac{q_0}{\sin q_0}-(1+\beta\theta_0)\right\}}\qquad[24]$$

7. The Ignition Time

Figure 5 shows the relation between τ and θ_0 given by equation 23 for several δ and μ. Although it is not shown for each curve in *Figure 5*, τ has a maximum and decreases when θ_0 becomes larger than a certain value which depends on δ and μ. Of course it is not an actual case, and this contradiction must be caused by extending the approximation $\beta=1+0{\cdot}3691\,\theta_0+0{\cdot}0908\,\theta_0^2$ to the region where θ_0 is too large.

It is apparent from *Figure 5* that when the specimen goes into self-ignition, the temperature increases very rapidly at a certain time. This time can be reasonably defined as the ignition time τ_{ig}. However, the time τ'_{ig} at which the temperature arrives at the critical temperature (1·61) is not so different from τ_{ig}, as *Figure 5* shows, and so τ'_{ig} can be approximately considered to be the ignition time. Values of τ'_{i} are shown in *Figure 6* for various δ and μ.

8. Application to the Self-ignition of Sawdust

One of the authors (K.A.) made an experimen about the self-ignition of woody materials. Sawdust was contained in a spherical wire gauz and was heated in a uniform temperature fiel of an electric furnace. The physical constant for this sawdust were studied by the same autho by several other experiments and are reported a follows:

$c=0{\cdot}44$ cal.g^{-1} °C^{-1},
$\rho=0{\cdot}14$ g.cm^{-3},

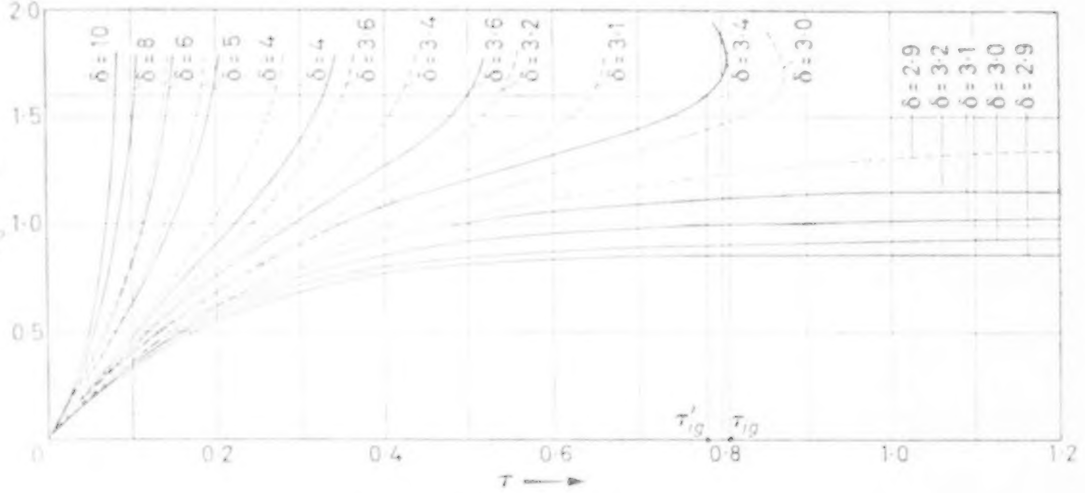

Figure 5. θ_0/τ *for several* δ *and* μ.
Solid curves: $\mu=\infty$
Dotted curves: $\mu=15$

$E=26\cdot1$ kcal.mol^{-1},

$k=1\cdot4\times10^{-4}$ cal.cm^{-1}.s^{-1}.°C^{-1},

$A=1\cdot46\times10^{9}$ cal.cm^{-3}.s^{-1},

and

$\alpha=4\cdot4\times10^{-4}$ cal.cm^{-2}.s^{-1}.°C^{-1}

The experiments were carried out for several ambient temperatures and radii of sphere.

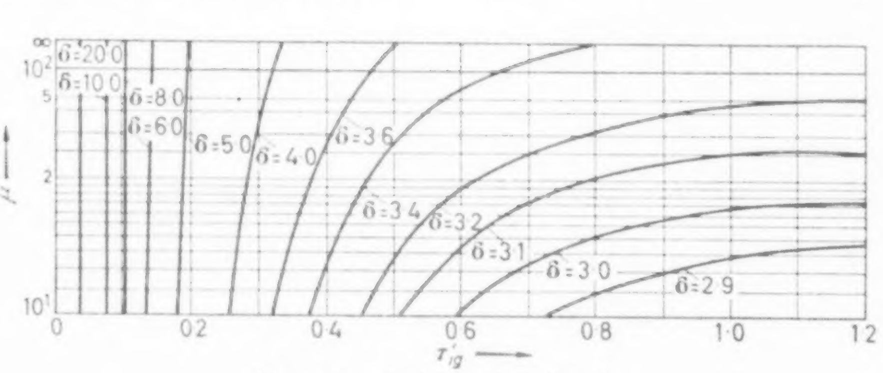

Figure 6. τ'_{ig} *for various* δ *and* μ

Figure 7 shows the experimental results[9] of two cases of

(*1*) $T_a=196$°C, $r=3\cdot70$ cm

and

(*2*) $T_a=179$°C, $r=5\cdot25$ cm

together with the theoretical curves (solid lines) corresponding to them. The experimental and the theoretical results show very good agreement with respect to the qualitative behaviour of temperature rise with time, but with respect to the magnitude of ignition time the results fall short of our expectation.

This might be due partly to the fact that the physical constants used are not known exactly, and partly to the extended application of equation 12 to the non-steady state. As mentioned previously, a state having the centre-temperature θ_0 is attained after the preceding successive states which have the lower centre-temperatures. So in calculating β by equation 12 for the state of θ_0 at an instant τ, some other smaller value should be used instead of β. In other words, β should be smaller than the value given by equation 12. Then τ would be larger than has been shown in *Figure 7*, and the experimental and theoretical results could be expected to show good agreement. However, the main reason for this discrepancy may be, as P. H. Thomas pointed out in his private communication, that the consumption of material by chemical reaction was not taken into consideration. A in equation 1 is not a true constant but decreases with time. If the equation is solved considering this change of A, the calculated ignition time must be larger than that obtained in our present theory and would coincide with the actual ignition time, but further investigations are required to resolve this point.

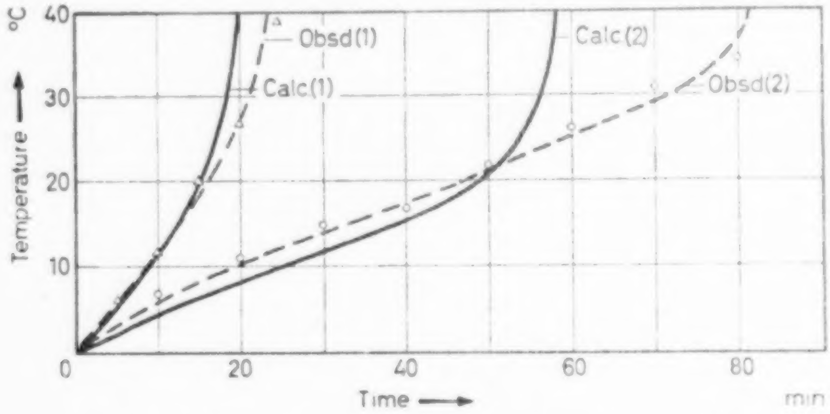

Figure 7. Observed and calculated temperature rise with time.
(1): $T_a = 196°C$, $r = 3·70$ cm, $\delta = 5·23$, $\mu = 11·6$
(2): $T_a = 179°C$, $r = 5·25$ cm, $\delta = 3·94$, $\mu = 16·5$

References

[1] FRANK-KAMENETZKY, D. A. *Diffusion and Heat Exchange in Chemical Kinetics* (translated by N. THON). Princeton University Press, 1955
[2] CHAMBRÉ, P. L. *J. chem. Phys.* 1952, **20,** 1795
[3] CLEMMOW, D. M. and HUFFINGTON, J. D. *Trans. Faraday Soc.* 1956, **52,** 385
[4] GENENSKY, S. M. *J. Res. Nat. Bur. Stand.* 1957, **59,** 79
[5] THOMAS, P. H. *Trans. Faraday Soc.* 1958, **54,** 60
[6] HICKS, B. L. *J. chem. Phys.* 1954, **22,** 414
[7] COOK, G. B. *Proc. Roy. Soc.* 1958, **246,** 154
COOK, G. B. *Sixth Symposium (International) on Combustion*, p 626. Reinhold: New York, 1956
[8] CHANDRASEKHAR, S. and WARES, G. W. *Astrophys. J.* 1949, **109,** 551
[9] AKITA, K. *Rep. Fire Res. Inst. Japan*, 1959, **9,** 1

Recent Developments and Notes

Spanish Investigations on Combustion

Members of the Instituto Nacional de Tecnica Aeronautica Esteban Terrades, Madrid, have published several monographs on some of the chemical and physical aspects of flames of burning gases and liquids.

G. Millan and I. Da Riva have made a study of the distribution of radicals in laminar flames. Part I of this work is concerned with the criterion of validity of the steady-state assumption [*AFOSR TN 59–626*; *ASTIA 217811*, 36 pp. Jan. 1959]. It is shown that the applicability of this assumption depends on the value of a certain dimensionless parameter in which the effects of reaction and diffusion of the radicals are combined. A method of recurrence is developed which enables successive approximations for the distribution of the radicals to be obtained from that corresponding to the steady state. A study is made of a mathematical model which, preserving all the properties of the flames, enables an easy comparison of the exact solution with the approximate ones obtained by means of the proposed methods.

In Part II of the work [*AFOSR TN 59–627*; *ASTIA 217812*; 51 pp. Jan. 1959] the criterion of validity of the steady-state assumption is applied to various cases corresponding to flames studied by different authors. By use of the criterion set out it is shown that this assumption is sufficiently approximate to calculate the concentration of the radicals in ozone and hydrogen flames and for the hydrogen radical in the hydrogen–bromine flame, but not for the bromine radical in this flame, nor for the hydrazine flame.

G. Millan, I. Da Riva and S. Sanz have applied the method proposed by R. P. Probert [*Phil. Mag.* 1946, **37**, 95] for studying the evaporation of fuel sprays to the analysis of the combustion of a spray burning in an oxidizing atmosphere [*AFOSR TN 59–629*; *ASTIA 217814*; 27 pp. Jan. 1959]. The conditions used were those corresponding to starting and stopping the injection of the fuel, as well as to continuous running, and also to periodical injections of short duration. The Mugele–Evans function of size distribution [*Industr. Engng Chem.* (*Industr.*) 1951, **43**, 1317] was used since it gives a maximum size drop which is more realistic than a few very large drops predicted by other formulae. Some general qualitative conclusions are given as to the most suitable characteristics of a spray. In two other monographs C. Sanchez Tarifa and P. Perez del Notario describe respectively theoretical and experimental investigations on the combustion of monopropellant droplets [*AFOSR TN 59–463*; *ASTIA 215268*, 51 pp. Dec 1958: *AFOSR TN 59–628*; *ASTIA 217813*, 24 pp. Jan. 1959].

Heat Transfer in Gas Turbine Combustion

A. H. Lefebvre, of Rolls-Royce Ltd, and M. V. Herbert, of the National Gas Turbine Establishment, have recently reviewed the heat transfer processes in gas turbine combustion chambers with a view to applying existing knowledge for the derivation of an equation for flame-tube metal temperatures [*Chart. mech. Engr*, 1959, **6**, 423]. At higher pressures the main problem in aircraft combustion chambers is that of providing a flame tube to withstand the combined effects of high buckling load and high metal temperature.

Broadly, the flame tube is heated by radiation and convection from the hot gases inside and is cooled by radiation to the outer casing and by convection to the annulus air. Heat transferred by radiation to the outer casing is generally small compared with that transferred by convection and can often be neglected at low values of temperatures.

The heat transferred internally is the most difficult of the four transfer processes to estimate. The assumption is made that it is proportional to the difference in temperature between the flame tube wall and the glass adjacent to it, and to some power of the Reynolds number consistent with established convection theory for conditions of extreme turbulence. The situation is complicated by considerable radial temperature gradients which result in the gases adjacent to the walls being below the average temperature level. The external convection component may be estimated accurately from the relationship for convective heat transfer in pipes, in which the Nusselt and Reynolds numbers are based on the hydraulic mean diameter of the annulus air space.

The separate equations for the four relevant heat transfer processes may be combined to give a general equation from which the effect on primary-zone wall temperatures of variations in fuel/air ratio, pressure, inlet temperature and air mass flow may be calculated. Flame-tube temperatures are found to increase with *increase* in pressure and inlet temperature, and with *decrease* in air mass flow and flame-tube size. The highest flame-tube temperatures for identical conditions are found in the tubo-annular design of combustion chamber. Lower temperatures are obtained in tubular and annular systems because annulus velocities are generally higher.

Cold-starting in Diesel Engines

At a meeting of the Automobile Division in conjunction with the Internal Combustion Engine Group of the Institution of Mechanical Engineers, held in London in December 1959, A. E. W. AUSTEN and W. T. LYN presented a paper describing some investigations on cold-starting phenomena in high-speed diesel engines [*Chart. mech. Engr*, 1959, **6**, 428].

During continuous cranking without fuelling the peak cylinder temperature and pressure are uniform, or decrease slightly, whereas with fuelling there is a considerable rise in peak pressure in the first cycles followed by a slight but steady rise as cranking proceeds. This pressure rise does not appear to be due to left-over fuel. Firing after a period of cranking is due mainly to the increase of compression temperature and pressure resulting from the effect of the accumulated fuel in improving sealing and increasing compression ratio. When cranking speed is increased the criterion for ignition is that the time available shall be as great as the delay period corresponding to the temperature attained. Using an extrapolation of available ignition delay data and measured compression temperatures it is shown that the temperature falls short of the value required for ignition as the cranking speed is reduced. Over a range of cranking speeds this can be offset by an increase of cranking time; and the temperature, deduced from the pressure, at the point of firing is consistent with the delay data.

Engine and Fuel Problems

L. RAYMOND, Chief Automotive Engineer, Research, Socony Mobil Oil Company, Inc., New York, and President of the Society of Automotive Engineers, gave an address to the Automobile Division of the Institution of Mechanical Engineers in the early part of 1959, in which he put forward some of the engineering challenges to American engine and petroleum research [*Chart. mech. Engr*, 1960, **7**, 48]. Perhaps the most obvious challenge is in the development of more efficient engines and higher octane gasolines. As long as knock was the principal form of uncontrolled combustion, the attainment of knock-free combustion from the fuel standpoint was dependent upon higher octane numbers. Compression ratio, dependent primarily on improvements in fuel anti-knock quality, has increased from about 5·1 in 1930 to about 9·4 at the present time, and premium grade research octane number has increased from 74 to 98 in the same period. For engines at the present time of 10 : 1 compression ratio and for engines in the near future of even higher ratio, other forms of uncontrolled combustion must be overcome.

In engines with these higher compression ratios, surface ignition effects decidedly tend to become as significant a measure of fuel and engine performance and development as anti-knock characteristics. As both temperatures and speeds have increased, these more severe manifestations of erratic combustion, including pre-ignition, rumble, thud, dieseling, slow knock and after-running have become important and new knowledge is required to solve the problems which they present. Surface ignition may place a ceiling on the most efficient use of such engines unless overcome and it may necessitate a different basis for fuel selection than that of research octane numbers. A further contribution to relief of surface ignition lies in the lubricating oil, in respect of reducing detrimental carbonaceous combustion chamber deposits and in modifying the chemical composition and the glow or ignition characteristic. From the engine designer's standpoint, the problems to be solved for the future involve the control of rate of pressure development, reduction of combustion chamber deposits, elimination of hot spots, control of clearance volume, ample structural strength and rigidity, adequate starting and ignition systems and improved thermal efficiency.

International Journal of Heat and Mass Transfer

The publication of a new monthly periodical of special interest to workers in the fields of fuel technology and chemical engineering, *International Journal of Heat and Mass Transfer*, began in January this year [Pergamon Press Ltd, 4 and 5 Fitzroy Square, London, W.1; subscription rates, £7 per annum to libraries and institutions, £5 5*s* 0*d* to private individuals]. The six editors include Dr A. J. Ede, National Engineering Laboratory, East Kilbride, Scotland, and Professor D. B. Spalding, Imperial College of Science and Technology, London, two others being in the U.S.A., one in Germany and one in the U.S.S.R. The co-chairmen of the Honorary Editorial Advisory Board are Professor E. R. G. Eckert, of the University of Minneapolis, and Professor O. A. Saunders, F.R.S., of the Imperial College of Science and Technology, London.

In addition to papers on original research, a section of the Journal will be devoted to discussions of previously published papers and there will appear in each issue a bibliography of recent papers on heat and mass transfer listed by title, author and source.

Heat Exchange in Cyclone Combustion Chambers

A study of heat exchange in vertical cyclone chambers has been described by J. L. Marshak [*Teploenergetika*, Nov. 1958, 20]. The author's objective was to obtain a formula to calculate the heat transfer in vertical, pulverized coal-fired, cyclone pre-combustion chambers of steam boilers, and the experiments were carried out at the Zakamst thermoelectric station. The boiler capacity was 250 t/h, 30 atm steam, superheated at 420°C. The furnace consisted of four vertical combustion chambers, each 2 m in diameter and 4 m long, formed of external pinned 83/5 mm steel tubes, at 132 mm intervals. The radial fins, 10 mm in diameter and 12 to 15 mm long, were helically staggered, at 32 mm axial intervals and 18° inclination.

For the efficiency of the radiation screens the author obtained the formula

$$\phi=(0{\cdot}53-0{\cdot}25\times10^{-3}t_s)\,(1{\cdot}36-0{\cdot}06A)$$

where t_s is the mean temperature °C of the slag, approximately 50°C below the slag fusion temperature or 100°C below the flame temperature, and A is the slag content of fired coal, in parts of unity.

With the notations t_a and t_n for the adiabatic combustion and the flame temperatures in °C, the author arrives at the empirical formula

$$\theta=(t_n+273)/(t_a+273)=T_n/T_a=\exp(-1{\cdot}12B_0^{1/2})$$

for B_0, the Boltzmann number, between 1·5 and 4·4, and consequently to the following approximate expression of the unit heat transfer

$$q_1=(BV_cT_a/H)\exp(-1{\cdot}12B_0^{1/2})$$

where H is the radiation screen surface, B the fuel burned per hour, and V_c the mean thermal capacity of the gases leaving the furnace. This formula is recommended by the author for cyclone combustion chambers [L. G. Hamburger, *Appl. mech. Rev.* 1960, **13**, 142].

Protection of Gas Plant from Corrosion

A joint symposium on 'The Protection of Gas Plant and Equipment from Corrosion', sponsored by the Institution of Gas Engineers, The Society of Chemical Industry Corrosion Group and the College of Advanced Technology, Birmingham, is to be held at the College, Costa Green, Birmingham 4, on 22 and 23 September 1960.

There is to be presentation and discussion of papers on the fundamentals of corrosion and protection; organic protective coatings; protection of structural steel against corrosion; corrosion of cast iron in the gas industry; principles and applications of cathodic protection; protection of gas service pipes and fittings; corrosion and the gas consumer; sprayed metal coatings in the gas industry.

Full particulars may be obtained from A. S. **Blower**, Department of Chemistry, College of Advanced Technology, Suffolk Street, Birmingham 1.

Domestic Oil Burning

A review entitled *Literature pertaining to the art and science of oil burning for residential applications* [*A.P.I. Publ. No. 1537*, Mar. 1960, 110 pp] has recently been published by the American Petroleum Institute. It has been prepared for the A.P.I. by combustion technologists under the direction of D. W. **Locklin** and C. F. **Speich** at the Battelle Memorial Institute, to provide a guide to technical literature relating particularly to distillate fuel oil combustion for residential heating equipment and similar low-capacity oil-fired applications. There are about 300 abstracts of literature dealing with aspects ranging from the fundamental physics and chemistry of fuel oil combustion to the latest developments in equipment. The Fuel Oil Committee of the A.P.I. Division of Marketing has authorized the preparation of this review in support of its current programme to stimulate research on oil burners throughout industry. During the past year a study has been conducted by the Battelle Memorial Institute to determine the long-range research needed by the oil-heating industry. Copies of this review may be obtained free of charge from the Division of Marketing, American Petroleum Institute, 1271 Avenue of the Americas, New York 20, N.Y.

International Clean Air Conference

The diamond Jubilee of the formation in 1899 of the Coal Smoke Abatement Society, now called the National Society for Clean Air, was celebrated in October 1959 by a three-day International Clean Air Conference held in London. Seventy eight papers were discussed in four sessions, dealing with: (*i*) national air pollution problems, legislation and education, (*ii*) technical problems, (*iii*) observations, investigations and measurement of air pollution, (*iv*) research and international cooperation.

The *Proceedings* of the conference are shortly to be published and will contain in addition to the papers presented, the sessional reviews by rapporteurs and a full record of the discussions and replies from the authors. The price will be 30*s* per copy, plus 2*s* 6*d* to cover packing and postage. Enquiries should be addressed to the National Society for Clean Air, Palace Chambers, Bridge Street, London, S.W.1.

New Smokeless Fuels

The Beaver Committee on Air Pollution which issued its report in November 1954 agreed that 19 million tons of coal which are burned every year in houses in black areas will have to be replaced. Since then there has been a decided movement of public demand for various smokeless fuels through the successive winters, which points to the need of a policy for the development of such fuels. A statistical analysis of this trend and a description of new smokeless fuels which are being developed by the National Coal Board were presented to the International Clean Air Conference held in London in October 1959, in a paper by J. **Bronowski**, Director-General of Process Development, National Coal Board [see note above]. He pointed out that the largest increase has been in the demand for oil, not the cheapest smokeless fuel, and the overriding requirement by the public would appear to be the convenience of the fuel, in handling and storing, in easy lighting and good performance in burning, and in amount and character of the ash. The sales, however, of all the premium smokeless fuels, for the open fire and for closed stoves, have been rising quite rapidly; over 70 per cent increase in the last four years in the sales of such fuels for the open fire. The fuels under consideration are Coalite, Rexco, Cleanglow and Phimax, for open grates, and anthracite, Phurnacite and Welsh dry steam coal, for closed stoves. It should be noted that the quantities of smokeless fuel which are being sold are still quite marginal.

The development of new smokeless fuels to replace up to 19 million tons of household coal necessary for the implementation of the Clean Air Act is a long-term undertaking, say over the next five or ten years. For solving the short-term problem, between now and 1965, there must be improvisation in the sense of using existing plants to manufacture premium fuels although not designed for this purpose. Cleanglow and Phimax are fuels made in this way during the past two years and more recently Warmco.

The author described two new premium fuels which the National Coal Board is now developing, first, briquettes made from a char which has been produced in a fluid bed, and second, briquettes made from coal and subsequently treated by mild heat. A full development programme has been formulated to put the research findings into effect. Substantial plants for these two processes are now contracted for and are expected to produce the first commercial samples of the new fuels to test the public response in the winter of 1960–61. These plants are being constructed respectively at Birch Coppice in the West Midlands Division and, probably, at Graigola in the South Western Division. These new processes have still to be tried in competition with one another and with existing processes.

Assessment of Domestic Smoke

R. Dickinson and D. E. Kimber, of the British Coal Utilisation Research Association, presented two papers to the International Clean Air Conference held in London in October 1959 [see note above], one on the design of a new type of electroprecipitator for measuring the smoke emission from domestic appliances and the other reporting the results of the use of this apparatus.

The authors set out on their investigations from the point of view that the actual weight of smoke discharged into the atmosphere is the overriding factor in pollution and therefore domestic smoke emission should be assessed in gravimetric terms. Inferential techniques have mostly been used for this purpose, assuming either that the concentration of smoke is proportional to its optical density, or that the total weight of smoke can be obtained by measuring the weight of smoke in a relatively small sample of flue gases. Neither of these methods can be regarded as very reliable. The instrument described in the first of these papers was developed in order to enable the smoke to be removed from the whole of the flue gases and its weight to be determined directly.

In the electroprecipitator described the system of charging and precipitation in a single stage is used, the electric field causing the corona discharge being also used to effect the precipitation. Various arrangements of electrodes and earthed surfaces were investigated and it was decided that the only arrangement which would provide sufficient surface area was a nest of tubes, each having an electrode in the form of a wire along its vertical axis. The best design of an instrument consisting of a nest of parallel tubes is obtained when the tubes are hexagonal in cross section. This enables them to be fitted together in a honeycomb formation and makes it possible for the free area of the instrument to approxmate to the overall cross sectional area, thus ensuring the least disturbance to the flow of the gases. Further, a larger overall collecting area is obtained than with tubes of circular cross section in an instrument of the same external dimensions. The instrument is 23 in. high, 13 in. in diameter, and weighs about 15 lb.

The authors have shown that the precipitator is capable of removing more than 97 per cent of the smoke from a charge of coal on a domestic appliance under normal conditions. It can be regarded therefore as an ideal standard of reference for the gravimetric measurement of domestic smoke. Tests are described in which it has been possible to establish the level of smoke emission from conventional bituminous fuels in conventional appliances. Work is now being carried out on the variation in smoke emission with the yield of volatile matter from different fuels and on the effect of various devices for reducing smoke emission.

Fuel Dust Surface Area

The size distribution and surface area of airborne particles are important factors in their dispersion, their fog-inducing tendencies and their detrimental effects upon health. It is highly desirable, therefore, to have a method as direct as possible for recording the surface area of particles. Recent work by the British Thomson-Houston Co. Ltd has resulted in the development of an electrostatic dust monitor which records the surface area of dust sampled per second and is sensitive to the small as well as to the large particles in the range 0·1 to 1·0 micron in diameter. This instrument was described by D. H. Grindell at the International Clean Air Conference held in London in October 1959 [see note above].

The principles employed are similar to those of the electrostatic precipitator, the flow of charged dust particles to the outer tube surrounding the charged axial wire constituting a current proportional to the total external surface area of the dust sampled by the monitor per second. The reading of current may be converted by calculation to surface area of dust passing each square foot of chimney duct per second. This is done in terms of the amplifier gain, the corona current and particle dielectric constant. Alternatively, the apparatus can be calibrated against the weight of dust per unit volume of gas determined by a gas-filtering technique.

Smoke from Low-temperature Furnaces

In a paper presented to the International Clean Air Conference in London in October 1959 [see note above] on the emission of smoke from low-temperature metallurgical furnaces, M. W. Thring, Professor of Fuel Technology and Chemical Engineering, University of Sheffield, referred to several investigations by his students which have recently been completed or are now proceeding in his Department.

J. S. Gerrard found that soot made by the pyrolysis of acetylene would not burn at an appreciable rate below 720°C and that variation in the particle size of the soot had a greater effect on the rate of combustion than had the temperature.

B. G. Clamp, using water and air models, has investigated the mixing of secondary air jets over a fuel bed and confirmed that the larger the number of jets the greater the entrainment and the higher the combustion efficiency. By the use of formulae the path of the jet can be predicted and it can be ascertained, therefore, whether there will be sufficient penetration to cover the bed.

S. G. McConnell has examined the relationship between the smoking tendency of a coal and its composition. Over the range of 15 to 40 per cent yield of volatile matter (d.a.f.) the relationship of weight per cent smoke on d.a.f. coal = 0·17 (volatile matter—3·4) was found. Over this range of coals, at an air–smoke temperature of 750°C, a fixed percentage of smoke is burned when a certain proportion of the air theoretically necessary to burn all the volatiles is admitted, for example, 60 per cent of theoretical air always burns about 88 per cent of the smoke which would be obtained if no air were used. Gas chromatography is being used to analyse the combustion gases.

To determine whether atmospheric pollution is aggravated by the presence of sulphur dioxide in soot particles, D. Watson is investigating the reaction between coal smoke and sulphur dioxide in a heated flue. The percentage of sulphur in the soot is found to increase, but there is no measurable increase in free acidity, nor is any sulphur dioxide desorbed on standing. It would thus seem that this process cannot account for the highly acid smuts emitted from some chimneys.

From other work carried out in the Department a few years ago, particularly by G. R. Mattocks and by G. Underwood, it can be concluded that if the volatile matter distilled from coal during burning can be prevented from undergoing pyrolysis in regions of high temperature, the formation of carbon is not severe and the smoke can be burned at temperatures between 700° and 800°C. There need be no smoke pollution from low-temperature furnaces and smoky atmospheres are not necessary for the correct treatment of steel.

Flow and Reaction Rates in Turbulent Flames

R. P. Barbor, J. D. Larkin, H. E. van Rosenberg and C. W. Shipman have described the results of experiments on the combustion of propane-air mixtures using two ramjet-type combustion chambers, one operating at atmospheric pressure, and the other at 0·2 atmosphere [*J. Amer. Inst. chem. Engrs*, 1959, **5**, 37]. Static pressure, total pressure, and gas sampling measurements were made at several points in the turbulent two-dimensional flow field downstream from the bluff-body flameholder. Curves are given showing a detailed mapping of the flow field, composition, velocity, eddy viscosity and reaction rate.

Assuming that with the sampling velocity equal to the flow velocity the sample composition would represent the true local composition, local concentrations of carbon dioxide, carbon monoxide, oxygen and unburnt material were determined by Orsat analysis. The local density was computed from the composition by assuming flame zone properties that are consistent with the wrinkled laminar flame model. The local velocity was determined from the static and total pressures, and the streamline directions were calculated from the velocities and densities by computing the mass flow rate across transverse areas. It was then possible, by numerical differentiation, to evaluate the convective mass flux term in the turbulent diffusion equation, and to solve for an effective chemical reaction rate, which includes the turbulent diffusion rate and the rate of production of burnt gas. By similar numerical techniques, a turbulent momentum equation was solved for the eddy viscosity, and the turbulent mass diffusivity was computed by assuming a turbulent Schmidt number of unity. It was then possible to evaluate the turbulent diffusive flux in order to obtain the true chemical reaction rate.

Evidence was obtained that the turbulent Schmidt number exceeds unity in regions where strong turbulence is generated by the walls or the bluff body; the local concentrations of reactants and products were found to be determined by the local oxygen concentration, and the sampling velocity exhibited a great effect upon the measured composition in non-homogeneous regions [F. A. Williams, *Appl. mech. Rev.* 1960, **13**, 209].

Theory of Detonation Velocity

A theory of detonation velocity has been put forward by J. A. Fay in which the dependence of detonation velocity of gases on the diameter of the confining tube is attributed to divergence of flow between shock front and Chapman–Jouguet plane [*Physics of Fluids*, 1959, **2**, 283]. Divergence is due to the effect of the turbulent boundary layer adjacent to the wall of the confining tube. Because the velocity of flow and density are higher in the boundary layer than in the main stream, the fluid in the boundary layer has a larger mass flow per unit area than the main stream. Thickness of the boundary layer increases with distance from the shock front, so that the flow within the main stream diverges. The effect of the boundary layer is expressed in terms of an increase of effective cross-sectional area of the detonation wave.

Equations of continuity, momentum and energy are those appropriate for quasi-one-dimensional flow in a channel of slowly enlarging cross-sectional area. The expression for the increase of the effective area due to the boundary layer is incorporated into the equations. Making use in addition of the equation of state and the Chapman–Jouguet condition, expressions for the velocity deficit $(U^0 - U / U^0)$, where U is the observed detonation velocity and U^0 is the ideal velocity, are obtained in terms of diameter and the effective area increase at the Chapman–Jouguet plane. The position of the Chapman–Jouguet plane is deduced from a derived expression for a generalized Chapman–Jouguet condition, an assumed chemical rate law, and experimental measurements of relaxation distance within the reaction zone.

Computed velocity deficits for a stoichiometric hydrogen–oxygen mixture with and without monatomic diluents, hydrogen in air, and acetylene with oxygen, differed by from 12 to 41 per cent from observed deficits. The initial pressure was 1 atm and the tube diameter 2 cm.

This is reasonably good agreement. In addition, experimental results which indicate a reaction zone thickness varying inversely with the initial pressure for oxy–hydrogen mixtures are in agreement with the measurements of A. J. Mooradian and W. E. Gordon [*J. chem. Phys.* 1951, **19,** 1166], which showed velocity deficits to be inversely proportional to the initial pressure, if Fay's theory is accepted [M. W. Evans, *Appl. mech. Rev.* 1960, **13,** 218].

U.S.S.R. Patents and Inventions

The first issue of the complete English translation of *U.S.S.R. Patents and Inventions* has recently been made [1959, **1,** Nos. 1/2; 173 pp; Pergamon Press Ltd, 4 and 5 Fitzroy Square, London, W.1]. This is a journal of abstracts published by the Committee for Inventions and Discoveries of the Council of Ministers of the U.S.S.R. The executive editor is I. V. Makarov and the translation editor is E. Bishop. The English translation will be published monthly and the annual subscription is £50. Subscriptions will also be accepted for individual sections at rates of £10 or £15, depending upon the particular section. An authoritative English translation of any Russian patent specification or a photostat copy of the original can also be supplied by the publishers.

B.C.U.R.A. Publications

The twenty first anniversary of the British Coal Utilisation Research Association was celebrated in 1959 and amongst the events to mark this is the recent issue of the *Bibliography of Publications 1938–1959*. This comprises a classified list, complete to April 1959, of all publications by B.C.U.R.A. staff, alone or with outside collaborators, that have been freely available to members of the Association.

A full classified subject index gives a ready guide to the wide variety of topics studied; in all there are some 1 200 entries. Included in the *Bibliography* are details of the patents taken out by the Association, the books it has published, and the translations that it has prepared. Copies are available from the Liaison and Publications Officer, B.C.U.R.A., Randalls Road, Leatherhead, Surrey, price 5*s* post free.

Rocket Engine Problems

A lecture given early last year by S. L. Bragg, Chief Performance Engineer (Rocket Division), Rolls-Royce Ltd, to the Royal Aeronautical Society on performance problems in large rocket engines has now been published in a revised form [*J. Roy. aero. Soc.* 1960, **64,** 131].

Liquid propellant engines at present being built for use with ballistic missiles and of possible use for launching satellites are considered. About 50 tons can be taken as a typical thrust level for such engines and at a specific impulse of 240 lb sec/lb this corresponds to a propellant flow of 450 lb/sec. Jet velocity would be about 7 500 ft/sec and kinetic energy in the jet represents nearly $0{\cdot}75 \times 10^6$ h.p. Best performance is obtained when the working temperatures in the combustion chamber are about 3 500 K, consequently cooling of the thrust chamber walls presents a grave problem. Since the calculated heat transfer rate to the walls at the throat may be about 9 B.t.u./in^2 sec, in order to prevent exceeding the melting points of most metals, regenerative wall cooling, using one of the propellants, is essential.

When the proportion of hydrocarbon fuel near the thrust chamber walls is increased to counteract overheating, it is found that the cooling effect is much greater than would be expected from simple heat transfer theory. This is due to a thin film of soot deposited on the walls during running if the mixture ratio is rich. The soot has a very low conductivity and acts as a thermal insulator, a layer 0·002 in. thick can be responsible for a temperature drop of several hundred degrees. To this fuel-rich layer at the walls may be attributed the apparent combustion inefficiency of rocket engines. A possible cause of the apparent inefficiency is inhomogeneity in the exhaust due to variation in the mixture ratio which could result from the presence of a fuel-rich mixture at the walls.

With regard to combustion instability, there are two main types, low frequency and high frequency. The former, referred to as 'chugging' is caused by the finite time, or 'combustion delay', which elapses between the injection of the propellants and their combustion. This delay is associated with the time necessary for atomization, vaporization and ignition. High frequency instability, or 'screaming', is an acoustic resonance of the combustion chamber, usually in the tangential swashing mode analogous to 'screech' or 'howl' on reheat systems. Whilst 'chugging' does not usually cause immediate disintegration of the thrust chamber, the results of 'screech' are devastating, the chamber possibly being destroyed in less than a second.

Consequently for the solution of these problems important requirements include an injector designed to secure as thorough mixing as possible of the propellants; smooth starting, involving the prevention of accumulation of both propellants in the chamber before ignition; control of the engine at the desired thrust level, preferably by throttling the turbine, either by varying the supply of propellant to the gas generator or by throttling the gases upstream of the nozzles; more important still is control of the propellant mixture ratio, or rather the overall ratio in which the propellants are used; and cut-off repeatability.

Fuel Abstracts and Current Titles

The Institute of Fuel has announced the issue of a new publication *Fuel Abstracts and Current Titles*. It will be a monthly classified summary of world literature on the scientific and technical aspects of all fuels and their usage, and it will be supported by comprehensive annual author and subject indexes.

The publication is to be a development of that formerly prepared by the Department of Scientific and Industrial Research, which ceased in December **1958**. The classification headings in the new publication will be the same as those in the former one.

This new publication will be obtainable, commencing **15** May **1960**, from The Institute of Fuel, **18** Devonshire Street, Portland Place, London, W.1, or through any bookseller, the annual subscription being **£12 12*s*.** The Institute is now expanding its editorial staff to deal with the preparation of this work. The aim of the publishers is to provide the best possible abstract service at a minimum cost as a duty to research and industry. Any credit balance will be used first to improve the publication, and secondly to reduce the price.

Working of the Clean Air Act

The National Society for Clean Air is making an extensive inquiry into the working of the Clean Air Act by means of a questionary addressed to all local authorities administering the Act, both in England and Wales and in Scotland [*Smokeless Air*, Spring **1960**, No. **113**, 173].

The inquiry has been drawn up on the advice of local authority representatives on the Society's Executive Council and it is designed to ascertain how well the Act is working in practice, to what extent the various provisions are being used, and how effective they are.

It is intended to report on the returns to the questionary at the Society's conference at the Royal Hall, Harrogate, **5** to **7** October next, when two full sessions will be devoted to the presentation and discussion of sectional reports.

Flame Traps

At the research meeting of The Institution of Gas Engineers held in London in November **1959**, a paper was presented by **P. A. CUBBAGE**, Midlands Research Station, The Gas Council, reviewing the effectiveness of different types of flame traps for use with town gas–air mixtures, and at the same time reporting an investigation to develop an effective trap consisting of an arresting element and a fuel cut-off device mounted in a housing [The Gas Council, *Res. Commun. No. GC 63*, **1959**].

The experimental work carried out included the measurement of speeds of flame propaga- flame traps for use with town gas–air mixtures, for a range of pipe sizes and for different pipe layouts. One of the objectives was to obtain experimental evidence whether detonations could occur in industrial pipe layouts. It is reported that under certain industrial conditions when the gas concentration is between **10** and **28** per cent by volume, detonations can occur with flame velocities of **5 000** to **7 000** ft/sec. Consequently traps to be effective, must protect against such types of combustion.

The performance of a number of commercially available traps was examined. Two of these were considerably better than the others and one of this pair was chosen for further development. It consisted of a crimped ribbon flame arrester in a housing. The arrester was made by winding two metal ribbons, one flat and the other crimped, on a central pin to form a circular element. A detailed study of this type of arrester over a range of crimp sizes, depths and diameters, showed that the housing was an important factor in the functioning of the arrester. Sufficient information was obtained to enable traps with this type of arrester to be designed to provide the full protection required. The design of flame traps on this basis is given in detail in the paper.

Modern Explosives

The late WILFRID TAYLOR, who died in July 1958 and was Joint Deputy Research Manager in the Nobel division of Imperial Chemical Industries Ltd, had been for many years one of the foremost authorities in this country on explosives and had an international reputation. He joined the Research Department in the Nobel Division of I.C.I. at Ardeer in 1928, so that practically the whole of his working life was spent on explosives and detonator problems.

His manuscript for a monograph on *Modern Explosives* was practically complete at the time of his death and some of Dr TAYLOR's colleagues have collaborated to finish the work which has now been published [The Royal Institute of Chemistry: *Lectures, Monographs and Reports, 1959, No. 5,* 63 pp]. The main sections are: explosion and detonation; explosive characteristics; intrinsically explosive substances; evolution of commercial explosives; physical phenomena of detonation; the physical action of explosives; the hydrodynamic theory of detonation; reaction mechanisms; coal mining explosives; special applications of explosives.

W. A. KIRKBY

Western States Section of the Combustion Institute, Spring Meeting

The programme arranged for the Spring Meeting (25 and 26 April) at Lockheed Research Laboratory, Palo Alto, California, of the Western States Section of the Combustion Institute included the presentation of twelve papers entitled:

Calculation of the adiabatic flame temperatures of afterburning rocket exhausts as a function of altitude. F. P. BOYNTON and J. T. NEU

Thermal lag of solid carbon in rocket nozzle flow. F. S. SIMMONS and F. G. SPADARO

Determination of temperature, velocity and concentration profiles in the mixing layer between a rocket exhaust jet and the surrounding supersonic air stream. J. VASILIU

The extinguishing of rocket motor afterburning. D. G. MILLER and M. C. ABRAMS

Ion production and removal in flames. H. F. CALCOTE

The reaction between oxygen atoms and diborane. F. P. FEHLNER and R. L. STRONG

Burning velocity and the structure of flames near extinction limits. C. H. YANG

Calculation of flame speed and droplet burning rates of hydrazine monopropellant. J. W. BJERKLIE and H. B. WELLMAN

Rate of combustion from free surfaces of liquid hydrocarbons. W. L. FONS

Fireclimate patterns and fire behaviour. C. M. COUNTRYMAN

Effects of mass fires on personnel in shelters. A. W. MCMASTERS and A. BROIDA

A performance chart for three-component jet engine combustion systems. W. UNTERBERG

Secretary of the Western States Section is G. S. BAHN, 16902 Bollinger Drive, Pacific Palisades, California, from whom further details can be obtained.

FUEL

Readers of *Combustion and Flame* may like to know that a *Note* on 'Vacuum science and technology' appeared in the March issue of *Fuel,* and a further *Note* on the 'Gas Council's new film catalogue' was published in the May issue of that journal.

Letter to the Editors

Letters to the Editors on points of scientific interest related to combustion and flames are invited. The Editors do not hold themselves responsible for opinions expressed in correspondence. Anonymous contributions cannot be accepted.

Prediction of the Emissivity of Large Hydrocarbon Flames from the Mie Theory

PREDICTION of the emissivity of hydrocarbon flames is a problem of great practical interest in industrial heat transfer. Gas emissivity can be calculated from the curves of H. C. HOTTEL and R. B. EGBERT[1] but the bulk of the flame emissivity is often due to the presence of small carbon particles. In an investigation on the oil-fired furnace at IJmuiden[2], a relationship between the emissivity and the soot concentration on the flame axis was obtained of the form

$$\varepsilon_f = 1 - \exp[-A_1 C_a L] \quad \ldots . [1]$$

where ε_f is the total emissivity of the flame, A_1 is a constant, C_a is the soot concentration on the flame axis, and L is the path length in the flame. To separate the effects of gas and soot emissivity this can be modified to

$$\varepsilon_{\text{soot}} = \{1 - \exp[-A_1 C_a L]\}\,(1 - \varepsilon_g) \quad . . [2]$$

where ε_g is the emissivity of the gaseous components.

This relationship is only applicable to geometrically similar flames as it neglects the concentration gradients within the flame and also such factors as carbon particle size and radiation wavelength which are both known to affect extinction coefficients.

The reported values of carbon particle size in laboratory diffusion flames[3] lie mainly between 80 and 500 Å, and M. LEVEQUE[4] in an examination of the IJmuiden flame found a wide range of particle size with most particles of a diameter between 300 and 450 Å. The particles are always spherical.

A consideration of Planck's radiation law reveals that for a black body at the temperatures of industrial flames 80 per cent of the emitted radiation lies in a small band about 4μ wide. However, the emission from a gas turbine flame examined by D. J. WEEKS and O. A. SAUNDERS[5] shows a deficiency in the region above 2·5μ. This shifts the mean wavelength to a lower value and reduces the width of the radiation band (see *Table 1*).

Table 1

Temp. °*K*	*Mean wave length* μ	*80% of the energy lies in the range,* μ	*Source*
1 493	2·75	1·64–6·3	*Planck's law*
1 493	1·9	1·3 –2·5	*Weeks and Saunders*[5]
2 073	1·98	1·18–4·54	*Planck's law*

It was therefore thought that a theoretical approach might clarify the problem. For a random array of spherical particles of diameter from 0 to d_1

$$\ln(I_0/I) = cL\,(\pi/4)\sum_{0}^{d_1} E_z N_z d_z^2 \quad \ldots . [3]$$

where I_0 is the incident radiation, I is the emergent radiation, E_z is the area extinction coefficient of a particle of diameter d_z, and N_z is the number of particles per unit weight. For spherical carbon particles of density 2 g/cm³

$$N_z d_z^2 = 3/\pi d_z \quad \ldots . [4]$$

The area extinction coefficient E_z is a function of the radiation wavelength and the diameter and physical properties of the particle. The solution for a single spherical particle was first presented in a comprehensive form by G. MIE[6] and this subject has been reviewed by P. G. W. HAWKSLEY[7] who has tabulated the general expressions involved. For carbon particles under the conditions considered, $x \ll 1$, $mx \ll 1$. Hence

$$E = \frac{24xn^2k}{(n^2+n^2k^2)^2+4(n^2-n^2k^2+1)} = x\mathrm{f}(n,\,k) \qquad \ldots . [5]$$

where $x = \pi d/\lambda$, λ is wavelength, d is particle diameter, n is the real refractive index of soot, $k = K\lambda/4\pi$, K is the linear absorption coefficient of soot, and $m = n(1-ik)$.

Unfortunately, accurate values of the refractive index and absorption coefficient of amorphous carbon are not available but the values of H. SENFTLEBEN and E. BENEDICT[8] for carbon in the visible spectrum provide data of the right order of magnitude without affecting the argument. Thus

$$n = 1{\cdot}95$$

$$k = 0{\cdot}338$$

and

$$E = 0{\cdot}87\pi d/\lambda \qquad \ldots . [6]$$

It must be noted that whereas k is dependent on the wavelength λ, $\mathrm{f}(n,\,k)$ in equation 5 is insensitive to changes in λ and varies only 10 per cent in the range to which it is applied.

Substituting equations 4 and 6 in 3

$$\ln\,(I_0/I) = 0{\cdot}615\pi cL/\lambda \qquad \ldots . [7]$$

and the dependence on particle size is eliminated.

It can be seen from *Table 1* that the mean wavelength will only vary over a range of 30 per cent. Thus for a typical wavelength of $1{\cdot}9\mu$ and equating absorptivity with emissivity

$$\varepsilon = 1 - \exp\,[-0{\cdot}01017cL] \qquad \ldots . [8]$$

where c is the mean soot concentration in mg/litre at the flame temperature and L is the path length in cm.

Equation 8 is of the same form as the IJmuiden formula where k_1 is 0·0025. If it is assumed that the soot concentration in the IJmuiden flame has the same profile as $\cos\theta$ between $-\pi$ and $+\pi$ its mean value will be half the axial concentration.

Thus one obtains the empirical relation

$$\varepsilon_f = 1 - \exp\,[-0{\cdot}005cL] \qquad \ldots . [9]$$

Equation 9 may be regarded as the general practical equation in the light of present knowledge. The derived equation 7 indicates the lack of dependence on particle size and the nature of the dependence on the wavelength of the radiation. The value of the 'constant' in equation 8 is of the same order as has been experimentally determined, but an accurate knowledge of the refractive index and absorption coefficient of soot is required before a true comparison can be made. It should be noted that the derived equations only apply accurately when the measuring instrument subtends a small angle at the flame and an increase in the angle subtended will lead to higher experimental emissivities.

We should like to thank Professor M. W. Thring for advice in the preparation of this note and for permission to publish it.

P. J. FOSTER
I. A. MCGRATH

Department of Fuel Technology
and Chemical Engineering,
University of Sheffield

(*Received April 1960*)

References

[1] HOTTEL, H. C. and EGBERT, R. B. *Trans. Amer. Soc. mech. Engrs*, 1941, **63**, 297

[2] Flame Radiation Research Joint Committee *Report of the Sixth Performance Trials*

[3] *B.C.U.R.A. Mon. Bull.* 1958, **32**, No. 12

[4] Flame Radiation Research *Doc. D2/f/2*, 1952

[5] WEEKS, D. J. and SAUNDERS, O. A. *J. Inst. Fuel*, 1958, **31**, 247

[6] MIE, G. *Ann. phys. Lpz.* 1908, **25**, 377

[7] *B.C.U.R.A. Mon. Bull.* 1952, **26**, Nos. 4 and 5

[8] SENFTLEBEN, H. and BENEDICT, E. *Ann. phys., Lpz.* 1919, **60**, 297

Interpretation of the Anti-knock Performance of Hydrocarbons in Gasoline Engines in Terms of their Combustion Characteristics

K. C. SALOOJA

'Shell' Research Ltd, Thornton Research Centre, P.O. Box 1, Chester

(Received March 1959)

The information on the combustion characteristics of hydrocarbons, previously reported, leads to a better insight into the anti-knock performance of hydrocarbons in gasoline engines. The results show that the overall extent of reaction taking place before ignition relates very closely to the knock-limited performance of the fuel. The effects of the addition of tetraethyl-lead and of hydrocarbon components whose value in terms of blending octane number is not predictable from the intrinsic octane number, can be readily interpreted from their effects on the extent of pre-flame reactions. Furthermore, the performance changes brought about by alterations in engine speed or operating temperature are shown to be governed by the changes in the resistance to ignition (as judged by the ignition temperature/lag relationship and also by the influence of mixture strength on this) and with the changes occurring in the extent of pre-flame reaction.

A BETTER understanding of the relationship between the anti-knock performance of fuels in gasoline engines and their combustion characteristics is of interest to both engine designers and fuel technologists. Numerous attempts have been made to interpret the wide differences in the anti-knock performance of different fuels in terms of their combustion characteristics. These attempts, however, have had only limited success. Many investigators, who have sought the interpretation of engine performance in terms of basic combustion characteristics determined under simple laboratory conditions at atmospheric pressure, have claimed that a correlation exists between the engine performance of fuels and their minimum ignition temperatures. The early investigators who reported such a correlation have been referred to by W. HELMORE[2]. In recent years this correlation has again been pointed out by C. E. FRANK and A. U. BLACKHAM[3], and by D. E. SWARTS and M. ORCHIN[4]. This correlation, however, has only been satisfactory for hydrocarbons belonging to the same structural category. Even here, the correlation is poor in the case of olefins and *cyclo*paraffins. It is mainly with aromatic and some paraffinic hydrocarbons that there is a broad correlation between the engine performance and the minimum ignition temperature.

The combustion characteristics of hydrocarbons, which have been investigated recently and reported in an earlier paper[1], do, however, correlate well with their anti-knock qualities. These combustion characteristics have been determined in terms of both chemical and physical parameters and include: (*i*) the extent of pre-flame reaction, (*ii*) the minimum ignition temperature for a given lag, (*iii*) the ignition temperature/lag relationship, and (*iv*) the effect of fuel/air ratio on (*i*), (*ii*) and (*iii*). Apart from correlating with anti-knock performance, these characteristics help to interpret successfully the influence on the anti-knock performance of such factors as the speed and operating temperature of engines. Furthermore, the influence of anti-knock agents and of hydrocarbon components, whose value in terms of blending octane number is not predictable from their intrinsic octane numbers, can be satisfactorily interpreted from their effects on combustion characteristics.

The afore-mentioned combustion character-under the conditions considered, $x \ll 1$, $mx \ll 1$. Hence

$$E=\frac{24xn^2k}{(n^2+n^2k^2)^2+4(n^2-n^2k^2+1)}$$
$$=x\mathrm{f}(n,\,k) \qquad \ldots\ldots [5]$$

where $x=\pi d/\lambda$, λ is wavelength, d is particle diameter, n is the real refractive index of soot, $k=K\lambda/4\pi$, K is the linear absorption coefficient of soot, and $m=n(1-ik)$.

Unfortunately, accurate values of the refractive index and absorption coefficient of amorphous carbon are not available but the values of H. SENFTLEBEN and E. BENEDICT[8] for carbon in the visible spectrum provide data of the right order of magnitude without affecting the argument. Thus

$$n=1{\cdot}95$$
$$k=0{\cdot}338$$

and

$$E=0{\cdot}87\pi d/\lambda \qquad \ldots\ldots [6]$$

It must be noted that whereas k is dependent on the wavelength λ, $\mathrm{f}(n,\,k)$ in equation **5** is insensitive to changes in λ and varies only **10** per cent in the range to which it is applied.

Substituting equations **4** and **6** in **3**

$$\ln\,(I_0/I)=0{\cdot}615\pi cL/\lambda \qquad \ldots\ldots [7]$$

and the dependence on particle size is eliminated.

It can be seen from *Table 1* that the mean wavelength will only vary over a range of **30** per cent. Thus for a typical wavelength of $1{\cdot}9\mu$ and equating absorptivity with emissivity

$$\varepsilon=1-\exp\,[-0{\cdot}01017cL] \qquad \ldots\ldots [8]$$

where c is the mean soot concentration in mg/litre at the flame temperature and L is the path length in cm.

Equation **8** is of the same form as the IJmuiden formula where k_1 is $0{\cdot}0025$. If it is assumed that the soot concentration in the IJmuiden flame has the same profile as $\cos\theta$ between $-\pi$ and $+\pi$ its mean value will be half the axial concentration.

Thus one obtains the empirical relation

$$\varepsilon_f=1-\exp\,[-0{\cdot}005cL] \qquad \ldots\ldots [9]$$

Equation **9** may be regarded as the general practical equation in the light of present knowledge. The derived equation **7** indicates the lack of dependence on particle size and the nature of the dependence on the wavelength of the radiation. The value of the 'constant' in equation **8** is of the same order as has been experimentally determined, but an accurate knowledge of the refractive index and absorption coefficient of soot is required before a true comparison can be made. It should be noted that the derived equations only apply accurately when the measuring instrument subtends a small angle at the flame and an increase in the angle subtended will lead to higher experimental emissivities.

We should like to thank Professor M. W. Thring for advice in the preparation of this note and for permission to publish it.

P. J. FOSTER
I. A. MCGRATH

Department of Fuel Technology
and Chemical Engineering,
University of Sheffield

(*Received April 1960*)

References

[1] HOTTEL, H. C. and EGBERT, R. B. *Trans. Amer. Soc. mech. Engrs*, 1941, **63**, 297
[2] Flame Radiation Research Joint Committee *Report of the Sixth Performance Trials*
[3] *B.C.U.R.A. Mon. Bull.* 1958, **32**, No. 12
[4] Flame Radiation Research *Doc. D2/f/2*, 1952
[5] WEEKS, D. J. and SAUNDERS, O. A. *J. Inst. Fuel*, 1958, **31**, 247
[6] MIE, G. *Ann. phys. Lpz.* 1908, **25**, 377
[7] *B.C.U.R.A. Mon. Bull.* 1952, **26**, Nos. 4 and 5
[8] SENFTLEBEN, H. and BENEDICT, E. *Ann. phys., Lpz.* 1919, **60**, 297

Interpretation of the Anti-knock Performance of Hydrocarbons in Gasoline Engines in Terms of their Combustion Characteristics

K. C. SALOOJA

'Shell' Research Ltd, Thornton Research Centre, P.O. Box 1, Chester

(Received March 1959)

The information on the combustion characteristics of hydrocarbons, previously reported, leads to a better insight into the anti-knock performance of hydrocarbons in gasoline engines. The results show that the overall extent of reaction taking place before ignition relates very closely to the knock-limited performance of the fuel. The effects of the addition of tetraethyl-lead and of hydrocarbon components whose value in terms of blending octane number is not predictable from the intrinsic octane number, can be readily interpreted from their effects on the extent of pre-flame reactions. Furthermore, the performance changes brought about by alterations in engine speed or operating temperature are shown to be governed by the changes in the resistance to ignition (as judged by the ignition temperature/lag relationship and also by the influence of mixture strength on this) and with the changes occurring in the extent of pre-flame reaction.

A BETTER understanding of the relationship between the anti-knock performance of fuels in gasoline engines and their combustion characteristics is of interest to both engine designers and fuel technologists. Numerous attempts have been made to interpret the wide differences in the anti-knock performance of different fuels in terms of their combustion characteristics. These attempts, however, have had only limited success. Many investigators, who have sought the interpretation of engine performance in terms of basic combustion characteristics determined under simple laboratory conditions at atmospheric pressure, have claimed that a correlation exists between the engine performance of fuels and their minimum ignition temperatures. The early investigators who reported such a correlation have been referred to by W. HELMORE[2]. In recent years this correlation has again been pointed out by C. E. FRANK and A. U. BLACKHAM[3], and by D. E. SWARTS and M. ORCHIN[4]. This correlation, however, has only been satisfactory for hydrocarbons belonging to the same structural category. Even here, the correlation is poor in the case of olefins and *cyclo*paraffins. It is mainly with aromatic and some paraffinic hydrocarbons that there is a broad correlation between the engine performance and the minimum ignition temperature.

The combustion characteristics of hydrocarbons, which have been investigated recently and reported in an earlier paper[1], do, however, correlate well with their anti-knock qualities. These combustion characteristics have been determined in terms of both chemical and physical parameters and include: (*i*) the extent of pre-flame reaction, (*ii*) the minimum ignition temperature for a given lag, (*iii*) the ignition temperature/lag relationship, and (*iv*) the effect of fuel/air ratio on (*i*), (*ii*) and (*iii*). Apart from correlating with anti-knock performance, these characteristics help to interpret successfully the influence on the anti-knock performance of such factors as the speed and operating temperature of engines. Furthermore, the influence of anti-knock agents and of hydrocarbon components, whose value in terms of blending octane number is not predictable from their intrinsic octane numbers, can be satisfactorily interpreted from their effects on combustion characteristics.

The afore-mentioned combustion characteristics, reported in the earlier paper, were measured for the following eight typical C_6–C_8 hydrocarbons: *n*-heptane, methyl*cyclo*hexane, *iso*octane, di*iso*butylene, benzene, toluene, *m*-xylene and ethylbenzene. In the present paper the relative performance of these hydrocarbons in gasoline engines* has been interpreted in terms of the combustion characteristics.

Correlation with Anti-knock Performance in Engines

The relative anti-knock performance of different fuels, under any given set of engine operating conditions, can be directly related to the extent of pre-flame reactions. Those hydrocarbons which undergo less reaction in the pre-flame stages perform better in the engine than those which react more extensively. This is so irrespective of the structural category to which the hydrocarbons belong, and is true almost without regard to the minimum ignition temperatures of the hydrocarbons so long as these are not too far apart.

As an illustration, the ignition temperatures of di*iso*butylene and methyl*cyclo*hexane are in the same range. However, methyl*cyclo*hexane, which undergoes far more overall pre-flame reaction than di*iso*butylene, has a much lower octane rating and critical compression ratio. *iso*Octane ignites at an appreciably higher temperature than di*iso*butylene, yet di*iso*butylene, which suffers relatively less reaction in the pre-flame stages has a higher 'Research' octane rating. Ethylbenzene and *iso*octane both ignite in the same temperature range. Ethylbenzene, however, undergoes less pre-flame reaction than *iso*octane and its 'Research' octane rating, too, is higher. Again, at the high end of the ignition temperature scale, benzene, toluene and *m*-xylene ignite at comparable temperatures, but benzene, which suffers the least extent of pre-flame reaction, performs best.

The anti-knock quality of different hydrocarbons in terms of their octane numbers by both the 'Research' and 'Motor' methods and the critical compression ratios is shown in *Tables 1* and *2*.

That it is the extent of pre-flame reaction rather than the minimum ignition temperature that should provide the more exact correlation with the engine performance is understandable since the ignition temperatures, in the manner in which they are usually determined in open vessels, cannot possibly reflect the tendencies of fuels to auto-ignite in internal combustion engines where the fuel–air charge is subjected to increasing pressure and temperature in the compression stroke before the passage of the spark and again under more severe conditions in the 'end-gas region' ahead of the approaching flame front. A fuel capable of undergoing greater pre-flame reaction would produce more

Table 1. CFR Octane Ratings of unleaded hydrocarbons*[5]

Hydrocarbon	*Research method* 'F_1'	*Motor method* 'F_2'
n-*Heptane*	0	0
*Methyl*cyclo*hexane*	74·8	71·1
iso*Octane*	100·0	100·0
Diisobutylene	105·3	88·6
Benzene	—†	—†
Toluene	120·1	103·5
m-*Xylene*	117·5	115·0
Ethylbenzene	107·4	97·9

*Octane ratings above 100 are according to the ASTM (Wiese) scale.

†The value for benzene is too high to be rated satisfactorily in the CFR engine.

Table 2. Critical compression ratios of unleaded hydrocarbons in General Motors single cylinder variable-compression engine[5]

Hydrocarbon	*Critical compression ratios*			
	600 rev/min		*2000 rev/min*	
	Jacket: 212°F *Air : 100°F*	*350°F* *150°F*	*212°F* *100°F*	*350°F* *150°F*
n-*Heptane*	3·0	—	3·8	3·0
*Methyl*cyclo*hexane*	4·55	4·0	5·9	4·9
iso*Octane*	7·3	6·6	9·0	7·1
Diisobutylene	11·95	7·3	8·55	5·7
Benzene	—	—	—	—
Toluene	15	11·35	13·5	9·0
m-*Xylene*	15·5	11·5	12·3	9·3
Ethylbenzene	13·5	8·2	9·3	6·9

---

*The information on the anti-knock performance of different hydrocarbons in gasoline engines has been taken from the API Project 45 data[1].

heat and pressure rise and would consequently carry the charge to the point of ignition more readily than one which undergoes less reaction. Thus, irrespective of minor differences in ignition temperatures, fuels with widely different extents of pre-flame reactions would differ markedly in their tendencies to auto-ignite and knock in engines. It is not surprising therefore that, for all types of hydrocarbons, the extent of pre-flame reactions provides a satisfactory correlation with engine performance.

Such a correlation between engine performance and extent of pre-flame reaction has also been indicated in engine experiments by E. R. Retailliau, H. A. Ricards, Jr and M. C. K. Jones[6]. These authors took the average engine temperature before ignition as the criterion of pre-flame reaction and showed that, under both firing and cycling conditions, *iso*octane undergoes more reaction than benzene, and a blend of *iso*octane containing 25 per cent *n*-heptane more reaction than *iso*octane itself.

Correlation with Temperature Sensitivity of Fuels in Engines

It is well known that an increase in the running temperature of an engine lowers its knock-limited performance (*Table 2*). The degree to which the knock-limited compression ratio must be reduced on increasing the jacket and air temperature, however, varies with the nature of the fuel. Comparing, for instance, *iso*octane, ethylbenzene and di*iso*butylene, the reduction of critical compression ratio is less with *iso*octane than with the other two hydrocarbons for a given increase in temperature. The studies of their combustion characteristics have strongly indicated that the pre-flame reactions of *iso*octane are far more resistant to self-ignition than those of ethylbenzene or di*iso*butylene. (This is judged from the slope of the ignition temperature versus lag curves and from the effect of fuel concentration on ignition temperature under different isolag conditions.) For instance, for the same rise in temperature, the ignition lags of ethylbenzene and di*iso*butylene are shortened much more than with *iso*octane. In other words, the same rise in temperature renders ethylbenzene and di*iso*butylene much more readily ignitable than *iso*octane. These observations are in line with the observed temperature sensitivities of these hydrocarbons in the engine.

Comparing toluene and *m*-xylene, the studies of combustion characteristics have shown that the pre-flame reactions of *m*-xylene are more resistant to self-ignition than those of toluene and this again is in line with the temperature sensitivities in the engine of these two hydrocarbons. The same increase in temperature reduces the critical compression ratio of *m*-xylene to a level which is still higher than that of toluene. This lower temperature sensitivity of *m*-xylene is further reflected by the relative differences in the 'Research' and 'Motor' octane ratings. The octane rating of *m*-xylene drops from 117·5 to only 115·0, whereas for toluene the drop is from 120·1 to 103·5.

Correlation with Effects of Engine Speed Variation on Performance

Since engines have to operate over a wide range of speed, much attention has been given to the relative sensitivities of different fuels to changes in engine speed. As a result considerable data have been accumulated which show very marked differences between different fuels in this respect. As the engine speed increases, *n*-paraffins, most of the *cyclo*paraffins and some *iso*paraffins and olefins improve in anti-knock performance, whereas aromatics and most of the highly branched paraffins and olefins depreciate in their performance. Apart from these broad differences amongst hydrocarbons of different structural categories, even amongst *n*-paraffins and aromatics, there are often marked differences between individual hydrocarbons.

Amongst the hydrocarbons under discussion, as shown in *Table 2*, *n*-heptane and methyl*cyclo*hexane appreciate in their performance when the engine speed is increased from 600 to 2 000 rev/min. *iso*-Octane also improves in performance at the higher speed, whereas di*iso*butylene and ethylbenzene depreciate markedly. With both toluene and *m*-xylene, the engine performance falls considerably at the higher speed.

To understand the reasons for the widely different effects that an increase in engine speed produces on the performance of different fuels, one must follow the manner in which the increase in engine speed affects the combustion processes of an individual hydrocarbon. An increase in engine speed, when all other operating conditions are kept the same, could be considered to affect the combustion processes in the engine in the following ways:

(*1*) The temperatures at which combustion takes place in the engine tend to be higher at faster speeds even when the jacket temperature and the other operating conditions are kept the same. This is due to the greater number of heat cycles per unit time which result in a higher combustion chamber surface temperature. The increase in the running temperature of the engine would tend to lower the performance of various fuels in accordance with their temperature sensitivies.

(*2*) At higher speeds the duration of combustion cycles would decrease. This would have the following effects:

  (*i*) The extent of pre-flame reactions would decrease owing to shorter times being available for these reactions to take place. The reduction in the extent of pre-flame reactions should lead to an improvement in the engine performance.

  (*ii*) The stability characteristics of the pre-flame reactions with respect to self-ignition would be affected: those hydrocarbons which have a relatively stable pre-flame reaction stage and offer greater resistance to ignition at shorter reaction times would tend to improve in their engine performance at higher speeds. Any improvement on this account, as also on account of (*i*) above, would be offset somewhat by the increase in the running temperature of the engine.

With *n*-heptane and methyl*cyclo*hexane, which undergo extensive pre-flame reactions, the effect of a large increase in engine speed would primarily be that of a marked reduction in the extent of the pre-flame reactions. This, by itself, should lead to a corresponding improvement in the engine performance. There would, however, be some depreciation in the performance due to an increase in the effective engine temperature at the higher speed. The net effect could be that of an improvement in the performance of the fuel, such as is observed.

In comparison with *n*-heptane and methyl*cyclo*hexane, *iso*octane, di*iso*butylene and ethylbenzene undergo little pre-flame reaction and as a result have much higher critical compression ratios. In accordance with the relative extents of pre-flame reaction, at an engine speed of 600 rev/min and jacket and air temperatures of 212° and 100°F, ethylbenzene has the highest critical compression ratio value (13·5), followed by di*iso*butylene (11·95) and *iso*octane (7·3). With little pre-flame reaction taking place in these hydrocarbons, the effect of increasing engine speed on the extent of pre-flame reactions would be much less pronounced than that with *n*-heptane or methyl*cyclo*hexane. However, what little improvement could occur on this account at higher speeds would be greatest with *iso*octane which undergoes more pre-flame reaction than either di*iso*butylene or ethylbenzene.

At higher engine speeds, the depreciating influence due to a rise in the effective engine temperature would be more marked with ethylbenzene and di*iso*butylene than with *iso*octane. The studies on the combustion characteristics of these hydrocarbons, as mentioned in the previous section, have clearly shown that the inherent temperature sensitivity of *iso*octane is very much less than that of either ethylbenzene or di*iso*butylene.

Consideration of the results on the stability characteristics of the pre-flame reactions towards self-ignition of these hydrocarbons particularly with respect to reaction time, which is reduced by an increase in engine speed, indicates that at shorter residence times *iso*octane has a markedly greater stability towards ignition than has either di*iso*butylene or ethylbenzene. For instance, as shown in the previous paper[1], for the reduction of the ignition lag even from four to two seconds, *iso*octane has to be raised in temperature by about 28° at about 520°C, whereas, for a similar reduction in ignition lag of ethylbenzene, the temperature needs to be raised by only 13° at 525°C and with di*iso*butylene by only 11° and that moreover at a much lower temperature level, about 490°C. Furthermore, the previous studies have shown that whereas the ignition temperature of *iso*octane is raised when the fuel concentration is increased at shorter isolags, the ignition temperatures of di*iso*butylene and ethylbenzene are lowered under identical experimental conditions. Thus, in view of the greater resistance to ignition of *iso*octane its performance at higher engine speeds would be expected to be less severely affected than that of either di*iso*butylene or ethylbenzene.

Yet another factor to be borne in mind, while comparing hydrocarbons with widely varying critical compression ratios such as *iso*octane, di*iso*butylene and ethylbenzene, is that at higher compression ratio levels the rate of reaction of the pre-flame processes would be higher. Consequently, the depreciating influence on the basis of critical compression ratios alone would be in the order: ethylbenzene > di*iso*butylene > *iso*octane.

In the light of all the foregoing considerations, the performance of *iso*octane with increasing speed would be expected to improve more, or be less adversely affected, than that of either di*iso*butylene or ethylbenzene. This is in agreement with the observed engine performance of these hydrocarbons. The critical compression ratio for *iso*octane is increased appreciably as the engine speed is raised from 600 to 2 000 rev/min, whereas, with di*iso*butylene and ethylbenzene, it actually falls under similar conditions.

Toluene and *m*-xylene, which undergo little pre-flame reaction and that too at a much higher temperature level than that in the case of di*iso*butylene, *iso*octane or ethylbenzene, indeed have higher critical compression ratios than those for the other hydrocarbons. The combustion characteristics of toluene and *m*-xylene are somewhat similar to each other and so also is the effect of increasing engine speed, which causes a depreciation in the engine performance in both cases.

This effect of increasing engine speed on the performance of toluene and *m*-xylene is more like that observed with ethylbenzene and di*iso*butylene than that of *iso*octane which appreciates in performance at higher speeds. The combustion characteristics of toluene and *m*-xylene, particularly with regard to the stability of the pre-flame reactions towards self-ignition, however, have more similarities with those of *iso*octane than with those of di*iso*butylene and ethylbenzene. The depreciation with increasing speed for toluene and *m*-xylene as against the appreciation observed with *iso*octane, might well be due to the rather large depreciating factor involved in the former case on account of a higher rate of reaction of pre-flame processes at higher compression ratios. [The critical compression ratios are very much higher for toluene and *m*-xylene (15·0 and 15·5 respectively) than for *iso*octane (7·3).]

Correlation with Blending Properties of Fuels

The improvement that takes place in engine performance on adding a high quality component to one of poor quality is often quite different from that expected from the known characteristics of the individual components. For example, benzene by itself has a much higher anti-knock quality than di*iso*butylene, yet the addition of di*iso*butylene to a fuel causes much greater improvement in its performance than does the addition of the same amount of benzene. The differences in the blending characteristics of various hydrocarbons which are indicated by their 'blending octane numbers' are tabulated in *Table 3*.

In order to determine whether the blending octane numbers of different hydrocarbons in the engine are reflected in the combustion properties under examination, a series of experiments was carried out on blends of *n*-heptane with 20 per cent *iso*octane, benzene and di*iso*butylene. For these experiments the same method and technique were used as had been adopted for studies on pure hydrocarbons described in the previous paper[1]. The results different effects that an increase in engine speed produces on the performance of different fuels, one must follow the manner in which the increase in engine speed affects the combustion processes of an individual hydrocarbon. An increase in engine speed, when all other operating conditions are kept the same, could be considered to affect the combustion processes in the engine in the following ways:

(*1*) The temperatures at which combustion takes place in the engine tend to be higher at faster speeds even when the jacket temperature and the other operating conditions are kept the same. This is due to the greater number of heat cycles per unit time which result in a higher combustion chamber surface temperature. The increase in the running temperature of the engine would tend to lower the performance of various fuels in accordance with their temperature sensitivies.

(*2*) At higher speeds the duration of combustion cycles would decrease. This would have the following effects:

  (*i*) The extent of pre-flame reactions would decrease owing to shorter times being available for these reactions to take place. The reduction in the extent of pre-flame reactions should lead to an improvement in the engine performance.

  (*ii*) The stability characteristics of the pre-flame reactions with respect to self-ignition would be affected: those hydrocarbons which have a relatively stable pre-flame reaction stage and offer greater resistance to ignition at shorter reaction times would tend to improve in their engine performance at higher speeds. Any improvement on this account, as also on account of (*i*) above, would be offset somewhat by the increase in the running temperature of the engine.

With *n*-heptane and methyl*cyclo*hexane, which undergo extensive pre-flame reactions, the effect of a large increase in engine speed would primarily be that of a marked reduction in the extent of the pre-flame reactions. This, by itself, should lead to a corresponding improvement in the engine performance. There would, however, be some depreciation in the performance due to an increase in the effective engine temperature at the higher speed. The net effect could be that of an improvement in the performance of the fuel, such as is observed.

In comparison with *n*-heptane and methyl*cyclo*hexane, *iso*octane, di*iso*butylene and ethylbenzene undergo little pre-flame reaction and as a result have much higher critical compression ratios. In accordance with the relative extents of pre-flame reaction, at an engine speed of 600 rev/min and jacket and air temperatures of 212° and 100°F, ethylbenzene has the highest critical compression ratio value (**13·5**), followed by di*iso*butylene (11·95) and *iso*octane (7·3). With little pre-flame reaction taking place in these hydrocarbons, the effect of increasing engine speed on the extent of pre-flame reactions would be much less pronounced than that with *n*-heptane or methyl*cyclo*hexane. However, what little improvement could occur on this account at higher speeds would be greatest with *iso*octane which undergoes more pre-flame reaction than either di*iso*butylene or ethylbenzene.

At higher engine speeds, the depreciating influence due to a rise in the effective engine temperature would be more marked with ethylbenzene and di*iso*butylene than with *iso*octane. The studies on the combustion characteristics of these hydrocarbons, as mentioned in the previous section, have clearly shown that the inherent temperature sensitivity of *iso*octane is very much less than that of either ethylbenzene or di*iso*butylene.

Consideration of the results on the stability characteristics of the pre-flame reactions towards self-ignition of these hydrocarbons particularly with respect to reaction time, which is reduced by an increase in engine speed, indicates that at shorter residence times *iso*octane has a markedly greater stability towards ignition than has either di*iso*butylene or ethylbenzene. For instance, as shown in the previous paper[1], for the reduction of the ignition lag even from four to two seconds, *iso*octane has to be raised in temperature by about 28° at about 520°C, whereas, for a similar reduction in ignition lag of ethylbenzene, the temperature needs to be raised by only 13° at 525°C and with di*iso*butylene by only 11° and that moreover at a much lower temperature level, about 490°C. Furthermore, the previous studies have shown that whereas the ignition temperature of *iso*octane is raised when the fuel concentration is increased at shorter isolags, the ignition temperatures of di*iso*butylene and ethylbenzene are lowered under identical experimental conditions. Thus, in view of the greater resistance to ignition of *iso*octane its performance at higher engine speeds would be expected to be less severely affected than that of either di*iso*butylene or ethylbenzene.

Yet another factor to be borne in mind, while comparing hydrocarbons with widely varying critical compression ratios such as *iso*octane, di*iso*butylene and ethylbenzene, is that at higher compression ratio levels the rate of reaction of the pre-flame processes would be higher. Consequently, the depreciating influence on the basis of critical compression ratios alone would be in the order: ethylbenzene > di*iso*butylene > *iso*octane.

In the light of all the foregoing considerations, the performance of *iso*octane with increasing speed would be expected to improve more, or be less adversely affected, than that of either di*iso*butylene or ethylbenzene. This is in agreement with the observed engine performance of these hydrocarbons. The critical compression ratio for *iso*octane is increased appreciably as the engine speed is raised from 600 to 2 000 rev/min, whereas, with di*iso*butylene and ethylbenzene, it actually falls under similar conditions.

Toluene and *m*-xylene, which undergo little pre-flame reaction and that too at a much higher temperature level than that in the case of di*iso*butylene, *iso*octane or ethylbenzene, indeed have higher critical compression ratios than those for the other hydrocarbons. The combustion characteristics of toluene and *m*-xylene are somewhat similar to each other and so also is the effect of increasing engine speed, which causes a depreciation in the engine performance in both cases.

This effect of increasing engine speed on the performance of toluene and *m*-xylene is more like that observed with ethylbenzene and di*iso*butylene than that of *iso*octane which appreciates in performance at higher speeds. The combustion characteristics of toluene and *m*-xylene, particularly with regard to the stability of the pre-flame reactions towards self-ignition, however, have more similarities with those of *iso*octane than with those of di*iso*butylene and ethylbenzene. The depreciation with increasing speed for toluene and *m*-xylene as against the appreciation observed with *iso*octane, might well be due to the rather large depreciating factor involved in the former case on account of a higher rate of reaction of pre-flame processes at higher compression ratios. [The critical compression ratios are very much higher for toluene and *m*-xylene (15·0 and 15·5 respectively) than for *iso*octane (7·3).]

Correlation with Blending Properties of Fuels

The improvement that takes place in engine performance on adding a high quality component to one of poor quality is often quite different from that expected from the known characteristics of the individual components. For example, benzene by itself has a much higher anti-knock quality than di*iso*butylene, yet the addition of di*iso*butylene to a fuel causes much greater improvement in its performance than does the addition of the same amount of benzene. The differences in the blending characteristics of various hydrocarbons which are indicated by their 'blending octane numbers' are tabulated in *Table 3*.

In order to determine whether the blending octane numbers of different hydrocarbons in the engine are reflected in the combustion properties under examination, a series of experiments was carried out on blends of *n*-heptane with 20 per cent *iso*octane, benzene and di*iso*butylene. For these experiments the same method and technique were used as had been adopted for studies on pure hydrocarbons described in the previous paper[1]. The results are shown in *Figure 1*. The extent of reaction at different temperatures has been plotted in terms of the concentration of carbon monoxide in the gaseous products. The concentration of carbon dioxide was also measured along with that of carbon monoxide but since carbon dioxide was formed in much smaller amounts than the latter and furthermore its manner of formation at all the pre-flame stages followed the same pattern as that for the latter, the results are presented only in terms of carbon monoxide produced. For a rough comparison with the results on blends of *n*-heptane with *iso*octane, benzene and di*iso*butylene, the results obtained with *n*-heptane alone, using the same amount of *n*-heptane as present in the mixtures, are shown by the broken line in *Figure 1*. The results clearly show that the presence of 20 per cent benzene has hardly any effect on the extent of pre-flame reactions or on the ignition temperature of *n*-heptane. The presence of *iso*octane tends to cause some inhibition in the pre-flame reaction and a slight lowering in ignition temperature. Di*iso*butylene, however, markedly reduces the extent of overall pre-flame reaction and also lowers the ignition temperature. However, it has already been shown that, unless the differences in ignition temperatures are large, it is the extent of pre-flame reactions that primarily provides the correlation with the engine performance of fuels.

Table 3. CFR Blending Octane Ratings of unleaded hydrocarbons[5]*

Hydrocarbon	*Research method*	*Motor method*
n-*Heptane*	0	0
*Methyl*cyclo*hexane*	104	84
iso*Octane*	100	100
Di*iso*butylene	168	151
Benzene	99	91
Toluene	124	112
m-*Xylene*	145	124
Ethylbenzene	124	107

*Hydrocarbon 20 per cent in a 60/40 *iso*octane/*n* heptane mixture.

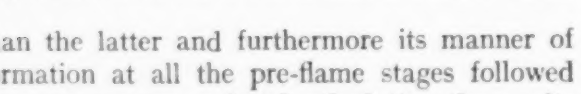

Figure 1. Pre-flame reactions as influenced by blending different hydrocarbons with n-*heptane. Effect of temperature on carbon monoxide production up to ignition point*

The results obtained in the present experiments on the extent of pre-flame reaction using mixtures of *n*-heptane with benzene, *iso*octane and di*iso*butylene thus fall in broad agreement with the observed blending octane numbers.

C. Walcutt and E. B. Rifkin[7], who carried out experiments in motored engines, also arrived at similar conclusions with regard to the superior blending octane rating of di*iso*butylene. They estimated the total heat released prior to autoignition and regarded it as the criterion of the extent of pre-flame reactions. On comparing various blends of *n*-heptane and di*iso*butylene with the corresponding blends containing *n*-heptane and *iso*octane, they showed that there was much less heat released in the *n*-heptane/di*iso*butylene blends.

Correlation with Influence of Tetraethyl-lead

Addition of relatively small amounts of tetraethyl-lead to poor quality fuel is well known to bring about a phenomenal improvement in its engine performance. In an attempt to investigate whether such influence of tetraethyl-lead on engine performance could be interpreted in terms of any effects on the combustion characteristics, experiments were carried out using *n*-heptane as the fuel. The extent of pre-flame reactions and the variation of ignition lag with temperature were first determined in a clean reaction chamber in the manner described previously[1]. A small amount (about 1 g) of lead oxide was then dropped into the chamber and the experiment repeated. (It has already been shown by G. H. N. CHAMBERLAIN and A. D. WALSH[8] that the effect produced by the addition of tetraethyl-lead can be reproduced by carrying out the combustion experiments in the presence of lead oxide.) The results obtained in the absence of lead oxide and again in its presence are shown in *Figures 2* and *3*. The presence of lead oxide strongly inhibited the pre-flame reactions and it also raised the ignition temperature by over 100°C. This effect thus corresponds to the observed improvement in engine performance.

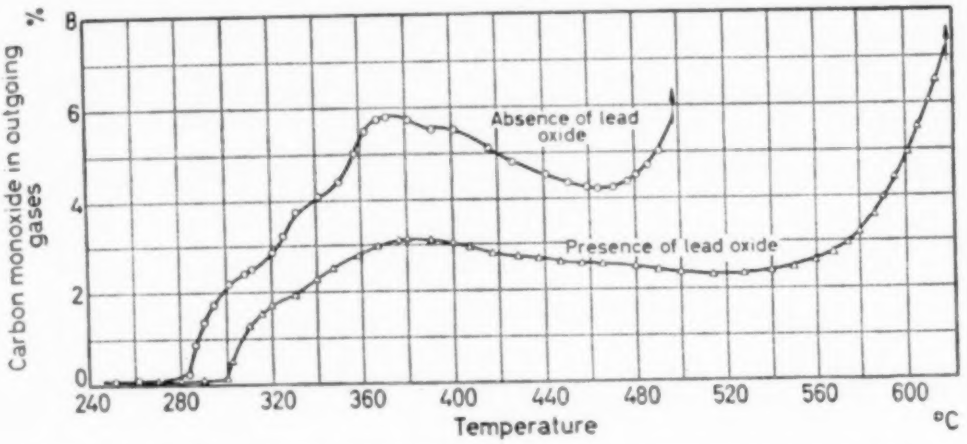

Figure 2. Influence of lead oxide on the combustion characteristics of n-*heptane. Effect of temperature on carbon monoxide production up to ignition point*

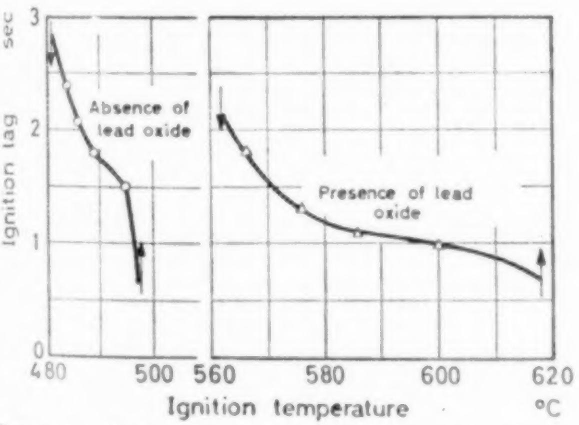

Figure 3. Influence of lead oxide on the ignition characteristics of n-*heptane. Effect on the ignition lag/temperature relationship*

Further work on the combustion characteristics of different fuels, both in the absence and presence of various blending agents and anti-knock compounds, is in hand.

The author wishes to thank the Directors of 'Shell' Research Ltd for permission to publish this work.

References

[1] SALOOJA, K. C. *Combustion & Flame,* 1960, **4,** 117
[2] HELMORE, W. *The Science of Petroleum,* Vol. IV, p 2970. Oxford University Press: London, 1938
[3] FRANK, C. E. and BLACKHAM, A. U. *Industr. Engng Chem.* (*Industr.*), 1952, **44,** 862
[4] SWARTS, D. E. and ORCHIN, M. *Tech. Note Nat. Adv. Comm. Aero., Wash., No. 3579* (1955)
[5] American Petroleum Institute, Research Project 45, Eighteenth Annual *Report,* 30 June 1956
[6] RETAILLIAU, E. R., RICARDS, H. A., Jr. and JONES, M. C. K. *S.A.E. quart. Trans.* 1950, **4,** 438
[7] WALCUTT, C. and RIFKIN, E. B. *Industr. Engng Chem.* (*Industr.*), 1951, **43,** 2844
[8] CHAMBERLAIN, G. H. N. and WALSH, A. D. *Proc. Roy. Soc. A,* 1952, **215,** 175

WHE
degr
simp
reac
of th
a sin

CH$_3$

+ NO

ONO
|
CH$_2$

+ NO

In
nitro
of th
react
dyna
of th
(olef
state

The Flame Decomposition of Some Substituted Ethyl Nitrates

J. Powling, W. A. W. Smith and J. Thynne

Explosives Research and Development Establishment, Waltham Abbey, Essex

(Received April 1959)

Detailed reaction product concentration profiles have been obtained for the decomposition flames of 2-hydroxyethyl nitrate, 2-methoxyethyl nitrate and 2-ethoxyethyl nitrate stabilized in a simple flat flame burner. The reactions in the flames at atmospheric pressure do not proceed to equilibrium, and the temperatures (measured in 24 mm diameter tubes) just behind the flame fronts are 910°, 490° and 450°C, respectively, for the above esters, the 2-ethoxyethyl nitrate requiring about 60°C preheat for stable burning. The rates of burning of the liquids are given for pressures up to 1300 to 2000 $\mathrm{lb/in}^2$. *Up to about 800* $\mathrm{lb/in}^2$ *2-methoxyethyl nitrate burns faster than 2-hydroxyethyl nitrate, in spite of a considerably lower heat of explosion and flame front temperature. The primary products of reaction, i.e. those sampled where the decomposition of the original ester was just complete, can be readily accounted for on the basis of the mechanism previously put forward for the flame reactions of ethyl nitrate and the propyl nitrates. The essential feature of this mechanism is the abstraction of a hydrogen atom from the nitric ester by* NO_2 *or* HONO, *and simple rearrangement of the resulting hydrogen-deficient ester molecule directly to the observed aldehydic products. The primary products of six mononitrate flames and those of two dinitrates are compared.*

Introduction

Whereas certain aliphatic dinitrates appear[1] to degrade in their decomposition flames in the simple unimolecular fashion exemplified by reactions 1 and 2 below, the reaction products of the mononitrates are not easily described by a similar mechanism.

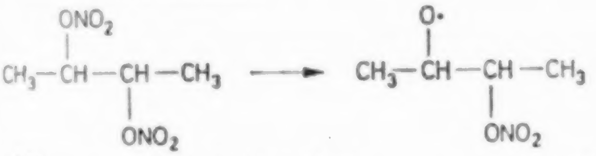

$$CH_3\text{—}\underset{ONO_2}{CH}\text{—}\overset{ONO_2}{CH}\text{—}CH_3 \longrightarrow CH_3\text{—}\overset{O\cdot}{CH}\text{—}\underset{ONO_2}{CH}\text{—}CH_3$$

$$+NO_2 \longrightarrow 2CH_3CHO+2NO_2 \quad \ldots\ [1]$$

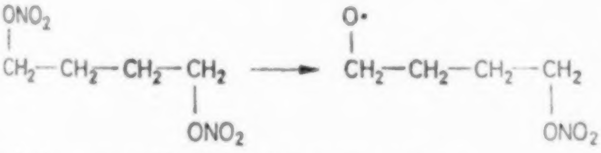

$$\overset{ONO_2}{CH_2}\text{—}CH_2\text{—}CH_2\text{—}\underset{ONO_2}{CH_2} \longrightarrow \overset{O\cdot}{CH_2}\text{—}CH_2\text{—}CH_2\text{—}\underset{ONO_2}{CH_2}$$

$$+NO_2 \longrightarrow 2H_2CO+CH_2{:}CH_2+2NO_2 \quad \ldots\ [2]$$

In the above dinitrates high concentrations of nitrogen dioxide can be observed in a thin zone of the flame front, and the final products of reaction at atmospheric pressure (not in thermodynamic equilibrium) are identical with those of the appropriate nitrogen dioxide–aldehyde–(olefin) mixture. In an earlier report[2] it was stated that the products of the ethyl nitrate decomposition flame could be better accounted for if it were assumed that nitrogen dioxide attack was not confined to the products of an initial fission of the nitric ester but occurred extensively on the nitric ester itself. It was suggested that the greater part of the degradation of the nitric ester was brought about by the removal of a hydrogen atom by NO_2, HONO, or $CH_3\cdot$, and that unimolecular fission of the nitrate to a radical and NO_2 was only the initiating step. The stationary concentration of nitrogen dioxide in this flame was nowhere great enough to be observed. The products of the flames of normal and *iso*propyl nitrate have been described[3] by a similar mechanism, but an alternative explanation, based on the unimolecular degradation of the esters to alkoxy radicals and NO_2, could not be confidently excluded in this case. Again, in contrast to the dinitrates, the stationary concentrations of nitrogen dioxide were very small. The reaction schemes postulated for these mononitrates may be found elsewhere[2, 3].

To examine the possibilities of a more extensive application of such a mechanism, the combustion of three further mononitrates of significantly different chemical structure (within the limited range of energy suitable for examination in the laboratory) has now been studied. These are 2-methoxyethyl nitrate, $CH_3OCH_2CH_2ONO_2$; 2-ethoxyethyl nitrate, $CH_3CH_2OCH_2CH_2ONO_2$ and 2-hydroxyethyl nitrate, $HOCH_2CH_2ONO_2$.

Experimental Method

Preparation of the nitric esters

2-Hydroxyethyl nitrate—This compound (ethylene glycol mononitrate) was prepared by adding 1·13 mole of ethylene bromohydrin to 1 mole of silver nitrate dissolved in acetonitrile. Separation of silver bromide began almost at once and the temperature rose in two hours to 45°C. The mixture was cooled to room temperature and showed no further tendency to heat up. It was allowed to stand for six days in the dark, filtered, and the silver bromide washed with acetonitrile. The combined filtrate and washings were distilled at 20 mm of mercury to about half their volume and allowed to stand for three days. Silver bromide was again filtered off and washed; at this stage the total recovery of silver was 98·4 per cent. The combined filtrate and washings were evaporated at reduced pressure and the residual 2-hydroxyethyl nitrate distilled in a vacuum. The yield was 95 per cent; b.pt 57·5°C/1 mm Hg.

2-Ethoxyethyl nitrate—98 per cent nitric acid (117 ml) was cooled below 5°C and 4·5 g urea slowly added. 2-Ethoxyethanol (45 g) was added dropwise over a period of 20 minutes with good stirring and cooling, so that the temperature remained below 0°C. After allowing to stand for 10 min at −2°C, the nitration mixture was drowned in 1 kg of 50/50 ice/water and then extracted three times with 75 ml of methylene chloride. The combined extracts were washed twice with 50 ml of 3 per cent sodium carbonate solution and twice with 50 ml of water. The solution was dried overnight with anhydrous sodium sulphate and the methylene chloride distilled off at atmospheric pressure. The residual 2-ethoxyethyl nitrate distilled off at 63·5°C and 15 mm Hg (Yield: 87 per cent).

2-Methoxyethyl nitrate—This was prepared in a somewhat similar manner except that a sulphuric acid–nitric acid nitrating mixture was used, and the nitrate was separated, rather than extracted with methylene chloride, from the drowned nitration mixture. B.pt 57°C/22 mm Hg.

Flame stabilization and probe sampling

The flames were studied at atmospheric pressure, using a flat flame burner and a simple probe sampling technique similar to that used in the decomposition of the other nitrates[1-3]. Steady decomposition flames very close to the (stationary) liquid surface were obtained with all the esters. Difficulties encountered were a tendency of the 2-methoxyethyl nitrate to boil at the surface, which made sampling at close distances tedious, and the deposition of tarry materials on the burner jacket, which obscured the flame.

Rates of burning

The rate of regression of burning liquid surface was measured at elevated pressures in 4·5 mm diameter glass tubes, and at atmospheric pressure in 24 mm diameter tubes. The rate of burning/pressure curves for the three esters are given in *Figure 1*.

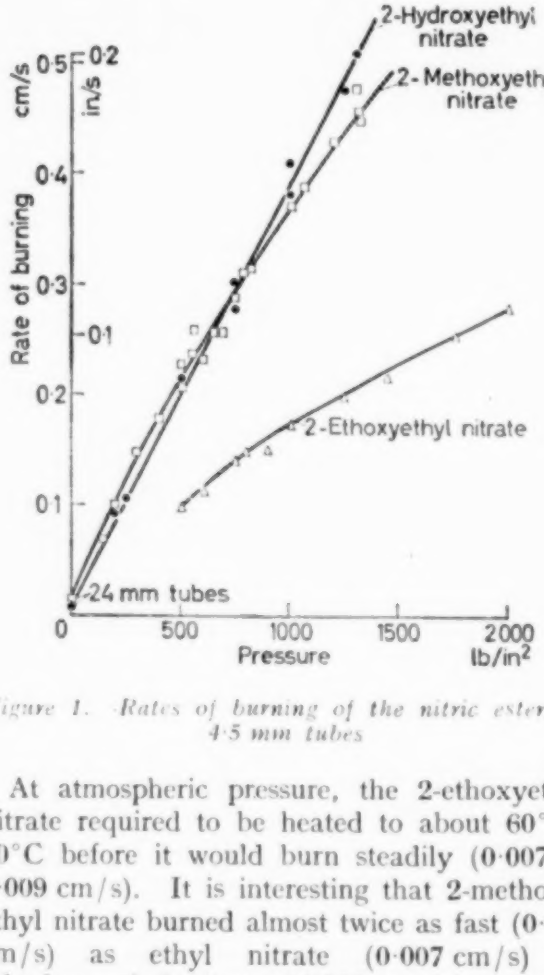

Figure 1. Rates of burning of the nitric esters in 4·5 mm tubes

At atmospheric pressure, the 2-ethoxyethyl nitrate required to be heated to about 60° to 80°C before it would burn steadily (0·007 to 0·009 cm/s). It is interesting that 2-methoxyethyl nitrate burned almost twice as fast (0·013 cm/s) as ethyl nitrate (0·007 cm/s) or 2-hydroxyethyl nitrate (0·0067 cm/s), in spite of a much lower heat of explosion and flame front temperature. However, at pressures above 200 lb/in² and 800 lb/in², respectively, the rates of burning of the latter esters are greater.

Flame temperature measurement

Flame temperatures were measured with platinum/platinum–10 per cent rhodium thermocouples, butt-welded from wires of 0·05 mm diameter and covered with a thin layer of silica to reduce catalytic action. The liquid surface was allowed to burn past the stationary thermocouple, and the e.m.f. recorded on a potentiometric recorder. Knowledge of the liquid consumption rate and of the recorder chart speed gave a reliable temperature distribution, with the exception that the surface tension of the liquid made it impossible to record the real temperature within ~1 mm from the liquid surface. The temperature distributions are given in *Figure 2*.

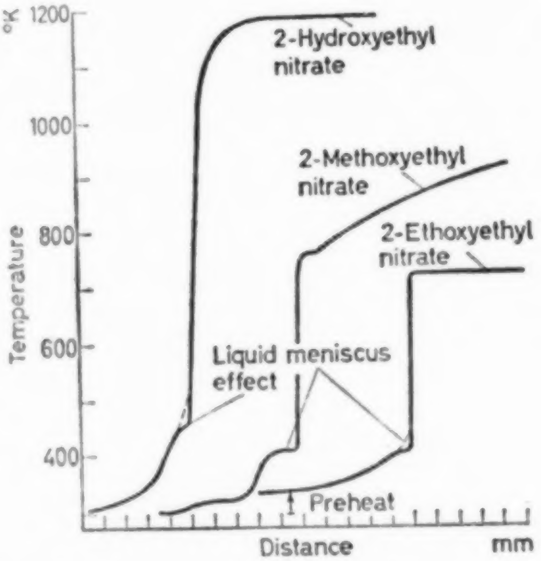

Figure 2. Temperature recordings through the liquid nitric ester flames

Analysis of combustion products

The products from the flames were drawn (via a fine silica probe situated at a measured distance from the liquid surface) through a cold isopentane trap at −120°C, and the non-condensable fraction collected over mercury. Infra-red analyses were then performed on the gas sample, and hydrogen and nitrogen, which are transparent in the infra-red, were estimated chromatographically using a 120 cm activated charcoal column. The cold trap was removed and an i.r. analysis of the fraction vaporizing between −120°C and room temperature was obtained. The condensate was then weighed and divided into parts as necessary. Typical treatment of a liquid would involve:

(*i*) Infra-red analysis at 120°C—by this means less volatile products such as H_2CO, HCO_2H, CH_3OH and nitro compounds could be estimated. Water, in amounts encountered, can be estimated only approximately in this way.

(*ii*) Water content was estimated by the Karl Fischer method.

(*iii*) The third fraction was titrated for acid, and the aldehyde content estimated by the sodium sulphite method.

The products of the combustion were also examined using a Metropolitan Vickers MS 3 mass spectrometer, when certain specific components were being sought.

Results

The distributions of reaction products in the three nitric ester flames are shown in *Figures 3* to *5*. The number of moles of reaction product derived from 100 moles of the nitric ester is plotted against the distance of the sampling probe from the burning liquid surface. A mass balance between reactant and products had to be made because, with these esters, considerable amounts of unidentified material (of low volatility) were found in the liquid fraction. The atom balances were poor, therefore. They indicated the presence of unidentified nitrogenous material in the cases of 2-methoxyethyl nitrate and 2-ethoxyethyl nitrate, but not in that of 2-hydroxyethyl nitrate. It is thought that most of the polymeric residue is derived from the rather reactive aldehydes, methoxyacetaldehyde, ethoxyacetaldehyde and glycollic aldehyde, which would be expected as major degradation products of the above nitric esters. These aldehydes might be expected to polymerize and react with other materials in the trap. The unknown material has arbitrarily been given the molecular weight of the appropriate aldehyde, so that, if the assumption that it is derived from the aldehyde is accepted, the amount of the latter is indicated on the plots in *Figures 3* to *5*.

Discussion

Each ester will be considered under a separate heading; the 2-methoxyethyl nitrate will be

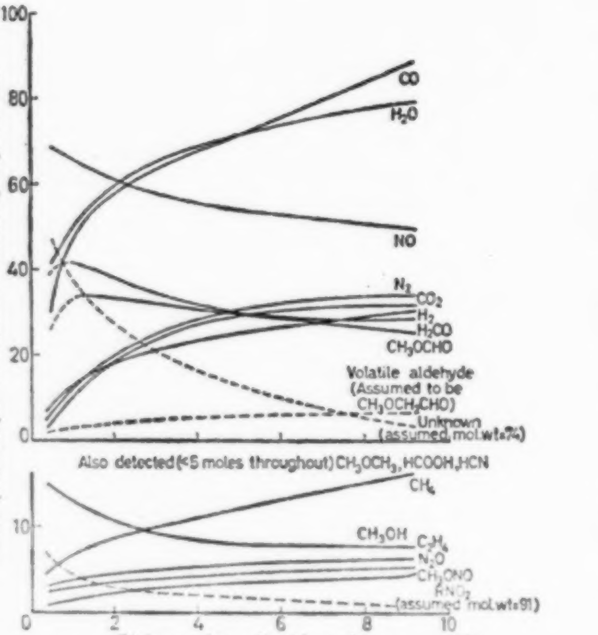

Figure 3. Product distribution in the 2-methoxyethyl nitrate flame

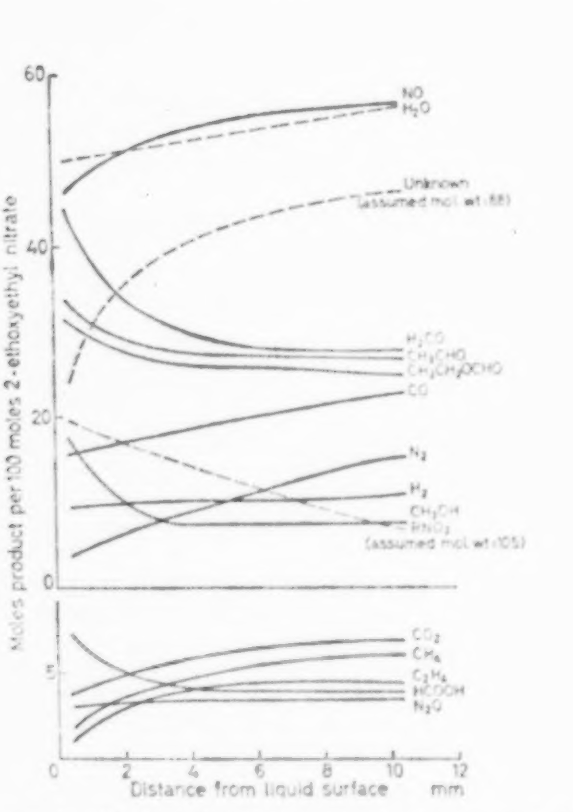

Figure 4. Product distribution in the 2-ethoxyethyl nitrate flame

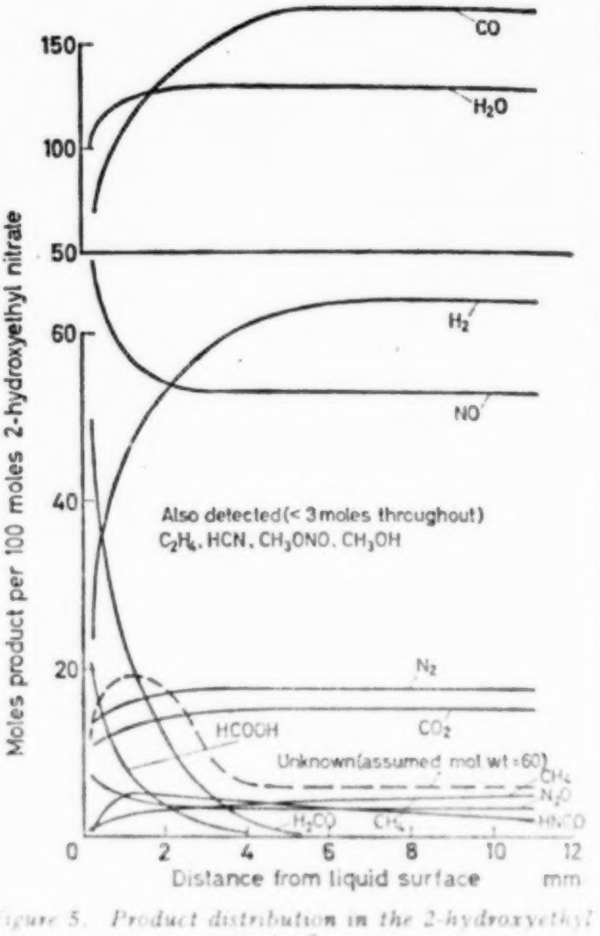

Figure 5. Product distribution in the 2-hydroxyethyl nitrate flame

taken first, and then the other two esters will be discussed more briefly by analogy.

2-Methoxyethyl nitrate

The major products of very rapid reaction in the flame front are nitric oxide, carbon monoxide, water, formaldehyde, methyl formate, a large amount of the unidentified material and a smaller, but significant, quantity of methanol. The absence of 2-methoxyethanol and of nitrogen dioxide, and the presence of only minor quantities of dimethyl ether, is of some importance.

The initiating step in the degradation of the nitric ester is considered to be the rupture of the weakest bond in the molecule, the —O—N— bond (reaction 3) and could be expected[4] to be followed by further breakdown of the alkoxy radical at the high temperatures (400° to 500° C) involved, according to reaction 4 and perhaps 5.

$$CH_3OCH_2CH_2ONO_2 \longrightarrow CH_3OCH_2CH_2O\cdot + NO_2 \quad \ldots. [3]$$

$$CH_3OCH_2CH_2O\cdot \longrightarrow CH_3OCH_2\cdot + H_2CO \quad \ldots. [4]$$

$$CH_3OCH_2\cdot \longrightarrow CH_3\cdot + H_2CO \quad \ldots. [5]$$

The absence of 2-methoxyethanol, and the presence of only the small amounts of dimethyl ether, suggests either that the radicals produced in reactions 3 and 4 rapidly degrade before their expected hydrogen-capturing reactions can take place, or that the main decomposition reaction involves a chain mechanism in which only a few initiating steps are required in order to bring about the subsequent breakdown of many nitric ester molecules. The relatively small amount of methane, an unknown amount of which is always produced from the thermal decomposition of methyl formate, adds support to the view that the number of initiating steps is relatively small.

Of particular interest is the production of large amounts of methyl formate, which cannot be satisfactorily accounted for on the basis of unimolecular decomposition of the nitric ester. Its appearance can, however, be described in a simple way by a reaction completely analogous to that proposed as an important step in the degradation of ethyl nitrate. It was suggested that ethyl nitrate was attacked by nitrogen dioxide (or HONO or $CH_3\cdot$) with consequent loss of a hydrogen atom. If an α-hydrogen were removed, the reactions would be simply:

$$NO_2 + CH_3CH_2ONO_2 \longrightarrow HONO + [CH_3\dot{C}HONO_2]$$

$$[CH_3\dot{C}HONO_2] \longrightarrow CH_3CHO + NO_2 \quad \ldots. [6]$$

If, however, a β-hydrogen atom were lost, the remaining radical would immediately rearrange and decompose thus

$$[\dot{C}H_2CH_2ONO_2] \longrightarrow$$

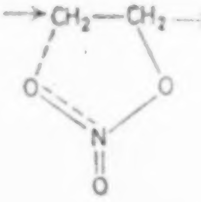

$$\longrightarrow 2H_2CO + NO \quad \ldots. [7]$$

If reactions analogous to 6 and 7 occur in the decomposition of methoxyethyl nitrate, two different, but characteristic, products would be methoxyacetaldehyde and methyl formate, respectively.

$$NO_2 + CH_3OCH_2CH_2ONO_2 \longrightarrow [CH_3OCH_2\dot{C}HONO_2] + HONO \quad \ldots. [8]$$

$$\downarrow$$

$$CH_3OCH_2CHO + NO_2 \quad \ldots. [8a]$$

$$NO_2 + CH_3OCH_2CH_2ONO_2 \longrightarrow [CH_3O\dot{C}HCH_2ONO_2] + HONO \quad \ldots [9]$$

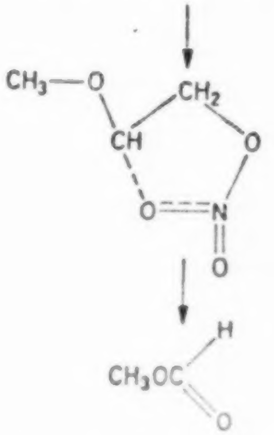

$$+ H_2CO + NO \quad \ldots. [9a]$$

It is difficult to determine how much of the reaction might proceed by reaction 8, since methoxyacetaldehyde could not be prepared for reference spectra and calibration. The alkoxyacetaldehydes are known[5] to be difficult to prepare and keep. Infra-red spectra revealed the presence of an unknown aldehyde in the vapour fraction, and a small amount of a substance giving mass peaks at 74 and 73 was present. Not a great deal of methoxyacetaldehyde could have been present in the vapour phase, but a large amount of a substance of low volatility was always found in the liquid fraction, and it is thought that this was probably a polymer of methoxyacetaldehyde with some formaldehyde. The monomer was not regenerated when heated to 120°C in the infra-red hot cell. If the unknown aldehyde and the polymer are assumed to be due to methoxyacetaldehyde, then more than 40 mole per cent of the nitrate decomposes to this substance. More than 30 mole per cent of methyl formate was found, and

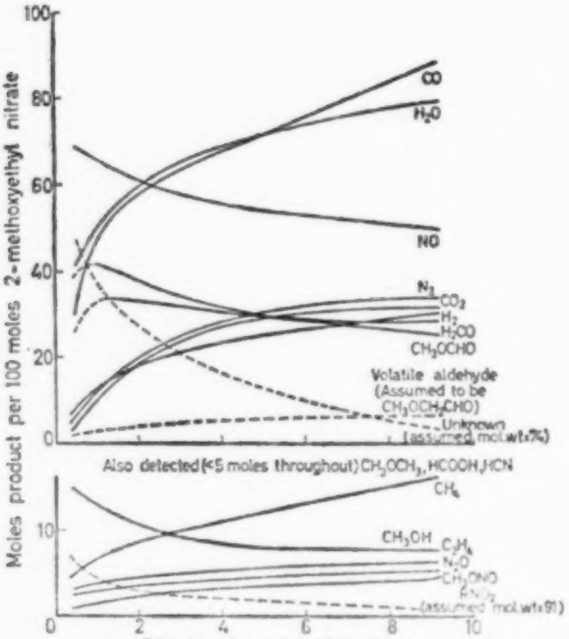

Figure 3. Product distribution in the 2-methoxyethyl nitrate flame

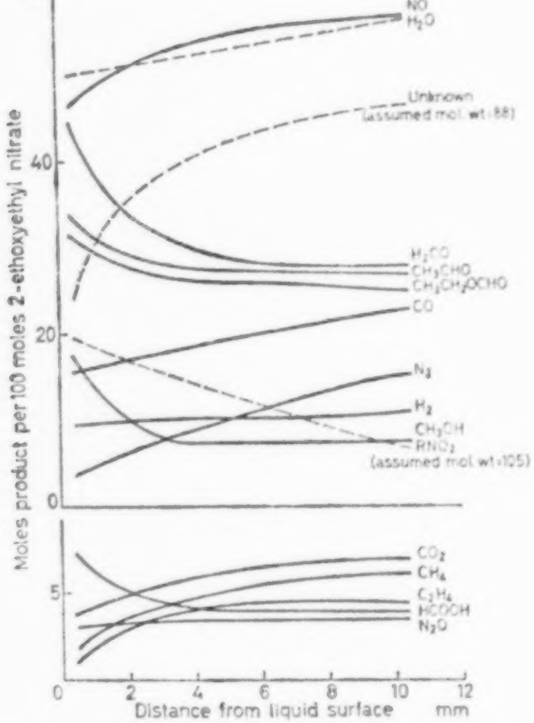

Figure 4. Product distribution in the 2-ethoxyethyl nitrate flame

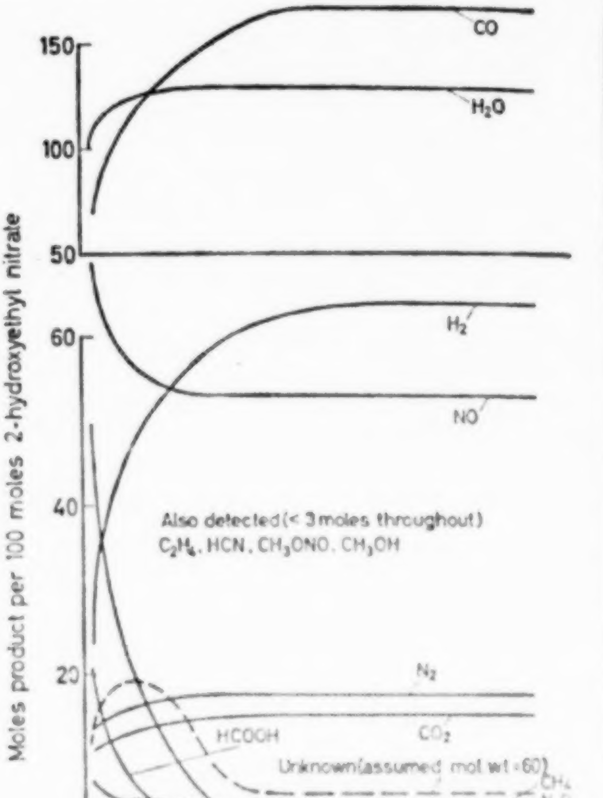

Figure 5. Product distribution in the 2-hydroxyethyl nitrate flame

taken first, and then the other two esters will be discussed more briefly by analogy.

2-Methoxyethyl nitrate

The major products of very rapid reaction in the flame front are nitric oxide, carbon monoxide, water, formaldehyde, methyl formate, a large amount of the unidentified material and a smaller, but significant, quantity of methanol. The absence of 2-methoxyethanol and of nitrogen dioxide, and the presence of only minor quantities of dimethyl ether, is of some importance.

The initiating step in the degradation of the nitric ester is considered to be the rupture of the weakest bond in the molecule, the —O—N— bond (reaction 3) and could be expected[4] to be followed by further breakdown of the alkoxy radical at the high temperatures (400° to 500°C) involved, according to reaction 4 and perhaps 5.

$$CH_3OCH_2CH_2ONO_2 \rightarrow CH_3OCH_2CH_2O\cdot + NO_2 \quad .\,.\,.\,.\ [3]$$

$$CH_3OCH_2CH_2O\cdot \rightarrow CH_3OCH_2\cdot + H_2CO \quad .\,.\,.\,.\ [4]$$

$$CH_3OCH_2\cdot \rightarrow CH_3\cdot + H_2CO \quad .\,.\,.\,.\ [5]$$

The absence of 2-methoxyethanol, and the presence of only the small amounts of dimethyl ether, suggests either that the radicals produced in reactions **3** and **4** rapidly degrade before their expected hydrogen-capturing reactions can take place, or that the main decomposition reaction involves a chain mechanism in which only a few initiating steps are required in order to bring about the subsequent breakdown of many nitric ester molecules. The relatively small amount of methane, an unknown amount of which is always produced from the thermal decomposition of methyl formate, adds support to the view that the number of initiating steps is relatively small.

Of particular interest is the production of large amounts of methyl formate, which cannot be satisfactorily accounted for on the basis of unimolecular decomposition of the nitric ester. Its appearance can, however, be described in a simple way by a reaction completely analogous to that proposed as an important step in the degradation of ethyl nitrate. It was suggested that ethyl nitrate was attacked by nitrogen dioxide (or HONO or $CH_3\cdot$) with consequent loss of a hydrogen atom. If an α-hydrogen were removed, the reactions would be simply:

$$NO_2 + CH_3CH_2ONO_2 \rightarrow HONO + [CH_3\dot{C}HONO_2]$$

$$[CH_3\dot{C}HONO_2] \rightarrow CH_3CHO + NO_2 \quad .\,.\,.\,.\ [6]$$

If, however, a β-hydrogen atom were lost, the remaining radical would immediately rearrange and decompose thus

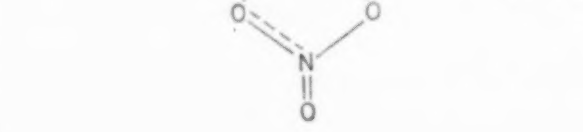

.... [7]

If reactions analogous to **6** and **7** occur in the decomposition of methoxyethyl nitrate, two different, but characteristic, products would be methoxyacetaldehyde and methyl formate, respectively.

$$NO_2 + CH_3OCH_2CH_2ONO_2 \rightarrow [CH_3OCH_2\dot{C}HONO_2] + HONO \quad .\,.\,.\,.\ [8]$$

$$\downarrow$$

$$CH_3OCH_2CHO + NO_2 \quad .\,.\,.\,.\ [8a]$$

$$NO_2 + CH_3OCH_2CH_2ONO_2 \rightarrow [CH_3O\dot{C}HCH_2ONO_2] + HONO \quad .\,.\,.\ [9]$$

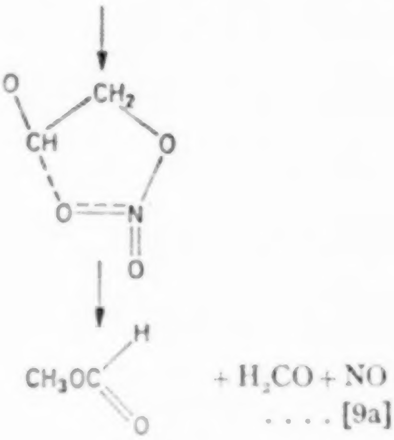

.... [9a]

It is difficult to determine how much of the reaction might proceed by reaction **8**, since methoxyacetaldehyde could not be prepared for reference spectra and calibration. The alkoxyacetaldehydes are known[5] to be difficult to prepare and keep. Infra-red spectra revealed the presence of an unknown aldehyde in the vapour fraction, and a small amount of a substance giving mass peaks at 74 and 73 was present. Not a great deal of methoxyacetaldehyde could have been present in the vapour phase, but a large amount of a substance of low volatility was always found in the liquid fraction, and it is thought that this was probably a polymer of methoxyacetaldehyde with some formaldehyde. The monomer was not regenerated when heated to 120°C in the infra-red hot cell. If the unknown aldehyde and the polymer are assumed to be due to methoxyacetaldehyde, then more than 40 mole per cent of the nitrate decomposes to this substance. More than 30 mole per cent of methyl formate was found, and probably some had already pyrolysed. Thermal decomposition of this material in a silica vessel at 600°C showed that it produced, very approximately, 90 per cent ($CO+CH_3OH$) and 10 per cent (CO_2+CH_4). This reaction, and the pyrolysis of formaldehyde, could account for the observed hydrogen, methane, carbon monoxide and methanol. Water would result from reactions of HONO produced in reactions 8 and 9. For example,

$$HONO+CH_3OCH_2CH_2ONO_2 \longrightarrow H_2O + NO + [CH_3O\dot{C}_2H_3ONO_2] \quad \ldots . [10]$$

A small amount of a nitro compound of low volatility was estimated by assuming the same extinction coefficient at 6·30 microns as for nitromethane. Its infra-red spectrum and its mass spectrum were compatible with the structure $CH_3OCH_2NO_2$, but this material was not successfully prepared, so no positive identification could be made. The postulated reaction scheme for 2-methoxyethyl nitrate, which will describe the appearance of all the observed reaction products, and which is completely analogous to that suggested for ethyl nitrate, is summarized below:

$$CH_3OCH_2CH_2ONO_2 \longrightarrow CH_3OCH_2CH_2O\cdot + NO_2 \text{ (initiation)} \quad \ldots . [3]$$

$$CH_3OCH_2CH_2O\cdot \longrightarrow \dot{C}H_3 + 2H_2CO \quad \ldots . [4 \text{ and } 5]$$

$$\dot{C}H_3 + CH_3OCH_2CH_2ONO_2 \longrightarrow CH_4 + [CH_3O\dot{C}_2H_3ONO_2] \quad \ldots . [11]$$

$$NO_2 + CH_3OCH_2CH_2ONO_2 \longrightarrow HONO + [CH_3O\dot{C}_2H_3ONO_2] \quad \ldots . [8]$$

$$HONO + CH_3OCH_2CH_2ONO_2 \longrightarrow H_2O + NO + [CH_3O\dot{C}_2H_3ONO_2] \quad \ldots . [10]$$

$$[CH_3O\dot{C}_2H_3ONO_2] = [CH_3OCH_2\dot{C}HONO_2] \longrightarrow CH_3OCH_2CHO + NO_2 \quad \ldots . [8a]$$

$$[CH_3O\dot{C}_2H_3ONO_2] = [CH_3O\dot{C}HCH_2ONO_2] \longrightarrow CH_3OCHO + H_2CO + NO \quad \ldots . [9a]$$

An overall equation for the initial stages of the reaction according to the above scheme, with a chain length of ten, would be

$$CH_3OCH_2CH_2ONO_2 \longrightarrow 0{\cdot}1CH_4 + 0{\cdot}8H_2CO + 0{\cdot}6CH_3OCHO + 0{\cdot}3CH_3OCH_2CHO + 0{\cdot}4H_2O + 1{\cdot}0NO \quad \ldots . [12]$$

No adequate check is possible however, because, even in the earliest samples taken, some oxidation and pyrolysis of aldehydes had occurred and part of the nitric oxide had been reduced.

2-Ethoxyethyl nitrate

This ester has a less favourable oxygen balance than the 2-methoxyethyl nitrate, but a stable flame can be obtained at atmospheric pressure by preheating. The flame temperature at the point of complete disappearance of the nitrate is not much different from that of the 2-methoxyethyl nitrate if the minimum amount of preheat for stable burning is given.

The products of greatest interest from this ester are formaldehyde, ethyl formate and acetaldehyde. The amount of carbon monoxide is much smaller than usual and indicates that not much pyrolysis of aldehydes has occurred. No ethoxyethanol, methylethyl ether or nitrogen dioxide could be detected, and less than 0·5 mole of ethane per 100 moles of nitric ester was present. Significant amounts (~20 mole per cent) of a high-boiling nitro compound were found. Its mass spectrum was consistent with the fragments expected from $CH_3CH_2OCH_2NO_2$, but this could not be prepared for comparison.

Initiation is again taken to be fission of the weakest bond

$$CH_3CH_2OCH_2CH_2ONO_2 \longrightarrow CH_3CH_2OCH_2CH_2O\cdot + NO_2 \quad \ldots . [13]$$

The absence of 2-ethoxyethanol suggests that the alkoxy radical breaks down rapidly

$$CH_3CH_2OCH_2CH_2O\cdot \longrightarrow CH_3CH_2O\dot{C}H_2 + H_2CO \quad \ldots . [14]$$

The absence of methylethyl ether and the low concentrations of ethane and ethylene would be evidence to suggest that, in fact, no large proportion of the nitric ester decomposed according to reaction 13 because none of the expected products of the resulting alkoxy radical would have been produced:

$$CH_3CH_2O\dot{C}H_2 + RH \longrightarrow CH_3CH_2OCH_3 + R\cdot \quad \ldots [15]$$

$$CH_3CH_2O\dot{C}H_2 \longrightarrow CH_3CH_2\cdot + H_2CO \quad \ldots [16]$$

However, if the nitro compound is indeed $CH_3CH_2OCH_2NO_2$, then it is possible that it was formed by combination of $CH_3CH_2OCH_2\cdot$ and NO_2, although this reaction would have to be very much faster than the hydrogen-abstracting reaction **15** since the concentration of both $CH_3CH_2OCH_2\cdot$ and NO_2 must be very small, whereas 'RH' is always large. The amount of stable hydrocarbon from the alkoxy radical (reaction **16**) cannot in this case be taken as some guide to the reaction chain length. On the other hand, the nitro compound may well have been produced by a bimolecular reaction 17, below, which is not a chain-terminating process.

$$NO_2 + CH_3CH_2OCH_2CH_2ONO_2 \rightarrow CH_3CH_2OCH_2NO_2 + H_2CO + NO_2 \quad \ldots [17]$$

The ethyl formate is produced by reactions analogous to **9** and **7**:

$$NO_2 + CH_3CH_2OCH_2CH_2ONO_2 \rightarrow HONO + [CH_3CH_2O\dot{C}HCH_2ONO_2] \quad \ldots [18]$$

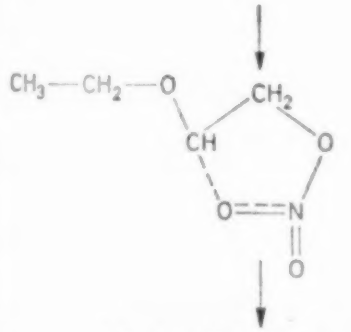

$$CH_3CH_2OCHO + H_2CO + NO \quad \ldots [18a]$$

Two other hydrogen-stripping reactions would appear to be equally probable in this ester. One of them could account for the acetaldehyde observed in large amounts

$$NO_2 + CH_3CH_2OCH_2CH_2ONO_2 \rightarrow [CH_3\dot{C}HOCH_2CH_2ONO_2] + HONO \quad \ldots [19]$$

The radical $CH_3\dot{C}HOCH_2CH_2ONO_2$, produced in reaction **19**, could rearrange, by way of either of the two forms below, to give acetaldehyde, formaldehyde and nitric oxide:

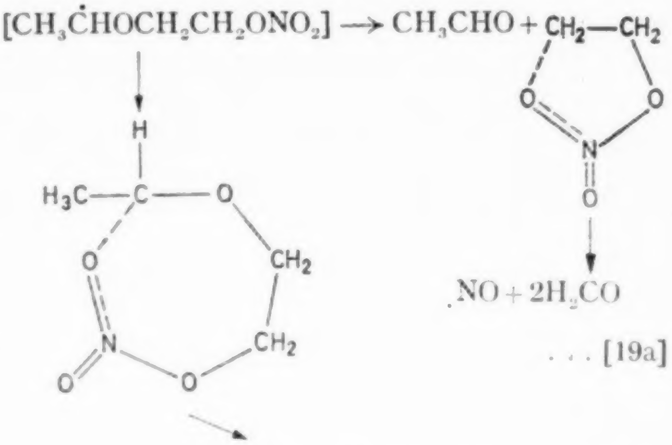

$$[CH_3\dot{C}HOCH_2CH_2ONO_2] \rightarrow CH_3CHO + $$

$$NO + 2H_2CO \quad \ldots [19a]$$

$$CH_3CHO + 2H_2CO + NO \quad \ldots [19b]$$

The other hydrogen-stripping reaction (**20** below) would produce ethoxyacetaldehyde. The large amount of polymeric substance in the liquid fraction might well be due to this unstable aldehyde, but no positive infra-red evidence could be obtained for this suggestion, because of the interference of acetaldehyde, formaldehyde, ethyl formate and water.

$$NO_2 + CH_3CH_2OCH_2CH_2ONO_2 \longrightarrow HONO + [CH_3CH_2OCH_2\dot{C}HONO_2] \quad [20]$$

$$\downarrow$$

$$CH_3CH_2OCH_2CHO + NO_2 \quad [20a]$$

A reaction scheme closely similar to that for the 2-methoxyethyl nitrate, but with the additional reactions to account for the acetaldehyde (reaction **19**) and the nitro compound (e.g. reaction **17**), will account for the main identified products. The large amounts of unknown substance from this more complex ester (see *Figure 4*) upset attempts to describe the reaction more fully. Beyond the flame front, it would seem that, in this cool-burning ester, polymerization of aldehydic products is faster than their pyrolysis. In *Figure 4* it may be seen that the curves of the aldehydes and of the unknown polymeric material are inversely related to each other. The nitro compound decomposes steadily in the product gases.

2-Hydroxyethyl nitrate

The decomposition products of this ester are all simple molecules and do not provide much evidence about the course of the flame degradation unless examined in relation to the other nitrates, when abnormally large amounts of formic acid, hydrogen, carbon monoxide, water and carbon dioxide are seen to be produced (*Figure 5*). No methanol or glycol is observed, and, although the amount of hydrogen is larger than commonly observed in the flame front of similar nitric esters, the trend of the hydrogen curve in *Figure 5* indicates that its initial concentration (when the decomposition of the nitric ester is just complete) is much smaller.

The amount of 2-hydroxyethyl nitrate consumed according to reaction 21 (plus reactions 22 and 23) is again probably not large:

$$HOCH_2CH_2ONO_2 \longrightarrow HOCH_2CH_2O\cdot + NO_2 \quad \ldots . [21]$$

$$HOCH_2CH_2O\cdot \longrightarrow HOCH_2\cdot + H_2CO \quad \ldots . [22]$$

$$HO\dot{C}H_2 \longrightarrow H\cdot + H_2CO \quad \ldots . [23]$$

It is suggested that the observations are better explained by a mechanism similar to that of the other mononitrates, with reaction 21 being the initiating step in a chain process, the main reactions being 24 and probably 25 below:

$$NO_2 + HOCH_2CH_2ONO_2 \longrightarrow HONO + [HO\dot{C}HCH_2ONO_2] \qquad [24]$$

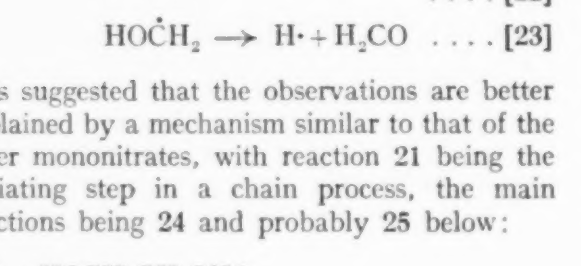

$$\longrightarrow HCOOH + H_2CO + NO \ \ldots [24a]$$

$$H_2O + CO \text{ or } H_2 + CO_2$$

$$NO_2 + HOCH_2CH_2ONO_2 \longrightarrow HONO + [HOCH_2\dot{C}HONO_2] \quad \ldots . [25]$$

$$\downarrow$$

$$HOCH_2CHO + NO_2 \quad \ldots . [25a]$$

Again, the relative extent of reaction 25 could not be estimated because of the difficulty of analysing for polymerized glycollic aldehyde in the trap, and of the rapidity of the pyrolysis of the aldehydes in this flame. The 'unknown' in *Figure 5* has been given the molecular weight of glycollic aldehyde. Synthetic samples of glycollic aldehyde, both as the anhydrous solid and as the hydrated form, were examined spectroscopically. It was considered that the latter was the form in which it was most likely to occur in the liquid products, but this, when heated to 120°C, gave a negligible vapour-phase i.r. spectrum. Its spectrum as a thin film was compared with that of the liquid products, but the latter consisted of broad featureless bands due to the mixture of water, formaldehyde and formic acid, which were also present in the samples in which the unknown occurred. Thus, no positive inference as to the presence or absence of the aldehyde in the products could be made.

HNCO is an interesting and unusual minor product of this particular flame, but there are no clues regarding its mode of formation.

The reaction scheme for this ester would be summarized as follows:

$$HOCH_2CH_2ONO_2 \longrightarrow H\cdot + 2H_2CO + NO_2 \quad \ldots . [21, 22 \text{ and } 23]$$

$$H\cdot + HOCH_2CH_2ONO_2 \longrightarrow H_2 + [HO\dot{C}_2H_3ONO_2] \quad \ldots . [26]$$

$$NO_2 + HOCH_2CH_2ONO_2 \longrightarrow HONO + [HO\dot{C}_2H_3ONO_2] \quad [24 \text{ or } 25]$$

$$HONO + HOCH_2CH_2ONO_2 \longrightarrow H_2O + NO + [HO\dot{C}_2H_3ONO_2] \ldots [27]$$

$$[HO\dot{C}_2H_3ONO_2] \longrightarrow HCOOH + H_2CO + NO \quad \ldots . [24a]$$

$$\searrow HOCH_2CHO + NO_2 \quad \ldots [25a]$$

Reactions behind the flame fronts

In all the flames examined, relatively slow reactions follow in the wake of the very fast reactions occurring in the flame front. The former are largely aldehyde pyrolyses, and do not result in any further heat release, unless nitric oxide becomes involved in the reaction and is reduced. This reduction of nitric oxide is an important feature in relation to the rate of energy release in nitric ester combustion, and has been discussed elsewhere[1, 6]. In all nitric ester flames in which formaldehyde is observed to be decomposing, nitric oxide is reduced at a rate which seems (from the concentration curves) to be related to the rate of aldehyde pyrolysis. In the 2-hydroxyethyl nitrate the decomposition of formaldehyde is rapid, and the associated reduction of nitric oxide stops at about the point when the aldehyde has disappeared. The continued temperature rise resulting from this nitric oxide reduction is seen as a 'rounding off' of the temperature profile in *Figure 2*.

In the 2-methoxyethyl nitrate flame, the temperature is lower and the aldehyde pyrolyses are slower. Nitric oxide is reduced continuously, the nitric oxide curves and those of the formaldehyde and methyl formate being roughly parallel over the range covered (*Figure 3*). The flame temperature continues to rise fairly steeply beyond the flame front (*Figure 2*). The situation with regard to nitric oxide reduction in the 2-ethoxyethyl nitrate is complicated by the early production and subsequent slow decomposition of significant amounts of a nitro compound; nitric oxide is produced more rapidly than it is decomposed to nitrogen. Aldehyde pyrolyses, as judged by the production of carbon monoxide, are not rapid in the cool-burning ester, but the increase in the amount of unknown material (tarry residue) with distance from the flame front (*Figure 4*) indicates extensive polymerization of the aldehydes. No temperature rise occurs beyond the flame front in this ester. The propyl nitrates, burning with similar flame temperature, produce larger amounts of more stable nitro compounds[3] which slow down the rate of heat release and reduce the burning rate. In the 2-ethoxyethyl nitrate and the propyl nitrates, the temperature acquired in the flame front at atmospheric pressure is insufficient for rapid aldehyde pyrolysis and the associated nitric oxide-reducing actions. The overall chemical changes brought about by those and other reactions occurring in the wake of the flame front may be deduced from *Figures 3* to *5*.

A comparison of the initial products from a number of nitric ester flames

Since extension of this analytical study of the effect of chemical structure on degradation mechanisms in nitric ester flames is not contemplated at the present time, it was considered useful to summarize and compare briefly the results for the eight esters examined. The primary reaction products (i.e. the products at the point in the flame at which virtually all the original nitric ester has disappeared) from these esters are listed in *Table 1*.

Some of the values for the less volatile components should be regarded as semiquantitative because the complexity of the mixtures in which they were encountered would have made a better estimate unprofitably time-consuming. It was hoped that at least a semiquantitative answer for *all* the significant stable reaction products of every ester could be obtained, and it is considered that this has been achieved in all cases except the three more difficult esters reported in the present paper. The aldehyde mixtures produced in these alkoxy nitrates gave polymeric materials not readily analysed and sometimes representing a large proportion of the products.

It is considered that the divers products from all these mononitrates, in contrast to the two dinitrates studied, can be more reasonably and more completely described by a degradation mechanism which does not require extensive unimolecular breakdown of the nitric ester into alkoxy radical and nitrogen dioxide, but which depends upon hydrogen abstraction from the esters by radicals and reactive species, particularly NO_2 and HONO. Such a mechanism presents no difficulty in describing the appearance of the major products from all the mononitrates examined. It is more difficult to understand why nitrogen dioxide and radical attack on butane-2,3-diol dinitrate[1] is not as rapid as in the mononitrates.

In the mononitrate flames at atmospheric pressure, no evidence has been found for the production of alkoxy radicals, insofar as the appropriate alcohol has not been observed. It is probable that such alkoxy radicals as are produced in the initiating steps are broken down to alkyl radical and aldehyde at the high temperature involved[9]. The low pressure ethyl nitrate flame (temperature about 560°C) has, however, recently been shown[7] to yield up to

Table 1. *Primary products of some nitric ester flames*

Nitric ester	$CH_3CH_2ONO_2$	$HOCH_2CH_2$-ONO_2	$CH_3OCH_2CH_2$-ONO_2	$CH_3CH_2OCH_2$-CH_2ONO_2	$(CH_3)_2CHONO_2$	$CH_3CH_2CH_2$-ONO_2	$CH_3CH(ONO_2)$-$CH(ONO_2)CH_3$	$CH_2(ONO_2)$-$CH_2CH_2CH_2$-(ONO_2)
Product	*Moles of product per 100 moles of nitric ester*							
HCHO	52	48	34	43	24	88	0	**132***
HOCHO	0	18·6	2·4	4·5	0	0	—	**~4***
CH_3OCHO	—	0	29	0	—	—	—	—
C_2H_5OCHO	—	0	0	30	—	—	—	—
CH_3CHO	10·5	0	0	33	53	28	**176***	**1·7**
$(CH_3)_2CO$	0	0	0	0	14·0	0	0	**0**
H_2	21	29	(8)	10·0	2·1	12·4	12·8	**20**
CH_4	22	0·8	6·4	2·6	17·4	11·5	14·7	**3·7**
C_2H_6	0	0	0	<0·5	0	0	0	**0**
CH_3OCH_3	0	0	2·5	0	—	—	—	—
$C_2H_5OCH_3$	—	—	—	0	—	—	—	—
CO	62	91	37	16·5	22	34	82	**139**
NO_2	0	0	0	0	0	0	**46***	**40***
NO	78	66	68	51	42	53	100	**104**
N_2O	1·4	7·0	3·2	3·8	2·0	2·0	1·2	**3·0**
N_2	8·9	15·4	6·1	4·3	<9·5	<21	19	**21**
HCN	0	0·2	0·3	0	0	0	0	**4·0**
CH_3NO_2	0·6	0	0	0	35	—	0	**0**
CH_3ONO	0·8	2·4	0·4	<2	12·8	4·9	6·8	**0**
$C_2H_5NO_2$	0	0	0	0	0	39	0	**0**
C_2H_5ONO	0	0	0	<1·6	0	3·6	0	**0**
$CH_3OCH_2NO_2$(?)	—	—	(~6)	—	—	—	—	—
$C_2H_5OCH_2NO_2$(?)	—	—	0	(~19)	—	—	—	—
H_2O	61	114	41	51	7·1	71	88	**125**
CO_2	6·7	11·5	4·8	4·6	7·2	3·8	26	**15·7**
CH_3OH	3·4	0	8·0	12·9	24	0	0	**0**
C_2H_4	1·4	0·6	5·2	1·5	0	19	0·06	**47**
Unknown	—	12(*mol. wt* 60)	44(*mol.wt* 74)	27(*mol.wt* 88)	—	—	—	—
T_f†, °K	1060	1180	760	~720	670	~570	990	**1020**
T_m‡, °K	1175	1180	>900	~720	(>720)	(>750)	990	**1060**
Burning rate§, *cm/s*	0·007	0·0067	0·013	~0·008	*Unstable*	*Unstable*	0·005	**0·0035**

*Roughly corrected for nitrogen dioxide reaction in the traps.
†Temperature just behind the flame front.
‡Maximum temperature reached at atmospheric pressure under conditions employed.
§At atmospheric pressure: 24 mm diameter glass tubes.

15 mole per cent ethanol. Alkyl radicals and hydrogen atoms, produced either from the alkoxy radical from the original ester or by radical attack of early reaction products such as aldehydes, are also expected to abstract a hydrogen atom from the nitric ester, but, according to the reaction scheme suggested here, none of these are regenerated when the hydrogen-deficient nitric ester radical decomposes, the only reactive species produced being NO_2.

It is not considered that reactions of the type

$$\begin{tikzcd} R\cdot + NO_2 \arrow[r] \arrow[dr] & RO\cdot + NO \\ & RNO_2 \end{tikzcd}$$

take place to any major extent for the following reasons. ROH, expected to be produced by hydrogen abstraction by RO·, is rarely a significant product. The concentrations of R· and NO_2 are very small, and although the activation energy for reaction may be sufficiently low to make this a possible competitor with $R\cdot + RONO_2 \rightarrow RH$, etc., and $NO_2 + R'ONO_2 \rightarrow HONO$, etc., for which the activation energy may be 7 to 10 kcal and 15 to 20 kcal respectively[8], the products of other equally probable reactions (e.g. $2R\cdot \rightarrow$ products, $R\cdot + NO \rightarrow$ products) are not generally observed. Where the NO_2 concentration is known to be large, and CH_3CHO is pyrolysing to CH_4 and CO (the butane-2,3-diol dinitrate system), no CH_3NO_2 or CH_3OH (from $CH_3O\cdot$ reactions) is observed. In fact, it has not been possible to detect any significant amounts of nitro compound, nitrites or hydrogen cyanide in flames of nitrogen dioxide and numerous fuels which might be expected to produce methyl radicals in a similar temperature range[3]. There is much evidence for the occurrence of these reactions at lower temperatures[4]. Significant quantities of nitro compounds are produced only in the two cool-burning nitric esters. It is of interest to take nitro compound formation as an example, and compare the behaviour of 2-methoxyethyl nitrate and *iso*propyl nitrate. If it were considered that unimolecular breakdown of the nitric esters was a major reaction in flames, and that the alkoxy radicals degraded to aldehyde and simple alkyl radical (see P. GRAY and A. WILLIAMS[9] and A. F. TROTMAN-DICKENSON[8], p 306), the products of these two esters might be expected to be similar, apart from the aldehyde produced:

$$CH_3OCH_2CH_2ONO_2 \rightarrow CH_3\cdot + 2H_2CO + NO_2 \quad \ldots\ldots [26]$$

$$(CH_3)_2CHONO_2 \rightarrow CH_3\cdot + CH_3CHO + NO_2 \quad \ldots\ldots [27]$$

No nitromethane is found in the products of the 2-methoxyethyl nitrate flame, and only minor quantities of other nitro compounds and nitrites, whereas the yields in *iso*propyl nitrate are very high.

The authors are grateful to Mr J. V. Griffiths for preparing the 2-hydroxyethyl nitrate and the 2-ethoxyethyl nitrate.

References

[1] POWLING, J. and SMITH, W. A. W. *Combustion & Flame*, 1958, **2**, 157

[2] NEEDHAM, D. P. and POWLING, J. *Proc. Roy. Soc. A*, 1955, **232**, 337

[3] POWLING, J. and SMITH, W. A. W. *Combustion & Flame*, 1957, **1**, 308

[4] GRAY, P. *Trans. Faraday Soc.* 1955, **51**, 1367

[5] DRAKE, N. L., DURALL, H. M., JACOBS, T. L., THOMPSON, H. T. and SONNICHSEN, H. M. *J. Amer. chem. Soc.* 1938, **60**, 73

[6] ARDEN, A. E. and POWLING, J. *Combustion & Flame*, 1958, **2**, 55

[7] HICKS, J. A. E.R.D.E., Waltham Abbey, Essex (to be published)

[8] TROTMAN-DICKENSON, A. F. *Gas Kinetics*. Butterworths: London, 1955

[9] GRAY, P. and WILLIAMS, A. *Spec. Publ. chem. Soc., Lond., No. 9*, 1958, 97

Mo
in
up
hav
tha
wh
nev
me
obj
app
mol
or
don
Ro
rep
of
the
bro
hal
are
of
car
sin
bus

Chlorine Inhibition of Carbon Monoxide Flames

H. B. Palmer and D. J. Seery

Department of Fuel Technology, College of Mineral Industries, Pennsylvania State University

(Received April 1959)

Chlorine and bromine reduce the burning velocities of hydrogen-containing carbon monoxide flames supported by air, oxygen and nitrous oxide, with the qualification that if the hydrogen content is low, the effect of chlorine upon nitrous oxide-supported flames can become an acceleration caused by chlorine catalysis of nitrious oxide decomposition. Measurements of the reduction of S_u by chlorine over a wide range of carbon monoxide–air compositions show that the relative change in $(S_u)^2$ with an increment of chlorine is, at most, only weakly dependent upon the carbon monoxide–air ratio or upon the hydrogen content. The effect of carbon tetrachloride reported by Drozdov and Zeldovich is found to be identical to the equivalent amount of chlorine. A lower limit to the chain length in the absence of inhibitor is established to be 55, with the probable actual chain length appearing to be more like 1000. 'The radical-free' contribution to the burning velocity appears to be 1 cm/sec or less, if it exists at all. Chlorine inhibition can be expressed by a simple equation having the form typical of chain inhibition. An approximate analysis of a hypothesized mechanism for hydrogen-catalysed carbon monoxide combustion in the presence and absence of inhibitor leads to predicted inhibition consistent with the empirical result for small chlorine additions. Hydrogen chloride is apparently the principal inhibitor in the flame, impeding propagation by reacting with hydroxyl radicals. Some information concerning the rate constant of the principal inhibition reaction can be gleaned from the analysis.

Introduction

Most investigations of flame inhibition reported in the literature, which have been summarized up to 1956 by R. Friedman and J. B. Levy[1], have made use of organic halides. One supposes that this is dictated by practical considerations when thinking in terms of fire extinguishing; nevertheless, if one wishes to discover the mechanism of flame inhibition, an avowed objective of a number of published studies, it appears that one should use the simplest possible molecules as inhibitors, viz. the pure halogens or the hydrogen halides. Indeed this has been done in some work discussed in ref. 1. W. A. Rosser, H. Wise and J. Miller[2] have recently reported detailed measurements of the inhibition of methane–air flames, in which were included the effects of chlorine, bromine and hydrobromic acid as well as a number of organic halides. With the thought that simple molecules are the ones to examine, we have studied some of the effects of chlorine and bromine upon carbon monoxide flames. The hope was that since the kinetics of carbon monoxide combustion are somewhat better understood than those of hydrocarbons, firmer conclusions regarding inhibitor action might be reached. Particular attention has been given to the effect of chlorine upon the burning velocities of hydrogen-containing carbon monoxide–air flames. So far as we can determine, no quantitative measurements of inhibition of carbon monoxide flames by chlorine have previously been reported in the literature. We also report here some qualitative observations which seem to be of interest.

The materials used were: 'C.P.' grade carbon monoxide* (two tanks; one with less than 150 p.p.m. hydrogen, very dry; the other with 45 p.p.m. hydrogen, very dry); 'Commercial' grade carbon monoxide (98% CO, 2·04% H_2, very dry); dry air (11 p.p.m. water max.); 'Extra dry' grade oxygen (99·6 per cent min.); 98·0 per cent pure nitrous oxide; 99·85 per cent pure chlorine; and 99·9 per cent bromine†. Most of the flame observations were made using a bunsen tube of 1·28 cm i.d., approximately 1 m long. A 3 cm i.d. jacket was available for experiments in control of the secondary atmosphere. Standard mixing and metering devices were employed. The materials were used without further purification except for removal of iron pentacarbonyl from the carbon monoxide by means of a glass chip-packed column held at 320°C.

---

*All cylinder gases were obtained from the Matheson Co.

†The J. T. Baker Co.

Results and Discussion

Some of the qualitative observations may be mentioned before giving the numerical data on burning velocities. They may be summarized as follows:

Commercial CO ($2{\cdot}04\%$ H_2)

(*1*) Flames with air were inhibited by both chlorine and bromine to a roughly similar degree. There was a hint that quite rich flames were slightly accelerated by very small chlorine additions. Effects of small halogen additions on the flame spectra were to weaken slightly both the OH radiation and the continuum. With larger amounts—several per cent—a 'tail' appeared on the outer cone that had a colour (no spectra were taken here) appropriate to halogen recombination continua, viz. yellow-red, and also appropriate to halogen band spectra[3].

(*2*) Addition of oxygen accelerated the flames, as expected.

(*3*) Nitrous oxide addition had at first very little effect; with larger additions, acceleration was produced. Characteristic NO + O radiation was observed in the outer cone. Flames supported entirely by nitrous oxide had a higher burning velocity than air-supported flames. They were inhibited by chlorine, but not strongly.

C.P. CO (45–150 p.p.m. H_2)

(*1*) Flames with air were inhibited by both chlorine and bromine. Air-supported flames burned stably only in a moist secondary atmosphere (we discuss the atmospheric effects elsewhere[4]). Halogen addition appeared to weaken somewhat both the OH radiation, which was not strong to begin with, and also the continuum. With bromine addition, three weak emission bands of BrO were identifiable in the outer cone. The characteristic halogen radiation appeared in the outer cone with larger halogen additions.

(*2*) Oxygen addition accelerated the burning. Flames supported by oxygen alone could be burned successfully in a dry atmosphere.

(*3*) Nitrous oxide addition weakly accelerated the flames at first; with large additions, inhibition finally resulted. Flames with nitrous oxide alone burned faster than flames with air and could be burned in a dry atmosphere. Radiation from NO + O was strong in the outer cone. Addition of chlorine to these flames had the following curious effect: small amounts inhibited the flames very slightly; at a critical amount of chlorine, the outer cone faded from sight, including the NO + O radiation, and there was a virtually discontinuous increase in burning velocity when this occurred. Further chlorine addition accelerated the combustion and turned the flame to a brilliant white. With very large amounts of chlorine, inhibition finally appeared. We did not succeed in adding enough chlorine to bring the flame to blowoff, although a great deal was added (several per cent).

These qualitative observations are largely what one would expect. The catalysis of carbon monoxide flames by hydrogen or water vapour is a well-known fact. Halogens can react in various ways with hydrogen-containing species and remove them, at least momentarily, from a reaction sequence in which they may have been involved. Particularly if the reaction sequence is a chain, as is accepted here, such momentary removal breaks the chain and reduces the reaction rate. The halogens are largely dissociated or converted to HX molecules by the time they reach the radiation zone. It is hence not to be expected that the diatomic halogen molecules act as inhibitors, but rather the atoms or else HX molecules, or both. In the formation of HX molecules, H atoms are generated so that it is conceivable that with sufficient hydrogen and a small amount of inhibitor, there could be slight acceleration, as observed in rich flames of commercial carbon monoxide. With larger amounts of halogen, the chain-breaking comes rapidly to dominance and inhibition results. Weakening of both OH radiation and the CO+O continuum is to be expected if H or OH or both are removed by halogens because of the coupled effects of the reaction pair

$$H+O_2 \longrightarrow OH+O$$

and

$$OH+CO \longrightarrow CO_2+H$$

Halogen recombination radiation is to be expected in the outer cone because in the equilibrium gases a sizeable fraction of the halogen is present as atoms.

Oxygen accelerates the flame because of the $H+O_2$ chain-branching reaction. Nitrous oxide addition provides a new source of O atoms through the decomposition reaction

$$N_2O \longrightarrow N_2+O$$

it can participate in the chain via

$$H+N_2O \longrightarrow N_2+OH$$

and it can react directly with carbon monoxide in the exothermic reaction

$$CO+N_2O \longrightarrow CO_2+N_2$$

However, this last is not a chain reaction, and the reaction with H is not a chain-branching reaction (in contrast to $H+O_2$); furthermore, nitrous oxide decomposition has the effect of diluting the flame somewhat with nitrogen. Hence the effect of nitrous oxide addition is not pronounced. The inhibition observed with large nitrous oxide additions to C.P. carbon monoxide–air flames must have represented an approach to the lean limit.

Nitric oxide is produced from nitrous oxide in the secondary reaction

$$N_2O+O \longrightarrow 2NO$$

giving rise to the NO+O continuum. Oxygen will also be produced[5] via

$$N_2O+O \longrightarrow N_2+O_2$$

Hydrogen-containing, nitrous oxide-supported carbon monoxide flames may be expected to be inhibited by halogens. However, the situation here is complicated by the halogen-catalysed decomposition of nitrous oxide, which is in competition with H-species removal as a sink for halogen atoms. When there is much hydrogen available, as in commercial carbon monoxide, there is continuous but rather weak inhibition by halogens because of the plentiful supply of hydrogen for the reaction

$$H+N_2O \longrightarrow N_2+OH$$

a very exothermic reaction and surely a very fast one. With C.P. carbon monoxide, however, the initial inhibition is soon overwhelmed by the catalysis of the nitrous oxide decomposition. There is some controversy over the kinetics of this halogen-catalysed reaction[6,7], but fortunately there is agreement on the initial step, which is all that need concern us. It is

$$Cl+N_2O \longrightarrow N_2+ClO$$

In the presence of carbon monoxide, the ClO may be expected to react in the very exothermic reaction

$$ClO+CO \longrightarrow CO_2+Cl$$

regenerating the chlorine so that an excellent chain results. There appears to be no multiplicity problem in the reaction of ClO with carbon monoxide and it should be very fast. The ultimate inhibition of this system by sufficient halogen may be attributed to a combination of the effects of dilution and of heat extraction because of the necessity of having a considerable concentration of halogen atoms in the burnt gases. It may be expected that the arrival at dominance of the chlorine-catalysed nitrous oxide decomposition will be rather abrupt, so that a nearly discontinuous change in flame characteristics occurs at this point. The nitrous oxide also no longer acts as a source of NO+O, so that the NO+O radiation disappears. The brilliant white colour, which certainly merits more detailed examination, may well be the halogen recombination spectrum, spread out over the entire visible region.

Effect of chlorine on burning velocity

The results of our measurements, made with the visible cone frustum method[8], are given in *Tables 1* and *2* and some of the data have been plotted in *Figure 1*. The precision of the data for C.P. carbon monoxide–air is not as good as that for commercial carbon monoxide, partly because of the thicker reaction zones and lower

Table 1. Burning velocities of commercial carbon monoxide–air mixtures with added chlorine

Mole % CO	*Mole %* Cl_2	S_u *cm/sec*	*Mole %* CO	*Mole %* Cl_2	S_u *cm/sec*	*Mole %* CO	*Mole %* Cl_2	S_u *cm/sec*
25·5	0	24·7	37·6	0	36·1	46·2	0	42·9
	0·08	22·8		0·07	32·9		0·06	40·4
	0·14	23·8		0·15	33·6		0·13	37·8
	0·22	22·7		0·26	30·9		0·20	33·7
	0·34	22·4		0·51	28·3		0·41	34·2
	0·49	19·9		0·79	26·6		0·75	29·8
	0·63	19·1		1·28	26·6		1·21	26·5
	0·81	18·2		2·05	24·5		1·81	23·1
29·0	0	32·2	41·2	0	36·1	54·8	0	37·8
	0·09	32·0		0·08	33·4		0·05	40·1
	0·35	28·9		0·29	30·0		0·10	40·2
	1·00	22·4		0·60	29·0		0·19	34·0
	1·48	18·2		1·12	24·4		0·27	32·2
	2·04	15·5		2·08	20·0		0·58	27·0
							0·86	25·3
							1·26	22·1
37·4	0	38·0						
	0·10	32·5						
	0·22	30·9						
	0·63	28·6						
	1·13	27·3						
	1·97	19·2						

burning velocities, and partly because of the pronounced effects of the secondary atmospheric moisture[4]. For this reason, further examination of the data will be confined principally to the commercial carbon monoxide results.

It can first be remarked that the effect of chlorine addition is in general a continuous reduction in burning velocity, with the strongest relative effect occurring at small additions, a characteristic of most inhibitions. The inhibition is comparable to that observed by Rosser, Wise and Miller[2] in methane–air. One per cent chlorine reduces the burning velocity of carbon monoxide–air by 30 to 40 per cent. The rate of change of S_u of methane–air with chlorine addition reported by Rosser *et al.* predicts a lowering of about 20 per cent by 1 per cent chlorine, slightly dependent upon the composition of the combustible mixture. These authors found bromine a much more effective inhibitor than chlorine in methane–air, whereas our (qualitative) observations indicate that the two are comparable in their effects on carbon monoxide–air.

In an effort to reach more general conclusions about the inhibition, we have plotted the data in various ways. One of the more successful of these is shown in *Figure 2*, which is a plot of the square of the relative burning velocity versus the square root of the mole per cent chlorine in the unburnt gas. In this figure are included the results of N. P. Drozdov and Y. B. Zeldovich[9] for addition of carbon tetrachloride to carbon monoxide–oxygen (stoichiometric) containing 1·8 per cent water vapour. The agreement with our data is strikingly good and seems to imply that addition of a CCl_4 molecule is essentially equivalent to adding two Cl_2s. This equivalence has been assumed in the plotting. The line indicating the average behaviour was drawn by eye. The square of the relative burning velocity was chosen as the ordinate because this should correspond to the relative rate of reaction in the flame[10], assuming only slight effects upon transport phenomena. For additions of chlorine up to 1 mole per cent, equilibrium calculations show that the change in flame temperature is

*Table 2. Burning velocities of C.P. carbon monoxide–air mixtures with added chlorine**

Mole % CO	*Mole %* Cl_2	S_u *cm/sec*	*Mole %* CO	*Mole %* Cl_2	S_u *cm/sec*	*Mole %* CO	*Mole %* Cl_2	S_u *cm/sec*
31·0	0	14·9	34·5	0	12·8	45·7	0	15·0
	0·08	12·6		0·08	13·7		0·10	13·9
	0·21	12·8		0·14	11·8		0·24	13·1
	0·26	11·9		0·21	11·4		0·49	11·7
				0·30	11·7		0·83	10·1
				0·42	11·6		1·18	8·4
				0·51	11·7		1·60	5·8
				0·58	10·7			
32·0	0	17·0	38·5	0	15·4	48·7	0	11·4
	0·08	16·1		0·08	13·5		0·06	11·6
	0·19	15·7		0·20	13·0		0·12	10·9
	0·40	15·4		0·42	11·3		0·20	10·4
	0·89	9·9		0·66	10·7		0·33	11·7
	1·09	9·5		1·35	9·0		0·54	10·5
				1·70	6·5		0·77	9·1
							1·24	6·1
32·4	0	19·4	41·9	0	13·6			
	0·09	17·2		0·07	12·4			
	0·16	18·3		0·11	11·7			
	0·31	17·3		0·13	12·2			
	0·56	16·4		0·20	11·7			
				0·28	9·8			
				0·58	9·3			
				0·89	7·5			

*These velocities are functions of the atmospheric humidity (see text).

slight, the principal effect showing up in rich (50–60 per cent) mixtures, where phosgene formation raises the final flame temperature by as much as 30°K. Even this change should be small in its effect on reaction rates relative to the effect of halogen in stopping chains. The point is that to a reasonable approximation, the effect of halogen addition can be regarded as an isothermal effect on the reaction kinetics.

In this light, the results in *Figures 1* and *2* provide some information about the chain length in the absence of inhibitor. Making use of the coincidence of the carbon tetrachloride results and our own, it is seen that 9 per cent chlorine will reduce $(S_u/S_u^0)^2$ to about 1×10^{-3} of its initial value. On the face of it this would imply an uninhibited chain length of at least 1 000; but a system containing 9 per cent chlorine is by no means isothermal with the uninhibited system, and absolute concentrations of reactants are also appreciably decreased by such a quantity of additive, so that the result should be accepted with caution. An approximate lower limit to the chain length may be found by making use of the C.P. carbon monoxide results. An S_u of 5·8 cm/sec was reached with chlorine addition to the 45·7 per cent carbon monoxide flame, in which the effects on composition and temperature were not great. If this is compared to the value, 42·9 cm/sec, found for uninhibited 46·2 per cent commercial carbon monoxide, the ratio of reaction rates is $(42{\cdot}9/5{\cdot}8)^2 = 55$. The chains in the commercial carbon monoxide should hence have a length of more than 55, at least at 46 per cent carbon monoxide. The previous result leads us to believe that the uninhibited chain length is much greater than 55, but this is at any rate a rather firm value as a lower bound.

There is no indication in *Figure 2* that extrapolation will yield $S_u = 0$ at any chlorine concentration, no matter how large. One might say

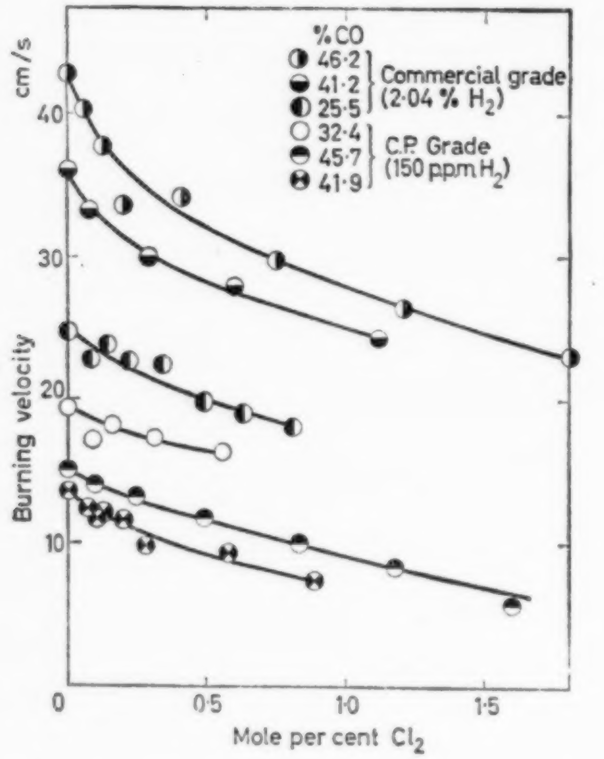

Figure 1. Effect of chlorine addition on carbon monoxide–air burning velocities at several concentrations of carbon monoxide. The C.P. carbon monoxide–values are not true burning velocities for C.P. carbon monoxide–dry air (see ref. 4)

that there must then be a ‘radical-free’ contribution[11] to the burning mechanism; but if so, it is apparently 1 cm/sec or less, rather than the 17 cm/sec value chosen by C. TANFORD and R. N. PEASE. There is of course the possibility that chlorine might inhibit both the radical-free mechanism and the radical–chain mechanism, but it is difficult to imagine how such an inhibition could function. Or it might be supposed that there is a residual contribution at large chlorine contents from an ‘H-free’ mechanism that would not be affected by chlorine. If it exists, it appears again that the S_u produced by such a mechanism cannot exceed about 1 cm/sec.

Although the plot of $(S_u/S_u^0)^2$ against $[Cl_2]^{\frac{1}{2}}$ is reasonably satisfactory for examining trends, it does not provide a satisfying mathematical expression for the behaviour, i.e. satisfying from the chemical standpoint. If chlorine is a chemical inhibitor, one might hope to find a relation of the type

$$(S_u/S_u^0)^2=(1+\alpha[Cl_2]^x)^{-1}$$

which has a form typical of chain inhibition[12]. In *Figure 3* are shown the experimental $(S_u/S_u^0)^2$ values plotted against mole per cent chlorine, where we have included Zeldovich's carbon tetrachloride points. Within the uncertainty of the data, a single curve expresses the behaviour up to 2 per cent chlorine addition. It is given by the above expression with $x=1$, $\alpha=1{\cdot}2$.

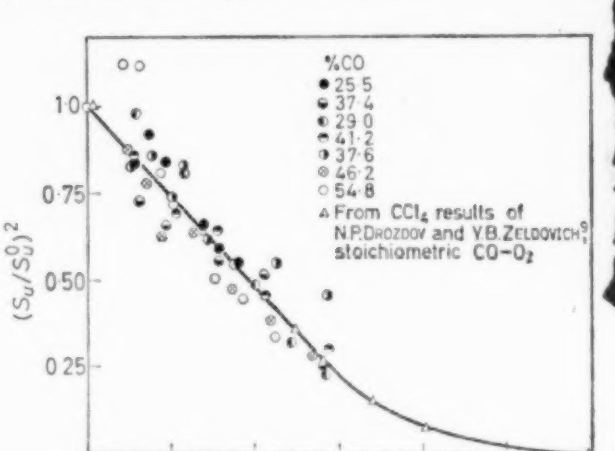

Figure 2. Dependence of square of relative burning velocity upon square root of unburnt gas chlorine content. The results of Drozdov and Zeldovich included in the plot are not from their raw data but were picked off their curve

$\alpha=1{\cdot}3$ is almost equally satisfactory, but $\alpha=1{\cdot}1$ and $\alpha=1{\cdot}4$ are less so. There may be a slight trend with composition over the range studied (25 to 55 per cent carbon monoxide); it is most evident in the two richest mixtures (46 and 55 per cent), where the points consistently lie somewhat below the line except for the two points representing acceleration at low chlorine addition in 55 per cent carbon monoxide–air.

The C.P. carbon monoxide results conform reasonably well to the plot in *Figure 3*, but with much larger scatter. This conformity can actually be seen quite well from *Figure 1*, so the C.P. results are not shown in *Figure 3*. Although moisture entered the C.P. flames from the secondary atmosphere during the inhibition measurements, these flames still contained much s hydrogen, whether as H_2, H_2O, H or OH, an did the commercial carbon monoxide mes. Hence the similarity in behaviour of P. carbon monoxide is interesting in its cation that the ***relative*** inhibition effect of a en total chlorine concentration is independent of hydrogen content. It has previously been noted that dependence upon the carbon monoxide and oxygen concentrations in the unburnt gas is at most quite weak.

If an interpretation of the experimental results n terms of the flame kinetics is to be attempted, he empirical expression for inhibition must be related to conditions within the reaction zone. As a first step it is noted that the half-life of Cl_2 with respect to dissociation into atoms at 000°K should be of the order of 100 microonds, by analogy to Br_2 dissociation[13]. The action of Cl with H_2 is very fast[5], so Cl_2 introduced into the unburnt gas can be expected to be converted almost completely to a mixture Cl and HCl before it reaches the flame reaction zone. Thus 1 mole of Cl_2 is replaced by 2 moles of (Cl + HCl) in the reaction zone. Converting the inhibition equation to units of concentration in moles/cm³ at the flame temperature

$$(S_u^0/S_u)^2 = 1 + 0{\cdot}6 \times 10^7 \{[Cl] + [HCl]\}$$

where 2 000°K has been taken as a typical temperature. This equation should have some meaning in terms of the kinetics in the flame.

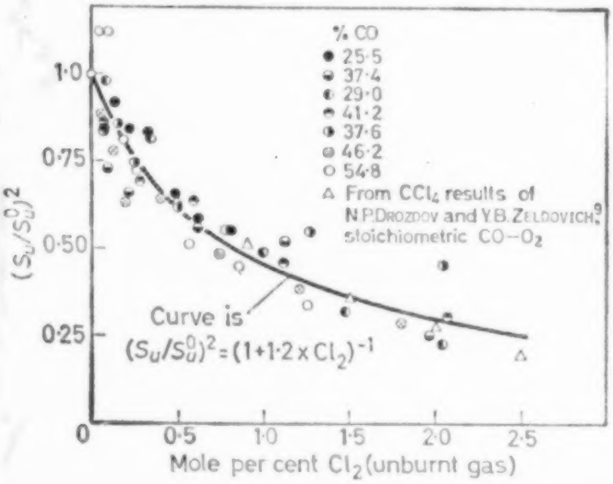

igure 3. Dependence of the square of the relative burning velocity upon the unburnt gas chlorine content

In the hydrogen-containing flame, we presume the most important reactions to be:

$$OH + CO \longrightarrow CO_2 + H, \text{ propagation} \quad \ldots [1]$$

$$H + O_2 \longrightarrow OH + O, \text{ branching} \quad \ldots [2]$$

$$O + H_2 \longrightarrow OH + H, \text{ branching} \quad \ldots [3]$$

$$H + OH + M \longrightarrow H_2O + M, \text{ ending} \quad \ldots [4]$$

Selection of reaction **4** as the only important ending reaction is based upon the recent work of E. M. Bulewicz and T. M. Sugden[14], who found the rate constant of this reaction to be some 100 times that of the H + H + M reaction at typical flame temperatures. This was in the presence of water as the third body, so it is possible that the rate constant ratio might differ in the carbon monoxide flame system; however, it seems likely that reaction 4 should still be strongly favoured over H atom recombination.

The rate of burning of carbon monoxide will be the rate of reaction 1; i.e.

$$R = k_1 [CO] [OH]$$

If the concentration of OH is assumed to be steady in the burning velocity-determining region of the flame, the rate of reaction 1, to which the square of the burning velocity is assumed to be proportional, is

$$R = k_1 [CO] \{k_2 [H][O_2] + k_3 [O][H_2]\} / \{k_1 [CO] + k_4 [H][M]\}$$

An order-of-magnitude calculation shows that $k_1 [CO] \gg k_4 [H][M]$. This is to be expected since, in the absence of inhibition, the ratio of the rates of reactions 1 and 4 will be the chain length. Reaction 1 is exothermic, with a low activation energy (Hirschfelder's rule[18] predicts $E_1 \fallingdotseq 5{\cdot}5$ kcal), and should have a rate constant $k_1 \fallingdotseq 10^{13}$ cm³/mole sec at 2 000°K. The total gas concentration is $[M] \fallingdotseq 6 \times 10^{-6}$ mole/cm³ at 1 atm and 2 000°K. For a typical starting concentration of carbon monoxide, its concentration in the reaction zone should be of the order of 10^{-6} to 10^{-7} mole/cm³. $k_4 \fallingdotseq 2 \times 10^{17}$ cm⁶/mole² sec at 2 000°K[14]; and [H] in the flame zone, which is of course dependent upon the overall hydrogen content, should be typically between 10^{-10} and 10^{-8} mole/cm^3 for commercial carbon monoxide, making allowance for the fact[15, 16] that its concentration should exceed considerably its equilibrium concentration. Then the typical range for $k_1[CO]$ is from 10^6 to 10^7, and that for $k_4[H][M]$ is from about 10^2 to 10^4. Thus the chain length in the absence of inhibition should be somewhere between 10^2 and 10^5. We previously concluded experimentally that it was certainly greater than 55 and probably greater than 1 000.

From the equation for the propagation rate expressed in terms of [OH] and [CO], it appears that the likely effect of an inhibitor will be to reduce the steady-state concentration of OH. This may occur by direct reaction with OH, or, as seen from the above equation for the steady-state propagation rate, by reaction with H, O, O_2 or H_2 as well. The most probable reactions seem to be the following:

$$Cl + OH \rightarrow HCl + O \quad \ldots . [5]$$

$$HCl + OH \rightarrow H_2O + Cl \quad \ldots . [6]$$

$$Cl_2 + OH \rightarrow HCl + ClO \quad \ldots . [7]$$

$$Cl + H + M \rightarrow HCl + M \quad \ldots . [8]$$

$$HCl + H \rightarrow H_2 + Cl \quad \ldots . [9]$$

$$H + Cl_2 \rightarrow HCl + Cl \quad \ldots . [10]$$

$$H_2 + Cl \rightarrow HCl + H \quad \ldots . [11]$$

$$Cl + O + M \rightarrow ClO + M \quad \ldots . [12]$$

$$HCl + O \rightarrow OH + Cl \quad \ldots . [13]$$

Such an array of reactions presents a discouraging prospect for any success in finding a theoretical expression that may conform to the experimental results. Largely in the hope of stimulating further work on the matter, the following attempt at a kinetic analysis is presented.

Let us make the arbitrary assumption that reaction 6 is the only inhibition reaction of importance; i.e. hydrogen chloride is the dominant inhibitor and its prime function is to remove hydroxyl from the system, forming water*. Actually, as one considers the reactions suggested, there seems to be some merit in the assumption. The reverse of reaction 6 is difficult, whereas the reverse of 5 is easy, and is indeed listed as reaction 13; and reactions 9 and 11 form a similar pair. Reaction 6 has the advantage over 7 and 10, which involve Cl_2, that there will be very little chlorine in the reaction zone; and, being a 2-body reaction, 6 may be favoured over 8 and 12, both of which are 3-body reactions, provided its collision efficiency is fairly high and its activation energy low. According to the Hirschfelder rule[18], $E_6 \doteqdot 5{\cdot}5$ kcal, so the low activation energy requirement seems to be fulfilled. (Note that $E_{-6} \doteqdot 20$ kcal by this rule.) The steric requirements for reaction 6 may, however, be rather stringent.

Of course it is not permissible to ignore the effect of a sizeable chlorine addition upon $[H_2]$, since hydrogen chloride formation must consume hydrogen. Therefore we shall restrict matters to the case of small chlorine addition, where it should be a good approximation to treat $[H_2]$ as unchanged by the addition, and assume all the chlorine to be converted to hydrochloric acid prior to entering the reaction zone. It is assumed, then, that the only major change in the steady-state concentration of hydroxyl is produced by the removal reaction 6. Including this reaction in the steady-state expression, we have

$$R' = k_1[CO]\{k_2[H][O_2] + k_3[O][H_2]\} / \{k_1[CO] + k_4[H][M] + k_6[HCl]\}$$

Comparing rates

$$\frac{R}{R'} = 1 + \frac{k_6[HCl]}{\{k_1[CO] + k_4[H][M]\}}$$

which has the same form as the experimental equation. Recalling that the second term in the denominator is much smaller than the first, the equation becomes

$$R/R' = 1 + \{k_6/k_1[CO]\}[HCl] = 1 + 0{\cdot}6 \times 10^7 [HCl]$$

It follows that

$$k_6/k_1[CO] = 0{\cdot}6 \times 10^7$$

---

*The implication that water vapour behaves as an inert gas is not intended. But it does seem certain that the reforming of OH from H_2O by reaction with Cl, O or H will be rather slow ($E_{act.} = 20$ kcal) relative to other reactions of importance, so that in effect reaction 6 removes OH from the system.

or, recalling that k_1[CO] was estimated to be between 10^6 and 10^7, one finds

$$k_6 = 6 \times 10^{12} \text{ to } 6 \times 10^{13} \text{ cm}^3\text{/mole sec at } 2000^\circ\text{K}$$

With the previous estimate for $E_6 = 5{\cdot}5$ kcal, the ollision factor is

$$A_6 = 2{\cdot}5 \times 10^{13} \text{ to } 2{\cdot}5 \times 10^{14} \text{ cm}^3\text{/mole sec}$$

This range is such as to indicate a collision efficiency of at least 0·1.

The result of this crude kinetic analysis seems together rather reasonable. It is tempting to onclude that hydrochloric acid is in fact the principal inhibitor in the flame and that its major effect is rapid reaction with hydroxyl. But we have avoided the serious problem (among others) of accounting for the fact that the empirical inhibition equation holds rather well over a much wider range of chlorine addition than is implied by the theoretical analysis.

The final comment may be made that the inhibition equation as derived requires, ostensibly, that k_6/k_1[CO] be a constant. This can be approximately so only if k_1 is a stronger function of temperature than k_6. As [CO] increases from stoichiometric to rich, the temperature falls, assuming the reaction zone temperature to parallel the equilibrium temperature. If it is assumed to *equal* the equilibrium temperature, and if it is assumed that the carbon monoxide concentration in the reaction zone is *proportional* to the unburnt carbon monoxide concentration times the appropriate temperature ratio, then a computation shows that the activation energy E_1 must be some 9 kcal greater than E_6, or about 14 kcal. N. N. SEMENOV[17] quotes a value of 10 ± 3 kcal for this reaction. An $E_1 = 14$ kcal necessitates a revision downward by a factor of about 10 of the previous estimates for k_1[CO], the uninhibited chain length, and k_6, all of which remain seemingly reasonable in magnitude.

This work was supported in part by a grant from the Experiment Station, College of Mineral Industries, The Pennsylvania State University.

References

[1] FRIEDMAN, R. and LEVY, J. B. *W.A.D.C. tech. Rep. No. 56-568*, Wright Air Development Center, Wright-Patterson Air Force Base, Ohio, 28 November 1956. Regrettably, this excellent review has not, to our knowledge, appeared in the open literature

[2] ROSSER, W. A., WISE, H. and MILLER, J. *Seventh Symposium (International) on Combustion*, p 175. Butterworths: London, 1959

[3] GAYDON, A. G. *The Spectroscopy of Flames*, Chapman & Hall: London, 1957

[4] PALMER, H. B. and SEERY, D. J. Paper submitted to *Combustion & Flame*

[5] For a discussion of nitrous oxide decomposition, see TROTMAN-DICKENSON, A. F. *Gas Kinetics*. Butterworths: London, 1955

[6] BENSON, S. W. and BUSS, J. H. *J. chem. Phys.* 1957, **27**, 1382

[7] KAUFFMAN, F., GERRI, N. J. and PASCALE, D. A. *J. chem. Phys.* 1956, **24**, 32

[8] DERY, R. J. Unpublished work; as discussed by HARRIS, M. E., GRUMER, J., VON ELBE, G. and LEWIS, B. *in the Third Symposium on Combustion, Flame and Explosion Phenomena*, p. 80. Williams and Wilkins: Baltimore, 1949

[9] DROZDOV, N. P. and ZELDOVICH, Y. B. *Zh. fiz. Khim., Mosk. (J. phys. chem., Moscow)*, 1943, **17**, 134

[10] FENN, J. B. and CALCOTE, H. F. in the *Fourth Symposium (International) on Combustion*, p 231. Williams and Wilkins: Baltimore, 1953

[11] TANFORD, C. and PEASE, R. N. *J. chem. Phys.* 1947, **15**, 861

[12] FROST, A. A. and PEARSON, R. G. *Kinetics and Mechanism*. Wiley: New York, 1953

[13] PALMER, H. B. and HORNIG, D. F. *J. chem. Phys.* 1957, **26**, 98

[14] BULEWICZ, E. M. and SUGDEN, T. M. *Trans. Faraday Soc.* 1958, **54**, 1855

[15] FENIMORE, C. P. and JONES, G. W. *J. phys. Chem.* 1958, **62**, 178

[16] KASKAN, W. E. *Combustion & Flame*, 1958, **2**, 229

[17] SEMENOV, N. N. *Usp. fiz. Nauk S.S.S.R. (Adv. phys. Sci., Moscow)*, 1940, **24**, No. 4, 433; English translation: *Tech. Memor. Nat. Adv. Comm. Aero., Wash., No. 1026*, September 1942

[18] HIRSCHFELDER, J. O. *J. chem. Phys.* 1941, **9**, 645

Mechanisms of Extinction of Liquid Fires with Water Sprays

D. J. Rasbash, Z. W. Rogowski and G. W. V. Stark

Department of Scientific and Industrial Research and Fire Offices' Committee Joint Fire Research Organization, Fire Research Station, Boreham Wood, Herts.

(Received May 1959)

An investigation has been carried out on the extinction by means of water sprays of fires of liquids burning in a vessel 30 cm in diameter. The effect on the ease of extinction of (1) *the nature of the liquid,* (2) *the time between the ignition of the fire and the application of the spray,* (3) *the properties of the sprays and* (4) *the direction of application of the spray have been studied. It was found that liquids like kerosine, which can be extinguished by being cooled to the fire point, or by being diluted, like alcohol, could be extinguished reliably by certain water sprays, although in some cases the extinction took a long time. For liquids like petrol and benzole extinction depended primarily on whether or not stable flames close to the burning liquid surface were easily established following the application of spray. These stable flames were very difficult to extinguish and were usually established readily when the preburn time was very short (less than 6 to 10 seconds) and also when the spray was applied in a horizontal direction across the fire. Over the range of conditions under which extinction took place, the extinction time decreased as the rate of flow and the entrained air current in the spray increased and generally also as the drop size of the spray decreased; the effect of drop size for the petrol, benzole and alcohol fires was very marked. There was evidence that for petrol and benzole fires heat transfer between the flame and the water drops, resulting in either cooling of the flames or the formation of steam, played a part in the extinction.*

Introduction

Water spray is often used to extinguish or control fires involving flammable liquids but little is known about how the properties of sprays influence their action on these fires or on the mechanisms of extinction. In this paper an account is given of the effect of water sprays on the extinction of fires in different liquids burning in a combustion vessel 30 cm in diameter. The objects of the investigation were (*a*) to determine the way the properties of both the fire and the sprays influenced the ease of extinction and (*b*) to obtain information on the extinction processes.

Experimental

Apparatus

Most of the tests were carried out with sprays produced by two fixed batteries of impinging jets which were mounted 175 cm above the combustion vessel, as shown in *Figure 1*. The drop size, the rate of flow and the entrained air

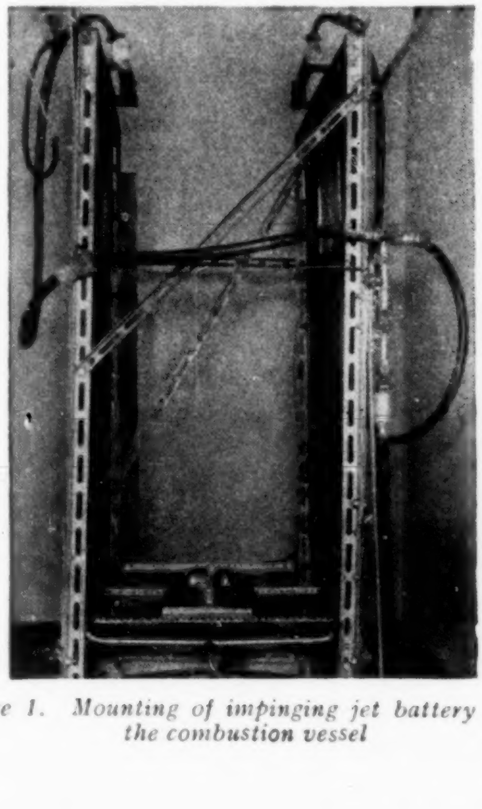

Figure 1. Mounting of impinging jet battery above the combustion vessel

current of the spray at the combustion vessel were varied by varying the diameter of the jets used, the number and the position of the jets, and the pressure at the batteries; a description of these batteries and the sprays they produced has been given elsewhere[1,2]. A few tests were also carried out with sprays from single nozzles. In all tests the top surface of the burning liquid was maintained at 2·0 cm from the top edge of the vessel. Six different liquids were used in the tests: alcohol, petrol, benzole, kerosine, gas oil and transformer oil. The latter three liquids were primed respectively with 10, 10 and 40 cm^3 of hexane prior to ignition. All the liquids except alcohol floated as a layer 6 cm deep on water.

Measurements of fire and spray properties

Measurements were made[3] of the rate of burning, the temperature distribution below the surface, the mean flame dimensions, the upward flame velocity and the flame temperature of the burning liquids. (*Figure 2* shows the fires in alcohol, petrol and benzole after burning for 2 minutes.) With all sprays, the mean flow rate of water spray to the combustion vessel, the drop size of the spray, the entrained air current and the spatial pattern of the spray at the combustion vessel were measured.

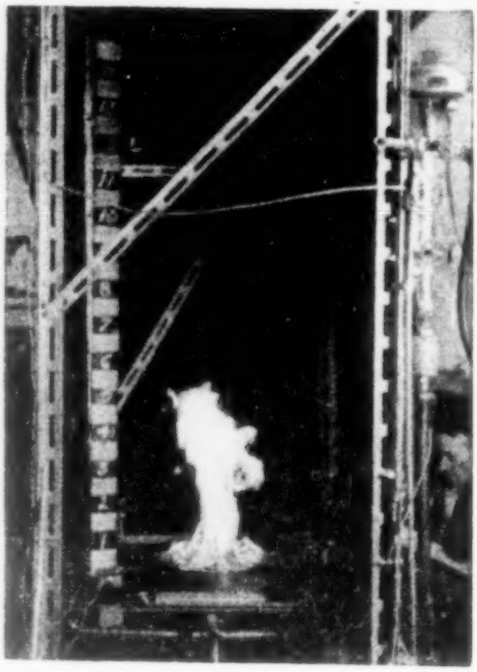

Figure 2(a). Appearance of fires after 2 min burning (alcohol)

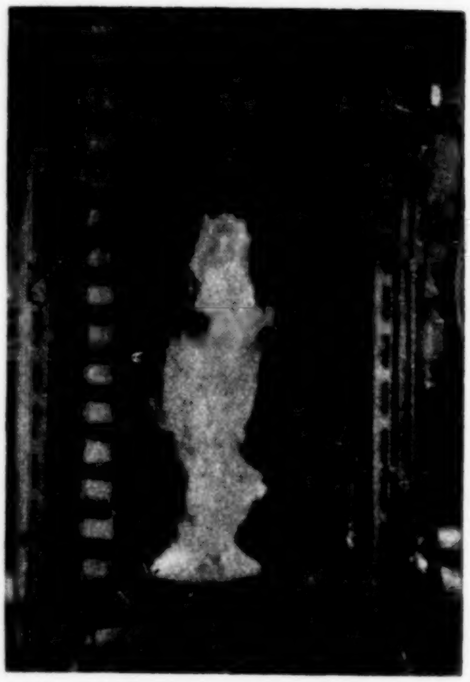

Figure 2(b). Appearance of fires after 2 min burning (petrol)

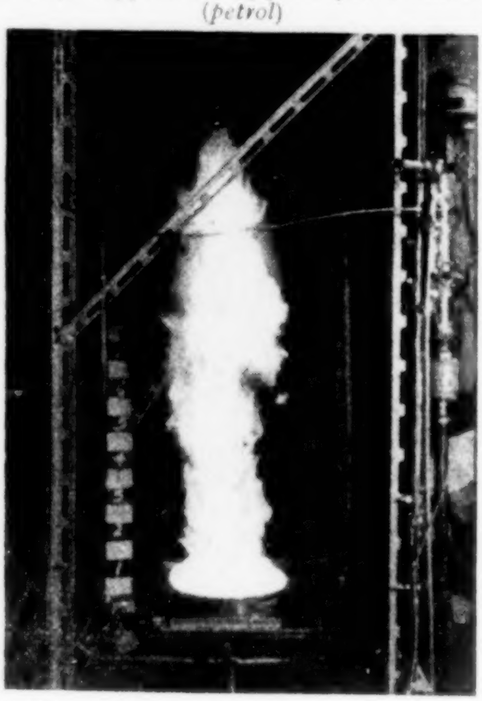

Figure 2(c). Appearance of fires after 2 min burning (benzole)

Most of the tests were carried out with one or other of five sprays, whose properties are given in *Table 1*.

Extinction Tests

The effects of four factors were investigated: (*1*) the nature of the burning liquid, (*2*) the time between the ignition of the fire and the application of spray (preburn time), (*3*) the spray properties and (*4*) the direction of application of the spray.

Four groups of tests were carried out, in each of which one of the above factors was the main item varied. The spray was allowed to act on the fire until extinction was obtained or until the test was stopped by extinguishing the fire by snuffing with a flat plate. The extinction time was recorded and observations were made on the effect of the sprays on the flames. The temperature of the liquid at a point 1 or 3 mm below the liquid surface was recorded.

Results

Effect of nature of burning liquids

Tests with all six burning liquids at preburn times of 2, 5 and 8 minutes were carried out with sprays A, B and C; these sprays differed mainly in drop size. With all liquids, except alcohol, there was an upsurge of flame less than a second after applying the sprays, mainly due to the splashing and sputtering caused by the spray. *Figure 3* shows the upsurge on applying spray C to the kerosine fire. During the application of the sprays the flames behaved in one of two characteristic ways (*a*) or (*b*):

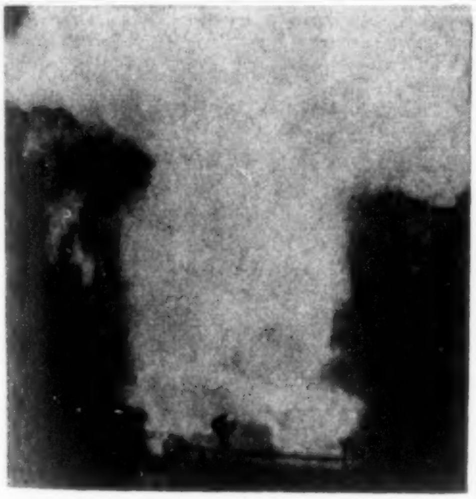

Figure 3. Upsurge of flame on applying spray C to a kerosine fire

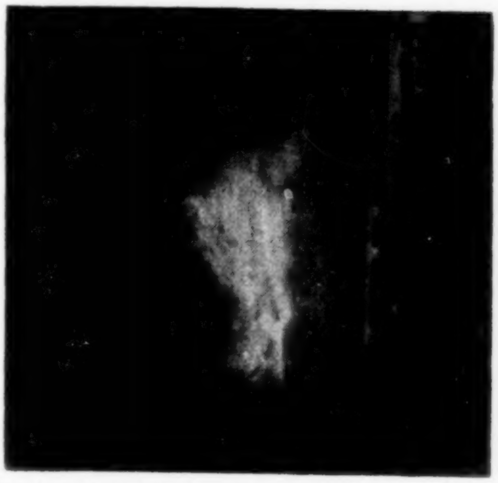

Figure 4. Partial clearance of flame from liquid surface

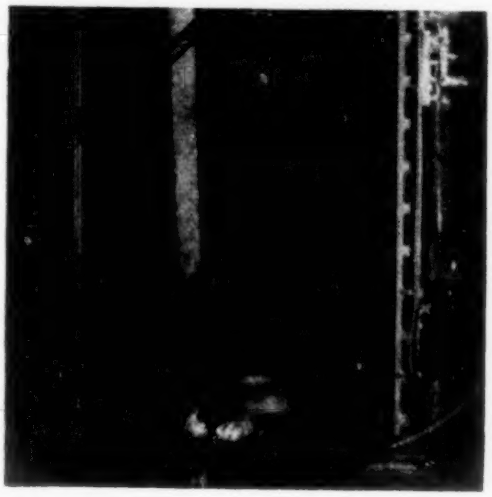

Figure 5. Full clearance of flame from liquid surface

(*a*) The flames were unstable. The size and shape varied continuously and there were frequent clearances from part or even the whole of the liquid surface as shown in *Figures 4* and *5*. These clearances were usually followed by flash back (*Figure 6*) but sometimes a full clearance was followed by extinction.

(*b*) A comparatively stable flat flame was established near the surface of the burning vessel as shown in *Figure 7*. According to the burning liquid, sudden clearances of flame from the surface were either infrequent or absent.

With few exceptions, the hydrocarbons followed behaviour (*a*) although quite often the

Table 1. Properties of selected sprays produced by the impinging jet battery at 85 lb/in² pressure

Designation	Diameter of jets used in battery in.	Mass median drop size mm	Sauter mean drop size mm	Mean volume drop size* mm	Entrained air velocity cm/s	Mean flow rate to fire area† $g\,cm^{-2}\,min^{-1}$	Estimated heat transfer rate from flame at 1000°C to spray drops cal cm^{-3} (of flame) s^{-1}
A	1/32	0·28	0·230	0·157	344	1·6	0·44
B	1/16	0·39	0·323	0·228	338	1·6	0·19
C	7/64	0·49	0·430	0·250	376	1·6	0·14
D	1/32	0·37	0·317	0·208	487	4·0	0·31
E	3/64	0·29	0·252	0·173	355	1·6	0·41

*$[\Sigma nD^3/\Sigma n]^{1/3}$.

†Divide by 5 to give gal $ft^{-2}\,min^{-1}$.

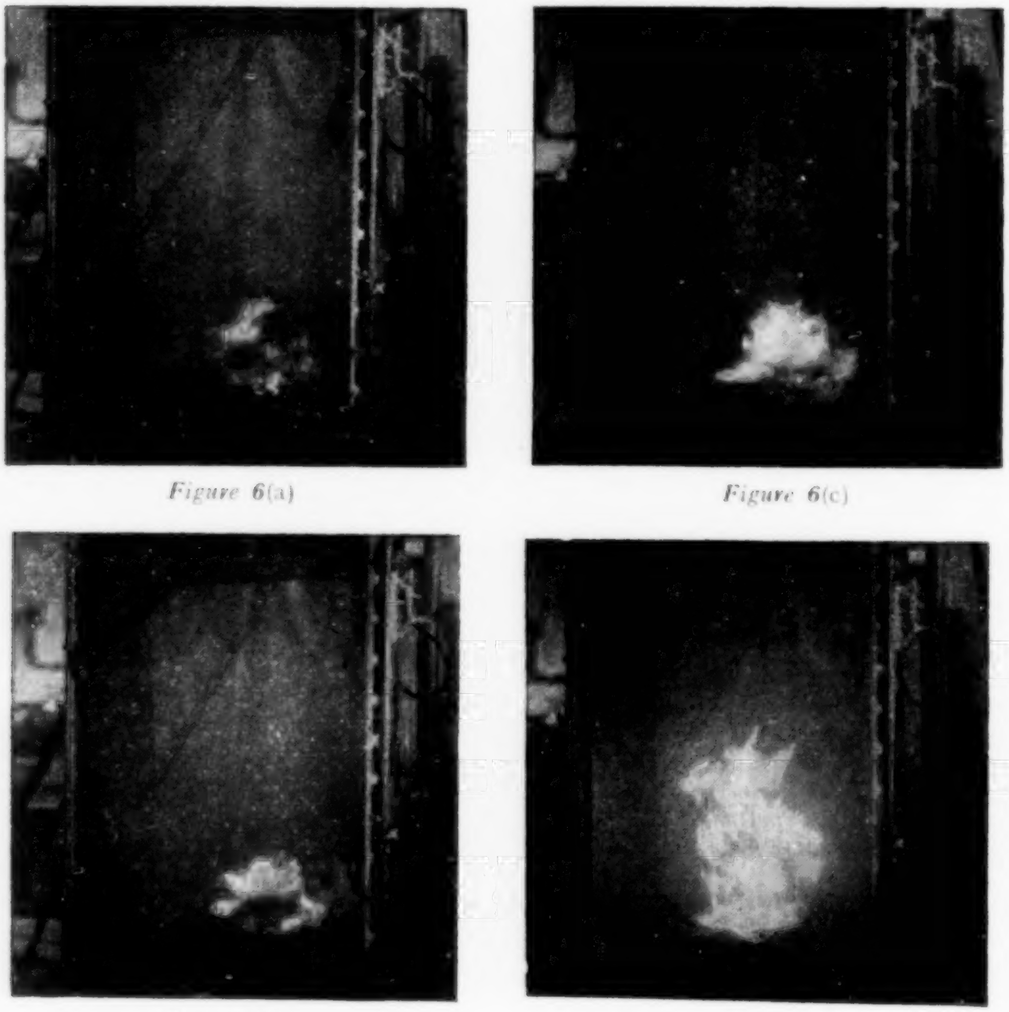

Figure 6(a)

Figure 6(c)

Figure 6(b)

Figure 6(d)

Clearance of flame followed by a flash back

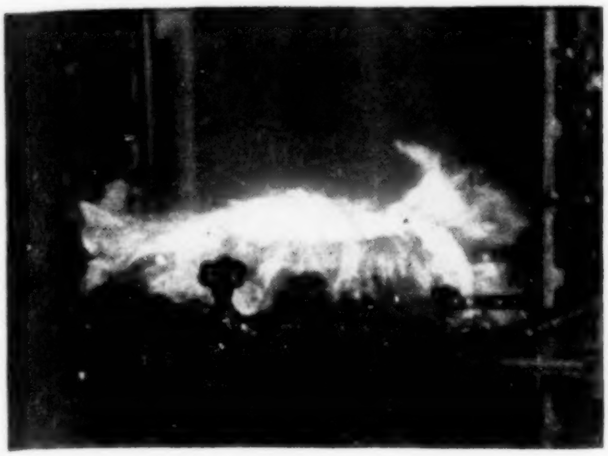

Figure 7. Flat stable flame near liquid surface (behaviour b)

behaviour changed from (*a*) to (*b*) if extinction had not taken place within about 10 seconds. In nearly all the tests on alcohol, the fires followed behaviour (*b*). It may be mentioned here that the structure of the alcohol fire differed from that of the hydrocarbon liquids. With the former there was a thin vapour zone and with the latter a thick vapour zone[3]; the relevance of this observation will be discussed later. When the kerosine, gas oil and alcohol fires were following behaviour (*b*) extinction followed a gradual reduction in the size of the flames and in the area of the vessel covered by the fire; after extinction the liquid could not be ignited immediately by a taper. However, petrol and benzole fires following this behaviour were extinguished after one of the sudden clearances of flame.

Table 2 gives extinction times in replicate tests for the three sprays acting against the six liquids, and *Table 3* gives results of further tests carried out mainly to provide extra information on some parts of *Table 2* where there were wide differences between the replicate tests. The following conclusions may be drawn from *Tables 2* and *3*:

(*1*) Over the range of conditions covered, the sprays could bring about extinction reliably, except spray C on benzole and petrol.

(*2*) The extinction time decreased as the volatility of the liquids decreased.

Table 2. Extinction time (seconds) of different liquids with water sprays

Spray	*Preburn time min*	*Replicate*	*Alcohol (74 proof methylated spirit)*	*Benzole*	*Petrol*	*Kerosine (fire point 60° to 68°C)*	*Gas oil (fire point 104° to 115°C)*	*Transformer oil (fire point 175° to 180°C)*
A	2	i	8·6	6·1	9·3	1·6	5·5	3·6*
		ii	1·4‡	9·7	10·6	3·2	2·4	3·6*
	5	i	15·4	14·0	12·4	5·8	5·5	7·5
		ii	1·6‡	11·5	10·0	6·5	6·6	6·0*
	8	i	1·7‡	8·5	16·0	7·9	7·9	7·4
		ii	1·3‡	14·2	8·6	7·3	8·6	9·2
B	2	i	89·2	46·1	59·0	24·2*†	4·2	3·2*
		ii	163	47·9	49·6	21·4*†	6·0	3·4*
	5	i	217	169	39·8	9·5	6·2	7·0
		ii	254	52·0	45·2	7·8	9·0	6·5
	8	i	80·0	39·2	10·6	10·2	7·8	9·1
		ii	160	70·0	46·6	10·5	8·6	7·2
C	2	i	510	>240†	215†	46·4*†	14·4*†	2·8
		ii	465	>240†	249†	54·7*†	2·6	4·3*
	5	i	475	>240†	152†	6·8	3·4	3·2
		ii	509	2·1	235†	301*†	5·4	3·2
	8	i	525	211†	2·2	5·6	2·6	2·6
		ii	509	71·0†	158†	4·5	4·2	3·4

*Extinction preceded by the liquid being cooled to the fire point.
†Hydrocarbon fire in which type (*b*) behaviour was established after a period of spray application [all other tests type (*a*) behaviour only].
‡Alcohol fire in which type (*b*) behaviour was not established [all other tests, type (*b*) behaviour only].

Table 3. Extinction times in additional tests

Spray	Liquid	Preburn time min	Extinction time in extra replicate tests s	Extinction time from Table 3 s	Spray	Liquid	Preburn time min	Extinction time in extra replicate tests s	Extinction time from Table 3 s
A	Alcohol	2	8·0	8·6, 1·4‡	B	Kerosine	5	7·4	9·5, 7·8
A	Alcohol	5	12·3, 15·2	15·4, 1·6‡		Kerosine	8	8·8, 11·5, 8·7, 10·7	10·2, 10·5
A	Benzole	8	13·9	14·2, 8·5					
A	Petrol	2	10·0, 9·2, 7·8	9·3, 10·6		Gas oil	2	5·0, 12·2*†	4·2, 6·0
	Petrol	5	9·0	12·4, 10·0	C	Petrol	8	8·6, 19·2, 57†, 164†, >480†	2·2, 158†
A	Kerosine	5	4·3	5·8, 6·5					
A	Gas oil	5	5·5	5·5, 6·6		Kerosine	5	89*†, 5·5, 5·6, 5·7	6·8, 301*†
B	Kerosine	2	4·6	24·2*†, 21·4*†		Kerosine	8	4·9, 5·7	4·5, 5·6

*Extinction preceded by cooling to the fire point.
†Hydrocarbon fire in which type (*b*) flames were established.
‡Alcohol fire in which type (*b*) flames were not established.

(*3*) With benzole, petrol and alcohol the extinction time decreased with increasing fineness of spray.

(*4*) Quite different extinction times were often obtained in replicate tests. This was most noticeable when there was a tendency for a change to take place from type (*a*) to type (*b*) behaviour, long extinction times being associated with the latter behaviour.

Effect of preburn time

Table 4 shows results of tests with sprays A, C and D on the petrol and benzole fires at a wide range of preburn times. The outstanding feature of these results was the difficulty in extinguishing the petrol and benzole fires when the preburn time was very short. It was characteristic of the behaviour of the fire in tests with no extinction that before the spray application the vapour zone was thin and that type (*b*) burning was established immediately on applying the spray to the fire. The stable flame which was formed with sprays A and D was small and was concentrated round the inside edge of the vessel as shown in *Figure 8*; with spray C, however, at 2 seconds preburn the flames were pushed immediately into the shape shown in *Figure 7*.

Tests with a range of preburn times were also carried out with sprays C and E on the kerosine fire; the results are shown in *Figure 9*. With spray C extinction occurred either in a short period following the application of the spray during which the flames followed type (*a*) behaviour, or after a long subsequent period of type (*b*) behaviour. In the latter case the

Table 4. Extinction time (seconds) of petrol and benzole fires at low preburn times

Spray	Fire	Preburn times (s)								
		1	2	4	6	8	10	15	30	>30
A	Petrol	>60* >60*	>480* >60*	>60* 34·2*	> 60* 2·5, 0·9	3·2 1·9	4·6 3·2	2·6, 1·7 3·7	3·3 5·7	See Tables 2 and 3
A	Benzole	>60*	—	>60*	>60*, >60*	>60*, >60* 2·4	1·0, 1·7 1·4, 2·5	3·7 5·4	—	
C	Petrol	—	>60*, >60* > 60*	—	—	—	—	—	—	
D	Petrol	0·2 0·3	>30* 8·2*	1·0 1·5	>30* 0·7	1·0 1·3	>30* 0·7	0·7 1·6	1·2 2·0	See Figure 10

*Type (*b*) behaviour was established immediately after applying the spray.

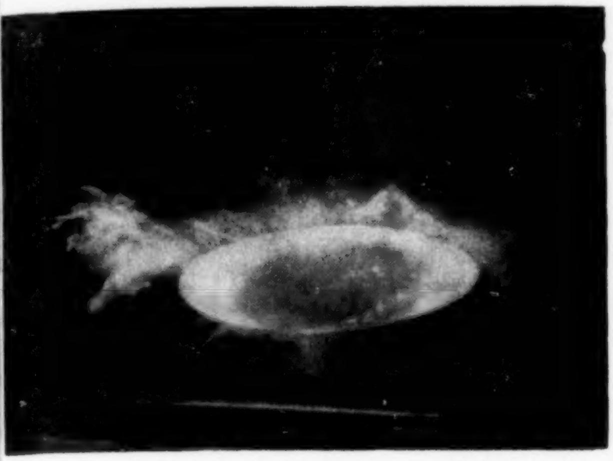

Figure 8. Action of spray A on a petrol fire preburn time less than six seconds

temperature near the surface was reduced to the fire point. The chance of rapid extinction increased as the preburn time increased and rapid extinction was obtained in all tests in which the preburn was longer than five minutes. With spray E the flames followed type (*a*) behaviour in all tests except two at a preburn time of 30 seconds in which type (*b*) behaviour was obtained on applying the spray. The kerosine fire began to form a thick vapour zone after a preburn time of 15 to 20 seconds.

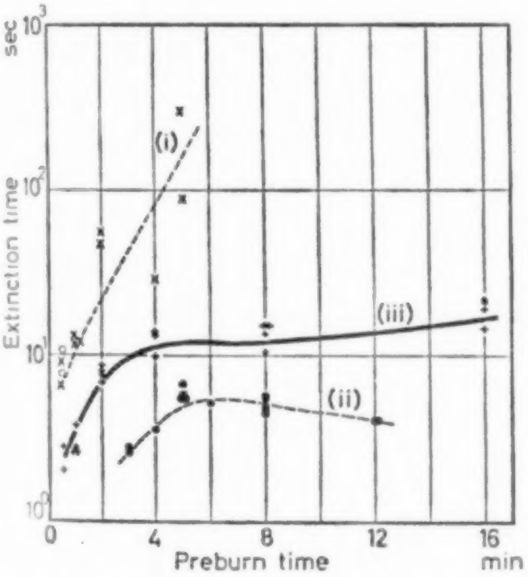

Figure 9. Effect of preburn time on extinction time of a kerosine fire

(i) — × — — × — Extinctions with spray C preceded by establishment of type (*b*) flames and cooling to the fire point.

(ii) — ● — — ● — Extinctions with spray C not preceded by establishment of type (*b*) flames and cooling to the fire point.

(iii) — + —— + — Extinctions with spray E not preceded by establishment of type (*b*) flames and cooling to the fire point

○ Tests with spray E in which type (*b*) flames were formed on applying the spray.

Effect of spray properties

Tests with sprays having a wider range of properties than those in *Table 1* were carried out on the kerosine and petrol fires. In these tests the preburn times were 8 and 5 minutes respectively. With most sprays only one or two tests were carried out, but with some sprays extra tests were made to give an estimate of reproducibility.

Figure 10 shows the extinction time obtained with sprays of different rates of flow plotted against the mass median drop size of the spray. All the sprays were produced by impinging jet batteries at a pressure of 85 lb/in². *Figure 10*(a) shows all the results for petrol. However, although the pattern of the spray at the combustion vessel was reasonably uniform in all the tests, the residual variation of spray pattern had an effect on the results for kerosine. For clarity, therefore, results for this liquid have been plotted separately according to spray pattern in *Figures 10*(b) and (c); 'central' and 'non-central' sprays were respectively those in which the peak flow rate occurred inside and outside the central half of the vessel area.

With both fuels an increase in rate of flow gave a marked reduction of extinction time. The petrol fire also showed a fairly consistent and marked decrease in extinction time as the drop size of the spray decreased; however, there is evidence of an increase in extinction time when the finest sprays were used at the lowest rates of flow. The latter phenomenon occurred with kerosine as well, but kerosine differed from petrol in that there was a decrease rather than an increase in extinction time for 'non-central' sprays as the drop size increased between 0·39 and 0·49 mm at the flow rate of 1·6 g cm^{-2} min^{-1}. *Figure 10* also shows that longer extinction times were obtained when sprays were of the 'central' type than when they were of the 'non-central' type.

The varying flow rates at the fire area shown in *Figure 10* were obtained by increasing the number of pairs of jets used in the battery. Under these conditions the entrained air in the spray also increased by a factor proportional to the square root of the rate of flow at the fire area[1]. It is not clear from *Figure 10* therefore, whether the increased efficiency of the sprays accompanying the increase in rate of flow was due to the larger amount of water delivered or to the extra amount of air incidentally entrained into the spray. The fact that the entrained air could have a substantial effect on the extinction time is shown by the results in *Table 5* in which extinction times with pairs of sprays differing mainly in entrained air current are compared. It will be noted that in every case the sprays with the larger entrained air velocity gave shorter extinction times.

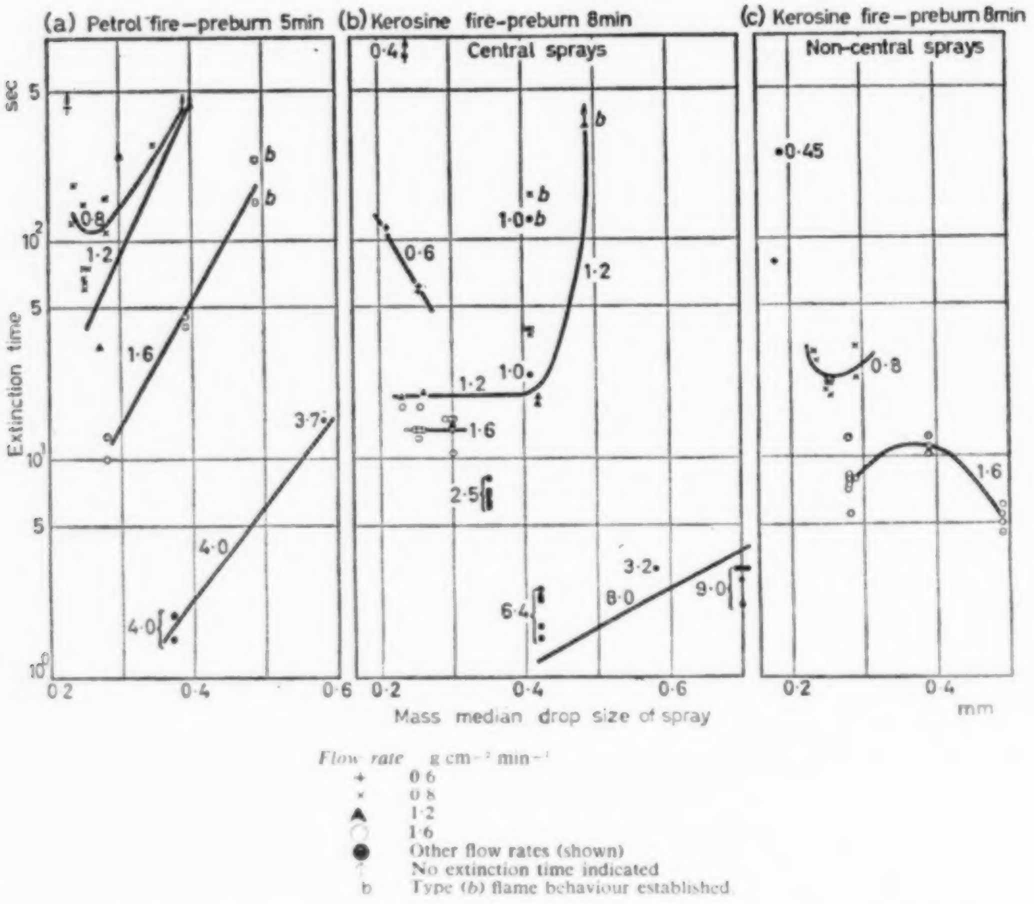

Figure 10. Effect of spray properties on the extinction of liquid fires

A quantitative estimate of the effect of spray properties on the extinction time of the petrol and kerosine fires was obtained by carrying out regression analyses. These analyses did not cover all the tests carried out; it was of course impossible to include any results in which no extinction was obtained. Moreover, for the kerosine fire, extinctions which were preceded by cooling to the fire point were not included as these were shown by *Figure 9* to form a different population from the other extinctions obtained. However, from the remaining tests equations 1 and 2 were obtained for the petrol and kerosine fires respectively.

$$Y = 6{\cdot}1 \times 10^{11} M^{-2{\cdot}1} D^{4{\cdot}3} A^{-3{\cdot}0} \quad \ldots . [1]$$

$$Y = 2{\cdot}6 \times 10^{9} M^{-0{\cdot}5} D^{0{\cdot}9} A^{-3{\cdot}2} \quad \ldots . [2]$$

where Y denotes extinction time (seconds), M is

Table 5. ***Effect of entrained air current on extinction time***

Burning liquid	*Method of producing spray*	*Spray properties*			*Extinction time*
		Mass median drop size mm	*Rate of flow* $g\,cm^{-3}\,min^{-1}$	*Entrained air velocity* cm/s	s
Kerosine 8 min preburn	*I.J. 1/64 in. jets, 30 lb/in²*	0·29	0·8	160	60·0
	I.J. 3/64 in. jets, 85 lb/in²	0·29	0·8	233	23·6, 32·0
	I.J. 1/32 in. jets, 30 lb/in²	0·36	1·2	204	69·0
	I.J. 1/64 in. jets, 85 lb/in²	0·30	1·2	310	14·2
Petrol 5 min preburn	*Proprietary nozzle, 100 lb/in²*	0·41	1·9	226	70, 198, >240
	I.J. 1/16 in. jets, 85 lb/in²	0·39	1·6	338	39·8, 45·2
	Proprietary nozzle, 100 lb/in²	0·45	1·7	157	>240, >240
	I.J. 7/64 in. jets, 85 lb/in²	0·49	1·6	376	152, 235

I.J. = impinging jet battery.

flow rate ($g\,cm^{-2}\,min^{-1}$), D is the mass median drop size (mm), and A is the entrained air current (cm/s).

The above equations refer to a uniform pattern of spray at the fire area and a preburn time of five minutes. They show that the extinction time decreased with increase in flow rate and decrease in drop size but that the extent of these effects varied somewhat for the two liquids. They also indicate that there was a pronounced reduction in the extinction time as the entrained air current increased and the effect was very similar for the two liquids. It must be remembered in applying these equations, that as long as sprays are produced in a given manner, then there is a strong dependence of the entrained air current on the rate of flow of water spray and if the total effect of rate of flow is to be estimated this must be taken into account.

Effect of direction of application

The effect of the direction of application of spray was investigated by applying sprays by hand to the standard petrol fire from single pairs of 1/32 and 1/16 in. impinging jets. If the sprays were applied horizontally across the fire no extinctions were obtained and a stable flame covered the surface of the liquid (*Figure 11*). An increase in the angle of projection from 0° to 30° to the horizontal gave an increase in the intensity of this flame chiefly because of extra fuel splashed into the flames when the water drops hit the petrol surface. At angles greater than 30° a clearance of some of the flames was often obtained, and at an angle of 60° or more extinction was frequently obtained.

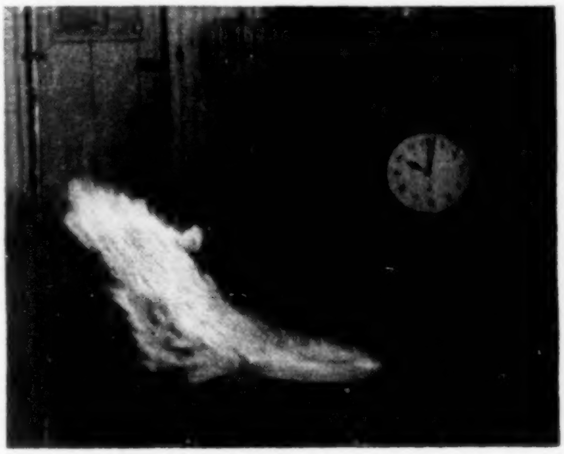

Figure 11. Spray from 1/32 in. impinging jets applied horizontally to fire

Table 6 shows extinction times obtained when the sprays were applied at an angle of 60° to the horizontal at a distance of 2 ft 6 in. and at preburn times of 2, 30 and 300 seconds. *Table 6* shows:

(*1*) that with both sprays it was sometimes found difficult to extinguish the fire when the preburn time was 2 seconds

(*2*) that in spite of a much smaller flow rate, the finer spray gave more rapid extinctions than the coarser spray.

The conditions of application in the above tests were somewhat different from those which were described in the previous sections. Broadly speaking, however, the establishment of the stable flame caused by a small angle of attack was akin to the occurrence of type (*b*) behaviour, and the occurrence of clearances and flash-backs when the angle was steep was akin to type (*a*) behaviour.

Discussion

Mechanisms of extinction

The extinctions may be divided into two groups. First, there are those which were preceded by a gradual reduction in the size of the flames and after which there was difficulty in re-igniting the liquid. Secondly, there are those which were preceded by a rapid clearance of a large volume of flame followed within a short time by the rapid disappearance of the remaining flame, and after which the liquid could be re-ignited immediately. The extinctions in the first group occurred usually after type (*b*) behaviour was established and there is little doubt that the mechanism of extinction was the reduction of the rate of evolution of combustible vapour from the liquid to below the value required to support flame. With the hydrocarbon liquids this reduction occurred by cooling the liquid to the fire point and with the alcohol by diluting the surface layers; further information on this type of extinction for hydrocarbon liquids has been given elsewhere[4]. In the second group extinction took place by the action of the spray on the flames. The way in which this occurred is not obvious but on the basis of available information a tentative hypothesis of the mechanism has been developed below.

Effect of heat transfer between flames and drops on extinction

Most of the facts concerning the direct extinction of the flames may be accounted for if it is assumed that the extinction depends on a heat transfer process between the flames and the drops.

First, the way in which the time of extinction depends on the rate of flow and the drop size is broadly such as might be expected from the dependence of the heat transfer on these properties. It may be shown[5] that the heat transfer will vary with the spray properties as in equation 3.

$$H \propto M_f^{1\cdot0} D_f^{-(1\cdot5 \text{ to } 2\cdot0)} V^{0\cdot5 \text{ to } 1\cdot0} \quad \ldots [3]$$

where H denotes heat transfer per unit volume of flame in unit time, M_f is the flow rate of spray through unit cross-sectional area of flame, D_f is the appropriate representative drop size and V is the drop velocity.

The heat transfer increases with an increase in the flow rate and a decrease in the drop size of the spray. If heat transfer contributes in an important way to the extinction process it would be expected that a variation in the above spray properties should have the reverse effect on the extinction time. This is shown to be so by regression equations 1 and 2.

Secondly, the amount of heat transfer which could take place between the flames and the drops was of the same order as that required to extinguish the flames. Thus to cool the flame, it may be postulated that the rate of heat transfer (H) required per unit volume of flame

Table 6. Extinction of petrol fire by hand application of spray from single pairs of impinging jets; angle of attack 60° to horizontal; pressure 96 lb/in²

Size of jets *in.*	*Total flow to fire area* *g/min*	*Mass median drop size* *mm*	*Extinction times* *s*		
			2 s preburn	*30 s preburn*	*300 s preburn*
1/32	268	0·21	1·1, 49·4 0·6, 4·4 11·3, 5·0	7·5, 8·5 12·5, 7·1 4·7, 16·5	22·8, 6·7 28·5, 13·4 5·0, 8·6
1/16	1438	0·36	>120 (6 *tests*)	21·0, 25·0 32·2, 12·6 32·0, >120	>120 (5 *tests*) 108·2

would be of the same order as the burning intensity of the flame (I) which is the rate of heat production per unit volume of flame[2]. It may also be shown[6] that a rate of heat transfer equal to $I/5$ would be required if all the heat transferred results in the formation of steam. This, however, would take place only if the water drops were at the wet bulb temperature in the flame (about 75°C). Mean values of I for the petrol fires were obtained from the flames shown in *Figures 2*(b) and *11* by dividing the heat of combustion of the fuel that entered the flame by the flame volume. The estimates were 0·45 and 2·5 cal $\text{cm}^{-3}\,\text{s}^{-1}$; these two values may be taken to represent respectively the burning intensity of the large flames that existed before the application of spray and the burning intensity of the flat stable flames which could sometimes be formed during the application of spray. Values of H between 0·1 and 0·5 cal $\text{cm}^{-3}\,\text{s}^{-1}$ were calculated[2] for sprays A to E (see *Table 1*); these values are of the same order as the above values of I or $I/5$.

The above calculation of the intensity of combustion also indicates why the flames could be extinguished under some conditions but not under others. When a flat flame was established near the surface of the burning liquid, it burned at about six times the intensity of a flame which occupied a large volume above the surface. On the other hand, for a given spray the heat transfer from the flames to the drops would not vary by a factor greater than about 1½ to 2, since this heat transfer would depend mainly on the flame temperature. Thus when a flat flame was established [type (*b*) behaviour] it was more difficult with a given spray to obtain clearances which could lead to extinction than when this type of flame was not established.

Factors affecting the flames

The above considerations of heat transfer do not explain why the flames should behave in different ways under different conditions, nor do they account for the influence of the entrained air current. Equation 3 shows that for given values of D_f and M_f the heat transfer should decrease as the velocity of the drops increases. Now, with most of the sprays used in the above tests, the velocity of those drops in the spray that made the greatest contribution to the heat transfer, was approximately the same as that of the entrained air current[1]. It might thus be expected that an increase in the entrained air current of the spray should decrease the heat transfer to the drops and therefore increase the extinction time; in fact a marked reduction in extinction time was noted.

The property of the fire which appeared to have the most influence on the behaviour of the flames was the thickness of the zone of vapour between the surface of the liquid and the flames. When this zone was thick or tended to be thick the application of the spray brought about type (*a*) flame behaviour; when it was thin, type (*b*) behaviour resulted. This suggests that the instability in the flames characteristic of type (*a*) behaviour was due to some action of the spray which could be exerted best when a thick vapour zone was present. A powerful effect was certainly exerted by the entrained air current, and probably accounts for the effect of the latter property on extinction. This air current could push the thick vapour zone either to the edge of the vessel or over the edge of the vessel thus helping to give partial and full clearances respectively. Alternatively it could mix by turbulent diffusion with the thick vapour zone and dilute it to such an extent as to make it non-flammable. With a thin vapour zone of the order of boundary layer thickness, however, neither of the above actions could be exerted so easily and a stable form of flame [type (*b*) behaviour] could be established.

Mechanism of rapid extinction of flames

The following hypothesis of the mechanism of the rapid extinction of the flames which occurred when type (*a*) behaviour was established is based on the above discussion. A local clearance in a large diffusion flame could take place perhaps as a result of heat transfer between the flames and the drops. Because of action between the entrained air current and the vapour zone this clearance would continue until a large part of the vessel area was free of flame. However, a small flame could still become established inside or outside a part of the edge of the vessel; this remnant of the flame was finally extinguished by heat transfer between the flames and the spray drops.

The sharp distinction between the effect of the air current and the heat transfer suggested in the above mechanism must be somewhat arbitrary even for the one shape of fire investigated in these experiments. For a surface of any given shape and oriented in a given way to an air current, it has been generally found that there is a limiting velocity of the air current above which a flame cannot be stabilized[7]. In this context an extinguishing agent may be defined as an agent which when present in the air stream reduces this upper limit, and it is likely that there will be a critical concentration of extinguishing agent which will not allow a flame to be stabilized under any air flow conditions. At the moment information on this aspect of the performance of extinguishing agents is lacking; its absence limits the extent to which the results of the present investigation may be interpreted in a fundamental manner. However, it would be expected that in the above tests the turbulence and velocity of the prevailing air current would in themselves have influenced the amount of heat transfer to the drops necessary to bring about final extinction.

Practical implications

Water is by far the most common material available for extinguishing fires and also the one which is most easily handled. It is very desirable therefore to use it as an extinguishing agent wherever it can be relied upon. The above tests show that water sprays with a wide range of spray properties are capable of extinguishing liquid fires.

However, if a spray cannot act on a liquid in such a way as to bring about a suppression of adequate vapour evolution from the liquid, then reliance must be placed on its ability to extinguish the flame. The above investigations have shown that this is very sensitive to the way in which the spray is applied and to the preburn time; it is likely that this ability would also be sensitive to other factors such as the shape and size of the surfaces associated with the fire. It may be concluded that water sprays with properties similar to those covered in the above tests are not reliable for the extinction of fires in liquids like petrol and benzole. Nevertheless, a water spray system can serve a useful purpose if it holds a fire in check or reduces the size of the fire until sufficient quantities of a better extinguishing agent can be brought into use. The results indicate that many of the sprays tested might be expected to perform this function.

The work described in this paper forms part of the programme of the Joint Fire Research Organization of the Department of Scientific and Industrial Research and Fire Offices' Committee; the paper is published by permission of the Director of Fire Research. The illustrations are Crown Copyright and appear by permission of H.M.S.O.

References

[1] RASBASH, D. J. 'The properties of sprays produced by batteries of impinging jets'. *Fire Research Note No. 181*, 1955. Department of Scientific and Industrial Research and Fire Offices' Committe Joint Fire Research Organization: London

[2] RASBASH, D. J. and ROGOWSKI, Z. W. 'The extinction of open fires with water spray. Part I. The effect of water spray on a kerosine fire 30 cm diameter'. *Fire Research Note No. 58*, 1953 See ref. 1

[3] RASBASH, D. J., ROGOWSKI, Z. W. and STARK G. W. V. *Fuel, Lond.* 1956, **35**, 94.

[4] RASBASH, D. J. and ROGOWSKI, Z. W. *Combustio & Flame*, **1957**, **1**, **453**

[5] RASBASH, D. J. and ROGOWSKI, Z. W. 'The effec of water sprays on a petrol fire of 30 cm diameter'. *Fire Research Note No. 185*, **1955**. See ref. 1

[6] RASBASH, D. J. and ROGOWSKI, Z. W. 'Th extinction of open fires with water spray. Part II The effect of drop size of spray on the extinction o different liquid fires'. *Fire Research Note No. 162* **1955**. See ref. 1

[7] SPALDING, D. B. 'Heat and mass transfer in th combustion of liquid fuels'. *Proceedings* of th General Discussion on Heat Transfer **1951**, Sectio IV, p **345**. Institution of Mechanical Engineers London; American Society of Mechanical Engineers: New York

Heterogeneous Combustion of Multicomponent Fuels

B. J. Wood, H. Wise and S. H. Inami

Department of Chemical Physics, Stanford Research Institute, Menlo Park, California

(Received May 1959)

The variation of burning-rate coefficient (the time-rate of change of drop cross-sectional area) as a function of composition was determined for single drops of a group of binary fuel mixtures. The results indicate that during combustion the composition of a multicomponent fuel drop changes by a process of simple batch distillation. Drops of fuel mixtures containing components of widely different boiling points demonstrated instability during combustion. Motion pictures of these burning drops reveal the formation of bubbles which expand and burst in the liquid phase. It is suggested that these effects are due to radiative heat transfer from the flame envelope to the liquid, resulting in local vaporization of the more volatile components within the drop. Surface temperatures of burning drops of pure compounds were measured for a drop suspended from a thermocouple junction and for a fuel-wetted, porous, Alundum sphere. The values obtained from these measurements are in close agreement with those calculated on the basis of a spherico-symmetric model of a burning drop.

Nomenclature

The following symbols, listed with their meanings, have been used:

c_p	Specific heat (constant pressure) of air at temperature T_e, cal/g °C
i	Stoichiometric mixture ratio, $(Y_a/Y_f)_{\text{stoich.}}$
Q	Heat of combustion (fuel vapour to gaseous products), cal/g
L	Heat of vaporization (sensible heat plus latent heat), cal/g
T_a	Temperature of ambient air, °K
T_c	Adiabatic flame temperature, °K
T_e	Log mean temperature, °K $T_e \equiv (T_c - T_a)/2{\cdot}3 \log (T_c/T_a)$
T_s	Temperature at drop surface, °K
Y	Weight fraction of specified component
Y_a	Weight fraction of oxygen in air, 0·232
Y_f	Weight fraction of fuel
ε	Burning-rate coefficient (diameter squared/sec), cm^2/sec
λ_e	Thermal conductivity of air at temperature T_e, cal/sec cm °C
ρ	Density of liquid, g/cm^3.

Introduction

Liquid fuels of industrial importance generally are mixtures of chemical compounds which possess individually different physical and chemical properties. The burning characteristics of such multicomponent mixtures when dispersed as liquid aerosols have not been investigated in detail. Combustion of a binary fuel mixture over a large planar liquid surface produces a gradual change in the composition of the liquid phase[1]; on the other hand, combustion of a fuel mixture on a wick immersed in the fluid consumes the fuel without change in liquid composition[2]. No deductions concerning the behaviour of a multicomponent burning drop can be made from these observations, because in such a system the conductive heat flux increases with decreasing drop size, and the convective effects in the liquid phase are affected by the geometry.

Because of the small mass of fluid involved, the variation in the burning-rate coefficient (the time-rate of change of drop diameter squared), ε, was chosen as a means of examining the type of vaporization process occurring on the drop surface. For pure fuels the burning-rate coefficient remains constant during the lifetime of the drop[3]. Similarly, for a binary fuel mixture composed of compounds with individually different burning-rate coefficients, the drop cross-sectional area decreases linearly with time if the composition of the liquid phase does not vary during combustion. A fuel drop, however, the constituents of which exhibit different burning-rate coefficients and vaporize selectively during combustion, would be expected to exhibit a non-linear decrease in cross-sectional area with time. Consequently, measurement of the burning-rate coefficients of binary mixtures offers a suitable means of analysing the vaporization process occurring during combustion. Burning-rate coefficients for three binary systems (heptane and butanol-1; 2,2,4-trimethylpentane and butanol-1; dibutyl ether and pentanol-1) were determined by means of a photoelectric shadowgraph apparatus which directly measures the variation of cross-sectional area of a single burning drop as a function of time[4]. The drops, which had an initial diameter of the order of 1 800 microns, were suspended in air from the enlarged tip (approximate diameter: 1 000 microns) of a quartz fibre, and were ignited with the flame of an alcohol burner. Drops of this size proved to be sufficiently small so that the effect of convective heat transfer could be neglected; the mass burning rate, therefore, was proportional to the drop diameter[5,6].

There are two basic mechanisms by which fuel can vaporize from the surface of a burning drop made up of a multicomponent solution. First, the vapours leaving the surface may have a composition identical to that of the liquid phase, i.e. non-equilibrium distillation. Secondly, a thermodynamic equilibrium may be established at the interface between liquid and vapour so that the components vaporize from the burning drop in continuously varying composition ratios, each of which is uniquely determined by the instantaneous temperature of the liquid phase. We assume there exists a uniform composition within the liquid at every instant, such as could be produced by convective mixing within the drop. El Wakil and co-workers observed[7] that the fluid within a drop evaporating in a heated air stream circulates rapidly enough to eliminate temperature gradients in the liquid. Similar observations demonstrating circulation within the liquid of a burning drop were made by us.

Results

Our experiments, conducted in air at a pressure of one atmosphere, indicate that the burning-rate coefficient does, indeed, vary during the burning lifetime of a drop composed of two pure compounds. Typical burning-rate curves for various mixtures of the system butanol–heptane are depicted in *Figure 1*. The pure fuel drops exhibit linear changes of cross-sectional area with time, i.e. their burning-rate coefficients remain constant during the drop lifetime. On the other hand, the burning-rate curve produced by the fuel mixture containing equimolar quantities of each constituent exhibits curvature. At the beginning of combustion, the slope approaches that of the azeotropic composition (25 mol per cent butanol), while near the end, that of pure butanol. The initial and final values of the burning-rate coefficients of all the fuel mixtures studied are summarized in *Figure 2*. The results indicate that the composition of the liquid phase changes during combustion in a manner which can be described as a batch distillation process (in which the liquid and the vapour are in equilibrium with respect to composition and temperature) rather than as a non-equilibrium distillation. For mixtures which contain a relatively small mol fraction of their more volatile components, the experimental data suggest constant burning rates. This effect is probably due in part to the loss of the volatile component from the liquid phase preceding drop ignition, and to ignition-produced perturbations which obscure observation of the rate of decrease in drop cross-sectional area at the onset of combustion.

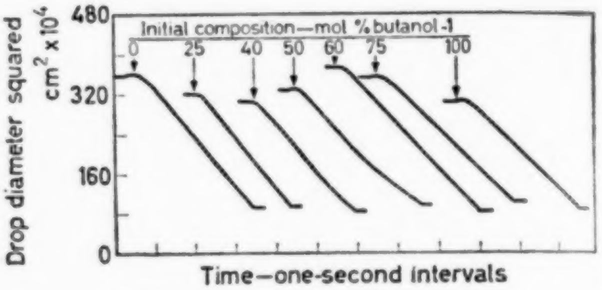

Figure 1. Burning-rate curves for various mixtures of butanol-1 and heptane in air

In order to characterize definitely the mechanism of the vaporization process, a theoretical analysis was attempted, based on the assumption that the composition of the drop at any time during the burning lifetime could be characterized from the equilibrium distillation curves for the system at atmospheric pressure. Such an assumption requires that: (*1*) the ignition lag of the drop be small, so the liquid/vapour interface rapidly attains thermodynamic equilibrium with its immediate surroundings, (*2*) the temperature of the interface be sufficiently close to the normal boiling point of the system to permit composition to be estimated from ordinary distillation curves for one-atmosphere pressure, and (*3*) the composition of the liquid phase be homogeneous.

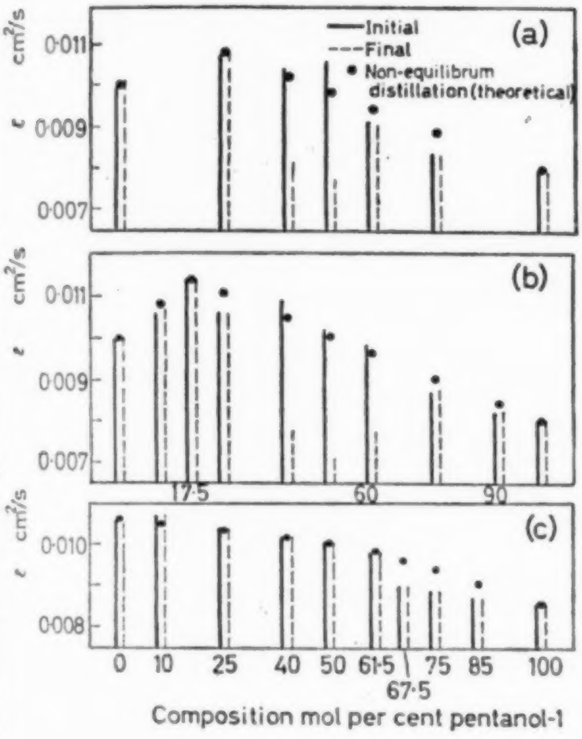

Figure 2. Burning-rate coefficients for various binary fuel mixtures in air: (a) *heptane–butanol-1,* (b) *2, 2, 4-trimethylpentane–butanol-1,* (c) *dibutyl ether–pentanol-1*

An examination of the burning curves for the pure compounds (*Figure 1*) shows that the extent of the time-span between ignition and the beginning of steady-state combustion occupies approximately 15 per cent of the total burning lifetime of the drop. We assume that a similar ignition lag holds for binary fuel drops.

Calculations of the drop surface temperature based on the burning-rate equations derived for the spherico-symmetric model of a burning drop[8] indicated that the true surface temperature of a drop of pure fuel burning in air is approximately 15 per cent lower than the normal boiling point of the liquid (*Table 1*). Actual surface temperature measurements were made by burning pure fuel drops suspended from a thermocouple in such a manner that the junction rested close to the surface within the drop. The thermocouple wires were insulated from the hot zone of the flame by a non-catalytic ceramic coating. Additional surface temperature measurements were made by means of a fuel-wetted porous sphere[6], at the lower surface of which was situated a thermocouple junction. A mass of pendent fluid surrounding the thermocouple junction was established on the lower half of the porous sphere. As the excess fluid burned, the thermocouple junction pierced the liquid film. The temperature indicated at this departure was taken as the surface temperature of the burning drop. The experimental results agree closely with the calculated values of surface temperature (*Table 1*). Thus, it is evident that the estimation of the time-variation of composition of a drop on the basis of ordinary distillation curves can be regarded as a first approximation.

The Rayleigh equation, which relates the composition of a residue in a simple batch distillation to the mol fraction of the original distilland remaining at any given instant[9], was used to calculate a series of composition

Table 1. Surface temperatures of liquid drops burning in air

Fuel	*B.pt* °C	*Surface temperature, °C*		
		Theory (ref. 8)	*Porous Sphere Expt*	*Hanging Drop Expt*
Ethanol	78·4	68	72·5	72
Butanol-1	118	101	108	105
Pentanol-1	138·1	117	124	125
Octanol-1	194·5	161	163	171
2, 2′-Oxydiethanol	244	211	215	226
Heptane	98·4	84	84	82
Octane	125·7	—	108	104
Kerosine	225*	185†	202	—

*Mean boiling point.
†Calculated on the basis of a pure hydrocarbon of b.pt 225°C.

values corresponding to arbitrarily selected mol fractions of the liquid drop yet unburnt*. The unburnt mol fraction of fuel is a function of the cross-sectional area of the drop. By assuming an average molecular weight for the fuel mixture, the composition of the liquid phase as a function of time after ignition may be calculated explicitly from the experimental burning-rate curves. Sets of composition values corresponding to periods of time elapsed after ignition for specific burning drops of binary fuels were thus obtained.

For a burning-drop model in which a spherical flame envelope is maintained around the liquid sphere, heat and mass transfer considerations lead to an expression of the burning-rate coefficient in terms of thermodynamic properties of the drop and transport properties of the gas film between drop and flame. As the gaseous region between the fuel and the reaction zone of a diffusion flame has been shown to consist predominantly of nitrogen, carbon dioxide and water vapour for a number of representative organic fuels[10, 11] we may consider that the transport properties of the gaseous envelope around a burning drop are independent of liquid composition within the category of ordinary organic fuels. In addition, we note that the quotient of heat of combustion and stoichiometric mixture ratio (Q/i) for the fuels employed in this investigation is essentially a constant (*Table 2*). At any instant during the combustion process the theoretical burning-rate coefficient[6] for the binary mixture containing components 1 and 2 is

$$\varepsilon_{1,2}=\frac{8\lambda_e}{(Y_1\rho_1+Y_2\rho_2)c_e}\ln\left\{1+\frac{1}{(Y_1L_1+Y_2L_2)}\left[\frac{Y_aQ}{i}-c_e(T_s-T_a)\right]\right\} \quad \ldots\ldots [1]$$

Burning-rate coefficients for drops of the pure constituents of the mixtures were calculated from this equation using the numerical values given in *Table 2*. The adiabatic flame temperatures of these fuels are nearly identical; so for all cases λ_e and c_e were evaluated for air at the logarithmic mean temperature between T_c and T_a.

Table 2. Properties of fuels used in in calculation of ε*

Fuel	ρ (g/cm^3)	L (cal/g)	Q (cal/g)	i (g/g)	Q/i (cal/g)	*B.pt* (°C)
Butanol-1	0·810	207·0	8051	2·59	3110	118
Heptane	0·684	121·6	10720	3·51	3060	98
2, 2, 4-Trimethylpentane	0·692	106·8	10672	3·51	3040	99
Pentanol-1	0·818	201	8420	2·72	3100	138
Dibutyl ether	0·773	185	8850	2·87	3080	142

*Transport properties of vapour film were taken as those of air at the log mean temperature between the flame and ambient temperature[15]; $c_e=0{\cdot}271$ cal/g °C. $\lambda_e=1{\cdot}56\times10^{-4}$ cal/sec cm °C. Since the drops were burned in air at one atmosphere, $Y_a=0{\cdot}232$.

By introducing the composition values obtained from the Rayleigh equation into equation 1, the instantaneous burning-rate coefficients for burning drops of binary mixtures of interest were calculated. Examples of these values are presented in the form of theoretical burning-rate curves in *Figure 3*. Superimposed on the theoretical curves are points taken from the burning-rate measurements of drops of identical initial composition. In view of approximations made in selecting the vapour film properties used in the theoretical equation, the amount of agreement is satisfactory. One may conclude that after a brief ignition lag, a simple equilibrium batch distillation is an adequate description of the vaporization process which a two-component drop undergoes during combustion.

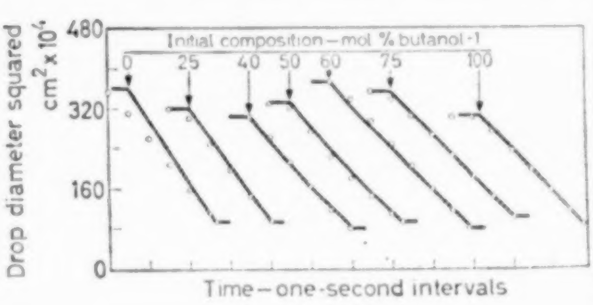

Figure 3. Theoretical burning-rate curves for various mixtures of butanol-1 and heptane in air (circles indicate experimental points)

---

*The liquid–vapour equilibrium diagrams, needed for this analysis, were determined in our laboratory for the fuel mixtures employed in this study. These distillation curves are presented in N.A.S.A. *Technical Note No. D-206*, see ref. 16.

In the light of these experiments, it is not surprising that the burning curves for drops of some multicomponent fuels of practical importance are quite linear. The explanation lies in the fact that the thermodynamic characteristics of all the components are such that the individual burning-rate coefficients vary over a narrow range. The practical fuels kerosine and jet fuel JP-4, for example, exhibit this characteristic (*Figure 4*).

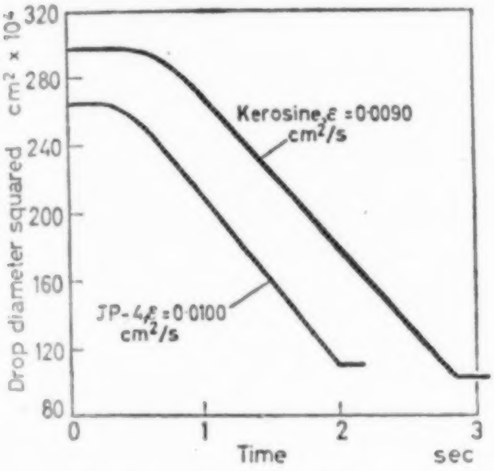

Figure 4. Burning-rate curves for kerosine and jet fuel JP-4 in air

Multicomponent fuel drops, composed of mixtures of aliphatic hydrocarbons with carbon chains varying between seven and sixteen atoms in length, were frequently observed to exhibit an unsteadiness while burning. We have termed this phenomenon 'disruptive combustion'. Visually, it appears as an oscillation of the burning drop on its supporting fibre, accompanied by ejection of small quantities of liquid fuel as an aerosol in random directions.

By photographing such burning drops with a motion picture camera, the phenomenon of disruptive combustion was shown to be associated with the formation of minute bubbles or vapour pockets in the liquid phase. The photographs of *Figure 5* are successive frames which reveal the formation and disintegration of such a disturbance. Frame I shows the quietly burning drop 1·149 sec after ignition; the dark spots are highlights produced by the strong side illumination of the drop. The beginning of a bubble is visible in the upper right quadrant of the drop in Frame II, and the subsequent growth of the disturbance can be followed in Frames III to V. The bubble apparently burst before Frame VI was exposed, and within the elapsed time of the next two frames the drop returned to quiescent combustion. The burning curve (*Figure 6*) for the same drop photographed in this sequence clearly shows the disruptions. In this case a small loss of material from the liquid phase had a negligible effect on the characteristic burning rate.

It is probable that this phenomenon is associated with the transfer of radiant energy from the flame into the interior of the drop. Calculations of temperature profiles have indicated that under conditions of absorption of incident radiant energy the temperature inside a drop can exceed that on the surface[12]. The contribution of radiative heat transfer to a burning drop was demonstrated experimentally by enhancing the absorptivity of the fuel. Unfortunately, compounds such as acetonitrile and phenylacetonitrile which absorb in the spectral region in which hydrocarbon flames emit strongly (∼4·5 microns), are quite insoluble in fuels such as those employed in this investigation. The addition of a particulate black dye which forms a slurry appeared to be the only way to change significantly the absorptivity of the hydrocarbon fuel drops[13]. To magnify the effect which a change in fuel absorptivity would produce in a burning drop, a fuel mixture was selected which burned quietly, but which possessed a wide boiling range and therefore a susceptibility to disruptive combustion. Small quantities of Apiezon W black wax were added to a 50–50 volume per cent mixture of nonane and tetradecane. Microscopic examination of the filtered solution, brown in colour, indicated that the colouring matter existed in the form of a particulate colloidal suspension within the drop. Absorption spectrograms of the coloured solution showed a small, uniform increase in optical density over the clear fuel in the 4 to 5 micron wavelength region*. Drops of the coloured solution burned values corresponding to arbitrarily selected mol fractions of the liquid drop yet unburnt*. The unburnt mol fraction of fuel is a function of the cross-sectional area of the drop. By assuming an average molecular weight for the fuel mixture, the composition of the liquid phase as a function of time after ignition may be calculated explicitly from the experimental burning-rate curves. Sets of composition values corresponding to periods of time elapsed after ignition for specific burning drops of binary fuels were thus obtained.

---

*It is possible, of course, that addition of colloidal carbonaceous material to the fuel may somewhat extend the spectral range of the flame emission.

For a burning-drop model in which a spherical flame envelope is maintained around the liquid sphere, heat and mass transfer considerations lead to an expression of the burning-rate coefficient in terms of thermodynamic properties of the drop and transport properties of the gas film between drop and flame. As the gaseous region between the fuel and the reaction zone of a diffusion flame has been shown to consist predominantly of nitrogen, carbon dioxide and water vapour for a number of representative organic fuels[10, 11] we may consider that the transport properties of the gaseous envelope around a burning drop are independent of liquid composition within the category of ordinary organic fuels. In addition, we note that the quotient of heat of combustion and stoichiometric mixture ratio (Q/i) for the fuels employed in this investigation is essentially a constant (*Table 2*). At any instant during the combustion process the theoretical burning-rate coefficient[6] for the binary mixture containing components 1 and 2 is

$$\varepsilon_{1,2}=\frac{8\lambda_e}{(Y_1\rho_1+Y_2\rho_2)c_e}\ln\left\{1+\frac{1}{(Y_1L_1+Y_2L_2)}\left[\frac{Y_aQ}{i}-c_e(T_s-T_a)\right]\right\}\quad\ldots\ldots[1]$$

Burning-rate coefficients for drops of the pure constituents of the mixtures were calculated from this equation using the numerical values given in *Table 2*. The adiabatic flame temperatures of these fuels are nearly identical; so for all cases λ_e and c_e were evaluated for air at the logarithmic mean temperature between T_c and T_a.

*Table 2. Properties of fuels used in in calculation of ε**

Fuel	ρ *(g/cm³)*	*L* *(cal/g)*	*Q* *(cal/g)*	*i* *(g/g)*	*Q/i* *(cal/g)*	*B.pt* *(°C)*
Butanol-1	0·810	207·0	8051	2·59	3110	118
Heptane	0·684	121·6	10720	3·51	3060	98
2, 2, 4-Trimethylpentane	0·692	106·8	10672	3·51	3040	99
Pentanol-1	0·818	201	8420	2·72	3100	138
Dibutyl ether	0·773	185	8850	2·87	3080	142

*Transport properties of vapour film were taken as those of air at the log mean temperature between the flame and ambient temperature[15]; $c_e = 0{\cdot}271$ cal/g °C. $\lambda_e = 1{\cdot}56\times10^{-4}$ cal/sec cm °C. Since the drops were burned in air at one atmosphere, $Y_a = 0{\cdot}232$.

By introducing the composition values obtained from the Rayleigh equation into equation 1, the instantaneous burning-rate coefficients for burning drops of binary mixtures of interest were calculated. Examples of these values are presented in the form of theoretical burning-rate curves in *Figure 3*. Superimposed on the theoretical curves are points taken from the burning-rate measurements of drops of identical initial composition. In view of approximations made in selecting the vapour film properties used in the theoretical equation, the amount of agreement is satisfactory. One may conclude that after a brief ignition lag, a simple equilibrium batch distillation is an adequate description of the vaporization process which a two-component drop undergoes during combustion.

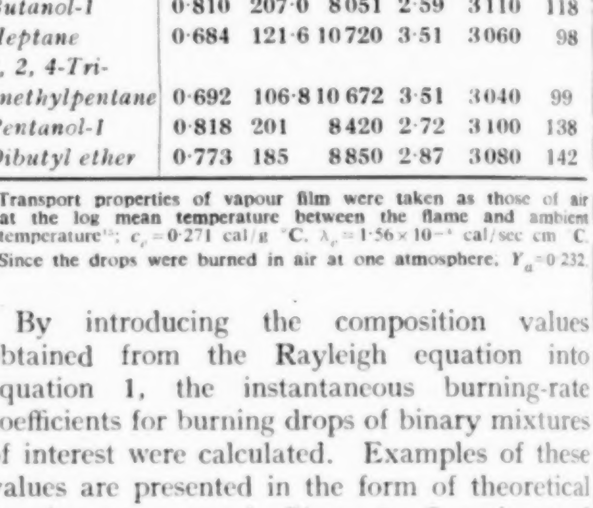

Figure 3. Theoretical burning-rate curves for various mixtures of butanol-1 and heptane in air (circles indicate experimental points)

---

*The liquid-vapour equilibrium diagrams, needed for this analysis, were determined in our laboratory for the fuel mixtures employed in this study. These distillation curves are presented in N.A.S.A. *Technical Note No. D-206*, see ref. 16.

In the light of these experiments, it is not surprising that the burning curves for drops of some multicomponent fuels of practical importance are quite linear. The explanation lies in the fact that the thermodynamic characteristics of all the components are such that the individual burning-rate coefficients vary over a narrow range. The practical fuels kerosine and jet fuel JP-4, for example, exhibit this characteristic (*Figure 4*).

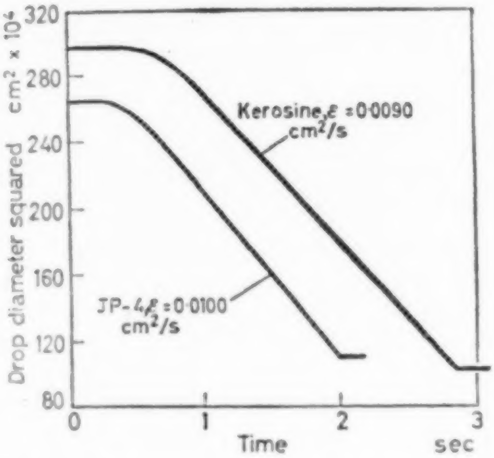

Figure 4. Burning-rate curves for kerosine and jet fuel JP-4 in air

Multicomponent fuel drops, composed of mixtures of aliphatic hydrocarbons with carbon chains varying between seven and sixteen atoms in length, were frequently observed to exhibit an unsteadiness while burning. We have termed this phenomenon 'disruptive combustion'. Visually, it appears as an oscillation of the burning drop on its supporting fibre, accompanied by ejection of small quantities of liquid fuel as an aerosol in random directions.

By photographing such burning drops with a motion picture camera, the phenomenon of disruptive combustion was shown to be associated with the formation of minute bubbles or vapour pockets in the liquid phase. The photographs of *Figure 5* are successive frames which reveal the formation and disintegration of such a disturbance. Frame I shows the quietly burning drop 1·149 sec after ignition; the dark spots are highlights produced by the strong side illumination of the drop. The beginning of a bubble is visible in the upper right quadrant of the drop in Frame II, and the subsequent growth of the disturbance can be followed in Frames III to V. The bubble apparently burst before Frame VI was exposed, and within the elapsed time of the next two frames the drop returned to quiescent combustion. The burning curve (*Figure 6*) for the same drop photographed in this sequence clearly shows the disruptions. In this case a small loss of material from the liquid phase had a negligible effect on the characteristic burning rate.

It is probable that this phenomenon is associated with the transfer of radiant energy from the flame into the interior of the drop. Calculations of temperature profiles have indicated that under conditions of absorption of incident radiant energy the temperature inside a drop can exceed that on the surface[12]. The contribution of radiative heat transfer to a burning drop was demonstrated experimentally by enhancing the absorptivity of the fuel. Unfortunately, compounds such as acetonitrile and phenylacetonitrile which absorb in the spectral region in which hydrocarbon flames emit strongly (∼4·5 microns), are quite insoluble in fuels such as those employed in this investigation. The addition of a particulate black dye which forms a slurry appeared to be the only way to change significantly the absorptivity of the hydrocarbon fuel drops[13]. To magnify the effect which a change in fuel absorptivity would produce in a burning drop, a fuel mixture was selected which burned quietly, but which possessed a wide boiling range and therefore a susceptibility to disruptive combustion. Small quantities of Apiezon W black wax were added to a 50–50 volume per cent mixture of nonane and tetradecane. Microscopic examination of the filtered solution, brown in colour, indicated that the colouring matter existed in the form of a particulate colloidal suspension within the drop. Absorption spectrograms of the coloured solution showed a small, uniform increase in optical density over the clear fuel in the 4 to 5 micron wavelength region*. Drops of the coloured solution burned

---

*It is possible, of course, that addition of colloidal carbonaceous material to the fuel may somewhat extend the spectral range of the flame emission.

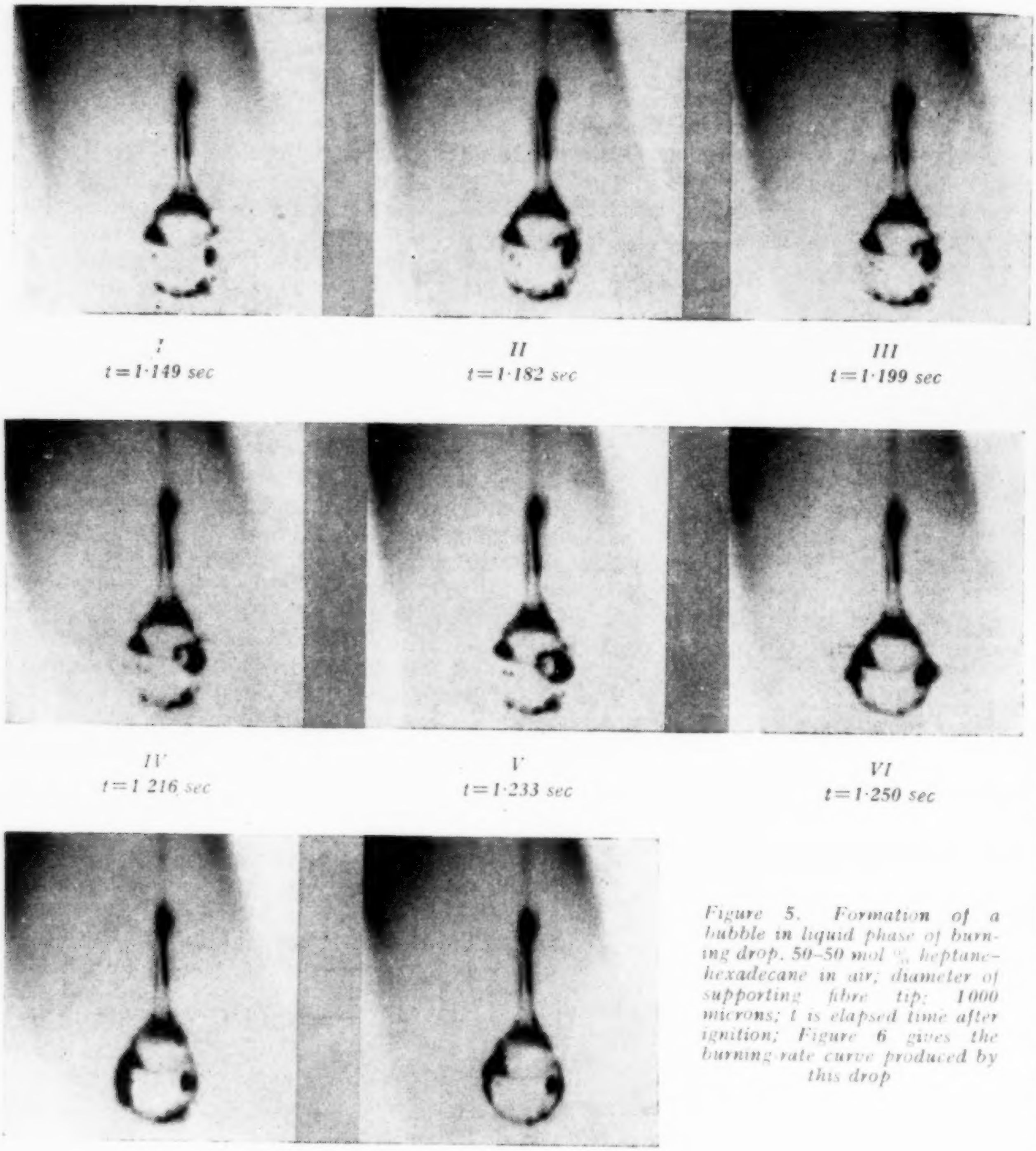

I
$t=1{\cdot}149$ sec

II
$t=1{\cdot}182$ sec

III
$t=1{\cdot}199$ sec

IV
$t=1{\cdot}216$ sec

V
$t=1{\cdot}233$ sec

VI
$t=1{\cdot}250$ sec

VII
$t=1{\cdot}267$ sec

VIII
$t=1{\cdot}284$ sec

Figure 5. Formation of a bubble in liquid phase of burning drop. 50–50 mol % heptane–hexadecane in air; diameter of supporting fibre tip: 1000 microns; t is elapsed time after ignition; Figure 6 gives the burning-rate curve produced by this drop

disruptively. To preclude the possible explanation that the particulate material within the drop provided nuclei for bubble formation, a parallel experiment was carried out in which finely ground alumina was dispersed in the fuel. The addition of these white reflective particles did not affect the quiescent combustion of the nonane–tetradecane mixture.

It appears, therefore, that radiant energy transfer to a liquid drop may result in the formation of a local hot zone within the liquid phase. If the drop is composed of fuels which boil over a sufficiently large range of temperature and are blended in a suitable quantitative ratio, this hot zone will cause the lower-boiling constituents to vaporize rapidly and disrupt the liquid/vapour interface. Apparently, internal circulation is not sufficient to eliminate these inhomogeneities caused by radiant heat transfer. Also, it is to be noted that, although radiative heat flux is independent of drop size, conductive heat flux from the flame to the liquid increases with decreasing drop diameter. Thus, the process of batch distillation observed in our measurements may change to one of non-equilibrium vaporization for drops much smaller than those employed in our studies. Under these conditions, the rates of convective transfer of mass and energy within the liquid phase may be slow in comparison to the mass burning rate. The diminished role of radiative heat transfer in small drops would decrease the likelihood of disruptive burning; but the diminution of convective mixing within the liquid phase would augment the tendency of a drop to burn disruptively as a result of increased conductive heat flux. Hence the dependence of disruptive combustion on drop diameter cannot be predicted quantitatively.

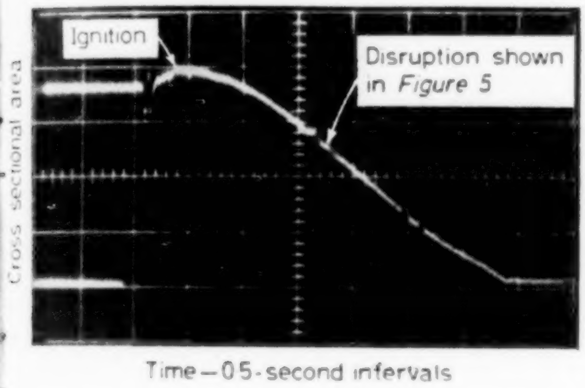

Figure 6. Burning-rate curve for binary fuel showing disruptive combustion. 50–50 mol % heptane–hexadecane in air. Compare with Figure 5

An estimate of the disruptibility of fuel drops in a combustion chamber should not be based entirely on the burning characteristics of single drops, for, in practice, a major portion of the radiant heat seen by a fuel cloud arises from the hot walls of the chamber. The spectral characteristics of such hot-wall radiation are quite different from the energy spectrum of a flame.

Discussion

It appears likely that the formation of tarry residues and carbonaceous 'cenospheres' from burning drops of heavy fuel oils is in part a consequence of the mechanism of batch distillation. Specifically, it has been shown that for those fuels for which the ratio of burning rate to thermal diffusivity of the liquid is small, the temperature at the centre of the droplet rapidly attains the surface temperature[14]. The effect of heat release or absorption, due to chemical reaction within the drop, on the mass burning rate and on the tendency of the fuel to form non-volatile reaction products may provide an answer to the query of optimum drop size in combustor sprays. If the separation of heavy fractions due to distillation is the principal cause of solid residues, it may be desirable to have extremely fine aerosols. In this connection, it may be possible to enhance atomization by using fuels which burn disruptively, provided, of course, that the disruption of the individual fuel drops does not interfere with the macroscopic stability of the combustion process.

This paper presents results obtained in a research project sponsored by the National Aeronautics and Space Administration, and in part presented at Berkeley in June 1958 to the Western States Section of the Combustion Institute.

References

[1] BLINOV, V. J. 'Change in the composition of binary liquid mixtures on burning'. *Dokl. Akad. Nauk S.S.S.R.* 1953, **89**, 101

[2] BURGOYNE, J. H. and RICHARDSON, J. F. 'Extinguishing burning at a wick by the use of non-inflammable liquids'. *Fuel, Lond.* 1950, **29**, 93

[3] WISE, H. and AGOSTON, G. A. *The Burning of a Liquid Droplet*, p 124. Advances in Chemistry Series, American Chemical Society: Washington, D.C., 1958

[4] WOOD, B. J. and WISE, H. 'Measurement of the burning constant of a fuel drop'. *J. appl. Phys.* 1957, **28**, 1068

[5] GODSAVE, G. A. E. 'Studies of the combustion

of drops in a fuel spray—the burning of single drops of fuel'. *Fourth Symposium (International) on Combustion*, p 818. Williams and Wilkins: Baltimore, 1953

[6] Wise, H., Lorell, J. and Wood, B. J. 'The effects of chemical and physical parameters on the burning rate of a liquid droplet'. *Fifth Symposium (International) on Combustion*, p 113. Reinhold: New York, 1955

[7] El Wakil, M. M., Priem, R. J., Brikowski, H. J., Myers, P. S. and Uyehara, O. A. 'Experimental and calculated temperature and mass histories of vaporizing fuel drops'. *Tech. Note Nat. Adv. Comm. Aero., Wash., No. 3490*. January 1956

[8] Lorell, J., Wise, H. and Carr, R. E. 'Steady-state burning of a liquid droplet II'. *J. chem. Phys.* 1956, **25**, 327

[9] Perry, J. H. *Chemical Engineers' Handbook*, p 580. McGraw-Hill: New York, 1950

[10] Smith, S. R. and Gordon, A. S. 'Studies of diffusion flames I'. *J. phys. Chem.* 1956, **60**, 759

[11] Smith, S. R. and Gordon, A. S. 'Studies diffusion flames II'. *J. phys. Chem.* 1956, **60**, 105

[12] Hottel, H. C., Williams, J. C. and Simpso H. C. 'Combustion of droplets of heavy liqui fuels'. *Fifth Symposium (International) on Combustion*, p 101. Reinhold: New York, 1955

[13] Berlad, A. H. and Hibbard, R. R. 'Effect radiant energy on vaporization and combustion liquid fuels'. *Res. Memor. Nat. Adv. Comm. Aero. Wash., No. E52I09*, November 1952

[14] Wise, H. and Ablow, C. M. 'Burning of a liqui droplet III. Conductive heat transfer within th condensed phase during combustion'. *J. chem Phys.* 1957, **27**, 389

[15] Agoston, G. A., Wood, B. J. and Wise, H 'Influence of pressure on the combustion of liqui spheres'. *Jet Propulsion*, 1958, **28**, 186

[16] Wood, B. J., Wise, H, and Inami. S. H. 'Heterogeneous combustion of multicomponent fuels' *Tech. Note Nat. Aero. Space Admin. No. D-206* Washington, D.C., November 1959.

Kinetic Parameters for the Hydrogen and Ethylene Flames from Flashback Measurements

B. FINE

Lewis Research Center, National Aeronautics and Space Administration, Cleveland, Ohio

(Received May 1959)

Values for the flame activation energy and an overall reaction order have been obtained for premixed hydrogen–oxygen and ethylene–oxygen flames with nitrogen and with argon as diluents; the values come from measurements of the change with pressure and flame temperature of the critical boundary velocity gradient for flashback. Measurements have been made for rich and stoichiometric hydrogen flames and for lean and stoichiometric ethylene flames. For hydrogen flames with nitrogen diluent an overall order of 2·3 is found; for ethylene flames with nitrogen diluent, the order obtained is 1·8. With argon diluent, values for the order are about 10 per cent lower for each flame. With nitrogen diluent the flame activation energy apparently increases with flame temperature; this increase is not found with argon diluent. For hydrocarbon flames the assumption that the initial equivalence ratio equals the effective equivalence ratio in the flame leads to an order of reaction with respect to oxygen that is considerably larger than unity. For hydrogen flames, that assumption is consistent with an oxygen order of unity.

Introduction

IN SEVERAL previous studies, the change of various properties of burner flames with pressure has been related to an overall order for the chemical reaction taking place within the flame[1, 2]. Frequently, the pressure dependence of the flame property increased with flame temperature. Thus, if one assumed that the flame reaction was described by a constant activation energy, the overall order likewise increased with flame temperature.

The present study is an attempt to examine in greater detail this apparent change of reaction order with flame temperature through measurement of the flashback of laminar burner flames. Measurements have been made with independent variation of pressure and flame temperature. This should permit a simultaneous determination of the overall order and activation energy for a flame reaction involving fuel and oxygen. In addition flashback measurements with variation of equivalence ratio have been made in an attempt to determine orders with respect to individual components of the initial mixture. Data are presented for premixed hydrogen–oxygen and hydrocarbon–oxygen flames with nitrogen, with argon, and with helium as diluents.

Theoretical Background

The critical boundary velocity gradient for flashback, g, has often been related to ϖ, the mean flame reaction rate, by the relation[1, 3]

$$ga \propto \varpi \qquad \ldots . [1]$$

where, for lean and stoichiometric flames, a is the volume concentration of fuel in the initial mixture and ϖ is defined as

$$\frac{1}{(T_f - T_0)} \int_{T_0}^{T_f} \omega \, dT$$

where T_f is the flame temperature and T_0 the initial gas temperature. Within the approximation of equation1, g gives a measure of ϖ independent of transport processes within the flame. Thus, if equation 1 is valid, the change of g with various experimental conditions should be related in a particularly simple fashion to the various parameters describing the flame reaction.

One may assume[4] that the mean flame reaction rate can be represented as

$$\varpi = k\mathbf{a}_1^m\mathbf{a}_2^n\mathbf{a}_3^l F_{\mathrm{III}}(T_f) \qquad \ldots [2]$$

where $\mathbf{a}_1$, $\mathbf{a}_2$ and $\mathbf{a}_3$ are, respectively, the effective volume concentrations of fuel, oxygen and diluent in the flame zone, k is a constant and F_{III} is some function of flame temperature. The fact that ϖ depends on initial temperature as well as flame temperature will be neglected here. In terms of mole fractions, x_i, equation 2 can be written as

$$\varpi = k'\mathbf{x}_1^m \mathbf{x}_2^n \mathbf{x}_3^l P^{m+n+l} F_{\text{II}}(T_f) \quad \ldots . [3]$$

where P is pressure and F_{II} is another function of flame temperature. If one combines equations 1 and 3 and introduces the equivalence ratio

$$\phi = (x_1/x_2)/(x_1/x_2)_{\text{stoich.}} \quad \ldots . [4]$$

one obtains

$$g \propto \mathbf{x}_1^{m+n} \mathbf{x}_3^l \mathbf{x}_1^{-1} (\phi)^{-n} T_0 P^{m+n+l-1} F_{\text{I}}(T_f) \quad . [5]$$

For any reactant whose proportion in the initial mixture is equal to or less than stoichiometric, the effective mole fraction, $\mathbf{x}_i$, will be proportional to the initial mole fraction x_i, differing by a factor of order of magnitude

$$(RT_f^2/E)/(T_f - T_0)$$

where E is an activation energy for the overall flame reaction[4]. For a reactant whose proportion in the initial mixture is greater than stoichiometric, the initial and effective mole fractions can be related by expressions of the form

$$\begin{aligned} \mathbf{x}_2 &= x_2 - \delta_2 x_1 \quad (\phi < 1) \\ \mathbf{x}_1 &= x_1 - \delta_1 x_2 \quad (\phi > 1) \end{aligned} \quad \ldots . [6]$$

where the δs describe the depletion of fuel or oxygen due to reaction in the flame zone[3]. Then the change of flashback gradient with, for example, oxygen concentration can be represented as

$$g \propto (x_2 - \delta_2 x_1)^n \quad (\phi < 1) \quad \ldots . [7]$$

If either δ_2 or the range of variation of x_2 is not too large, equation 7 can be approximated by

$$g \propto (x_2)^{n'} \quad \ldots . [8]$$

If δ_2, in addition to being reasonably small, is also positive, then $n' > n$. By use of equation 8, equation 5 can be written in terms of initial mole fractions as

$$g \propto x_1^{m+n-1} x_3^l (\phi)^{-n'} T_0 P^{m+m+l-1} F(T_f) \quad . [9]$$

Thus, the relation between n', an empirically determined exponent, and n, the order of reaction with respect to oxygen, depends on the relation between the initial equivalence ratio and the effective equivalence ratio in the flame zone.

Equation 9 applies only to lean and stoichiometric flames. However, one may derive an equation analogous to equation 9 for rich or stoichiometric flames. The result is

$$g \propto x_2^{m+n-1} x_3^l (\phi)^{m'} T_0 P^{m+n+l-1} F(T_f) \quad . . [10]$$

Here, m' is another empirical constant related in some fashion to the fuel order m, depending on the relation between initial and effective equivalence ratios.

If one defines the overall reaction order as

$$r = l + m + n \quad \ldots . [11]$$

then, for a given initial mixture, equations 9 or 10 can be written as

$$g \propto P^{r-1} F(T_f) \quad \ldots . [12]$$

Logarithmic differentiation with respect to pressure gives

$$\frac{\mathrm{d} \log g}{\mathrm{d} \log P} = (r-1) + \frac{\mathrm{d} \log F(T_f)}{\mathrm{d} \log P} \quad \ldots . [13]$$

in which the last term is generally a small correction. Equation 13 in turn can be written

$$\frac{\mathrm{d} \log g}{\mathrm{d} \log P} = (r-1) + \left[\frac{\partial \log F(T_f)}{\partial \log T_f}\right]_P \frac{\mathrm{d} \log T_f}{\mathrm{d} \log P} \quad . [14]$$

in which $[\partial \log F(T_f)/\partial \log T]_P$ depends on the flame temperature and activation energy E. According to the thermal quenching theory of A. E. Potter, Jr and A. L. Berlad[2] that derivative can be set approximately equal to $1{\cdot}125\, E/RT_f$. In order to evaluate the two unknowns r and $[\partial \log F(T_f)/\partial \log T_f]_P$ in equation 14, one needs independent determination of the change of g with pressure and flame temperature.

Expressions for the change of g with flame temperature can be obtained from consideration of equations **9** and **10**. Thus, if $l=0$ (that is, the reaction does not depend on inert constituents) the quantity

$$Y_1 = g\phi^{n'} x_1^{1-r} T_0^{-1}$$

should depend on flame temperature alone for lean and stoichiometric flames. For rich and stoichiometric flames, the quantity

$$Y_2 = g\phi^{-m'} x_2^{1-r} T_0^{-1}$$

should have the same dependence on flame temperature. These correlating functions Y_1 and Y_2 are similar in form to those devised by R. S. BROKAW and M. GERSTEIN[5] for correlating burning velocity, quenching distance and minimum ignition energy with flame temperature. Then, if g is obtained experimentally at constant pressure, a plot of either Y_1 or Y_2 against T_f^{-1} should give an activation energy and a value of $[\partial \log F(T_f)/\partial \log T_f]_P$. However, the value of r used in the correlation must be consistent with equation **13**. Since r is unknown, both r and $[\partial \log F(T_f)/\partial \log T_f]_P$ must be obtained in some simultaneous fashion. The resulting values of the overall order will be largely independent of the aforementioned assumption that $l=0$, since that assumption affects only the small correction term in equations **13** or **14**.

Experimental

The gas metering system, low-pressure combustion chamber and procedure for producing flashback have been described previously[1,6]. The main burner was a brass tube, 125 cm long and 1·89 cm in diameter which was water-cooled near the lip. In the present study, burner diameter was varied by using inserts 0·928, 1·016 and 1·459 cm in diameter.

Hydrogen (98–99 per cent H_2) and technical grade ethylene (95 per cent C_2H_4) were used as fuels. Oxidant mixtures were prepared by separately metering the flow of oxygen and diluent and mixing the flowing gases or were commercially prepared. All gases were obtained from tanks and used without further purification.

The critical boundary velocity gradient for flashback was computed as

$$g = 8\bar{U}/D$$

where $\bar{U}$ is the mean stream velocity at flashback and D the burner diameter[7].

Results

Description of results

Figures 1 to *4* show log g plotted against log pressure for stoichiometric hydrogen–oxygen–nitrogen flames (*Figure 1*), rich and stoichiometric hydrogen–oxygen–argon flames (*Figure 2*), lean and stoichiometric ethylene–oxygen–nitrogen flames (*Figure 3*) and lean and stoichiometric ethylene–oxygen–argon flames (*Figure 4*).

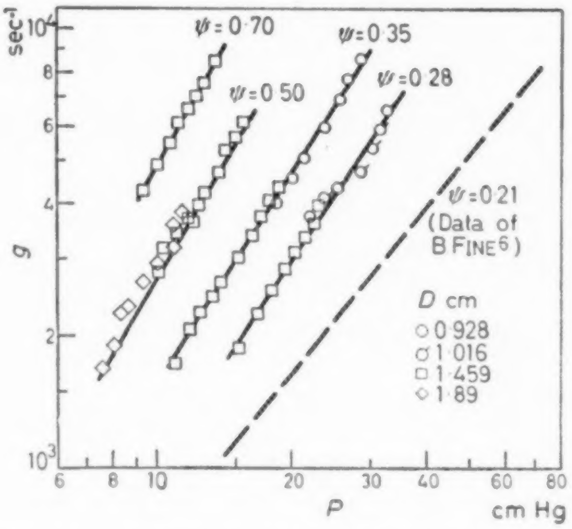

Figue 1. Flashback of stoichiometric H_2–N_2–O_2 *flames*

Figure 3 contains, in addition, results obtained by J. E. GARSIDE, J. S. FORSYTH, and D. T. A. TOWNEND[8] for stoichiometric ethylene–air flames. The higher values obtained in their study may be a result of their having used a burner whose lip was not cooled. One curve in *Figure 4* involves the use of helium rather than argon as diluent. However, it was established previously[1] that substitution of helium for argon did not change the critical flashback gradient.

Compositions of the various initial mixtures are designated by the equivalence ratio, ϕ, defined in equation 4 and the oxidant strength ψ defined as

$$\psi = x_2/(x_2 + x_3)$$

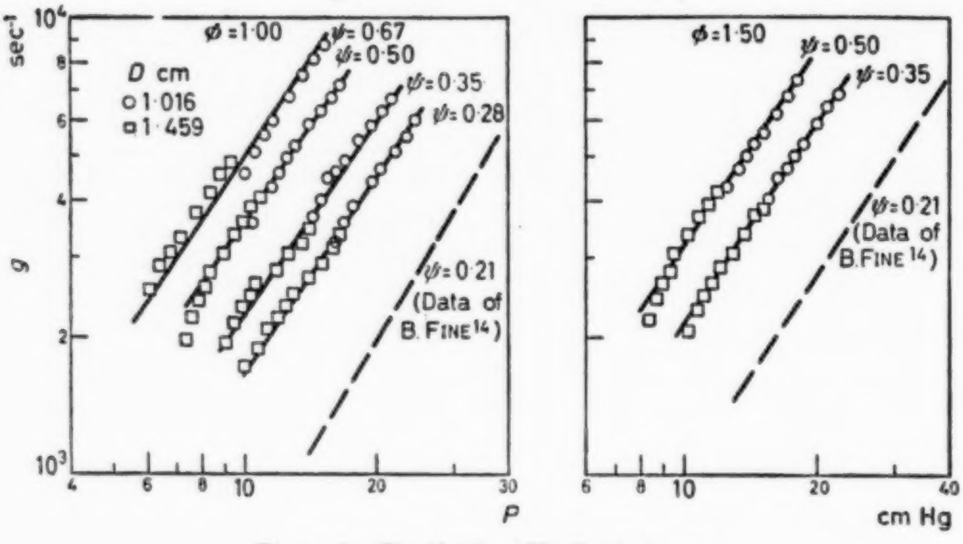

Figure 2. Flashback of H_2–O_2–A *flames*

Log-log pressure slopes, obtained from the data of *Figures 1* to *4*, are presented in *Tables 1* and *2*. They are given to two decimal places, although the significance of the second place is somewhat doubtful. Also shown in *Tables 1* and *2* are flame temperatures, calculated from a self-consistent set of thermal data by the method of ref. 9. Values shown for d log T_f/d log P are based on flame temperatures at 1 and 0·1 atmosphere.

It can be seen from *Figures 1* to *4* that critical flashback gradients are always independent of burner diameter where argon is used as diluent. A few exceptions have been found, however, with nitrogen as a diluent. For lean ethylene flames (*Figure 3*) at an oxidant strength of 0·67, values of g at constant pressure decreased with decreasing burner diameter even for the two largest burners available. The magnitude of the decrease was about 20 per cent. In

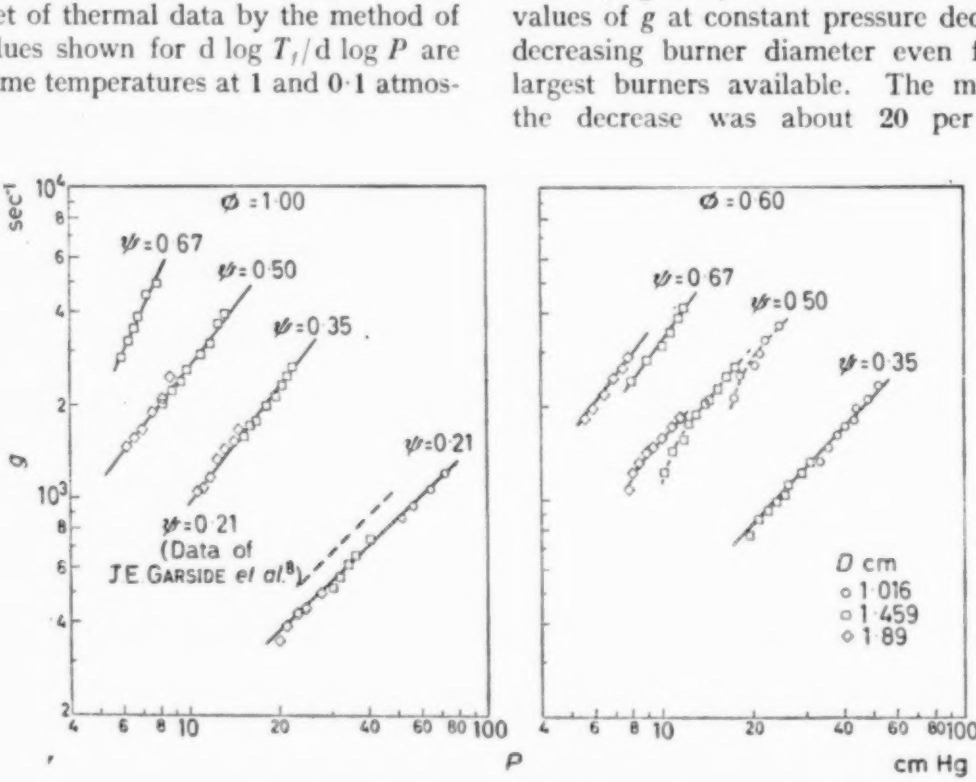

Figure 3. Flashback of C_2H_4–O_2–N_2 *flames*

Table 1. Correlation of critical flashback gradient g with flame temperature for hydrogen–oxygen flames; pressure, 15 cm of mercury

ψ	ϕ	*Diluent*	x_1	T_0 °K	T_f °K	$\frac{10^4}{T_f}$ °K^{-1}	$\frac{d \log T_f}{d \log P}$	g sec^{-1}	$\frac{d \log g}{d \log P}$	r	m'	Source of g	$\left[\frac{\partial \log F(T_f)}{\partial \log T_f}\right]_P$
0·21	1·50	N_2	0·129	298	2 230	4·484	0·0120	1 500	1·35		1·32	*Ref. 1*	—
0·21	1·00		0·148	298	2 322	4·307	0·0157	1 140	1·35	2·28	—	*Ref. 6*	3·4
0·21	1·50		0·129	659	2 430	4·115	0·0184	4 800	ca. 1·4		1·18	*Ref. 10*	—
0·28	1·00		0·180	298	2 500	4·000	0·0209	1 880	1·54	2·43		*This work*	5·3
0·28	1·60		0·148		2 371	4·218	0·0172	2 160	1·33		1·16	*Ref. 3*	—
0·35	1·00		0·205		2 602	3·843	0·0298	2 930	1·55	2·35	—	*This work*	6·8
0·49	1·44		0·205		2 691	3·716	0·0327	4 800	1·55		0·69	*Ref. 3*	—
0·50	1·00		0·250		2 726	3·668	0·0355	5 450	1·72	2·31	—	*This work*	11·4
0·70	↓	↓	0·292	↓	2 809	3·560	0·0391	10 000	1·79	2·21	—	*This work*	14·9
0·21	1·00	A	0·148	298	2 527	3·957	0·0275	1 300	1·50	2·24	—	*Ref. 14*	9·6
0·21	1·50		0·129		2 467	4·053	0·0207	1 750	1·49			*Ref. 14*	—
0·28	1·00		0·180		2 631	3·801	0·0326	2 930	1·44	2·14	—	*This work*	9·3
0·35	1·00		0·205		2 695	3·711	0·0351	3 910	1·40	2·09	—		9·0
0·35	1·50		0·171		2 652	3·771	0·0312	3 800	1·46		0·92		—
0·50	1·00		0·250		2 774	3·605	0·0383	6 200	1·39	2·13	—		8·8
0·50	1·50		0·200		2 725	3·670	0·0335	5 600	1·43		0·74		—
0·67	1·00	↓	0·285	↓	2 824	3·541	0·0399	8 875	1·50	2·16	—	↓	8·6

accordance with the conclusions of a previous discussion[3] of this effect only data for the larger of the two burners ($d = 1{\cdot}89$ cm) are used in the calculations which follow. For an oxidant strength of 0·50, results are complicated by partial quenching at low Reynolds numbers. However, at sufficiently high Reynolds numbers, it is seen that critical flashback gradients are still somewhat dependent on burner diameter, decreasing slightly with decreasing burner size. For stoichiometric ethylene and hydrogen flames with nitrogen diluent, at oxidant strengths near 0·7, data were obtained in only one burner. It is possible then that these values are too low by 20 per cent or more. This could not be checked because bigger burners could not be used.

Usually the log-log pressure slopes are constant for any single initial mixture. The most pronounced exception is noted in *Figure 3* where quenching at low Reynolds numbers apparently affected the results for $\psi = 0{\cdot}50$ and $\phi = 0{\cdot}60$.

Table 2. Correlation of critical flashback gradient g with flame temperature for hydrocarbon–oxygen flames; pressure 10 cm of mercury

ψ	ϕ	*Fuel*	*Diluent*	x_1	T_0 °K	T_f °K (10 *cm* Hg)	$\frac{10^4}{T_f}$ °K^{-1}	$\frac{d \log T_f}{d \log P}$	g sec^{-1}	$\frac{d \log g}{d \log P}$	r	n'	Source of g	$\left[\frac{\partial \log F(T_f)}{\partial \log T_f}\right]_P$
0·21	1·00	C_2H_4	N_2	0·0654	298	2 291	4·365	0·0165	180	0·92	1·81	—	*This work*	3·4
0·21				↓	615	2 400	4·165	0·0209	550	1·0	1·81		*Ref. 15*	9·1
0·35				0·104	298	2 586	3·867	0·0294	950	1·19	1·79	—	*This work*	14·1
0·50				0·143		2 728	3·664	0·0340	2 690	1·31	1·69	—		18·3
0·67	↓			0·182		2 811	3·557	0·0391	8 300	2·07	—	—	↓	—
0·50	0·80			0·118		2 664	3·754	0·0331	2 250	1·14	1·63	1·74	*Ref. 10*	15·6
0·35	0·60			0·0654		2 331	4·290	0·0153	420	1·02	1·91	1·45	*This work*	7·4
0·50				0·0909		2 552	3·949	0·0270	1 540	ca. 1·1	1·78	1·82		11·8
0·67	↓	↓		0·118		2 675	3·738	0·0331	3 940	1·31	1·74	1·76	↓	17·1
0·50	1·00	C_2H_2	↓	0·0909		2 691	3·716	0·0250	1 400	1·15	1·73	—	*Ref. 1*	17·1
1·00	0·85	↓	O_2	0·145	↓	2 829	3·534	0·0406	5 000	1·40	—	—	*Ref. 1*	—
0·21	1·00	C_2H_4	A	0·0654	298	2 512	3·981	0·0286	339	1·07	1·63	—	*This work*	15·6
0·35				0·104		2 682	3·729	0·0352	1 500	1·07	1·56	—		14·6
0·50				0·143		2 782	3·595	0·0386	3 230	1·11	1·57	—		14·1
0·67	↓			0·182		2 843	3·517	0·0407	6 050	1·09	1·54	—		13·9
0·50	0·50			0·0770		2 563	3·902	0·0292	1 370	1·05	1·59	1·31		15·9
0·67	0·70	↓	↓	0·128	↓	2 767	3·614	0·0377	4 450	1·08	1·54	1·38	↓	14·3

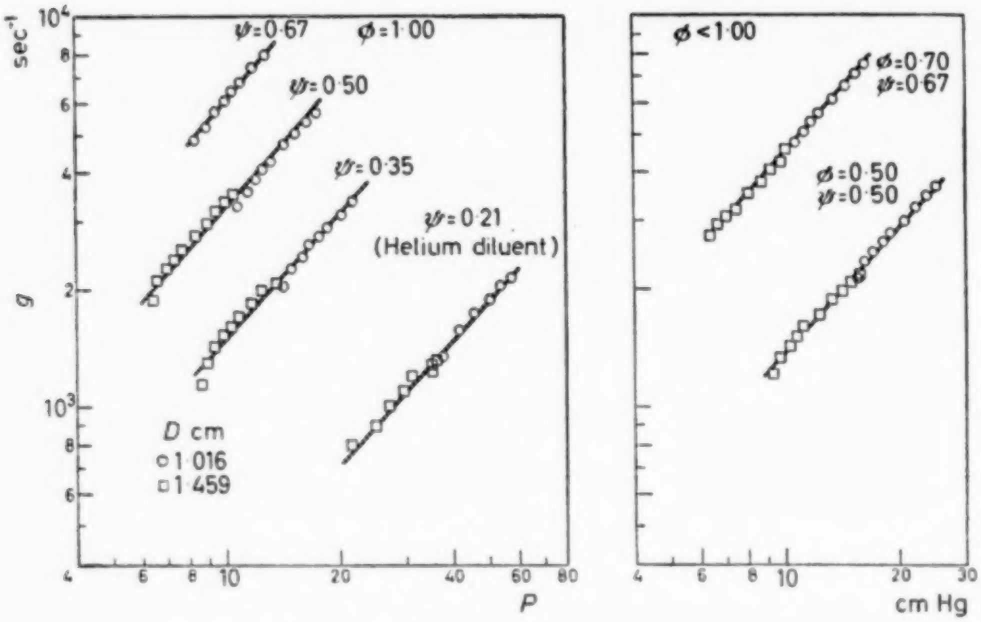

Figure 4. Flashback of C_2H_4–O_2–A *flames*

It should be noted that, with nitrogen as diluent, pressure slopes increase significantly for both hydrogen and ethylene flames with increasing levels of flame temperature. This is the effect which had been previously observed in a less systematic fashion[1]. With argon as diluent, however, no progressive change is found in the pressure slopes with flame temperature or equivalence ratio. The pressure slopes appear to depend only on the fuel type, being larger for hydrogen flames than for ethylene flames.

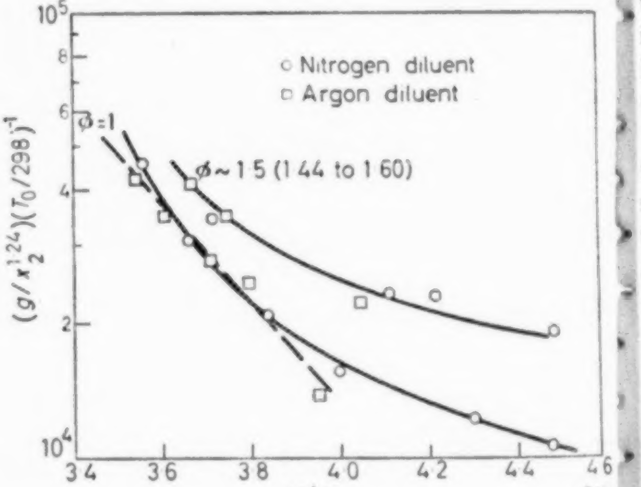

Figure 5. Correlation of g with flame temperature for rich and stoichiometric hydrogen–oxygen flames

Results for hydrogen flames

Table 1 shows values of g taken from *Figures 1* and *2* at a pressure of 15 cm of mercury; also shown are corresponding values of initial oxygen mole fraction and of flame temperature. The data include stoichiometric flames and flames near an equivalence ratio of 1·5. *Figure 5*, in turn, shows a plot against $1/T_f$ of

$$\log [g(T_0/298)^{-1}x_2^{1-r}]$$

This quantity represents either of the correlating functions Y_1 or Y_2 for stoichiometric flames. As an approximation for r, 2·24 was chosen. This is about the value obtained from the variation with pressure of flashback, burning velocity or quenching distance for hydrogen–air flames[1]. It is seen that the stoichiometric points lie on a smooth curve independent of the diluent, with the possible exception of the point for $\psi = 0{\cdot}21$ with argon as diluent; this point is low by about 10 per cent. The data on the rich side describe a second curve which lies above the first and is likewise roughly independent of the diluent. The displacement of the rich points from the stoichiometric curve should permit determination of m' in the correlating function Y_2. Values obtained for each rich point are shown in *Table 1*. The values of m' are not constant, but decrease with increasing flame temperature; this is a consequence of the fact that the two curves are not parallel. Thus, the increase in $\log [g(T_0/298)^{-1}x_2^{1-r}]$ with equivalence ratio agrees only qualitatively with the prediction of theory. The failure to obtain a constant value of m' must be attributed to an error either in applying the theory or, possibly, in calculating flame temperatures. There is no likely justification for citing the results as evidence either for a change of reaction order with respect to hydrogen or a change in the degree of depletion of hydrogen in the flame zone with temperature.

It is apparent that both plots in *Figure 5* show much curvature, considerably more than can be accounted for by pre-exponential terms in $F(T_f)$. One interpretation of this curvature would be that the flame activation energy increases with flame temperature. However, at least for flames with nitrogen as diluent, one may relate the curvature in the plots against $1/T_f$ and the change of pressure slope with flame temperature. Thus, in *Figure 5*, for stoichiometric flames, one may take slopes along the appropriate curve and evaluate rough but adequate values of $[\partial \log F(T_f)/\partial \log T_f]_P$ for any value of T_f. These values are shown in *Table 1* for stoichiometric hydrogen–oxygen–nitrogen flames. When these values are used in equation **14**, they permit determination of a better set of approximations to r. These values, given in *Table 1*, show no trend with flame temperature and average about 2·3. This value is sufficiently close to the original assumed value (2·24) that no further approximation is necessary.

Although the data with argon and with nitrogen as diluents generally correlate well, there is no real evidence that the argon data, as plotted in *Figure 5*, will show curvature when considered alone. This situation is somewhat indeterminate because the range of flame temperatures covered with argon as diluent is much smaller than that with nitrogen. However, if we admit that the point for $\psi = 0{\cdot}21$ with argon as diluent does lie significantly below the stoichiometric nitrogen curve, then all five stoichiometric points with argon as diluent are adequately described by a straight line corresponding to an activation energy of 43 kcal/mole. Since $[\partial \log F(T_f)/\partial \log T_f]_P \approx 1{\cdot}125E/RT_f$, one may use equation **14** to obtain a set of values for r. As shown in *Table 1*, these are independent of flame temperature and average $r = 2{\cdot}15$. The small difference in overall order between flames with nitrogen and those with argon as diluents is probably due to oversimplification in application of the theory.

Since the plots of $\log [g(T_0/298)^{-1}x_2^{1-r}]$ against $1/T_f$ are not parallel with change of equivalence ratio, the slopes will depend on equivalence ratio as well as on flame temperature. Therefore, unless there is some compensating change in $d \log T_f / d \log P$, the value of r will depend on equivalence ratio. In practice, however, no significant change in overall order is found between equivalence ratios of unity and about 1·5.

In summary, then, flashback data for stoichiometric hydrogen–oxygen–argon flames are described by a constant activation energy and a constant overall order based on a pressure slope for the critical flashback gradient which is independent of flame temperature. The use of nitrogen as diluent gives a variable pressure slope and an apparently variable activation energy whose effects combine to give a constant overall order.

Results for ethylene flames

Table 2 shows values of g taken from *Figures 3* and *4* at a pressure of 10 cm of mercury. Also shown are corresponding values of initial mole fraction of fuel and flame temperature. The range of data includes stoichiometric and lean ethylene–oxygen flames with nitrogen and argon diluents. It also includes results for propane–oxygen–nitrogen flames taken from ref. 1 and for ethylene–air flames at elevated initial temperature taken from ref. 10. The data shown in *Table 2* are plotted in *Figure 6* as the correlating function Y_1 against $1/T_f$. As a first approximation, it was assumed that $r = 2$.

Values of n' were obtained in the same way that values of m' were obtained for hydrogen flames. The quantity $(g/x_1)(T_0/298)^{-1}$ was plotted against $1/T_f$. Then values of n' were determined so that results for lean flames fell on the curve described by the results for stoichiometric flames.

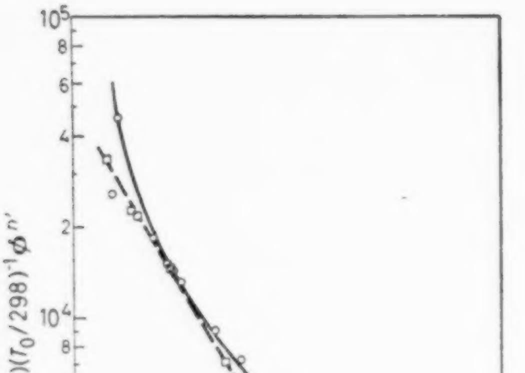

Figure 6. Correlation of g with flame temperature for lean and stoichiometric hydrocarbon–oxygen flames

As with hydrogen flames, the data show a rough correlation with change of diluent. However, the data for nitrogen diluent alone show considerable curvature, whereas those for argon diluent follow a straight line whose slope corresponds to an activation energy of about 70 kcal/mole. This behaviour is similar to that found for hydrogen flames.

The point for stoichiometric propane–oxygen–nitrogen with $\psi = 0{\cdot}50$ falls in line with the data for ethylene flames; this suggests that the correlation may be more or less general for hydrocarbon flames. However, the point for propane–oxygen ($\psi = 1{\cdot}00$) at an equivalence ratio of 0·85 falls considerably below the nitrogen curve. The reason for this is not known.

Values obtained for n' are shown in *Table 2*. The values obtained with nitrogen as diluent are reasonably constant and average 1·69; the two values obtained with argon diluent are quite close to each other and average 1·35. Thus, the behaviour of hydrocarbon flames with change of equivalence ratio is much simpler than for hydrogen flames.

With nitrogen diluent the plot against $1/T_f$ for hydrocarbons shows about the same degree of curvature as that for the hydrogen data. The fact that, for a given flame temperature, $[\partial \log F(T_f)/\partial \log T_f]_p$ is actually greater for hydrocarbon than for hydrogen flames is consistent with the usual observation that apparent activation energies are greater for hydrocarbon flames than for hydrogen flames. By evaluating slopes at given values of T_f and using equation 14, one may once again obtain a set of good approximations to r. These are shown in *Table 2*. (No orders were calculated at the highest temperatures, since the slope of the curve was too large to permit evaluation of

$$[\partial \log F(T_f)/\partial \log T_f]_p$$

with any accuracy.) The values obtained average 1·77 and show no trend with temperature. This average value agrees well with values estimated from other flame properties[5, 11].

For argon diluent, the computation of

$$[\partial \log F(T_f)/\partial \log T_f]_p$$

in the determination of the overall order is based on the straight line through the corresponding data and the assumption that

$$[\partial \log F(T_f)/\partial \log T_f]_p \approx 1{\cdot}125E/RT_f$$

The values obtained for r shown in *Table 2* average 1·57, independent of flame temperature. Thus, for both hydrogen and hydrocarbon flames, the value obtained for the overall reaction order is slightly less with argon as diluent than with nitrogen.

In summary, several points of similarity are found in the correlation of critical flashback gradients with pressure and flame temperature for hydrogen and hydrocarbon flames. For both flames with nitrogen as diluent, the log-log pressure slope of the critical flashback gradient increases with flame temperature. This increase is offset by a corresponding increase in the apparent activation energy, so that the overall order is independent of flame temperature. For both flames with argon as diluent, the log-log pressure slope and apparent activation energy are independent of flame temperature and yield an overall order which is likewise constant. The orders obtained with argon as diluent are about 10 per cent lower than those with nitrogen as diluent.

Discussion of Results

Comparison with other data

The most striking result of treating flashback data in terms of a Semenov-type theory is the apparent increase of the flame activation energy with temperature for flames diluted with nitrogen. It is of interest, then, to see whether data for other properties of burner flames yield such a result when treated in a similar way. Correlations of burning velocity for hydrocarbon–oxygen–nitrogen flames reported by R. S. Brokaw and M. Gerstein[5] and by E. S. Golovina and G. G. Fyodorov[12] show no curvature; the quenching distance correlation of Brokaw and Gerstein likewise shows no curvature. Thus the curvature appears to be specific to flashback measurements with certain diluents which include nitrogen but not argon or helium.

The activation energies obtained with argon as diluent are about twice as large as those generally assumed or determined from other properties of flames with nitrogen as diluent[12]. Since burning velocity and quenching distance have not been measured over a large range of flame temperature with argon as diluent, direct comparison is not possible in this case.

Significance of m' and n' values

In a previous report[3] values of m', n' and r were obtained for hydrogen–oxygen–nitrogen flames. The value of r was obtained from the same data and in almost the same manner as in this article. However, in that report n was obtained by observing the change of g as nitrogen was progressively replaced by oxygen at a constant lean mole fraction of hydrogen. It was found that the flame temperature changed by less than 50°K between $\phi = 1{\cdot}00$ and $\phi = 0{\cdot}35$. A recalculation of flame temperatures in terms of more recent thermal data has yielded values which vary by less than 30°K over that range of composition. The value previously obtained for n', 0·92, suggested that the order with respect to oxygen was close to unity. Certainly, the oxygen order could not be much larger than unity; if it were, equations 7 and 8 show that δ_2 would be negative and, thus, the effective mole fraction of oxygen in the flame would be greater than in the initial mixture. It is possible that the oxygen order is significantly less than unity. This would imply, on the basis that the overall order was 2·3, that the order with respect to hydrogen was at least twice as large as that for oxygen.

If it is assumed that δ_2 in equation 7 is negligibly small, then, for hydrogen flames the order with respect to oxygen is about 0·9. In that case, the value predicted for m, the order with respect to hydrogen, is about 1·4. This value was actually obtained in ref. 3 from measurement of the change of g as nitrogen was progressively replaced by hydrogen at constant mole fraction of oxygen for equivalence ratios greater than unity. It was hoped that in this procedure as well as in the other, flame temperature would remain nearly constant. However, it was observed that, in this case, flame temperatures increased by more than 60°K between $\phi = 1{\cdot}00$ and $\phi = 1{\cdot}59$. The effect of this temperature change was neglected. Recalculation of temperatures has shown that the increase was actually somewhat larger, about 90°K. Detailed examination of *Table 1* and *Figure 5* will show that this increase in flame temperature is closely related to the failure of the correlation of hydrogen flames with equivalence ratio for equivalence ratios greater than one. It should be pointed out, then, that the failure to correlate successfully flashback data for rich hydrogen–oxygen flames with change of flame temperature does not impair the validity of orders of reaction determined in ref. 3, since those values could have been obtained without use of data for rich flames.

A few points may be noted with regard to the values of n' found for hydrocarbon flames.

The expected order of reaction with respect to oxygen is about unity. That n' is significantly larger than unity both with nitrogen and with argon as diluents suggests that the effective equivalence ratio in the flame zone is significantly smaller than the initial equivalence ratio. This follows from equations **7** and **8**. In this respect, the behaviour of hydrocarbon and hydrogen flames appear to be different. The fact that the value of n' obtained in ref. **3** for hydrogen flames was very close to unity' indicated that initial and effective equivalence ratios were equal. For hydrocarbon–oxygen–nitrogen flames, on the other hand, if one assumes that the flame reaction is first order in oxygen, an initial equivalence ratio of, for example, 0·6 corresponds to an effective equivalence ratio of 0·42. This effective degree of depletion in the flame zone of the reactant in excess agrees well with that found by Weil and Ellington from measurement of methane–oxygen–nitrogen burning velocities (equations 11 of ref. **13**).

References

[1] FINE, B. *Combustion & Flame*, 1958, **2**, 253

[2] POTTER, A. E., Jr and BERLAD, A. L. *Sixth Symposium (International) on Combustion*, p 27 Reinhold: New York, 1957

[3] FINE, B. *Nat. Aero. Space Admin. Memor. No. 12 23–58E*, 1959

[4] SEMENOV, N. N. *Usp. fiz. Nauk S.S.S.R.* (*Ad phys. Sci., Moscow*), 1940, **24**, 433; translation a *Tech. Memor. Nat. Adv. Comm. Aero., Wash. No. 1026*, 1942

[5] BROKAW, R. S. and GERSTEIN, M. *Sixth Symposiu (International) on Combustion*, p 66. Reinhold: New York, 1957

[6] FINE, B. *Tech. Note Nat. Adv. Comm. Aero Wash, No. 3833*, 1956

[7] LEWIS, B. and VON ELBE, G. *Combustion, Flam and Explosions of Gases*, p 279. Academic Press New York, 1951

[8] GARSIDE, J. E., FORSYTH, J. S. and TOWNEND D. T. A. *J. Inst. Fuel*, 1945, **18**, 175

[9] HUFF, V. N., GORDON, S. and MORRELL, V. E. *Rep. Nat. Adv. Comm. Aero., Wash., No. 1037*, 1951

[10] FINE, B. *Industr. Engng Chem.* (*Industr.*), 1959, **51**, 564

[11] LONGWELL, J. P. and WEISS, M. A. *Industr Engng Chem.* (*Industr.*), 1955, **47**, 1634

[12] GOLOVINA, E. S. and FYODOROV, G. G. *Sixth Symposium (International) on Combustion*, p 88 Reinhold: New York, 1957

[13] WEIL, S. A. and ELLINGTON, R. T. 'A study of the fundamentals of combustion'. *Rep. Illinois Inst. Technol. No. 1*, 1956

[14] FINE, B. *Tech. Note Nat. Adv. Comm. Aero., Wash., No. 4031*, 1957

[15] DUGGER, G. L. *Rep. Nat. Adv. Comm. Aero., Wash., No. 1061*, 1952

Activation Energy and Reaction Order in Methane–Oxygen Flames

H. VANDENABEELE, R. CORBEELS and A. VAN TIGGELEN

Department of Inorganic Chemistry, University of Louvain, Belgium

(Received June 1959)

Flame propagation velocities and temperatures have been measured in preheated and unpreheated methane–oxygen mixtures at different mixture strengths and varying dilutions with nitrogen. An activation energy of 38 kcal can be derived from these measurements. The order of the reaction with respect to oxygen is 1·4 and with respect to methane, –0·4. These parameters (orders and activation energy) are ascribed to the branching process. The reaction mechanism is discussed.

Introduction

THE general relation which has been proposed[1] for the flame propagation velocity can be put in the following formula

$$V_0=\frac{K_0T_0}{T_m^{1/2}}\left[\frac{(A)^a\,(B)^b}{P^{a+b}}\exp\left(-\frac{E}{RT_m}\right)\right]^{\frac{1}{2}}\quad\ldots[1]$$

where T_0 denotes the room temperature at which the gas flows are measured, T_m is the mean temperature of flame front and

$$T_m=T_i+0{\cdot}74\,(T_f-T_i)$$

Here T_f is the flame temperature and T_i the initial temperature of the unburnt gases, (A) and (B) are the partial pressures of oxidant and fuel, respectively. P denotes total pressure, and a and b are respectively the reaction orders with respect to oxidant and fuel; E is the overall activation energy of the branching reaction. It should be borne in mind that the sum $(a+b)=i$ corresponds to the total overall order of the branching process minus unity since the branching is also first order with respect to the chain carrier concentration[1].

From the point of view of reaction kinetics two important parameters are to be measured: activation energy E and reaction orders a and b.

Determination of activation energy

The determination of an activation energy involves in principle the observation of a series of experiments which are identical in respect of concentration and pressure but which occur at different temperatures. This, of course, can be done, for example, by preheating the gases which feed the burner; it suffices then to measure T_i, T_f and V_0.

For such a series of experiments equation 1 can be written in a logarithmic form

$$\log V_0+\tfrac{1}{2}\log T_m$$
$$=\text{constant}-E\log e/2RT_m\quad\ldots.[2]$$

Plotting the LHS against $1/T_m$, a straight line must be obtained and its slope gives the value of E. This method has its limitation: the temperature of the preheated gases must remain below a certain value to prevent any slow reaction which would alter the mixture composition.

A second method has a wider applicability: the flame temperature can be lowered by the addition of an inert gas. If the physical properties of the inert gas do not differ too much, the value of K_0 (in equation 1) remains unaffected, and we have

$$V_0=\frac{K_0T_0}{T_m^{1/2}}\left[\frac{(A)^a\,(B)^b}{[(A)+(B)]^i}\,\frac{[(A)+(B)]^i}{P^i}\exp\left(-\frac{E}{RT_m}\right)\right]^{\frac{1}{2}}\quad\ldots.[3]$$

In this equation the symbols (A) and (B) are used for partial pressures and $i=(a+b)$.

If we consider now a series of mixtures at increasing dilution but with a constant ratio of fuel/oxidant, we then have that $[(A)^a+(B)^b]/[(A)+(B)]^i$ remains constant and since

$$Y^i=\frac{[(A)+(B)]^i}{P^i}=\left(\frac{100-\%\,\text{inert}}{100}\right)^i$$

we obtain finally

$$\log V_0 + \tfrac{1}{2} \log T_m - \tfrac{1}{2}\, i \log Y = \text{constant} - E \log e / 2RT_m \quad \ldots . [4]$$

Once again E is given graphically by plotting the LHS against $1/T_m$.

The only difficulty lies in the choice of the value of i, the total order with respect to the reacting gases. A linearity test[2, 3] makes it possible in certain cases to choose between some possible values of i; all ambiguity will disappear from the determination of a and b as explained in the next paragraph.

Determination of reaction order

The simplest method of determining the partial reaction orders is to compare the reaction velocities in mixtures which differ only by the partial pressure of the substance for which the order is to be determined; all other conditions must be kept identical (temperature, total pressure and partial pressures of the other reacting species).

This method cannot be applied to flames since the flame temperature depends precisely on the composition of the mixture. The only way to compensate the change of temperature, when modifying the composition, is to preheat the gas mixture: the preheating must be such as to make the mean temperature constant for the whole series of experiments. Therefore the initial temperature T_i will have to be adjusted to obtain a flame temperature T_f which, in combination with T_i, obeys the relation

$$\text{constant} = T_m = T_i + 0{\cdot}74\ (T_f - T_i)$$

When the series of experiments corresponds to (B) constant and (A) variable, or vice versa, the following equations may respectively be written:

$$\log V_0 = \text{constant} + \tfrac{1}{2} a \log (A) \quad \ldots [5]$$

or

$$\log V_0 = \text{constant}' + \tfrac{1}{2} b \log (B) \quad \ldots [6]$$

The order a (or b) will be derived graphically by plotting $(\log V_0)$ against $\log (A)$ [or $\log (B)$]. Evidently in order to keep (A) [or (B)] constant while (B) [or (A)] varies, a certain amount of inert gas M must be added such that

$$(A)\% + (B)\% + (M)\% = 100$$

This means that in a series where (A) increases and (B) remains constant, (M) must decrease complementarily and the order a will be derived from the results obtained.

The eventual existence of a reaction order with respect to the total pressure will be derived from a series of experiments performed with the same mixture but at different pressures: the burner must, of course, be enclosed in a vessel maintained at the different desired pressures.

However, in most cases[4], the burning velocity does not seem to vary much with pressure: it means that the order c with respect to pressure should be near to zero. Most likely the slight dependence of V_0 on pressure, which is sometimes observed, is rather to be explained either by the variation of physical factors included in the constant K_0 in equation 1, or by the variation of flame temperature when the pressure is modified.

The partial orders a and b are not necessarily constant when the composition of the burning mixture varies between wide limits; this results from the fact that equation 1 is a simplified form of a more general equation[1] which will be discussed in the last part of this paper. The possible variation of a and b (while their sum, $a+b$, remains constant and equal to i) when the ratio of fuel to oxidant is modified can be shown from a general analysis of all values of V_0 and T_m in terms of general reaction kinetics after the determination of the activation energy as explained above. Equation 3 can be written as

$$\frac{V_0 T_m^{1/2}}{K_0 T_0} [\exp (E/RT_m)]^{\frac{1}{2}} = \left[\frac{(A)^a\,(B)^b}{P^{a+b}}\right]^{\frac{1}{2}}$$

Knowing that $a+b=i$ we obtain, after a few transformations, the logarithmic equation

$$2 \log V_0 + \log T_m + 0{\cdot}4343E/RT_m - i \log (B)/P = 2 \log K_0 T_0^{+}\ a \log [(A)/(B)] \quad \ldots . [7]$$

Once the activation energy is known, the LHS of this equation can be calculated for any mixture, that is for any ratio of fuel to oxidant and any dilution of a given fuel–oxidant mixture. If we then plot the values of the LHS against $\log [(A)/(B)]$, a curve can be obtained; the slope of this curve at any given ratio

$(A)/(B)$ gives the order a with respect to oxygen at the given composition. By subtracting a from i the corresponding order b with respect to the fuel is obtained directly.

It should be pointed out that in all flames (except those of hydrogen) which have been studied the value of i is equal to unity[2, 3]. This value has also been verified in the results which have been obtained in this work. In a theoretical paper[1] it was shown that the sum $(a+b)$ represents the global apparent order minus unity of the branching reaction.

The principles which are emphasized here have been applied to a complete experimental study of methane–oxygen flames.

Experimental

Flame velocities were determined by the total area method applied to the schlieren cone[5] for all flames in mixtures where the preheating temperature remained less than about 500°K. At higher preheating temperatures the schlieren image can no longer be distinguished from the luminous cone and it was necessary, for these flames, to calculate the flame velocity from the inner surface of the conical image obtained by photographing the flame.

The coalescence of schlieren and luminous image, as soon as the temperature of the fresh gases becomes larger than about 500°K, corresponds to our previous observations concerning the mean temperature of the region where the schlieren image is formed; some estimations[5] were made according to which this temperature lies between 500 and 600°K. The exact position of the schlieren image has been investigated by F. J. WEINBERG[6].

The preheating was achieved by placing the whole length of the circular burner (about 1 m) in a constant temperature oven. Up to one half of its length the burner was filled with obstacles of inert material: the gas flow was made laminar in the second half of the tube whose opening was conical. The measurement of the preheating temperature was made, after each measurement of flame velocity, by means of a thin thermocouple placed 1 mm deep in the burner immediately after having extinguished the flame.

Flame temperatures were measured by the classical sodium line reversal method[5]: sodium salt was introduced with one of the mixture constituents (nitrogen) by means of a heated sodium borate bead. All gases were commercial, purity 99 per cent.

The gas flows were measured at room temperature (293°K) by means of frequently calibrated rotameters.

Results

(a) *Unpreheated mixtures*

Table 1 contains all our experimental results obtained from experiments on unpreheated methane–oxygen mixtures.

Table 1. Flame temperatures and burning velocities in unpreheated mixtures
$T_i = 293°K$

$\frac{CH_4}{CH_4+O_2}$	% N_2	T_f °K	T_m °K	V_0 cm/s
0·27	57·5	2370	1830	87·5
0·27	60	2330	1800	77·5
0·27	62·5	2265	1752	65
0·27	65	2180	1689	51
0·30	57·5	2460	1896	100·5
0·30	60	2415	1863	90·5
0·30	62·5	2350	1815	76
0·30	65	2275	1759	61
0·33	57·5	2520	1941	104
0·33	60	2480	1911	94
0·33	62·5	2410	1859	81
0·33	65	2325	1796	66

(b) *Preheated mixtures*

Since the gas flows are always measured by means of rotameters at room temperature, the flame velocities, V_0, are not the values which should represent the flame velocity with respect to the gases measured at the initial T_i temperatures. These values are not mentioned in *Tables 2* and *3*, since the application of formulae 2, 5 and 6 in the next section implies only the knowledge of V_0. The results reported in *Table 2* concern flames with constant concentration of methane (10 per cent) and different concentrations of oxygen (from 20 to 35 per cent); for each different oxygen content the preheating temperatures T_i varied from about 350°K to about 700°K.

In *Table 3* are given the results of flames in mixtures where the percentage of oxygen was kept constant while the percentage of methane

Table 2. ***Flame temperatures and burning velocities in preheated mixtures. Percentage of methane constant at 10 per cent***

$\frac{CH_4}{CH_4+O_2}$	% N_2	T_i °K	T_f °K	T_m °K	V_0 cm/s
0·308	67·5	356	2245	1754	54
		407	2280	1793	57
		501	2300	1832	63
		579	2333	1877	70
		654	2387	1936	80
0·286	65	382	2270	1779	66
		455	2310	1828	72
		545	2327	1864	81
		609	2360	1905	90
		702	2392	1953	104
0·25	60	353	2314	1804	76
		421	2342	1843	81
		507	2382	1894	89
		580	2407	1932	97
		678	2445	1986	111
0·222	55	354	2324	1813	88
		426	2355	1853	93
		512	2400	1909	100
		588	2435	1955	108
		680	2463	1999	121

Table 3. Flame temperatures and burning velocities in preheated mixtures. Percentage of oxygen constant at 25 per cent

$\frac{CH_4}{CH_4+O_2}$	% N_2	T_i °K	T_f °K	T_m °K	V_0 cm/s
0·242	67	475	2162	1723	54
		606	2230	1808	73
		737	2285	1883	91
0·286	65	382	2270	1779	66
		455	2310	1828	72
		545	2327	1864	81
		609	2360	1903	90
		702	2392	1953	104
0·305	64	343	2346	1825	75
		388	2370	1855	80
		484	2400	1902	92
		571	2445	1958	102
0·333	62·5	346	2422	1882	85
		383	2448	1901	89
		463	2466	1945	97
		539	2492	1984	106

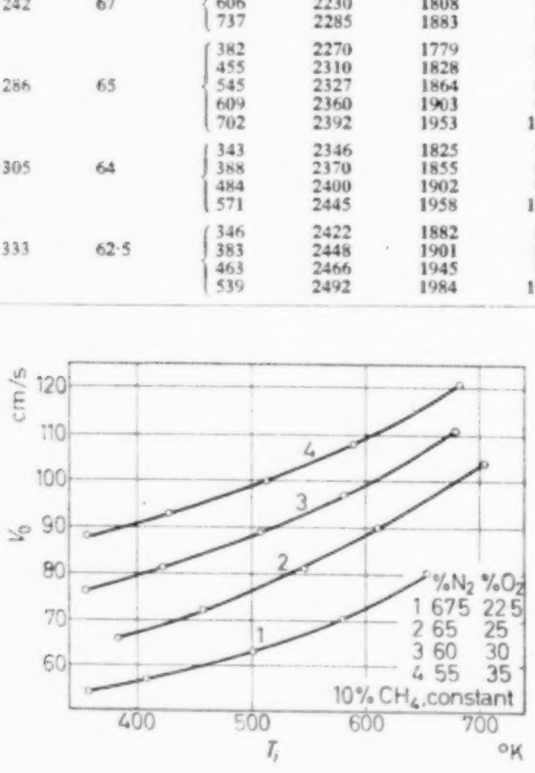

Figure 1. Burning velocities at constant methane concentration versus initial temperature

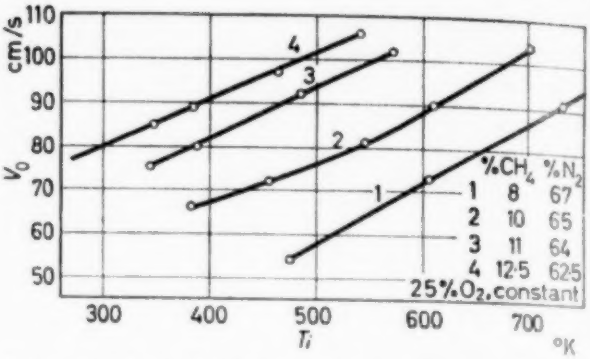

Figure 2. Burning velocities at constant oxygen concentration versus initial temperature

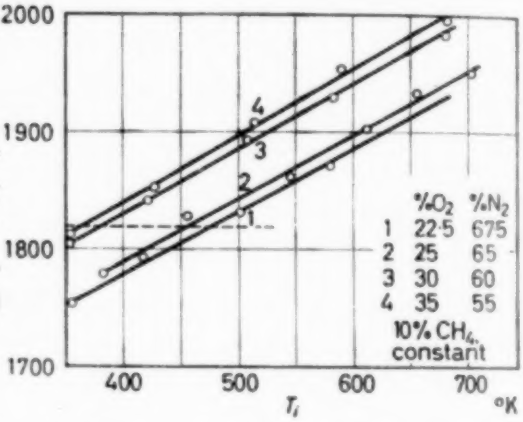

Figure 3. Mean temperature of flame front versus initial temperature at constant methane concentration

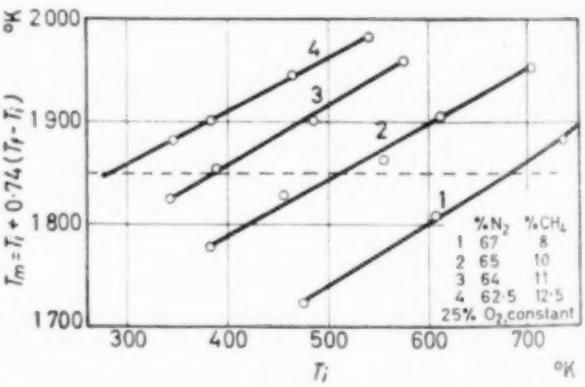

Figure 4. Mean temperature of flame front versus initial temperature at constant oxygen concentration

and T_i were varied. The respective results are plotted in *Figure 1* (constant percentage of methane) and in *Figure 2* (constant percentage of oxygen) where V_0 is given as a function of T_i. *Figures 3* and *4* are the corresponding graphs of T_m as a function of T_i.

Choosing one given temperature T_m (or more) on the T_m versus T_i graphs (dotted line) the corresponding T_i can be re-introduced in the V_0 versus T_i graphs where the V_0 velocities are interpolated. This method allows the establishment of *Table 4*.

Table 4. Interpolated data at three constant temperatures of flame front

T_i °K	% O_2	% N_2	V_0 cm/s	
365	35	55	88	T_m = 1820 °K % CH_4 = 10
381	30	60	78	
457	25	65	72	
476	22·5	67·5	62	
504	35	55	99	T_m = 1900 °K % CH_4 = 10
523	30	60	90	
602	25	65	88	
622	22·5	67·5	75	
T_i °K	**% CH_4**	**% N_2**	**V_0 cm/s**	
282	12·5	62·5	78	T_m = 1850 °K % O_2 = 25
386	11	64	80	
512	10	65	78	
681	8	67	83	
379	12·5	62·5	88	T_m = 1900 °K % O_2 = 25
472	11	64	90	
603	10	65	89	
760	8	67	95	

Discussion

Activation energies have been derived from our experimental results by the two methods explained in the introduction. From the experiments at increasing dilution (*Figure 5*) the activation energy is found equal to 39·5 kcal.

From the experiments at increasing initial temperature (*Figures 6* and *7*) the activation energy is found equal to about the same value, 36·5 kcal. The agreement between the two values obtained is as good as can be expected. A mean value of 38 kcal will be taken as representative.

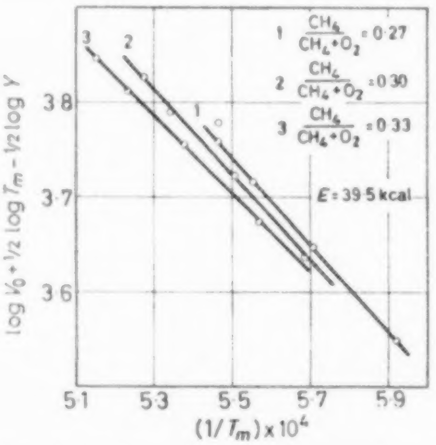

Figure 5. Activation energies from series of diluted mixtures

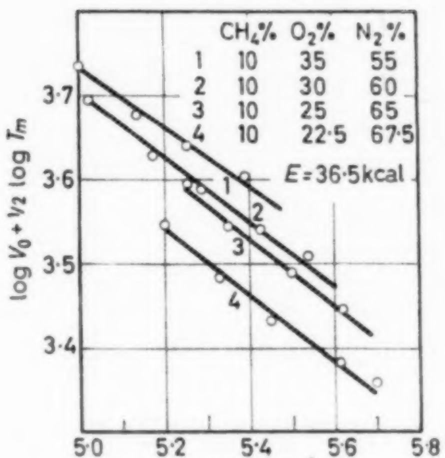

Figure 6. Activation energies from series of preheated mixtures at constant methane concentration

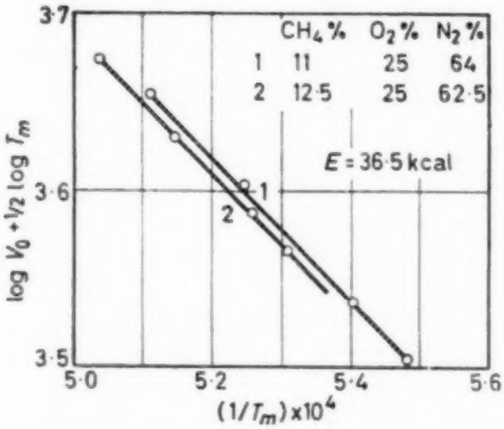

Figure 7. Activation energies from series of preheated mixtures at constant oxygen concentration

The reaction orders a and b are given directly by the application of equations 5 and 6 to the data reported in *Table 4*. The corresponding plots are represented in *Figure 8*; the orders are respectively: $a = 1{\cdot}4$ (order with respect to oxygen) and $b = -0{\cdot}3$ (order with respect to methane). As expected, the sum $(a+b)$ is about equal to one.

When the formula 7 is applied to the data of *Table 1* one finds that $a = 1{\cdot}4$ and $b = 1 - 1{\cdot}4$

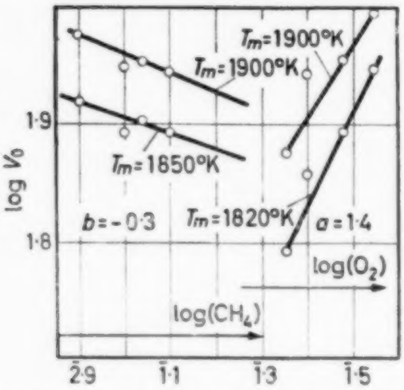

Figure 8. Order of branching reaction with respect to oxygen and methane from data on preheated mixtures

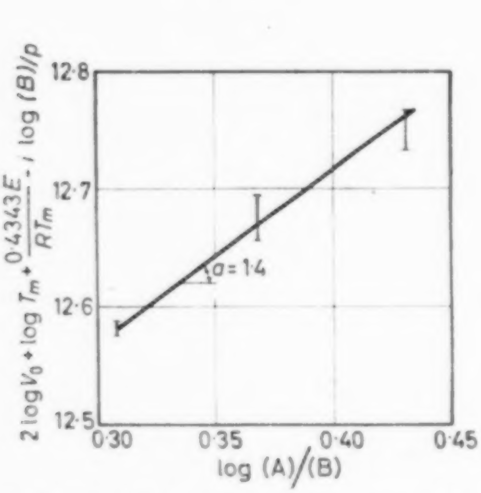

Figure 9. Order of branching reaction with respect to oxygen from data on unpreheated mixtures

= −0·4: this is shown in *Figure 9*. It will be noted that the orders do not, in this case, vary with the composition: almost a straight line is obtained in *Figure 9*. It might be surprising, at first sight, that the order with respect to methane is negative; however, the explanation is to be found on the basis of the theoretical equation for the flame propagation velocity given in ref. 1

$$V_0 = \frac{4T_0}{\pi}\left[\frac{2R}{3M_R}\right]^{\frac{1}{2}}\left[\frac{\delta}{T_m}\right]^{\frac{1}{2}} = K_0 T_0 \left[\frac{\delta}{T_m}\right]^{\frac{1}{2}} \quad . . [8]$$

where R is the gas constant in ergs, and M_R is the mean molecular weight of the chain carriers. The probability that any collision suffered by any chain carrier leads to a branching reaction is represented by δ.

In the propagation of a chain reaction there are usually (at least) two chain carriers whose formation alternates in the propagating reaction steps: however, very often only one of those chain carriers designated by X (or Y) is able to generate new carriers. If now its lifetime is given by τ_X, the probability that a given chain carrier is really an X (or a Y) radical is given by τ_X/τ (or τ_Y/τ) where τ represents the sum of the lifetimes of the two (or more) alternating active species. Therefore τ is also equal to the total duration of one link of the chain.

Furthermore the chain branching process has to occur with a well defined initial species: either a fuel (B) or an oxidizer (A) molecule. Finally sufficient energy has to be available in the collision. The three conditions are stated in the expression for δ

$$\delta = \frac{\tau_X \text{ or } \tau_Y}{\tau} \times \frac{(A) \text{ or } (B)}{P} \exp\left(-E_r/RT_m\right) \quad . . . . [9]$$

where E_r represents the true activation energy of the elementary branching process. As shown previously[1] τ_X/τ and τ_Y/τ must be represented by one of the two equations:

$$\frac{\tau_Y}{\tau} = \frac{(A)\exp\left(-E_{p'}/RT_m\right)}{(A)\exp\left(-E_{p'}/RT_m\right) + (B)\exp\left(-E_p/RT_m\right)} \quad . . . . [10]$$

$$\frac{\tau_X}{\tau} = \frac{(B)\exp\left(-E_p/RT_m\right)}{(A)\exp\left(-E_{p'}/RT_m\right) + (B)\exp\left(-E_p/RT_m\right)} \quad . . . . [11]$$

E_p and $E_{p'}$ are the activation energies of the propagation steps, both smaller than E_r. If we put $(A) = (O_2)$ and $(B) = (CH_4)$ and if we use equation 10 for τ_Y/τ, δ is given by

$$\delta = \frac{(O_2)^2 \exp\left[-(E_r + E_{p'})/RT_m\right]}{P\{(O_2)\exp\left[-E_{p'}/RT_m\right] + (CH_4)\exp\left[-E_p/RT_m\right]\}}$$

The apparent orders *a* and *b* will be somewhere between the two extreme cases:

First case

$$(CH_4) \exp[-E_p/RT_m] \gg (O_2) \exp[-E_{p'}/RT_m]$$

$$\delta = \frac{(O_2)^2 \exp[-(E_r + E_{p'})/RT_m]}{P\,(CH_4) \exp[-E_p/RT_m]}$$

$$a = 2 \text{ and } b = -1$$

Second case

$$(O_2)\exp[-E_{p'}/RT_m] \gg (CH_4)\exp[-E_p/RT_m]$$

$$\delta = \frac{(O_2)}{P} \exp[-E_r/RT_m]$$

$$a = 1 \text{ and } b = 0$$

Intermediate case

$$\delta = \frac{(O_2)^a\,(CH_4)^b \exp[-E/RT_m]}{P}$$

where a exceeds unity and b is negative, but still $a+b=1$.

To conclude from these considerations it may be assumed that our experimental results can very easily be explained in terms of classical reaction kinetics. This means, however, that the mechanism of chain propagation in methane–oxygen mixtures has to be reconsidered.

In particular the two following mechanisms do not explain our observations on the reaction order of the branching process:

$$\left.\begin{array}{l} CH_4 + OH \longrightarrow CH_3 + H_2O \\ CH_3 + O_2 \longrightarrow CH_2O + OH \end{array}\right\} \text{B. Lewis and G. von Elbe}^{7}$$

$$\left.\begin{array}{l} CH_4 + O \longrightarrow CH_2 + H_2O \\ CH_2 + O_2 \longrightarrow CH_2O + O \end{array}\right\} \text{R. G. W. Norrish and S. G. Foord}^{8}$$

If the first mechanism is accepted, it means that the branching reaction ought to be $OH + O_2 \longrightarrow ?$; with the second scheme this would be replaced by the branching reaction $O + O_2 \longrightarrow ?$. Neither of these two reactions could possibly lead to branching; if we suppose they could we should be compelled to admit that the branching process would be exactly the same in hydrogen–oxygen flames.

However, by means of the formation of peroxide radicals, according to the mechanism suggested by A. D. WALSH[9], the following reactions might be proposed:

$$\left\{\begin{array}{l} CH_3 + O_2 \longrightarrow CH_3O_2 \\ \quad \text{and also } CH_2O + OH \\ CH_3O_2 + CH_4 \longrightarrow CH_3O_2H + CH_3 \\ \quad \text{and also } OH + CH_4 \longrightarrow H_2O + CH_3 \end{array}\right.$$

From the observed orders, the chain branching has to occur between an oxygen molecule and a chain carrier which was also formed in a collision with oxygen: therefore we would suggest the following branching reaction

$$CH_3O_2 + O_2 \longrightarrow \text{chain branching}$$
(any process producing two radicals)

The formation of stable peroxide radicals in the methane–oxygen flame might explain the presence of peroxide compounds in the reaction products collected on the cooled walls by methane combustion at low pressure[10]. On the other hand N. N. SEMENOV has discussed the relative importance of different mechanisms[11] and comes to identical conclusions about the peroxide theory.

The large value of the reaction order with respect to oxygen and the negative order with respect to methane agree with some recent observations[12] on the slow combustion of methane at relatively higher temperatures (up to 1 100°C): the observed orders are 1·5 for oxygen and −0·5 for methane. The continuous change occurring in the overall orders from the values observed at lower temperatures[13, 14] (1·7 for methane and 0·3 for oxygen at 600°C) to those observed at higher temperatures corresponds to the fact that, at increasing temperatures, the overall kinetics gains more and more the characteristics of the branching process.

A last but important conclusion can be derived from the observed facts; it concerns the absolute value of the flame propagation velocities in all methane–oxygen–nitrogen mixtures.

The intercept of the straight line on the vertical axis in *Figure 9* should give the value of the constant ($2 \log K_0 T_0$); this value can also be calculated theoretically according to the following expression of $K_0 T_0$

$$K_0 T_0 = \frac{4T_0}{\pi} \left[\frac{2R}{3M_B}\right]^{\frac{1}{2}}$$

In this equation M_R might be taken equal to the molecular weight of the OH radicals; this value was shown[15] to be valid for hydrocarbon–oxygen flames and it means that the OH radical is probably the longest living free radical in the flame front, that one by which the hydrocarbon molecules are primarily attacked in a process of hydrogen abstraction and water formation. The last equation gives for 2 log K_0T_0 a theoretical value of 11·7 which is very near indeed to the value of 12·1 which is given by the intercept in *Figure 9*.

To resume this discussion, all burning velocities in methane–oxygen–nitrogen mixtures are given with a very good approximation by the following relation

$$V_0 = \frac{4T_0}{\pi}\left[\frac{2R}{3M_R}\right]^{\frac{1}{2}}\left[\frac{(O_2)^{1\cdot 4}\exp\left[-38000/RT_m\right]}{T_mP\,(CH_4)^{0\cdot 4}}\right]^{\frac{1}{2}}$$

or more simply by

$$V_0 = 10^6\left[\frac{(O_2)^{1\cdot 4}\exp\left[-38000/RT_m\right]}{T_mP\,(CH_4)^{0\cdot 4}}\right]^{\frac{1}{2}}$$

The theoretical basis of this relation implies the branching reaction in a reaction between oxygen and a peroxide radical.

The authors express their thanks to the Air Force Office of Scientific Research of the Air Research and Development Command (U.S.A.F.)–European Office which sponsors this research [Contract No. AF61(514)–1245], and to the Fonds National de la Recherche Scientifique for its financial support to the laboratory. Two of them (H.V. and R.C.) are also indebted to the I.R.S.I.A. for a postgraduate fellowship.

References

[1] VAN TIGGELEN, A. *Mem. Acad. R. Belg. Cl. Sci.* 1952, **27**, 1. See also VAN TIGGELEN, A. and DECKERS, J. *Sixth Symposium (International) on Combustion*, p 61. Reinhold: New York, 1957

[2] VAN WONTERGHEM, J and VAN TIGGELEN, A. *Bull. Soc. chim. Belg.* 1955, **64,** 99

[3] VAN WONTERGHEM, J. and VAN TIGGELEN, A. *Bull. Soc. chim. Belg.* 1955, **64,** 780

[4] GAYDON, A. G. and WOLFHARD, H. G. *Flames, their Structure, Radiation and Temperature*, p 75. Chapman and Hall: London, 1953

[5] VAN WONTERGHEM, J. and VAN TIGGELEN, A. *Bull. Soc. chim. Belg.* 1954, **63,** 235

[6] WEINBERG, F. *Fuel, Lond.* 1955, **34,** S84; 1956, **35,** 161

[7] LEWIS, B. and VON ELBE, G. *J. Amer. chem. Soc.* 1937, **59,** 976

[8] NORRISH, R. G. W. and FOORD, S. G. *Proc. Roy. Soc. A*, 1936, **157,** 503

[9] WALSH, A. D. *Trans. Faraday Soc.* 1946, **42,** 269

[10] EVERETT, A. J. and MINKOFF, G. J. *Third Symposium (International) on Combustion*, p 390. Williams and Wilkins: Baltimore, 1953

[11] SEMENOV, N. N. [*Some Problems in Chemical Kinetics and Reactivity*], pp 71 and 163. Translated by M. BOUDART. Princeton University Press, 1958

[12] KOZLOV, G. I. *Seventh Symposium (International) on Combustion*, p 142. Butterworths: London, 1959

[13] VANPEE, M. and GRARD, F. *Fifth Symposium (International) on Combustion*, p 484. Reinhold: New York, 1955

[14] HOARE, D. E. and WALSH, A. D. *Fifth Symposium (International) on Combustion*, p 467. Reinhold: New York, 1955

[15] VAN WONTERGHEM, J., SLOOTMAEKERS, P. J. and VAN TIGGELEN, A. *Bull. Soc. chim. Belg.* 1956, **65,** 899

The Formation of Polycyclic Aromatic Hydrocarbons and Carbon Deposits from Normal and Reversed Diffusion Flames

A. J. LINDSEY

Department of Chemistry, Sir John Cass College, Jewry Street, London, E.C.3

(Received June 1959)

Polycyclic aromatic hydrocarbons have been determined in the carbonaceous deposits from normal and reversed diffusion flames of a number of pure gaseous and liquid hydrocarbons used as fuels. Many of these compounds have not previously been detected or determined in partial combustion products of the fuels used, and it has been demonstrated that they are always present in such deposits whatever fuels are used. It is suggested that they may originate from simple radicals such as CH *which are known to be present in such flames, and that they may be precursors of the carbon with which they are always associated in the flame deposits.*

IN A study by J. R. ARTHUR and D. H. NAPIER[1] it was suggested that new information on carbon formation in flames might be obtained by isolating some of the intermediate stages in the chain of reactions proceeding in the flames. Two types of diffusion flame were studied; (*a*) reversed or inverted flames (flames of air burning in the fuel gas) and (*b*) normal diffusion flames burning at low pressures. The tarry combustion products were examined by various methods but no definite compounds were reported present.

More recently, using the microgramme method[2,3] of determining polycyclic aromatic hydrocarbons by elution chromatography and ultra-violet (u.v.) spectrophotometry, it has been shown that the major portion of soluble material associated with these carbon deposits consists of such hydrocarbons[4]. An independent qualitative study has demonstrated their presence in the deposits from normal diffusion flames[5], and they are also found in a wide variety of soots and other partial combustion products[6-10]. At least one theory of the formation of carbon in flames[11,12] postulates them to be precursors of carbon. It was therefore decided to make a quantitative study of the hydrocarbon content of the deposits from diffusion flames using a wide variety of gaseous and liquid fuels.

Experimental

Gaseous fuels were burnt in air at atmospheric pressure at a simple Pyrex glass jet 3 mm in diameter [*Figure 1*(a)]. The pressure and flow of gas was adjusted to produce a steady normal diffusion flame (10 to 15 mm high). The solid carbonaceous deposit was collected on a water-

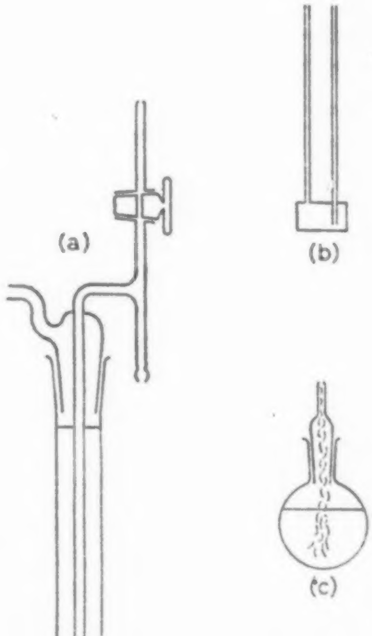

Figure 1. Flame burners

Table 1. Polycyclic aromatic hydrocarbons in carbon deposits from diffusion flames of gaseous fuels

Hydrocarbon	*Percentages in carbon deposits from various fuel gases*					
	Methane	*Ethane*	*Propane*	n-*Butane*	*Ethylene*	*Acetylene*
Acenaphthylene	0·273	0·230	0·290	0·300	0·142	0·110
Fluorene	0·210	0·052	0·073	0·089	0·019	0·032
Phenanthrene	0·590	0·076	0·125	0·100	0·010	0·070
Anthracene	1·00	0·109	0·250	0·230	0·008	0·042
Pyrene	1·90	0·024	0·024	0·051	0·009	0·042
Fluoranthene	0·650	0·009	0·012	0·049	0·022	0·015
1,2-Benzanthracene			0·058			
1,2-Benzpyrene	0·040		0·018	0·110		
3,4-Benzpyrene	0·610	0·035	0·018	0·110	*Trace*	*Trace*
Anthanthrene	0·180	*Trace*	0·029	0·022	*Trace*	*Trace*
Coronene	0·190	0·039	0·036	0·020		*Trace*
Totals	5·643	0·574	0·933	1·081	0·210	0·311

cooled brass target of the type previously used for such work[1] [*Figure 1*(b)]. It was held just within the tip of the flame and at intervals the deposit was scraped off and was freed from moisture by leaving it in a desiccator over sulphuric acid. The weighed dry deposit was extracted to exhaustion with *cyclo*hexane in a Soxhlet extractor, made up to known volume, and two aliquot portions were chromatographed on activated alumina brought into equilibrium with the vapour of either 70 per cent or 50 per cent sulphuric acid[2]. The columns were 10 mm in diameter and 100 mm long and about 50 fractions each of 3 ml were collected from each. The spectrum of every fraction was plotted between 250 and 500 mμ on a Beckman D.K.2 recording spectrophotometer and the amounts of each polycyclic aromatic hydrocarbon were calculated from the recorded absorbances of all the fractions containing it. These amounts are given in *Table 1*.

For liquid fuels a Pyrex glass lamp [*Figure 1*(c)] was constructed with a wick made from twisted strands of glass wool. Thus no combustion products other than those from the fuel were produced. The lamp orifice was about 2 mm in diameter and the wick height was adjusted to give a steady flame about 10 mm high. The carbon deposits were collected and examined in exactly the same way as for gaseous fuels and the amounts found are given in *Table 2*.

The apparatus employed for the preparation of reversed flame condensate was similar to that described by Arthur and Napier[1]. The fuel gas was led into a glass cylinder A (*Figure 2*) and excess was burned at the jet B. A current of air from a small compressor was filtered

Table 2. Polycyclic aromatic hydrocarbons in carbon deposits from diffusion flames of liquid fuels

Hydrocarbon	*Percentages in carbon deposits from various liquid fuels*									
	Benzene	*Toluene*	o-*Xylene*	p-*Xylene*	*Ethylbenzene*	p-*Cymene*	*Cumene*	*Styrene*	cyclo-*Hexene*	cyclo-*Hexan*
Acenaphthylene	0·310	0·330	0·090	0·150	0·080		0·065	0·048	0·137	0·050
Fluorene	0·092	0·350	0·090	0·083	0·120	0·052	0·110	0·086	0·060	0·055
Phenanthrene	0·310	0·290	0·100	0·140	0·190	0·040	0·210	0·130	0·090	0·130
Anthracene	0·051	0·110	0·150	0·067	0·057	0·045	0·038	0·031	0·010	0·035
Pyrene	0·078	0·055	0·023	0·034	0·016	0·034	0·025	0·014	0·060	0·090
Fluoranthene	0·130	0·090	0·070	0·050	0·033	0·055	0·058	0·038	0·039	0·060
1,2-Benzanthracene	0·021	0·010				0·026	0·012			
1,2-Benzpyrene	0·016	0·012	0·007	0·012	0·020	0·031	0·012	0·007	0·010	
3,4-Benzpyrene	0·030	0·034	0·030	0·045	0·058	0·060	0·010	0·015	0·040	0·010
Anthanthrene	0·007	0·006			0·014	0·015			0·016	
Coronene	0·015	0·009	0·003	0·010	0·010	0·010	0·005	0·003	0·010	0·00
Totals	1·060	1·296	0·563	0·591	0·598	0·368	0·545	0·372	0·472	0·43

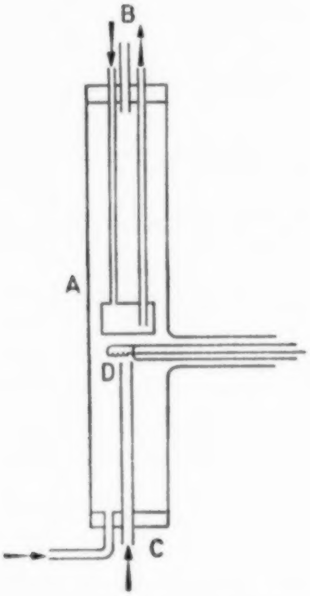

Figure 2. Arrangement of burner

through cotton wool and passed into the burner D after control of its pressure and flow at C. Combustion was initiated by means of an electrically heated platinum spiral igniter which could then be withdrawn from the flame. The products of incomplete combustion were condensed on a brass target similar to that used for normal flames. At intervals the deposits were removed, dried and analysed exactly as described above for normal diffusion flame deposits, and the quantities of each of the various polycyclic aromatic hydrocarbons found are shown in *Table 3*.

Table 3. Polycyclic aromatic hydrocarbons in carbon deposits from reversed diffusion flames

Hydrocarbon	*Percentages in carbon deposits from various fuels*			
	Methane	*Ethane*	*Propane*	*n-Butane*
Acenaphthylene	0·909 (0·057)	0·426	0·450	0·315
Fluorene	0·345 (0·036)	0·813	0·289	0·109
Phenanthrene	0·534 (2·680)	0·409	0·150	0·125
Anthracene	1·054 (2·120)	0·257	0·225	0·270
Pyrene	1·800 (6·450)	0·065	0·075	0·056
Fluoranthene	0·720 (2·260)	0·139	0·072	—
1,2-Benzanthracene	— (0·182)	—	—	—
1,2-Benzpyrene	— —	0·090	0·165	0·052
3,4-Benzpyrene	0·561 (1·660)	0·070	0·180	0·119
Anthanthrene	0·153 (0·710)	0·050	0·033	0·056
Coronene	0·108 (0·382)	0·020	0·057	0·040
Totals	6·184 (16·537)	2·339	1·696	1·142
Totals (normal flames)	5·643	0·574	0·933	1·081

Discussion

Examination of the analytical results recorded in *Tables 1* and *2* reveals no regular trends with various fuel materials in passing from one compound to another of related structure, although it generally appears that greater proportions of polycyclic aromatic hydrocarbons are found in the deposits from the simpler fuels. But a series of polycyclic aromatic hydrocarbons is obtained from every fuel, however simple or complex it may be, and this points to the existence of a simple and essential stage in the synthesis of these compounds in all the flames.

The analytical results obtained for normal and reversed flames (*Table 3*) show that, with all the fuels employed, greater total proportions of polycyclic aromatic hydrocarbons were found in the carbonaceous deposits from reversed flames than in normal diffusion flame deposits. This is probably because intermediate reaction products in such flames are carried by diffusion and convection into the non-oxidizing atmosphere which forms the outer envelope of the flame and are thus protected from the more complete combustion characteristic of the outer envelope of the normal diffusion flame.

Methane gives rise to greater proportions of polycyclic aromatic hydrocarbons than the other gaseous fuels. It was, however, difficult to keep methane reversed flames alight with air of ordinary composition, but with enriched air containing a total of 30 per cent of oxygen by volume much more stable flames were produced[4]. These more stable flames gave rise to much increased amounts of aromatic hydrocarbons in the carbonaceous deposit as shown in parentheses in *Table 3*.

All the fuels studied with either reversed or normal flames produced the same series of polycyclic aromatic hydrocarbons in the flame deposits. A simple explanation is that the formation of these compounds is similar in all the flames studied and, since these compounds are produced in greatest proportions in methane flames, it appears reasonable to assume that an essential stage in their production could well be the simplest radical CH.

Well-established spectroscopic evidence exists for the presence of the CH radical in flames[13] and such radicals could well be the primary stage and then condense to a variety of molecules. Later stages are in part conjecture but whatever mechanism is proposed it has to explain the presence of acetylene and benzene in all hydrocarbon flame condensates and the ubiquitous array of polycyclic aromatic hydrocarbons of increasing molecular weight up to that of coronene. Acetylene and benzene give a whole series of polycyclic aromatic compounds and carbon at temperatures similar to those existing in the diffusion flames. R. E. Ferguson, by burning propane-2-^{13}C, demonstrated that carbon does not arise preferentially from a two-carbon fragment of the fuel molecule[17], and thus deduced that acetylene, which has been said to be the last stable precursor of carbon in flames[18], is not formed from a carbon pair. Thus, if it is the immediate precursor of carbon it must arise from a more complicated process than simple degradation of the fuel. It is most simply reasoned that acetylene must have a one-carbon precursor, and a likely unit is the CH radical. The mechanism for the production of aromatic hydrocarbons could thus be either directly from CH radicals or indirectly via acetylene. For molecules larger than benzene it is necessary to assume dehydrogenation processes at the high temperatures of the flame and subsequent reactions between the larger radicals so formed. However, there is no need to assume the direct formation of radicals such as C_6H_5CH or $C_6H_5{<}\genfrac{}{}{0pt}{}{CH}{CH}$ from compounds such as toluene or the di-substituted alkyl benzenes, because no preferential formation of polycyclic aromatic hydrocarbons having structures to be expected from such sources was observed when these compounds were used as fuels (*Table 2*).

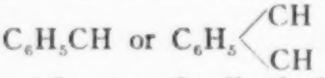

The experimental results show that the polycyclic compounds are always associated with much larger amounts of carbon (about 100 times) and it may be that these compounds are partly precursors of the carbon and partly formed in the same pyrosynthetic process. Several theories of the formation of carbon deposits in flames have been proposed but some of these take no account of the polycyclic aromatic hydrocarbons always associated with carbon deposits. Thus the well-known Swan bands in the spectra of hydrocarbon flames have been ascribed[14, 15] to the radical C_2 and it has been suggested that solid carbon occurs by a polymerization process from these radicals[16].

It appears likely that carbon originates in flames by a number of processes and that the polycyclic aromatic hydrocarbons which have been shown to be associated with the carbon deposits from a wide variety of fuels could well be its precursors. Further studies of diffusion flames and pyrolytic reactions of intermediate combustion products are proceeding as part of a comprehensive study of incomplete combustion.

The author wishes to thank the Medical Research Council for supporting these investigations by the loan of apparatus and provision of technical assistance and materials. He also acknowledges the generous gift of specimens of some pure hydrocarbons from the British Petroleum Co. Ltd, Petroleum Division.

References

1 Arthur, J. R. and Napier, D. H. *Fifth Symposium (International) on Combustion*, pp 303–315. Reinhold: New York, 1955

2 Lindsey, A. J. *Analyt. chim. Acta*, 1959, **20**, 175

3 Lindsey, A. J. *Analyt. chim. Acta*, 1959, **21**, 101

4 Arthur, J. R., Commins, B. T., Gilbert, J. A. S., Lindsey, A. J. and Napier, D. H. *Combustion & Flame*, 1958, **2**, 267

5 Badakhshan, A., Garner, F. H. and Long, R. *Combustion & Flame*, 1958, **2**, 437

6 Cooper, R. L. and Lindsey, A. J. *Chem. & Ind.* **1953**, 1177

7 Commins, B. T., Cooper, R. L. and Lindsey, A. J. *Brit. J. Cancer*, 1954, **8**, 296

8 Gilbert, J. A. S. and Lindsey, A. J. *Brit. J. Cancer*, 1957, **11**, 398

9 Tebbens, B. D., Thomas, J. F. and Mukai, M. *Amer. Med. Ass. Ind. Health*, 1956, **13**, 567

10 Tebbens, B. D., Thomas, J. F. and Mukai, M. *Amer. Med. Ass. Ind. Health*, 1957, **14**, 413

11 Gaydon, A. G. *Spectroscopy and Combustion Theory*. Chapman and Hall: London, 1948

12 Parker, W. G. and Wolfhard, H. G. *J. chem. Soc.* **1950**, 2038

13 Gaydon, A. G. and Wolfhard, H. G. *Proc. Roy. Soc.* 1949, **199**, 89

14 Pretty, W. E. *Proc. Roy. Soc.* 1928, **40**, 71

15 Gaydon, A. G. and Wolfhard, H. G. *Proc. Roy. Soc.* 1950, **201**, 561

16 Smith, E. C. W. *Proc. Roy. Soc.* 1940, **174**, 110

17 Ferguson, R. E. *Combustion & Flame*, 1957, **1**, 431

18 Arthur, J. R. *Nature, Lond.* 1950, **165**, 557

The Spontaneous Ignition of Aliphatic Amines

C. F. Cullis and B. A. Khokhar

Department of Chemistry, Imperial College of Science and Technology, London

(*Received July 1959*)

A comparative study has been made of the spontaneous ignition of primary, secondary and tertiary aliphatic amines. In all cases the tendency to explode increases continuously with the proportion of amine in the mixture and it appears that the ignition pressure is not appreciably affected by the presence of the partial products of slow combustion. The results are discussed and it seems probable that the explosions are largely thermal in nature.

Although the slow combustion of aliphatic amines has in recent years been extensively investigated[1-4] there appears to be little information available regarding the ignition characteristics of such compounds. H. J. Emeleus and L. J. Jolley[5] studied the ignition of methylamine–oxygen mixtures between 400° and 600°C and found that for all the mixtures examined the ignition pressure (P) is related to the ignition temperature (T) by an equation[6] of the form

$$\ln P/T = A/T + B \qquad \ldots . [1]$$

However, there was shown to be an abrupt change in the value of A at about 490°C and this suggests that two different mechanisms can operate according to the temperature.

In the present investigation, an attempt has been made to extend our knowledge of the mechanism of spontaneous ignition of amine–oxygen mixtures. Amines are of special interest as they are powerful inhibitors of combustion processes[7-9] and it might therefore be expected that their ignition behaviour would exhibit certain differences from that of other fuels.

Experimental

The apparatus consisted essentially of a spherical Pyrex reaction vessel, 7·2 cm in diameter, which was maintained at a suitably elevated temperature, and which was connected both to a mercury manometer and to a spherical premixing vessel, 14·2 cm in diameter, which was kept throughout at 25°C. To provide a pressure release in the event of explosion, the mercury manometer was of the open type and in addition a safety trap was inserted between the manometer and the reaction vessel. The 'sharing factor' between the reaction vessel and the premixing vessel was accurately determined under a wide range of conditions of temperature and pressure. Thus, if the pressure of a combustible mixture in the premixing vessel before sharing was known, that developed in the reaction vessel after sharing could easily be calculated.

To determine the ignition limits, amine–oxygen mixtures of known composition and at relatively high pressures were prepared manometrically in the premixing vessel. A tap connecting this with the reaction vessel was momentarily opened and then closed again. If there was slow reaction at the temperature used, both vessels were evacuated and the temperature was raised. A fresh amine–oxygen mixture of the same composition and at the same pressure was then prepared in the premixing vessel and admitted to the reaction vessel at a higher temperature. This procedure was repeated at increasing temperatures until explosion occurred. After each explosion, the reaction vessel was evacuated and the combustible mixture remaining in the premixing vessel was again used, giving progressively lower pressures until slow reaction was observed. Explosion was denoted by a sudden depression of the meniscus of the mercury manometer, accompanied by a bright flash of light. A much milder pressure pulse indicated the passage of a cool flame.

Results

Ethylamines

Ignition diagrams for three triethylamine–oxygen mixtures [*Figure 1*(a)] indicate the occurrence of regions of slow combustion, of single and multiple cool flames and of true explosion. With a mixture containing 16·7 per cent of amine and with a total pressure of 200 mm, explosion first occurs at 264°C. The ignition diagrams for mixtures containing 9·1 and 4·8 per cent of triethylamine are found to be generally similar but with the leaner mixtures ignition only takes place at somewhat higher temperatures and pressures. Explosion is preceded by a measurable induction period during which a small increase in pressure is generally observed. The length of the induction period decreases markedly with temperature and with the proportion of oxygen in the mixture [*Figure 1*(a)]. Cool flames are encountered between 280° and 375°C. Two successive cool flames are observed only between 315° and 330°C and with the richest mixture investigated.

Figure 1(b) shows the ignition diagrams of some diethylamine–oxygen mixtures under comparable conditions of temperature, pressure and mixture composition. Explosion takes place, however, at considerably higher temperatures and is less violent than with triethylamine. Ignition is preceded by an induction period during which a small pressure increase sometimes occurs. Lean mixtures are again less explosive than rich mixtures and the length of the induction periods decreases with increasing temperature and oxygen content of the system [*Figure 1*(b)]. It will be seen that the induction periods with diethylamine are considerably longer than those observed under corresponding conditions with triethylamine.

Ethylamine–oxygen mixtures ignite only at relatively high temperatures as shown by the results in *Figure 1*(c). Explosions occur smoothly and are generally non-violent; they are preceded by measurable induction periods. No cool flames are observed with this compound.

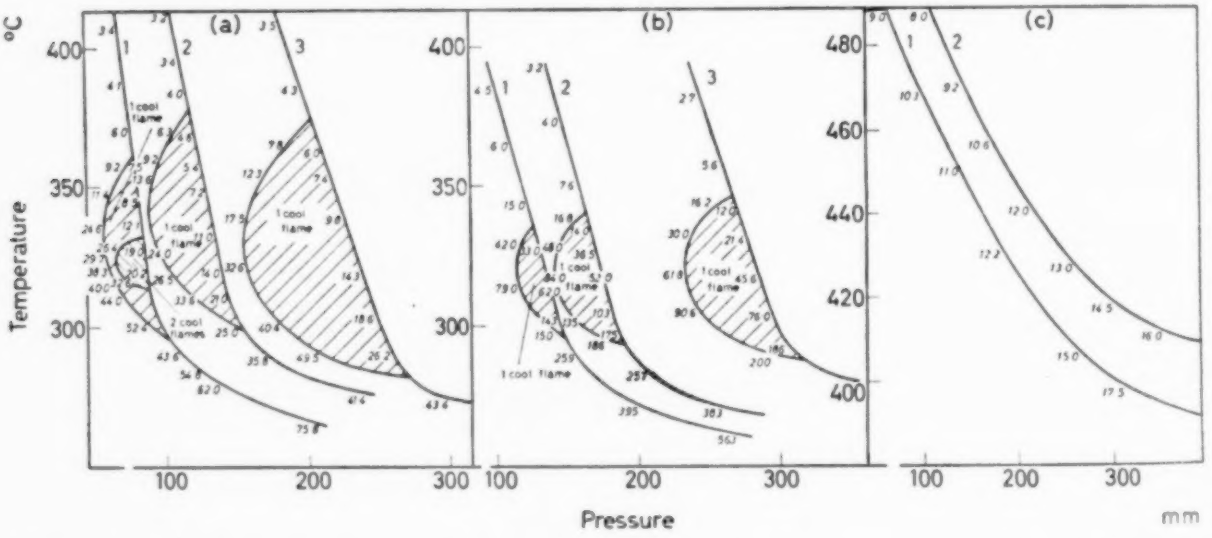

Figure 1. Ignition limits for mixtures of ethylamines and oxygen; (a) *Curve 1. 16·7 per cent triethylamine; curve 2. 9·1 per cent triethylamine; curve 3. 4·8 per cent triethylamine.* (b) *Curve 1. 25·0 per cent diethylamine; curve 2. 16·7 per cent diethylamine; curve 3. 9·1 per cent diethylamine.* (c) *Curve 1. 25·0 per cent ethylamine; curve 2. 16·7 per cent ethylamine. (The small italicized numerals represent the induction periods in seconds preceding explosion)*

Methylamines

The ignition diagrams for some trimethylamine–oxygen mixtures are shown in *Figure 2*(a). The induction periods preceding explosion are very short and decrease sharply as the temperature is increased. Explosions are much more violent than with triethylamine. In common with the first members of many other homologous series of organic compounds, trimethylamine does not give rise to cool flames.

Figure 2(b) shows the corresponding ignition diagrams for two diethylamine–oxygen mixtures. Under comparable conditions of temperature and pressure, explosion occurs at considerably higher temperatures and is less violent than with trimethylamine. The induction periods preceding explosion are much longer.

Influence of oxidation products

Examination of *Figures 1* and *2* shows that, with all the amines studied, lean mixtures are generally less prone to explosion than rich mixtures. The compositions of the mixtures used have been varied over a wide range and systems with both a stoichiometric deficit and a stoichiometric excess of amine have been investigated. The fact that the tendency to explode increases continuously with the amine concentration is somewhat surprising in view of the well known inhibiting effect of amines on combustion processes. A possible explanation of the observed behaviour is, however, that unchanged amine is not the only inhibitor but that even more effective inhibition is caused by reaction products which are formed more readily in lean than in rich mixtures. To investigate this possibility further, an attempt has been made to discover whether the ignition of amine–oxygen mixtures is inhibited by the oxidation products.

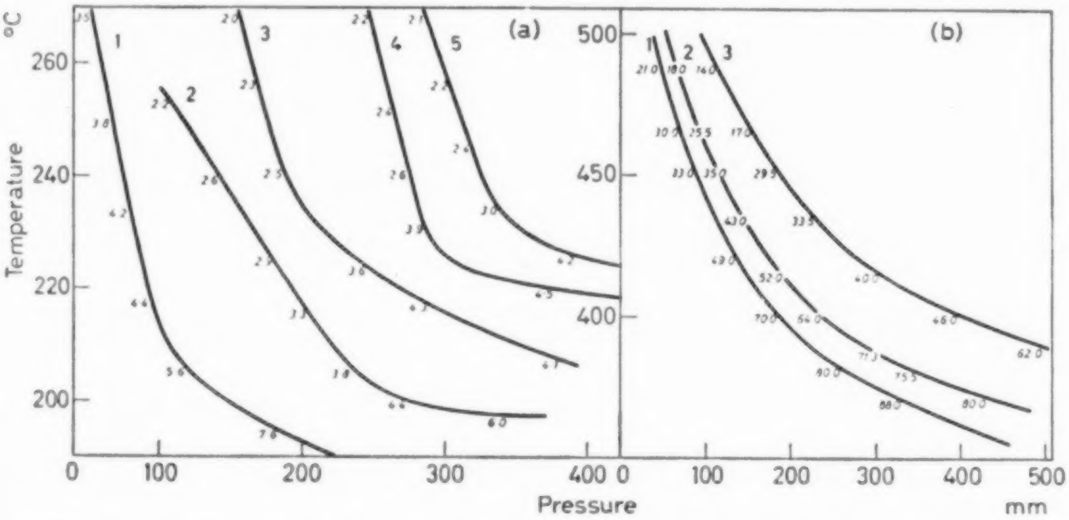

Figure 2. Ignition limits for mixtures of methylamines and oxygen. (a) *Curve 1. 50·0 per cent trimethylamine; curve 2. 16·7 per cent trimethylamine; curve 3. 9·1 per cent trimethylamine; curve 4. 6·2 per cent trimethylamine; curve 5. 5·4 per cent trimethylamine.* (b) *Curve 1. 25·0 per cent dimethylamine; curve 2. 16·7 per cent dimethylamine; curve 3. 9·1 per cent dimethylamine. (The small italicized numerals represent the induction periods in seconds preceding explosion)*

The behaviour of triethylamine and diethylamine was specially studied for this purpose. The procedure already described was used for the determination of ignition limits but in each run 50 mm of the amine–oxygen mixture was allowed to remain in the hot reaction vessel at the desired temperature for ten minutes before the remainder of the combustible mixture was admitted.

Some of the results obtained are shown in *Figure 3*. With both triethylamine and diethylamine, the position of the ignition limits is almost unchanged at low temperatures. This is no doubt due to the fact that under these conditions negligible reaction takes place during the preheating period. On the other hand, at the highest temperatures investigated, reaction will be very rapid and the amine will be readily burnt more or less completely to final products.

Now if it is assumed that these products are ammonia, carbon dioxide and steam:

$$(C_2H_5)_3N + 9O_2 \longrightarrow NH_3 + 6CO_2 + 6H_2O$$

$$(C_2H_5)_2NH + 6O_2 \longrightarrow NH_3 + 4CO_2 + 4H_2O$$

and since the mixtures used contained exactly the necessary stoichiometric amount of oxygen demanded by the above equations, then 50 mm of the combustible mixture admitted initially will produce about 65 mm of inert oxidation products. It will be seen from *Figure 3* that in both these systems the ignition limit at high temperatures is in fact raised by precisely this amount.

If partial oxidation products formed at intermediate temperatures were powerful inhibitors of the combustion of the amines, then the ignition limit would under these conditions be raised to an extent much greater than this. There is, however, no sign of such behaviour and it must therefore be concluded that, in contrast to the experimental findings with, for example, acetaldehyde–oxygen mixtures[8], the products of partial oxidation of triethylamine and diethylamine do not appreciably inhibit the explosive combustion of these compounds.

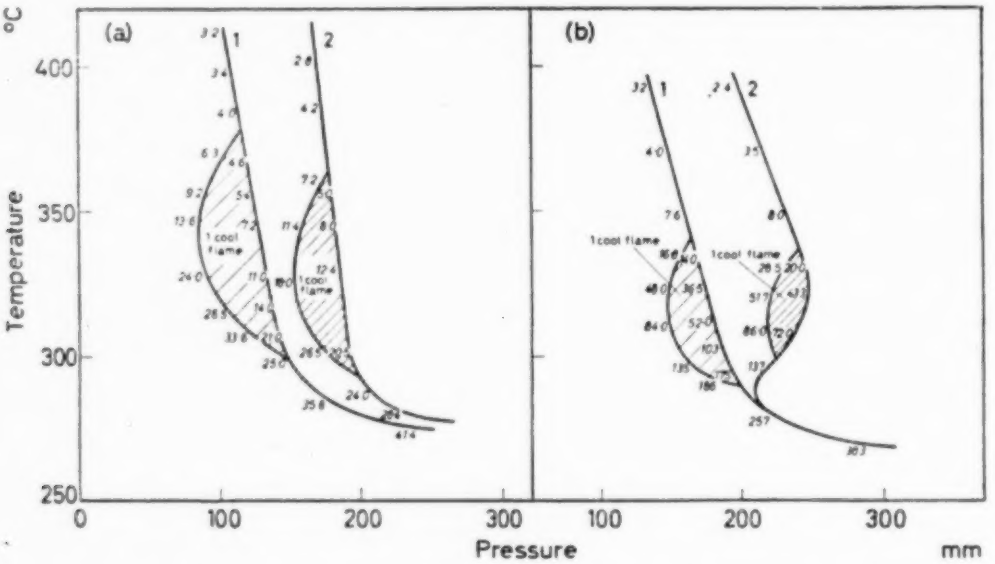

Figure 3. The influence of partial oxidation products on ignition limits of amine–oxygen mixtures. (a) *Curve 1. Normal ignition limits for mixture containing 9·1 per cent triethylamine; curve 2. Ignition limits obtained after 'preheating' 50 mm of the amine–oxygen mixture.* (b) *Curve 1. Normal ignition limits for mixture containing 16·7 per cent diethylamine; curve 2. Ignition limits obtained after 'preheating' 50 mm of the amine–oxygen mixture. (The small italicized numerals represent the induction periods in seconds preceding explosion)*

Discussion

The slow combustion of aliphatic amines has been extensively studied and it is known that the ease of oxidation decreases in the order: tertiary amines > secondary amines > primary amines. In the present investigation, it has been established that the order of ease of ignition is the same as the order of ease of slow oxidation and this suggests in a general way that the two types of combustion are in fact related. On the other hand, while the lower amines and other intermediate products of combustion of higher amines inhibit slow oxidation, such compounds apparently have little or no effect in controlling explosion in the present systems investigated.

Although the slow oxidation of aliphatic amines undoubtedly proceeds by a chain mechanism, it is by no means certain that the explosions encountered involve branching chains. In fact, with the amines studied in this work, very high reaction rates were ofte observed immediately prior to explosion and this leads to the belief that ignition may well be largely thermal in nature. The validity of equation 1 (which should theoretically hold both for thermal and branched-chain explosions) has been tested for all the systems studied and *Figure 4* shows that there exists a linear relationship (over the temperature range studied) between log P/T and $1/T$ for ethylamine, trimethylamine and dimethylamine. A sharp break appears, however, between 280° and 300°C in the plots for triethylamine and diethylamine and this is reminiscent of the behaviour shown by methylamine[5] and by a number of hydrocarbons and other organic compounds[10]. The values of A calculated from the gradients of the plots shown in *Figure 4* are given in *Table 1*. Below 300°C, the values for all the different amines are very similar. Above this temperature, however, the values of A for triethylamine and diethylamine are much smaller.

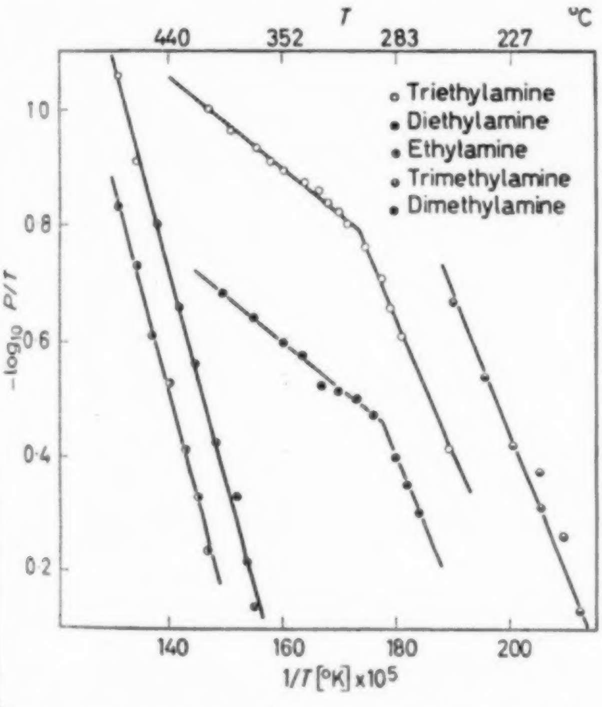

Figure 4. Test of the validity of the Semenov relationship for the ignition of amine–oxygen mixtures (16·7 per cent amine)

Table 1

Amine	*A (below 300°C)*	*A (above 300°C)*	*A (above 360°C)*
Triethylamine	2 310	787	
Diethylamine	2 330	781	
Ethylamine			3 673
Trimethylamine	2 428		
Dimethylamine			3 670

In complex oxidation reactions, deviations from the simple behaviour predicted by theory are not unexpected. With ethane[11], for example, under certain conditions explosion does not occur until slow reaction is practically complete. It may indeed represent the subsequent reaction of one or more of the products without any direct connection with the slow oxidation of ethane itself. The explosive combustion of amines takes place in a complex mixture of intermediate products, some of which exert a marked inhibiting influence on the slow oxidation. Whether explosion is thermal or due to chain-branching, the fact that amines inhibit slow oxidation must to some extent be reflected in the results for the explosive combustion despite the findings made in the preheating experiments (*Figure 3*). In these circumstances then it is perhaps not surprising that a relationship developed for an idealized case is apparently not strictly valid when applied to such a potentially complex system.

The authors would like to thank the Central Government of Pakistan for the award of a Research Scholarship to one of us (B.A.K.) and Shell Research Ltd for valuable financial assistance in the purchase of apparatus.

References

[1] CULLIS, C. F. and SMITH, L. S. A. *Trans. Faraday Soc.* 1950, **46**, 42

[2] CULLIS, C. F. and WILLSHER, J. P. *Proc. Roy. Soc. A*, 1951, **209**, 218

[3] CULLIS, C. F. and ISAAC, I. *Trans. Faraday Soc.* 1952, **48**, 218

[4] CULLIS, C. F. and WADDINGTON, D. J. *Proc. Roy. Soc. A*, 1958, **244**, 110; 1958, **246**, 91; 1958, **248**, 136

[5] EMELEUS, H. J. and JOLLEY, L. J. *J. chem. Soc.* **1936**, 1524

[6] SEMENOV, N. N. *Chemical Kinetics and Chain Reactions*. Oxford University Press: London, 1935

[7] CULLIS, C. F. and WADDINGTON, D. J. *Trans. Faraday Soc.* 1957, **53**, 1317

[8] CULLIS, C. F. and KHOKHAR, B. A. *Seventh Symposium (International) on Combustion*, p 171. Butterworths: London, 1959

[9] WADDINGTON, D. J. *Seventh Symposium (International) on Combustion*, p 165. Butterworths: London, 1959

[10] SAGULIN, A. B. *Z. phys. Chem. B*, 1928, **1**, 275

[11] SADOWNIKOW, P. *Phys. Z. Sowjet.* 1933, **4**, 743

Recent Developments and Notes

Firedamp Hazards in Mines

Safety in Mines Research 1958, the annual report recently issued on the work of the Safety in Mines Research Establishment (H.M.S.O.: London, 1960) contains short accounts of some interesting investigations on the ignition and combustion of firedamp and coal dust.

In researches concerned with locating the point of ignition of firedamp by a detonating explosive, photographs with a high-speed cine-camera indicate that the flame is well established within 0·5 msec of the detonation of the explosive, so that very high-speed photography is required to get detailed knowledge of the ignition process. There now appears to be hope that by using special films and by increasing the actinic value of the flame by adding a volatile metallic salt to the methane–air mixture, it will be possible to obtain records with exposures of a few microseconds.

Work on ignition hazards by sparks from aluminium and its alloys has been continued. A hard zinc alloy did not cause ignition at the highest velocity of which the apparatus delivering glancing blows was capable. The incendivity of aluminium was found to be intermediate between that of the zinc alloy and steel or brass, and this may be correlated with the melting point of aluminium which is between those of the zinc alloy and steel or brass.

In connection with ignition hazards from rocks, an extension of the work of M. J. BURGESS and R. V. WHEELER [1928] on frictional sparking has been started, consisting essentially of pressing a rock 'slider' with known force against the periphery of a rotating 12 in. diameter rock wheel in a methane–air mixture. The new experiments are designed to determine accurately the variation of time-to-ignition with load and rubbing speed.

Several recent large firedamp explosions in British mines have been due to ignitions of gas that had accumulated either in roof layers or in cavities. Small-scale models have now been made based on some of these explosions for the study of the inflammations of methane–air mixtures. Each model is geometrically scaled and is made from Perspex and wood so that the flame is visible and little heat is lost during its propagation. Air and methane are supplied so as to simulate the conditions thought to be prevailing at the time of the explosion. When such factors as pressure release and point of ignition are carefully controlled, the model shows a spread of flame similar to that known to have occurred in the mine explosion. Research is being continued to build up a theoretical basis for the modelling which promises to be of considerable value.

Coal Dust Hazards in Mines

In addition to the various investigations that are being carried out in the Safety in Mines Research Establishment (see note above) directly concerned with the suppression of coal dust explosions in mines, a study is being made of the mechanism of such explosions. This knowledge is required both for understanding how stone dusting impedes combustion, and for suggesting new methods of countering the danger. In the method being used, dust from a vibrating hopper is allowed to fall at a known rate through a vertical tube, 2$\frac{3}{4}$ in. in diameter, and is ignited near the bottom (open) end. A knowledge of the shape and speed of flame as it travels up the tube will enable the burning velocity of the dust cloud to be calculated, the burning velocity being defined as the volume of dust cloud burned in unit time per unit area of flame front.

The aerodynamics of coal dust explosions are being studied in a 4 in. square steel shock tube 40 ft long. Air pressure is built up behind a cellulose acetate diaphragm which on being pierced ruptures violently and a shock wave passes along the tube. The shock strength and duration of air flow behind the wave can be varied and by means of optical detectors the speed of the wave and hence the strength of the blast can be measured.

Combustion Research at Battelle

GORDON BATTELLE established in his will the Battelle Memorial Institute at Columbus, Ohio, as an organization for industrial research, mentioning specifically as one field of work, that of coal. Soon after the Institute was opened in 1929 work was extended to cover problems in the use of gas and oil, and now researches are being carried out in a number of branches of technology, including aeronautical engineering, air pollution control, nucleonics and reactors, and welding. In 1953 laboratories were opened at Frankfurt-am-Main and at Geneva in the following year. There is a staff of 2 200 at Columbus, and of 400 and 250 at the two latter places respectively. A survey of the different types of work carried out and now in progress has recently been published by H. R. HAZARD and A. A. PUTNAM [*J. Inst. Fuel,* 1960, **33,** 22]. The former is Assistant Chief of the Thermal Engineering Division and the latter is Consultant to the Aeronautics and Thermodynamics Division of the Institute.

The initial project in research at Battelle, carried on with the endowment funds of the Institute, concerned the combustion of pulverized coal and the radiation from its flames. The economic depression of the 1930s prevented the continuation of this work and Battelle now participates in similar work by membership in the American Committee of the International Flame Research Foundation whose researches are being carried on at IJmuiden. It is noteworthy that there is excellent order of agreement between the early results obtained at Battelle and recent ones at IJmuiden as regards the rate of burning of pulverized coal, although in the early work a premixed flame was used whilst a diffusion flame was used in Holland.

Substantial efforts have been made in the development of coal-fired equipment to improve performance, for both industrial and domestic purposes. One of these projects worthy of note is that on the development of such equipment for a gas turbine-driven locomotive. Other important projects undertaken for the coal industry include those related to improvements in production of water gas and producer gas.

Considerable attention has been given in recent years to the design and operation of incinerators for burning both domestic and industrial waste. Several researches have been devoted to the operation of air-breathing jet engines for aircraft propulsion, including work on a ceramic-lined pilot chamber for extending the altitude limits of turbojet combustors, the effect of combustion products containing boron trioxide on turbocompressors of a high-altitude test facility, and erosion in turbojet fuel nozzles using radioactive nozzle parts which were operated in a special high-temperature flow bench.

Rocket combustion studies have been undertaken not only in relation to rocket motors for free-flight vehicles but also as applied to industrial processes involving supersonic heat transfer as in the flame-hardening of metals.

There has been a continuing fundamental investigation of the physical and chemical aspects of combustion, the major support for which has come from the U.S. Government. Most of this research has to do at present with rocket combustion problems but there is also a considerable amount of work being carried out on liquid fuel combustion in ramjets and gas-turbine afterburners. A review is given of the researches on flame-stabilization, the burning characteristics of fuels, the suppression of combustion-driven oscillations, the effect of imposed physical influences on the burning velocity and stability of flame, and the spark ignition of fuel mists.

Optical Techniques in Combustion Research

A review has been written by F. J. WEINBERG, of the Department of Chemical Engineering, Imperial College of Science and Technology, London, of *Geometric–Optical Techniques in Combustion Research* and has been issued as a preprint of a contribution to *Progress in Combustion Science and Technology,* Vol. I, which is to be published by the Pergamon Press.

The optical methods discussed are all based on the change of direction which the light beam undergoes when 'transluminating' each part of the phenomenon studied. The sections of the review are: the geometric optics of flames;

'schlieren' methods; shadowgraphs; deflection mapping. Apart from the methods of physical optics, the background of the optics and combustion theory involved has been assumed. Theoretical issues and a more comprehensive account of applications of the techniques described are the subject of a monograph to be published by the author [*The Theory and Applications of the Optics of Flames*, Butterworths, London].

Future High-compression Engines

A James Clayton lecture was delivered by W. G. LOVELL, Senior Research Adviser, Ethyl Corporation, Detroit, Mich., at a meeting of the Automobile Division of the Institution of Mechanical Engineers in March 1960, in London. His subject was 'Some chemistry of future high-compression engines', and the author discussed some of the reasons why he believes there are going to be many high-compression Otto-cycle engines in the future [*Chart. mech. Engr.* 1960, **7**, 275]. The gains made in efficiency with higher compression ratios are difficult to evaluate and the author shows how the determination of engine friction, and thus the indicated efficiency of an engine, is subject to wide variation. This is reflected in the brake output which is of prime importance as far as ultimate efficiency is concerned. Whilst the cost of octane numbers in the fuel is likewise difficult to evaluate, the author thinks that gasoline with the appropriate hydrocarbon structure will be made at low cost in the future.

On the basis of cost of engine plus fuel, it does not seem likely that turbines, free-piston engines, or diesel engines will displace gasoline engines, unless, for example, a reasonably cheap material is found which will withstand a temperature of 2 760°C, in which event turbines might well become of pre-eminent importance.

In considering the various combustion irregularities, attention is drawn to the fact that the sensitive test fuels, those which have the greater difference between Research and Motor octane numbers, have relatively much less power-producing value under the more severe conditions of higher inlet-air temperature. In other words, they are actually the less valuable fuels under higher temperature engine conditions. These considerations become more important with higher compression engines, in which knock at part throttle becomes a problem.

Combustion chamber deposits increase octane number requirements, possibly on account of various thermal effects as well as reduction in the combustion chamber volume with consequent increase in compression ratio.

Other irregularities in combustion which are discussed include precombustion and the associated cool flames; incomplete burning with unburnt hydrocarbon products in the exhaust gases, and also chemical side reactions, resulting particularly in the formation of oxides of nitrogen, both of these creating pollution of the atmosphere.

There is a serious limitation in the hydrocarbons that can be used in the fuels for higher compression engines and the author considers that refining processes will have to be changed to produce the correct molecular structures. In connection with the use of anti-knock substances, the new metallic anti-knocks based on manganese have made available not only a new class of compounds but also a new phenomenon of increasing the activity of existing anti-knock compounds.

S.M.R.E. Bibliography

The second edition of *S.M.R.E. Bibliography* was published in January 1960 by the Safety in Mines Research Establishment [Ministry of Power, U.D.C. 016: 061·6: 622·8; 177 pp. 17*s* 6*d*]. This was compiled by E. B. SMITH and includes over 1 500 references to publications by the staff of this research organization and their associated workers, from 1908 to the end of 1959. In the former year the organization was founded under the auspices of the Mining Association of Great Britain, two years later it became the Home Office Experimental Station and in 1920 was transferred to the Mines Department of the Board of Trade. From then until 1943 the income of the Safety in Mines Research Board was derived almost entirely from the Miners' Welfare Fund. In this year financial responsibility began to be assumed by the Exchequer and in 1946 the establishment and activities of the Board were transferred to the Ministry of Fuel and Power. The present title of the organization was assumed in 1950.

Abnormal Hydroxyl Excitation in Flames

In an investigation by W. E. KASKAN, General Electric Research Laboratory, Schenectady, N.Y., the emission from the first four vibrational levels of $OH^2\Sigma^+$ and the concentrations of ground state $OH^2\Pi$ have been measured in a series of rich hydrogen–oxygen–nitrogen flames held on flat porous burners, as a function of distance from the burner [*J. chem. Phys.* 1959, **31**, 944]. The intensity of emission of each of the bands is proportional to the cube of the concentration of ground state OH, but the constant of proportionality depends on the band and the flame conditions. This dependence, as well as absolute intensity measurements, establish the fact that the radiation is non-thermal.

The dependence of the emission intensity on an integral power of OH strongly indicates that the excited OH is formed as a result of one or more of a set of possible radical recombination reactions. In general it is not possible to obtain a unique determination of the excitation mechanism for any band. The only exception to this is that definite evidence for the pre-association reaction

$$O + H \rightarrow OH^2\Sigma, \ v = 2$$

has been obtained. The vibrational distributions of excited OH are shown to be consistent with 'temperatures' from 3 000° to 5 000°K (compared with maximum flame gas temperatures of 1 600°K), which is probably to be expected from a reaction with the exothermicity of

$$H + OH + OH \rightarrow H_2O + OH^\star$$

It is concluded from this and from the general behaviour of the data, that this last reaction is most likely responsible for the non-thermal emission of all the bands, with the exception of that specifically known to be due to the pre-association reaction.

Detonation Reaction Zone Width

Reaction zone widths in the detonation waves of certain explosives have been derived from the relation of detonation rate to radius of charge by L. N. STESIK and L. N. AKIMOVA, Institute of Chemical Physics, U.S.S.R. Academy of Sciences, Moscow [*J. phys. Chem., Moscow*, 1959, **33**, 148]. A theoretical relation between detonation rate, charge radius and zone width was given some years ago by H. EYRING, R. POWELL *et al.* [*Chem. Rev.* 1949, **45**, 69] and by H. JONES [*Proc. Roy. Soc. A*, 1947, **189**, 415]. In both these investigations the curves for

$$D/D_i = \mathrm{f}(R)$$

have similar shapes, where D is the rate for a charge of radius R, and D_i is the ideal rate. These curves are all described by a function

$$D/D_i = \varphi(a/R)$$

where a is the zone width. The functions given by these investigators differ considerably and neither agrees well with experiment. The authors of the present paper have determined the function experimentally, using trotyl, hexogene, and mixtures of these, and a photographically recording mirror scanner to determine the relation between rate and radius for explosive charges of different diameters.

The experimental curve found for

$$D/D_i = \varphi\,(a/R)$$

differs considerably from the theoretical ones obtained earlier by the investigators mentioned above. The present investigators found that the reaction zone width varies with the radius of the charge.

Future of Aviation Engines

A James Clayton Lecture of the Institution of Mechanical Engineers was delivered in London in December 1959 by S. G. HOOKER, O.B.E., Technical Director (Aero), Bristol Siddeley Engines Ltd [*Chart. mech. Engr*, 1960, **7**, 208]. The subject was the future of air-breathing engines in aviation.

In regard to the growth of thrust, this has increased twentyfold in the past twenty years and recently thrusts in excess of 20 000 lb from development of the Rolls-Royce Conway and the Bristol Siddeley Olympus engines have been announced. It does not seem likely that thrusts much larger than this will be required for subsonic aircraft in Britain but for supersonic military aircraft a boost in thrust by means of afterburning or reheat may be necessary. Thrust exceeding 30 000 lb under sea-level static conditions can be made available from engines of the types mentioned above.

Specific fuel consumptions between 0·8 and 0·7 were obtained in engines with axial compressors in the early 1950s, and lower values have already been obtained. In a design of engine later than the Conway, in which there will be three times as much by-pass air, specific fuel consumptions between 0·6 and 0·5 lb/h.lb thrust developed will be achieved. By raising the compression ratio of this engine a value of less than 0·5 can be obtained. Such engines are real ducted-fan engines, and the development of this type will form the main effort of most aircraft engine companies in the next few years. The advantages of the ducted-fan engine over the conventional jet for civil aircraft are threefold: a lower noise level for a given thrust, a lower specific fuel consumption under cruising conditions, and a greater thrust output for a given weight of engine. These advantages arise from a reduction in jet velocity and an increase in mass flow to maintain the given thrust.

Thrust/weight ratio has increased from rather less than 2 lb for each lb of engine weight in the early Whittle centrifugal engines to between 6 and 7:1 in the Bristol Siddeley Orpheus engine in 1956. Modern designs indicate that ratios of about 14:1 can be achieved in specialized engines used for lifting purposes at take-off and landing.

In connection with the future of engines for supersonic flight, the author discusses the thermodynamic cycle of a typical ramjet engine. The compression ratio of modern jet engines is of the order of 12:1, and if a similar compression ratio can be obtained by forward speed alone, then a considerable simplification can be effected by eliminating the compressor and turbine of the normal jet engine. This principle is that of the ramjet engine in which compression ratios are sufficient to constitute the compression phase of a thermal cycle. So far ramjets have only been used for missile propulsion, but the author considers that their light weight, simplicity and inherent reliability will commend them more and more for use in aircraft as the speed of transport planes increases to three or four times the speed of sound.

For operation beyond the régime of a speed of 2 000 miles/h and altitude of 100 000 ft, the ramjet is the only possible propulsion unit for aircraft and for operation beyond these values, from about 3 000 to 5 800 miles/h and altitudes between 100 000 and 200 000 ft, some characteristics of hypersonic ramjet engines are discussed.

Flame Propagation at Low Pressures

An account has recently been published of a major investigation on the propagation of flame in gaseous mixtures at pressures less than atmospheric, carried out by J. COMBOURIEU, in the Laboratoire de Chimie Générale, Université de Paris, under the direction of Professeur P. LAFFITTE and presented as a thesis for the degree of Docteur ès Sciences Physiques [*Rev. Inst. franç. Pétrole*, 1960, **7–8**, 1–64, **9**, 65–102]. Apart from its theoretical interest, such an investigation has an obvious application in the operation of engines at high altitudes.

A preliminary study of flame propagation was made in closed tubes, with a view to elucidating the mechanism of extinction at low pressures in the region of partial propagation on the pressure/composition diagram. The interpretation of the results obtained was uncertain and it appeared necessary first to determine the fundamental speed of flame in tubes open at the ignition end and to study its variation with pressures less than atmospheric. Experiments were first carried out with propane–air mixtures at atmospheric pressure on the upward propagation of flame in vertical tubes open at the ignition end, similar to those of H. F. COWARD and F. J. HARTWELL [*J. chem. Soc.* **1932**, 1996, 2676] from which they deduced the fundamental speed of flame V_f in methane–air mixtures from the relation

$$V_f = V\Sigma / A$$

where V is the linear speed of uniform movement, Σ the area of the base of the flame, and A the area of the flame front. The stability and symmetry of the flame, however, were not sufficiently good for precise measurements and an apparatus was constructed for determining V_f at different low pressures in a constant pressure vertical combustion tube [see also J. COMBOURIEU, *J. chim. Phys.* **1956,** 963; R. GRAZIOTTI, J. COMBOURIEU and R. FOULATIER, *Vide, Paris,* **1957,** 220]. Photographs of the flame front profiles were obtained using an endless-film camera which was specially constructed. The records obtained gave sufficiently good measurements of the area of the flame front.

In the vertical tube the flame front was symmetrical with respect to the axis of the tube when the pressure p was less than a certain critical value, $p_{\lim}$, and for a given mixture and direction of propagation

$$p_{\lim}d^2 = \text{constant}$$

d being the diameter of the tube. At $p_{\lim}$ cooling of the flame by the tube wall attains a lower critical value, the dead space being very small between the base of the flame front and the wall. By working at $p_{\lim}$ it is then possible to determine, using at least two different tubes, the relationship, $V_f = p^n$, independently of any wall effect. Mixtures of air with propane, methane, ethylene and acetylene were used, as well as some methane–oxygen mixtures. In some mixtures the nitrogen of the air was replaced by helium or argon. The values of n range in general between $-0{\cdot}44$ for very slow flames near the limits of inflammability and 0 for rapid flames. Direction of flame propagation has no significant effect on the value of n. The author states that theories of flame propagation based on the diffusion of active radicals appear to explain certain anomalies met with in rich propane–air mixtures. The experimental criteria found for conditions of flame front stability are interpreted using similarity laws, in particular Reynolds number and Grashof number.

Heat and Mass Transfer

The first issue of the new *International Journal of Heat and Mass Transfer* appeared in June [see *Combustion & Flame,* 1960, **4,** 183]. There are ten original papers of which there are three each from the U.S.A. and the U.S.S.R., and one each from England, France, Germany and Switzerland. There is a bibliography on heat transfer, prepared at the Heat Transfer Laboratory, University of Minnesota, containing over 260 references, mostly for 1958 and 1959, with a few going back as far as 1955.

Two papers in the new journal are of particular interest in connection with the operation of propulsion systems and furnaces at the higher temperatures now increasingly necessary in many engineering systems. C. M. USISKIN and E. M. SPARROW, lately of the N.A.S.A., Lewis Research Center, Cleveland, Ohio, U.S.A., have made a complete formulation, including the local details of gas absorption–emission processes, for thermal radiation in a parallel plate enclosure [*Internat. J. Heat and Mass Transfer,* 1960, **1,** 28]. The approach made by these authors to the subject of non-isothermal radiating gas bodies is different from that of H. C. HOTTEL and E. C. COHEN [*J. Amer. Instn chem. Engrs,* 1958, **4,** 3] who provide interchange factors between finite-sized rectangular gas volumes situated at various orientations with respect to one another. In the present work the temperature is allowed to vary continuously throughout the gas, and energy conservation is therefore applied to *infinitesimal* volume elements. The emissive power of the gas may have an arbitrary dependence on temperature. The only parameter in the problem is kL, where k is the absorption coefficient and L the spacing between plates. Solutions of the governing integral equations are given for kL in the range 0·1 to 2·0. Temperature distributions and heat transfer results are given. For moderate values of kL, the temperature is uniform across the gas.

One-dimensional energy transfer in radiant media is considered in a paper by R. and M. GOULARD, Advanced Development Laboratories, Bendix Products Division, Indiana, U.S.A. [*Internat. J. Heat and Mass Transfer,* 1960, **1,** 81], who extend the mathematical expressions of radiant energy developed in astrophysics to include walls of arbitrary radiative properties in simple one-dimensional geometries. A steady infinite flat layer is considered with conduction and radiation present, the wall conditions being chosen so as to give a good model of a low-speed high-temperature boundary layer. The effect of radiation is to smooth out the temperature profiles and relieve the sharp temperature gradients at the cool wall. The application of this method yields a lower value of both components of the total heat flux, radiation plus convection, than calculated previously by assuming a temperature profile on the basis of conduction only. Such coupling of convective and radiative fluxes is governed by the magnitude of a non-dimensional parameter, depending on the physical properties and the flow geometry of the problem. This parameter is of the same family as the non-dimensional quantities discussed in a paper by V. N. ADRIANOV and S. N. SHORIN [*Izvest. Akad. Nauk S.S.S.R., Otdel tekh. Nauk*, **1958**, No. 5, 46; see *Combustion & Flame*, 1960, **4**, 84].

New Combustion Appliances

Outstanding developments in fuel efficiency were in evidence in some of the exhibits shown at the Fuel Efficiency and Power for Industry Exhibition, held at Olympia, London, from 27 April to 6 May.

An automatic coal stoking machine demonstrated an entirely new modulating control system which ensures that any fluctuation in the boiler load is provided for by graduating the coal and air supply automatically. This arrangement, coupled with controlled secondary air, should make the machine of particular value for burning bituminous solid fuel in smoke-controlled areas.

The distinctive feature of one new type of oil-fired air heater is the method of combustion. Instead of the conventional gas gun-burner, a combustion unit, especially designed for this form of heating and incorporating integrally the burner air supply and combustion chamber, is utilized.

A coal-fired packaged boiler for installation as a complete unit was displayed. This type of construction up to now has been regarded as having particular application to oil-fired units. Previously coal-fired boilers have been confined to the standard orthodox design of equipment, but in view of the accumulation in the country of coal supplies it is now logical that the proven simplicity of features inherent in packaging should be applied to coal-burning installations.

An impressive exhibit was a three-roller Lopulco mill for a power station. This mill, over 21 ft high and weighing 76 tons, illustrates the significant advance in mill design to provide an output of 25 tons of coal per hour from a single mill.

A unique design of a simple vertical boiler, claimed to represent the greatest advance for many years in this class, offers advantages such as high performance in fluctuating loads, maximum safety and low maintenance costs. Between the primary and secondary combustion chambers the inner lining of the boiler shell is necked to provide a throat through which all the combustion products must pass so as to promote mixing and complete combustion.

A new pressure jet oil burner recently developed for domestic hot water and central heating boilers of a wide range of capacities was exhibited. The noise level of this pressure jet burner has been reduced down to a point where it is no longer objectionable. At the same time combustion efficiency has been maintained with extremely low smoke emission thus contributing to a reduction in boiler cleaning.

Other noteworthy exhibits were a new portable injector equipment for oil firing top-fired continuous Hoffman kilns and side-fired Belgian kilns, and a static model of a new electro-precipitator designed especially for the iron and steel industry.

The Institute of Physics and the Physical Society

The incorporation of a new body on 17 May, under the name of *The Institute of Physics and The Physical Society*, marks the fulfilment of the desire expressed by the overwhelming majority of the members of the Institute and Society for their amalgamation.

The first President of the amalgamated body is Sir JOHN COCKCROFT and the four Vice-Presidents are Dr J. TOPPING, Dr W. H. TAYLOR, Professor R. W. DITCHBURN and Mr A. J. PHILPOT, each responsible to the Council for a defined area of the activities to be taken over by the new organization from its predecessors. The Presidents of the predecessors, Sir George Thomson and Mr J. A. Ratcliffe, are also members of the new Council. The other Officers are Dr J. Taylor, Honorary Treasurer and Dr C. G. Wynne, Honorary Secretary. The Secretary of the new body is Dr H. R. Lang and the headquarters are 47 Belgrave Square, London, S.W.1.

Accurate Measurement of Temperature

Robust equipment is being developed at the Mechanical Engineering Research Laboratory, East Kilbride, Glasgow, for measuring temperature under industrial conditions with an error of only a few millidegrees centigrade.

A new type of resistance thermometer is used. It contains two elements, one with a high temperature coefficient of resistance and the other with a low coefficient. The former is a copper wire wound on an insulated copper cylinder and the latter is minalpha wire wound on a cylinder of minalpha; in this way the effects of differential expansion are reduced.

The temperature is determined by means of a bridge circuit. An a.c. bridge with transformer ratio arms is particularly suitable since these arms can readily be made of high accuracy and the ratios are not affected by vibration or by variations in air temperature.

The existing equipment is intended for use in the range 0° to 100°C, but the method can also be applied to other temperature ranges. Further information is given in *N.E.L. Fluids Note No. 82*: 'A resistance thermometer and bridge of millidegree accuracy for field use', by W. H. P. Leslie and J. J. Hunter, available from the Laboratory.

New Instruments

Amongst the exhibits at the Instruments, Electronics and Automation Exhibition held at Olympia, London, in May, the following were noted for their application in combustion processes.

Transmitting signals from reciprocating, rotating or oscillating parts of a machine to stationary measuring equipment usually involves the use of intermittent contacts or flexible leads. Such devices have several disadvantages and to avoid these the British Internal Combustion Engine Research Association has developed a transistorized radio telemetering system, using small but robust encapsulated units.

Particularly suitable for diesel engines and gas turbines, the system was demonstrated on a sectioned working Petter AVA2 diesel engine. A transmitter complete with aerial is mounted inside a piston reciprocating in a cylinder, transmitting temperature indications. The piston, with a transducer mounted in its crown, comes in contact with a heating element at the top of the cylinder and a compressed air jet at the bottom of the cylinder, so producing a maximum contrast signal on the c.r.o. The transducer signal varies directly the carrier frequency of 2 Mc/s. At the receiving station the frequency variations are converted into voltage variations suitable for display on an oscilloscope screen.

A Venturi pneumatic pyrometer designed by the British Coal Utilisation Research Association gives almost instantaneous readings of gas temperatures in industrial furnaces, including those which are too high for suction pyrometers or accompanied by too much fume and slag for the suction type to have an appreciable life. It has been used for temperatures up to 2 200°C and could be used for even higher temperatures.

A stream of gas from the furnace is drawn into a water-cooled probe, 11 ft long by $2\frac{3}{4}$ in. diameter through a $\frac{1}{2}$ in. bore Venturi-type orifice, and then through a second cold Venturi. The temperature of the cooled gas is measured just after the cold Venturi. As it is important that the two orifice pressure drops be measured simultaneously, a simple analogue computer with pressure transducers is an essential part of the equipment. The computer output is then an e.m.f. proportional to the hot gas temperature.

The B.C.U.R.A. has also produced a recording dewpoint meter, an automatic version of the earlier manual meter. It consists of an air-cooled element carrying a thermocouple and a surrounding ring electrode between which an a.c. potential is maintained. The element is mounted on a probe and inserted in the gas stream. On cooling to the dewpoint temperature a liquid film condenses on the surfaces of the element and a current flows between the thermocouple and the ring. The signal produced activates a recorder and automatically shuts off the cooling air, allowing the element to warm up. The film evaporates and the cycle begins again and is repeated every 20 to 30 seconds, giving a continuous record of variations in the dewpoint temperature.

Theory of Flame Propagation

J. O. Hirschfelder and C. F. Curtiss, Theoretical Chemistry Laboratory, University of Wisconsin, Madison, have made a recent further contribution to the theory of flame propagation [*Appl. mech. Rev.* 1960, **13**, 231]. In this paper only one-dimensional steady-state flames are under discussion as a first step in an attempt to apply to practical systems the theory of flame propagation based on well-known aerodynamic equations which include the effects of chemical kinetics.

As previously, these authors define the cold boundary by the conception of a flameholder. The treatment begins with the observation that there is a maximum amount of heat which the flameholder can extract without extinguishing the flame. For smaller amounts of heat transfer from the flame to the flameholder there is both a stable burning mode with a relatively large flame speed and an unstable mode with a smaller flame speed. For steady-state flames a flameholder which extracts a small amount of heat from the fuel gases is necessary. The heat transfer to the flameholder determines the quenching distance and thus the position of the flame with respect to the flameholder.

The basic equations are those of conservation of each chemical species and of energy balance, and the diffusion equations; the equation of motion does not usually play an important part in one-dimensional flames. In order to calculate the flame velocity, therefore, there must be established equations for the boundary conditions, those at the flameholder and those far from the flameholder at the *hot* boundary. In a particular chemical system and set of initial conditions, there is only one value of the flame velocity for which there exists a solution of the flame equations which satisfies all the boundary conditions. Thus the flame velocity, or mass rate of flow, is an eigenvalue of the flame equations.

The expression obtained for flame velocity is in agreement with all treatments of flame propagation and indicates that the velocity is proportional to the square root of the reaction rate. Diffusion in simple flames is observed to decrease the flame velocity and in a typical case the authors calculate that the velocity in a system with no diffusion would be almost twice as large as in a system with a reasonable coefficient of diffusion. In the hottest part of the flame, where most of the reaction takes place, the free radicals are diffusing away from the flameholder so that, in the authors' opinion, the purely diffusional theories of flame propagation cannot be true.

Another recent paper on the theory of the rate of combustion of hydrocarbon mixtures that should be noted is that by K. Weiss, Institut für Theoretische Physik der Johannes-Gutenberg-Universität in Mainz [*Z. Elektrochem.* 1959, **63**, 1081]. A scheme is described which is based simply on the use of molecular formulae and, taking into account dissociation, equations are set up for determining burning velocity. A thermal theory of combustion, which was put forward some ten years ago by K. Bechert [*Ann. Phys., Lpz.* 1949, **4**, 191; 1950, **5**, 349. *Z. Elektrochem.* 1950, **54**, 239] and gave very good agreement between measured and predicted trends, has been used by Weiss for calculating the speed of combustion. The essential feature of his procedure is to designate the composition of the mixtures by a magnitude ε which has the value unity for stoichiometric mixtures and less or more than 1 for mixtures with excess of air or fuel respectively. In this way it is considered easier to compare properties such as flame speed and limits of ignition, which depend on mixture composition. The agreement between the values calculated as a function of ε and experimental values appears to be very good, both for weak and rich mixtures.

Safe Oil Heaters

A new British Standard for oil heaters was recently published [*B.S. 3 300* (1960): 'Kerosine (paraffin) unflued space heaters, cooking, and boiling appliances for domestic use']. The main feature in this standard is a really severe draught test and the appliances covered include radiant drip-feed heaters. Tests will have to be made by manufacturers by means of a wind-tunnel to ensure that heaters will not create a fire hazard even when exposed to draughts up to 26 ft/sec, that is 17 to 18 miles/hour. This is the rate recommended by the recent report of the Department of Scientific and Industrial Research. In order to limit as much as practicable the hazard which might result should an appliance be knocked over it is laid down that all heaters must include some provision for fixing them to the floor or wall to prevent them overturning. The fuel tanks of radiant heaters must also be made of corrosion-resistant materials to obviate another possible source of fire risk.

Diffusive Burning of Liquids

A paper on the rate of combustion from free surfaces of liquid hydrocarbons was presented by W. L. Fons, Pacific Southwest Forest and Range Experiment Station, Forest Service, U.S. Department of Agriculture, to the Spring Meeting of the Western States Section of the Combustion Institute, in California (see this Journal, **1960**, **4**, 190). The study was one of several planned to help in designing a model combustion system to represent the complex fuel and weather conditions in forest fires.

n-Hexane and *cyclo*hexane were burned in circular pans of ten different diameters from about 0·2 to 12 in., to learn the influence of diameter of the fuel surface on the rate of combustion. This work may be regarded as somewhat complementary to that of V. I. Blinov and G. N. Khudiakov [*Dokl. Akad. Nauk S.S.S.R.* (*N.S.*), 1957, **113,** (5), 1094], and H. C. Hottel's quantitative analysis of this latter work [*Appl. mech. Rev.* 1959, **12,** 876; see *Combustion and Flame*, 1960, **4,** 84]. The Russian investigators, however, used pans with diameters up to 22·9 m. The velocity of burning found by Fons when plotted against the diameter of pan gives a curve generally similar to those plotted by Hottel, decreasing with small pan diameters but increasing with diameters greater than about 5 in., corresponding respectively to the laminar flow régime and a transition régime. For still larger diameters the velocity increases still more in the turbulent flow régime obtaining in the larger pans discussed by Hottel up to about 36 in. in diameter, after which the burning velocity does not change.

Robot Supervision of Gas Supply

A new installation of electronic supervising equipment, capable of reporting any combination of conditions relating to the performance of Newbury gas holder station, Berkshire, has recently been set in operation by the Southern Gas Board. This station is the first one in the world to have robot equipment capable of supervising a complete district gas supply without any form of manual assistance. It is the result of extensive development work carried out jointly by F. Bell, the Board's Distribution Engineer, and the manufacturers, Sound Diffusion (Auto-Thermatic) Ltd, Portslade, Sussex, who also carried out the installation work. The system is known as Datofonic and is the first method of supervising control possible without the need for private telephone lines. The operating conditions at Newbury can be made known to the area control centre at Reading, 17 miles away, for the cost of an ordinary telephone call.

The equipment is completely automatic in operation and gives all its information verbally, thereby eliminating the need for decoding and display equipment in the control room. There are six main supervisory functions which the Datofonic equipment reports on simultaneously; (*i*) stock held in the 750 000 ft^3 gas holder, (*ii*) pressure of gas in grid main, (*iii*) pressure of gas in local medium pressure main, (*iv*) pressure of district supply, (*v*) electricity supply, (*vi*) booster operation. The equipment is put into operation by either an alarm condition being set up on the holder site or by interrogation from an outside telephone. When an alarm occurs the equipment automatically engages the site telephone exchange line and requests the manual exchange operator to make connection with the control room number of the Southern Gas Board at Reading. This request is made from a record which forms part of the equipment. Readings on all monitored items are continuously fed into the supervising equipment via tappings from appropriate recorders.

German Gas Turbine Developments

A paper by the late Professor Dr-Ing. K. Leist, of the Institute for Turbo-machines at the Rheinisch-Westfälische Technical University, Aachen, who died in May, was presented to the Sectional Meeting of the World Power Conference held in Madrid in June, giving an account of recent developments of gas turbines in the Federal Republic of Germany [*Brennst.-Wärmekr.* 1960, **12**, 267]. Since 1945 attention has been given in Germany particularly to the development of coal-fired stationary gas turbines, the question of fuel prices having a considerable influence on this.

A description is given of the 2 300 kW coal-fired plant operating successfully on a closed cycle as an industrial power plant at Ravensburg since 1956. This is probably the first plant of its kind and has provided experience for similar installations such as the thermal power plant at Coburg and Oberhausen using pit coal, and also plant in Moscow using brown coal. At Coburg the plant now being constructed for the municipal power supply is a 6 600 kW hot-air turbine to be fired with coal dust.

One firm which is building open-cycle gas turbines with outputs between 1 500 and 18 000 kW, for gaseous and liquid fuels, with and without heat exchanger, is developing a system of cooling the rotor blades by means of water whereby the gas temperature may be considerably increased. A trial turbine of this design is arranged for 1 000 kW.

An interesting example is given of gas turbines with free-piston gas generators with 1 000 h.p. per generator which have become widely established. This is a 1 250 kW compound plant with three gas generators and an exhaust heat gas boiler which has been in continuous operation at a cellulose mill since 1958, working for 6 000 hours per year with an average load of 80 per cent. The essential advantage of such installations is that the waste gases, owing to their much higher air content, can be utilized as preheated combustion air in a subsequent process.

Gas turbines are eminently suitable for small and medium power outputs and considerable attention has recently been given in Germany to developing units of under 300 h.p. to serve as small stationary plants. A 65 h.p. gas turbine which has recently begun to be manufactured, has been developed to drive fire pumps and other equipment of small dimensions, with vertical shaft if necessary. Compressor and turbine of this unit, built as a single-shaft machine, are of the semi-apertural radial design. The plant has an air flow rate of 0·6 kg/s, with a pressure ratio of the compressor of 3 : 1 and a speed of 45 000 rev/min. The fuel consumption at full load is about 600 g/h.p.h., and the unit including gearing weighs 65 kg. The air flows from the compressor outlet to the combustion chamber inlet in such a manner as to cool the chamber walls and the hollow turbine guide blades. The fuel, which is gasoline, kerosine, diesel oil or light fuel oil, is atomized by means of a centrifugal disc.

An interesting account is given of some of the major problems which are being investigated in several research institutes.

W. A. Kirkby

FUEL

Readers of *Combustion and Flame* may wish to know that the July issue of *Fuel* contained *Notes* dealing with:

Liquefied petroleum gases
Coke News
Air pollution problems and legislation
International cooperation in air pollution research
Reactivity of coke

while a further *Note* on the National Society for Clean Air may be found in the September issue of *Fuel*.

Publications

MATHEMATICAL ASPECTS OF SUBSONIC AND TRANSONIC GAS DYNAMICS

L. Bers. New York: Wiley; London: Chapman and Hall, 1958. *xv*+164 *pp*. $7.75 or 62*s*

The surveys in Applied Mathematics, of which this is the third volume, have been written as a joint project of the American Office of Naval Research and *Applied Mechanics Reviews*. They are intended to provide a coherent treatment of the subject, not for research specialists who must know the original papers, but for 'a broader, mathematically literate audience' who wish to be able to apply these results to other problems. In particular they also hope to put relevant Russian papers into the same picture. How far has the author succeeded in achieving these very laudable aims? He has himself contributed a large number of mathematical papers to the subject, many of them only available as N.A.C.A. *Technical Notes*, and sometimes he has even to give a reference to his own university lecture notes. He is a very clear expositor and the argument flows smoothly without excessive insertion of algebraic steps; it is frequently illustrated by clear diagrams. The fact that he is attempting to combine a large number of published papers is bound to intrude periodically when he refers briefly to the different treatment of a problem by Japanese, Russian or German authors. When a mathematical derivation is standard he tends to refer to several textbooks and may involve the reader in more background study than the latter will care to make. In order to keep the book in the field readily susceptible to mathematical treatment it is limited to two-dimensional steady potential flow and von Kármán's statement 'if there is really serious doubt about the answer, the mathematician is of little help' is acknowledged cheerfully and without contradiction. However, it is very satisfactory to the fluid flow physicist and engineer to see that he has so greatly aroused the interest of the mathematicians in a problem closely related to the practical experimental world.

M. W. Thring

SPACE TECHNOLOGY

Edited by H. S. Seifert. New York: Wiley; London: Chapman and Hall, 1959. *xvi*+1140 *pp*. 180*s*

Only five years ago space travel was still regarded by many scientists and engineers as rather improbable. Now the technology is so well established that it is possible to base a graduate lecture course on the subject, and for the contents of this course to fill a book of about a thousand pages.

Thirty eight authors, each an expert in his special field, have contributed and there is no doubt that the subject matter is authoritative. On the other hand, since little practical space flight has yet been achieved, the treatment is largely theoretical, so that whereas the specialist may find individual chapters helpful, the general reader may get no farther than the introduction to them.

Combustion specialists will naturally turn to the chapters on Rocket Propulsion. The first of these deals primarily with the idealized flow of a compressible gas, but it contains an interesting section on the flow pattern outside the exit of a rocket nozzle. The second chapter on liquid fuelled rocket engines is written in very general terms. The design of propellant injection arrangements is not discussed at all critically and the paragraph on combustion oscillations is disappointingly vague. The following chapter, on solid propellant motors, is much more definite and can be recommended as an excellent introduction to the subject. Later chapters deal with more advanced types of nuclear and ion rockets.

Other sections of the book deal with Flight Dynamics—satellite, lunar, and interplanetary trajectories—Communications, Guidance and Control, and Human Needs in Space. The last section covers the use of satellites for research in the upper atmosphere and the paragraphs on 'chemical aeronomy'—that is, the chemical reactions produced by the strong ultra-violet radiation at high altitudes—may interest combustion chemists. There is also a short finale in the shape of a panel discussion between Ramo, Porter, Wheaton and Kantrowitz on 'What the future holds'. Certainly the members of the panel were confident that it held manned space flight.

Although intended for graduate students, it would appear unlikely that any single reader could cope adequately with more than a small proportion of the text. The volume will therefore appeal more to the librarian than to the individual reader.

S. L. Bragg

EXPLOSIONS, DETONATIONS, FLAMMABILITY AND IGNITION

B. P. Mullins and S. S. Penner. London: Pergamon, 1959. *xi*+287 *pp*. 70*s*

This book is unusual in that it deals with the subject matter, which is mainly gaseous flames and explosions, from two quite different points of view. The first part by Professor Penner is a review of theoretical aspects of some problems of gas phase combustion, including explosion and flammability limits, ignition, detonation, quenching and chain reactions. Except perhaps for the chapter on detonation, a thorough knowledge of the background to the subject is taken for granted and little experimental information is provided to support the various theoretical approaches outlined. Emphasis is placed on the value of certain simplifications assumed by Schvab and Zeldovich for obtaining tangible results from general conservation equations and the author illustrates their utility in deriving relationships for droplet burning and heterogeneous combustion. The analysis although claimed to be more powerful than that of Spalding does not proceed as far in giving relationships of practical value.

In contrast, the second part of the book by Dr Mullins covers much the same field mainly from a phenomenological standpoint. Stress is laid on the practical usefulness of certain semi-empirical generalizations based on the concept that limiting 'combustion phenomena occur when the rate of heat developed by chemical transformation equals the rate of heat lost to the surroundings'. Although this dictum is unexceptionable and is well illustrated, the text might have benefited if a clearer indication were given wherever possible of the factors that control the rate of chemical transformation. This part of the book contains a wealth of information and stimulating ideas particularly on spontaneous and electrical ignition, combustion processes and flammability limits. However, its usefulness for engineers interested in explosion prevention is, apart from a source of references, limited by a lack of balance in the treatment of the various topics. For example, the reviewer found little reference to ignition by friction sparks or to safe gaps, and only two pages are devoted to dust explosions. On the other hand, a whole chapter is given over to flash points; this is perhaps too liberal, in spite of the importance of the subject, and it could well have been included in the chapter on flammability limits. An account of the use of water to extinguish fire forms part of a chapter on the use of water and air to prevent explosions. Since water is used far more frequently to extinguish fires than to prevent explosions, the emphasis could profitably have been reversed.

The contributions of the two authors are intended to be complementary, yet the connection between them is so tenuous that they might as well be two different books. There is little doubt that the book as a whole would have gained by a more ample cross referencing from one part to the other. As it stands the two parts although individually of great value, will appeal to two different audiences rather than the whole book appealing to a wide audience. The book would also have profited by the inclusion of full lists of symbols.

D. J. Rasbash

ROCKET PROPULSION

M. Barrère, A. Jaumotte, B. F. Fraeijs de Veubeke and J. Vandenkerckhove. London: Elsevier (D. Van Nostrand Co. Ltd., 358 Kensington High Street, W.14), 1959. *xxxi*+829 *pp.* 135*s*

In this book the authors attempt to cover a very wide field by giving a detailed account of the fundamentals of rocket propulsion and a description of the technological problems and developments of rocket motors during the past few years. Whilst the principles of rocket propulsion are now well established, the technology of rockets is still in its infancy and shows all the phenomenal growth of a well nurtured infant. A balance between these two aspects of the subject is not easy to achieve in a single work and although the results here are satisfactory, the presentation of the theory might with advantage have been more concise.

In the first chapter the main types of rocket motors are described with reference to some recent missiles as well as to that ubiquitous veteran rocket, the German V2. These descriptions are followed by what is termed the energy approach to rocket propulsion. This introduction is sound but not too well executed and some important equations are not set out as clearly as one might wish. Also the review, which follows, of the energy available from chemical propellants and other sources is too brief to be of much value. In contrast to this the theory of nozzles is dealt with exhaustively in the second and third chapters. Idealized flow conditions for homogeneous and heterogeneous systems are introduced first followed by what is termed aerothermochemistry of combustion products or, in other words, the properties and behaviour of real gases under rocket conditions. The overall performances of rockets and multi-stage missiles are considered also in the concluding chapters where the mathematical approaches to problems of achieving maximum performance are indicated.

Between these largely theoretical sections lie the chapters on rocket technology. Solid propellants and the internal ballistics and design of solid propellant motors are described in three chapters contributed by Dr Vandenkerckhove. Liquid propellant rockets are similarly dealt with by Dr Barrère who also contributes a chapter on test-bed techniques. Both authors are well informed and have drawn widely on their own experiences and on the large volume of papers published recently. It is not their fault that much of the material is *ad hoc* or that empirical relationships abound.

Rocket technology involves the application of several sciences and for that reason it is doubtful whether the style of this book will be wholeheartedly acclaimed by the pure chemist, pure aerodynamicist, or, if such exist, the pure engineer. Much of its value and appeal lies in the fact that it is a composite work produced by four specialists in different branches of the subject. Most readers will find interest in parts if not all of the book. The English translation is satisfactory, but the price is uncomfortably high.

W. G. Parker

IONIZATION PHENOMENA IN GASES

G. Francis. London: Butterworths, 1960. *vii*+300 *pp.* 60*s*

It is the intention of the author that this book should be complementary to the several existing treatises on the subject, and that this volume should discuss in most detail those branches and applications which have not hitherto been adequately treated, e.g. in astrophysics and in nuclear devices. The book is intended mainly for those near the end of a physics degree course, or for those about to commence research in the subject.

In the first three chapters the fundamental principles are reviewed. Thus the first chapter is a brief outline of the wave-mechanical treatment of atomic structure and spectroscopic theory. Then follows a review of the motion of particles in gases, with special emphasis on elastic and inelastic collisions involving electrons, ground state and excited atoms, and ions ionization by electron and atomic impact, thermal ionization, ionization by shock waves in gases, diffusion and de-ionization are discussed in detail. Since surface processes at electrodes are important in discharges the emission of ions and electrons from metal surfaces, and the various phenomena associated with the impact of atoms, electrons, ions and photons with surfaces are reviewed. In the third chapter the principles of similarity are developed for discharges between electrodes in gases, and their applications for the interpretation of experimental observations are discussed. In the remaining four chapters the basic principles are employed for the discussion of alternating and high frequency discharges, ionization and excitation in the upper atmosphere, high current discharges and thermonuclear effects, and plasma oscillations and waves. In spite of the advanced level and condensed form of the mathematical theories involved, the book is generally easy to read and has been carefully prepared, although in a few places the significance of some symbols is a little obscure.

It is evident from the foregoing outline of the contents of this book that research workers in the field of combustion are unlikely to be directly concerned with the main part of the volume. Nevertheless the subject matter of the introductory chapters is of prime importance to those concerned with ionization phenomena in flames. For them the large number of references to original papers and to more comprehensive treatises on the subject, which are listed at the end of each chapter, could be particularly useful.

C. W. Nutt

ROCKET PROPELLANT HANDBOOK

B. Kit and D. S. Evered. New York and London: Macmillan, 1960. 351 *pp*. $12.50 or 87*s* 6*d*

Rocket engineers and others who need information on rocket fuels spend a lot of time hunting for it through the jungle of scientific and technical journals and there is no doubt that a *Handbook* which gathers this knowledge together is timely and welcome.

Three difficult problems face the authors of a work of this kind. The first is the problem of selection of propellants, the second is the matter of additional information over and above the straightforward physicochemical data and the third is the problem of arrangement. As regards selection, the authors of this *Handbook* have made a reasonable choice. All the liquid propellants in common use are included together with some which have potentially higher performance, such as fluorine. The ingredients of solid propellants are to be found but information on solid propellants as such is understandingly meagre. To return to liquid propellants, monographs of considerable size have been written on many of the substances included, e.g. hydrogen peroxide, and it is not surprising that the drastic abridgement of general information required for a handbook of this size opens the door to criticism. Methods of manufacture are interesting, but not vital to the rocket engineer. If room is found for them the methods should be concise with emphasis on the principles of important productive processes. The prominence given to the barium peroxide process for hydrogen peroxide, for example, is misleading and to be told that air is obtainable in large amounts everywhere on the surface of the earth seems a bit unnecessary. The information on storage and handling of propellants is welcome although it is rather poorly presented. The description of water as a stabilizer for hydrogen peroxide is unusual and the recommendation that acetanilides should be available on all sites where hydrogen peroxide is handled suggests an academic rather than a practical outlook. Lastly, on the arrangement of material, the authors deserve praise for the many references which they have consulted and which they list at the end of each chapter together with a separate bibliography of further works. Most of the physical, chemical and performance data are given in separate tables for each propellant. This appears to be wasteful of space but may be the only practical method of presentation in view of the great diversity of facts available for each substance. Errors may be found and there are some inconsistencies, for example, in Appendix 1, it is stated that heats of combustion are usually given in btu/lb while in Appendix 2, these are tabulated in btu/lb mole, but such details will be put right in time no doubt and the book as a whole is a very useful one.

W. G. Parker

Letters to the Editors

Letters to the Editors on points of scientific interest related to combustion and flames are invited. The Editors do not hold themselves responsible for opinions expressed in correspondence. Anonymous contributions cannot be accepted.

On the Decomposition Flame of Solid Ozone–Oxygen Mixtures

IN AN earlier paper of the author[1] a theory was presented dealing with the decomposition flame of liquid ozone or mixtures of ozone and oxygen in a glass tube. The results were found in reasonably good agreement with available experimental results. This theory can be further extended, without any major modifications, to cover solid ozone–oxygen mixtures also.

In any experiment of this kind, the solid mixture will have to be kept in a tube which is cooled at the outside to a sufficiently low temperature T_1. A thin liquid layer is formed on top of the solid so that the flame zone is in contact with the liquid only. So the phenomenon is almost identical to the evaporation and decomposition of the liquid mixture and all formulae derived for that case apply here also. However, the numerical values for the initial temperature T_1 and the flame temperature T_f will be different and likewise the difference $h_0 - h_1$ between the enthalpy of the gas at temperature T_0 (surface temperature of the liquid) and the enthalpy of the solid at temperature T_1.

The quantities T_f and $h_0 - h_1$ can be computed by thermodynamic methods. Most of the data required for this are now available and a fairly good estimate can be made for the missing ones.

By a suitable technique, it is possible to avoid macroscopic phase separation during freezing of liquid ozone–oxygen mixtures so that the solid mixtures can be regarded as homogeneous substances*. It has been assumed further that the enthalpy of the mixture can be found simply by adding the enthalpies of the components. Complete data are available for oxygen[2]. For ozone, most data can be found in C. E. THORP's ozone bibliography[3]. The specific heat of liquid ozone has recently been determined by R. I. BRABETS and T. E. WATERMAN[4]. An estimated value for the heat of fusion (**500 cal/g**) and an exactly measured value for the density of solid ozone (**1·728 g/cm³**) are given in a paper by A. G. STRENG and A. V. GROSSE[5]. The only quantity which is at present unknown is the specific heat of solid ozone. Here the best basis for an estimate seems to be comparison with solid oxygen. The specific heat of solid oxygen is **0·35** cal/g °C between the melting point of this substance (**54**°K) and a transformation point at **43·5**°K. The same value was assumed for solid ozone between its melting point (81°K) and **43·5**°K. This seems to be justified in view of the fact that the specific heats per gramme are almost equal for liquid ozone and oxygen (**0·425** and **0·394** cal/g °C at **90**°K). For lower temperatures the assumption has been made that the enthalpy required for heating one gramme of the substance up to **43·5**°K is the same for ozone and oxygen (including the transformation heat). These assumptions are, of course, somewhat arbitrary since nothing seems to be known about transformations solid ozone might undergo at these low temperatures. Luckily, the influence of these assumptions on flame temperature and flame velocity is very small. For pure ozone, a **10** per cent change in the enthalpy increase from $T_1 = 20$°K up to the melting point would result in a change of the flame temperature of **8**° and of the flame velocity of **1·3** per cent only. For a **50** per cent mixture, the corresponding values would be **5**° and **2·0** per cent.

Numerical computations were carried out for pure ozone and for mixtures containing **50** and **75** mole per cent ozone at atmospheric pressure and for initial temperatures T_1 of **20**°K, 63°K (melting point of nitrogen) and **70**°K. The melting point curve of ozone–oxygen mixtures

---

*Private communication from Dr A. G. STRENG of Temple University.

Table 1. Flame temperatures and velocities

Variable	$y_{30}=0{\cdot}50$		$y_{30}=0{\cdot}75$			$y_{30}=1{\cdot}00$		
T_1 (°K)	20	63	20	63	70	20	63	70
T_0 (°K)	150·5	150·5	156·5	156·5	156·5	161	161	161
T_f (°K)	1371	1445	1894	1960	1969	2287	2339	2346
V_0 (cm/s)	20·2	26·9	74·2	85·6	87·2	130	140	143
V_1 (cm/s)	0·0380	0·0505	0·147	0·170	0·173	0·274	0·294	0·301
V_1* (cm/s)		0·0774			0·227			0·361

*Flame velocity of corresponding liquid mixture (initial temperature 90°K).

does not seem to be known at present but it can safely be assumed that at 70°K the 50 per cent mixture will be liquid. On the other hand it is not possible to state if the 75 per cent mixture is solid at that temperature but the flame velocity has been tentatively calculated.

The results are shown in *Table 1*. In this table y_{30} is the molar fraction of ozone in the unburnt mixture, V_0 is the linear flame velocity in the gaseous mixture at temperature T_0 while V_1 is the velocity in the solid, i.e. the velocity at which the flame will move down in the tube. Comparison with the values previously calculated for corresponding liquid mixtures[1] shows that the flame temperatures and velocities are considerably lower for the solid mixtures, in particular for the 50 per cent mixture. For pure ozone, the difference in flame temperature is not as great, owing to dissociation of the molecular oxygen into atomic oxygen. In addition, the temperature dependence of reaction rates and consequently of flame velocities is not as great at high as at low temperature.

For the sake of simplicity, the psychrometric effect has been disregarded here as well as in earlier publications of the author. It would make the flame velocity a few per cent lower.

The theory is believed to yield somewhat too low values for the flame velocities of liquid mixtures. The same should be true for solid mixtures.

The author wishes to express his thanks to Dr J. W. Broughton of the National Research Council for reading and commenting on the manuscript.

R. SANDRI

National Research Council,
Ottawa, Canada

(*Received February 1960*)

References

[1] SANDRI, R. *Combustion & Flame*, 1958, **2**, 348

[2] *Gmelin's Handbuch der anorganischen Chemie* (Oxygen Volume). Verlag Chemie, Weinheim/Bergstrasse

[3] THORP, C. E. *Bibliography of Ozone Technology*, Vol. II. Armour Research Foundation of Illinois Institute of Technology: Chicago, 1956

[4] BRABETS, R. I. and WATERMAN, T. E. *J. chem. Phys.* 1958, **28**, 1212

[5] STRENG, A. G. and GROSSE, A. V. *J. Amer. chem. Soc.* 1959, **81**, 805

Temperatures of Flames Burning on Porous Burners

IN A recent communication D. B. SPALDING and V. S. YUMLU[1] presented measurements of the heat transferred to a porous burner as a function of flow velocity for several combustible mixtures at atmospheric pressure. Their data are presented in the form of plots of the burning velocity S_{20} against Q, where S_{20} is the linear velocity of the unburnt gas measured at 20°C and Q is the heat transferred to the burner per unit volume of fuel. According to these data, there are two values of S_{20} for a single value of Q over limited ranges of Q for each of the mixtures discussed. The authors state that this finding is evidence in support of a theory of inflammability limits given by D. B. SPALDING[2], in which it is deduced that a single value of a heat loss parameter leads to two values for the burning velocity.

It might be inferred from these papers and an earlier one by J. P. BOTHA and D. B. SPALDING[3], that it is possible to calculate the temperatures of flames burning on porous burners from the values of Q. It is the purpose of this Note to point out that there is a large discrepancy between temperatures calculated from Q and those measured directly by the present author[4] on some of the same mixtures and over the same velocity range as reported by Spalding and Yumlu, and that the discrepancy remains large, even when other known heat losses are taken into account.

The temperature of a non-adiabatic flame can be easily calculated, just as with adiabatic flames, given the appropriate thermodynamic data, the magnitude of all of the heat losses, and by making a suitable assumption as to whether the flame gases are at equilibrium. With the flames for which Q values have been reported, the simplest set of assumptions which could be made would be to assume that Q was the only heat loss term and that the gases were at chemical equilibrium at the maximum temperature. This, in fact, is precisely what was done by Botha and Spalding[3]. As these authors pointed out, this procedure is formally equivalent to calculating an adiabatic flame temperature for the case where the amount of heat Q is removed from the unburnt gas.

With these assumptions, the flame temperature with heat loss Q can be calculated from

$$\int_{T_Q}^{T_a} C_p \, \mathrm{d}T = Q \qquad \ldots . [1]$$

where C_p is the heat capacity of the burnt products and Q is the heat removed by the porous plug, both for the same mass of gas; T_a is the adiabatic flame temperature corresponding to the reference initial condition (atmospheric pressure and 20°C here), and T_Q is the desired temperature of the flame burning on the porous burner.

Table 1. Flame temperature as a function of unburnt gas velocity, S_{20}, for three values of the equivalence ratio φ for hydrogen–air flames at one atmosphere. T_Q are deduced from the Q values of Spalding and Yumlu[1]; T_{TC} are from Kaskan[4] and the $\Delta T_{\rm rad}$ are the radiation corrections applied to obtain each T_{TC}

φ	S_{20} cm/s	T_Q °K	T_{TC} °K	$\Delta T_{\rm rad}$ °K
1·0	10·0	1755	1515	45
	9·0	1745	1495	44
	8·0	1745	1470	44
	7·0	1760	1450	43
	6·0	1780	1420	42
0·8	10·0	1625	1485	41
	9·0	1610	1465	40
	8·0	1600	1445	39
	7·0	1605	1425	38
	6·0	1625	1400	38
0·6	10·0	1475	1405	34
	9·0	1460	1390	34
	8·0	1450	1370	33
	7·0	1450	1355	33
	6·0	1470	1330	32

Some results of applying equation 1 to the Q values of Spalding and Yumlu, for the hydrogen–air mixtures with $\varphi = 1{\cdot}0$, $0{\cdot}8$, and $0{\cdot}6$, are given in *Table 1*. In *Table 1* are given:

(*a*) The flame temperatures we have calculated[5] from the Q values read off Fig. 3, ref. 1

(*b*) The corresponding temperatures read from Fig. 7, ref. 4

(*c*) The radiation correction added to the thermocouple temperature to get the temperature in (*b*) above.

It can be seen that the differences between the two temperatures for apparently identical flames are as large as 360°C, and always larger than the radiation correction applied to the thermocouple. It is clear that similar differences exist for the other mixtures common to references 1 and 4.

These large differences suggest that one cannot neglect other sources of heat loss. Thus, in equation 1 the single term Q should be replaced by a sum over all possible heat losses. The only significant terms in the sum one expects are those which represent losses from: (*a*) radiation, (*b*) incomplete reaction at the plane of maximum temperature, and (*c*) edge effects. On the basis of the data of Botha and Spalding[3], the last one can be disregarded since they obtained substantially the same results on 1 in. and on 2 in. diameter burners. Thus, only (*a*) and (*b*) need be considered.

Properly the radiation loss should be calculated by integrating the rate of emission from the time of leaving the burner surface to the time at the temperature maximum. Since this would require a more detailed knowledge of the structure of the flame than is available for these flames, it is simpler to estimate this loss from the far downstream rate of cooling. In these flames the rate of temperature decrease a few millimetres downstream of the plane of maximum temperature is constant, and agrees well (within 30 to 40 per cent) with what is calculated using the emissivities of water vapour given in the book by W. H. McAdams[6]. Hence, an approximate value for the radiation loss, in terms of a temperature decrease from that otherwise expected, is given simply by the product of the downstream temperature gradient and the distance from the burner surface to the plane of maximum temperature (2 to 3 mm here). This is probably an upper bound, since the average gas temperature in this region is low.

For the conditions listed in *Table 1*, in no case does this temperature decrease exceed 20°C. Thus, we conclude that radiation from water vapour cannot account for a significant proportion of the discrepancy.

To conclude the discussion of radiation two other points should perhaps be made for the sake of completeness, even though they may be obvious. The first is that there is no evidence for abnormally high (i.e. non-thermal) radiation from water vapour in hydrogen–air flames[7]. Hence, the use of data on thermal emission by water vapour is valid. The second point is that, of course, other radiation processes, some non-thermal, are occurring in these flames; however, these are not expected to be at all important in the present context. For example, the non-thermal ultra-violet emission of OH can easily be shown to be completely insignificant[8].

The heat loss due to incomplete combustion can be calculated given information on the composition of the flame gases at the temperature maximum. It has been shown by direct measurement of OH concentrations that there are excess radicals present in the gases downstream of the reaction zone in flames of this kind, and that the concentrations of H_2, H and O can be calculated from that of OH[9]. These four species are the only ones which need be accounted for in computing a heat loss. However, the temperature rise which would occur in these lean flames if all of these molecules were to recombine is quite insignificant in the present context. For example, if all the radicals (including H_2) present near the flame of run 5, Tables 1 and 4 of ref. 9 (which is for hydrogen–air, $\phi = 0{\cdot}8$, at 15 cm/s) were suddenly to recombine, we calculate that a temperature rise of only 27°C would occur. This particular run was chosen because the maximum radical concentration was relatively high, i.e. the measurement was probably made relatively near the flame. However, the maximum temperature probably occurred later when some radical decay had taken place, so that this source of uncertainty is insignificant.

In order to be able to judge more certainly the significance of these differences, the errors associated with the experiments should be discussed. Obviously the present author can only do this thoroughly with respect to his own work.

The presentation in ref. 4 involves essentially the comparison between two quantities determined by experiment; the flow velocity and the burnt gas temperature. Little more can be said at the present time about the accuracy of the first of these. However, to narrow the problem down, it can be said that the system of porous burner and silica-coated thermocouple has proved to give highly reproducible results in this laboratory. Not only did two observers, working with different pieces of apparatus, contribute the data in ref. 4, but since then at least three others in this laboratory have on various occasions verified the results reported therein*. Thus, the discussion of errors in this work is reduced, for practical purposes, to a consideration of the reliability of the temperature as determined by the thermocouples. This, in turn, can only involve the radiation correction, and catalytic effects, since the actual thermocouple temperatures were certainly known to within a few degrees.

Two uncertainties are involved in making the radiation correction; that in the thermal conductivity of the gases, and that in the emissivity of the coated thermocouple wire. As has been pointed out previously, the thermal conductivity of the gases was taken as that of air, which is almost certainly too low, so that from this cause the radiation corrections are too high. Nothing more can be said about the emissivity of the coated wire, but even if it were unity, there would remain a discrepancy in temperatures, and in general, the flame temperature would still be a single-valued function of velocity.

---

*With one exception. The curve in Fig. 8, ref. 4, for $(CO+H_2)$–air, $\phi = 0{\cdot}8$ was found to have been mislabelled. This should be $\phi = 0{\cdot}6$. There are also typographical errors in Figs. 3 and 5 in which 0·534 and 0·100 should read 0·834 and 1·00 respectively.

Concerning possible catalytic effects, all that has been shown is that a silica coating is less catalytic than the bare wire[4, 10]. To the extent that catalysis still occurs, the observed temperatures are too high and the differences in *Table 1* are enhanced.

The strongest evidence for the accuracy of the thermocouple data is the fact that they agree well with temperatures measured in other ways. Thus, the temperatures derived from the rotational distribution of ground state OH[11], the density measured by x-ray absorption[12], and the sodium reversal temperature[13] all agree with the thermocouple temperatures within 50°C or so, which is within the experimental error. Finally, the measured temperature of a blown off (i.e. adiabatic) methane–air flame agreed, within 20°, with the computed adiabatic flame temperature (see Fig. 2, ref. 4). It appears to us, therefore, that the accuracy of the silica-coated thermocouple data is quite firmly established.

To summarize, it does not appear possible to calculate the temperature of flames burning on porous burners from the Q values of Spalding and his co-workers, even if corrections are made for the heat losses known to occur. The burning velocity is a single-valued function of flame temperature, in contrast to its dependence on Q. In a private communication Dr Spalding has indicated that he too believes that the burning velocity is a single-valued function of flame temperature, but that heat losses other than to the burner allow S_{20} to be a double-valued function of Q. However, as we have tried to demonstrate here, the known heat losses do not appear large enough to account for the difference. Hence, there appears to be a real disagreement between the two experimentally determined quantities, the flame temperatures and the Q values.

The author wishes to express his gratitude to Mr G. J. Mullaney and Drs C. P. Fenimore, G. E. Moore and R. C. Millikan for helpful discussions of this problem, and to Dr D. B. Spalding for his helpful criticisms of an earlier version of this paper.

W. E. KASKAN

General Electric Research Laboratory,
Schenectady, New York, U.S.A.

(*Received April 1960*)

References

[1] SPALDING, D. B. and YUMLU, V. S. *Combustion & Flame*, **1959**, **3**, **553**

[2] SPALDING, D. B. *Proc. Roy. Soc. A*, **1957**, **240**, 83

[3] BOTHA, J. P. and SPALDING, D. B. *Proc. Roy. Soc. A*, **1954**, **225**, **71**

[4] KASKAN, W. E. *Sixth Symposium (International) on Combustion*, p **134**. Reinhold: New York, 1957

[5] For these calculations, we utilized extensive tables of the thermodynamic properties of the products of hydrogen–air combustion prepared by E. A. MICKLE and H. N. POWELL at the General Electric Company, Flight Propulsion Laboratory Department, Cincinnati, Ohio

[6] MCADAMS, W. H. *Heat Transmission*, 3rd ed., Fig. 4-15. McGraw-Hill: New York, **1954**

[7] GAYDON, A. G. *The Spectroscopy of Flames*, p 79. Chapman & Hall: London, **1957**; also unpublished observations in this laboratory

[8] KASKAN, W. E. *J. chem. Phys.* **1959**, **31**, 944

[9] KASKAN, W. E. *Combustion & Flame*, 1958, **2**, **286**

[10] LEAH, A. S. and CARPENTER, N. *Fourth Symposium (International) on Combustion*, p **274**. Williams & Wilkins: Baltimore, 1953

[11] KASKAN, W. E. *Combustion & Flame*, 1958, **2**, 229

[12] MULLANEY, G. J. *Rev. sci. Instrum.* **1958**, **29**, 87

[13] Unpublished work from this laboratory by C. P. FENIMORE, R. C. MILLIKAN and W. E. KASKAN

Note Added in Proof

A heat loss which was not considered above was that from diffusion. This term is difficult to estimate because of the many diffusing species and because the plane of $T_{\max}$ is not well defined. The assumptions that a loss results only from radical diffusion and that the radicals are equilibrated led, in two typical cases, to heat losses comparable with those from convection. Thus, diffusion is not negligible as we had thought, but no more important than the other terms considered, and our conclusions remain unchanged. That no large losses from the plane of $T_{\max}$ occur can also be inferred from the fact that the temperature gradients a few millimetres downstream are consistent with the radiation loss only, since large losses from $T_{\max}$ must appear eventually as large heat releases.

The Influence of Secondary Atmospheric Moisture upon Carbon Monoxide Flames

D. J. SEERY and H. B. PALMER

Department of Fuel Technology, College of Mineral Industries, The Pennsylvania State University, University Park, Pennsylvania

(*Received May 1959*)

Premixed CP grade carbon monoxide–dry air flames are highly sensitive to secondary atmospheric moisture, which diffuses into the reaction zone. This increases the burning velocity but does not change greatly the shape of its dependence upon composition. The curve appears to possess a maximum much nearer stoichiometric composition than is the case for commercial carbon monoxide. Shielding from atmospheric moisture produces new evidence that the burning velocity of pure carbon monoxide–air flames is approximately zero.

P. L. WALKER and C. C. WRIGHT[1] have reported a very slight increase in the critical boundary velocity gradient for flashback of commercial carbon monoxide (containing in this instance 1·01 per cent hydrogen)–air flames when the moisture content of the surrounding atmosphere was altered from a fairly dry condition to saturation. We report here some preliminary observations of the effect of atmospheric moisture upon air-supported premixed flames of CP grade carbon monoxide*. Observations included visual ones and measurements of the composition dependence of the burning velocity, S_u. The supporting air used in the work contained essentially no hydrogen and a maximum of 11 p.p.m. water vapour. The air in the laboratory contained about 0·6 per cent moisture by volume, typically, with fluctuations from day to day that carried it as low as about 0·3 per cent and as high as 1 per cent. Burning velocities were measured on bunsen tubes, using the visible cone frustum method[2]. The inner edge of the photographic image of a frustum of the visible cone was used. The frustum height typically covered between one third and one half of the cone height, mostly in the lower half of the cone. Flow control and measurements were accomplished with standard gas regulators and flowmeters. Iron pentacarbonyl [$Fe(CO)_5$] was removed from the carbon monoxide with a glass chip-packed column held at 320°C. The bunsen tubes were of Pyrex, uncooled, having length : diameter ratios greater than 60.

To check the method, measurements were first made of flashback characteristics and burning velocities of premixed commercial carbon monoxide–air flames. These were in adequate agreement with previous work reported in the literature and need not be reported here. It was found that introduction of steam into the air adjacent to the burner port had at most a slight effect upon the commercial carbon monoxide–air flames. In the case of the CP carbon monoxide†–dry air flames, however, the effect was to increase the burning velocity very greatly. It was obvious that substantial amounts of water or other hydrogen-containing species were diffusing into the reaction zone of the flame and accelerating the combustion. Introduction of a concentric stream of pre-purified nitrogen, dry air, or helium around the central tube decreased the burning velocity slightly; while a complete shielding of the flame from the atmosphere, produced by pulling the central tube down into a jacket with pure nitrogen, reduced the S_u so far that we were unable to stabilize such flames. The jacketing effect could be observed most clearly by using moist nitrogen initially and then allowing it to free itself of moisture by gradual introduction of dry nitrogen. The flame lengthened steadily and finally lifted off the burner or extinguished itself. The S_u value at extinction was estimated to be less than 5 cm/s for carbon monoxide–air at between 40 and 50 mole per cent carbon monoxide. This result appears to be supported by the recent work of R. A. Wires, L. A. Watermeier and R. A. Strehlow[3] on carbon monoxide–oxygen flames. A direct comparison is not possible because of their use of oxygen rather than air and because their observations were made exclusively on stoichiometric mixtures. The result appears to be in serious conflict with the only available published value of S_u for reportedly pure carbon monoxide–air, viz. 14·9 cm/s for 47 per cent carbon monoxide reported by G. McDonald[4]. Since we know that our carbon monoxide contained 45 p.p.m. hydrogen, it seems virtually certain that his contained more‡, or else he did not exclude the effect of moisture in the room atmosphere. It is of interest to note (*Figure 1*) that our S_u results for open flames of 47 per cent carbon monoxide–air range from about 11 cm/s to 15 cm/s, depending upon the atmospheric humidity.

---

*The Matheson Co. 99·5 per cent carbon monoxide, less than 150 p.p.m. hydrogen, very dry.

†These observations were made using CP grade carbon monoxide containing approximately 45 p.p.m. hydrogen.

As noted, it was not possible to obtain S_u data on the effectively shielded CP carbon monoxide–air flames because they could not be stabilized. The preliminary data reported here (*Figure 1*) are for carbon monoxide–air flames burning in the room atmosphere, or with partial protection by a concentric stream of nitrogen or helium. It is seen that the nitrogen- or helium-shielded results tend to lie somewhat, but not much, lower than the others. They are not very significant because, to preserve a stable flame on the burner, the velocity of the surrounding stream had to be so low as to offer almost no protection to the flame. The scatter in the room atmosphere results is largely due to variations in humidity, as may be seen in *Figure 2*, where sequences of data obtained on the same day are given distinguishing marks.

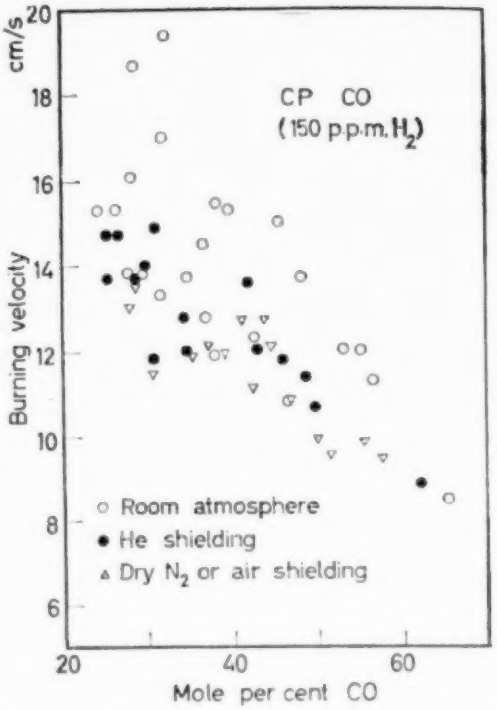

Figure 1. Burning velocity results for CP carbon monoxide (150 p.p.m. hydrogen)–dry air under three types of experimental conditions

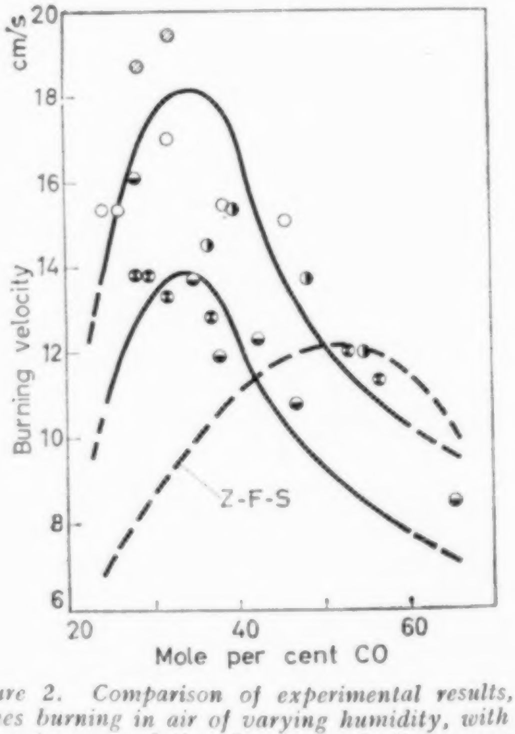

Figure 2. Comparison of experimental results, for flames burning in air of varying humidity, with two expressions correlating burning velocity, concentrations and temperature, as discussed in the text. Points obtained on the same day are given the same symbol

---

‡Although in ref. 4, McDonald does not cite the source of his carbon monoxide, the work reported appears to be part of a study of carbon monoxide combustion reported in *N.A.C.A. R.M. E53L08*, 5 February 1954, and in *N.A.C.A. R.M. E50C10*, 5 July 1950. In these reports, the carbon monoxide is described as having been prepared from anhydrous formic acid and concentrated sulphuric acid. It was dried very thoroughly, as was the air also. An apparatus diagram in *R.M. E53L08* appears to show the flame burning without any sort of jacket.

Further difficulty arose from variations in humidity during the course of a single day. Experimentally, the solution to humidity control is straightforward; further experiments will include this feature.

Despite the scatter in the experimental data, it is clear that the composition dependence of the S_u results for these flames is very different from that for commercial carbon monoxide–air flames, which exhibit an S_u maximum at about 50 per cent carbon monoxide, at atmospheric pressure[5-7]. R. FRIEDMAN and J. A. CYPHERS[8] have found that a modified expression based upon the flame theory of Y. B. ZELDOVICH, D. A. FRANK-KAMENETSKY and N. N. SEMENOV[9] correlates quite successfully the available experimental S_u data on hydrogen- or moisture-containing carbon monoxide flames. This modified Z–F–S expression may, to an adequate approximation (for present purposes), be written

$$S_u^2 \propto T_f^2\,[\mathrm{CO}]_{\mathrm{eff.}}\,[\mathrm{H_2O}]_{\mathrm{eff.}}^{0\cdot5}\exp\left(-20\,\mathrm{kcal}/RT_f\right)$$

where T_f is the computed adiabatic flame temperature and 'eff.' refers to the reaction zone, for which the concentrations are computed from those in the unburnt mixture using equations stated in both refs. 8 and 9. The result of fitting this expression to an $S_u = 12\,\mathrm{cm/s}$ at 47 per cent carbon monoxide is given by the dashed line in *Figure 2*. The unburnt concentrations of H-species, $(\mathrm{H_2})_u$ and $(\mathrm{H_2O})_u$, are here considered to be equivalent in their intrinsic effects[8] and to vary as $[\mathrm{CO}]_u$. Considering a fixed H-species content in the total mixture makes little difference in the shape because the most important variables are $[\mathrm{CO}]_{\mathrm{eff.}}$ and T_f.

If, as a refinement, we let the water vapour concentration in the reaction zone (taken to be the region of most intense luminosity) be determined by diffusion from the atmosphere, it is found that the magnitudes of the calculated S_us are increased but the shape of the curve remains essentially unaltered. Here the diffusion is considered to be free concentration diffusion across the stream boundary at an effective temperature equal to the numerical average of room temperature and T_f. The treatment is designed only to show trends and contains too many assumptions and approximations to warrant outlining it.

If one changes the $[\mathrm{CO}]_{\mathrm{eff.}}$ value from Semenov's value to one that considers it to be unburnt, for purposes of the correlation (i.e. $[\mathrm{CO}]_{\mathrm{eff.}} = [\mathrm{CO}]_u\,[T_0/T_f]$, then the result takes on a shape that conforms reasonably well to the data, as shown by the two solid lines in *Figure 2*. The two curves represent a threefold change in atmospheric humidity. Most of the experimental points lie between the two extremes or within experimental imprecision of them. The two very high points were obtained on a warm day when the outdoor relative humidity was 91 per cent.

It may be that the introduction of water into the flame by diffusion from the surroundings rather than by addition to the unburnt gases works in some unknown way to shift the composition dependence of S_u in these flames, but this is not very appealing. It seems to us more likely that there is a chemical significance in the need to consider the carbon monoxide as unburnt in the correlation, and that the shape of the composition dependence obtained here is probably representative of that for carbon monoxide–air flames having a very low H-species content, irrespective of its source. As hydrogen or water vapour is added to the unburnt mixture, then, there should be a gradual shift in the location of the maximum S_u from around 35 per cent to the usual 50 per cent. It will be interesting to explore this question experimentally.

This work was supported in part by a grant from the Experiment Station, College of Mineral Industries, The Pennsylvania State University.

Note Added after Acceptance of Paper

T. G. SCHOLTE and P. B. VAAGS[10] have recently reported burning velocities of carbon monoxide–hydrogen–air mixtures, including supposedly hydrogen-free, dry carbon monoxide–air. For this they find $S_u = 14{\cdot}5 \pm 1\,\mathrm{cm/s}$ over the range, 40 per cent to 55 per cent carbon monoxide. Since this conflicts with our low hydrogen result and apparently supports McDonald's result[4], we have collected in *Figure 3* the results of several independent investigations, correlated as

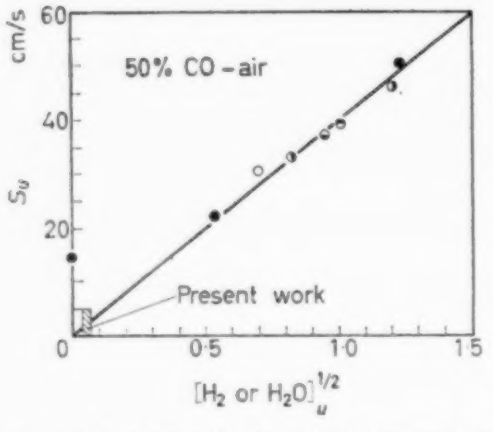

Figure 3. Burning velocity of 50 per cent carbon monoxide–air as a function of hydrogen or water vapour concentration (in volume per cent) in the unburnt mixture. Key: ● T. G. SCHOLTE *and* P. B. VAAGS[10]; ◐ G. JAHN[5]; ◓ D. J. SEERY *and* H. B. PALMER, *unpublished work;* ◒ P. L. WALKER, JR *and* C. C. WRIGHT[6]; ○ R. EDSE *and* W. A. STRAUSS[7]

S_u for 50 per cent carbon monoxide–air versus the square root of the percentage of hydrogen or water vapour in the unburnt gas, the same kind of relation as used by Scholte and Vaags. While the correlation is purely empirical, the upper points certainly suggest a straight line through the origin, or very close to it. Our result for very low $[H_2+H_2O]$, although regarded only as an upper limit value, clearly supports the line as drawn.

Inasmuch as Scholte and Vaags took great pains to dry their mixtures, the only conclusion that we can draw is that preparation of carbon monoxide by decomposing formic acid in the presence of sulphuric acid yields some hydrogen (and carbon dioxide). Free energy-wise, these products are favoured for the pure decomposition reaction, and even in the presence of concentrated sulphuric acid they exist in substantial amounts at equilibrium. In practice, kinetic considerations presumably enter that tend to promote further the yield of carbon monoxide and water vapour. The correlation in *Figure 3* indicates that carbon monoxide prepared in this way contains about 0·25 per cent hydrogen. Scholte and Vaags state that their carbon monoxide was 'completely free of hydrogen' but do not state the analytical method used and its accuracy. If in fact an accurate analysis was made, and if it showed the hydrogen to be, say, less than 100 p.p.m. then we are at a loss to explain the discrepancy between their result (and McDonald's) and ours. Our hydrogen analysis was that provided by the Matheson Co., in the case of the 45 p.p.m. hydrogen to be, say, less than 100 p.p.m., then performed the analysis by gas chromatography. The precision of these data is probably about ±20 per cent. The compressed air was assumed to have a normal composition. Its maximum moisture content was computed from the dew point stated by the Matheson Co.

References

1 WALKER, JR, P. L. and WRIGHT, C. C. *Fuel, Lond.* 1952, **31**, 37
2 DERY, R. J. Unpublished work; as discussed by HARRIS, M. E., GRUMER, J., VON ELBE, G. and LEWIS, B. in the *Third Symposium on Combustion, Flame, and Explosion Phenomena*, p 80. Williams and Wilkins: Baltimore, 1949
3 WIRES, R. A., WATERMEIER, L. A. and STREHLOW, R. A. *J. Phys. Chem.* 1959, **63**, 989
4 MCDONALD, G. *J. chem. Phys.*, 1952, **20**, 1947
5 JAHN, G. *Der Zündvorgang in Gasgemischen.* Oldenbourg: Berlin, 1934; data as presented in LEWIS, B. and VON ELBE, G. *Combustion, Flames and Explosions in Gases.* Academic Press: New York, 1951. Jahn's data include the two cases, H_2O content 1·35 per cent and (H_2+H_2O) content 2·85 per cent
6 WALKER, JR, P. L. and WRIGHT, C. C. *Fuel, Lond.*, 1952, **31**, 45. H_2 content of the CO, 1·82 per cent
7 EDSE, R. and STRAUSS, W. A. *J. chem. Phys.* 1956, **25**, 1241. H_2 content of the CO, 0·97 per cent
8 FRIEDMAN, R. and CYPHERS, J. A. *J. chem. Phys.* 1956, **25**, 448
9 SEMENOV, N. N. *Advanc. phys. Sci., Moscow*, 1940, **24**, No. 4; translated into English as *N.A.C.A. tech. Memor. No. 1026*, September 1942
10 SCHOLTE, T. G. and VAAGS, P. B. *Combustion & Flame*, 1959, **3**, 503 and 511

Ignition of Cellulosic Materials by Radiation

D. L. SIMMS

Fire Research Station, Boreham Wood, Hertfordshire

(Received June 1959)

The ignition of cellulosic materials by radiation has been examined. Ignition occurs first in the gas phase ; flame is shown to appear well away from the surface. Of the factors affecting ignition, external draughts and the supply of volatiles are likely to determine whether ignition can occur and the thermal properties, the time at which it will occur ; the size of the area irradiated may affect both. The ignition time has been correlated satisfactorily with the thermal properties over a large range of intensities by assuming that ignition occurs when the temperature of the solid reaches a certain fixed value.

Introduction

THE ease with which cellulosic materials such as wood, paper and cotton fabrics may be ignited is important in determining the growth of fires. As most of the heat transfer in well-developed fires is by radiation, which is, moreover, a convenient and easily measured method of transferring heat, it has been used as the source of heat in these as in earlier experiments[1].

Three sources of radiation are used at the Fire Research Station: a 1 ft square gas-fired radiant panel[2] which is a diffuse source, and two sources from which the radiation is focused by an ellipsoidal mirror, one being a tungsten filament lamp[3], the other a carbon arc[4]. Some comparative details are given in *Table 1* below.

When specimens are exposed to radiation the surface first darkens, then chars and volatiles issue from it; at high rates of heating they may burst into flame. The experiments have been restricted to this type of ignition which was defined earlier[1] as spontaneous ignition, that is, ignition of the volatiles without the presence of an extraneous igniting source, and they examine some of the factors affecting the ignition time and the minimum intensity of irradiation at which ignition occurs.

The materials tested were either thin (0·02 to 0·065 cm) or thick (>1 cm) and are listed in *Tables 2* and *3*, respectively. Before exposure to radiation they were dried in an oven at 95°C for 24 hours and then allowed to cool over phosphorus pentoxide.

Specimens were exposed to radiation of different intensities and the times at which ignition occurred spontaneously were measured. The specimens were then removed from the radiation; below a certain intensity, ignition of the volatiles did not occur although specimens were observed to glow. Flaming persisted after removal of the radiation for most of the thin materials, *Table 2*, except for those irradiated at high intensities.

Table 1. Characteristics of sources in use

Source	*Approximate radiating temperature* °*K*	*Area receiving not less than 90 per cent maximum radiation* cm^2	*Range of intensities* ($cal\ cm^{-2}\ s^{-1}$)
Gas-fired radiant panel[2]	1 000	60	0 *to* 3
Tungsten filament lamp–ellipsoidal mirror[3]	3 000	0·5	1 *to* 5
Carbon arc–ellipsoidal mirror[4]	4 000	3	1·5 *to* 12

Table 2. Thin materials which behave as slabs with a linear temperature gradient. The specific heat of all these materials is taken[5] as 0·34 cal g^{-1} °C^{-1}. All properties are taken as the values applying at room temperature*

Material	*Colour*	*Density (g/cm^3) ρ*	*Thermal conductivity[6] ($cal\,cm^{-1}s^{-1}\,°C^{-1} \times 10^4$) K*	*Thickness cm 2l*	*Source of radiation*	*Range of intensities of irradiation ($cal\ cm^{-2}\ s^{-1}$) I*	*Symbol in Figure 7*
Cotton	*Black*	0·57	1·8	0·045	*Carbon arc[4]*	1·7 *to* 13·5	●
					1 ft² radiant panel[2]	1·2 *to* 2·3	■
Cotton	*White*	0·57	1·8	0·045	*1 ft² radiant panel*	1·0 *to* 1·8	○
Filter paper	*Black*	0·53	1·7	0·02	*Carbon arc*	1·2 *to* 12·9	▲
Denim	*Khaki*	0·52	1·6	0·06	*1 ft² radiant panel*	1·3 *to* 1·9	▼
Drill	*Blue*	0·46	1·5	0·065	*1 ft² radiant panel*	1·3 *to* 2·0	△
Drill	*Black*	0·39	1·4	0·056	*1 ft² radiant panel*	1·5 *to* 1·9	□
Gaberdine	*Olive*	0·59	1·9	0·029	*1 ft² radiant panel*	1·1 *to* 2·0	▽

Table 3. Thick materials which behave as semi-infinite solids. The specific heat of all these materials is taken[5] as 0·34 cal g^{-1} °C^{-1}. All properties are taken as the values applying at room temperature*

Material	*Colour*	*Density (g/cm^3) ρ*	*Thermal conductivity[7] ($cal\,cm^{-1}s^{-1}\,°C^{-1} \times 10^4$) K*	*Source of radiation*	*Range of intensities of irradiation ($cal\,cm^{-2}s^{-1}$) I*	*Symbol in Figure 8*
Oak	*Natural*	0·7	3·9	*Carbon arc[4]*	2·4 *to* 14·0	○
	Black (candle)			*Carbon arc*	1·9 *to* 2·9	◆
	Black (carbon)			*Carbon arc*	1·5 *to* 2·5	●
Fibre insulating board	*Natural*	0·25	1·7	*Carbon arc*	2·4 *to* 12·0	△
	Natural			*1 ft² radiant panel[2]*	1·2 *to* 2·1	·
	Black (carbon)			*Carbon arc*	1·7 *to* 7·1	▲
	Black (candle)			*Carbon arc*	2·0 *to* 3·6	+
Cedar	*Natural*	0·4	2·4	*Carbon arc*	1·9 *to* 12·0	□
	Natural			*1 ft² radiant panel*	1·6 *to* 2·1	■
	Black (candle)			*Carbon arc*	1·4 *to* 2·9	◇
	Black (candle)			*1 ft² radiant panel*	1·7 *to* 2·4	×
Mahogany	*Natural*	0·6	3·4	*Carbon arc*	1·9 *to* 12·0	▽
	Black (candle)			*Carbon arc*	1·9 *to* 12·0	▼

*See page 297

Factors Affecting Ignition of Materials

Effect of absorptivity of surface of specimen[8]
The absorptivity of a surface at very low rates of heating is independent of the rate of heating and only varies with the quality of the incident radiation, but in heating a material to ignition, the irradiated surface darkens and the absorptivity is dependent on exposure time. Empirical absorption factors corresponding to different exposure times may be obtained[8] by comparing the intensities of irradiation required to ignite the natural material with those required with the material artificially blackened by carbon black. Absorption factors for materials for radiation from the carbon arc source are shown in *Figure 1*.

Effect of area of specimen irradiated[9, 10]
The smaller the area irradiated, the greater the least intensity at which ignition occurs[9] [*Figures*

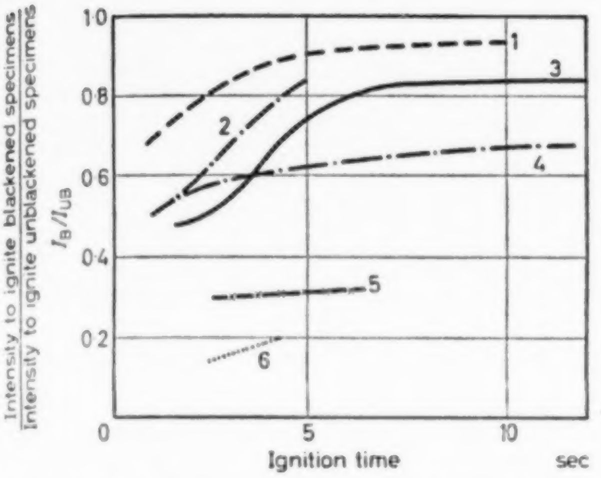

Figure 1. Variation of absorptivity with time (carbon arc source). 1 Natural mahogany, 2 Natural fibre insulating board, 3 Natural cedar, 4 Natural oak, 5 White cotton, 6 White filter paper

2(a) and 2(b)] and the greater the ignition time[10]. By plotting $1/(\text{area})^{\frac{1}{2}}$ [the choice of $1/(\text{area})^{\frac{1}{2}}$ as the function is one of convenience] against the ignition time, and extrapolating the results to intercept the time axis when $1/(\text{area})^{\frac{1}{2}}$ is zero, the ignition times of an infinite area at different intensities of irradiation may be estimated. A typical example for one material is given in ***Figure 3***. The lines have been drawn to cut the abscissa at right angles as the rate of decrease of ignition time with increasing area decreases rapidly when the area becomes large.

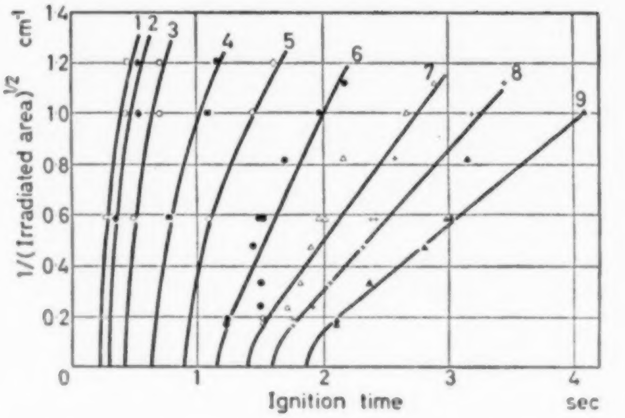

Figure 3. Variation of ignition time with irradiated area, with intensity of irradiation: 1 10·0, 2 8·0, 3 6·0, 4 4·0, 5 3·0, 6 2·4, 7 2·0, 8 1·8 and 9 1·6 cal cm^{-2} s^{-1}

The factor to convert the ignition times on the carbon arc apparatus to those for an infinite area is given in *Figure 4*.

The size of the area irradiated affects both the temperature rise of the specimen and the conditions in the stream of volatiles issuing from the surface. The experiments have been designed so that lateral conduction in the specimen is negligible[11]. Although the convective heat losses from the irradiated area on the surface are dependent on the area irradiated, the likely variation is small compared with the total heat loss, so that the rate of rise in temperature of the specimen only changes slightly;

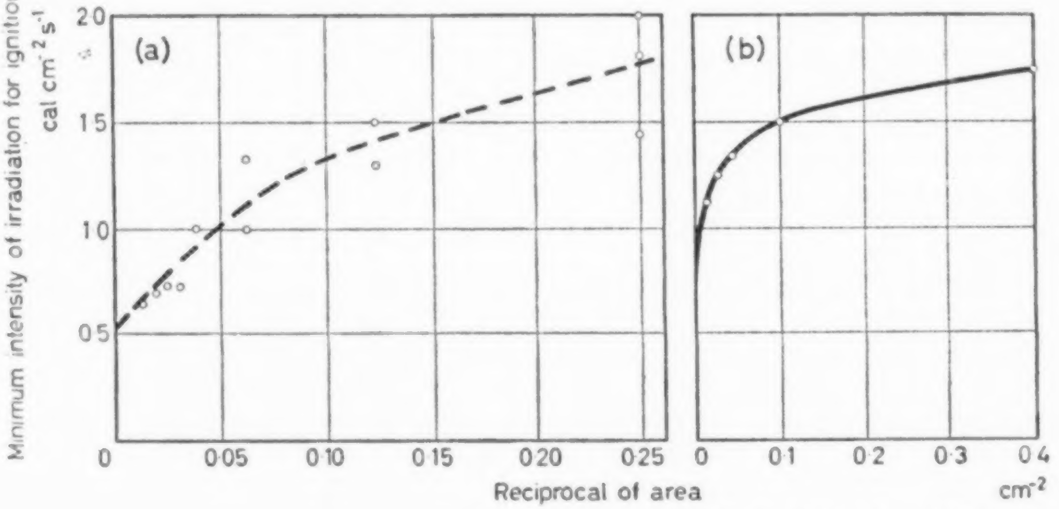

Figure 2(a). Area effect for white cotton

Figure 2(b). Area effect for fibre insulating board

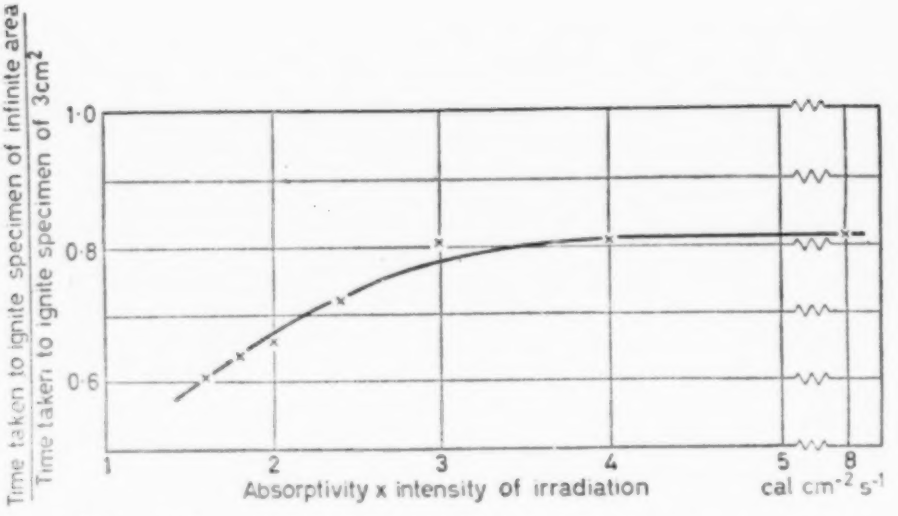

Figure 4. Conversion factor for ignition times (carbon arc source)

any differences in ignition times are therefore due to different flow patterns in the volatile stream.

Volatile stream

Slow motion photographs of ignition by means of the tungsten source[3] are shown in *Figure 5*. The flame first appears in the volatiles some distance above the heated surface, near the point at which the volatile stream becomes turbulent.

Turbulence occurs sooner with both the carbon arc apparatus and the radiant panel than with the tungsten lamp source. This is partly because of the draughts associated with the operation of the first two, the velocity of the draught from the panel being about **25** cm/s, and partly because the increased size of the volatile stream associated with larger irradiated areas assists the onset of natural turbulence. This disturbance of the volatile stream with these two sources[12] is the cause of the lowering of the minimum intensity at which ignition occurs but, if ignition would otherwise occur, disturbing the volatiles does not hasten it.

Because the flame first appears in the volatile stream, a complete statement of whether ignition is or is not possible must take into account the conditions there, but these are not yet formulated completely. A criterion for ignition based on a critical rate of emission of volatiles from the surface of the specimen has been suggested[13]. The rate is dependent on the temperature of the irradiated specimen; if this temperature rises rapidly, the rate of production of volatiles is large compared with the critical rate so that ignition may then be discussed in terms of the thermal balance of the specimen[14]. Some of the limitations of this approach due to the neglect of the chemical aspects of the problem are discussed later (p 299).

Because the rate of evolution of chemical heat is limited at any instant by the temperature of the specimen, the higher the rate of external heating the less significant the chemical heating will be. In the present analysis chemical are discussed later (p 299).

Thermal Balance of the Solid

Calculation of temperature rise

The temperature rise θ of an opaque inert slab, irradiated on one face of absorptivity 1 by an intensity of irradiation I, thickness $2l$, at time t, losing heat from both faces by Newtonian cooling, is a complex function[17]. Useful approximations, given in *Figure 6*, may be made for a range of values of two dimensional groups[14], the Fourier number kt/l^2 and the Biot number hl, and these define mathematically thin and thick materials where k is the thermal diffusivity $= K/\rho c$, K is the thermal conductivity, ρ is the density, c is the specific heat of

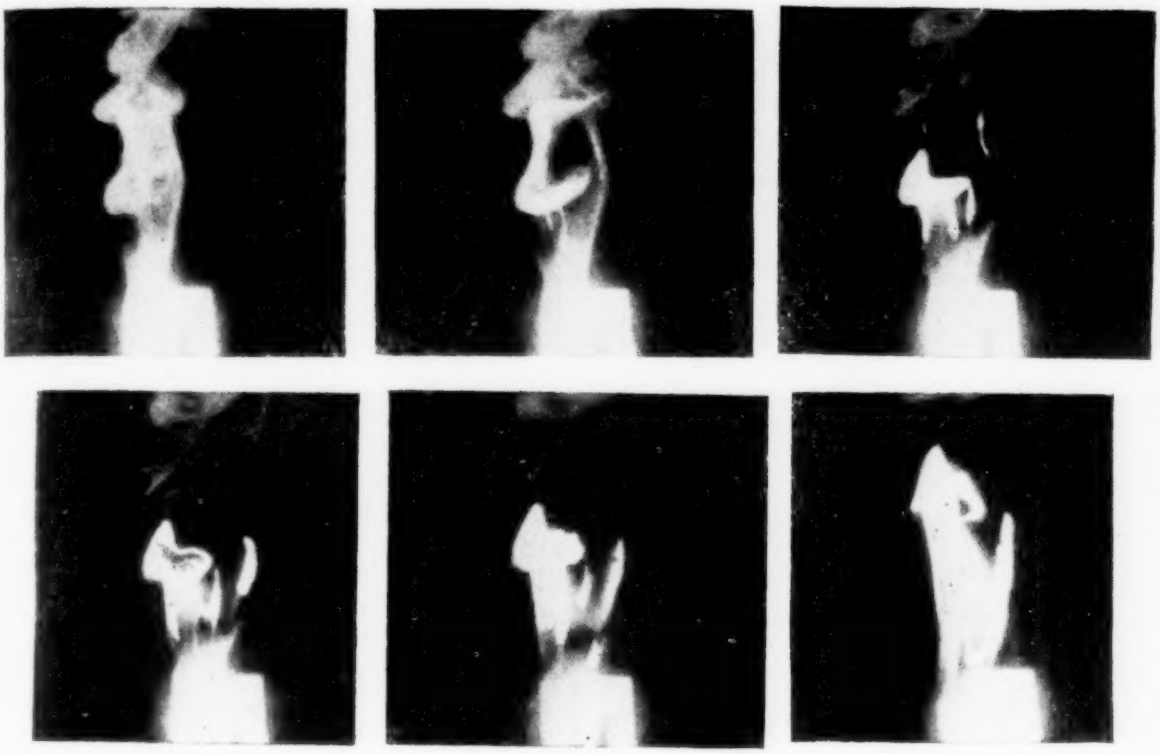

Figure 5. Successive stages in the ignition of wood by irradiation. Frames ~0·01s exposure. Note ignition occurs above specimen outside the radiation field

the material, $h=H/K$, and H is the Newtonian cooling constant. Note that K, ρ and c are taken as independent of temperature.

Slab with linear temperature gradient (*thin materials*)—When hl and kt/l^2 have values in the region *A* of *Figure 6*, there is a linear temperature gradient through the solid[14] and the mean temperature θ_m may be shown[14] to be

$$\theta_m=\frac{I}{2H}[1-\exp(-Ht/\rho cl)] \quad \ldots\ldots [1]$$

where $Ht/\rho cl$ is a dimensionless group obtained from the Biot and Fourier numbers by eliminating the thermal conductivity, K.

Semi-infinite solid (*thick materials*)—For values of hl and kt/l^2 in the region B of *Figure 6* the surface temperature θ_F is the same as that for an infinite solid and may be shown[14] to be

$$\theta_F=(I/H)\,(1-\exp\beta^2\operatorname{erfc}\beta) \quad \ldots\ldots [2]$$

where $\beta=h(kt)^{\frac{1}{2}}$. β is a dimensionless group obtained from the Biot and Fourier numbers by eliminating the thickness $2l$.

Experimental results

Ignition data for materials in the form of non-uniform slabs are given in *Table 2* and for semi-infinite solids in *Table 3*. The data have been corrected for the effects of absorptivity[9] and area[11] before being used in the correlations of *Figures 7* and *8*.

Correlation of results

Experimental results may be correlated in terms of the groups of properties in equations 1 and 2, but it is more useful to plot the results in terms of two dimensionless variables, namely the energy modulus $It/2l\rho c\theta$ which represents the ratio of the energy received by the surface to the heat content of the specimen at ignition, and the cooling modulus $Ht/\rho cl$ which represents the ratio of the energy lost by cooling, to the heat content. In terms of these groups, equation 1 for slabs with linear temperature gradients may be rearranged as

$$\frac{It}{2l\rho c\theta_m}=\frac{Ht}{\rho cl}\Bigg/\left[1-\exp-\frac{Ht}{\rho cl}\right] \quad \ldots\ldots [3]$$

This is shown in *Figure 7*.

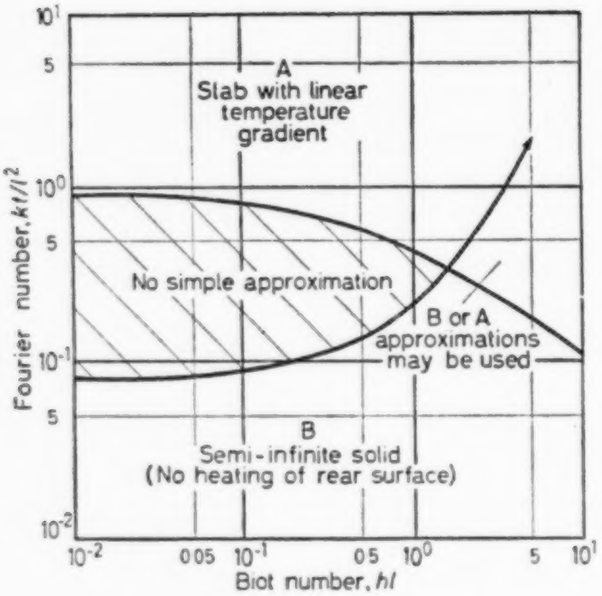

Figure 6. Role of dimensionless groups in determining temperature rise

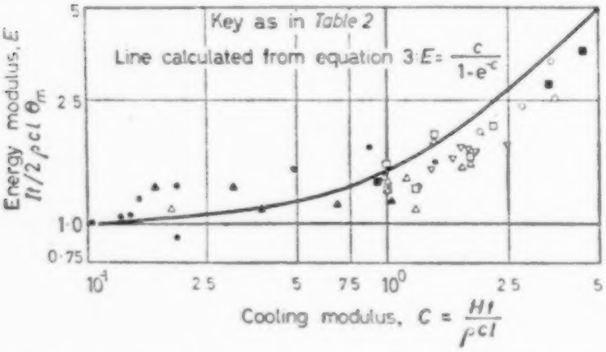

Figure 7. Correlation if ignition times for slab with linear temperature gradient (thin materials). Range of intensities of irradiation: 1 to 14 cal cm^{-2} s^{-1}. Range of thicknesses; 0·02 to 0·065 cm. Range of ignition times; 1 to 20s. Correlating temperature, θ_m: 525°C

Equation 2 for semi-infinite solids may be arranged as

$$\frac{It}{\rho c(kt)^{\frac{1}{2}}\theta_F} = \frac{Ht}{\rho c(kt)^{\frac{1}{2}}} \Big/ (1 - \exp \beta^2 \operatorname{erfc} \beta) \quad . . [4]$$

This is shown in *Figure 8*.

Equation 4 contains the same variables as equation 3 except that $(kt)^{\frac{1}{2}}$ replaces the thickness of the slab in the formation of the dimensionless groups and θ_F replaces θ_m.

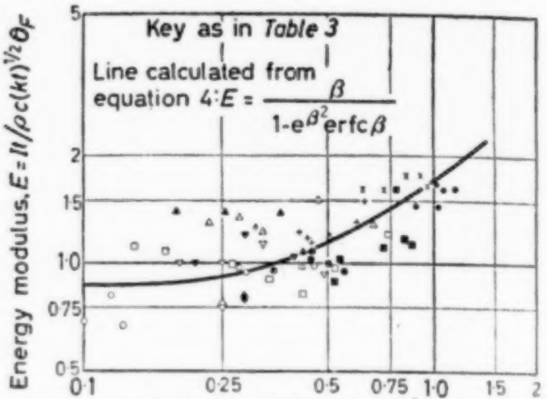

Figure 8 Correlation of ignition times for semi-infinite solids (thick materials). Range of intensities of irradiation: 1·2 to 14 cal cm^{-2} s^{-1}. Range of densities: 0·25 to 0·7g/cm^3. Range of ignition times: 2 to 30s. Correlating temperature, θ_F: 525°C

Slab with linear temperature gradient—When the cooling modulus $Ht/\rho cl$ tends to zero, then from equation 3

$$It/2l\rho c\theta_m \longrightarrow 1 \quad . . . . [5]$$

Hence from values of $It/2l\rho c\theta_m$ for small values of $Ht/\rho cl$, a first approximation to θ_m may be obtained and the appropriate value chosen for the Newtonian cooling constant H for that temperature range. The value of θ_m is then adjusted to give the best fit between the experimental points and equation 3. The correlation obtained in *Figure 7* is adequate considering the assumptions made and the experimental variations, in particular, the effect due to the size of the irradiated area.

Semi-infinite solids—When the cooling modulus $Ht/\rho c(kt)^{\frac{1}{2}}$ tends to zero, then from equation 4

$$\frac{It}{\rho c(kt)^{\frac{1}{2}}\theta_F} \longrightarrow \frac{\pi^{\frac{1}{2}}}{2} \quad . . . . [6]$$

Hence from the values of $It/\rho c(kt)^{\frac{1}{2}}\theta_F$ for small values of the cooling modulus $Ht/\rho c(kt)^{\frac{1}{2}}$, a first approximation to θ_F may be obtained and the appropriate value chosen for the Newtonian cooling constant H for that temperature range. The value of θ_F is then adjusted to give the best fit between the experimental points and equation 4 (*Figure 8*).

Discussion

Ignition times

In this series of experiments, ignition was not obtained below 1 cal cm^{-2} s^{-1}, but above this level the ignition time may be obtained for slabs (thin materials) from *Figure 7* or from equation **3** and for semi-infinite solids (thick materials) from *Figure 8* or from equation **4**. The best fit between the experimental results and these equations is obtained with a value of 525°C for θ_F or θ_m.

The effect of diathermancy on the temperature rise has been neglected in the present analysis. Because diathermancy reduces the temperature gradients within the solids, the mean temperature and the surface temperature of the slab may be more nearly equal than the present analysis suggests so that a possible reason for obtaining a satisfactory correlation in terms of the mean temperature θ_m, instead of the surface temperature θ_F, may simply be the neglect of diathermancy. Similarly, as the surface temperature of a semi-infinite solid when ignition occurs is lower with diathermanous materials than with blackened materials, which are opaque[18], diathermancy may be the cause of the scatter in the correlation of *Figure 8*.

With long ignition times, where chemical heating is most likely to be significant, ignition may occur a little sooner than would be expected from the external heating alone (*Figure 7*).

A large part of ignition behaviour may therefore be understood in terms of the thermal balance in the solid.

Minimum intensity for ignition

The rate of heat loss from a semi-infinite solid at 525°C in equilibrium is approximately 0·6 cal cm^{-2} s^{-1}; this equilibrium condition corresponds to the critical intensity of irradiation at which ignition is just possible[1]. Since the correlating temperature is 525°C for all the cellulosic materials tested here, this suggests that the critical intensity should be independent of the species of wood[1]. Specimens which are losing heat from both faces would, however, be expected to require a higher critical intensity.

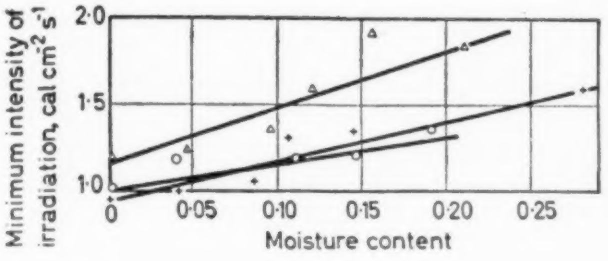

Figure 9(a). *Effect of moisture content on minimum intensity of irradiation for ignition.* ○ *Columbian pine,* △ *Mahogany,* + *Fibre insulating board*

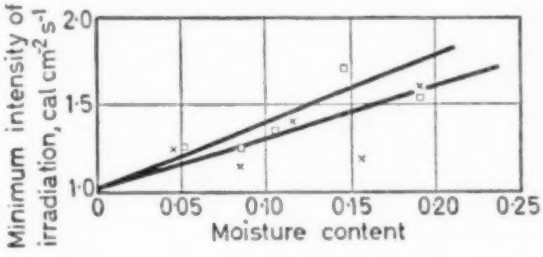

Figure 9(b). *Effect of moisture content on minimum intensity of irradiation for ignition*

Ignition after a long time would be expected at intensities of irradiation just above 0·6 cal cm^{-2} s^{-1}. The lowest level at which ignition has been obtained in the present experiments is about 1 cal cm^{-2} s^{-1} corresponding to an ignition time of about 30 seconds, although some specimens took longer. The difference between the critical intensity predicted from the theory on page 297 and the minimum intensity found in practice may be due to neglecting the fact that the supply of volatiles is limited.

Preliminary heating for extended periods at temperatures between 120° and 180°C drives off some of the volatiles, leading to an increase in the minimum intensity required for ignition proportional to the loss in weight[19]. This temperature region is below that at which ignition is possible. This suggests that any factor prolonging the period between the surface reaching the temperature at which volatiles are emitted and the surface reaching that at which ignition takes place, tends to increase the probability of exhaustion of volatiles and may increase the minimum intensity of irradiation required for ignition.

One such factor is the size of the area irradiated, and the minimum intensity required for ignition does increase with decreasing size

[*Figures* 2(a) and 2(b)]. Another is the moisture content[19, 20], the minimum intensity for ignition increasing with increasing moisture content [*Figures* 9(a) and 9(b)]. Equations 1 and 2 suggest that another factor should be the density but the experimental evidence is insufficient to confirm any increase of minimum intensity required, although the failure to ignite Iroko in the experiments reported earlier[1] may be due to its high density.

Conclusions

Ignition by radiation of some cellulosic materials such as wood and paper has been shown to occur in the gas phase. Factors such as external draughts and exhaustion of volatiles appear to determine whether ignition can occur rather than the time at which it occurs.

Data for cellulosic materials covering a large range of intensities, densities and thicknesses have been satisfactorily correlated by regarding spontaneous ignition in the time range of 1 to 30 s as occurring when the temperature of the solid reaches a certain fixed value.

The work described in this paper forms part of the programme of the Joint Fire Research Organization of the Department of Scientific and Industrial Research and Fire Offices' Committee; the paper is published by permission of the Director of Fire Research. The author would like to thank his many colleagues who have both shared in the work and discussed the results. The illustrations are Crown Copyright and appear by permission of H.M.S.O.

References

[1] LAWSON, D. I. and SIMMS, D. L. 'The ignition of wood by radiation'. *Brit. J. appl. Phys.* 1952, **3** (9), 288

[2] SIMMS, D. L. and MILLER, J. E. 'Some radiation characteristics of a gas-fired panel'. *Fire Research Note No. 217*, 1955. Department of Scientific and Industrial Research and Fire Offices' Committee Joint Fire Research Organization: London.

[3] *Fire Research 1952*, p 13. H.M. Stationery Office: London, 1958

[4] HINKLEY, P. L. 'A source of high intensity radiation employing an arc lamp and an ellipsoidal mirror'. *Fire Research Note No. 270*, 1956. See ref. 2

[5] DUNLAP, F. 'The specific heat of wood'. *Forest Service Bul. No. 110*. U.S. Department of Agriculture: Washington, 1912

[6] SAUER, F. H. *Ignition of Black Alpha-cellulose Papers by Thermal Radiation. Square Wave Pulse.* U.S. Department of Agriculture. Forest Service. Division of Fire Research: Berkeley, 1956

[7] MACLEAN, J. D. 'The thermal conductivity of wood'. *Trans. Amer. Soc. Heat. Vent. Engrs*, 1941, **47**, 1184

[8] SIMMS, D. L., LAW, M. and HINKLEY, P. L. 'The effect of absorptivity on the ignition of materials by radiation'. *Fire Research Note No. 308*, 1957. See ref. 2

[9] SIMMS, D. L. 'The minimum intensity for the spontaneous ignition of cellulosic materials'. *Fire Research Note No. 361*, 1958. See ref. 2

[10] SIMMS, D. L. *et al.* 'The effect of size of irradiated area on the spontaneous ignition of materials. Part I. The effect on ignition time'. *Fire Research Note No. 307*, 1957. See ref. 2

[11] THOMAS, P. H. 'Some conduction problems in the heating of small areas on large solids'. *Quart. J. Mech.* 1957, **10** (Part 4), 482

[12] SIMMS, D. L. 'The influence of external air movements on the ignition of materials by radiation'. *Fire Research Note No. 305*, 1957. See ref. 2

[13] BAMFORD, C. H., CRANK, J. and MALAN, D. H. 'The combustion of wood'. *Proc. Camb. phil. Soc.* 1946, **42**, Part 2 (June), 166

[14] SIMMS, D. L. 'The correlation of ignition time with the physical properties of materials. Part I. Spontaneous ignition of cellulosic materials'. *Fire Research Note No. 319*, 1958. See ref. 2

[15] LAWRENCE, E. K. 'Analytical study of flame initiation'. *M.Sc. Thesis.* Massachusetts Institute of Technology: Cambridge, Mass., 1952

[16] THOMAS, P. H. and SIMMS, D. L. 'Thermal damage to solids by radiation and chemical decomposition'. *Fire Research Note No. 331*, 1958. See ref. 2

[17] CARSLAW, H. S. and JAEGAR, J. C. *The Conduction of Heat in Solids*, Section 43. Oxford University Press: London, 1951

[18] GARDEN, R. 'Temperatures attained in wood exposed to high intensity thermal radiation'. *Fuels Res. Lab. tech. Rep. No. 3.* Massachusetts Institute of Technology: Cambridge, Mass., 1953

[19] SIMMS, D. L. and ROBERTS, V. E. 'Effect of prolonged heating on the subsequent spontaneous ignition of oak'. *J. Inst. Wood Sci.* (To be published)

[20] THOMAS, P. H., SIMMS, D. L. and LAW, M. 'The effect of moisture content on the spontaneous ignition of wood by radiation'. *Fire Research Note No. 280*, 1955. See ref. 2

Gaseous Explosions in Vented Ducts

D. J. RASBASH and Z. W. ROGOWSKI

Fire Research Station, Boreham Wood, Hertfordshire

(*Received June 1959*)

Pentane and propane–air mixtures have been exploded in nine straight steel ducts with openings at one end. The ducts were either of 1 ft square section or of 3 in. or 6 in. diameter circular section and varied in length from 6 to 30 ft. The size of the opening varied within the range $K=1$ to 64 where K is the ratio of cross sectional area of the duct to the area of the opening. Pressure was recorded and with the longer ducts the progress of the flame was also recorded using ionization gaps. For eight of the ducts with ignition remote from the opening and $32>K>2$ the maximum pressure recorded (P_m Lb/in^2) was approximately independent of the duct and was given by $P_m=aK$ where 'a' was a coefficient which varied between 0·85 and 1·5. The flame speed also reached a maximum value after the flame had travelled 6 to 12 diameters. With the narrowest tube tested measuring 12 ft long × 3 in. diameter, higher pressures and flame speeds were obtained than with the other vented ducts although this tube gave a lower pressure with the unvented duct. With all ducts, flame speeds and pressures were very much smaller when ignition was near the vent. A relation is given for the rate of combustion in the ducts as a function of the Reynolds number in the unburnt gas and the pressures developed are discussed on the basis of the combustion rate in the ducts.

FLAMMABLE vapours and gases are handled in many industrial plants and while it is essential in such plant to ensure that, as far as possible, the vapour concentration is well outside the limits of flammability, it is also desirable that the plant should be constructed so as to minimize the damage which could be caused by an explosion. One way of reducing explosion damage is to provide relief vents but it is often difficult to apply this method in practice because of the lack of information on the pressures developed in vented explosions. Some, mainly empirical, data are available, particularly for explosions in short cylindrical vessels; this work has been reviewed by K. N. PALMER[1]. In addition, P. A. CUBBAGE and W. A. SIMMONDS[2] have carried out extensive tests on explosions in vented drying ovens of approximately cubical shape, and these tests form an excellent basis for the design of relief vents for this type of equipment. However, it has not been found possible to calculate venting requirements from fundamental principles, and with a large range of systems of considerable industrial importance even the necessary empirical data are scanty. Examples of the latter systems are the various arrangements of ducts that are commonly met with in practice. A series of vapour explosions has therefore been carried out in ducts of different shapes with open vents of different sizes in one end of the ducts. To assist in the interpretation of the results, measurements of the flame speed were made in addition to pressure measurements. The results are given and discussed in this paper.

Experimental

List of symbols

A to J	Letters to designate ducts
K	Vent ratio, equivalent to $\dfrac{\text{Cross sectional area of duct}}{\text{Area of vent}}$
L	Duct length
α	Ratio of duct length to duct width or diameter
P_m	Maximum pressure (Lb/in^2) reached in an explosion
S	Stoichiometric concentration of vapour
U	Flame speed relative to unburnt gas
U_0	Fundamental burning velocity
V	Dimensionless rate of combustion
R_e	Reynolds number of unburnt gas into which flame is propagating.

Apparatus

The ducts used are listed in *Table 1*. A to D were circular steel ducts designed to withstand pressures of 350 Lb/in^2. Ducts E to J were of 1 ft square cross section; they were made from $\frac{1}{8}$ in. thick sheet steel and could withstand pressures up to 10 to 20 Lb/in^2. The vents were holes with sharp, right-angle edges, cut in the centre of flanges which could be bolted to the ends of the ducts. The size of the vents was defined by a factor K equal to the ratio of the cross sectional area of the duct to the area of the vent. For ducts A to D, a range of vent sizes from $K=1$ to $K=\infty$ (i.e. completely open end to completely closed end) were used. For ducts E to J, vents of size $K=1$, 2 and 4 only were used.

Table 1. Ducts and vents used

Duct designation	*Shape of duct and vents used*	*Duct diameter or width W (in.)*	*Duct length L (ft)*	*Ratio $L/W = \alpha$*
A	*Circular*	3	6	24
B	*Circular*	3	12	48
C	*Circular*	6	6	12
D	*Circular*	6	12	24
E	*Square*	12	6	6
F	*Square*	12	12	12
G	*Square*	12	18	18
H	*Square*	12	24	24
J	*Square*	12	30	30

Pentane–air mixtures were used as the combustible gas in the tests with ducts A to D. A measured amount of pentane was introduced as vapour and the mixture circulated with a fan. With the closed ducts, a range of concentrations of vapour was used but in the tests with vents, the concentration of vapour was 1·17 or 1·33 S, S being defined as the percentage of vapour in the stoichiometric mixture. A propane–air mixture was used for ducts E to J. A prepared mixture of concentration 1·25 S was blown through the ducts for a sufficient time to give ten changes of volume.

The quiescent mixture was ignited with an induction spark at a point on the axis 6 in. from one end of the duct. A piezoelectric gauge[3] and a capacity gauge were used to measure the pressure for the explosions in ducts A to D, and E to J respectively; the capacity gauge was used for the latter ducts since these were sited in the open air and the capacity gauge was less sensitive to outside weather conditions than the piezoelectric gauge. The flame speed was obtained using ionization gaps placed at intervals of approximately 3 ft along the ducts. These gaps projected a distance of $\frac{3}{4}$ in. into ducts A to D and $1\frac{1}{2}$ in. into ducts E to H. In some initial tests with duct C, the vent was covered by thin typing paper which was slit across two diameters at right angles immediately before the explosion[4]. However, evidence was obtained subsequently that under some conditions the paper in the vent influenced the course of the explosions, particularly when the vent was near the ignition source. In most of the tests described below a covering was placed over the vent and removed one to two seconds before firing, although a few tests in which slit paper was used have been included for duct C.

Results

Closed ducts

The pressure records obtained with closed ($K=\infty$) ducts A, C and D were similar in form to each other and also to those obtained for closed tubes by other workers. An example is given in *Figure 1*(a); the records were characterized by vibrations which increased in amplitude as the mean pressure rose to a fairly sharp peak. With duct B, however, the records were somewhat different [*Figure 1*(b)]; particularly violent and complicated vibrations occurred when the flame was in the second half of the duct, but there was usually no sharp peak. *Figure 2* gives the maximum pressure rise plotted against the vapour concentration; the pressures plotted refer to the mean curve running through the middle of the vibrations. *Figure 2* shows that:

(*1*) For a given mixture, the maximum pressure decreased as α, the ratio of the length to the diameter of the duct, increased.

(*2*) The 6 in. diameter ducts (C and D) gave a 'plateau' of approximately equal maximum pressures over a wide range of concentrations, whereas the 3 in. ducts (A and B) gave a definite peak with a 1·17 S mixture.

(*3*) In all cases there was evidence of a discontinuity in the curve when the concentration was between 1·5 and 1·8 S, the discontinuity becoming more pronounced as the ratio α increased.

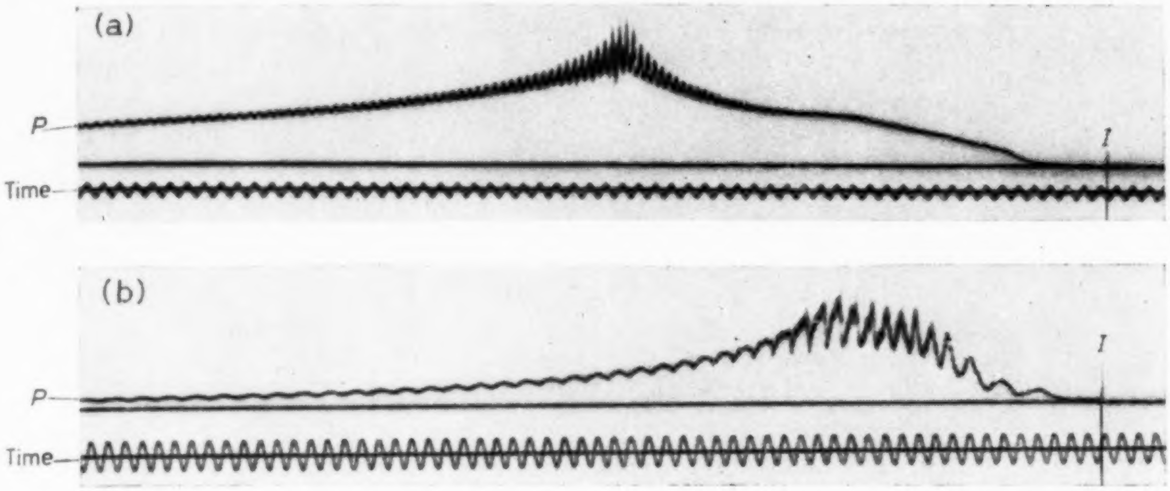

Figure 1. Pressure records for closed ducts. P is the pressure record. I denotes ignition. P_m represents maximum pressure (Lb/in²) to highest peak. Time trace at 100 c/s. (a) *Duct C: 1·33S, $P_m=110$;* (b) *Duct B: 1·33S, $P_m=67$*

Relief vent remote from ignition source

Pressure—For values of $K \geqslant 2$ the pressure records were often characterized by long periods in which the rate of change of pressure was constant; the maximum pressure occurred either at the beginning or end of these periods. A few examples of these pressure records are given in *Figures 3*(a), (b) and (c). Although vibrations were often recorded, the amplitudes of these were not usually large in comparison with the mean pressure rise. However, this was not so with duct *B* in which intense vibrations were often obtained in the vented explosions (*Figure 3*(d).

Figure 4 shows the maximum pressure P_m plotted against K for all tests in which ignition was remote from the vent $K \geqslant 2$. If there were vibrations, the maximum pressure taken was the peak vibration pressure. No difference was found between the maximum pressures recorded with the gauge either near or remote from the vent and for ducts *A* to *D*, there was little difference in the pressures recorded using 1·17 *S* and 1·33 *S* mixtures; the points recorded in

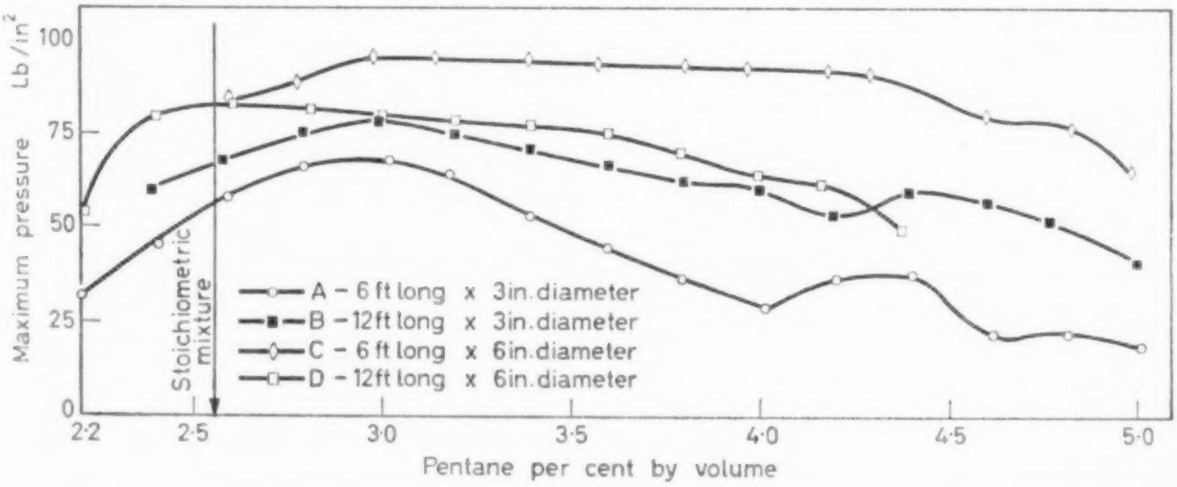

Figure 2. Maximum pressures in circular ducts; no vents. Each point is the mean of at least two traces

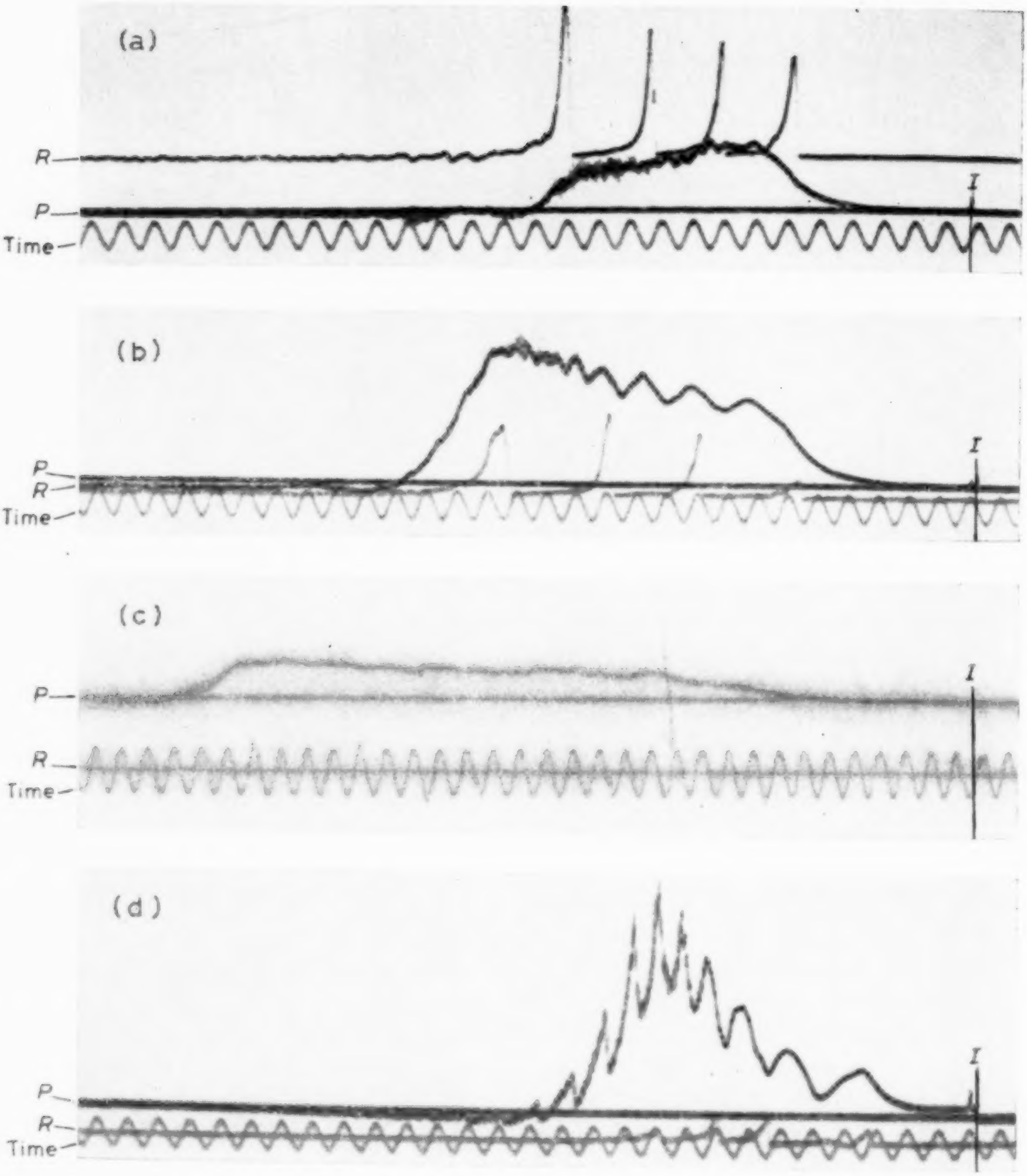

Figure 3. Pressure records with vents remote from ignition source—R denotes ionization gap record: (a) *Duct D: K=4, P_m=4·4;* (b) *Duct D: K=8, P_m=9·5;* (c) *Duct J: K=4, P_m=4·6;* (d) *Duct B: K=8, P_m=29·9. Time trace at 100 c/s in each case*

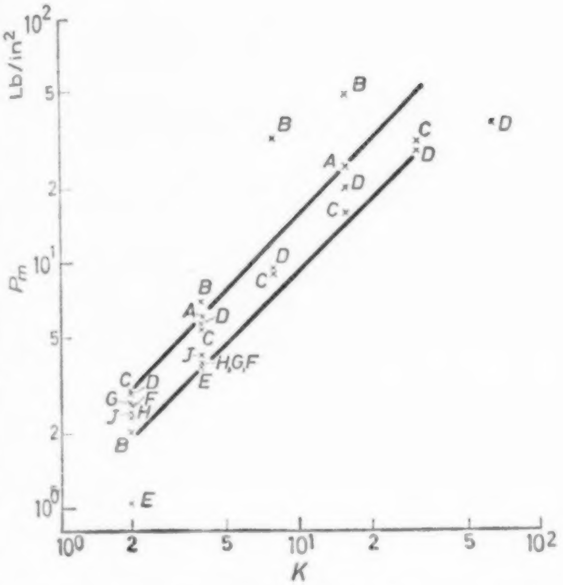

Figure 4. Relation between vent size and maximum pressure with vent remote from ignition source and duct data as in Table 1

Figure 4 for a given duct and vent are therefore the mean values of all the tests carried out. *Figure 4* shows that for $2<K<32$ most of the points fall between two parallel lines represented by the equation

$$P_m = aK \qquad \ldots . [1]$$

where a is a factor which varied between 0·85 and 1·5.

The exceptions were some points for high values of K with duct B which fell above the lines and a point for $K=2$ with duct E which fell below the lines. Duct B gave very disturbed pressure records, and it will be seen later that duct E was not long enough to allow the development of high flame speeds. It must also be expected that the relation in equation 1 will break down for high values of K since the pressure must approach that measured in a closed vessel as K approaches infinity.

Figure 5 shows the results for $K=1$ plotted against α for all ducts. The pressure increased as α increased. There was little difference between the peak pressures at the two ends of the duct with $\alpha \leqslant 12$ but substantial differences were obtained at greater values of α. For a given value of α there was no significant difference in the behaviour of circular and square ducts.

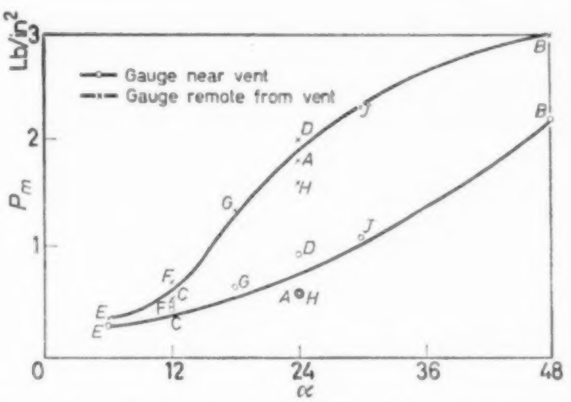

Figure 5. Maximum pressure in open-ended cylindrical and square ducts with vent remote from ignition source

Flame speed—*Figure 6* shows the mean flame speed between the ignition source and the vent plotted against K for all the ducts. The mean flame speed decreased as α decreased. For a given value of α there was little difference between the mean flame speed in ducts of different diameter. The flame speed along the ducts is shown in *Figures 7* to *11*. *Figures 7* and *8* give the flame speeds for ducts B and D respectively for all values of K and *Figures 9*, *10* and *11*, the flame speeds for ducts E to H for values of $K=1$, 2 and 4 respectively. The

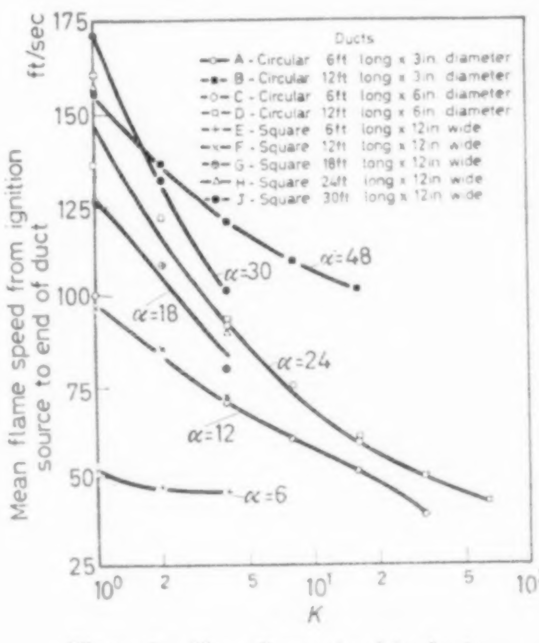

Figure 6. Mean flame speed in ducts

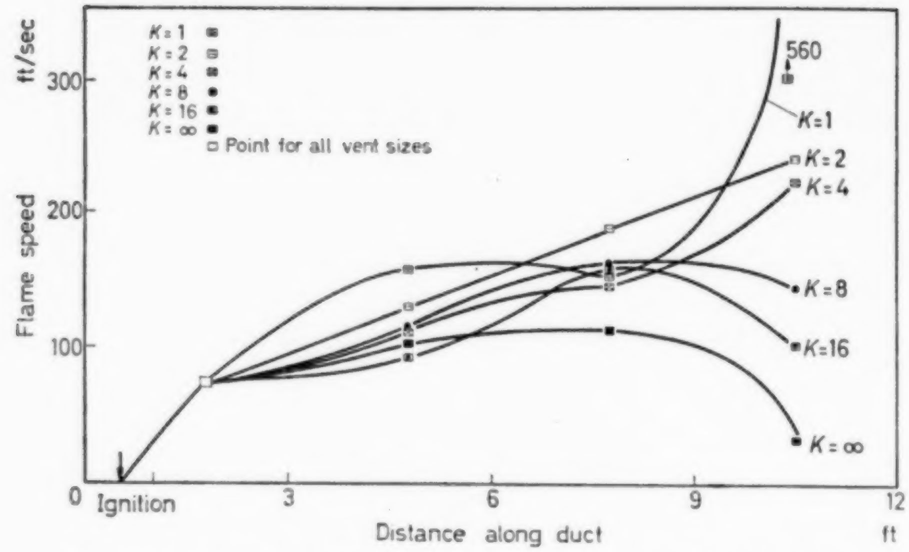

Figure 7. Flame speed in circular duct with vent remote from ignition source. Duct B—Circular 12 ft long × 3 in. diameter

points shown in these figures are mean flame speeds between neighbouring ionization gaps. The figures show that with $K=1$, the flame speed increased more or less continuously for all ducts. With the exception of duct *B*, the flame speed for all other values of *K* reached its maximum after travelling 6 to 12 duct diameters and then decreased. For $K=2$, 4 and 8, fairly constant values of the flame speed were obtained as the flame approached the vent; these flame speeds were independent of the duct but decreased with *K*. Explosions in duct *B* were exceptional in that maximum flame speeds occurred much farther along the duct. There was also no consistent decrease in flame speed as *K* increased, nor any tendency for a constant value of the flame speed to be established.

Relief vent near ignition source

The pressure records obtained for explosions

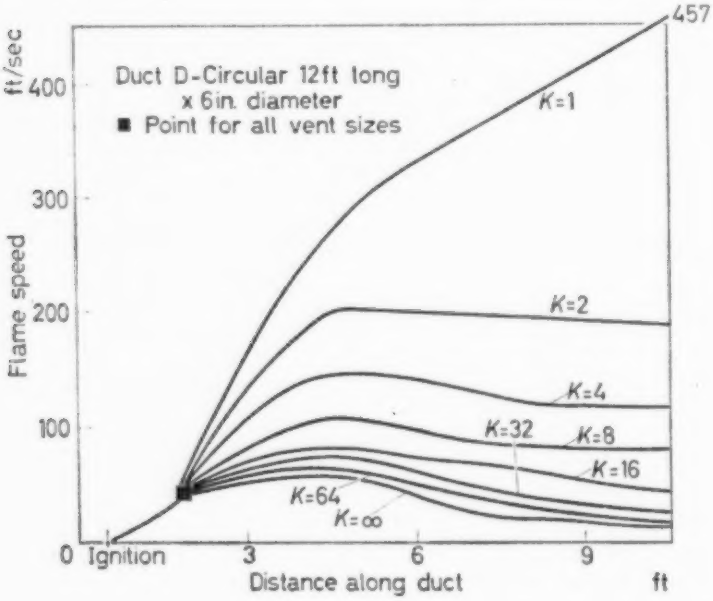

Figure 8. Flame speed in circular duct with vent remote from ignition source

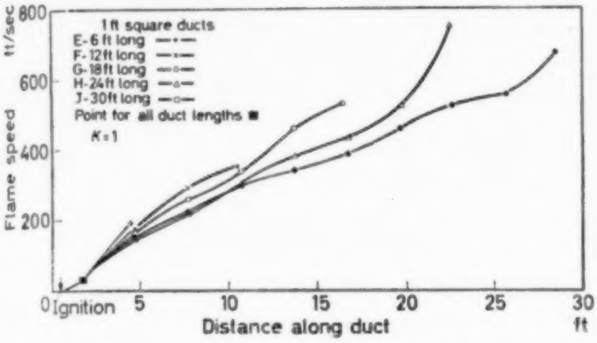

Figure 9. ***Flame speed in open-ended square ducts with vent remote from ignition source***

with vents near the ignition source could be divided into two groups. For values of $K \geqslant 8$ the pressure rose quickly to a peak value, which was in general the maximum pressure obtained, and then dropped somewhat for the rest of the explosion. For values of $K \leqslant 4$ the pressure dropped to atmospheric after the initial rise and acoustic vibrations were established which had an amplitude either comparable to or larger than the initial pressure rise. For $K=1$ there was usually no apparent initial pressure rise. Examples of these pressure records are given in *Figure 12*.

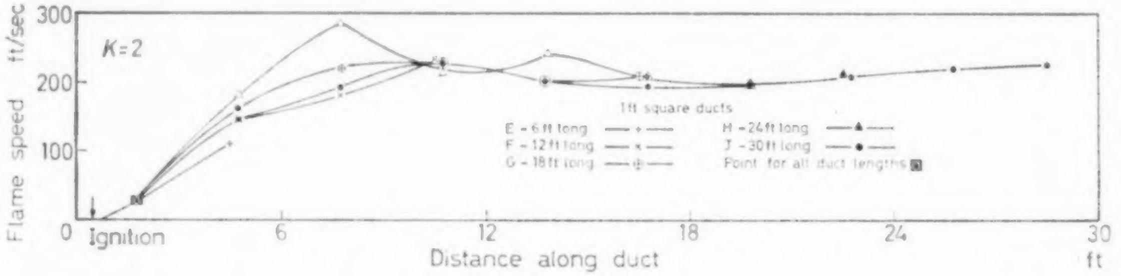

Figure 10. Flame speed in square ducts with vent remote from ignition source

Figure 13 shows the maximum pressure P_m plotted against K for $K \geqslant 4$. The maximum pressure for $K=4$ refers only to the initial pressure rise. The mean relation between P_m and K for ignition remote from the vent is also given for comparison. The pressures reached were much smaller when the vent was near the ignition source than when it was remote, the difference increasing as K decreased. The pressure also decreased as W, the duct diameter or width increased although for a given value of W the length of the duct had little effect.

Figure 14 shows the maximum amplitude of the acoustic vibrations that occurred with low values of K, plotted against K. The amplitude increased as K increased, and in the explosions in the circular ducts, reached values up to ± 5 Lb/in^2. With the square ducts, however, the amplitude was much less. The amplitude also in general decreased as the duct length increased. It was found that the vibrations could be suppressed if the closed flange opposite the vent was replaced by a flexible diaphragm or a slab of a certain material with a honeycomb structure. However, the amplitude of the vibrations was not appreciably decreased if the

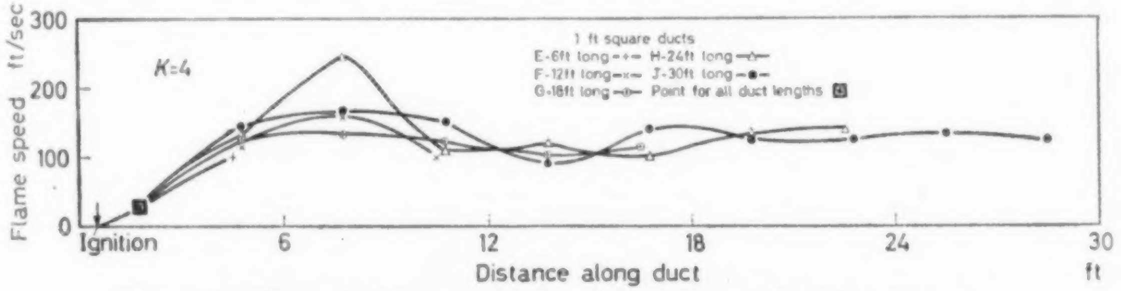

Figure 11. Flame speed in square ducts with vent remote from ignition source

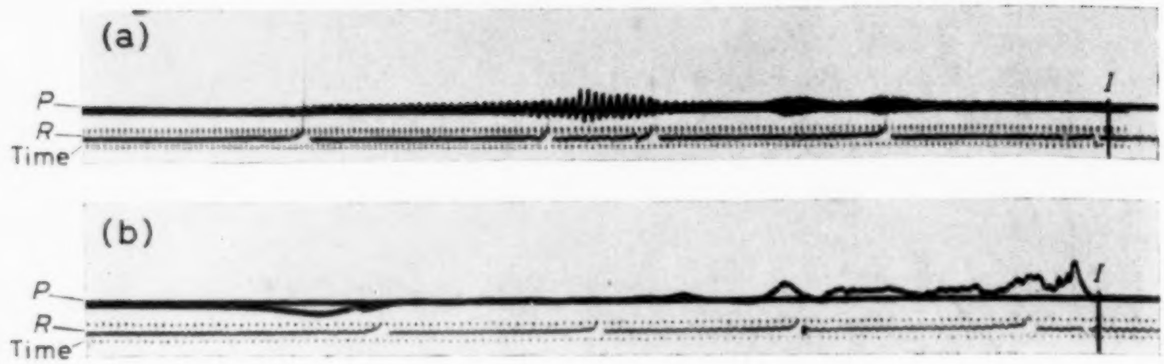

Figure 12. Pressure records with vents near ignition source. P is the pressure record, R the ionization gap record, I the ignition, and P_m represents maximum pressure (Lb/in²). (a) *Duct D: $K=2$; $P_m=\pm 1{\cdot}4$.* (b) *Duct D: $K=16$; $P_m=3{\cdot}0$. Time trace at 50 c/s for both*

flange was bolted in place behind the materials, even when a gap was left between the flange and the materials.

The flame speeds in these tests with the vent near the ignition source were generally between 3 and 6 ft/sec. However, higher flame speeds of up to 10 to 15 ft/sec were obtained for $K=1$ when the flame was in the region remote from the vent; it was when the flame was in this region that acoustic vibrations were most pronounced. Higher flame speeds were also obtained with very small vents.

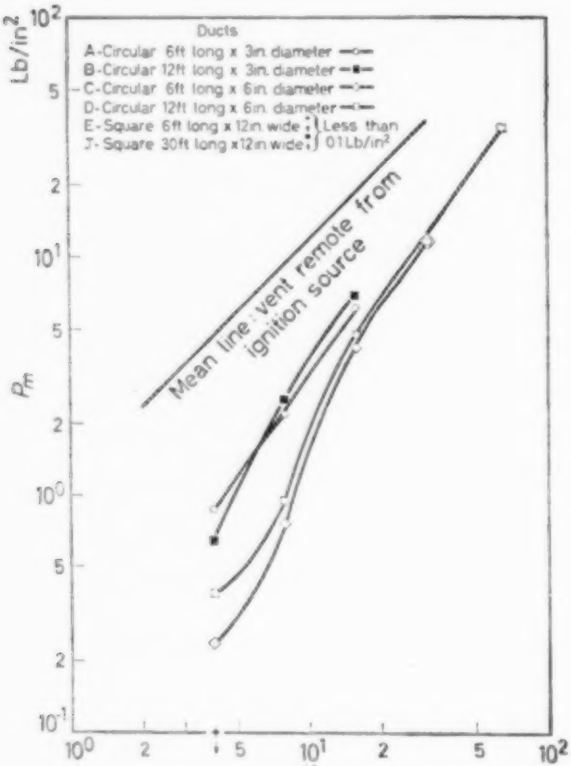

Figure 13. Effect of vent size on maximum pressure with vent near ignition source

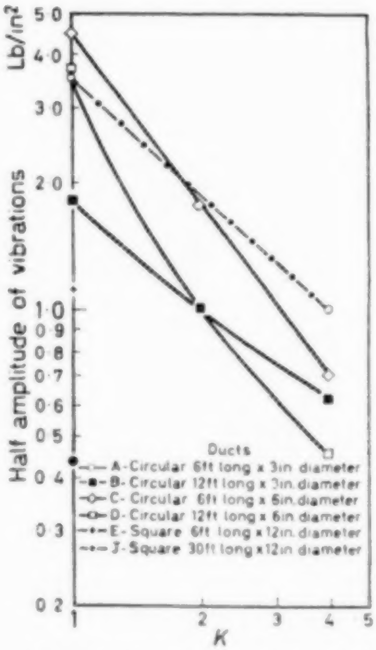

Figure 14. Effect of vent size on pressure caused by acoustic vibrations

Discussion

The above results give empirical relationships for the maximum pressures and the flame speeds

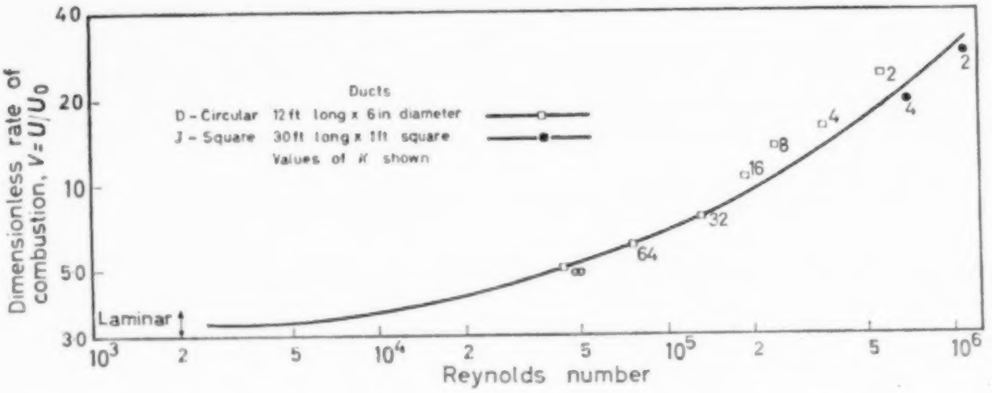

Figure 15. Effect of Reynolds number in unburnt gas on dimensionless rate of combustion

for explosions in ducts of various shapes and with different degrees of venting. To interpret these results, and to allow their extrapolation to systems which have not been tested, it is necessary to have some insight into the factors which control the pressure reached in a vented vessel. These factors may be divided into two groups: those which govern the rate at which the volume in the gas vessel is increased or expanded, and those which govern the rate at which the gas may be discharged. The most important factor in the first group is the rate of combustion at the flame front and it is very desirable from this point of view to have as fundamental and comprehensive a relation as possible between the rate of combustion and the aerodynamic and shape factors of the system. In the particular instance of flame travelling in empty ducts it might be expected that there would be a relationship between the rate of combustion and the Reynolds number in the unburnt gas ahead of the flame, since the turbulence in this gas would be a function of the Reynolds number. The cooling of the burnt gas behind the flame will also affect the rate at which the volume of gas is increased. The factors which govern the discharge of gases from the system are the friction and inertia of the gases and the discharge characteristics of the vent.

Rate of combustion

It was possible, where both pressure and flame speed records were available, to estimate the rate of combustion as the flame passed any given point in the duct and also the corresponding speed of the unburnt gas ahead of the flame. This calculation was carried out for the tests with ducts *D* and *J* for a point one quarter of the length of the duct from the vent and with ignition remote from the vent. It was necessary in the calculation to take into account not only the flame speed but also the way in which pressure was changing and the cooling of the burnt gas behind the flame; fuller details of the calculation will be given elsewhere. *Figure 15* shows *V*, which was a dimensionless rate of combustion, plotted against the Reynolds number of the unburnt gas immediately ahead of the flame. *V* was obtained by dividing U the calculated velocity of the flame relative to the unburnt gas by U_0 the fundamental burning velocity at the pressure and temperature of the unburnt gas. It was assumed on the basis of information in the literature that U_0 increased as the 1·6 power of the absolute temperature and inversely as the fourth root of the absolute pressure, and that the gas ahead of the flame was compressed adiabatically; the values of U_0 calculated in this way varied between 1·3 and 1·6 ft/sec. The results for the two ducts and different values of *K* fall about a single curve. Moreover, when this curve is extrapolated back to a Reynolds number of 2 500, a value of *V* equal to 3 to 4 is obtained which is the expected value for ducts under laminar conditions. It should be noted that *Figure 15* does not give the ratio of turbulent burning velocity to laminar burning velocity since the area of the flame has not been taken into account.

It was noted in the results that there was a considerable similarity in the flame speed and maximum pressure measurements for explosions in all the ducts with the exception of duct *B* (12 ft long × 3 in. diameter). It may therefore be expected that it is unlikely that the relationship between burning rate and Reynolds number given in *Figure 15* for ducts *D* (12 ft long × 6 in. diameter) and *J* (30 ft long × 1 ft square) would differ appreciably for the other ducts, with the exception of duct *B*. It was not possible to calculate reliable rates of combustion for the latter duct since it was not possible to estimate the effect on the cooling of the burnt gases of the intense vibrations which were set up during the combustion. However, approximate calculations indicated that values of *V* were between two to three times larger than the values expected from *Figure 15*. These high rates of combustion may have been due to the vibrations imposing their own turbulence on the system; on the other hand both the high rates of combustion and the vibrations may have been the result of some other factor.

Discharge of gases from the ducts

In the present experiments it was found that for values of $K \geqslant 2$ (i.e. vent areas less than half the cross section of the duct) there was no significant difference in the maximum pressure between the ends of the ducts. For these values of *K*, therefore, the effect of inertia and the friction of the moving gas on the discharge of the gases was small in comparison with the restriction caused by the vent.

From the calculated values of the velocity of the unburnt gas ahead of the flame it was possible to estimate the rate at which gas was arriving at the vent. In addition, on the basis of discharge formulae[5, 6] it was also possible to estimate from the pressure in the duct the rate at which gas was being discharged at the vent. These two rates are compared in *Figure 16* for the tests with duct *D* when the flame was 3 ft from the vent. Within the error of measurements and the approximation in the calculations there was good agreement between the calculated rates. This not only acts as a check on the rates of combustion, but also suggests that, knowing these rates and the appropriate corrections for cooling caused by the walls, it

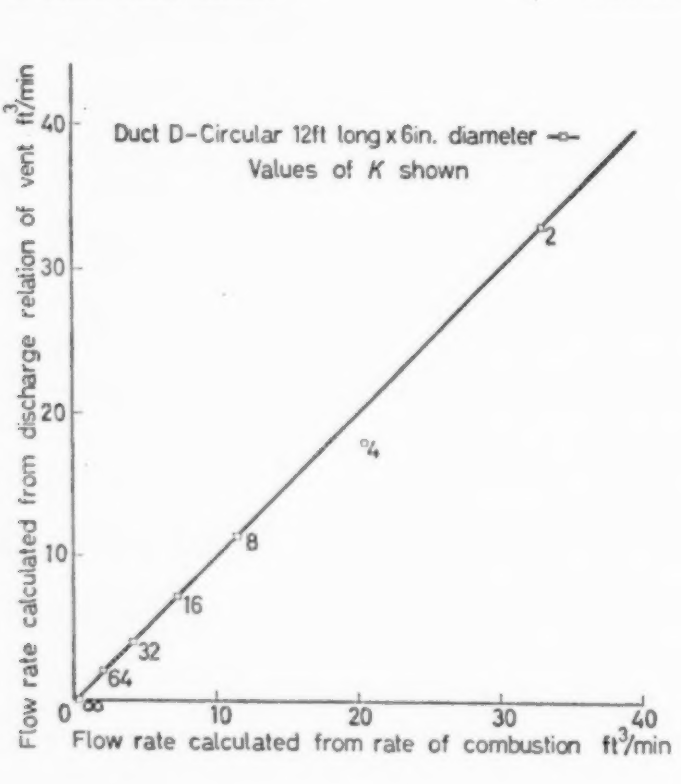

Figure 16. Comparison of calculated flow rates at vent (the line represents equality between calculated values)

should be possible to calculate the maximum pressure that may be obtained. It would be necessary to use a stepwise procedure and to allow for the fact that there will, in general, be two flame fronts one moving towards the vent and one away from the vent.

For values of $K \geqslant 4$ very much lower pressures were obtained when the ignition source was near the vent. There are two reasons for this. First, the rate of combustion was much smaller when the gas was ignited near the vent; this resulted in the volume of gases flowing towards the vent being about one fifth to one half of that when ignition was remote from the vent, the fraction increasing as K decreased. Secondly, the gases moving through the vent were hot burnt gases rather than cold unburnt gases and for a given volume of gas flowing through an orifice, the pressure drop across the orifice is approximately directly proportional to the gas density. Allowing for the cooling of the gases, both these factors combined should result in the pressure for vents remote from the ignition source being about 10 to 60 times greater than for vents close to the ignition source, the factor increasing as the vent size increases. The observed differences were generally not as great as this except for the 12 in. square ducts. The reason is that in all tests the gas was ignited at a point 6 in. from the vent and, in the initial stages of the explosion, unburnt gas was pushed through the vent. This accounts for the increase in pressure as the duct diameter was reduced and also for the fact that the peak pressures occurred very early in the explosions with ignition near the vent.

When $K=1$, there was no restriction to discharge caused by the vents. It was estimated that the friction along the ducts when the ignition was remote from the vent was responsible for a pressure drop equal to about one twentieth or one fifth of the measured difference in pressure between the ends of the ducts, whereas the inertia of the gas columns ahead of the flame could be responsible for the whole of the pressure drop. This indicates that, under the conditions investigated, the inertia rather than the friction of the gas column, controlled the discharge of the gases when one end of the ducts was fully open.

Practical implications

It is outside the scope of this paper to discuss in detail the practical implications of this work or to compare the results obtained with those of other investigations. The results may be applied directly to the design of vents for duct-shaped vessels with ratios of length to diameter within the range tested, and which may contain gases with a burning velocity similar to those of propane–air mixtures; some precautionary remarks should, however, be made. First, the results apply to open vents in the ends of the ducts. Work which will be described elsewhere has shown that substantially higher pressures may be obtained if vents are placed on the side of ducts, i.e. when the gases to be vented have to turn through a right angle. Also, if the vent is covered by a bursting disc the maximum pressure will be at least the bursting pressure of the disc[4]. Secondly, the results apply only to initially quiescent gas in empty ducts; the insertion of objects in the duct or the pre-existence of turbulence will be expected to alter the pattern of turbulence ahead of the flame and give different combustion rates. Thirdly, the maximum pressures given for vented ducts cover only a narrow range of combustible mixture strengths. In a few cases which have not been described, tests were carried out with a range of combustible mixtures varying in concentration from 0·9 to 1·55 S. The mixture which gave the highest pressures varied between 1·0 and 1·3 S. However, with the exception of tests in duct B, in no single test with any mixture was the maximum pressure greater than that given by the following form of equation 1 for $K \geqslant 2$.

$$P_m = 1{\cdot}75K \qquad \ldots . [2]$$

Lastly, the pressures given are for ignition 6 in. from the end of the duct. It will be expected from the considerations in the previous section that the highest pressure will be obtained when the ignition is near such a point that flame would reach both ends of the duct at the same time. From the relative values of the rates of combustion when propagation is taking place away from and towards a vent, it may be expected that, at the optimum position for ignition, pressures of the order of 20 to 40 per cent higher than those given by equation 2 might be obtained for vents of size $K \leqslant 8$. This prediction has been confirmed by further tests.

Much smaller pressures were obtained when a relief vent was near the ignition source than when it was remote from this source. This difference may be ascribed basically to the fact that burnt gas rather than unburnt gas was vented when ignition took place near the vent. When burnt gas is vented, the unburnt gas ahead of the flame is left relatively undisturbed. As a result the rate of combustion does not increase substantially over that expected for conditions of laminar flow. Moreover, as mentioned above, a given volume flow rate of burnt gas may be vented at a much lower pressure than unburnt gas. These views lead to an important practical principle that vents should be so disposed in a plant that burnt gas rather than unburnt gas should be ejected through them. A way in which this can be applied in practice for venting ducts is to install frequent small vents or to have an almost continuous strip of venting along the duct, instead of large vents at infrequent intervals. In this way flame cannot travel far before it passes a vent and allows burnt gases to be vented. Further work on testing this principle is in progress.

The work described in this paper forms part of the programme of the Joint Fire Research Organization of the Department of Scientific and Industrial Research and Fire Offices' Committee; the paper is published by permission of the Director of Fire Research. Messrs A. Kelly and J. Card assisted in the experiments.

References

[1] Palmer, K. N. 'Progress Review No. 38. A review of information on selected aspects of gas and vapour explosions'. *J. Inst. Fuel*, 1956, **29** (186), 239–309

[2] Cubbage, P. A. and Simmonds, W. A. 'An investigation of explosion reliefs for industrial drying ovens. I. Top reliefs in box ovens. II. Back reliefs in box ovens: reliefs in conveyor ovens'. *Gas Counc. Res. Commun. Nos. GC 23* (1955) and *GC 43* (1957)

[3] Margerson, S. N. A. and Robinson, H. 'A piezoelectric recording manometer'. *Saf.-i-Mines Res. Rep. No. 82* December 1953

[4] Rasbash, D. J. and Rogowski, Z. W. 'The venting of explosions in duct systems. Part II. The venting of explosions in a pentane–air mixture in a duct 6 ft long × 6 in. diameter'. Department of Scientific and Industrial Research and Fire Offices' Committee Joint Fire Research Organization. *F.R. Note No. 298* (1957)

[5] Perry, J. H. (Ed.) *Chemical Engineers Handbook*, 3rd ed., p 403. McGraw-Hill: New York and London, 1950

[6] Finniecombe, J. R. 'Flow through standard nozzle, orifice plates and Venturi tubes'. Emmot and Co. Ltd: Manchester, 1948

Structure and Propagation of Laminar Flames near a Heat Sink

TZE-NING CHEN and TAU-YI TOONG

Massachusetts Institute of Technology, Cambridge 39, Mass., U.S.A.

(*Received June 1959*)

This paper presents the results obtained in a theoretical investigation of the problem of laminar flame propagation near a heat sink, the temperature of which may be either high or low as far as the chemical reaction rate is concerned. The results presented consist of two parts : first, effects on the burning velocity of an adiabatic laminar flame due to a change in the temperature of the unburnt mixture ; and secondly, effects on the structure and the burning velocity of a laminar flame when the rate of heat loss per unit volume inside the flame in the direction normal to the mixture velocity and the rate of heat loss per unit area at the hot boundary in the direction parallel to the flow are prescribed by arbitrary functions. In all cases, the burning velocity is found to vary approximately with the temperature of the combustion product at the hot boundary according to an expression of the following form $S_u \sim \exp\,(-T_c/T_b)$ *where* S_u *is the burning velocity,* T_b *is the temperature of the combustion product, and* T_c *is a characteristic temperature, the value of which depends on the specific case under consideration. Some of these observations have also been found to agree with the experimental results. For the special case where heat loss occurs only at the hot boundary in the direction parallel to the flow, there is a lower limit for the temperature of the combustion product, below which no steady-state solution for the burning velocity can be found. This limit is in addition to the one deduced from stability considerations.*

Introduction

IN AN earlier paper[1] by the senior author, it has been shown that a flame can be stabilized in the boundary layer of a steady stream of a combustible gas over a smooth surface when the tendency for the flame to propagate at the local burning velocity is in stable equilibrium with the fluid motion. Also, it has been found that flame stabilization can be realized in a high-speed stream by raising the surface temperature. Thus, a promising step toward the prediction of the flameholding characteristics of such a smooth surface is to study the problem of flame propagation in the neighbourhood of this surface.

Figure 1, taken from the work of T. Y. TOONG[1], shows a steady laminar flow of a combustible mixture over an isothermal flat plate. According to the boundary-layer theory, the viscous, thermal and chemical effects are predominant in a region of a developing boundary layer, which starts to grow in thickness from the leading edge, whereas the fluid outside of this region can be assumed to be unaffected by the presence of the flat plate.

Two cases are illustrated in *Figure 1* with the corresponding velocity and temperature profiles of the combustible mixture and the burning velocity profiles. In case (a), the wall temperature, T_w, is maintained at the free-stream mixture temperature, T_∞, which is assumed to be low as far as the chemical reaction rate is concerned; and in case (b), the wall temperature is maintained at a value somewhere between the mixture temperature and the corresponding adiabatic flame temperature T_+^0. Because of the presence of the flat plate as a heat sink and possibly also as a sink for active particles, the burning velocity decreases rapidly to zero in *Figure 1*(a) within a distance equal to the quenching distance. In *Figure 1*(b), as the distance normal to the wall decreases, the burning velocity is shown first to increase due to the effect of increasing mixture temperature* and then to decrease rapidly to zero when the quenching effect becomes more predominant. Thus, for the case of *Figure 1*(a), the flame

---

*The effect of increasing mixture temperature would be somewhat augmented or offset by that due to a change in the mixture composition resulting from chemical reaction in the hot boundary layer. It has been shown[1], however, that this latter effect is relatively small if the flame is stabilized at a small distance from the leading edge of the flat plate.

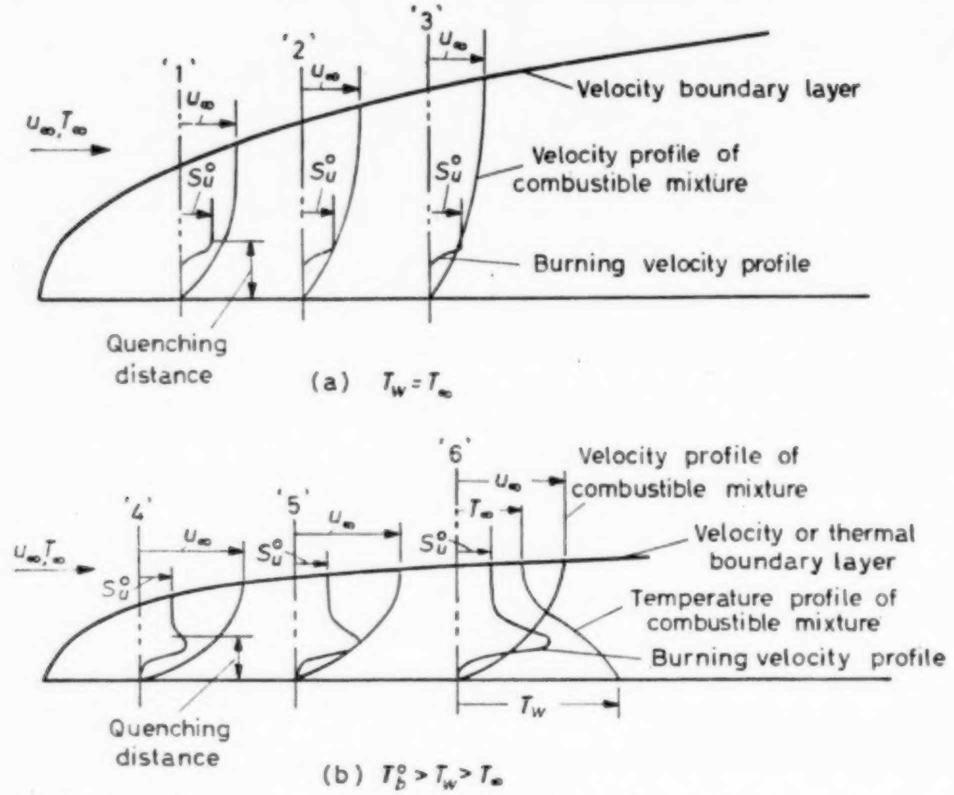
'1'
'2'
'3'
u_∞, T_∞
u_∞
S_u°
Velocity boundary layer
Velocity profile of combustible mixture
Burning velocity profile
Quenching distance
(a) $T_w = T_\infty$
'4'
'5'
'6'
Velocity or thermal boundary layer
Temperature profile of combustible mixture
T_∞
T_w
(b) $T_b^\circ > T_w > T_\infty$

Figure 1. Schematic diagram showing mechanism of flame stabilization by means of a smooth surface

propagation problem under investigation becomes one of the study of the quenching effect on the structure and the burning velocity of a laminar flame; and for the case of ***Figure 1***(b), in addition to the quenching effect, it is also necessary to study the effect due to a change in the temperature and the composition of the combustible mixture at different positions inside the hot boundary layer.

A quasi-one-dimensional method is developed in this paper for the determination of the structure and the burning velocity of laminar flames near a heat sink. The equations of conservation of mass and energy are solved by means of an iteration scheme, which is found to converge reasonably rapidly. The burning velocity is then determined as an eigenvalue, which gives the exact solution satisfying the conservation equations and the appropriate boundary conditions.

The results presented consist of two parts: first, effects on the burning velocity of an *adiabatic* laminar flame due to a change in the temperature of the unburnt mixture; and secondly, effects on the structure and the burning velocity of a laminar flame when the rate of heat loss per unit volume inside the flame in the direction normal to the mixture velocity and the rate of heat loss per unit area at the hot boundary in the direction parallel to the flow are prescribed by different arbitrary functions.

Analysis

(1) *Basic equations*

For a steady, one-dimensional, laminar flow of a reacting mixture of two components of equal specific heats at constant pressure (viz. the combustible component and the product of combustion), with heat losses in the direction normal to the flow, the equations of conservation of mass and energy are as follows:

$$\rho u \frac{\mathrm{d}c_A}{\mathrm{d}x} - \frac{\mathrm{d}}{\mathrm{d}x}\left(\rho D \frac{\mathrm{d}c_A}{\mathrm{d}x}\right) + k_A = 0 \quad \ldots . [1]$$

$$\rho u = \rho_u u_u = \rho_b u_b = \text{constant} \qquad \ldots .[2]$$

$$\rho u c_p \frac{\mathrm{d}T}{\mathrm{d}x} - \frac{\mathrm{d}}{\mathrm{d}x}\left(\lambda \frac{\mathrm{d}T}{\mathrm{d}x}\right) + q_L - q k_A = 0 \quad ..[3]$$

where u_u is the so-called burning velocity or S_u and q_L represents the rate of heat loss per unit volume of the mixture in the direction normal to the flow. Other symbols are defined below:

ρ	mass density of mixture
u	velocity in x direction
c_A	mass fraction of combustible component 'A'
x	distance in flow direction
D	binary diffusion coefficient
k_A	mass rate of consumption of combustible component 'A' per unit volume
c_p	specific heat at constant pressure
T	absolute temperature
λ	thermal conductivity
q	enthalpy of combustion per unit mass of combustible component.

Subscripts u and b refer to the initial unreacted and final reacted conditions, respectively.

It is to be noted that diffusion in the direction normal to the flow is not considered in equation **1**.

The boundary conditions for c_A and T are the following:

$$\left.\begin{aligned} &\text{For } x = x_u : c_A = c_{Au}, \frac{\mathrm{d}c_A}{\mathrm{d}x} = 0,\ T = T_u, \frac{\mathrm{d}T}{\mathrm{d}x} = 0 \\ &\text{For } x = x_b : c_A = c_{Ab}, \frac{\mathrm{d}c_A}{\mathrm{d}x} = 0,\ T = T_b, \\ &\qquad\qquad\qquad\qquad \frac{\mathrm{d}T}{\mathrm{d}x} = \left(\frac{\mathrm{d}T}{\mathrm{d}x}\right)_b \end{aligned}\right\} \quad \ldots .[4]$$

Here T_b is the temperature of the combustion product at the burnt boundary, as given by the relation

$$\rho_u S_u c_p (T_b^0 - T_b) = \int_{x_u}^{x_b} q_L \,\mathrm{d}x - \lambda \left(\frac{\mathrm{d}T}{\mathrm{d}x}\right)_b \quad \ldots .[5]$$

with the last term in equation **5** representing the rate of heat transfer per unit flow area at the burnt boundary in the direction parallel to the flow. (Superscript ^{0} here refers to the adiabatic case.)

Examination of the second-order ordinary differential equations **1** and **3** and their boundary conditions (equation **4**) indicates that this is an eigenvalue problem. The eigenvalue parameter ρu and the burning velocity S_u can be determined from the solution of these equations.

(2) *Method of solution*

For the case where the diffusion coefficient is equal to the thermal diffusivity (or the Lewis number is unity) and the values of the thermal conductivity and specific heat at constant pressure are constant, equations **1**, **3** and **4** suggest the following possible relationship between the mass fraction c_A and the temperature T at any position of the flame*:

$$\begin{aligned} &\rho_u S_u (q c_A + c_p T) - \lambda \left(\frac{\mathrm{d}T}{\mathrm{d}x}\right)_b \exp\left[-\frac{\rho_u S_u c_p}{\lambda}(x_b - x)\right] \\ &\quad + \int_{x_u}^{x} q_L \,\mathrm{d}x + \left(\frac{\lambda}{\rho_u S_u c_p}\right) q_L + \left(\frac{\lambda}{\rho_u S_u c_p}\right)^2 \frac{\mathrm{d}q_L}{\mathrm{d}x} \\ &\quad + \left(\frac{\lambda}{\rho_u S_u c_p}\right)^3 \frac{\mathrm{d}^2 q_L}{\mathrm{d}x^2} + \ldots\ldots = \rho_u S_u (q c_{Au} + c_p T_u) \end{aligned} \quad \ldots .[6]$$

Further assumptions required by the boundary conditions indicated by equation **4** are:

$$\exp\left[-\frac{\rho_u S_u c_p}{\lambda}(x_b - x_u)\right] \ll 1 \quad \ldots [7]$$

$$\left[q_L + \frac{\lambda}{\rho_u S_u c_p} \frac{\mathrm{d}q_L}{\mathrm{d}x} + \ldots\ldots\right]_u = 0 \quad \ldots [8]$$

and

$$\left[q_L + \frac{\lambda}{\rho_u S_u c_p} \frac{\mathrm{d}q_L}{\mathrm{d}x} + \ldots\ldots\right]_b = 0 \quad \ldots [9]$$

It is to be noted that equation **7** is valid in most cases. However, the actual distribution of the rate of heat loss per unit volume inside the flame may not necessarily satisfy equations **8** and **9**.

In view of the complexities involved in equations **6**, **8** and **9**, and the possibility that the actual value of the Lewis number may be different from unity, the following simplified expression is used instead of equation **6** in the present investigation

---

*Equation 6 can be obtained by eliminating k_A from equations 1 and 3 and solving the resulting differential equation together with the boundary conditions given by equation 4.

$$\rho_u S_u (q c_\Lambda + c_p T) - \lambda \left(\frac{\mathrm{d}T}{\mathrm{d}x}\right)_b \exp\left[-\frac{\rho_u S_u c_p}{\lambda}(x_b - x)\right] + \int_{x_u}^{x} q_L \,\mathrm{d}x = \rho_u S_u (q c_{\Lambda u} + c_p T_u) \quad \ldots.[10]$$

Here, the rate of heat loss per unit volume in the direction normal to the flow must satisfy the following conditions at the two boundaries:

$$q_{Lu} = q_{Lb} = 0 \quad \ldots.[11]$$

Thus, the problem becomes one of solving either equation **1** or **3** together with equations **4** and **10**.

Integration of equation **3** between any section x inside the flame and the burnt boundary b gives

$$\rho_u S_u c_p (T_b - T) - \lambda \left(\frac{\mathrm{d}T}{\mathrm{d}x}\right)_b + \lambda \frac{\mathrm{d}T}{\mathrm{d}x} + \int_{x}^{x_b} q_L \,\mathrm{d}x - \int_{x}^{x_b} q k_\Lambda \,\mathrm{d}x = 0 \quad \ldots.[12]$$

With $(\mathrm{d}T/\mathrm{d}x)_u = 0$, $\int_{x_u}^{x_b} q_L \,\mathrm{d}x$ given by equation **5** and $x = x_u$ equation **12** yields

$$S_u = \frac{q}{\rho_u c_p (T_b^0 - T_u)} \int_{T_u}^{T_b} \frac{k_\Lambda \,\mathrm{d}T}{(\mathrm{d}T/\mathrm{d}x)} \quad \ldots.[13]$$

Since k_Λ is usually a function of c_Λ and T, the integral on the RHS of equation **13** can be evaluated with the aid of equation **10** if $\mathrm{d}T/\mathrm{d}x$ is known as a function of T (and so follow therefrom x and $\int q_L \,\mathrm{d}x$ as functions of T). $\mathrm{d}T/\mathrm{d}x$ can be determined as a function of the temperature by the use of equation **12** in the following form

$$\frac{\mathrm{d}T}{\mathrm{d}x} = \left(\frac{\mathrm{d}T}{\mathrm{d}x}\right)_b - \frac{\rho_u S_u c_p}{\lambda}(T_b - T) - \frac{1}{\lambda}\int_{x}^{x_b} q_L \,\mathrm{d}x + \frac{q}{\lambda}\int_{T}^{T_b} \frac{k_\Lambda \,\mathrm{d}T}{\mathrm{d}T/\mathrm{d}x} \quad \ldots.[14]$$

Thus, an iterative procedure can be formulated on the basis of equations **13** and **14** to solve for the correct values of S_u and $\mathrm{d}T/\mathrm{d}x$.

To start the iteration, a first approximation for $\mathrm{d}T/\mathrm{d}x$ is obtained by neglecting the heat losses q_L and $(\mathrm{d}T/\mathrm{d}x)_b$ as well as the convective term $\rho_u S_u c_p \,\mathrm{d}T/\mathrm{d}x$ in equation **3**. This procedure is justified by the fact that the iteration scheme to be described below is convergent and correct solutions can be obtained even if the iteration is started with an arbitrary temperature distribution. Thus

$$\left(\frac{\mathrm{d}T}{\mathrm{d}x}\right)_1 = \left[\frac{2}{\lambda}\int_{T}^{T_b^0} q k_\Lambda \,\mathrm{d}T\right]^{1/2} \quad \ldots.[15]$$

where the subscript $_1$ denotes the first approximation. A first approximation of the burning velocity can then be obtained by introducing equation **15** into equation **13** and a second approximation of $\mathrm{d}T/\mathrm{d}x$ obtained from equation **14** by the use of this iterated value of S_u and the first approximation of $\mathrm{d}T/\mathrm{d}x$. Thus, a second approximation of S_u can be obtained from equation **13**; and so forth.

It has been shown by T. Y. Toong and T. N. Chen in an earlier work[2] that the iteration scheme described above gives results which converge quite rapidly to the correct answer in an alternating manner.

An alternative iteration method has been used by G. Klein[3] in the computation of adiabatic burning velocities. For the present problem where heat loss is taken into consideration, the corresponding equations become the following:

$$S_u = \left[\rho_u c_p \int_{T_u}^{T_b} \left(\frac{\mathrm{d}T}{\mathrm{d}x}\right) \mathrm{d}T\right]^{-1} \left[\frac{\lambda}{2}\left(\frac{\mathrm{d}T}{\mathrm{d}x}\right)_b^2 + \int_{T_u}^{T_b} (q k_\Lambda - q_L)\,\mathrm{d}T\right] \quad \ldots.[16]$$

and

$$\frac{\mathrm{d}T}{\mathrm{d}x} = \left[\left(\frac{\mathrm{d}T}{\mathrm{d}x}\right)_b^2 + \frac{2}{\lambda}\int_{T}^{T_b} (q k_\Lambda - q_L)\,\mathrm{d}T - \frac{2\rho_u S_u c_p}{\lambda}\int_{T}^{T_b} \left(\frac{\mathrm{d}T}{\mathrm{d}x}\right) \mathrm{d}T\right]^{1/2} \quad \ldots.[17]$$

(3) *Non-dimensional working equations*

Let the overall reaction-rate expression for $T > T_u$ be represented by one of the first order of the Arrhenius type, such that

$$k_A = K\rho c_A \exp(-E/RT) \qquad \ldots\ldots [18]$$

where K is the specific reaction rate, E is the activation energy and R is the universal gas constant. Also, let

$$k_A = 0 \text{ for } T = T_u \qquad \ldots\ldots [19]$$

With the assumptions of perfect gas, constant pressure and constant molecular weight, equation **18** is further reduced to

$$k_A = K\rho_u c_A (T_u/T) \exp(-E/RT) \qquad \ldots [20]$$

Also, for convenience, introduce the following dimensionless variables:

$$\theta = T/T_b^0 \qquad \ldots\ldots [21]$$

$$\theta_a = E/RT_b^0 \qquad \ldots\ldots [22]$$

$$\delta = x/(\lambda \exp\theta_a/K\rho_u c_p \theta_u)^{1/2} \qquad \ldots\ldots [23]$$

$$\phi = S_u/(\lambda K \theta_u/\rho_u c_p \exp\theta_a)^{1/2} \qquad \ldots\ldots [24]$$

$$Q_L = q_L \exp\theta_a/K\rho_u c_p T_u \qquad \ldots\ldots [25]$$

$$Q = q/c_p T_b^0 \qquad \ldots\ldots [26]$$

and

$$\psi = k_A \exp\theta_a/K\rho_u\theta_u \qquad \ldots\ldots [27]$$

Thus, the working equations **5, 10, 13, 14, 15, 16, 17, 19** and **20** become

$$\phi(1-\theta_b) = \int_{\delta_u}^{\delta_b} Q_L \, d\delta - \left(\frac{d\theta}{d\delta}\right)_b \qquad \ldots\ldots [5a]$$

$$\phi(Qc_A + \theta) - \left(\frac{d\theta}{d\delta}\right)_b \exp[-\phi(\delta_b - \delta)] + \int_{\delta_u}^{\delta} Q_L \, d\delta = \phi(Qc_{Au} + \theta_u) \qquad \ldots\ldots [10a]$$

$$\phi_r = \frac{Q}{1-\theta_u} \int_{\theta_u}^{\theta_b} \frac{\psi \, d\theta}{(d\theta/d\delta)_r} \qquad \ldots\ldots [13a]$$

$$\left(\frac{d\theta}{d\delta}\right)_{r+1} = \left(\frac{d\theta}{d\delta}\right)_b - \phi_r(\theta_b - \theta) - \int_{\delta}^{\delta_b} Q_L \, d\delta + Q \int_{\theta}^{\theta_b} \frac{\psi \, d\theta}{(d\theta/d\delta)_r} \qquad \ldots\ldots [14a]$$

$$\left(\frac{d\theta}{d\delta}\right)_1 = \left[2 \int_{\theta}^{\theta_b} Q\psi \, d\theta\right]^{1/2} \qquad \ldots\ldots [15a]$$

$$\phi_r = \left[\int_{\theta_u}^{\theta_b} \left(\frac{d\theta}{d\delta}\right)_r d\theta\right]\left[\frac{1}{2}\left(\frac{d\theta}{d\delta}\right)_b^{-1\ 2} + \int_{\theta_u}^{\theta_b} (Q\psi - Q_L) \, d\theta\right] \qquad \ldots\ldots [16a]$$

$$\left(\frac{d\theta}{d\delta}\right)_{r+1} = \left[\left(\frac{d\theta}{d\delta}\right)_b^2 + 2\int_{\theta}^{\theta_b} (Q\psi - Q_L) \, d\theta - 2\phi_r \int_{\theta}^{\theta_b} \left(\frac{d\theta}{d\delta}\right)_r d\theta\right]^{1/2} \qquad \ldots\ldots [17a]$$

$$\psi = 0 \text{ for } \theta = \theta_u \qquad \ldots\ldots [19a]$$

and

$$\psi = \frac{c_A}{\theta} \exp\left[-\theta_a\left(\frac{1}{\theta} - 1\right)\right] \qquad \ldots\ldots [20a]$$

In the above equations, the subscript $_r$ refers to the rth approximation.

(4) *Limiting value of temperature of combustion product*

Elimination of $(d\theta/d\delta)_b$ in equations **5a** and **16a** gives the following quadratic equation in terms of the burning velocity

$$(1-\theta_b)^2\phi^2 - 2\left[(1-\theta_b)\int_{\delta_u}^{\delta_b} Q_L \, d\delta + \int_{\theta_u}^{\theta_b} \left(\frac{d\theta}{d\delta}\right) d\theta\right]\phi + \left[\int_{\delta_u}^{\delta_b} Q_L \, d\delta\right]^2 + 2\int_{\theta_u}^{\theta_b} (Q\psi - Q_L) \, d\theta = 0 \qquad . [28]$$

In order to have a real solution for the burning velocity, it is necessary that

$$\left[(1-\theta_b)\int_{\delta_u}^{\delta_b} Q_L \, d\delta + \int_{\theta_u}^{\theta_b} \left(\frac{d\theta}{d\delta}\right) d\theta\right]^2 \geqslant (1-\theta_b)^2 \left\{\left[\int_{\delta_u}^{\delta_b} Q_L \, d\delta\right]^2 + 2\int_{\theta_u}^{\theta_b} (Q\psi - Q_L) \, d\theta\right\} \qquad \ldots\ldots [29]$$

Or

$$\left[\int_{\theta_u}^{\theta_b}\left(\frac{\mathrm{d}\theta}{\mathrm{d}\delta}\right)\mathrm{d}\theta\right]^2+2\,(1-\theta_b)\left[\int_{\delta_u}^{\delta_b}Q_L\,\mathrm{d}\delta\right]\left[\int_{\theta_u}^{\theta_b}\left(\frac{\mathrm{d}\theta}{\mathrm{d}\delta}\right)\mathrm{d}\theta\right]$$

$$+2\,(1-\theta_b)^2\int_{\theta_u}^{\theta_b}Q_L\,\mathrm{d}\theta\geqslant 2\,(1-\theta_b)^2\int_{\theta_u}^{\theta_b}Q\psi\,\mathrm{d}\theta \qquad \ldots.[29a]$$

Equations 29 and 29a indicate that it is possible that no real solution of the burning velocity exists for a given distribution of the heat losses, Q_L and $(\mathrm{d}\theta/\mathrm{d}\delta)_b$, and a given value of the temperature of the product θ_b.

For the case where the heat loss occurs only at the hot boundary (or $Q_L=0$), equation 29a is reduced to

$$\theta_b\geqslant 1-\left[\int_{\theta_u}^{\theta_b}\left(\frac{\mathrm{d}\theta}{\mathrm{d}\delta}\right)\mathrm{d}\theta\right]\Big/\left[2\int_{\theta_u}^{\theta_b}Q\psi\,\mathrm{d}\theta\right]^{1/2} \qquad \ldots.[30]$$

In other words, there is a lower limit for the temperature of the combustion product, below which no steady-state solution for the burning velocity can be found.

For the case where the heat loss occurs only in the direction normal to the flow [or $(\mathrm{d}\theta/\mathrm{d}\delta)_b=0$], no such limiting value for θ_b as described above seems to exist.

It is to be noted that the lower limiting value of the temperature of the combustion product discussed here is different from the one obtained by D. B. SPALDING[4] and by E. MAYER[5] from stability considerations. The former limit, shown as point A in *Figure 8*, is given by equation 30; while the latter limit, shown as point B in the same figure, corresponds to the point of tangency of two curves, (*a*) and (*b*), both representing the rate of heat loss per unit flow area at the hot boundary. Here, curve (*a*) is calculated from the flame theory and curve (*b*) shows the variation of the actual heat loss to the environment at the limiting situation. Since the shape of the curve (*b*) depends on the way in which a particular experiment is performed, it follows that point B would vary accordingly. However, point A represents an absolute limit for the temperature of the combustion product below which there is no steady flame no matter how the experiment is conducted.

Although equation 28 suggests the possibility of having two values of the burning velocity at a given value of θ_b, under certain conditions, it can be shown that the larger one of these values approaches infinity as the temperature of the combustion product approaches the adiabatic value. It is physically meaningless and must therefore be discarded.

Results

The results presented in this paper consist of two parts: first, effects on the burning velocity of an *adiabatic* laminar flame due to a change in the temperature of the unburnt mixture; and secondly, effects on the structure and the burning velocity of a laminar flame when the rate of heat loss per unit volume inside the flame in the direction normal to the mixture velocity and the rate of heat loss per unit area at the hot boundary in the direction parallel to the flow are prescribed by arbitrary functions. These results were calculated by the use of the iteration schemes described above and will be separately discussed below.

(1) *Effect of initial mixture temperature*

In this case, both Q_L and $(\mathrm{d}\theta/\mathrm{d}\delta)_b$ are assumed to be zero. Thus, the problem becomes one of the determination of the *adiabatic* burning velocity at different values of the initial mixture temperature.

As indicated in the analysis, the overall reaction-rate expression is assumed to be one of the first order of the Arrhenius type (or $n=1$). Furthermore, for simplicity, c_{Au} and c_{Ab} are taken to be unity and zero, respectively, and the temperature rise $(T_b^0-T_u)$ and the pressure are assumed to be constant as T_u varies.

Figures 2(a) and *2*(b) show the variation of the adiabatic burning velocity as a function of the initial mixture temperature and that of the reciprocal of the adiabatic flame temperature, respectively. The values with superscript ⋆ correspond to a case where $\theta_u=0{\cdot}15$ and $\theta_a=8$. Also, the mean thermal conductivity is assumed to vary as the square root of the arithmetic

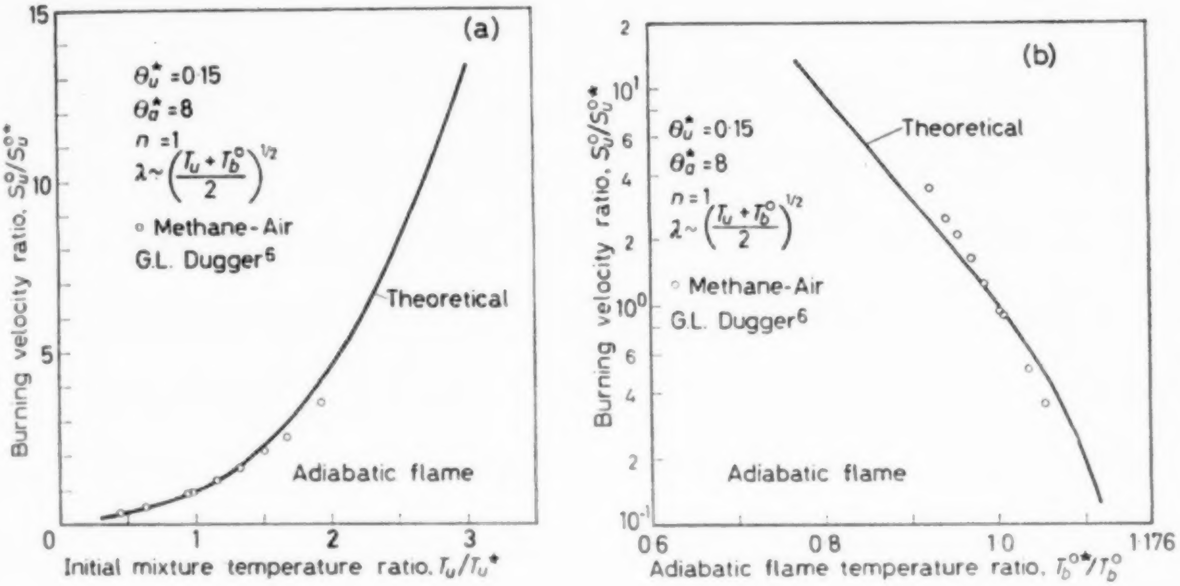

Figure 2(a) *Figure 2*(b)

Figure 2. Effect of initial mixture temperature on burning velocity: (a) $S_u^\circ\star$ *versus* $T_u/T_u\star$; (b) $S_u^\circ/S_u^\circ\star$ *versus* $T_b^\circ\star/T_b^\circ$

mean of the temperatures at the hot and the cold boundaries.

Figure 2(b) shows that the variation of the burning velocity in the high-temperature region can be approximated by an expression of the following form

$$S_u \sim \exp(-T_c/T_b) \qquad \ldots . [31]$$

where T_c is a characteristic temperature, the value of which depends on the specific case under consideration.

It is further observed in *Figure 2*(b) that the burning velocity decreases very rapidly as the adiabatic flame temperature drops to its limiting value corresponding to zero value of the initial mixture temperature.

Included in *Figure 2* are also the experimental data of G. L. DUGGER[6] for methane–air flames. Although the quantitative agreement may be fortuitous, the correct trend of variation is clearly indicated.

(2) *Effect of heat loss*

The working equations presented in the analysis indicate that the structure and the propagation speed of a laminar flame for given temperatures at the hot and cold boundaries depend on the distribution of the heat loss inside the flame, Q_L, and at the hot boundary $(d\theta/d\delta)_b$. In order to further a basic understanding of these effects, they have been separately investigated in this paper.

(a) *Effect of* Q_L—In this case, $(d\theta/d\delta)_b$ is assumed to be zero and the distribution of Q_L to be of the following form

$$\int_{\delta_u}^{\delta} Q_L \, d\delta = \phi\,(1-\theta_b)\left(\frac{\theta-\theta_u}{\theta_b-\theta_u}\right)^m \qquad \ldots . [32]$$

where m is a constant. This relationship corresponds to a case where the fraction of total heat loss per unit time per unit flow area is a function of the fraction reacted. It is to be noted that the boundary conditions required by equation **11** are hereby satisfied.

Figure 3 shows the variation of the fraction of the total heat loss per unit time per unit flow area versus the reactedness $(\theta-\theta_u)/(\theta_b-\theta_u)$ for three different values of m; viz. **0·5**, **1** and **2**. The corresponding variation of the burning velocity is plotted in *Figure 4* versus the reciprocal of the temperature of the combustion product for $\theta_u = 0{\cdot}15$ and $\theta_a = 8$. (Other conditions involved here are: $c_{Au} = 1$, $c_{Ab} = 0$, constant pressure and constant mean thermal

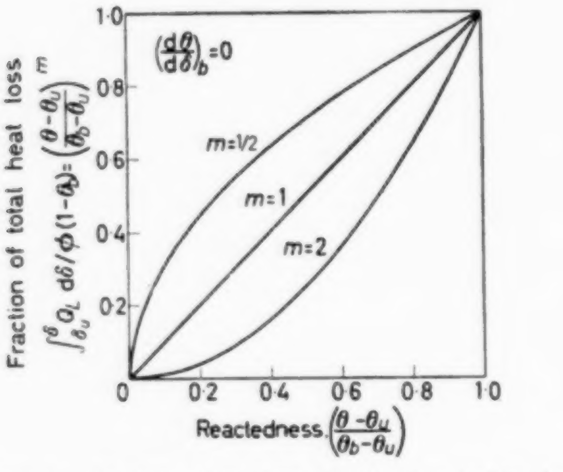

Figure 3. Arbitrary heat loss distribution inside the flame in the direction normal to the mixture velocity with $(d\theta/d\delta)_b = 0$

conductivity.) The reference values S_u^0 and T_b^0 correspond to the adiabatic case. Although the heat-loss distribution is quite different for the three cases, the change in the burning velocity is only **50** per cent at $\theta_b = 0{\cdot}5$.

As the value of m decreases, equation **32** indicates that a greater fraction of the heat loss occurs near the unburnt boundary, thus giving a smaller value of the mass fraction c_A at a given temperature according to equation **10a**. The resulting decrease in the reaction rate accounts for the drop in the burning velocity for decreasing value of m.

Figure 4 further shows that the three curves can each be approximated by a straight line in a semi-log plot. In other words, the variation of the burning velocity can again be represented by an expression in the form of equation **31**. The strong temperature dependence of the burning velocity is thus clearly indicated.

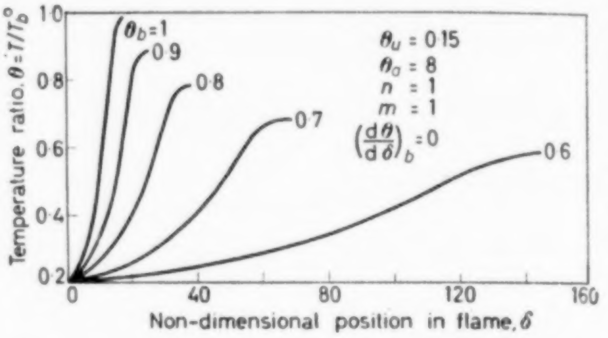

Figure 5. Temperature profiles in flames with heat loss

Figure 5 presents the temperature profiles inside the flame for $m = 1$ and at several specific values of θ_b. Because of the asymptotic nature of these profiles at the boundaries, the zero value of δ is arbitrarily set to correspond to a value of 0·2 for θ. The strong temperature dependence of the flame thickness is also indicated.

Figure 6 presents the temperature profiles at $\theta_b = 0{\cdot}8$ and for $m = 0{\cdot}5$, **1** and **2**. Contrary to the usual observation that a small flame thickness corresponds to a case of a high burning

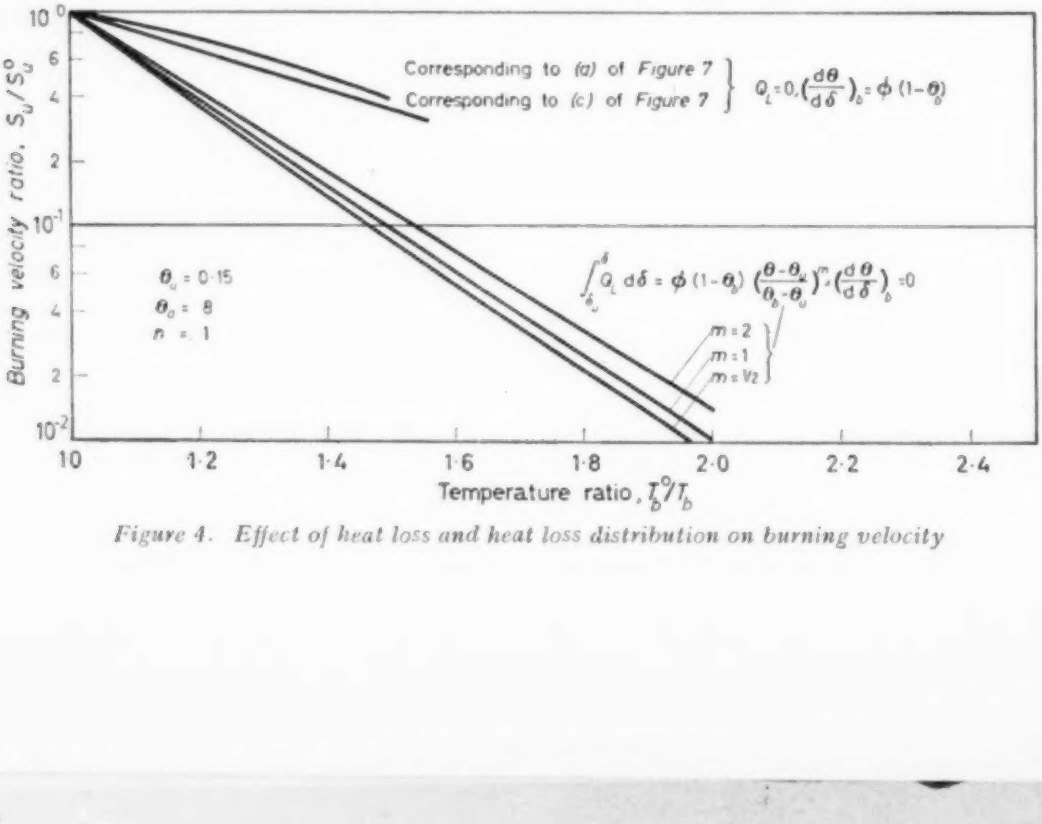

Figure 4. Effect of heat loss and heat loss distribution on burning velocity

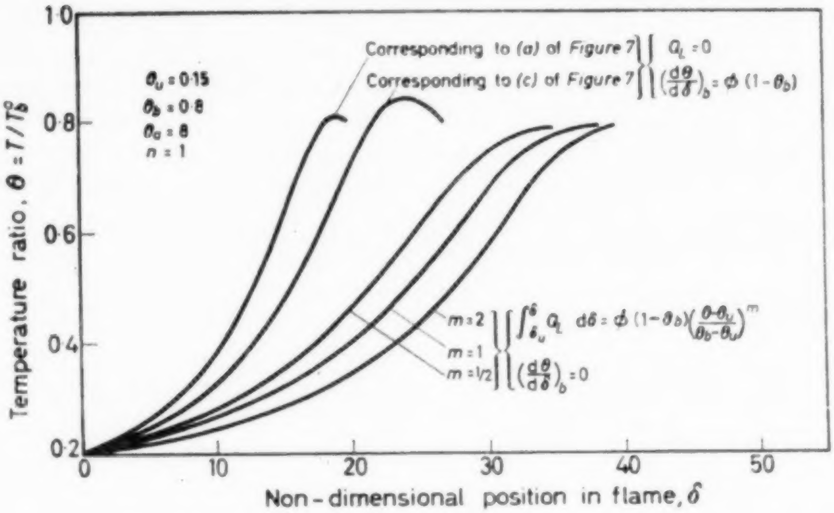

Figure 6. Temperature profiles in flames with heat loss

velocity, the flame thickness here decreases with decreasing value of m or of burning velocity. The physical explanation is that, when the value of m becomes smaller, a larger curvature in the temperature profile is needed near the unburnt boundary to allow for the larger fraction of the heat loss occurring there. Apparently, the corresponding decrease in the burning velocity is not sufficient to offset this tendency.

(b) *Effect of* $(d\theta/d\delta)_b$—In this case, Q_L is assumed to be zero and the heat loss occurs only at the hot boundary.

Some difficulty arises in the computation of the burning velocity due to the presence of a distance parameter δ in an exponential term in equation **10a**. Examination of this exponential term, however, indicates that its value is practically zero for a major portion of the flame and increases rapidly to unity as δ approaches δ_b. Thus, a first approximation is to assume a discontinuous jump in the value of this term from zero to unity at the hot boundary, such that equation **10a** becomes

$$Qc_A + \theta = Qc_{Au} + \theta_u \quad \text{for } \delta < \delta_b \quad \ldots [33]$$

and

$$\phi\,(Qc_A + \theta) - (d\theta/d\delta)_b = \phi\,(Qc_{Au} + \theta_u) \quad \text{for } \delta = \delta_b \quad \ldots . [34]$$

Since equation **33** would give a value of c_A at a given temperature larger than the correct one, the burning velocity so calculated would also be larger than the correct value because of the larger reaction rate resulting therefrom.

It has been noted earlier in the study of the effect of the distribution of heat loss inside the flame that the burning velocity increases as the heat loss becomes more predominant near the burnt boundary. It is thus expected that at a given value of θ_b the burning velocity for $Q_L = 0$ would be greater than that for $Q_L > 0$. Therefore, the assumption made above concerning the term $\exp[-\phi\,(\delta_b - \delta)]$ would give an upper bound in the value of the burning velocity for a given value of θ_b.

One objectionable feature of this assumption, however, is that the mass fraction c_A would increase with decreasing temperature according to equation **33** near the burnt boundary, where the temperature drops due to a negative value of $(d\theta/d\delta)_b$. This is indicated by an arrow beside curve (a) in *Figure 7*. In principle, this undesirable feature can be eliminated if a new solution is obtained on the basis of curve (b), which is calculated from equation **10a** by the use of the results obtained from curve (a). This procedure can also be repeated, if necessary, by successive correction of the exponential term in equation **10a**, to obtain a solution of any high degree of accuracy. However, the work is rather tedious. Experience shows that a solution very close to the correct one can be obtained on the basis of curve (c) in *Figure 7* (for $c_{Au} = 1$ and $c_{Ab} = 0$), the two segments of which are represented by the following equations:

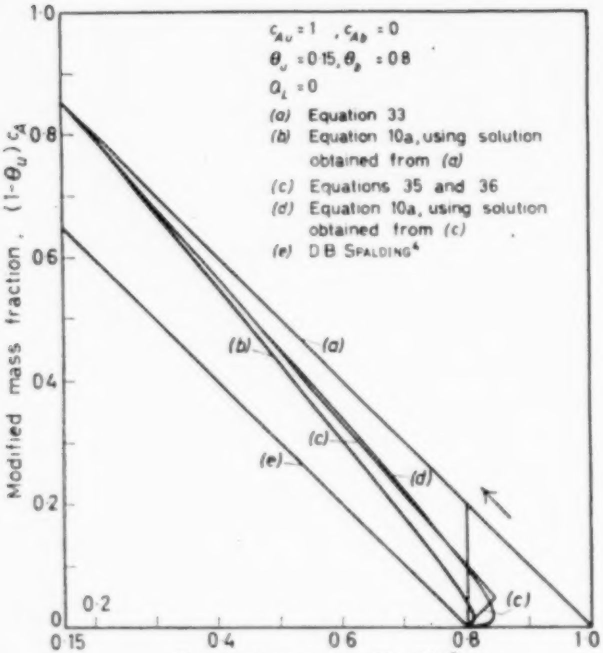

Figure 7. Variation of mass fraction of combustible component with temperature inside a flame

$$(1-\theta_u)\,c_A+\left[\frac{1+\theta_b-2\theta_u}{2\,(\theta_b-\theta_u)}\right]\theta=1+\frac{\theta_u\,(1-\theta_b)}{2\,(\theta_b-\theta_u)}\cdot \quad [35]$$

and

$$(1-\theta_u)\,c_A=\theta-\theta_b \qquad \ldots\ldots [36]$$

It is to be noted that the segment of curve (*c*) calculated from equation **35** gives a value of $(1-\theta_b)/2$ for the ordinate at $\theta=\theta_b$.

Curve (*d*) in *Figure 7* shows the variation of the modified mass fraction of the combustible component versus the temperature, calculated from equation 10a by the use of the results obtained from curve (*c*). The agreement of these two curves shows that the solution based on curve (*c*) must be very close to the correct one.

In a similar investigation, D. B. Spalding[4] assumed a value of unity for the exponential term throughout the entire flame. This result is represented by curve (*e*) in *Figure 7*. The burning velocity so calculated would be smaller than the correct value. Furthermore, the mass fraction c_A would become negative in the region where the temperature is higher than the temperature of the combustion product.

Figure 4 shows also the effects of $(d\theta/d\delta)_b$ on the burning velocity when the mass fraction of the combustible component varies with the temperature according to curves corresponding to curves (*a*) and (*c*) in *Figure 7*. Although curve (*a*) is rather arbitrary, the results obtained therefrom agree quite well with the more correct ones based on curve (*c*).

Again, the curves of burning velocity versus the reciprocal of the temperature of the combustion product can be approximated by straight lines in a semi-log plot.

Figure 6 shows also the corresponding temperature profiles inside the flame for $\theta_b=0{\cdot}8$ for the case where $Q_L=0$. Again a good agreement between the results obtained from curves (*a*) and (*c*) of *Figure 7* is demonstrated.

(3) *Limiting value of temperature of combustion product*

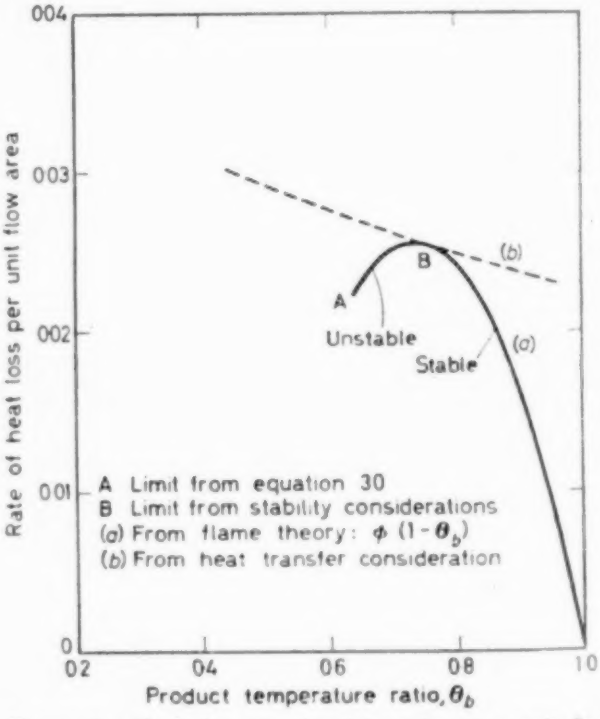

Figure 8. Variation of rate of heat loss per unit flow area with temperature of combustion product, showing lower temperature limits

Curve (*a*) of *Figure 8* shows the variation of the rate of heat loss per unit flow area versus the temperature of the combustion product for the case where $Q_L=0$ and the mass fraction of the combustible component varies with the temperature according to a curve represented by curve (*c*) in ***Figure 7***. As discussed earlier in the section on analysis for the case where $(d\theta/d\delta)_b \neq 0$, there is a lower limit for the temperature of the combustion product, below which no steady-state solution can be found for the burning velocity. This is indicated by point A in ***Figure 8***. The limit obtained from stability considerations of D. B. SPALDING[4] and E. MAYER[5] is indicated by point B, where curve (*a*) touches an arbitrary curve (*b*), which represents the variation of the rate of heat loss per unit flow area to the environment at the hot boundary with the temperature of the combustion product at the limiting situation. The stable and unstable regions are also shown.

Conclusions

The results presented in this paper show that, when the overall reaction-rate expression is of the Arrhenius type, the burning velocity considering heat losses varies approximately with the temperature of the combustion product according to the following expression

$$S_u \sim \exp(-T_c/T_b) \qquad \ldots . [31]$$

where T_c is a characteristic temperature, the value of which depends on the distribution of the heat loss. A strong temperature dependence of the burning velocity is thus indicated.

For the special case where heat loss occurs only at the hot boundary in the direction parallel to the flow, there is a lower limit for the temperature of the combustion product, below which no steady-state solution for the burning velocity can be found. This limit is in addition to the one deduced from stability considerations.

For the same temperature of the combustion product, the burning velocity decreases as greater fraction of the heat loss occurs near the unburnt boundary. However, contrary to the usual observation, the flame thickness does not necessarily increase accordingly.

For the adiabatic case at different initial mixture temperature, the same type of expression given above can be used to represent the variation of the burning velocity in the high-temperature region.

The work reported here was supported by a research grant (NSF–G3274) from the National Science Foundation.

The assistance of Mr Robert L. deJong in the computation of the results is gratefully acknowledged.

References

[1] TOONG, T. Y. *Combustion and Propulsion Third AGARD Colloquium*, pp 581–97. Pergamon: London, 1958

[2] TOONG, T. Y. and CHEN, T. N. Unpublished *Report No. 24.63*. Massachusetts Institute of Technology, 1956

[3] KLEIN, G. *Phil. Trans. A* 1957, **249,** 389

[4] SPALDING, D. B. *Proc. Roy. Soc. A*, 1957, **240,** 83

[5] MAYER, E. *Combustion & Flame*, 1957, **1,** 438

[6] DUGGER, G. L. *Tech. Rep. Nat. Adv. Comm. Aero., Wash., No. 1061*, 1952

A Theory of Flame Extinction Limits[*]

A. L. Berlad and C. H. Yang

Convair Scientific Research Laboratory, San Diego, California, U.S.A.

(*Received July 1959*)

A theory of flame extinction limits is formulated, which includes consideration of heat losses by conduction and radiation at every point of the temperature profile of the flame. The proper selection of boundary conditions is examined. In addition to the prescription of characteristic flame burning velocities (as in the adiabatic theory) this theory predicts flame extinction limits. Calculation of extinction limits are made for propane–oxygen–nitrogen flames.

Introduction

Well defined existence limits as well as burning velocities are general characteristics of flame systems. Experimentally, it has been found that:

(*1*) Flames propagating in a long tube filled with premixed gaseous reactants exhibit nearly steady burning velocities.

(*2*) Sufficiently large heat abstraction from normally vigorous flames causes flame extinction or quenching[1].

(*3*) Well defined fuel–oxidant mixture ratio and pressure limits exist. Outside of these limits stable flame propagation is not possible[2].

It is thus evident that a theoretical treatment of the flame phenomenon must account for all the above characteristics.

Recent contributions to the theory of non-adiabatic flame propagation have considered these phenomena for the case of laminar, premixed, gaseous flames[3, 4]. This paper presents a non-adiabatic flame theory which is consistent with the above stated general characteristics of flame systems.

Mathematical Model of the Flame

(a) *Conservation equations and reaction rate*

A reacting medium is assumed to be contained in an infinitely long tube of diameter, *d*. The tube axis is taken to be coincident with the x axis. The reactants are in a gaseous, homogeneous premixed state. The tube wall is assumed to be kept at a constant temperature, T_u, and a flame is assumed to be propagating in the tube with a stationary temperature profile as shown in *Figure 1*. For simplicity the temperature profile of the gas is represented by an average value, T, at each cross section of the tube. The actual radial temperature distribution at any cross section of the tube will usually be of the shape shown in *Figure 2*.

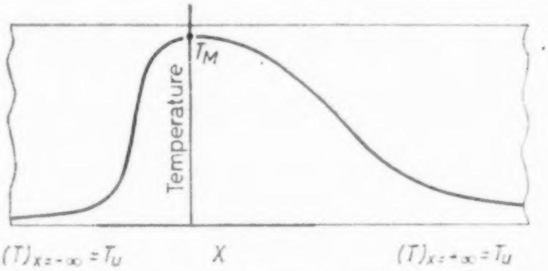

Figure 1. Average temperature profile of the flame

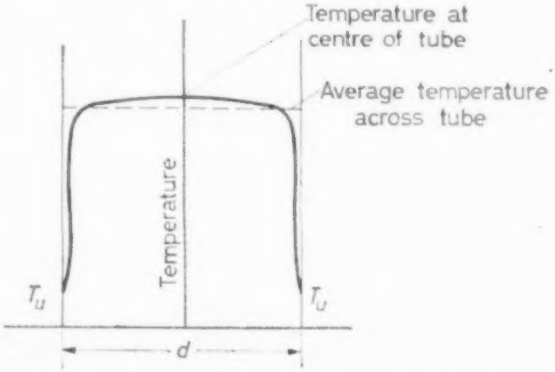

Figure 2. Temperature distribution at a typical cross section of the tube

---

[*] Paper presented at the March 1959 meeting of the Western States Section (U.S.A.) of the Combustion Institute. Abstract: *Combustion & Flame*, 1959, **3**, 265

An average value, T, as shown in the same figure with the dotted line is assumed to characterize the actual distribution. Heat losses and heat release by chemical reaction can then be approximated by functions of this average temperature at each cross section. Similarly, the concentrations of reactants are distributed at each cross section of the tube. Average values are also used here for simplicity.

Let us neglect kinetic energy of the flow and the pressure variations. Consider a reaction

$$A + B \longrightarrow \text{products}$$

Using average values, T, α and β for temperature, concentration of reactant A and concentration of reactant B at each cross section of the tube, the energy conservation equation (using D. B. SPALDING's notation[5]) can be written as follows

$$\frac{d^2\tau}{dx^2} - \frac{cG}{k}\frac{d\tau}{dx} = -\Phi(\alpha, \beta, \tau), + l(\tau) \quad \ldots . [1]$$

Equations for the conservation of mass, considering diffusion, become:

$$\delta_A \frac{d^2\alpha}{dx^2} - \frac{cG}{k}\frac{d\alpha}{dx} = \Phi(\alpha, \beta, \tau) \quad \ldots . [2]$$

$$\delta_B \frac{d^2\beta}{dx^2} - \frac{cG}{k}\frac{d\beta}{dx} = \Phi(\alpha, \beta, \tau) \quad \ldots . [3]$$

where $\tau = (T - T_u)/(T_a - T_u)$, is the dimensionless temperature, T is the average temperature at each cross section of the tube (°K), T_u is the temperature at the wall of the tube (°K), T_a the adiabatic flame temperature of the mixture (°K), x the tube axis (cm), c the average specific heat of mixture at constant pressure (cal/g.°K), G the mass flow rate (g/cm^2.s), and k the thermal conductivity (cal/cm.°K.s).

The transformed heat release rate is

$$\Phi = [\dot{M}_A''' H]/[k(T_a - T_u)]$$

where $\dot{M}_A'''$ denotes the mass of reactant A consumed by chemical reaction per unit volume per unit time (g/cm^3.s), H is the standard heat of reaction of reactant A (cal/g), $\alpha = M_A/M_{A,u}$ is the dimensionless concentration of reactant A, M_A is the mass of reactant A per unit mass of mixture, $M_{A,u}$ the mass of reactant A per unit mass of unburnt mixture, $\beta = M_B/rM_{A,u}$ with r the mass ratio of reactant A to reactant B of the unburnt mixture, $\delta_A = D_A\rho c/k$, the Lewis number for reactant A, $\delta_B = D_B\rho c/k$, for reactant B, D_A is the diffusion coefficient for reactant A (cm^2/s), ρ_u is the density of unburnt mixture (g/cm^3), and ρ is the local gas density (g/cm^3).

The transformed heat loss is

$$l = L/k(T_a - T_u)$$

where L denotes the heat loss from unit volume to surroundings (cal/cm^3.s). If the reacting mixture is stoichiometric the rate of the reaction will be approximated by an expression which is of the first order in each of the reactant concentrations. The Arrhenius rate function may be written as follows

$$\dot{M}_A''' = K_1 \alpha\beta M_{A,u}^2 \rho^2 \exp(-E/RT) \quad \ldots [4]$$

where K_1 is a constant. Equation 4 can be approximated by

$$\dot{M}_A''' = K\alpha\beta\tau^m\rho^2 M_{A,u}^2 \simeq K\alpha\beta\rho_u^2 T_u^2 \tau^{m-2} M_{A,u}/T_a^2 \quad \ldots . [5]$$

where K is a constant. Expression 5 is easier to handle than expression 4. Spalding also has used a similar simplified rate law[5].

(b) *Boundary conditions*

The boundary conditions at the 'cold boundary' for the non-adiabatic considerations are the same as for the adiabatic theory:

$$\left\{\begin{array}{l} \tau = 0, \; d\tau/dx = 0 \\ \alpha = 1, \; \beta = 1 \end{array}\right\} \quad \ldots . [6]$$

On the other hand, the state of the mixture after burning is completed does not seem to be as critical a boundary condition here as in the adiabatic case. In the adiabatic theory the flame temperature reaches its maximum when burning is completed. In the non-adiabatic system the flame temperature cools to the temperature of its surroundings when burning is completed. This point at which burning is completed is usually relatively distant from the peak temperature. It is therefore unlikely that the conditions at this point can critically affect the existence of the flame.

A close examination of the temperature profile of a flame reveals that the additional boundary condition for the non-adiabatic theory can be easily obtained. It is easy to see from the temperature profile that the range from T_u to T_m is a critical one. The heat release rate in this range is related to the reaction rate and to the amount of time available for reaction. The amount of time available for reaction is related to the mass flow rate G. For a given reaction rate, when T is restricted to be monotonically increasing it is conceivable that there can be critical limits beyond which the heat release rate cannot balance the heat loss rate. In other words, flames cannot exist beyond such limits.

The additional boundary condition for the non-adiabatic case can therefore be stated as follows:

$$\tau=\tau_m,\ \mathrm{d}\tau/\mathrm{d}x=0 \qquad \ldots.[7]$$

where $\tau_m=(T_m-T_u)/(T_a-T_u)$ and T_m is the maximum temperature in the flame.

The problem now becomes a mathematical one of seeking the eigenvalue, G (mass flow) in conservation equations **1**, **2** and **3** with the above imposed boundary conditions **6** and **7**. When the eigenvalue G (mass flow) is obtained the flame structure is completely determined. The problem is very similar to the adiabatic theory of flames in which one also seeks an eigenvalue G (mass flow) of a similar set of conservation equations but without the heat loss term.

There is only one additional requirement that the present consideration must fulfil; namely, the conservation equations with heat losses must also prescribe the flame extinction limits. We are going to demonstrate this by obtaining approximate solutions for these equations in two special cases.

(*i*) For Lewis number $\delta_A=\delta_B=0$

(*ii*) For Lewis number $\delta_A=\delta_B=1$.

Approximate Solution of Flame Equations and Extinction Limits of Flame

(i) *For* $\delta_A=\delta_B=0$

Combine equations **2** and **3**. Integrate and apply the boundary condition $\alpha=1,\ \beta=1$. We have

$$\beta=\alpha \qquad \ldots.[8]$$

Substitute $\Phi(\alpha,\beta,\tau)$ and β in equation **2** from equations **5** and **8** and integrate. Apply boundary condition $\tau=0,\ \alpha=1$. This yields

$$\alpha=\frac{1}{1+\int\frac{K\rho_u^2M_{A,u}T_u^2\tau^{m-2}}{T_a^2G}\,\mathrm{d}x} \qquad \ldots.[9]$$

Substitute $\Phi(\alpha,\beta,\tau)$ and β in equation **2** from **5**, **8** and **9** into equation **1** and integrate from $\tau=0$ to $\tau=\tau_m$. Apply boundary conditions, $\tau=0,\ \mathrm{d}\tau/\mathrm{d}x=0$ and $\tau=\tau_m,\ \mathrm{d}\tau/\mathrm{d}x=0$. We obtain

$$\tau_m=\left(1-\frac{1}{1+\int\frac{K\tau^{m-2}\rho_u^2T_u^2M_{A,u}}{T_a^2G}\,\mathrm{d}x}\right)-\int\frac{L(T)}{cG(T_a-T_u)}\,\mathrm{d}x \qquad \ldots.[10]$$

The first term represents the integrated heat release while the second term represents the integrated heat loss.

We can obtain an approximate solution of equation **1** by letting τ be represented by a gaussian error function

$$\tau=\tau_m\exp(-x^2/2\sigma^2) \qquad \ldots.[11]$$

where τ_m and σ are undetermined parameters and represent maximum temperature and 'flame depth' respectively. The gaussian function has known characteristics that the actual solution must satisfy, namely[6]: $\tau\longrightarrow 0,\ x\longrightarrow -\infty$ and T is a monotonically increasing function in the range between $x=-\infty$ and $x=0$. The gaussian function also satisfies the boundary conditions of the problem, namely, $x=-\infty,\ \mathrm{d}\tau/\mathrm{d}x=0$ and $x=0,\ \mathrm{d}\tau/\mathrm{d}x=0$.

The heat losses can be divided into two parts, conduction loss and radiation loss. The conduction loss from the mixture to the wall of the tube is proportional to the temperature difference between the wall and gas and can be written as follows[7]

$$L_c=(gk/2d^2)(T-T_u) \qquad \ldots.[12]$$

where d denotes diameter of tube, and g is the geometric factor involved in channel quenching.

The radiation exchange between wall and gas is proportional to $(T^4 - T_u^4)$. Since the major part of the radiation occurs at temperatures much greater than T_u, the radiation loss can be approximated as

$$L_r = N\varepsilon' T^4$$

where N is a constant and ε' is the emissivity of the gas.

ε' is usually a function of temperature. Thus, an average value may be computed for a given temperature range. ε' also changes with the diameter of the tube but it changes only slightly. For simplicity, $N\varepsilon'$ will be regarded as a constant here, so that

$$\begin{aligned} L_r &= N\varepsilon' T^4 \\ &= N\varepsilon' (T_a - T_u)^4 [\tau^4 + 4\tau^3\nu + 6\tau^2\nu^2 + 4\tau\nu^3 + \nu^4] \end{aligned}$$

where $\nu = T_u/(T_a - T_u)$. Since ν is usually much smaller than unity we have

$$L_r \simeq N\varepsilon' (T_a - T_u)^4 (\tau^4 + 4\tau^3\nu + 6\tau^2\nu^2) \qquad \ldots\ldots [13]$$

Substitute equations **11**, **12** and **13** into equation **10** and integrate. We then have

$$\begin{aligned} \tau_m = &\left[1 - \frac{1}{1 + \dfrac{K\rho_0^2 T_u^2 \tau_m^{m-2} M_{A,u}}{T_a^2}\left(\dfrac{\pi}{2m-4}\right)^{\frac{1}{2}} \dfrac{\sigma}{G}}\right] \\ &- \frac{gk}{2cd^2}\left(\frac{\pi}{2}\right)^{\frac{1}{2}} \tau_m \frac{\sigma}{G} \\ &- \varepsilon\left[\frac{1}{2}\left(\frac{\pi}{2}\right)^{\frac{1}{2}} \tau_m^4 + 4\nu\left(\frac{\pi}{6}\right)^{\frac{1}{2}} \tau_m^3 + 3\nu^2 (\pi)^{\frac{1}{2}} \tau_m^2\right]\frac{\sigma}{G} \end{aligned} \qquad \ldots\ldots [14]$$

where $\varepsilon = (T_a - T_u)^3 N\varepsilon'/k$. In equation **14** the undetermined parameters σ and G appear as a single parameter σ/G. The first term on the RHS of equation **14** represents the total heat release in the range from $\tau = 0$ to $\tau = \tau_m$. The second and third terms represent total conduction and radiation losses respectively. If the energy conservation law is to be preserved, equation **14** will always have to be satisfied. In other words, a flame cannot exist beyond extinction limits simply because the above relationship, i.e. the energy conservation law, cannot be satisfied. Temperature, flame depth and mass flow must all take positive values. This means that the parameters τ_m and σ/G must always be positive.

Now, if the diameter of the tube d in equation **14** is decreased, the second term (conduction loss) increases rapidly while the third term (radiation loss) remains unchanged. Since the first term approaches unity as a limit when σ/G is very large, the above expression will cease to hold for positive values of τ_m. Thus, there must exist a minimum value for d beyond which a positive value of τ_m cannot be obtained for any positive value of σ/G. This is obviously the 'quenching limit'. At such a limit the second term, i.e. conduction loss, is always dominating.

On the other hand, if we keep the diameter of the cylinder sufficiently large, the conduction loss term of the above equation becomes less important. Suppose we now reduce the fuel content in the mixture, that is, we reduce the value of $M_{A,u}$ in the above expression. The value of the first term becomes zero when $M_{A,u}$ reaches zero. Then τ_m will be negative since the heat loss terms are negative. There must exist a minimum value of $M_{A,u}$, beyond which positive values of τ_m are no longer obtainable for any positive value of σ/G. This is the so-called 'inflammability limit' at which the third term, i.e. radiation loss, becomes important.

If we reduce the pressure of the mixture, the value of ρ_0 will then decrease. The first term of the above expression will behave just as if the value of $M_{A,u}$ is reduced. The third term (radiation loss) also decreases as ρ_0 is reduced. The second term remains unchanged when the tube diameter is fixed. Obviously, there will be a minimum value of ρ_0 for a positive τ_m, as before. This is the 'pressure limit'. It is interesting to note that the conduction loss may be dominating for the pressure limit even though the diameter of the tube is usually considered large.

Computations have been made for extinction limits of stoichiometric propane–oxygen–nitrogen flames. Results are set out in *Table 1*. All the calculated extinction limits are italicized in *Table 1* and some experimental results are taken from the literature for comparison[2, 15–17]. (For details of calculation see appendix.)

Calculated results are very close to experi-

Table 1. Extinction limits calculated for stoichiometric C_3H_8–O_2–N_2 *flames*

Extinction limit	*Max. temp.* T_m, °*K*	$\frac{\sigma}{G}$	*Pressure* *P* *atm*	*Tube diameter* *d, cm*	*Composition* C_3H_8:O_2:N_2 *moles*	*Conduction loss* %	*Radiation loss* %	*Experimental results*[2, 15–17]
Quenching propane–air	1 680	1·92	1	*0·31*	1 : 5 : 18·8	0·992	0·008	*d*=0·31 *cm*
Inflammability propane–vitiated ***air***	1 200	288	1	5·00	*1 : 5 : 35·7*	0·603	0·397	C_3H_8:O_2:N_2 =1 : 5 : 32·2
*Pressure propane–**air***	1 680	44·2	*0·066*	5·00	1 : 5 : 18·8	0·845	0·155	*P*=0·046 *atm*
Quenching propane–oxygen	2 070	0·05	1	*0·031*	1 : 5 : 0	—	—	*d*=0·034 *cm*

mental values even though diffusion is omitted by taking the Lewis number equal to zero and the complicated kinetics are represented by simplified, truncated kinetics. It is also to be noted that the conduction loss (99 per cent) is indeed the dominating factor in the case of quenching. In the case of inflammability limit, radiation loss becomes more important. However, both the conduction and the radiation losses are approximately of the same order of magnitude when the tube diameter is kept at 5 cm. This is contradictory to the general belief that the radiation loss dominates in such experiments. For example, it has been found[8] that the inflammability limit for a propane–oxygen–helium flame is 1·92 per cent propane whereas the corresponding limit for a propane–oxygen–argon flame is 1·79 per cent propane. In both cases, the oxygen/inert ratio was identical. The only significant difference between these two systems is that helium and argon have different transport properties. These determine the conduction heat losses of the individual flames. It is thus obvious that the conduction heat losses have affected the inflammability limits of these flames.

(ii) *For* $\delta_A = \delta_B = 1$

Subtract equation 3 from equation 2 and integrate; this yields

$$\alpha - \beta = u_1 \exp[(cG/k)x] + u_2$$

where u_1 and u_2 are arbitrary constants. u_1 must be zero because physically the value of $\alpha - \beta$ must always be bounded. Apply the boundary condition, $\alpha = 1$, $\beta = 1$. We then have

$$u_2 = 0 \text{ and } \beta = \alpha \qquad \ldots . [15]$$

Combine equations 1 and 2 and integrate. Observing the following boundary conditions at $\tau = 0$:

$$\mathrm{d}\tau/\mathrm{d}x = 0; \quad \mathrm{d}\alpha/\mathrm{d}x = 0; \quad \alpha = 1$$

we obtain

$$\tau + \alpha = 1 + \frac{\int \exp[-(cG/k)x] \int l(\tau)\,\mathrm{d}x\,\mathrm{d}x}{\exp[-(cG/k)x]}$$

Integrate by parts to obtain

$$\tau + \alpha = 1 - \frac{k}{cG}\int l(\tau)\,\mathrm{d}x + \\ + \frac{k}{cG}\exp(cG/k)x \int \exp[-(cG/k)x]\, l(\tau)\,\mathrm{d}x \qquad \ldots . [16]$$

The above equation will reduce to $\tau + \alpha = 1$ when the heat loss approaches zero. $\tau + \alpha = 1$ is a well known relationship established in the adiabatic theory of flames.

For Lewis number of unity substitute equations 5, 11–13, 15 and 16 into equation 1. Integrate and apply the boundary conditions 6. There then results

$$\frac{cG}{k}\tau_m = \int_{-\infty}^{0} \left[\frac{c}{k} \cdot \frac{K\rho_u^2 M_{A,u} T_u^2}{T_a^2}\left(1 - \frac{k}{cG}\int l(\tau)\,\mathrm{d}x\right.\right.$$

(equation continued overleaf)

$$+\frac{k}{cG}\exp(cG/k)\,x\int\exp[-(cG/k)x]\,l(\tau)\,\mathrm{d}x-\tau\Big)^2$$

$$\tau^{m-2}-\frac{L(T)}{k(T_a-T_u)}\Big]\,\mathrm{d}x \qquad \ldots.[17]$$

The gaussian error function is not integrable for variable limits. Thus, an exponential curve is used for evaluating the integrals in equation 16.

Let the new approximation be

$$\tau=\tau_m\exp sx$$

Equate the area under this curve from $-\infty$ to 0 and the area of the gaussian curve in the same range. Thus

$$s=(1/\sigma)(2/\pi)^{\frac{1}{2}}$$

Equation 17 can be reduced to

$$G\tau_m=\int_{-\infty}^{0}\frac{K\rho_0^2T_u^2M_{A,u}}{T_a^2}$$

$$(1-[S_1+1]\tau-S_2\tau^2-S_3\tau^3-S_4\tau^4)^2\,\tau^{m-2}\,\mathrm{d}x$$

$$-\frac{gk}{2cd^2}\left(\frac{\pi}{2}\right)^{\frac{1}{2}}\tau_m\sigma-\varepsilon\left[\frac{1}{2}\left(\frac{\pi}{2}\right)^{\frac{1}{2}}\tau_m^4+4\nu\left(\frac{\pi}{6}\right)^{\frac{1}{2}}\tau_m^3\right.$$

$$\left.+3\nu(\pi)^{\frac{1}{2}}\right]\sigma \qquad \ldots.[18]$$

where:

$$S_1=\frac{gk\pi^{\frac{1}{2}}\sigma}{2.2^{\frac{1}{2}}cd^2G}\left(1+\frac{1}{\pi^{\frac{1}{2}}cG\sigma/2^{\frac{1}{2}}k-1}\right)$$

$$S_2=$$

$$\frac{3(T_a-T_u)T_u^2N\varepsilon'\pi^{\frac{1}{2}}\sigma}{3.2^{\frac{1}{2}}cG}\left(1+\frac{1}{(\pi^{\frac{1}{2}}/3.2^{\frac{1}{2}})(cG\sigma/k)-1}\right)$$

$$S_3=$$

$$\frac{4.\pi^{\frac{1}{2}}(T_a-T_u)^2T_uN\varepsilon'\sigma}{3.2^{\frac{1}{2}}cG}\left(1+\frac{1}{(\pi^{\frac{1}{2}}/3.2^{\frac{1}{2}})(cG\sigma/k)-1}\right)$$

$$S_4=\frac{(T_a-T_u)^3N\varepsilon'\pi^{\frac{1}{2}}\sigma}{4.2^{\frac{1}{2}}cG}\left(1+\frac{1}{(\pi^{\frac{1}{2}}cG\sigma/4.2^{\frac{1}{2}}k)-1}\right)$$

Thus

$$\frac{G}{\sigma}=$$

$$\frac{K\rho_0^2M_{A,u}\pi^{\frac{1}{2}}\tau_m^{m-3}}{2^{\frac{1}{2}}T_a^2}\left(\frac{1}{(m-2)^{\frac{1}{2}}}-\frac{2(S_1+1)}{(m-1)^{\frac{1}{2}}}\tau_m+\ldots.\right)$$

$$-\frac{gk}{2cd^2}$$

$$(\tfrac{1}{2}\pi)^{\frac{1}{2}}\tau_m-\varepsilon[\tfrac{1}{2}(\tfrac{1}{2}\pi)^{\frac{1}{2}}\tau_m^4-4\nu(\tfrac{1}{6}\pi)^{\frac{1}{2}}\tau_m^3+3\nu^2(\pi)^{\frac{1}{2}}]$$

$$\ldots.[19]$$

The existence of flame extinction limits in equation 19 is as explicit as in equation 14. G/σ for physical reasons must always be positive. τ_m always takes a positive value between zero and one. When the diameter of the tube is smaller than the quenching distance, the second term on the RHS of equation 19 becomes so large that G/σ cannot be positive regardless of what value τ_m takes between zero and one. At the inflammability or pressure limit, the value of the constant $M_{A,u}$ or ρ_0 will be reduced when the fuel concentration or pressure of the gas is reduced. $M_{A,u}$ or ρ_0 will reach a limiting value when a positive value of G/σ is no longer obtainable in equation 19. This limit is then the composition or the pressure limit of the mixture.

Determination of Flame Velocity

Various methods are used in adiabatic theory for calculating burning velocities[5, 9, 10] for near-adiabatic flames. These methods can also be adapted for calculating the burning velocities in the non-adiabatic case. In a forthcoming paper[18] analogue computers are used to calculate burning velocity and the structure of flames near the extinction limits.

Discussion

(*1*) It is easy to extend this simplified formulation to two- or three-dimensional temperature fields and more complicated kinetics. Simple solutions are of course improbable for the more generalized cases. Machine integration, however, can be used. The prediction of basic characteristics of the flame should remain unchanged.

(*2*) G. Dixon-Lewis and G. L. Isles[11] in a recent paper showed experimentally that the inflammability limit of a flame can be extended without limit by imparting heat to the flame from the boundary.

From the present theory one can see that all the extinction limits exist only when the boundary conditions of the flame are fixed. The heat imparted from the top plate to the flame in the Dixon-Lewis and Isles experiments compensated for the reduction of heat generation due to a decrease of initial fuel concentration in the mixture. There is no difficulty in balancing either equation **14** or equation **19** as long as the heat generation term in these equations is compensated by the heat imparted from the top plate. Actually one can extend or shrink any of the extinction limits at will by changing the boundary conditions, as was done in the experiments of Dixon-Lewis and Isles.

(3) In calculating the extinction limits for various stoichiometric flames a truncated reaction rate is used. The actual kinetics for a propane–oxygen reaction are, of course, very complicated. The fact that the calculated results shown in ***Table 1*** came very close to the experimental results does not mean that the actual detailed kinetics are not important in such calculations. It merely shows that the actual detailed kinetics, in this case, can be closely approximated by such a single gross one for the extinction limit calculations.

APPENDIX

Calculation of Extinction Limits of Propane–Oxygen–Nitrogen Flames

It has been pointed out in the text that the flame extinction limits are prescribed by equation **14** for the case where the Lewis number is zero. For calculating the extinction limits of propane–oxygen–nitrogen flames we have used equation **14**. For calculating quenching distance for a flame system one guesses the quenching distance, d', and substitutes it into equation **14**. If τ_m is given, then the rest of the parameters which are functions of temperature (except σ/G) can be estimated in equation **14**. For a given value of τ_m (between zero and one) one can solve for the undetermined parameter, σ/G, from this equation.

For values of d' which are larger than the quenching distance of the flame one can always obtain real positive values of σ/G. But when d' is decreased, it reaches a critical value below which a positive real value of σ/G is no longer obtainable, no matter what value is given for τ_m. This minimum value is the calculated quenching distance.

For inflammability and pressure limits, the same procedure can be followed. The mixture is usually contained in a tube of fixed diameter. Instead of trying different values of d' as in the quenching case one tries different values of ρ_0 and $M_{A,u}$ in the first term of equation **14**, for pressure and inflammability limit respectively.

In all the calculations for propane–oxygen–nitrogen extinction limits, the temperature (T_u) at the wall of the tube is assumed to be **300**°K. Other parameters in the equation may be estimated as follows:

(1) *Mean thermal conductivity, k*
k is approximately proportional to $T^{3/4}$

$$k=\frac{k_0\int_{T_u}^{T_m}\left(\frac{T}{T_u}\right)^{3/4}\mathrm{d}\left(\frac{T}{T_u}\right)}{\int_{T_u}^{T_m}\mathrm{d}\left(\frac{T}{T_u}\right)}=\frac{4k_0}{7}\,\frac{\left(\frac{T_m}{T_u}\right)^{7/4}-1}{\frac{T_m}{T_u}-1}$$

where k_0 is a constant, taken to be $0{\cdot}0568\times10^{-3}$ in this case.

(2) *The geometric factor, g*
The factor g which relates the quenching behaviour of channels of various geometric shapes is given in ref. 7.

$$g=32 \text{ for cylindrical tubes}$$

(3) *Standard heat of reaction, H*
For propane H is taken[12] to be $1{\cdot}11\times10^4$ cal/g.

(4) *Specific heat of gas at constant pressure, c*
An average value of **0·36** is taken for the propane–oxygen–nitrogen flames and an average of value **0·96** for the propane–oxygen flames.

(5) *Reaction rate constants, K and m*
For the stoichiometric propane–oxygen–nitrogen flame the reaction rate given in equation **4** can be reduced to

$$\dot{M}_A''' = K'\alpha\beta\rho^2M_{A,u}^2\exp(-E/RT)$$

For $\delta_A=\delta_B=0$, and $\beta=\alpha$

$$\dot{M}_A''' = K'\alpha^2\rho^2M_{A,u}^2\exp(-E/RT)$$

It is difficult to find accurate data of reaction rates of various fuels. W. H. Avery[13] gives a value of **40 000** calories for the activation energy of hydrocarbon–air reactions and a maximum space heating rate of 3 to 5×10^8 BTU/ft^3.h in a highly stirred reactor. The reactor temperature can be computed[13] to be $T_{\text{opt.}} = 1\,760°\text{K}$ and the reaction constant, K', can then be estimated to be within the range of 2 to 4×10^{14}. A mean value of 3×10^{14} is used in this calculation.

$$\dot{M}_A'''' = 3 \times 10^{14} \alpha^2 \rho^2 \exp(-20\,000/T)$$

The reaction rate should be reduced to the form of equation **5**.

$$\dot{M}_A'''' = K \alpha^2 \rho^2 \tau^m$$

Since the reaction rate is a very steep function of temperature, the rate in the neighbourhood of the highest temperature of the flame is of more importance than at other temperatures. τ_m and the first derivative with respect to τ are therefore matched for every flame, in satisfaction of equation **5**. Thus

$$|K' \alpha^2 \rho^2 \exp(-E/RT)|_{T=T_m} = |K \alpha^2 \rho^2 \tau^m|_{T=T_m}$$

and

$$\left.\frac{\mathrm{d}(K' \alpha^2 \rho^2 \exp[-E/RT])}{\mathrm{d}T}\right|_{T=T_m} = \left.\frac{\mathrm{d}(K \alpha^2 \rho^2 \tau^m)}{\mathrm{d}T}\right|_{T=T_m}$$

m and K can be evaluated for any value of T_m:

$$m = \frac{E \tau_m (T_a - T_u)}{R T_m^2}$$

and

$$K = \frac{K' \exp(-E/RT_m)}{\tau_m^m}$$

where $\qquad \tau_m = (T_m - T_u)/(T_a - T_u).$

(6) *Average radiation loss parameter,* ε

A formulation for the radiant energy exchange between a gas (containing carbon dioxide and water vapour) and its bounding surfaces is given by W. H. McAdams[14]

$$\frac{q}{A} = 0{\cdot}173 \left(\frac{\varepsilon_s + 1}{2}\right) \left[\varepsilon_g \left(\frac{T_g}{100}\right)^4 - \alpha_g \left(\frac{T_u}{100}\right)^4\right]$$

where q denotes the rate of heat transfer by radiation in BTU/h, A is the area of surface in ft^2, ε_g is the emissivity of gas at T_g (dimensionless), T_g the temperature of gas (°R), α_g the emissivity of the gas at T_u (dimensionless), and ε_s is the absorptivity of the wall; dimensionless and assumed to be 0·90.

$$\frac{q}{A} = 1{\cdot}24 \times 10^{-5} \left[\varepsilon_g \left(\frac{T_g}{500/9}\right)^4 - \alpha_g \left(\frac{T_u}{500/9}\right)^4\right] \text{ cal/s.cm}^2$$

For maximum $T_g \gg T_u$

$$\frac{q}{A} \simeq 1{\cdot}24 \times 10^{-5} \left(\varepsilon_g \left[\frac{9}{500}(T_a - T_u)\right]^4\right) \left(\tau^4 + 4\tau^3 \left[\frac{T_u}{T_a - T_u}\right] + 6\tau^2 \left[\frac{T_u}{T_a - T_u}\right]^2\right)$$

For a 1 atm propane–air flame within the temperature range of 500° to 2 400°K, ε_g can be closely approximated, linearly (from McAdams's[14] tables). For 5 cm tubes

Let $\nu = T_u/(T_a - T_u)$

$$\varepsilon_g = 0{\cdot}0939 - (0{\cdot}055/1450)\,T$$

$$\varepsilon_g = 0{\cdot}0825 - 0{\cdot}0704\,\tau$$

$$q/A = 1{\cdot}24 \times 10^{-5}\,(0{\cdot}0825 - 0{\cdot}0704\,\tau)\,(\tau^4 + 4\tau^3\nu + 6\tau^2\nu^2) \times [9\,(2155 - 300)/500]^4$$

$$q/A = 19{\cdot}4\,(0{\cdot}0825 - 0{\cdot}0704\,\tau)\,(\tau^4 + 4\tau^3\nu + 6\tau^2\nu^2)$$

The total radiation loss per unit cross sectional area of the tube is

$$\int_{-\infty}^{0} \frac{q \pi d}{A \pi (\frac{1}{2} d)^2}\,\mathrm{d}x$$

$$\therefore \int_{-\infty}^{0} l\,\mathrm{d}x = \frac{4}{kd\,(T_a - T_u)} \int_{-\infty}^{0} \frac{q}{A}\,\mathrm{d}x$$

Thus for ε, the average radiation loss parameter, one obtains

$$\varepsilon = \frac{123{\cdot}2}{kd\,(T_a - T_u)\,\tau_m} \int_{\frac{1}{2}\tau_m}^{\tau_m} (0{\cdot}0825 - 0{\cdot}0704\,\tau)\,\mathrm{d}\tau$$

References

[1] Friedman, R. *Third Symposium (International) on Combustion*, p 110. Williams and Wilkins: Baltimore, 1949

[2] Lewis, B. and von Elbe, G. *Combustion, Flames and Explosions of Gases*. Academic Press: New York, 1951

[3] Spalding, D. B. *Proc. Roy. Soc. A* 1957, **240**, 83

[4] Mayer, E. *Combustion & Flame*, 1957, **1**, 438

[5] Spalding, D. B. *Combustion & Flame*, 1957, **1**, 287

[6] ROSEN, J. B. *Fourth Symposium (International) on Combustion*, p 210. Williams and Wilkins: Baltimore, 1953

[7] BERLAD, A. L. and POTTER, A. E. *Fifth Symposium (International) on Combustion*, p 728. Reinhold: New York, 1955

[8] POTTER, A. E., Jr and BERLAD, A. L. *J. phys. Chem.* 1956, **60**, 97

[9] HIRSCHFELDER, J. O. and CURTISS, C. F. *Third Symposium (International) on Combustion*, p 121. Williams and Wilkins: Baltimore, 1949

[10] ROSEN, G. *Seventh Symposium (International) on Combustion*, p 339. Butterworths: London, 1959

[11] DIXON-LEWIS, G. and ISLES, G. L. *Seventh Symposium (International) on Combustion*, p 475. Butterworths: London, 1959

[12] ROSSINI, F. D. *et al. Circ. U.S. Bur. Stand. No. C461*, 1947

[13] AVERY, W. H. *Fifth Symposium (International) on Combustion*, p 86. Reinhold: New York, 1955

[14] MCADAMS, W. H. *Heat Transmission*, p 64. McGraw-Hill: New York, 1942

[15] BERLAD, A. L. *J. phys. Chem.* 1954, **58**, 1023

[16] COWARD, H. F. and JONES, G. W. *Bull. U.S. Bur. Min. No. 503*. U.S. Government Printing Office: Washington, 1952

[17] SIMON, D. M., BELLES, F. E. and SPAKOWSKI, A. E. *Fourth Symposium (International) on Combustion*, p 126. Williams and Wilkins: Baltimore, 1953

[18] YANG, C. H. 'Burning velocity and the structure of flames near extinction limits'. To be published

On

THE
the d
good
obser
R. P
refere
ZELD
great
MART
in th
the t
in eq
their
H. S
that
igniti
obser
their
The v
prese
Symp
analy

Fi
ref. 5
schlie
with
Fig.
time
the c
the s
the p
diagr

On the Development of Detonation with Pre-ignition

A. K. Oppenheim, R. A. Stern and P. A. Urtiew

Department of Aeronautical Sciences, University of California, Berkeley

(Received September 1959)

Importance of pre-ignition to the development of detonation is examined on the basis of a wave dynamic analysis of schlieren photographs obtained by Schmidt, Steinicke and Neubert. Present results complement those published at the Seventh Combustion Symposium for the case without pre-ignition. Although a definite stimulating effect of pre-ignition has been noticed, characteristic features of both solutions being the same, it is concluded that progress of the process, expressed in terms of intermediate states that must be attained in the course of its development, is essentially the same in both cases.

Introduction

The question of how essential is pre-ignition to the development of detonation has occupied a good deal of attention ever since the original observations of W. Payman[1] and of W. A. Bone, R. P. Fraser and W. H. Wheeler[2]. With reference to more recent publications, Y. B. Zeldovich and A. S. Kompaneets[3] attach great importance to pre-ignition, while F. J. Martin[4] claims that he has never observed it in the course of his detailed optical studies of the transition from slow burning to detonation in equimolar acetylene–oxygen mixtures. In their detailed experimental study, E. Schmidt, H. Steinicke and U. Neubert[5, 6] demonstrated that detonation can be developed without pre-ignition, although its appearance was often observed. Consequently in the publication of their results they included records of both cases. The wave-dynamic analysis of the first has been presented by us at the Seventh Combustion Symposium[7]. Submitted here is a similar analysis of the second case.

Figure 1 is an inverted version of Fig. **52** in ref. 5. It summarizes the observations made by schlieren photographs obtained by Schmidt *et al.* with a rotating drum camera and published as Fig. 51 in ref. **5** and Fig. **14** in ref. **6**. The time scale has been inverted to comply with the current practice of using for wave diagrams the space/time plane with time increasing in the positive direction of the ordinate. The diagram depicts the following world lines. The first shock propagating at an absolute velocity of **481** m/s is followed by the second shock propagating at **675** m/s. They merge forming a shock with a velocity of **529** m/s. The primary flame accelerates until the establishment of detonation (D) with an apparent velocity of an order of **2 400** m/s and a retonation (**R**) propagating at approximately **1 300** m/s. This occurs in the vicinity of the interaction between the primary and the secondary flame front that appears as a result of pre-ignition behind the shock wave, and, according to the interpretation of Schmidt *et al.*, propagates in the opposite direction. Intersecting the primary shock wave and flame front system are the world lines of shocks initiated by exploding a percussion cap outside the tube. This has been done by the experimenters in an attempt to provide more information on the initial state of the reacting gas mixture.

The experiment was performed with a mixture of **9** per cent propane, **49·2** per cent oxygen and **41·8** per cent nitrogen. This is only one per cent more propane in combination with the same oxygen–nitrogen mixture as in the case analysed in ref. **7**, so most of the thermochemical data summarized in *Table 1*[5] can be considered to be still applicable.

Analysis

The record of *Figure 1* has been analysed by the vector polar method as described in our previous publication[7]. Such an analysis yields

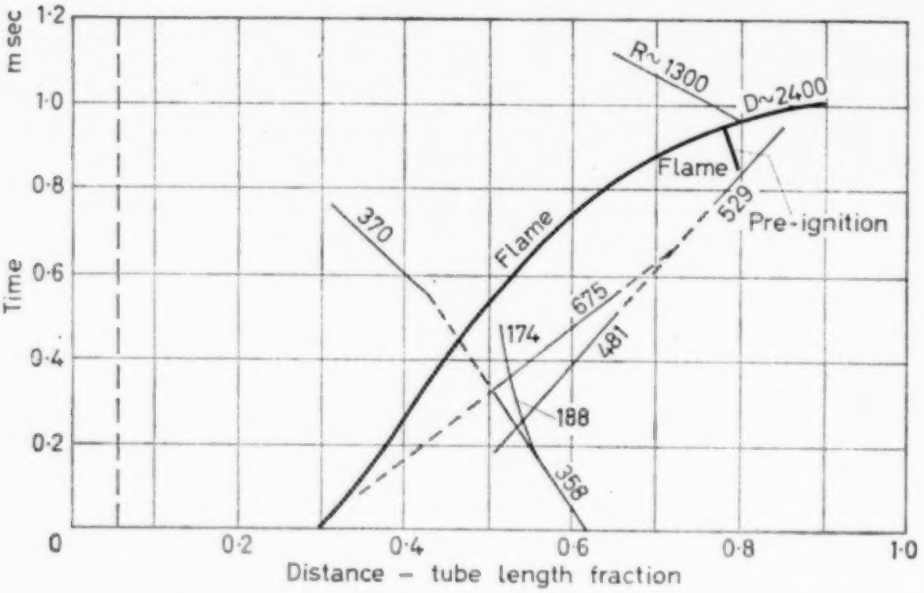

Figure 1. Wave world lines observed by E. Schmidt et al.[5]

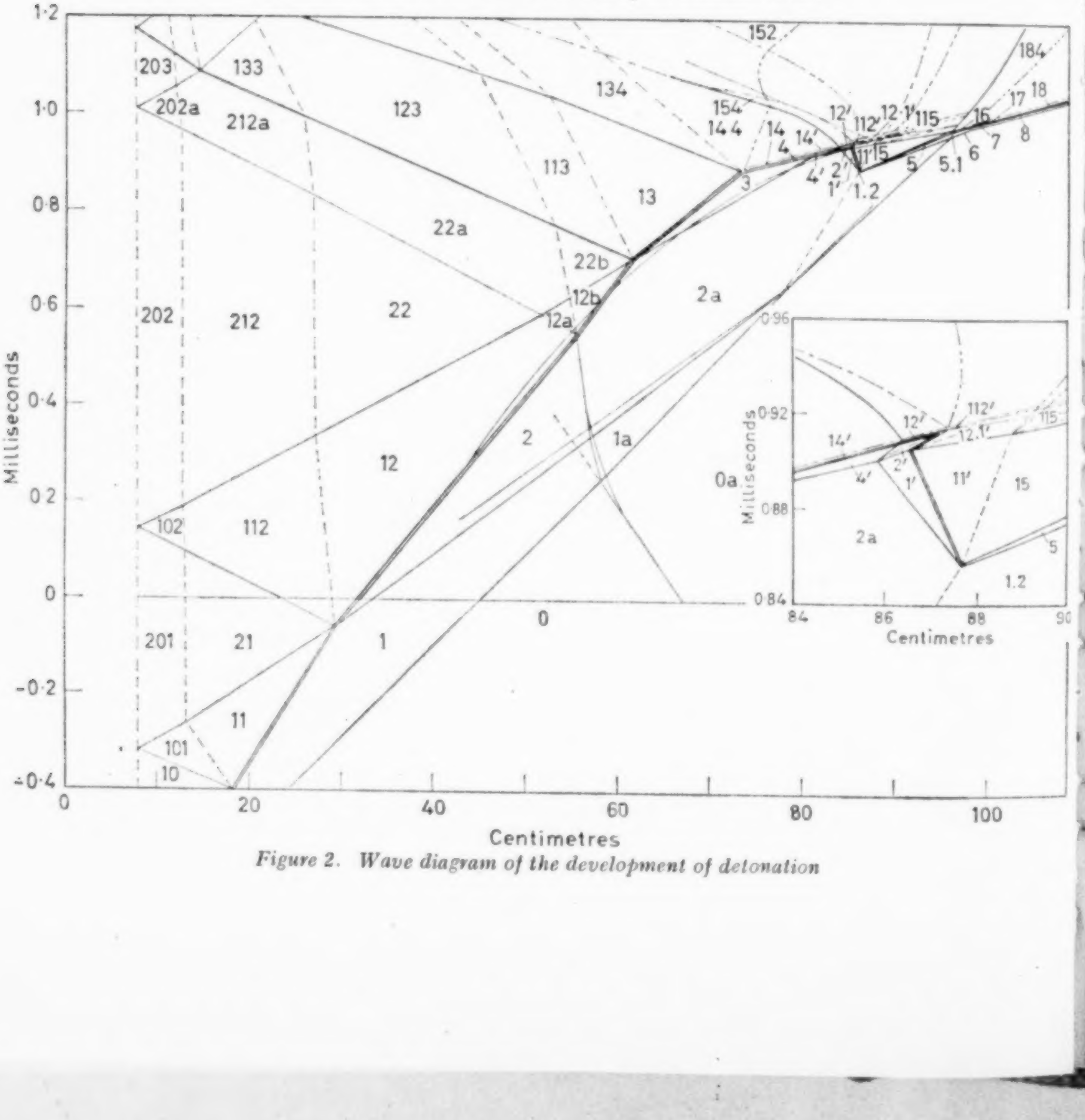
Milliseconds
1·2
1·0
0·8
0·6
0·4
0·2
0
-0·2
-0·4
0
20
40
60
80
100
Centimetres
203
133
152
184
202a
212a
123
134
154
144
14
14'
12'
112'
12·1'
115
16
17
18
4
4'
2'
1'
1.2
11'
15
5
5.1
6
7
8
113
13
3
22a
22b
12b
12a
2a
202
212
22
2
1a
0a
12
102
112
0
201
21
1
11
101
10
0·96
0·92
0·88
0·84
84
86
88
90
Milliseconds
Centimetres
14'
12'
112'
12.1'
115
2'
4'
1'
11'
15
2a
5
1.2

Figure 2. Wave diagram of the development of detonation

essentially specific information on the compatibility of wave trains resulting from a given interaction process, subject to restrictions imposed by the conservation principles of gas dynamics. The analysis is based upon the premise that all the changes of state are brought about only by the action of waves whose thickness (distance from the uniform state in front to the uniform state behind) is finite and sufficiently small in comparison with other dimensions in the flow field to render frictional and local heat transfer effects negligibly small. Consequently no other processes are considered except those of shocks, deflagrations and rarefaction waves. The major assumption concerning the substance is that it behaves essentially as a perfect gas with constant specific heats whose ratio is $\gamma_1 = 4/3$ in the unburnt and $\gamma_2 = 1{\cdot}3$ in the burnt régime.

Figure 2 represents the solution in space/time with *Figures 3* and *4* as the corresponding state diagrams of the process. The coordinates of the latter are: $P = \ln(p/p_0)$, $U = u/a_0$, and $\sigma = (s - s_0)/R$, where p is the pressure, u the mass flow velocity, a the velocity of sound, s the entropy, and R the gas constant, while subscript $_0$ denotes the initial state of reactants.

In *Figure 2* double lines represent the world lines of flame fronts, single lines are the shock waves, broken lines are contact discontinuities, chain-dotted lines are the leading edges of rarefaction fans, while the chain-double-dotted lines are their trailing edges.

As described in ref. 7 the use of the P/U plane is essential for the solution, since each wave interaction process creates a régime of uniform pressure and velocity which is represented by a single point in this plane. Each of these points is determined by the intersection of the appropriate polars representing the loci of states that can be produced by waves resulting from the interaction. The point of

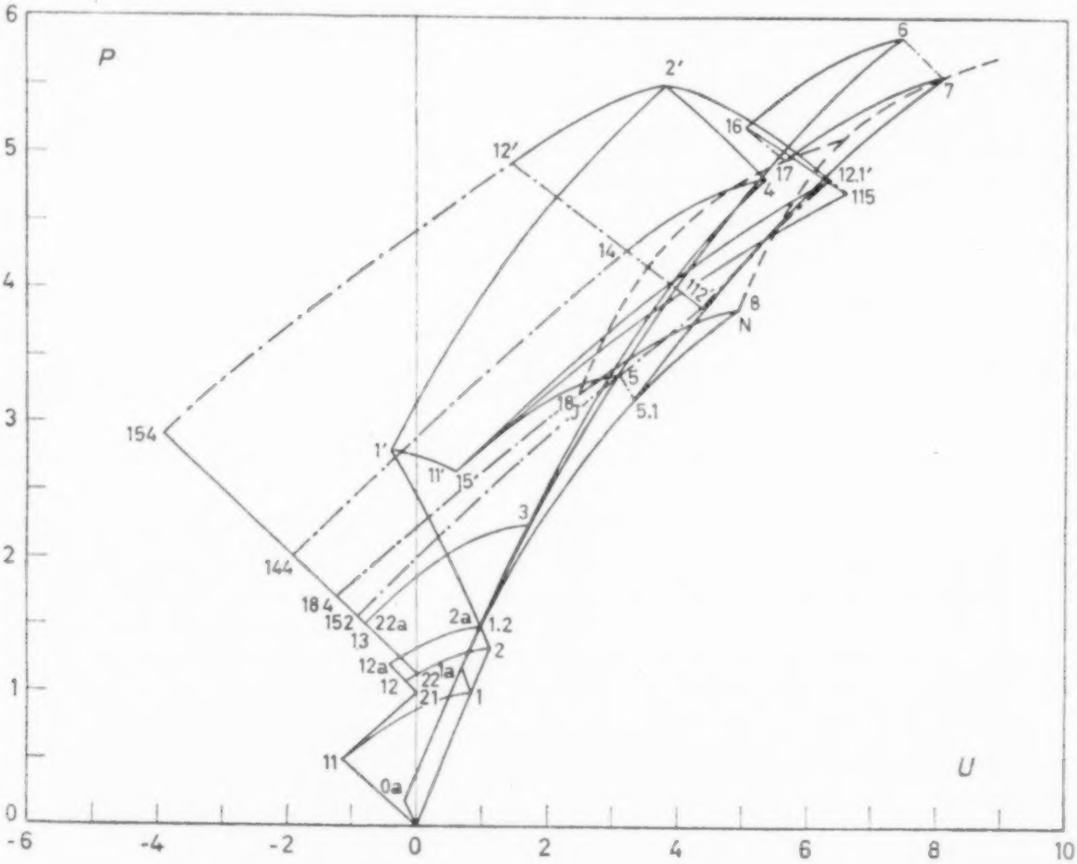

Figure 3. *State diagram in the pressure/velocity plane*

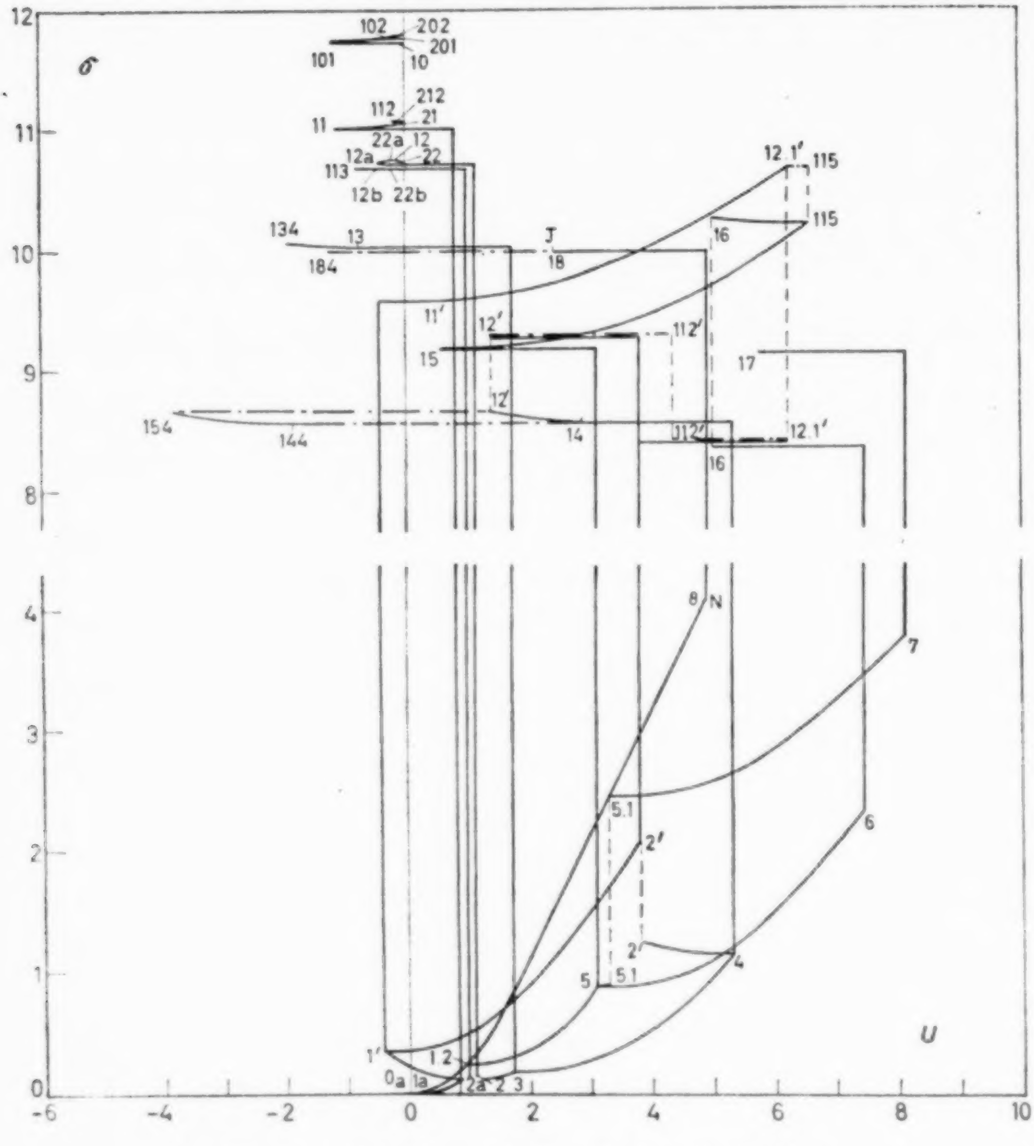

Figure 4. State diagram in the entropy/velocity plane

intersection satisfies the dynamic compatibility conditions for the resulting wave system and determines therefore the solution of the interaction.

To complete the information on the solution we present the hodograph of the process in the entropy/velocity plane, *Figure 4*, rather than the velocity of sound/velocity plane that was utilized in our previous publication[7]. The use of the σ/U plane to complement the P/U plane is, in our case, equivalent to that of the A/U plane $[A=\ln(a/a_0)]$, since for a perfect gas with constant specific heats

$$\sigma=[2\gamma/(\gamma-1)]\,A-P$$

while the entropy of formation generated across the flame front is nearly an order of magnitude larger than any of the entropy changes brought about by the action of other waves.

Solution

The solution is based upon the observed world line of the first shock which has been adopted as reference with other world lines construed so as to fit best the record of *Figure 1*. In order to demonstrate the fit the remaining world lines of *Figure 1* have been redrawn and are shown as thin lines on *Figure 2*.

The world lines accompanying the initiation of the process were not reported by Schmidt at all. They had to be reconstructed in the direction of negative time with reference to the datum of *Figure 1*. This was necessary in order to ascertain overall compatibility of all subsequent wave systems in relation to the initial state of the burnt gases which, in *Figures 2, 3* and *4*, is denoted by number **10**. It has been determined by assuming that it is obtained from zero state of the undisturbed reactants by constant pressure combustion.

Shock waves propagating through the burnt gases, such as those producing states **112**, **22**, **113**, **134**, etc., were not observed because of the poor resolution of schlieren photography in the vicinity of the luminous flame zone. They had to exist, however, as brought out by this analysis, in order to satisfy the dynamic compatibility conditions of the resulting wave systems.

Initial flame acceleration

Similarly as before[7], the process of initial flame acceleration is associated with the generation of shock **1*** propagating into the reactants and shock **101** producing state **11** in the products. By reflection from the closed end shock **101** produces eventually shock **21** which interacts with flame **11** resulting in shock **2**, flame **12** and reflected shock **112**. Contact surfaces generated by the interactions are so weak that waves reflected from them can be neglected. Shock **112** produces by reflection and interaction with contact surfaces shock **22** which interacts with flame **12** or, more precisely, shock **22b** interacting with flame **12b**—the small change having been brought about by the independently produced percussion wave. This results in shock **3**, which, because of its proximity to the combustion zone, could not have been observed by schlieren technique.

Again, similarly as in the previous case[7], the rapid acceleration of the combustion front that is then observed can be rationalized only by postulating the existence of shock **4** propagating into state **3** and followed by a deflagration producing state **14**. This is not yet a detonation, the propagation velocity of deflagration **14** being somewhat lower than that of shock **4**.

The explanation of the origin of wave system **4–14** is outside the scope of the present study. It could have been the result of some secondary wave system which might have existed in the régime of the burnt gases without being detected on schlieren photographs. Such a system could have been initiated at the time of ignition with a flame moving to the left accompanying the primary flame moving to the right; or it could result from shock reflections occurring at contact discontinuities which were neglected for the solution of the primary wave system; it could have originated also directly as a result of coalescing pressure waves generated by the combustion front **13** itself. For the present purpose it is sufficient to note that it must exist in order to explain the observed direction of the flame world line.

Of more importance to our analysis is the fact that, in order to satisfy the dynamic compatibility conditions, the generation of the system **4–14** must be accompanied by the appearance of retonation shock **134–144** propagating into state **13** and of rarefaction fan **14–144** whose leading edge coincides with the trailing edge of the Chapman–Jouguet deflagration, **14**.

The merging of shock **3** with the shock–flame system **4–14** enhances the establishment of detonation, similarly as in the case without pre-ignition. It has been found, however, that its effect in the present case is not significant and extremely short lived. It produces only a small change in the directions of the shock and flame, the resulting system being denoted by **4′** and **14′**, and reinforces only slightly the rarefaction fan behind it.

Pre-ignition and the establishment of detonation

The details of the wave interaction processes associated with pre-ignition are shown in the expanded section of the time/space plane included as an insert in *Figure 2*.

---

*Note that wave fronts are denoted by the same numbers as the régimes which are created by their action.

The only way in which one could rationalize the direction of the pre-ignition flame as shown in *Figure 1* is by postulating that it is accompanied by a shock which propagates in front of it. Since this happens in the middle of the unburnt mixture, it must be associated with a similar shock/flame system sent in the opposite direction. This gives rise to shock **1′** followed by flame **11′** moving to the left and shock **5** followed by flame **15** moving to the right. In placing the origin of such wave train in the time/space diagram, the best fit with experimental observation was attained by letting it lag somewhat behind the leading shock producing state **1.2**, rather than having it start immediately at the front as implied in *Figure 1*. As the most reasonable we adopted for our purpose the point of intersection of the pre-ignition flame trace of *Figure 1* with the contact surface between régimes 2a and 1.2, determined in the wave diagram of the solution, *Figure 2*.

The effects of the interaction show up most dramatically in the pressure/velocity hodograph plane, *Figure 3*. The head-on collision between shocks **1′** and **4′** creates state **2′** of high pressure but relatively low velocity and, hence, removed farther away from the state of steady detonation than state **4′**. Propagating into this régime is the primary flame **12′** and the pre-ignition flame **12.1′**. When they coalesce, they are extinguished since behind them are only products of combustion. This gives rise to rarefaction fans which reinforce the system carried behind the primary combustion front. They have small effect, however, on the transmitted shock **115** propagating into state **15**, which soon catches up with the forward moving combustion front of the pre-ignition zone, establishing the shock–flame system **6–16**. The latter interacts with a contact surface generated by the merging of shocks **5** and **1.2**, producing detonation **7–17**. Finally system **7–17** catches up with shock **5.1** that propagates into the undisturbed (zero) state of reactants and comes out as the fully developed detonation **8–18**, that is, the shock producing the von Neumann spike, N, followed by deflagration producing the Chapman–Jouguet state, J.

Salient features of state diagrams

As pointed out before the key to the solution is the pressure/velocity hodograph, *Figure 3*. Besides its utility for the analysis of each interaction process it serves also a useful function as an illustration of the conditions which the multiwave system has to satisfy in order to attain the steady detonation process.

For any given mixture there exists in this plane a point representing the Chapman–Jouguet state, J, with the corresponding von Neumann spike, N. If the shock is weaker than that of the von Neumann spike, it moves faster than the Chapman–Jouguet deflagration that propagates behind it. If the shock is stronger, then the deflagration can move faster and catch up with it from behind. When this happens the reaction zone of the flame penetrates into the collision zone of the shock, the flame is temporarily extinguished while the shock is weakened by the rarefaction fan which has been carried behind the deflagration, and the whole wave system collapses until the steady state of the Chapman–Jouguet detonation is established.

Similar points can be found for detonations propagating into régimes that are created by a shock. The two broken lines stemming from points J and N in *Figure 3* represent the loci of such points. In consequence to their significance, points lying to the right of these lines in the P/U plane cannot be achieved by a shock–flame train propagating in the same direction. State **115** for instance was attained as a result of the collision between shock **2′** with flame **11′**. So the intermediate states that are reached during the progress of the process lie essentially to the left of the locus of detonation states, that is, in the direction of higher pressures and lower particle velocities. Since the same is true in our previous analysis[7], it appears that such a trend must be followed irrespective of whether the detonation is established with or without pre-ignition.

The solution in the entropy/velocity hodograph, *Figure 4*, is somewhat cleaner than that on the velocity of sound/mass velocity hodograph, which has been used in our previous publication[7]. The points are clustered into groups corresponding to régimes bounded by contact discontinuities. It is of interest to note that the highest entropy is generated in the immediate vicinity of the back wall. In agreement with the theory of the Hugoniot curve, entropies of states attained behind the accelerating flame are higher than that behind the fully developed detonation. It is this point that often confuses the student: how entropy can be depleted in a compatible manner within an adiabatic irreversible system. The solution presented in *Figure 4* provides a rational explanation of this point. The highest entropy generation is produced by the constant pressure reaction that starts the process. As the flame accelerates it generates less entropy. But the acceleration of the flame is accomplished by collisions with shocks. These generate contact discontinuities which provide the compatibility conditions permitting the establishment of a flow field with the required non-uniform entropy distribution.

Conclusions

From considerations of dynamic compatibility it appears that pre-ignition alone is not sufficient for the establishment of detonation. Although pre-ignition has definite stimulating effect on the development of the process, its history, expressed in terms of the intermediate states that must be attained in the course of its progress, is essentially the same irrespective of whether the detonation is achieved with pre-ignition or without. In particular such phenomena as pressure and wave velocity overshoot should occur in both cases.

This work was performed under the auspices of the Air Force Office of Scientific Research of the Air Research and Development Command under Contract AF 49(638)–166.

References

[1] PAYMAN, W. 'The detonation wave in gaseous mixtures and the pre-detonation period'. *Proc. Roy. Soc. A*, 1928, **120,** 90–109

[2] BONE, W. A., FRASER, R. P. and WHEELER, W. H. 'A photographic investigation of flame movements in gaseous explosions, Part VII—The phenomenon of spin in detonation'. *Phil. Trans.* 1935, No. 747, **235,** 29–68

[3] ZELDOVICH, Y. B. and KOMPANEETS, A. S. *Theory of Detonation,* 288 pp. Gosudarstvennoe Isdatel'stvo Tekniko Teoreticheskoi Literatury: Moscow, 1955

[4] MARTIN, F. J. 'Transition from slow burning to detonation in gaseous explosions'. *Physics of Fluids,* 1958, **1,** No. 5, 399–407

[5] SCHMIDT, E., STEINICKE, H. and NEUBERT, U. 'Flame and schlieren photographs of the combustion of gas–air mixtures in tubes'. *Forschungsh. Ver. dtsch. Ing. Nr. 431,* Ausgabe B, Band **7,** 31 pp. Deutscher Ingenieur-Verlag: Dusseldorf, 1951

[6] SCHMIDT, E., STEINICKE, H. and NEUBERT, U. 'Flame and schlieren photographs of combustion waves in tubes'. *Fourth Symposium (International) on Combustion,* pp 658-666. Williams and Wilkins: Baltimore, 1953

[7] OPPENHEIM, A. K. and STERN, R. A. 'On the development of detonation—Analysis of wave phenomena'. *Seventh Symposium (International) on Combustion,* pp 837–850. Butterworths: London, 1959

THI
eng
stre
dor
stre
as
coo
to
pro
i.e.
gre
pos
am
wh
of
dev
bef
Th
des
per

Fo
Co
div
(2)
ize
elo

---

*T
'T
A
do
ex
re
†P
9

The Design of Combustors for Ramjet Engines[*]

J. J. ZELINSKI[†], L. J. MATTHEWS III, F. FALK and E. C. BAGNALL

Applied Physics Laboratory, Johns Hopkins University, Silver Spring, Md

(*Received October 1959*)

A design procedure for ramjet combustors is developed. A model which describes the manner in which the combustor operates is discussed. Experimental programmes to support the model are described. The use of the model as a design tool is outlined. Experimental verification of the design procedure is given.

Introduction

THE function of the combustor in the ramjet engine is to increase the total energy of the gas stream which passes through it. When this is done by burning a fuel injected into the air stream, the combustor can include such devices as fuel injectors, flameholders, mixers and cooling shrouds. It is the task of the designer to select and arrange these various devices to produce the greatest overall specific impulse, i.e. the highest possible temperatures with the greatest possible fuel economy in the smallest possible volume while introducing the least amount of losses into the fluid. The extent to which the designer can predict the performance of each device will determine the amount of development effort which must be expended before a satisfactory combustor can be obtained. This paper describes a method of combustor design and demonstrates the degree to which it permits combustor performance to be predicted.

The Flame Jet Combustor Model

Form of model

Combustors for ramjet engines usually are divided into two groups: (*1*) baffles and (*2*) cans. The baffle combustor is characterized by a bluff body flameholder with all elements in a single plane. The can combustor in its simplest form is a perforated cone and is characterized by a stage-wise addition of fluid to the combustion zone. In the broad sense, however, it can be considered that one group is merely the extension of the other—the baffle flameholder is a steep-angled can or, conversely, the can is a sloped baffle. A description of the operation of one should then suffice for both. The work at the Applied Physics Laboratory has been directed mainly in recent years to can-type combustors but can be considered applicable to baffle-type combustors as well.

The basis for the analysis of ramjet combustors is the flame jet model. This model states that the fuel–air mixture which enters the combustion zone through holes in the combustor wall is stabilized by a recirculation zone around the periphery of the holes and burns within the combustion zone in a manner similar to a turbulent flame in free air. The performance of the combustor, then, is the summation of the performance of the individual flame jets burning in an environment established by all the flame jets. In other words, each turbulent flame jet is assumed to retain its identity within the combustion zone but there is interaction in that the pressure level and flow velocities are the result of the integrated performance of all flame jets.

List of symbols

The following symbols are used:

η	combustion efficiency
P	combustion chamber pressure [lb/in^2 abs., or atm]
T	air–fuel temperature [$^\circ$R]

---

[*] This paper has been extracted from *Bumblebee Report No. 285*, 'The design of combustors for ramjet engines', (Confidential), Applied Physics Laboratory, Silver Spring, Maryland. A more detailed discussion of the subject matter as well as several more examples of the design procedure can be found in the classified report.

[†] Present address: Space Technology Laboratories, P.O. Box 95 001, Los Angeles 45, California.

V	jet velocity [ft/s]
E	equivalence ratio; actual fuel–air ratio divided by stoichiometric fuel–air ratio
A	area [in^2]
S	jet length
d	hole diameter [ft]
$\dot{m}$	mass flow rate [lb/s]
v	volume
ρ	density
B	blocked area
δ	thickness of annular stream tube
n	exponent on 'equivalent disc diameter'
D	'equivalent disc diameter'; four times ratio of blocked area to wetted perimeter; equal to actual diameter of a disc [ft]
N	number of holes per combustion stage
K_T	Esso temperature correction factor for inlet air
I_a	air specific impulse
M	Mach number
γ	ratio of specific heats
f	stream thrust per unit area
$\bar{C}_D$	average hole discharge coefficient, use 0·5
R	gas constant
h	depth of recirculation zone
F	stream thrust
g	gravitational constant
θ	angle of can with horizontal
ε	angle of jet from the normal to the can surface
β	angle of jet from the horizontal

$\theta + \beta + \varepsilon = 90°$

Mach number functions—

$$P/P_t = [1 + \tfrac{1}{2}(\gamma - 1)M^2]^{[-\gamma/(\gamma-1)]}$$
$$f/P = 1 + \gamma M^2$$
$$\mathring{m} = g[\gamma/R]^{\frac{1}{2}} M[1 + \tfrac{1}{2}(\gamma - 1)M^2]^{\frac{1}{2}}$$
$$\phi(M) = [1 + \gamma M^2] \div M[2(\gamma + 1)\{1 + \tfrac{1}{2}(\gamma - 1)M^2\}]^{\frac{1}{2}}$$
$$F = fA$$

Subscripts—

cc	denotes combustion chamber
h	denotes hole
a	denotes air
f	denotes fuel
t	denotes total
r	denotes recirculation zone
0	denotes free stream quantities
re	denotes reaction zone

Realization of model

To establish the model as a quantitative design tool two experimental programmes have been carried out. The first served to determine the parameters which govern the burning rates of confined turbulent flame jets, and the second established the parameters which correlate combustion stability limits.

The investigation of burning rates of confined turbulent flame jets has been reported elsewhere[1]. The correlation of average combustion efficiency for each jet has been modified to

$$\eta = 1 - \exp\left[-0{\cdot}016\left(\frac{PT}{V}\right)^{3/4} E^{1/2}\left(\frac{A_{cc}}{A_h}\right)\left(\frac{S}{d}\right)\right] \quad [1]$$

where η denotes integrated heat release combustion efficiency, and (A_{cc}/A_h) is the ratio of combustion chamber area to total flameholder hole area.

The range of variables tested was:

P	4·90 to 9·80 lb/in^2 abs.
T	100° to 340° F
V	300 to 700 ft/s
d	1 to 3 in.
E	0·7 to 1·3
(A_h/A_{cc})	0·375 to 0·700
S	8 to 24 in.

To correlate combustion stability limit data[2] it was assumed that the combustion stability is controlled by the chemical kinetics of the recirculation zone gases in the wake of the flameholder. Assuming that the combustion stability of the recirculation zone gases is reaction-rate controlled, the correlating parameter is $(\dot{m}_a/P^2 v)_{re}$ where $\dot{m}_a$ is the air flow rate into the reaction zone, v is the volume of the reaction zone, and P is the static pressure. Using the model of the recirculation zone behind a disc of diameter D as shown in *Figure 1*, this parameter can be converted to more readily measured quantities (see list of symbols, above). It is

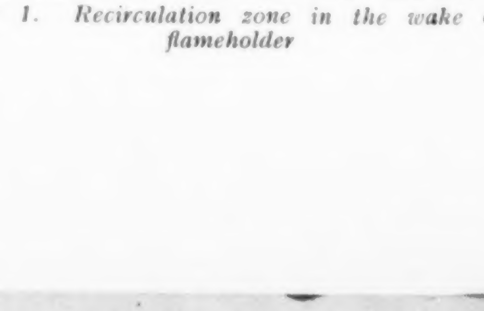

Figure 1. Recirculation zone in the wake of a flameholder

recognized that there is some dependence of δ upon h and consequently upon D; i.e. $\delta \propto h^n \propto D^n$ since $h \fallingdotseq 2D$ (see ref. 3). The correlating parameter can be shown to be proportional to $(\dot{m}_a/P^2D^3)\,(D^{n+1})$ where $\dot{m}_a$ is the total mass flow rate of air. Whether the reaction zone is made up of the total recirculation zone or only of a small mixing region within the recirculation zone is not clearly established at present. It has not been necessary to decide this point for the purpose of correlating the combustion stability data. Whether it be the total volume or some given fraction of the total volume, combustion stability can be correlated by the parameter $(\dot{m}_a/P^2D^3)$ if the chemical reaction rate controls.

To test this assumption of chemically controlled flame stabilization, the data of E. A. DEZUBAY[4] on the stability limits of discs were plotted as a function of $(\dot{m}_a/P^2D^3)$. The data were correlated as shown in *Figure 2* and showed the expected further dependence upon disc diameter.

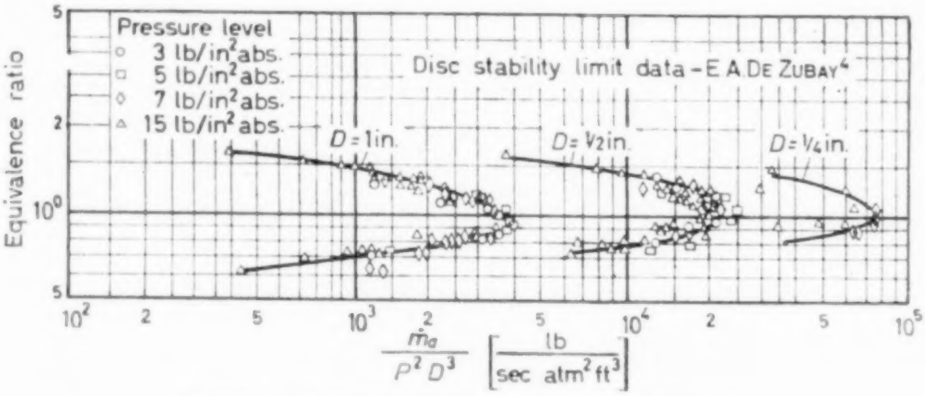

Figure 2. Correlation of combustion stability limits

To correlate the combustion stability limits of can-type flameholders a definition has been introduced to relate flameholders of various shapes to a common dimension. This dimension is the 'equivalent disc diameter', D, and is defined as four times the ratio of the blocked area to the wetted perimeter. For a can-type flameholder with an array of holes, the 'equivalent disc diameter' can be calculated from the representative section of *Figure 3* where the blocked area and the wetted perimeter are clearly marked. In this case the correlating parameter becomes $\dot{m}_a/P^2D^2d$, where d is the hole diameter. For three different configurations, the combustion stability limits can be correlated as shown in *Figure 4*.

To obtain a useful correlation of the combustion stability data for combustor design, the data were matched to the stability limit curve of the Esso spherical reactor[5]. The parameter which correlates the data is

$$\left(\frac{2}{\pi N K_T}\right)\left(\frac{\dot{m}_a}{P^2D^2d}\right)\left(\frac{5520D-625}{V^{0\cdot 88}}\right)$$

Figure 5 shows the final correlation.

Design Procedure

With the information on jet burning rates and combustion stability a can-type flameholder can be designed for a particular condition of operation. For a given engine geometry there will be designated the air flow rate, inlet air total temperature, the exit nozzle size, and the required overall combustion efficiency at a given equivalence ratio. Air and fuel are assumed to be pre-mixed upstream of the combustor, and the fuel–air distribution is specified. Choosing a blockage fixes the velocities through the holes, and all the parameters are known which determine the ratio of flame-jet length to hole diameter. The available combustion chamber length fixes the hole sizes, and the stability requirements fix the separation distances between holes.

Once the geometrical pattern has been chosen, the expected performance can be calculated by the same general procedure set down for the design. The effects of varying equivalence ratio, inlet air temperature, and air flow rate can be examined, and an estimate of the pressure drop through the combustor can be made. To calculate performance at a given condition of inlet air temperature, air flow rate and equivalence ratio, the combustion efficiency is chosen. This corresponds to a value of air specific impulse. The static pressure in the combustion chamber can then be calculated from

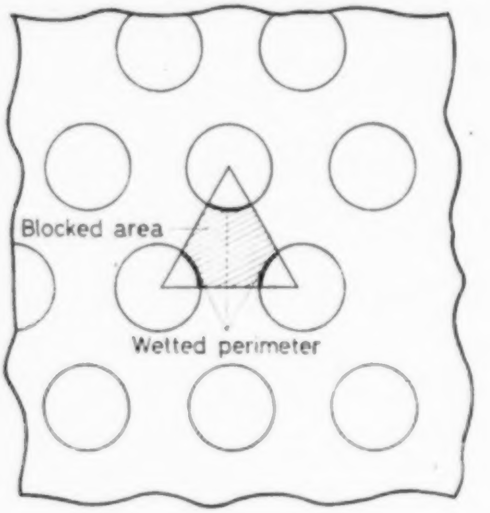

Figure 3. Representative area for calculating the 'equivalent disc diameter' of a can-type flameholder

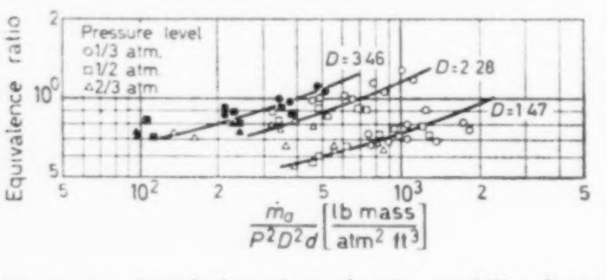

Figure 4. Correlation of combustion stability limits (can-type flameholder)

$$P_{cc}=\frac{I_a\dot{m}_a\phi(M_{cc})}{A_{cc}(1+\gamma_{cc}M_{cc}^2)} \qquad \ldots . [2]$$

where P is measured in lb/in^2 abs. and I_a in [lb force × s/lb mass of air]; M_{cc} is determined by the size of the sonic exit nozzle, γ_{cc} is the ratio of specific heats for burning gases in the combustion chamber, taken as 9/7, and $\phi(M_{cc})$ is the Mach number function[*].

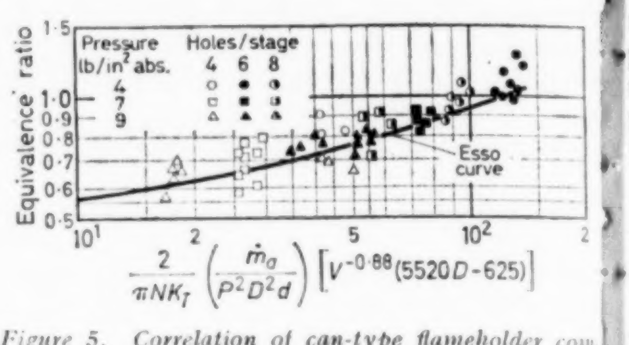

Figure 5. Correlation of can-type flameholder combustion stability limits

To calculate pressure change in the combustor due to burning, assume burning takes place in a constant area duct. Then

$$[I_a\times\phi(M)]_{\substack{\text{unburnt}\\ \text{gas}}}=[I_a\times\phi(M)]_{\substack{\text{burnt}\\ \text{gas}}} \qquad \ldots [3]$$

The I_a of the burnt gas is the chosen number, and the I_a of the unburnt gas is given by the inlet air temperature. The Mach number of the burnt gas is known from the nozzle size, and the Mach number of the unburnt gas can be found. The static pressure ratio of the unburnt to the burnt gas is given by

$$[(f/P)\ (P)]_{\text{unburnt}}=[(f/P)\ (P)]_{\text{burnt}} \qquad \ldots [4]$$

The values of f/P are Mach number functions, and the static pressure ratio can be found. Using the static pressure of the burnt gas previously determined, the static pressure of the unburnt gas can be calculated. A linear variation of static pressure can be assumed from the station downstream of the first row of holes to the entrance of the exit nozzle. The mass flow through each stage of the combustor can be calculated from

$$\dot{m}_{a+f}=P_{cc}A_h\bar{C}_D\overset{\circ}{m}/T_t^{\frac{1}{2}} \qquad \ldots . [5]$$

where P_{cc} denotes combustion chamber stati pressure at the stage, A_h is the total hole area o the stage, T_t is the total temperature of air–fue mixture entering the stage, and $\overset{\circ}{m}$ is a Mac number function, determined from total to static pressure ratio. The correct choice of upstream total pressure will account for the total mass flow. The Mach number is related to velocity by the relation

---

[*] For a discussion of the Mach number functions see OA *Memorandum 50*. New Mach Number Tables for Ramjet Flo Analysis, April 7, 1952, published by Convair, a Division o General Dynamics Corporation, Dangerfield, Texas.

$$V = M\,(\gamma RT)^{\frac{1}{2}}$$

where T is the static temperature (°R), $\gamma = 1{\cdot}4$, and $R = 1716$. With all the variables of equation 1 specified the combustion efficiency of each jet can be calculated. The over all combustion efficiency of the combustor is computed as the ratio of the heat released in all stable burning jets to the total available heat content.

The exprienced combustor designer will recognize that only the design of the flameholding element of the combustor has been described. The overall combustion efficiency must be evaluated on the basis of the efficiency of mixing of stable burning jets, unstable non-burning jets, by-pass cooling air, etc.

Scaling Parameters for Can Combustors

The experimental correlations of the factors controlling jet burning rates and combustion stability define the parameters by which combustors can be scaled. The geometry is similar when combustors have the same blockage (A_{cc}/A_h), the same ratio of combustion chamber length to hole diameter (S/d), and the same relationship of hole size to hole separation; i.e. the same 'equivalent disc diameter' (D). Premixed fuel–air mixtures are assumed, and similarity is established when two combustors have the same air–fuel distribution pattern at each stage of the combustor. Flow variables are duplicated by using the same exit constrictor area ratio, the same mass flow rate per unit cross-sectional area, and the same inlet air total temperature that are used in the full-scale configuration. To keep flow variables within the scale combustor the same as those within the full-scale combustor, a length term is duplicated; this term is the ratio of the volume within the flameholder proper to the cross-sectional area of the combustion chamber.

The ratio of the pressure–temperature product and the jet velocity (PT/V) is a term related to second-order reaction kinetics[6]. The exponent of this term is an indication of the degree of mass loading of the combustor. As the mass loading is increased to the point where the rate of mass addition is competitive with the rate of chemical reaction, changes in the parameters that affect chemical reaction (such as pressure and temperature) have an increasingly greater effect on overall combustion efficiency. The exponent on this term can vary from zero to infinity at blow-off. This is demonstrated by data from the Esso spherical reactor[5]. The variation of combustion efficiency is given for the condition at which blowout is approached by a change in pressure. This permits the pressure exponent to be determined. The pressure exponent of the reactor itself varies from 0·38 to 0·67. The slope of the theoretical curve increases rapidly to give an infinite slope at the low pressure end and a zero slope at high pressure. This indicates that the exponent on the (PT/V) term is different for different combustors. Experiments with baffles have shown an increasing dependence of combustion efficiency with pressure when the number of baffles in the duct is increased. Practical combustors, however, are operated in the region of high mass loading and show a marked dependence upon pressure. The value of 0·75 as the exponent of the (PT/V) term is recommended for design purposes.

Experimental Evaluation

In order to evaluate the design procedure, a full-scale combustor and a segment of the full-scale combustor were designed, built and tested. The full-scale combustor is pictured in *Figure 6*. It is a single-folded cone to permit separate fuel systems to each skirt and more efficient packaging. In this way a wide range of equivalence ratio operation is obtained, and the mixing of hot and cold gases is improved. The geometry is summarized in *Table 1*. A segment of the full-scale combustor is shown in *Figure 7*. It was tested in a rectangular 6 in. × 7 in. duct. To be consistent with the full-scale combustor it is identical to the full-scale model in (*1*) hole size at each stage, (*2*) ratio of total hole area to duct cross-sectional area, (*3*) ratio of hole area in the outer skirt to hole area in the inner skirt, (*4*) ratio of volume within the flameholder to cross-sectional duct area, and (5), as nearly as possible, the 'equivalent disc diameter' at each stage. For the 'two-dimensional' combustor segment, the leading edge is displaced from the centre to allow each skirt to intercept the fraction of total air more nearly in proportion to its hole area ratio.

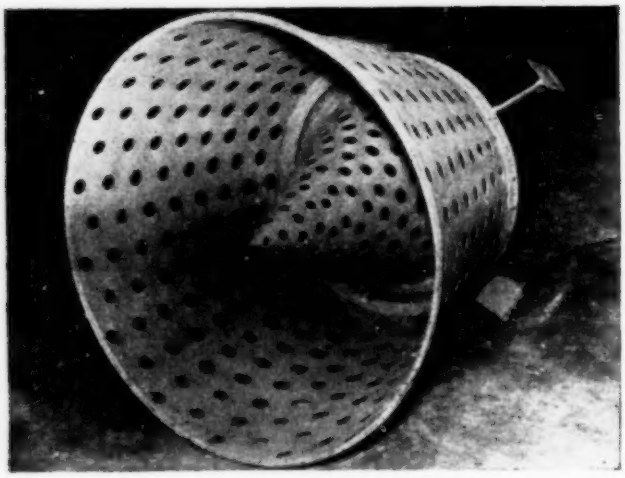

Figure 6. Full-scale combustor

Table 1. Full-scale combustor geometry
Leading edge at station zero
Combustion chamber exit at station 44

	Stage	*Station*	*Hole diameter in.*	*Holes per stage*	*Equivalent disc diameter in.*
Outer skirt	1	4·0	1·125	16	6·0
	2	5·8	1·125	16	4·6
	3	6·5	1·125	16	4·7
	4	7·8	1·125	16	4·8
	5	9·1	1·125	16	5·0
	6	10·3	1·125	16	5·1
	7	11·6	1·00	16	6·1
	8	12·9	1·00	16	6·3
	9	14·1	1·00	16	6·4
	10	15·4	1·00	16	6·6
	11	16·7	1·00	16	6·7
	12	17·9	1·00	16	6·9
	13	19·2	0·875	16	8·3
	14	20·5	0·875	16	8·4
	15	21·7	0·875	16	8·6
	16	23·0	0·875	16	11·4
Inner skirt	1	4·0	1·125	16	3·5
	2	5·4	1·00	16	3·5
	3	6·9	1·00	16	3·5
	4	8·5	0·875	16	3·5
	5	10·0	0·875	16	3·5
	6	11·6	0·750	16	3·5
	7	12·9	0·750	8	3·5
	8	13·7	0·750	8	3·5
	9	14·9	0·750	8	3·5
	10	15·9	0·625	8	3·5
	11	17·1	0·625	8	3·5
	12	18·6	0·625	8	3·5
	13	20·0	0·625	4	3·5
	14	21·3	0·500	3	3·5
	15	23·0	0·500	1	3·5

The performance of the segment was determined at an air flow rate of **2·07** lb/s, at an inlet air total temperature of **350**°F, with a homogeneous pentane–air mixture in a duct **44** in. long with a **65** per cent sonic exit constrictor. A comparison of the measured and calculated quantities is shown in *Table 2*. Air specific impulse was calculated from a combustion efficiency assuming complete mixing of hot gases. The static pressure gradient in the duct is shown in *Figure 8* for Runs 1, 2 and 3 listed in *Table 2*. The assumption of linear pressure gradient agrees well with the measured gradient.

The 'equivalent disc diameter' values were calculated for each stage of the combustor segment. The largest value of the parameter was used to determine combustion stability. The combustion stability data of *Figure 5* indicate stable burning at an equivalence ratio of 0·8; the actual blowout point was somewhere between an equivalence ratio of **0·8** and 0·86.

The agreement between full-scale combustor operation and combustor segment operation is shown in *Figures 9* and *10*. Air specific impulse for selected points at similar air flow rates and inlet air temperature is shown in *Figure 9*; static pressure distribution within the combustion zone of the full-scale combustor and combustor segment is shown in *Figure 10* for the condition of inlet air temperature of 350°F and air flow rate of **0·53** lb/s . in² of full duct area.

Detailed Calculation of Flow Parameters

The design procedure described has used an approximate method of calculating flow through the combustor. For flameholders with large blockages placed in a constant area duct this method of flow calculation is sufficiently accurate. A complete design procedure requires, however, a more accurate method of flow calculation which can take into account variable area and various degrees of blockage. Toward this end a set of equations has been developed which permits the calculation of all flow variables at each stage of the combustor. Calculations are shown for flow without heat release through a combustor segment.

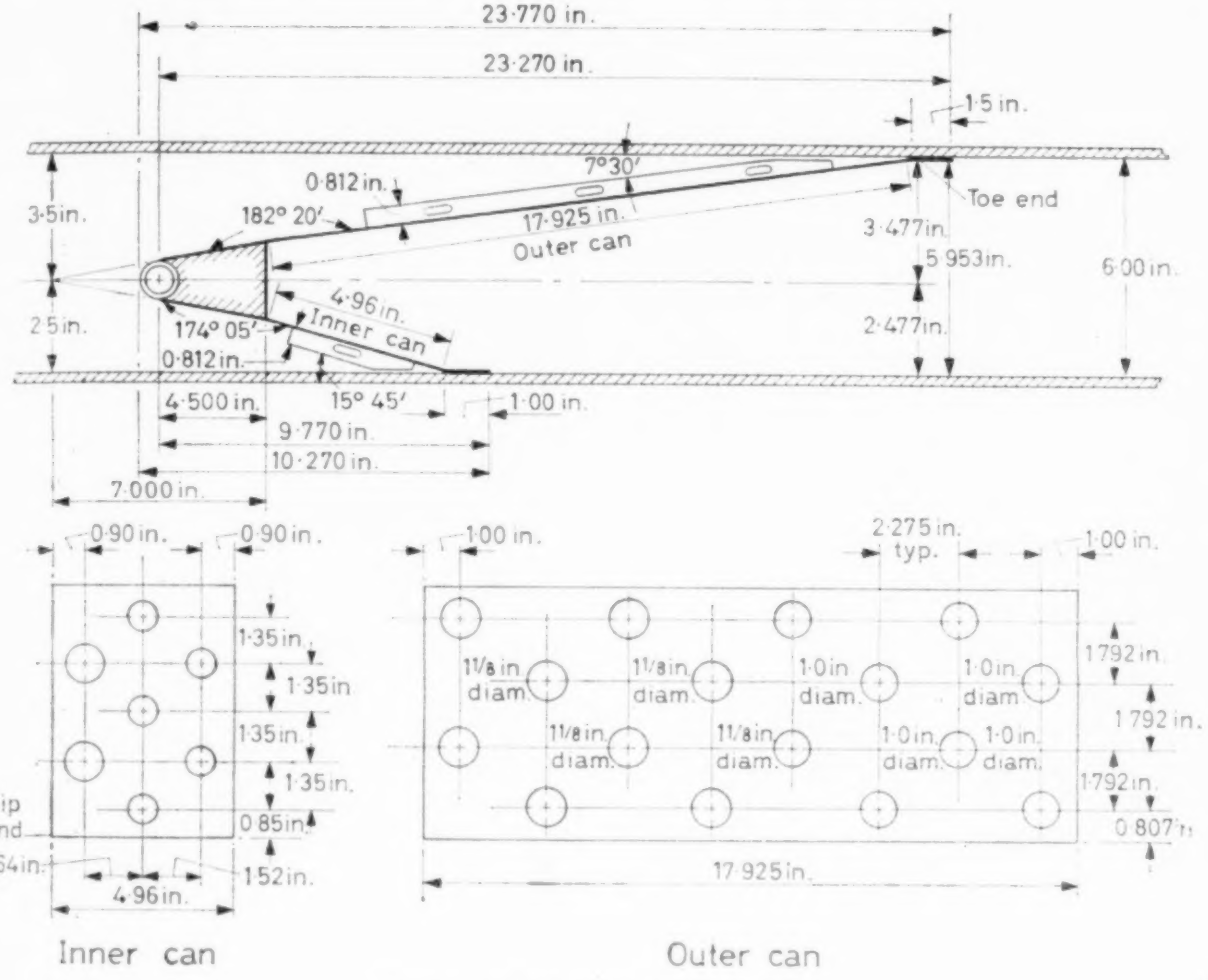
23·770 in.
23·270 in.
1·5 in.
7°30′
0·812 in.
182° 20′
17·925 in.
Outer can
Toe end
3·477 in.
5·953 in.
6·00 in.
3·5 in.
2·5 in.
4·96 in.
Inner can
174° 05′
0·812 in.
2·477 in.
4·500 in.
15° 45′
1·00 in.
9·770 in.
10·270 in.
7·000 in.
0·90 in.
0·90 in.
1·35 in.
1·35 in.
1·35 in.
1·35 in.
0·85 in.
Lip end
1·64 in.
1·52 in.
4·96 in.
1·00 in.
2·275 in. typ.
1·00 in.
1⅛ in. diam.
1·0 in. diam.
1·792 in.
1·792 in.
1·792 in.
0·807 in.
17·925 in.
Inner can
Outer can

Figure 7. Sketch of combustor segment

The calculations have been made for flow through a 'can-type' combustor. It is a two-dimensional configuration with matching hole patterns in the two plates, as shown in *Figure 11*. The effect on the flow parameters of jets which form when air passes through the perforations in the flameholder was considered. The three cases investigated were: (*a*) the immediate dissipation of the jets upon passing through the holes; (*b*) jets flowing at constant entry angle and dissipating after one stage; and (*c*) jets bending under the influence of the main stream and dissipating only if they penetrate to the centre line of the configuration—the

Table 2. Comparison of calculated and measured quantities in the combustor segment

Run No.	*Total mass flow rate lb/s*	*Equiv. ratio*	*Air total temp. °F*	*Air specific impulse*		*Exit total pressure lb/in² abs.*		*Upstream total pressure lb/in² abs.*	
				Meas.	*Calc.*	*Meas.*	*Calc.*	*Meas.*	*Calc.*
1	2·19	0·86	350	161	164	9·83	9·91	12·0	13·5
2	2·20	0·93	350	164	167·5	10·0	10·1	12·3	13·7
3	2·21	1·00	350	167	170	10·2	10·3	12·5	13·8
4	2·22	1·07	350	170	172	10·4	10·4	12·7	13·9
5	2·23	1·15	350	172	173	10·5	10·5	12·8	14·0

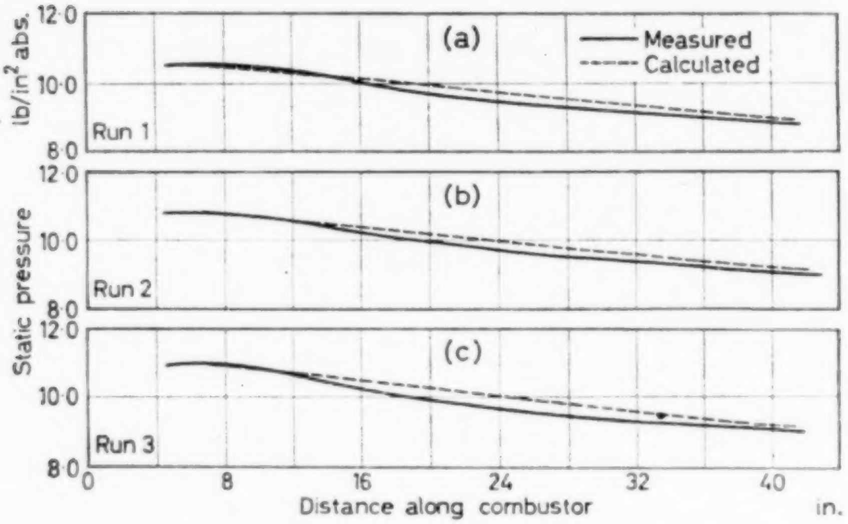

Figure 8. Comparison of measured and calculated static pressures in combustion zone of combustor segment

assumption being made that collision with opposing jets annihilates them. These cases are demonstrated in *Figure 12*.

Flow parameters were calculated in the following manner. For known parameters at station m, a mass flow through the holes was assumed. For the upstream stage at station n, this defined the mass flow rate, the Mach number, and the static pressure; total pressure and total temperature were assumed constant. Assuming that the total pressure of upstream stations m and n was equal to the total pressure of the mass flow through the hole, the Mach number and the angle at which the mass flowed through the hole (β in *Figure 12*) were calculated. At the downstream stage the static pressure of the mass flowing through the hole was found from the Mach number of the flow through the hole and the assumption of total pressure equal to upstream total pressure. Assuming static pressure of the flow through the hole the average of static pressure at downstream stations m and n defined the static pressure at downstream station n. A downstream force balance gave the stream thrust at station n, which led directly to a Mach number. With these quantities a mass flow at downstream station n was calculated which was the sum of the known mass flow at downstream station m and the assumed mass flow through the hole when the proper value was chosen.

When constant angle jets were considered, it was necessary to add equations defining the Mach number, the area and the stream thrust of the jet at downstream station n to effect a solution. With bending jets an additional equation defining the jet trajectory under conditions of cross-flow[7] was used.

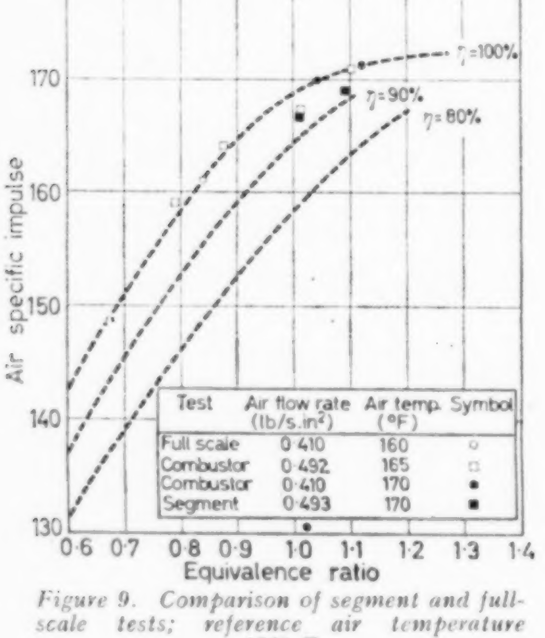

Figure 9. Comparison of segment and full-scale tests; reference air temperature 150° F

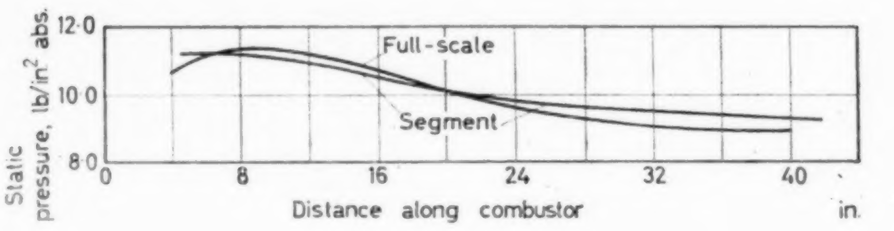

Figure 10. Comparison of static pressures in full-scale and segment tests

(a) Combustor section in 6in.x 7in.duct

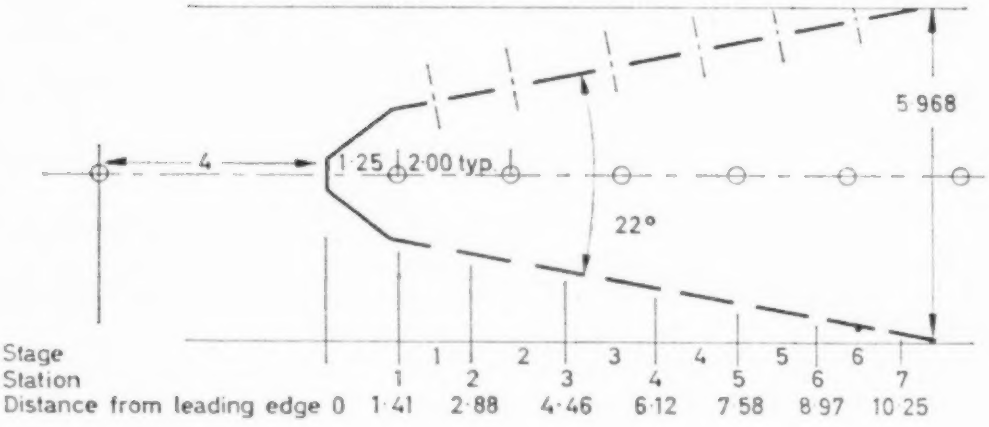
4
1·25
2·00 typ.
22°
5·968
Stage
1
2
3
4
5
6
Station
1
2
3
4
5
6
7
Distance from leading edge 0 1·41 2·88 4·46 6·12 7·58 8·97 10·25

(b) Hole pattern

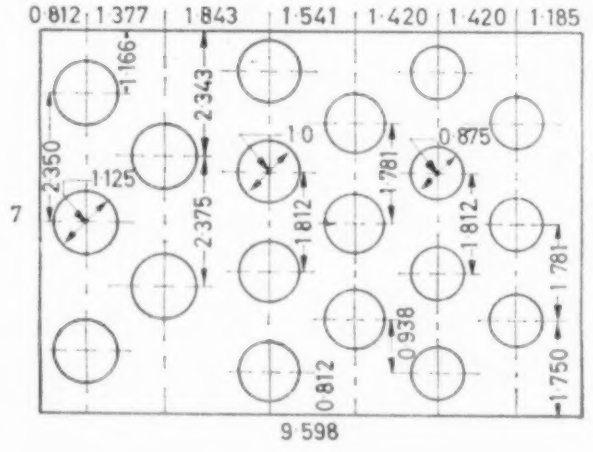
0·812
1·377
1·843
1·541
1·420
1·420
1·185
1·166
2·343
1·0
0·875
2·350
1·125
1·781
7
2·375
1·812
1·812
1·781
0·938
0·812
1·750
9·598

All dimensions in inches

Figure 11. Schematic of can-type combustor section

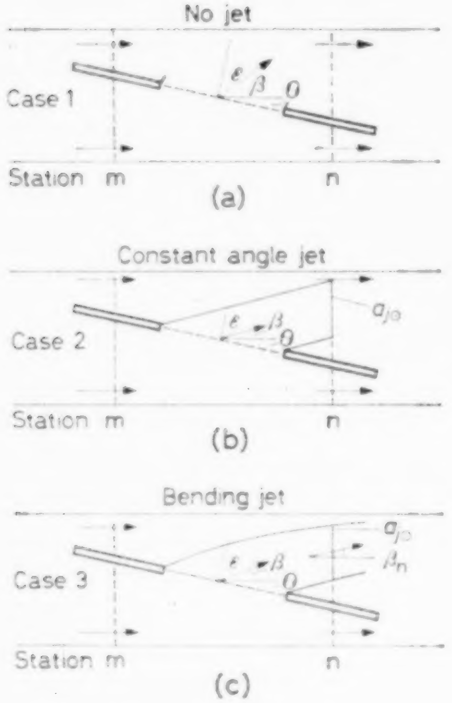

Figure 12. Generalized stage for calculation

In *Figure 13* are shown the results of the various assumptions. The calculations were carried out using the measured static pressure at the first downstream station and assuming a zero mass flow at this station. The free-stream measured conditions were mass flow rate of 1·96 lb/s, total pressure of 8·82 lb/in² abs., static pressure of 7·73 lb/in² abs., and total temperature of 577°R.

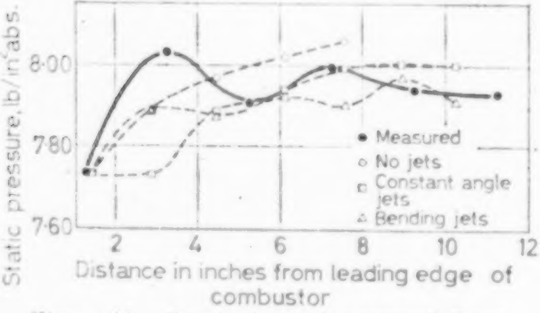

Figure 13. Comparison of measured downstream static pressures and those calculated by the three methods

The calculation of flow with bending jets was programmed for the IBM 650 computer[8] and the results are shown in *Figure 14*. In this calculation no assumption of downstream pressure was made; an iterative solution was carried out until total mass flow was conserved. The measured free-stream conditions were mass flow rate of 1·28 lb/s, total pressure of 8·06 lb/in² abs., static pressure of 7·56 lb/in² abs., and total temperature of 580°R.

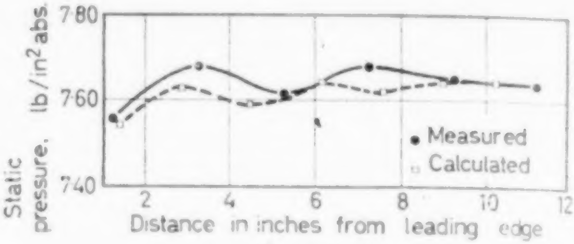

Figure 14. Comparison of measured and calculated downstream static pressures

An independent check on one of the calculated parameters, jet angle (ε), was made with experimental data on hole discharge coefficients[9]. The effective hole discharge coefficient in our study is taken as $C_D \cos \varepsilon$, where C_D is the 'contraction coefficient' equal to 0·60 and ε is the angle which the jet makes with the normal to the 'can' surface. A comparison with the experimental values is shown in *Table 3*. Agreement is within 6 per cent; since the conditions of flow were not exactly similar in the two experiments, this agreement is considered satisfactory.

Summary and Conclusions

This paper has described in brief the development of a procedure for designing combustors for ramjet engines. It began with a statement of a concept of operation of ramjet combustors—the flame jet combustor model. The model required two pieces of information before it

Table 3. Comparison of effective hole discharge coefficients

Stage	*Discharge coefficient, reference 9*	*Discharge coefficient, IBM calculation*
1	0·47 ± 0·01	0·51
2	0·46 ± 0·01	0·50
3	0·47 ± 0·01	0·51
4	0·49 ± 0·01	0·51
5	0·51 ± 0·01	0·54
6	0·57 ± 0·01	0·58

could be used as a design tool—the burning rates of confined turbulent flame jets and the conditions under which flames will stabilize on a flameholder. Experimental programmes were carried out to obtain this information. Using this concept of operation and the experimental data, a combustor was designed and tested, first as a segment and then in full scale. The results verified the design method.

With the procedure described it is possible to design ramjet combustors for particular applications and, also, to determine the improvements that can be made in existing designs.

This work was supported by the Bureau of Ordnance, Department of the Navy, Nord Contract 7386. Permission to publish this paper is gratefully acknowledged.

References

[1] Zelinski, J. J., Baker, W. T., Matthews, L. J. and Bagnall, E. C. *Proceedings of the Gas Dynamics Symposium on Aerothermochemistry*, pp **179–198**. Northwestern University: Evanston, Illinois, **1956**

[2] Zelinski, J. J., Walker, R. E. and Rosen, P. *APL/JHU CM–841*, **1955**. Also American Rocket Society *Preprint ARS–271–55*

[3] Zukoski, E. E. and Marble, F. E. *Proceedings of the Gas Dynamics Symposium on Aerothermochemistry*, pp **205–210**. Northwestern University: Evanston, Illinois, **1956**

[4] DeZubay, E. A. *Aero Digest* **1950**, **7**, **54**

[5] Longwell, J. P. and Weiss, M. A. *Industr. Engng Chem.* (*Industr.*), **1955**, **47**, **1634**

[6] Childs, J. H. and Graves, C. C. *Sixth Symposium (International) on Combustion*, pp **869–878**. Reinhold: New York, **1957**

[7] Walker, R. E. APL/JHU unpublished work

[8] Frier, J. L., Trimble, M. H., Sondheim, D. W. and Glover, D. 'Theoretical bending jet can solution for the Applied Physics Laboratory, The Johns Hopkins University', *OAL Memor. No.* **93**, 20 February 1957

[9] Dittrich, R. T. and Graves, C. C. 'Discharge coefficients for combustor-liner air-entry holes'. *Tech. Note Nat. Adv. Comm. Aero., Wash., No. 3663*, April 1956

Th

IN A
for th
point
engin
block
engin
bustic
broug
temp
vapo
aerod
techn
use o
insula
exces
reces
ever,
syste
to th
fuel,
than
relati
for th

Nu
dynar
sprea
publi
ZIEMI
has a
flame
resear

Sin
may
obser
summ
prove

Th
and I

The Ignition Delay Concept for Recessed Flameholders

L. A. Povinelli

School of Aeronautical Engineering, Turin Polytechnic, Italy

(*Received February 1960*)

Earlier work of Huellmantel, Ziemer and Cambel is considered in relation to tests on wake characteristics of recessed flameholders. Sodium injection was used, with propane–air. Recirculation lengths were found to be essentially constant with variations in velocity and equivalence ratio. The criterion of Zukoski and Marble is concluded to be applicable to recessed geometries.

In a recent article by G. L. **Dugger**[1], the need for the elimination of burner hardware drag was pointed out for high speed ramjets. Some engines now under development require less blockage or burner drag than lower speed engines in order to achieve comparable combustion efficiency and flame stability. This is brought about by the increase in inlet air temperature and the associated increase in fuel vaporization rate. Dugger suggests the use of aerodynamic flameholders and flame-spreading techniques as well as recessed geometries. The use of a ducted configuration with a ceramic-insulated combustor may serve to eliminate the excessive wall heating effects when employing recessed geometries in low speed ramjets. However, it is evident that more elaborate cooling systems will be required as speeds are increased to the hypersonic régime. Use of pentaborane fuel, having a flame velocity ten times greater than that of propane, may serve to decrease the relatively large downstream distance required for the meeting of the flame fronts.

Numerous papers have appeared on aerodynamic stabilization techniques and flame spreading. However, aside from the original publication by L. W. **Huellmantel**, R. W. **Ziemer** and A. B. **Cambel**[2], no additional work has appeared in the literature on recessed wall flameholders, although a certain amount of research has continued on the subject[3,4].

Since the application of recessed geometries may have merit for high speed ramjets, some observations made by the author during the summer of 1958 at Northwestern University may prove useful in design considerations.

The ignition delay concept of E. E. **Zukoski** and F. E. **Marble**[5] represents a blowoff criterion for bluff-body flame stabilizers. Hence, it was decided to investigate the wake characteristics of recessed flameholders. Recirculation lengths were measured for the three configurations shown in *Figure 1*, using the sodium injection technique. Commercial propane was used as the fuel, with air at ~75°F. The variation in recess depth was considered analogous to the change in bluff-body diameter. All experiments were conducted at Reynolds number values ~ 1×10^4, with a low degree of turbulence present in the approach stream. Further details on the apparatus may be found in ref. 2, since the same apparatus was employed by this

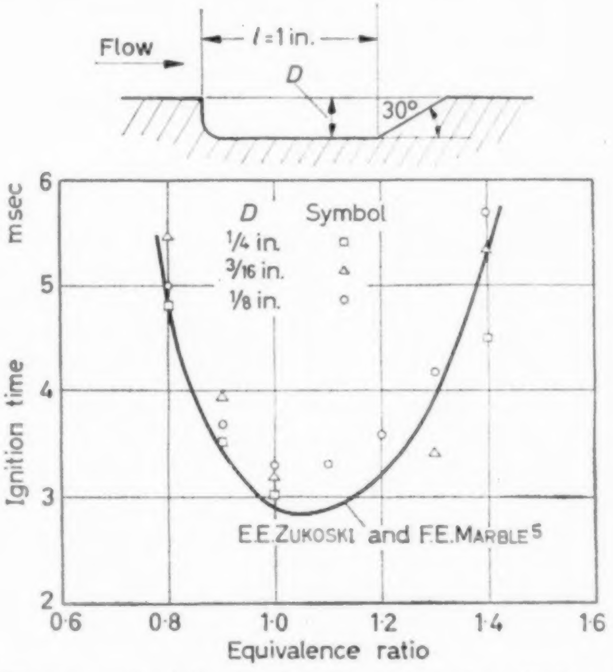

Figure 1. 'Ignition time' as a function of equivalence ratio

author. The recirculation lengths were found to be essentially constant with variations in velocity and equivalence ratio. A plot of the 'ignition time', that is, recirculation length/approach velocity, is shown in *Figure 1* as a function of equivalence ratio for the three test geometries. Velocity blowoff values used for computation are from ref. 2. The experimental curve of ref. 5 is shown for comparison. The ratio of recirculation length to recess depth was approximately equal to 5, which represents twice the value obtained by Zukoski and Marble. This L/D value might have been anticipated since one recess represents only half the flameholding perimeter. The value of the parameter, l, was considered sufficiently large, with these three geometries, so as not to influence the maximum length of the recirculation zone. Several wall flameholders having low l values were used previously[2], thereby effectively controlling the recirculation length. The flame stability limits for a majority of the geometries in ref. 2 may be predicted with a fair degree of accuracy, using the values of the ignition delay time from *Figure 1* and estimating the recirculation length from the available space. Thus it appears that the ignition times for recessed-wall flameholders are similar to those obtained by Zukoski and Marble with bluff bodies. Evidently, the blowoff criterion applies equally well to recessed geometries since the basic mechanism of stabilization is identical.

However, computations based on the results of W. T. SNYDER[6], who conducted experiments with a sudden expansion of 3/16 in. depth, yield delay times almost twice as large as those shown in *Figure 1*. These values are based on the widest stability limits presented in ref. 6 and a recirculation length of 1 $\frac{3}{16}$ in.*. This apparent discrepancy may be resolved by consideration of the flow characteristics involved in each set of experiments. The use of an approach length by Snyder, while studying turbulent boundary layer effects, may have caused a disturbance of the boundary layer initially existing on the floor of the test chamber. This disturbance may have caused the separated shear flow to have a greater thickness than that present in the work of Huellmantel *et al.* and of the present author. In the latter case, separation of the turbulent boundary layer from the trailing edge of the stabilizer without any flow disturbances results in a shear layer of minimum thickness. The mixing of reactants and products is therefore confined to a narrow region and the aerodynamic and chemical kinetic effects are correctly described by the Marble–Zukoski parameter. In this connection, one may visualize the reactants as having immediate contact with an energy source (recirculating gases) after separation from the stabilizer. However, with mixing occurring in a significantly thicker shear layer, the phenomenon of turbulent mixing may predominate, so that blowoff is primarily a function of the diffusional characteristics in the shear layer. One might conceive a model for this latter situation as one in which the reactants no longer have immediate contact with the energy source but must first diffuse through a buffer or mixing zone.

The ignition times of Zukoski and Marble are concluded to be identical for recessed flameholders and bluff-body stabilizers. For the case when boundary layer disturbances are present, these times may vary considerably. Obviously, the blowoff criterion of Marble and Zukoski is equally applicable to recessed geometries.

The author acknowledges the aid and encouragement of Professor Ali B. Cambel, of Northwestern University, and also thanks Dr P. Roy Choudhury (University of S. California) for his assistance in the laboratory.

References

1. DUGGER, G. L. 'Recent advances in ramjet combustion'. *Jet Propulsion*, 1959, **29**, 819
2. HUELLMANTEL, L. W., ZIEMER, R. W. and CAMBEL, A. B. 'Stabilization of premixed propane–air flames in recessed ducts'. *Jet Propulsion*, 1957, **27**, 31
3. POVINELLI, L. A. 'Development of helicopter tip jets'. *Final Report*. Armour Research Foundation Project D926, September 1957
4. POVINELLI, L. A. 'Combustion performance characteristics of a laboratory subsonic ramjet'. *J. R. aero. Soc.*, 1960, **64**, 564
5. ZUKOSKI, E. E. and MARBLE, F. E. 'Experiments concerning the mechanism of flame blowoff from bluff bodies'. *Proceedings* of the Gas Dynamics Symposium on Aerothermochemistry, Northwestern University, August 1955
6. SNYDER, W. T. 'The influence of approach boundary layer thickness on flame stabilization'. *Jet Propulsion*, 1958, **28**, 822

---

*Personal communication—W. T. SNYDER

The Theory of Flame Propagation in Branched and Unbranched Chain Systems

L. A. LOVACHEV

Institute of Chemical Physics, Academy of Sciences, Vorobyevskoye chaussée 2-b, Moscow V-133, U.S.S.R.

(Received May 1960)

An approximate method for the solution of a set of energy conservation and active centre diffusion equations, describing steady-state flame propagation by an unbranched one-centre chain reaction, is proposed. Calculated values for burning velocities and the distribution of active centres as a function of temperature are in agreement with those obtained by numerical integration. An approximate solution for the problem of flame propagation in an unbranched chain system involving two active centres is given. Theoretical burning velocity values for chlorine–hydrogen flames calculated from approximate formulae show a good fit with experimental results. Approximate formulae for burning velocities in unbranched chain systems are derived. The application of the formulae for the determination of elementary branched chain reaction rate constants from burning velocities as a function of temperature is illustrated by hydrogen flames.

DEVELOPMENT of the theory of flame propagation treating sets of differential equations for energy conservation and diffusion of active centres has begun only lately in the work of D. B. SPALDING, J. C. GIDDINGS, J. O. HIRSCHFELDER, E. S. CAMPBELL, L. M. SCHALIT, T. VON KÁRMÁN and S. S. PENNER[1-6]. All these authors considered simplified schemes of model branched chain reactions. Corresponding sets of equations were eventually integrated numerically. A number of important flame phenomena with chain reactions were found out by numerical integration, but it was not sufficient for establishing general laws.

Analytical relations connecting the burning velocity with initial and final parameters of gaseous mixtures and with chemical reaction rate functions had to be derived. These equations would permit investigations on kinetics of high temperature reactions, a problem most important for combustion theory.

The author[7-13] has attempted to set out a theory for flame propagation in branched chain systems. Corresponding relations were obtained by approximate solution of sets of appropriate differential equations.

Approximate Solution for a Thermal Problem at a Low Activation Energy of the Heat Release Process

Thermal theories discussed in detail by M. W. EVANS[14] use an equation for energy conservation describing the rate of heat release as a function of temperature alone. The burning velocity, u_0, is determined by the first integral of the equation for energy conservation

$$\frac{\mathrm{d}}{\mathrm{d}x}\left(\lambda\frac{\mathrm{d}T'}{\mathrm{d}x}\right)-u\rho c\frac{\mathrm{d}T'}{\mathrm{d}x}+\Phi(T')=0 \qquad \ldots . [1]$$

under boundary conditions:

$$x=-\infty,\ T'=T'_0,\ (\mathrm{d}T'/\mathrm{d}x)=0 \quad \ldots [2]$$

$$x=+\infty,\ T'=T'_b,\ (\mathrm{d}T'/\mathrm{d}x)=0 \quad \ldots [3]$$

Here u denotes the flow velocity (cm/s), ρ the density (g/cm^3), c the specific capacity at constant pressure (cal/g °C), λ the thermal conductivity of the mixture (cal/cm.s. °C), T the temperature (°K), $\Phi(T')$ the heat release rate, subscript $_0$ refers to the initial state of the unburnt mixture ($T'=T'_0$), and $_b$ to the state at the burning temperature ($T'=T'_b$).

By introducing $T=T'-T'_0$, $B=u\rho=u_0\rho_0$, and $p=\mathrm{d}T'/\mathrm{d}x$, and neglecting the term $(\mathrm{d}\lambda/\mathrm{d}T)(\mathrm{d}T/\mathrm{d}x)^2$ in view of its low magnitude (this can always be verified by calculation), we obtain from equation 1

$$p\,(\mathrm{d}p/\mathrm{d}T)-Bcp+\Phi(T)=0 \quad \ldots . [4]$$

under boundary conditions:

$$T=0,\ p=0 \qquad \ldots . [5]$$

$$T=T_b,\ p=0 \qquad \ldots . [6]$$

According to thermal theories[14], the activation energy involved in the expression for heat release $\Phi(T)$ is sufficiently high for $\Phi(T)$ to be neglected at low temperatures. This is well known. Another extreme case will be considered here, i.e. low activation energies of about 5 to 15 kcal/mole.

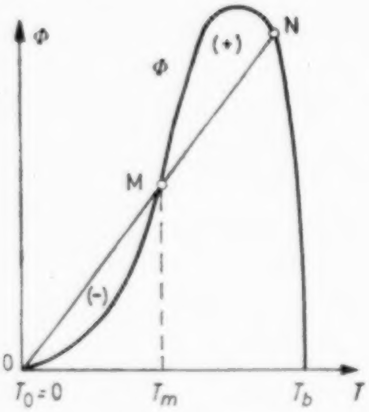

Figure 1. Linear approximation of the first part of the heat release curve, Φ, by a straight line 0MN, *at low activation energies*

A curve, Φ, for low activation energies is plotted in *Figure 1*. Approximation of the first part of Φ by the 0MN line, so that point M falls on curve Φ, shows that the area below Φ from $T=0$ to T_b will be defined without appreciable error. Sign $(-)$ denotes that part of the area, up to point M, which is superfluous in linear approximation, and sign $(+)$ the part that will be disregarded. At higher activation energy values a sharp maximum will be seen near $T=T_b$ and its approximation by a straight line will lead to a gross error (*Figure 2*). Determination of the T_m temperature represented by point M will be discussed later.

If linear approximation of curve $\Phi(T)$ is permissible, the formula of A. N. KOLMOGOROV, I. G. PETROVSKY and N. S. PISKUNOV[15] may be applied. It determines the lower eigenvalue spectrum end point of equation 4 under conditions 5 and 6. Problems demonstrating the uniqueness of solution 4 were treated in ref. 6, and briefly discussed in refs. 7 and 8.

Thus, according to the formula of Kolmogorov, Petrovsky and Piskunov:

$$B=u_0\rho_0=\frac{2}{c_0}\left[\lambda_0\Phi'(0)\right]^{\frac{1}{2}} \qquad \ldots.[7]$$

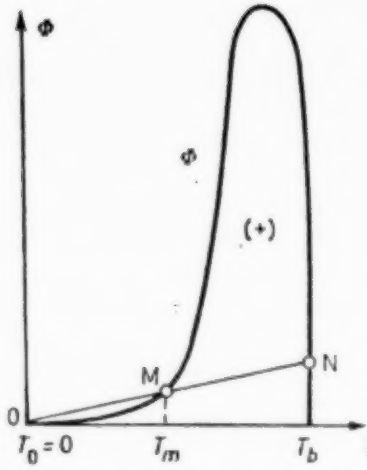

Figure 2. Linear approximation of Φ at high activation energies. This approximation would lead to a gross error, as the area under the curve, (+), is large compared with that below 0MN

where $\Phi'(0)$ is the Φ function derivative in point $T=0$. Under the given approximation $\Phi'(0)$ will be the slope angle of 0MN. Thus, in accordance with *Figure 1*, it may be written that

$$\Phi'(0)=\Phi(T_m)/T_m \qquad \ldots.[8]$$

Substituting equation 8 into 7 we obtain a relation for the burning velocity, u_0, at low activation energy values involved in the expression for the heat release rate function $\Phi(T)$:

$$u_0=\frac{B}{\rho_0}=\frac{2}{c_0\rho_0}\left[\frac{\lambda_0\Phi(T_m)}{T_m}\right]^{\frac{1}{2}} \qquad \ldots.[9]$$

If M is chosen so as to obtain, at $T=T_m$, the maximum temperature gradient, $p=p_m$, it follows from equation 4 that

$$Bc_mp_m=\Phi(T) \qquad \ldots.[10]$$

(at $p=p_m$, $p'_m=0$; subscript $_m$ corresponds to values at $T=T_m$). Substituting equation 10 into 9 we get

$$B=\eta p_m \qquad \ldots.[11]$$

where $\eta=4\lambda_0c_m/c_0^2T_m\simeq4\lambda_0/c_0T_m$.

Relation 11 showing that the mass burning velocity, B, is proportional to the p_m value, is independent of Φ. Thus it is valid for any function of the heat release rate. We shall use it for the solution of sets of differential equations.

Knowledge of the temperature corresponding to p_m is necessary for the solution of equation 9. Approximate relations for determination of T_m in the case of a simple model chain reaction scheme were obtained in refs. 7 and 8. However, comparing results obtained by various approximate formulae with those estimated by numerical integration, the author has shown to a high degree of precision that $T_m = 0{\cdot}5\,T_b$. The same may be shown by even less complicated means by determining u_0 from equation 9 at several different values of $T_m > 0{\cdot}5\,T_b$. As may be readily determined, at low activation energies u_0 values calculated at $T_m > 0{\cdot}5\,T_b$ will not differ much from those at $T_m = 0{\cdot}5\,T_b$.

Approximate Solution for a Model One-centre Unbranched Chain Reaction

An unbranched chain reaction may be represented as[1, 6–8]

$$A \longrightarrow 2P \quad \Phi_R = h_R R \qquad \ldots.[12]$$

(or $M + A \longrightarrow 2P + M$)

$$P + A \longrightarrow 2C + P \quad \Phi = Qn = hFn = hk\,(T)\,n_A n \qquad \ldots.[13]$$

$$2P + M \longrightarrow A + M \quad \Phi_W = h_W W\,(T)\,n^2 \qquad \ldots.[14]$$

Here A is the initial substance, P the active centre, and C the reaction product. Expressions for the heat release (absorption) rate are written on the right; h_i is the heat of reaction (cal/mole), R the rate of chain initiation (mole/cm^3 . s), k the chain propagation rate constant (g^2/cm^3 . mole.s), W the quadratic chain termination rate constant (g^2/cm^3 . mole.s), n_A and n concentrations of A and P, respectively (mole/g mixture), and $T = T' - T'_0$.

The corresponding set of differential equations, accounting for steady-flame propagation, comprises three equations:

$$\frac{\mathrm{d}}{\mathrm{d}x}\left(\lambda\,\frac{\mathrm{d}T}{\mathrm{d}x}\right) - Bc\,\frac{\mathrm{d}T}{\mathrm{d}x} + \Phi_R + \Phi + \Phi_W = 0 \quad \ldots.[15]$$

$$\frac{\mathrm{d}}{\mathrm{d}x}\left(\rho D_A\,\frac{\mathrm{d}n_A}{\mathrm{d}x}\right) - B\,\frac{\mathrm{d}n_A}{\mathrm{d}x} - R - kn_A n + W_1 n^2 = 0 \quad \ldots.[16]$$

$$\frac{\mathrm{d}}{\mathrm{d}x}\left(\rho D_P\,\frac{\mathrm{d}n}{\mathrm{d}x}\right) - B\,\frac{\mathrm{d}n}{\mathrm{d}x} + R - Wn^2 = 0 \quad \ldots.[17]$$

under boundary conditions:

$$T = 0,\ n = n_0,\ n_A = n_{A0},\quad \mathrm{d}T/\mathrm{d}x = \mathrm{d}n_A/\mathrm{d}x = \mathrm{d}n/\mathrm{d}x = 0 \quad \ldots.[18]$$

$$T = T_b,\ n = n_b,\ n_A = n_{Ab},\quad \mathrm{d}T/\mathrm{d}x = \mathrm{d}n_A/\mathrm{d}x = \mathrm{d}n/\mathrm{d}x = 0 \quad \ldots.[19]$$

where D_A and D_P are diffusion coefficients of the initial substance, A, and of the active centre, P, respectively (cm^2/s). The meaning of subscripts was given in the first section.

By assuming that in equation 15

$$\Phi > (\Phi_R + \Phi_W)$$

and in equation 16

$$kn_A n > (R - W_1 n^2)$$

which always takes place in flame, and that $\lambda = c\rho D_A$, it becomes possible to apply only one equation, 15 or 16, instead of the two, as under these conditions A will be a function of temperature alone, $n_A = n_A\,(T)$. Then $R = R\,(T)$ and $F = F\,(T)$. Initial substance concentrations will be considered hereafter as a function of temperature. Thus, introducing $D = \rho Dp$ and $p = \mathrm{d}T/\mathrm{d}x$ we obtain a set of two equations, temperature being the independent variable,

$$\lambda p\,(\mathrm{d}p/\mathrm{d}T) - Bcp + Qn = 0 \quad \ldots.[20]$$

$$Dp^2\,(\mathrm{d}^2n/\mathrm{d}T^2) - p\,[B - D\,(\mathrm{d}p/\mathrm{d}T)]\,(\mathrm{d}n/\mathrm{d}T) + R = 0 \quad \ldots.[21]$$

under boundary conditions:

$$T = 0,\ p = 0 \qquad \ldots.[22]$$

$$T = T_b,\ p = 0 \qquad \ldots.[23]$$

For the sake of simplicity and for fitting equation 21 into the reaction scheme of ref. 1, it was assumed that $Wn^2 = 0$. The solution at $Wn^2 \neq 0$ has been given in ref. 11.

In considering the results of numerical integration of equations 20 and 21 carried out by Spalding[1], it was found[7, 8] that the plot of n versus T would be approximated to high precision by a second order parabola. Thus the approximate solution for equation 21 was given as

$$n = n_0 + c_1 T + c_2 T^2 \qquad \ldots.[24]$$

where c_1 and c_2 were determined so as to get

$$n_b = n_0 + c_1 T_b + c_2 T_b^2 \qquad \ldots[25]$$

and $(\mathrm{d}n/\mathrm{d}T)=c_1+2c_2T$ and $(\mathrm{d}^2n/\mathrm{d}T^2)=2c_2$ obtained by differentiation of 24 satisfy equation 21 at $T=T_m$, at which temperature $p=p_m$ and $(\mathrm{d}p/\mathrm{d}T)_m=0$. Under these conditions we obtain from equation 21

$$D_m p_m^2 2c_2 - Bp_m(c_1+2c_2T_m)+R_m=0 \qquad \ldots .[26]$$

From equations 25 and 26:

$$c_1=\frac{R_m-Bp_ml}{Bp_m(2T_m-T_b)-2D_mp_m^2}, \quad c_2=l-c_1T_b \qquad \ldots .[27]$$

where $l=(n_b-n_0)/T_b$.

Substituting equation 27 into 24 we obtain an approximate solution for 21

$$n=(n_0+lT)-\frac{R_m-Bp_ml}{Bp_m(2T_m-T_b)-2D_mp_m^2}\times T(T_b-T) \qquad \ldots .[28]$$

Equation 28 is written down so as to obtain coincidence of the extreme points of its range of application with the exact solution, the derivatives in an intermediate $T=T_m$ point satisfying equation 21. High accuracy is ensured thereby. Choice of the intermediate point at $T=T_m$ greatly simplifies the ultimate result, and permits solution of equation 28, together with 20 by means of 11.

Equation 28 may now be substituted into 20. At $T=T_m$ we get

$$-Bc_mp_m+Q_m\left[t-\frac{R_m-Blp_m}{Bp_ms-2D_mp_m^2}r\right]=0 \qquad \ldots .[29]$$

where

$t=n_0+lT_m$, $s=(2T_m-T_b)$ and $r=T_m(T_b-T_m)$.

Substituting equation 11 into 29 we obtain an equation for determining p_m

$$c_m\eta(2D_m-\eta s)p_m^4-Q_m[t(2D_m-\eta s)-\eta lr]p_m^2-R_mQ_mr=0 \qquad \ldots .[30]$$

At $T_m=0{\cdot}5\,T_b$ (s being zero) equation 30 becomes

$$2c_m\eta D_mp_m^4-Q_m(2D_mt-\eta lr)p_m^2-R_mQ_mr=0 \qquad \ldots .[31]$$

Thus the burning velocity will be determined by the relation:

$$u_0=\frac{B}{\rho_0}=\frac{1}{\rho_0}\eta p_m \qquad \ldots .[32]$$

where p_m will be found from equation 30 or 31. Estimation of the error brought about by the assumption that $T_m=0{\cdot}5\,T_b$ was discussed in the preceding section of this paper.

The positive root of equation 31 is

$$p_m^2=\frac{Q_mt\omega}{2c_m\eta}\left[1+\left(1+\frac{2c_m\eta rR_m}{Q_mD_mt^2\omega^2}\right)^{\frac{1}{2}}\right] \qquad \ldots .[33]$$

where $2D_mt-\eta lr=2D_mt\omega$ and $\omega=1-2q/\kappa$, as

$$lT_m=t-n_0\simeq t, \quad D_0=D_mq, \quad \kappa=c_0D_0/\lambda_0,$$

$$q=(\mu_0/\mu_m)(T'_0/T'_m)^{(a-1)}$$

at $D_P\sim(T')^a$, and μ is the molecular weight of the mixture (g/mole).

By substituting equation 33 into 32 and making simple transformations, we finally obtain the relation for the burning velocity rate

$$u_0=\phi\xi\frac{1}{\rho_0}\left(\frac{n_bQ_m\rho_mD_{Pm}}{2c_mT_b}\right)^{\frac{1}{2}} \qquad \ldots .[34]$$

where

$$\phi=2\left[\frac{2q}{\kappa}\left(1-\frac{2q}{\kappa}\right)\right]^{\frac{1}{2}} \qquad \ldots .[35]$$

$$\xi=\left\{\tfrac{1}{2}\left[1+\left(1+\frac{16q\kappa c_mT_bR_m}{(\kappa-2q)^2n_b^2Q_m}\right)^{\frac{1}{2}}\right]\right\}^{\frac{1}{2}} \qquad \ldots .[36]$$

In deriving equations 34 to 36 it was assumed that $t=n_0+lT_m=(n_b+n_0)/2\simeq n_b/2$.

Discussion

The error in using equation 9 accounted for by linear approximation of the heat release function may always be estimated for a given $\Phi(T)$ function (*Figure 1*). It would be of interest to determine the error incurred in equation 28, as compared with the exact solution of equation 21. At the present time the latter may be obtained only by numerical integration of the system involving equations 20 and 21. This was made by Spalding for the hydrazine flame decomposition[1].

The dependence of n on T obtained by Spalding[1] is represented in *Figure 3* by the dotted line and denoted by n_S. The full line represents the same dependence, n_I, calculated at $B=\eta p_m$ from equation 28, where p_m was determined from equation 31. Equation 28 may be seen to give a result very near to that obtained in numerical integration. The good

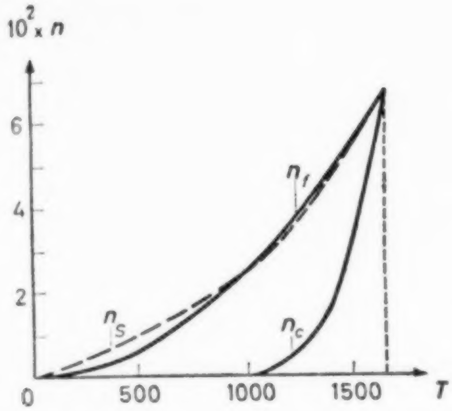

Figure 3. Active centre concentration, n, as a function of temperature in hydrazine decomposition: n_S—in flame, from results of numerical integration[1]; n_f—in flame, from equation 28; n_c—on spontaneous ignition or in flame, active centre diffusion being neglected[1] (g/g mixture)

agreement may be explained by the fact that two extreme and one intermediate point on the approximating parabola coincide with three points of the exact solution.

Figure 3 shows one more function $n_c = n_c(T)$ for spontaneous ignition in a closed vessel (ignition occurring simultaneously and uniformly throughout the volume). This function is obtained from a set of kinetic equations:

$$\rho\,(\mathrm{d}n_A/\mathrm{d}t) = k\,(T)\,n_A n \quad \ldots.[37]$$

$$\rho\,(\mathrm{d}n/\mathrm{d}t) = R\,(T) \quad \ldots.[38]$$

$$h\,(n_{A_0} - n_A) = cT \quad \ldots.[39]$$

integrated numerically by Spalding[1] for the very case of hydrazine decomposition for which the n_s function was obtained.

Under spontaneous ignition conditions, after solving equations 37 and 38 and eliminating the time, n_c may be represented as a function of temperature alone. This case of reaction development in flame would correspond to an idealized case of flame propagation with heat transfer through thermal conductivity, but without diffusion of active centres. Values of active centre concentrations given by the n_c function throughout the reaction time, up to the burning temperature, may be seen to be lower than the n_s value. This may be accounted for by the fact that active centres from regions near to the burning temperature are carried by the diffusion flow into moderate temperature regions. The same active centre concentration will be observed for any case at the burning temperature. Its value may be estimated by thermodynamic calculations.

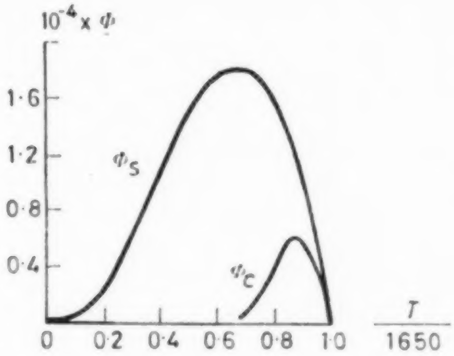

Figure 4. Heat release rate as a function of temperature in hydrazine decomposition[1]. Φ_c—on spontaneous ignition; Φ_S—in flame (cal/cm^3. s)

Figure 4 shows two heat release rate functions corresponding to n_c and n_S. Under spontaneous ignition (or in flame in the absence of active centre diffusion) the rate of heat release will be $\Phi_c = Qn_c$, and in flame $\Phi_S = Qn_S$. Since within the range from $T > 0$ to $T < T_b$, $n_S > n_c$, correspondingly $\Phi_S > \Phi_c$. Thus, other things being equal (including equal heat values), the rate of heat release in flame will exceed that taking place in spontaneous ignition. This is accounted for by the increased concentration of active centres in the intermediate temperature range, at the expense of diffusion from regions adjacent to that of the burning temperature. Φ_s and Φ_c functions shown in *Figure 4* were obtained by numerical integration in the work of Spalding[1].

Comparison of Φ_s and Φ_c shows that diffusion of active centres should by no means be neglected in the solution of problems concerned with flame propagation in branched chain systems. In other words equations for active centre diffusion have to be solved together with the equation for conservation of energy.

Burning velocities estimated from equation 34[1] were compared with those obtained by numerical integration[1]. All starting data were taken from the work of Spalding (see also ref. 8). The results obtained are summarized in *Table 1*.

Table 1. Theoretical burning velocity values in hydrazine decomposition (cm/s)

	$T_b'=1\,950°$K	$T_b'=1\,280°$K
Numerical integration[1]	160	11
From equation 34	147	7·35

The good agreement is accounted for by consistency of equation **28** with the exact solution, and by the fact that the approximate formula **9** gives a u_0 value that does not differ appreciably from the exact one. The activation energy involved in k and used in calculations leading to results summarized in *Table 1* was 7 kcal/mole.

The error given by equation **34** increases with lower burning temperatures, but remains quite permissible up to **1 300**°K, as can be seen from *Table 1*. The temperature of **1 300**°K usually corresponds to the combustion limit.

Approximate Solution for an Unbranched Chain Reaction Involving Two Active Centres

The reaction scheme, where A and B are initial substances, C the reaction product, and P_1 and P_2 active centres, was taken as in ref. **10**:

$$\mathrm{M+A \longrightarrow 2P_1+M},\quad \Phi_R=h_R R(T) \qquad \ldots .[40]$$

$$\mathrm{P_1+Z \longrightarrow C+P_2},\quad Q_1 n_1=h_1 F_1 n_1=h_1 k_1(T)\, n_Z n_1 \qquad \ldots .[41]$$

$$\mathrm{P_2+A \longrightarrow C+P_1},\quad Q_2 n_2=h_2 F_2 n_2=h_2 k_2(T)\, n_A n_2 \qquad \ldots .[42]$$

$$\mathrm{P_2+C \longrightarrow Z+P_1},\quad Q_3 n_2=h_3 F_3 n_2=h_3 k_3(T)\, n_C n_2 \qquad \ldots .[43]$$

$$\mathrm{P_1+C \longrightarrow A+P_2},\quad Q_4 n_1=h_4 F_4 n_1=h_4 k_4(T)\, n_C n_1 \qquad \ldots .[44]$$

$$\mathrm{2P_1+M \longrightarrow A+M},\quad X n_1^2=h_W W(T)\, n_1^2 \qquad \ldots .[45]$$

Conditions, definitions and units of measurement for expressions of heat release rates shown on the right remain similar to those mentioned before.

The following set of equations accounts for the given scheme:

$$\frac{\mathrm{d}}{\mathrm{d}x}\left(\lambda\frac{\mathrm{d}T}{\mathrm{d}x}\right)-Bc\frac{\mathrm{d}T}{\mathrm{d}x}+S_1 n_1+S_2 n_2+X n_1^2+\Phi_R=0 \qquad \ldots .[46]$$

$$\frac{\mathrm{d}}{\mathrm{d}x}\left(D_1\frac{\mathrm{d}n_1}{\mathrm{d}x}\right)-B\frac{\mathrm{d}n_1}{\mathrm{d}x}+G_2 n_2-G_1 n_1+R-W n_1^2=0 \qquad \ldots .[47]$$

$$\frac{\mathrm{d}}{\mathrm{d}x}\left(D_2\frac{\mathrm{d}n_2}{\mathrm{d}x}\right)-B\frac{\mathrm{d}n_2}{\mathrm{d}x}+G_1 n_1-G_2 n_2=0 \qquad \ldots .[48]$$

where $D_1=\rho D_{P_1}$, $D_2=\rho D_{P_2}$, D_{P_1} and D_{P_2} are diffusion coefficients of P_1 and P_2, $G_1=F_1+F_4$, $G_2=F_2+F_3$, $S_1=Q_1+Q_4$ and $S_2=Q_2+Q_3$.

By making use of the approximate method for the solution of diffusion equations, the active centre concentrations at $T_m=0{\cdot}5\,T_b$ may be written, in accordance with equations 47 and 48, as:

$$n_{1m}=t_1+(R_m+G_{2m}n_{2m}-G_{1m}n_{1m}-Bl_1 p_m)\,N_1 \qquad \ldots .[49]$$

$$n_{2m}=t_2+(G_{1m}n_{1m}-G_{2m}n_{2m}-Bl_2 p_m)\,N_2 \qquad \ldots .[50]$$

where $l_i=(n_{ib}-n_{i0})/T_b$, $t_i=n_{i0}+l_i T_m$ and $N_i=r/2D_{im}p_m^2$ It was assumed approximately in equations **49** and **50** that $Wn_1^2=0$.

By solving equations **49** and **50**, substituting n_{1m} and n_{2m} into **46** at $T=T_m$, and allowing for $B=\eta p_m$ we obtain a sixth power equation for p_m. It was given in ref. **10** and is similar to equations **30** and **31**. Approximate solution of this equation gives an approximate relation for the burning velocity:

$$u_0=\phi\xi\psi\frac{1}{\rho_0}\left(\frac{n_b Q_m \rho_m D_{Pm}}{2c_m T_b}\right)^{\frac{1}{2}} \qquad \ldots .[51]$$

$$n_b=(n_{1b}+n_{2b})\,\phi_D^2 \qquad \ldots .[52]$$

$$\phi_D^2=\frac{n_{1b}D_{1m}+n_{2b}D_{2m}}{(n_{1b}+n_{2b})}\,\frac{(G_{1m}+G_{2m})}{(G_{1m}D_{2m}+G_{2m}D_{1m})} \qquad \ldots .[53]$$

$$Q_m=\frac{S_{1m}G_{2m}+S_{2m}G_{1m}}{G_{1m}+G_{2m}} \qquad \ldots .[54]$$

$$D_{Pm}=\frac{n_{1b}D_{P1m}+n_{2b}D_{P2m}}{n_{1b}+n_{2b}} \qquad \ldots .[55]$$

$$\phi = 2\left[\frac{2q}{\kappa}\left(1-\frac{2q}{\kappa}\right)\right]^{\frac{1}{2}} \quad \ldots .[56]$$

Coefficients ξ and ψ* taking into account the effects of chain initiation and quadratic chain termination rates are estimated from the relations:

$$\xi = \left\{\tfrac{1}{2}\left[1+\left(1+\frac{16q\kappa c_m T_b R_m}{(\kappa-2q)^2 n_b^2 Q_m}\right)^{\frac{1}{2}}\right]\right\}^{\frac{1}{2}} \quad \ldots [57]$$

$$\psi = \left(1+\frac{q c_m T_b W_m}{\kappa Q_m}\right)^{-\frac{1}{2}} \quad \ldots .[58]$$

where

$$\frac{2q}{\kappa} = \frac{2q_1 q_2 (n_{1b}+n_{2b})}{n_{1b}\kappa_1 q_1 + n_{2b}\kappa_2 q_2}$$

$$D_i = \rho D_{Pi}, \quad \kappa_i = c_0 D_{i0}/\lambda_0,$$

and

$$q = (\mu_0/\mu_m)(T'_0/T'_m)^{a_i-1}, \text{ at } D_{Pi} \sim (T')^{a_i},$$
$$T_m = 0{\cdot}5\, T_b.$$

Theoretical burning velocities for a chlorine–hydrogen flame were obtained from equation **51** and are summarized in *Table 2* together with the results of E. Bartholomé[16]. Reaction rate constants found experimentally by kinetic methods independent of flame were taken from the results of A. F. Trotman-Dickenson[17] and are given in ref. **10** together with all starting data and parameters obtained by thermodynamic calculations.

Table 2. Experimental and theoretical burning velocities (cm/s) for chlorine–hydrogen mixtures

Source	$0{\cdot}6\,H_2+0{\cdot}4\,Cl_2$	$0{\cdot}5\,H_2+0{\cdot}5\,Cl_2$
Experimental results of E. Bartholomé[16]	405	350
From eq. 51 at $k_2'=10^{13{\cdot}7}$*	347	368
From eq. 51 at $k_2'=10^{13{\cdot}4}$*	252	278

*Two values of the pre-exponential factor of the constant for process $H+Cl_2 \rightarrow HCl+Cl$, $k_2'=10^{13{\cdot}7}$ cm³/mole. s, and $k_2'=10^{13{\cdot}4}$ cm³/mole . s were adopted in ref. 10, in accordance with ref. 17.

Relation **51** obtained for an unbranched chain reaction scheme **40** to **44** involving two active centres is written in the same form as equation **34**. It corresponds to a model reaction with a one-type active centre. This permits estimation of parameters for a model one-centre reaction, determined by processes **12** to **14**, from results for a real unbranched chain reaction scheme by means of **51** to **58**. Hence verification of equation **34** by the results of numerical integration shows the validity of **51** to **58** for the solution of a two-centre problem.

Thus, theoretical burning velocities calculated from equation **34** and the results of numerical integration of starting equations (*Table 1*) are in good agreement, as well as theoretical and experimental results (*Table 2*). This warrants the conclusion that the above theoretical treatment of flame propagation in unbranched chain systems gives a correct description of a real flame propagation process.

The results obtained provide confirmation for the possibility of determining true constants and activation energies for elementary processes from experimental relations for the burning velocity against burning temperatures. Let us simplify equation **54** by assuming that $F_3=F_4=0$, i.e. that the unbranched reaction proceeds only by two chain propagation steps **41** and **42**. Then:

$$Q_m = \frac{Q_{1m}F_{2m}+Q_{2m}F_{1m}}{F_{1m}+F_{2m}} = (h_1+h_2)\frac{F_{1m}F_{2m}}{F_{1m}+F_{2m}} \quad \ldots .[59]$$

If for instance, in mixtures with excess of Z, $F_{1m} > F_{2m}$ and $D_{1m}=D_{2m}$, the value of $Q_m \simeq (h_1+h_2)F_{2m}$, the constant k_2 and its activation energy, E_2, may be determined from u_0 as a function of T'_b. Once k_2 and E_2 values are known, k_1 and E_1 in mixtures with excess of A may be determined from u_0 as a function of T'_b.

As follows from equation **51** the slope angle in the plot $\log u_0^2$ versus $1/T'_b$ is dependent not only upon activation energy of processes **41** to **43**, but also upon the temperature dependence of active centre concentrations, n_b (relation **52**). (The effect of equation **40** may in practice be neglected.)

As may be seen, for example, from equation **40** the P_1 concentration function at the burning temperature will be determined by the heat of P_1 formation, which is usually high, whilst activation energies of the chain propagation processes 41 to 43 are relatively low. Consequently the temperature dependence of u_0 appears to be determined mainly by the n_b function, i.e. by the heat of formation of active centres.

---

*The relation for ξ and ψ was obtained on the basis of ref. 11.

Approximate Solution for a Model One-centre Branched Chain Reaction

The solution of this problem was given in refs. 11 and 13. The reaction scheme was assumed to be:

A ⟶ 2P (initiation),

$$\Phi_R = h_R R\,(T) \quad \ldots.[60]$$

P + A ⟶ 2C + P (propagation),

$$Qn = hFn = hk\,(T)\,n_A n \quad \ldots.[61]$$

P + A ⟶ C + 2P (branching),

$$Q_V n = h_V Vn = h_V k_V\,(T)\,n_A n \quad \ldots.[62]$$

(P ⟶ linear termination if $V < 0$)
2P ⟶ A (quadratic termination),

$$Xn^2 = h_W W\,(T)\,n^2 \quad \ldots.[63]$$

where A is the initial substance, C the reaction product, and P the active centre. Symbols and units have been given above.

At $\lambda = c\rho D_A$ the following set of equations will account for the chain reaction scheme[11]:

$$\frac{d}{dx}\left(\lambda\frac{dT}{dx}\right) - Bc\frac{dT}{dx} + \Phi_R + Q_{\Sigma} n + Xn^2 = 0 \quad \ldots.[64]$$

$$\frac{d}{dx}\left(D\frac{dn}{dx}\right) - B\frac{dn}{dx} + R + Vn - Wn^2 = 0 \quad \ldots.[65]$$

where $Q_{\Sigma} = Q + Q_V$.

The solution obtained from equations 64 and 65, taking into account the four processes 60 to 63, is given in refs. 11 and 13.

Less complicated relations may be obtained with $F_m \leqslant V_m$ on the basis of ref. 13, under the assumption that the initial and final active centre concentrations are zero ($n_0 = n_b = 0$). This simplification is possible, as the active centre concentration in the reaction zone is considerably higher than at the burning temperature. As shown before[7–10] the effect of conventional chain initiation rates upon the burning velocity is not important. The same conclusion may be drawn from relations obtained in refs. 11–13. Thus, on condition that $R_m = 0$, and $n_0 = n_b = 0$, we get a simple relation for the burning velocity

$$u_0 = \eta\frac{1}{\rho_0}\left[\frac{r\,(Q_{\Sigma m} + V_m h_W)\,W_m}{\eta c_m r W_m + 2D_m\,(Q_{\Sigma m} + 2V_m h_W)}\right]^{\frac{1}{2}} \quad \ldots.[66]$$

Assuming that $F_m = 0$, i.e. that a completely branched reaction takes place, we obtain

$$u_0 = \frac{4\lambda_0}{\rho_0 c_0}\left[\frac{c_0\,(h_V + h_W)\,V_m^2}{2\lambda_0 c_m T_b W_m + 2c_0 D_m\,(h_V + 2h_W)\,V_m}\right]^{\frac{1}{2}} \quad \ldots.[67]$$

This is consistent with the simplified reaction scheme of Giddings and Hirschfelder[2] involving only two processes:

2P ⟶ A, and P + A ⟶ C + 2P.

Flame propagation rate constants were estimated from equation 67 for three cases. The values of u_0 determined by numerical integration of the corresponding system of equations were taken from ref. 2. The results obtained are summarized in *Table 3*.

Table 3. Theoretical burning velocity values of u_0 (cm/s)

Source	$\kappa = c_0\rho_0 D_{V0}/\lambda_0$ 1	 2	 0
Numerical integration[2]	55·1	54·8	58·3
From eq. 67	59·7	58·5	60·9

As can be seen from *Table 3*, there is a good fit between the two sets of values. This provides confirmation for equation 67 and warrants its use in the determination of rate constants for elementary chain branching processes from the burning velocity as a function of temperature.

A somewhat modified reaction scheme, corresponding to the hydrogen oxidation reaction, may be represented in a simple form as a model one-centre reaction involving processes 2P ⟶ A and P ⟶ 3P. This modification would require substitution of $2V_m$ for all V_m in equation 67. Thus another relation will be obtained

$$u_0 = \frac{4\lambda_0}{\rho_0 c_0}\left[\frac{2c_0\,(h_V + h_W)\,V_m^2}{\lambda_0 c_m T_b W_m + 2c_0 D_m\,(h_V + 2h_W)\,V_m}\right]^{\frac{1}{2}} \quad \ldots.[68]$$

By neglecting the first term of the radicand denominator as compared with the first one (i.e. by assuming that $W_m = 0$ and $h_W = 0$), the relation for u_0 may be further simplified

$$u_0 = \frac{4\lambda_0}{\rho_0 c_0}\left(\frac{V_m}{D_m}\right)^{\frac{1}{2}} = \frac{4\lambda_0}{\rho_0 c_0}\left(\frac{k_{Vm} n_{Am}}{D_m}\right)^{\frac{1}{2}} \quad \ldots.[69]$$

Thus, if the ratio involving the radicand components of equation 68

$$M_W = \frac{\lambda_0}{2c_0 D_m}\,\frac{c_m T_b}{(h_V + 2h_W)}\,\frac{W_m}{V_m} \quad \ldots.[70]$$

is sufficiently low, and the term $\lambda_0 c_m T_b W_m$ may be neglected as compared with

$$2c_0 D_m\,(h_V + 2h_W)\,V_m$$

without surpassing the permissible error in u_0, the rate of quadratic chain termination may be disregarded, and u_0 may be determined from equation 69.

As stated in ref. 2 (*Table 3*), a considerable change in the active centre diffusion coefficient (with change in κ) exerts no important effect on u_0, the latter decreasing with increase in D_P. The nature of the u_0 change may be explained by equation 67. Numerical integration in ref. 2 was made under the assumption of a very high rate constant for quadratic chain termination, the first component of the denominator exceeding the second by a factor of 10 to 20. Thus the calculated u_0 value is almost independent of D_P.

C. E. Mellish and J. W. Linnett[18] report a ratio of burning velocity rates for two mixtures ($0{\cdot}21\,H_2 + 0{\cdot}11\,O_2$), the first with an addition of 0·68 of helium, and the second with 0·68 of argon. The experimental value of this ratio is $(u_0)_{He}/(u_0)_A = 2{\cdot}40$. From this value and at $\lambda_{He}/\lambda_A = 3{\cdot}76$, and $(D_P)_{He}/(D_P)_A = 1{\cdot}32$[13, 18], it is possible to obtain by equation 68 the value of $M_W = 0{\cdot}52$. The quadratic chain termination constant $k_{Wm} = W_m \mu_m / \rho_m^3 = 10^{17}$ cm^6/mole^2.s may be estimated from the experimental M_W value and equation 70. If the experimental ratio, $(u_0)_{He}/(u_0)_A$, were obtained for mixtures of a lower burning temperature, it would be higher than 0·52, and k_{Wm} could be determined to a higher degree of precision.

Approximate Solution for a Branched Chain Reaction Involving Three Active Centres

The hydrogen combustion reaction[19] is taken as an example of a chain reaction[12], chain termination processes being disregarded:

$$H_2 + O_2 \longrightarrow 2OH,$$
$$\Phi_{R1} = h_{R1} R_1\,(T) \quad \ldots.[71]$$

$$H_2 + M \longrightarrow 2H + M,$$
$$\Phi_{R2} = h_{R2} R_2\,(T) \quad \ldots.[72]$$

$$O_2 + O_2 \longrightarrow O + O_3,$$
$$\Phi_{R3} = h_{R3} R_3\,(T) \quad \ldots.[73]$$

$$OH + H_2 \longrightarrow H_2O + H,$$
$$Q_1 n_1 = h_1 F_1 n_1 = h_1 k_1\,(T)\,n_A n_1 \quad \ldots.[74]$$

$$H + O_2 \longrightarrow OH + O,$$
$$Q_2 n_2 = h_2 F_2 n_2 = h_2 k_2\,(T)\,n_Z n_2 \quad \ldots.[75]$$

$$O + H_2 \longrightarrow OH + H,$$
$$Q_3 n_3 = h_3 F_3 n_3 = h_3 k_3\,(T)\,n_A n_3 \quad \ldots.[76]$$

Here n_1, n_2 and n_3 denote concentrations in OH, H and O (mole/g mixture), n_A and n_Z concentrations in H_2 and O_2 (mole/g mixture), and the other definitions may be found in preceding sections. Diffusion coefficients of H_2, O_2 and H_2O are assumed to be equal to temperature conductivity ($\lambda = c\rho D_A = c\rho D_Z = c\rho D_c$), and consequently $R_i = R_i\,(T)$ and $F_i = F_i\,(T)$.

Under given conditions and with the adopted reaction scheme the system will comprise four equations:

$$\frac{d}{dx}\left(\lambda\frac{dT}{dx}\right) - Bc\frac{dT}{dx} + \Phi_R + Q_1 n_1 + Q_2 n_2 + Q_3 n_3 = 0 \quad \ldots.[77]$$

$$\frac{d}{dx}\left(D_1\frac{dn_1}{dx}\right) - B\frac{dn_1}{dx} + R_1 + F_2 n_2 + F_3 n_3 - F_1 n_1 = 0 \quad \ldots.[78]$$

$$\frac{d}{dx}\left(D_2\frac{dn_2}{dx}\right) - B\frac{dn_2}{dx} + R_2 + F_1 n_1 + F_3 n_3 - F_2 n_2 = 0 \quad \ldots.[79]$$

$$\frac{d}{dx}\left(D_3\frac{dn_3}{dx}\right) - B\frac{dn_3}{dx} + R_3 + F_2 n_2 - F_3 n_3 = 0 \quad \ldots.[80]$$

where $D_i = \rho D_{Pi}$, and D_{P1}, D_{P2} and D_{P3} are diffusion coefficients for OH, H and O (cm^2/s).

The u_0 function (cm/s) was obtained in ref. 12

$$u_0 = \frac{1}{\rho_0} \eta p_m \qquad \ldots . [81]$$

Here p_m is obtained from the eighth power equation given in ref. 12. Let us make a number of simplifying assumptions, including the allowance for relatively low chain initiation rates[7, 8, 10–12] ($R_1 = R_2 = R_3 = 0$), and neglect all terms containing active centre concentrations at the initial and burning temperatures. This would be possible for completely branched chain systems when the concentration of active centres in the reaction zone exceeds equilibrium values at the burning temperature, and burning velocities in practice do not depend on equilibrium active centre concentration. An approximate equation for p_m is then obtained

$$(F_{1m}\delta_1 + F_{2m}\delta_2 + F_{3m}\delta_3)\, p_m^4 + (F_{1m}F_{3m}\delta_1\delta_3)\, p_m^2 - F_{1m}F_{2m}F_{3m}2\delta_1\delta_2\delta_3 = 0 \qquad \ldots . [82]$$

where $\delta_i = T_m^2 / 2D_{im}$.

Apparently it will always be that $F_{1m}\delta_1 > F_{3m}\delta_3$, as $\delta_1 \simeq \delta_3$ and $k_{1m} > k_{3m}$. The inequality $k_{1m}n_{Am}D_{2m} > k_{2m}n_{Zm}D_{1m}$ will be unfulfilled only with lean mixtures, as the hydrogen atom diffusion coefficient is $D_{P2} \simeq 4D_{P1}$, and $k_{1m} > k_{2m}$[19]. Thus it may be assumed that $F_{1m}\delta_1 > (F_{2m}\delta_2 + F_{3m}\delta_3)$. Then from equation 82 we obtain

$$p_m^4 + F_{3m}\delta_3 p_m - 2F_{2m}F_{3m}\delta_2\delta_3 = 0 \qquad [83]$$

Hence

$$p_m^2 = \tfrac{1}{2}F_{3m}\delta_3 \left[\left(1 + \frac{8F_{2m}\delta_2}{F_{3m}\delta_3}\right)^{\frac{1}{2}} - 1 \right] \qquad \ldots . [84]$$

At $8F_{2m}\delta_2 < F_{3m}\delta_3$, expanding the radical in equation 84 into series, we get

$$p_m^2 = 2F_{2m}\delta_2 \qquad \ldots . [85]$$

Thus, even at $8F_{2m}\delta_2 / F_{3m}\delta_3 = 1$, the error in determining u_0 from equations 81 and 85 will be only 9 per cent, as compared with determinations from equations 81 and 84.

By substituting equation 85 into 81 we obtain a simple relation for u_0 at

$$8k_{2m}n_{Zm}D_{P3m} < k_{3m}n_{Am}D_{P2m}$$

$$u_0 = \frac{4\lambda_0}{\rho_0 c_0}\left(\frac{F_{2m}}{D_{2m}}\right)^{\frac{1}{2}} = \frac{4\lambda_0}{\rho_0 c_0}\left(\frac{k_{2m}n_{Zm}}{D_{2m}}\right)^{\frac{1}{2}} \qquad \ldots . [86]$$

This relation was given in ref. 12 and is consistent with that for a model one-centre problem, equation 69.

When $8F_{2m}\delta_2$ is slightly higher than $F_{3m}\delta_3$ determination of u_0, as well as of k_{2m} or k_{3m} from the experimental dependence of u_0 on burning temperature, should be made by equations 81 and 84.

When the radicand numerator in equation 84 is many times higher than the denominator, $8F_{2m}\delta_2 \gg F_{3m}\delta_3$, an approximate relation for p_m may be derived from equation 84. Substituting it into equation 81 we obtain

$$u_0 = \frac{4\lambda_0}{\rho_0 c_0}\left(\frac{k_{2m}n_{Zm}k_{3m}n_{Am}}{2D_{2m}D_{3m}}\right)^{\frac{1}{4}} \qquad \ldots . [87]$$

Solution of the burning velocity problem for hydrogen oxidation neglected quadratic chain termination. However, relations 86 and 87 permit determination of parameters and constants for a model one-centre reaction accounted for by equations 68 or 69. Thus, by making use of equations 68 to 70 it is possible to determine with equation 86 or 87 the effect of quadratic chain termination on the burning velocity in a real system involving three active centres. Besides, if equation 69 is consistent with equations 86 and 87, verification of equation 67 by the results of numerical integration (*Table 3*) proves that the given solution for the above-mentioned system is correct. This shows that equations 81, 86 or 87 may be applied for determination of elementary process rate constants from burning velocities as a function of the burning temperature.

Equation 86 was used for determination of the experimental rate constant for process 75 from u_0 as a function of temperature for two rich hydrogen–oxygen mixtures[12]. The values of $k_2^0 = k_2/\rho^2$ for the two mixtures were determined by equation 86 from the results of G. JAHN[20] and E. BARTHOLOMÉ[16], and appeared to be

$k_2^0 = 1{\cdot}32 \times 10^{14} \exp(-14\,000/RT')\ \mathrm{cm^3/mole.s}$

and

$k_2^0 = 4{\cdot}72 \times 10^{14} \exp(-16\,300/RT')\ \mathrm{cm^3/mole.s}$

respectively. Mixture compositions and starting data adopted in calculations were given in ref. 12.

The k_2^0 values thus obtained are in good agreement with the value of

$$k_2^0 = 1{\cdot}4 \times 10^{14} \exp(-16\,200/RT')$$

obtained by V. V. AZATYAN, V. V. VOEVODSKY and A. B. NALBANDYAN[21].

To get a more precise k_2^0 value it would be necessary to apply the above treatment to mixtures of a still higher hydrogen content (rich mixtures). After that the experimental k_3^0 value for process 76 might be determined from u_0 as a function of temperature in hydrogen-deficient mixtures.

The author is greatly indebted to Academician V. N. Kondratiev for much helpful advice and encouragement.

References

1 SPALDING, D. B. *Phil. Trans. A*, 1956, **249**, 1

2 GIDDINGS, J. C. and HIRSCHFELDER, J. O. *Sixth Symposium (International) on Combustion*, pp 199–212. Reinhold: New York, 1957

3 CAMPBELL, E. S., HIRSCHFELDER, J. O. and SCHALIT, L. M. *Seventh Symposium (International) on Combustion*, pp 332–8. Butterworths: London, 1959

4 GIDDINGS, J. C. and HIRSCHFELDER, J. O. *J. phys. Chem.* 1957, **61**, 738

5 VON KÁRMÁN, T. *Sixth Symposium (International) on Combustion*, pp 1–11. Reinhold: New York, 1957

6 VON KÁRMÁN, T. and PENNER, S. S. *Selected Combustion Problems*, Vol. I, pp 5–41. Butterworths: London, 1954

7 LOVACHEV, L. A. *Dokl. Akad. Nauk S.S.S.R.* 1958, **120**, 1287

8 LOVACHEV, L. A. *Izvest. Akad. Nauk S.S.S.R., Otdel khim. Nauk*, **1959**, No. 10, 1740

9 LOVACHEV, L. A. *Dokl. Akad. Nauk S.S.S.R.* 1959, **124**, 1271

10 LOVACHEV, L. A. *Dokl. Akad. Nauk S.S.S.R.* 1959, **125**, 129

11 LOVACHEV, L. A. *Dokl. Akad. Nauk S.S.S.R.* 1958, **123**, 501

12 LOVACHEV, L. A. *Dokl. Akad. Nauk S.S.S.R.* 1959, **128**, 995

13 LOVACHEV, L. A. *Dokl. Akad. Nauk S.S.S.R.* 1960, **131**, 876

14 EVANS, M. W. *Chem. Rev.* 1952, **51**, 363

15 KOLMOGOROV, A. N., PETROVSKY, I. G. and PISKUNOV, N. S. *Bulleten Moskovskogo Gosudarstvennogo Universiteta*, Razdel A, 1937, **1**, No. 6

16 BARTHOLMÉ, E. *Z. Elektrochem.* 1950, **54**, 169

17 TROTMAN-DICKENSON, A. F. *Gas Kinetics*, pp 182–5. Butterworths: London, 1955

18 MELLISH, C. E. and LINNETT, J. W. *Fourth Symposium (International) on Combustion*, pp 407–19. Williams & Wilkins: Baltimore, 1953

19 KONDRATIEV, V. N. *Kinetics of Chemical Gas Reactions*, p 514. U.S.S.R. Academy of Sciences: Moscow, 1958

20 JAHN, G. *Der Zündvorgang in Gasgemischen*, p 21. Oldenbourg: Munich and Berlin, 1934

21 AZATYAN, V. V., VOEVODSKY, V. V. and NALBANDYAN, A. B. *Dokl. Akad. Nauk S.S.S.R.* 1960, **132**, No. 4

Recent Developments and Notes

Conference on Waste Heat Recovery

The Institute of Fuel is arranging to hold a second 'Conference on Waste Heat Recovery from Industrial Furnaces' in Bournemouth from **15** to **19** May **1961**. The chairman of the organizing committee is G. N. CRITCHLEY, who occupied the same position in connection with the first conference on this subject in **1946**.

About 20 papers are to be presented in the following sessions: (*i*) fundamental principles, (*ii*) regenerators and recuperators, (*iii*) raising steam from waste heat and the use of waste heat steam, (*iv*) gas turbines as a means of recovering waste heat; possible future means of recovering waste heat, (*v*) heat recovery in the steel industry, (*vi*) heat recovery in industries other than the steel industry.

An exhibition of plant and equipment illustrating the recovery of waste heat will be arranged. A limited number of shell-type stands will be available for hire. Applications for specifications, plant and stand space, and prices, should now be made to The Secretary, The Institute of Fuel, 18 Devonshire Street, Portland Place, London, W.1.

Action of Inhibitors in Flames

A. VAN TIGGELEN and M. GROGNARD, Laboratoire de Chimie Inorganique, Université de Louvain, have published a paper on the theory of the action of inhibitors in flames [*Bull. Soc. chim. France*, **1959**, 1818]. Their contribution to this subject is based on the characteristic parameters of chain reactions and these are discussed in relation to the two separate effects produced by the addition of inhibitors, first the contraction of the range of inflammability, and secondly the reduction in flame speed.

The theoretical equations that A. VAN TIGGELEN and his co-workers have previously advanced for flame propagation are first reviewed [*Mém. Acad. R. Belg. Cl. Sci.* **1952**, **27**, 1; *C.R. 27^e Congr. int. Chim. industr., Bruxelles, 1954*, Vol. III, p 324; *Sixth Symposium* (*International*) *on Combustion*, p 61. Reinhold: New York, **1957**]. The authors of the present paper consider inhibition as a particular case in the general behaviour of ternary inflammable mixtures containing either one or two fuels. If the addition of a substance to a binary inflammable mixture results in the probability of chain branching being greater than in the absence of such substance, then the reaction is promoted and not inhibited. A well-known example of this is the addition of a small amount of hydrogen to mixtures of carbon monoxide and oxygen. This is essentially a ternary inflammable mixture and to all such, according to the authors, their general equations apply, and include the effects, whether promotion or inhibition, brought about by the addition of small amounts of substances.

Rocket Motor Afterburning

The programme for the Spring Meeting in April last at Lockheed Research Laboratory, Palo Alto, California, of the Western States Section of the Combustion Institute included several papers on different aspects of rocket combustion [for the list of papers presented see *Combustion and Flame*, **1960**, **4**, **190**].

One of these papers deals with the extinguishing of rocket motor afterburning, by D. G. MILLER and M. C. ABRAMS, of Convair Division of General Dynamics Corporation, Pomona, California. The reason for research on this subject is that it became established that a high-frequency electromagnetic wave can be severely attenuated when passing through a rocket exhaust flame. Radar attenuation measurements which were made through a flaming and a non-flaming rocket exhaust, have indicated that the rocket flame is the primary cause of this phenomenon. As this may result in a serious guidance problem on certain missiles methods of extinguishing rocket afterburning have been investigated, especially chemical flame quenchers.

Analysis of the jet–air mixing characteristics in the wake of the missile showed that the interaction of the rocket jet and the external air in the boat-tail cavity resulted in a hot circulation zone which acted as an artificial flameholder and piloted the visible jet flame. Attempts to reduce the jet–air mixing outside the jet exit by altering the missile configuration were unsuccessful and a programme was initiated to find a suitable substance to be injected into the jet–air mixing region of the rocket exhaust. A general discussion is given of the principles underlying this work and of the evaluation of chemical flame quenchers.

The test results indicated the feasibility of using iodine in the form of diiodomethane as an effective suppressor. The quantity of quencher required to eliminate rocket flame does not appear excessive and the amount necessary to prevent re-ignition may be less than the amount to quench the flame initially. The major problem in the use of a chemical quencher is the efficient injection of the material into the exhaust jet–air boundary where the flaming occurs.

Structure of Flames near Extinction Limits

A paper presented to the Spring Meeting in California, of the Western States Section of the Combustion Institute (see note above) by C. H. YANG, of Convair Scientific Research Laboratory, San Diego, California, was concerned with the phenomena of flames which are associated with heat losses to surroundings. These phenomena include quenching, inflammability and pressure limits, as well as the structure and burning velocity of flames. A general study of flame structure and burning velocity of non-adiabatic flames is made in this paper, using a one-dimensional model, and solutions were obtained by the use of analogue computers. The propane–air system was chosen for numerical computation.

The shape of the computed temperature and concentration profiles as well as the heat release curve are regarded as being in agreement with experimental measurements. It is shown that the structure of a flame near the inflammability limit differs considerably from that of a flame near the quenching limit. The reaction zone becomes larger as the proportion of inert gas in the mixture increases. The maximum temperature, however, is almost as high as the adiabatic temperature (cf. this volume, p 325).

Ionization in Flames

H. F. CALCOTE, AeroChem Research Laboratories, Inc., Princeton, New Jersey, made a further contribution to the subject of ionization in flames on which he has carried out work for some years, in a paper presented to the Spring Meeting in California, of the Western States Section of the Combustion Institute (see note above).

The observed ion concentrations are steady state values between ion-producing and ion-removal processes, consequently it is necessary to examine both rates to explain the relatively large concentrations of ions in hydrocarbon flames. New data obtained by Langmuir probes are presented, together with an important discussion and interpretation of these in terms of specific mechanisms. The experimental equipment consisted of a low-pressure flat-flame burner with means for measuring gas flows, a vacuum system, and a means for obtaining current–voltage probe curves. A special feature was the provision for maintaining the gas composition constant while varying either the total flow rate or pressure. The maximum positive ion concentrations were measured for several hydrocarbon–air or oxygen flames at pressures down to 33 mm of mercury. These values were obtained by setting the probe voltage at several volts negative and moving the probe through the flame front until a maximum current was observed. An interesting feature of these experiments is that the maximum ion concentration with respect to composition was found to occur very near to the stoichiometric mixture.

The experimental results are interpreted as giving ion recombination coefficients which are independent of pressure and equal to 2×10^{-7} cm^3/sec, that is, the rate of recombination is second order with respect to the ion concentration. The rate of ion formation is proportional to the square of the pressure so the formation process is second order. Below a pressure of about 66 mm of mercury ambipolar diffusion appears to be important and in interpreting ion decay processes behind the flame front diffusion must be considered.

The results are shown to be capable of interpretation in terms of chemi-ionization as regards ion production, for example by

$$CH + O \rightarrow CHO^{+} + e^{-}$$

The initially produced ion, present in only small concentrations, will then react with H_2O by an ion–molecule charge exchange reaction to produce the large quantity of H_3O^{+} which has already been observed by J. **Deckers** and A. **van Tiggelen**, and also by P. F. **Knewstubb** and T. M. **Sugden** [*Seventh Symposium (International) on Combustion*, 254, 247; Butterworths: London, 1959].

Gas Industry Register

The Register of the Gas Industry 1960 was published in June [Gas Publications Ltd, 240 *pp*, 25*s*]. The Directory Section contains full information as to the personnel of the Gas Division of the Ministry of Power, The Gas Council, the Gas Boards, and also of undertakings in Canada, Australia, New Zealand and Malta. The Technical Section contains succinct descriptions of the principles of the different types of gas production and associated processes, of distribution and utilization, together with a large amount of numerical information.

The Beilby Medal and Prize, 1961

Since 1930, at intervals of one or more years, awards have been made by the Administrators of the Sir George Beilby Memorial Fund, representing the Royal Institute of Chemistry, the Society of Chemical Industry and the Institute of Metals. Sir **George Beilby** had been President of each of these three bodies, and they jointly sponsored the appeal for subscriptions whereby the Fund was raised as a memorial to him after his death in 1925.

The awards are made to British investigators in science in recognition of independent original work of exceptional merit, carried out continuously over a period of years and involving the development and application of scientific principles in any field related to the special interests of Sir **George Beilby**, chemical engineering, fuel technology or metallurgy, in their modern interpretations. The awards are intended as an encouragement to younger men and women, preferably under age 40, who have done distinguished work of practical significance in any of these fields.

In 1958 two awards, each of 150 guineas, were made. It was then agreed that no further award would be made before 1960.

The Administrators have decided that henceforth each award shall consist of a gold medal as well as a substantial sum of money, and shall be known as 'The Beilby Medal and Prize' and specified as being 'For Advancement in Science and Practice'. Such an award will be offered at intervals of two years, but more than one may be made on the same occasion if there are several candidates of sufficiently outstanding merit.

Consideration will be given in due course to the making of an award (or awards) from the Fund in 1961. Outstanding work of the nature indicated may be brought to the notice of the Administrators, either by persons who desire to recommend the candidate or by the candidate himself, not later than 31 December 1960, by letter addressed to The Convenor of the Administrators, Sir George Beilby Memorial Fund, The Royal Institute of Chemistry, 30 Russell Square, London, W.C.1.

The letter should be accompanied by nine copies of a short statement on the candidate's career (date of birth, education and experience, degrees and other qualifications, special awards, etc., with dates) and of a list of titles, with references, of papers or other works published by the candidate, independently or jointly. Photographic copies of these documents are acceptable. Candidates are also advised to forward one reprint of each published paper of which copies are available.

Automatic Heat Treatment Line

The first completely automatic heat treatment line in Britain for carburizing, annealing, hardening and tempering has been installed by

AEI–Birlec Ltd at the Daventry works of British Timken, Division of The Timken Roller Bearing Co. The equipment has been built primarily for the heat treatment of tapered roller bearing cups and cones for vacuum brake rolling stock required for the railway modernization scheme.

The processes, which are in automatic sequence, are performed in four Birlec furnaces and these are linked by mechanical and hydraulic handling devices. The installation performs four processes, gas carburizing, sub-critical annealing, hardening and tempering. The components are loaded on to locating fixtures which are assembled four at a time on nickel–chromium trays, three of which form a furnace charge at every loading sequence.

The carburizing furnace, with a propane-enriched atmosphere, is heated by gas-fired radiant tubes arranged in four zones, each under independent and automatic temperature control. The first of these is a heating zone, the middle two are soaking zones, and the fourth is a diffusion zone. The furnace is rated at 3 500 ft^3/h. The tray loads pass through the furnace by a sequence of synchronized pushes from hydraulic cylinder mechanisms at the charge end of the furnace. After being discharged from the furnace the trays are transferred to an electrically heated pusher-type furnace, rated at 145 kW, supplied with a protective atmosphere from an exothermic generating plant, for sub-critical annealing. The components are next loaded by conveyors into the Birlec roller hearth furnace for hardening in an atmosphere from an endothermic generator. There are two heating zones in this furnace, with a total rating of 120 kW. Finally the components are fed into a continuous Birlec slat conveyor furnace, rated at 48 kW, for tempering.

By a correct selection of quenching operations with this continuous installation, it is possible to minimize the formation of scale on components during heat treatment and there is no necessity for any form of shot-blasting operation. Furthermore, by incorporating washing, rinsing and drying operations, degreasing of the components is avoided.

New Jet Fuel

According to a report in the German technical press a new jet engine fuel has been developed and put on to the market by Texaco Inc. [*BrennstChemie,* **1960**, **41,** No. 4, 37]. It has already undergone considerable testing in the laboratories of the leading aircraft engine manufacturers. The important property of the fuel is that of appreciable reduction in heat radiation in the combustion chamber, as the fuel burns with a comparatively low luminosity. Consequently as compared with the usual kerosine-type fuels the new fuel can attain a higher temperature during combustion without overheating the engine combustion chamber.

Waste Heat from the Diesel Engine

Waste heat from the diesel engine is of a sufficiently high grade as to be valuable for many purposes, although not at such a high energy level as to be very suitable for the direct generation of mechanical power in any large amount. The application of this waste heat, amounting to 60 to 70 per cent of the heat available in the fuel, for space heating and hot water supplies, has been considered in many papers and is a common practice in many stores, factories and offices. These and other methods of using waste heat from diesel and dual-fuel engines are discussed in a paper by N. D. WHITEHOUSE and A. STOTTER, of The English Electric Co. Ltd, presented to the Sectional Meeting of the World Power Conference held in Madrid last June. Attention is more especially directed by these authors to the use of engine waste heat for absorption refrigeration, for water distillation, and for heating sludge digester plant in sewage works.

The application of waste heat in an absorption refrigerator to cool the charge air of the diesel engine itself is examined in considerable detail as to costs, both for power generation alone, and also when combined with air conditioning. It is shown how, especially in tropical conditions, the rating of an engine may be increased by utilizing part of the cooling for the intake air of engines. It is concluded that charge refrigeration could advantageously be combined with power generation by diesel engines.

Melchett Medal, 1960

The award of the Melchett Medal for **1960** has been made by The Institute of Fuel to Professor H. C. Hottel, who is widely known for his contributions in the fields of fuel technology and chemical engineering, especially in connection with heat transfer. He has been a member of the staff of the Massachusetts Institute of Technology since **1924**, being Director of the Fuels Research Laboratory since **1934** and a Professor since **1941**. Professor Hottel is at present vice-president of The Combustion Institute.

World Power Conference, Melbourne, 1962

The Sixth Plenary Meeting of the World Power Conference is to take place in Melbourne, from **20** to **26** October, **1962**. The theme of the meeting is to be 'The Changing Pattern in Power'. Papers may be submitted only through the national committees or representatives of the World Power Conference. Further information may be obtained from The Secretary, British National Committee, The World Power Conference, **201–2** Grand Buildings, Trafalgar Square, London, W.C.2.

University Residential Course on Heat Transfer

The Department of Extramural Studies of the University of Sheffield in cooperation with Professor M. W. Thring, Professor of Fuel Technology and Chemical Engineering, is arranging a residential course on 'Heat Transfer: The Application of Fundamental Studies to Practical Problems', to be held from **19** to **25** March **1961** inclusive. The lectures and demonstrations will be given in the Department of Fuel Technology and Chemical Engineering, and accommodation for those attending will be provided in one of the Halls of Residence. The cost will be between **£21** and **£25**. A programme of the course and further particulars may be obtained from The Director of Extramural Studies, St John's, Crookes Valley Road, Sheffield **10**.

Burning Velocity of Turbulent Flames

G. de Soete and A. van Tiggelen, of the Laboratoire de Chimie Inorganique, Université de Louvain, have recently made a theoretical contribution to the study of the fundamental speed of flames under turbulent conditions [*Bull. Soc. chim. Fr.* **1960, 1127**]. Experimental work to test the equation put forward was carried out in the Reuil–Malmaison laboratories of l'Institut Français du Pétrole. Their paper deals with the recirculation of a portion of the burnt gas into the fresh gas, due to turbulence, resulting in an important modification of the fundamental speed of flame and consequently the speed of turbulent flame.

A new theoretical equation is deduced for the fundamental speed of flame from which it is possible to predict the modification which occurs when flame combustion passes from the laminar to the turbulent régime. It is shown that the flame speed may be either increased or reduced depending on the value of the energy of activation of the reaction, order of the reaction, and the flame temperature.

Industrial Chimney Heights

In a paper of unusual interest and importance, particularly in view of the implementation of the Clean Air Act, G. Nonhebel, Chemical Engineering Services, Imperial Chemical Industries Ltd, London, recently put forward before the Institute of Fuel recommendations on heights for new industrial chimneys [*J. Inst. Fuel*, **1960, 33, 479–495**; discussion **495–511**].

The paper represents a quantitative contribution to the subject to replace the previous empirical rules that will give designers and consultants a means of obtaining definite data for chimney height and at least provide thereby a basis for discussion with local authorities.

The major consideration in determining the heights of new chimneys, which have to be approved by local authorities, is the effect of the discharge at ground level. A review has been made by the author of the information which has been collected over a number of years by the use of several formulae to calculate the gas concentration and rate of dust fall under normal weather conditions. As a result of this survey recommendations are now made that the height of a new chimney serving a large plant should be such that the calculated 3-minute maximum concentration of sulphur dioxide at ground level should not exceed **40** parts per **100** million, by volume, in areas of heavy industry or high housing density and **50** p.p.h.m., in other areas. The calculated maximum rate of deposit of grit and dust which should not be exceeded is $\mathbf{1\,000}\ \mathrm{g}/\mathbf{100}\ \mathrm{m}^2$ month, with a wind blowing within an octant.

Since the formulae proposed do not apply to emissions from relatively low chimneys or small plants, recommendations based on experience are made for a sliding scale of heights from **60** to **120** ft for boiler plants of aggregate capacity **5 000** to **33 000** lb/h. It is found that the rate of dust deposit rather than ground-level concentration of sulphur dioxide is usually the factor which should control the height of boiler plant chimneys.

A study of the deposition rates of different size grades of dust in the gas stream leaving the chimney, shows the great importance in calculating chimney height of the quantities of particles larger than **76** microns, particularly those larger than **150** microns. Consequently it is recommended that the emission of particles or aggregates larger than **76** microns should be substantially prevented. Suggestions are made with regard to two other factors which require consideration, the rate of ground coverage by a film of deposited dust, and the distance from the chimney at which dusty plumes become substantially invisible.

In the considerable discussion which followed the presentation of the paper, attention was drawn to the fact that many formulae do not apply to inversion conditions and the difficulty of specifying such conditions mathematically. The shape of building must be regarded as very important as it may quite possibly be the cause of downward currents. It was also pointed out that there is a dependence of measured results on sampling time, which is complicated and requires to be more fully investigated.

Eighth Symposium on Combustion

The Eighth Symposium (International) on Combustion was held at the California Institute of Technology, Pasadena, California, from **28** August to **2** September **1960**. About **124** papers were presented and the subjects covered included: ions in flames, chemical kinetics, laminar and turbulent flames, shock waves, explosions and detonations in gases, liquids and solids, combustion of liquid and solid propellants in rocket engines, ammonium perchlorate propellants, nozzle flow with chemical reactions, relaxation phenomena and chemical reactions behind shock fronts, formation and combustion of solids, combustion spectroscopy, gas emissivities and radiant heat transfer, flameholding. Reference is made to some of the papers in the following notes.

Burning of Liquid Hydrazine

It has been suggested from time to time that the burning of liquids takes place in the gas phase, with no reactions occurring in the condensed phase, and there is some evidence that this may be applicable to liquid hydrazine. With a view to obtaining more data for its burning rates and more insight into the mechanism of its combustion, A. C. ANTOINE, Lewis Research Center, National Aeronautics and Space Administration, Cleveland, Ohio, carried out an investigation into the mechanism of the burning of liquid hydrazine, which he described in a paper to the Eighth Symposium on Combustion at Pasadena [see note above].

The burning rates were obtained using a strand burner. Liquid hydrazine was contained in Pyrex glass tubes and ignited at the surface by a hot wire. Heavy-wall tubes of **5·6**, **9·5** and **12·7** mm inside diameter were used. Three compositions were used: **100·0** per cent hydrazine, and **97·1** and **94·3** per cent hydrazine–water solutions. The decompositions were carried out in a nitrogen atmosphere between **1** and **17** atm.

Plotting the burning rates against pressure, the results for the **100·0** per cent concentration are of great interest. Except for deviations noted in the smaller tubes, the burning rates are proportional to pressure. This means, in keeping with observations at pressures below one atmosphere, that second-order kinetics prevail in the pressure range considered. There is, therefore, no rate-order transition around one atmosphere. In addition, a model for decomposition based on the gas phase reaction rate being controlling would be applicable. Heat is generated by exothermic decomposition in a vapour phase reaction zone a little above the surface of the liquid and is conducted back to the surface causing the liquid to heat and vaporize. The rate of regression of the surface is dependent on the rate of heat generation in the gas phase reaction zone and the thermal conductivity of the gaseous layer just above the surface. Applying the equations of R. FRIEDMAN, J. B. LEVY, and K. E. RUMBEL [Atlantic Research Corporation, *AFOSR—TN 59-173* (5 February 1959). *AD No. 211-313,* Contract No. AF 18 (600)-1502], and using a reaction rate of 0·36 moles/cm^3 sec for the one atmosphere reaction rate, a burning rate of 0·045 cm/sec was calculated. This value agrees well with the observed value.

It is evident that another mechanism must be used to account for the results for the 97·1 per cent concentration in the 9·5 and 5·6 mm tubes. It is more probable that the observed behaviour is better described by the mechanism proposed by M. GERSTEIN [*J. Amer. Rocket Soc.* **1959**, **29**, 514], that is, at low pressures a gas phase reaction is rate-controlling, whilst at high pressures the rate of evaporation of the liquid is controlling. The shapes of the curves for the 100·0 per cent concentration in the 9·5 and 5·6 mm tubes and for the 97·1 per cent concentration in the 12·7 mm tube cannot be solely explained by either of the two mechanisms mentioned above.

Direct Generation of Current from Combustion of Gas

S. WAY and R. L. HUNSTAD, Westinghouse Research Laboratories, Pittsburgh, Pennsylvania, read a paper to the Eighth Symposium on Combustion at Pasadena [see note above] on the direct generation of current from a combustion gas stream. The paper describes some experiments in which a hot combustion gas stream is caused to flow through a transverse magnetic field. By placing electrodes on opposite sides of the stream, so that flow velocity, magnetic field and electric field are all mutually perpendicular, electric power can be generated, as electrons are collected from the gas at the anode and then pass through an external circuit and back to the cathode where they re-enter the gas stream. Conductivity of the combustion gas is augmented by introduction of potassium, which, by virtue of its low ionization potential, yields an appreciable number of ions and free electrons, the concentrations being calculated by Saha's equation.

Operation of the generator hinges on the fact that the electric field $\bar{E}'$ relative to coordinates fixed in the moving gas is equal to the vector sum of the applied electric field $\bar{E}$ (resulting from the potentials established at the electrodes) and the vector $\bar{u} \times \bar{B}$ where $\bar{u}$ is gas velocity and $\bar{B}$ is magnetic induction. The electric force E' thus propels charges (electrons) transversely and produces the current drawn from the electrodes.

A combustion arrangement is used in which a fuel, consisting of a mixture of No. 2 furnace oil and 2-ethylpotassium hexoate, is burned with an oxygen–nitrogen mixture, at about 95 per cent oxygen equivalence ratio. The potassium atoms comprise about a 2 per cent fraction of the product gases. Product gas at approximate equilibrium composition enters the generator at about 2 800°K, 1·2 atm abs., in which state it has an electric conductivity of about 15 to 20 mhos/m. Magnetic fields of various strengths up to 14 000 gauss have been used. Open circuit voltages of over 80 V have been observed, and 6·4 kW has been generated.

Compression Waves and Chemical Reaction Rates in Gaseous Combustion

The amplification of compression waves during the course of gaseous combustion in a spherical vessel has been investigated by S. M. KOGARKO, Institute of Chemical Physics, U.S.S.R. Academy of Sciences, Moscow, who gave an account of his experiments to the Eighth Symposium on Combustion at Pasadena [see note above]. The gas mixtures were ignited by an electric spark at the centre of the sphere, 220 mm in diameter. Flame propagation was recorded on a high-speed rotating film, through a slit in the spherical vessel. The rise of pressure during combustion was recorded on the same film by means of a differential optical-mechanical indicator. Benzene and aviation gasoline were used as fuels. Experiments were carried out at initial pressures of 1 to 15 kg/cm^2. The mixture temperature was maintained at 65°C.

Combustion of fuel–air mixtures of any composition at initial pressures from 1 to 2 atm is accompanied by a smooth increase in pressure up to the maximum value. With certain mixture compositions a further increase in the initial pressure leads to a change in the nature of the combustion process. Variations in pressure connected with the propagation of compression waves within the mixture are observed in place of the smooth pressure rise, and the combustion process is accompanied by an acoustical effect. A compression wave propagates within the reaction products and the amplitude of this wave continuously increases as shown by the record of the rise of pressure with time.

In the combustion of benzene–air mixtures of composition $a = 1{\cdot}1$ and $a = 1{\cdot}2$, compression waves are not observed and one of these mixtures was used in order to find out if it is possible to amplify an artificial compression wave on interaction with the flame reaction zone. An artificial shock wave was created by exploding a small weighed portion of lead azide in the process of combustion of a benzene–air mixture having a composition of $a = 1{\cdot}2$. When the weight of the specimen was lower than a critical value, a compression wave was registered on the pressure record at the moment of the specimen explosion. The wave amplitude decreased with time and gradually became attenuated. On explosion of a specimen having a weight above the critical value, a continuous increase was observed in the amplitude of the compression wave arising, attaining a high value at the moment of completion of the combustion.

Under the experimental conditions the flame front propagated at a moderate (1·5 to 3·0 m/sec) and almost constant velocity. Thus there was no amplification of compression waves at the expense of progressive acceleration of the flame. Multiple interceptions of the flame front by the compression wave were observed during combustion.

It is suggested by the author that the amplification of the compression waves may be due to an increase in the chemical reaction rates in the combustion zone owing to an increase in density and temperature caused by the passage of the compression wave. Since the withdrawal of energy and matter by heat conduction and diffusion from the reaction zone into the ambient space remains unchanged during a certain (relaxation) time, there will be a rise of pressure in the reaction zone. Perturbations will occur at the boundaries of the combustion zone and being directed towards the compression wave front they will amplify the compression wave.

Apparent Flame Strength

A measurement which can be applied to diffusion flames for their characterization was described a short time ago by A. E. POTTER, Jr and J. N. BUTLER [*J. Amer. Rocket Soc.* 1959, **29**, 54]. The method consists of measuring the mass flow rate per unit area at which the diffusion flame between two opposed jets, one of fuel and the other of oxidant, is extinguished. This mass flow, called the *apparent flame strength*, is a measure of the maximum reaction rate in the diffusion flame and has special applicability to practical combustion systems which use highly reactive fuel–oxidant combinations as in rocket motors. A further paper on the subject was presented by A. E. POTTER Jr, S. HEIMEL and E. ANAGNOSTOU, Lewis Research Center, National Aeronautics and Space Administration, Cleveland, Ohio, to the Eighth Symposium on Combustion at Pasadena [see note above]. A recent theoretical treatment by D. B. SPALDING of the conditions necessary for the extinction of diffusion flames, takes into account forced convection and his new theory shows that the apparent flame strength is directly related to the maximum reaction rate in the diffusion flame.

The present paper is primarily an experimental one, and is concerned with the effect of various factors on the apparent flame strength. A complete study of the effect of jet diameter and spacing is presented, from which it is concluded that the apparent flame strength varies slightly with jet diameter, the variation agreeing with Spalding's theory only at very large diameters. The apparent flame strength for a number of fuel–oxidant systems (hydrogen–air, propane–nitrous oxide, propane–oxygen–nitrogen), in addition to those previously reported, was measured at one atmosphere pressure. All behaved normally, in that the values for the apparent flame strength were proportional to the mass burning rate of the stoichiometric mixture as predicted by theory, except hydrogen–air. For this flame, not only was the apparent flame strength anomalous, but the flame was stabilized at the mid-point between the jets when the mass flow of air exceeded that of hydrogen by a factor of three. This result is said to be qualitatively explained by Spalding's theory.

Combustion of Petroleum Fuels and Air Pollution

Several papers were read at the recent Conference of the National Society for Clean Air, held at Harrogate, 5 to 7 October, on the subject of air pollution by the combustion of petroleum fuels in a wide range of equipment, including domestic appliances, boilers, industrial furnaces, process plant, and also in road vehicles.

E. L. HOWE, BP Research Centre, British Petroleum Co. Ltd, described an investigation into the determination of 3,4-benzpyrene in the exhausts of appliances using petroleum products, ranging in size from a cooking ring to a water tube boiler. This is part of a research programme on the extent of the contribution of petroleum fuels to air pollution. Over a range of fuels, from liquefied petroleum gas to heavy fuel oil, the 3,4-benzpyrene content in the exhaust gases was less than $1{\cdot}0\,\mu g$, the limit of detection by the analytical method used. The quantity is likely to be less than 0·006 p.p.m. of fuel burnt.

The Hartridge–BP smoke meter was put forward by two speakers, D. LISTER, and G. J. WARING, in their papers on different aspects of the problem of preventing air pollution by diesel-engined road vehicles, as fulfilling the need for a portable instrument which gives an immediate reading of exhaust smoke emission and needs no special services for operation. It measures the obscuration of a beam of light falling on a photocell and showing this as a direct reading in percentage smoke. It is suggested that a new engine should have an exhaust of under 25 per cent obscuration, that the allowance for engine wear should be up to 45 per cent, and that 60 per cent should be the limit that could be allowed. This meter has been approved by the Air Pollution Panel of the British Motor Industry Research Association for research work. Reference was also made to the Bosch instrument which uses a filter paper disc through which gas is drawn by a sampling pump attached to the exhaust pipe.

In a paper by L. E. REED and S. C. WALLIN, Warren Spring Laboratory, D.S.I.R., describing experiments on methods of removing smoke from diesel engine exhaust gases, the conclusion is reached that no suitable filtering medium nor effective scrubbing device could be found. All methods which were capable of effecting a substantial reduction would be costly in operation and none is considered satisfactory for road transport. More emphasis should be given to the prevention of smoke than to devising methods of removing it.

Electrostatic Ignition Hazards

A monograph on *Conductive Flooring for Hospital Operating Rooms*, written by T. H. BOONE, F. L. HERMACH, E. H. MACARTHUR and RITA C. MCAULIFF, has recently been published [National Bureau of Standards *Monograph 11*, 1960; 16 *pp*]. The hazard which arises from sparks resulting from the accumulation of static electricity in places where explosive vapours are present is reduced most effectively, as is well known, by keeping the electrical resistance between all objects in the area so low that dangerous voltages are never attained. The investigation described in this monograph dealt with the characteristics and performance of conductive flooring materials as a primary factor in solving this problem.

It was found that the physical, chemical and general serviceable characteristics of available types of conductive flooring are comparable with those of non-conductive flooring. Care is required in the selection of instruments and methods used to measure the floor resistance, but the method specified by the National Fire Protection Association (60 Batterymarch Street, Boston 10, Mass., U.S.A.; 'Code for the Use of Flammable Anesthetics', *NFPA No. 56*, May 1960, 23–24) is regarded as reasonably simulating the actual conditions under which a floor functions in reducing electrostatic hazards.

Optical Methods for Flame Study

M. D. Fox and F. J. Weinberg, Department of Chemical Engineering, Imperial College of Science and Technology, London, have recently published a paper describing three optical methods for the investigation of flame combustion under turbulent conditions [*Brit. J. appl. Phys.* **1960**, **11**, 269]. All three methods are based on ray deflection consequent on variations in refractive index due to changes in temperature and composition of the medium across the flame front. The first of the methods is designed to give a measure of the extent of disorientation of flame, which may be regarded as a measure of the effect of turbulence on the flame front. This method gives a time-mean polar diagram of deflections over any desired zone of the flame. In the second method an instantaneous delineation of the flame front is obtained, producing a contour suitable for geometrical measurements, and the third method is used to record quantitatively the distribution of deflections in one direction over several selected regions of the field, intended to give information of time-mean distributions of gas properties.

Combustion Control in Steelmaking

The rate at which heat is transferred to the hearth of an open-hearth furnace can be increased by enlarging the area of bath covered by the flame. In the *Annual Report 1959 of The British Iron and Steel Research Association* reference is made to the use of twin burners in the BISRA model calorimeter-hearth furnace to obtain the extra bath coverage. The rate of heat transfer was thereby increased 30 per cent above that obtaining with a single burner at the same total fuel rate. It is suggested that the use of twin burners might be advantageous in open-hearth furnaces, but such a large increase in the rate of heat transfer may not be expected due to increased loss to the water cooling system of the twin burners and because of reduced furnace oxidation rate.

Waste gas analysis at several open-hearth furnaces has shown a wide variation in excess air from heat to heat, from reversal to reversal, and even within a reversal. Sampling and analysis equipment needed to determine excess air continuously has now reached a pitch of development adequate for automatic furnace combustion control.

A large part of the Physics Department's resources has been devoted to continuing research into air pollution. A simplified photoelectric smoke sampler has been constructed which will enable works staff and plant manufacturers to carry out operations satisfactorily without relying on visual assessments of chimney effluents. This sampler can be made in a portable form and used to indicate or record the smoke density of hot or cold flue gases whether dry or wet.

Development of the BISRA wet scrubbing system was discontinued in the middle of 1959, after an investigation had shown that the process could not compete on a basis of total costs when compared with an electroprecipitator operating continuously for a period of ten years. The wet scrubbing system, however, can be the more economic of the two for intermittent operation, as for example, during oxygen lancing. The relative merits of the two systems are now being further studied in the light of developments in iron- and steel-making processes.

Convective Mass Transfer

About seven years ago D. B. Spalding, Professor of Heat Transfer, Imperial College of Science and Technology, London, published his first formulation of the convective mass transfer problem [*Fourth Symposium (International) on Combustion*, p 847. Williams and Wilkins: Baltimore, 1953]. In this paper and some subsequent ones the differential equations of atomic and energy conservation were used, together with derivation of corresponding approximate solutions of the laminar boundary-layer equations, in connection with the combustion of liquid fuels. The formulation was later elaborated and Professor **Spalding** has now written a paper in which he develops this work, particularly as regards rigour of derivation and also in connection with the definition of the *transferred substance*. The result is that use of the method may be extended to processes, common in chemical engineering equipment, in which substances are transferred through the phase boundary simultaneously in both directions [*Internat. J. Heat Mass Transfer* 1960, **1**, 192].

It is shown that, provided that certain relations exist between the transport properties, every mass transfer problem, including those with simultaneous heat transfer and chemical reaction, can be expressed by relations of the 'Ohm's law' type: $\dot{m}'' = g \cdot B$, where $\dot{m}''$ is the required mass transfer rate through the surface, g is a surface conductance dependent on aerodynamic factors, and B is a dimensionless driving-force dependent on the thermodynamic properties of the main stream, of the fluid in contact with the phase boundary, and of the transferred substance.

The standard formulation is derived from the differential equations of conservation and flux and by reference to a wall-flux boundary condition.

The Turbo-furnace

The importance of reducing the emission of grit and dust from industrial plant is being increasingly recognized, particularly by designers of boiler plant using pulverized fuel, in the greater attention which is now being given to the possibilities of the slag-tap type of unit. The original objective in developing this type of boiler unit was that of disposal of ash in a more easily handled form, but present day units are being designed with the additional intention of being capable of burning a variety of fuels. With the dry-bottom type of unit, the design of superheaters and reheaters becomes complicated by this provision for alternative fuels. This problem is considerably simplified in the turbo-furnace which has proved to be one of the most successful of the American designs with slagging combustion chamber and is equally suitable for coal, oil or gas firing. The development of this new type of furnace has been described by J. D. **Williams**, John Brown Land Boilers Ltd [*J. Inst. Fuel*, **1960**, **33**, 328].

The prototype turbo-furnace was actually designed as a means of solving a fly-ash disposal problem in a West Virginian chemical plant. Its most novel features are the shape of the lower half of the combustion chamber and the disposition of the burners. The hearth, constructed entirely from refractory material, is completely separate from the boiler structure and pressure parts. The burners are arranged in both front and rear furnace walls, across the full width of the boiler unit. They are inclined downwards so that the centrelines of opposing burners intersect at a point some 6 ft above the refractory hearth. The slag-tap opening is placed at one end of the furnace. In a later design which is described a water-cooled hearth is used.

Two of the most important operational features of the turbo-furnace are the ability to burn any fuel and maintain the same furnace-exit gas temperature, and also the relatively high heat absorption in the furnace leading to somewhat lower exit temperatures than would be expected. Explanations are given to account for these features.

The first turbo-furnace to be ordered in the United Kingdom is an oil-fired unit for the Bankside B Power Station of the Central Electricity Generating Board. It is an 860 000 lb/h steam generator and reheater unit, to operate under standard 120 MW conditions of 1 600 lb/in² and 1 005°F final steam temperature.

VDI Symposium on Flow and Combustion

A second symposium on 'Flow and Combustion', organized by the Verein Deutscher Ingenieure, was held from 10 to 12 March last at Bad Kreuznach. Several papers presented dealt with model experiments, including one by Professor Dr-Ing. F. N. **Scheubel**, Director of the Versuchsanstalt für Strömungslehre und hydraulische Maschinen at the Technische Hochschule, Darmstadt, on flow experiments in models of boiler combustion chambers [*Brennst.-Wärmekr.* **1960, 12, 347**], and another by G. Hilgers and R. Wille on model flow experiments in relation to oil cracking plants. Two contributions were concerned with investigations on pulverized fuel flames in model furnaces, one by H. Effenberger, Institut für Wärmetechnik und Wärmewirtschaft of the Technische Hochschule, Dresden [*ibid*, **351**], and the other by R. H. Essenhigh, Department of Fuel Technology and Chemical Engineering, University of Sheffield [*ibid*, **356**]. A paper, by Professor Dr-Ing. F. Schuster, Gaswärme-Institut, Essen, and Technische Hochschule, Aachen, was devoted to considering the effect of heavy hydrocarbons on soot formation in gas flames [*ibid*, **359**].

In a review of the whole symposium [*ibid*, 337], Professor Dr-Ing. R. Wille, Director of the Hermann-Föttinger-Institut für Strömungstechnik at the Technische Universität, Berlin, refers to several other papers communicated of a theoretical and fundamental character and published in other journals. These include one by D. B. Spalding and D. Vortmeyer, on the stabilization of turbulent flames by recirculation; E. Le Grivès, on an investigation of the mixing and combustion processes of concentric streams; A. Martinengo and H. Gg. Wagner, on the self-ignition of hydrocarbons by adiabatic compression and by shock waves.

W. A. Kirkby

FUEL

Readers of *Combustion and Flame* may like to know that *Notes* appeared in the November issue of *Fuel* entitled:

Wantage Research Laboratory, U.K. Atomic Energy Authority

Gas research in France

Publications

FROZEN FREE RADICALS

G. J. Minkoff. New York and London;
Interscience, 1960. *ix*+148 *pp*. $5.00 or 36*s*

The experimental study of free radicals is inevitably a very difficult problem, since it is rarely possible to obtain high concentrations. However, the past few years have seen renewed interest in a technique first used by Dewar at the beginning of this century, for concentrating radicals by condensation in the solid form at very low temperatures in a matrix of more stable molecules. The renewal of interest must be partly due to the increased availability of very low temperature refrigerant, but is mainly due to the development of new and powerful methods for the study of radicals, such as electron-spin resonance. In this book the author has surveyed present knowledge in this rapidly expanding subject, in a systematic manner.

The introductory chapter explains and summarizes the reasons for the importance of radical studies in such widely different fields as combustion, biological reactions, spectroscopy, solid state physics, astronautics and astronomy.

The early history of the subject is briefly reviewed in the following chapter, from the exploratory work of Dewar on luminescence at low temperatures and attempts to prepare carbon monosulphide, to more recent attempts to elucidate the spectra and properties of active species in electrical discharges in common gases and vapours. The third chapter reviews the experimental techniques now available. In this a summary of the methods available for the production of radicals by heat, radiation or by electrical discharges is followed by discussion of the evolution and design of cells for the condensation of radicals. The chapter concludes with a brief review of the methods for the study of the properties of radicals, either in the condensed state, or whilst evaporating from the solid, by spectroscopy, mass spectrometry, calorimetry, etc. Chapter four is concerned with the basic principles and requirements of trapping radicals in frozen solids. The desired properties of the matrix are considered together with the fate of radicals produced by irradiation of frozen solids. Theories concerned with the concentration of free radicals attainable in the matrix are discussed in detail. The remaining three chapters review systematically and in detail, experimental studies and theories concerning individual radicals which have been studied by these techniques (H, O, I, N, radicals with H and O, C, N and H, etc.).

The volume is well prepared and in general easy to read, although in some places the condensation inevitable in a monograph of this size, may render it necessary for a reader unfamiliar with the subject to refer elsewhere for a complete understanding of some topics.

C. W. Nutt

CHEMICAL ENGINEERING PRACTICE

Volume 11. Works Design, etc.

Edited by H. W. Cremer and S. B. Watkins.
London: Butterworths; New York: Academic Press,
1959. *vi*+390+*xviii*. (*illus.*) **95*s* or $13.30**

Volume 11 of the series edited by Cremer and Watkins is devoted to the construction, organization and administration of a chemical factory. It discusses personnel, establishment of contracts, programming of erection and general factory legislation rather than the detailed design of chemical engineering equipment.

Chapters 1 and 2 and concerned with the location of the factory, the disposition of the equipment to form a production stream, and the buildings necessary to accommodate the equipment. It is unfortunate that the authors of the first chapter have used the definition 'unit process' to mean a unit of production when it conflicts with another definition meaning nitration or sulphonation, etc. However, these chapters include a brief discussion on the selection of the factory site in relation to raw materials, labour and finished products; and the various aspects of site surveying are touched upon.

Chapter 3 entitled 'Contracts and contract documents' is very short and merely introduces the reader to the types of contract usually made, and the general methods of selecting a contractor. The section on contract documents is very brief indeed and is covered in just over one page. However, chapter 4 on 'Factory construction' is fuller and is presented in an interesting manner. The list of 'sequence of operations' arranged in its reverse order gives the reader an immediate picture of the stages to be completed from the concept of the project to the installation and running-in of the plant.

Chapter 5 by Dr D. Hiscock is the most interesting part of this text. It gives a very comprehensive account of works administration ranging from the various facets of management to control of expenditure. The paragraphs on the principles of work study and job evaluation are instructive whilst the introduction to factory expenditure is well worth reading. Finally the two examples on costing that terminate the chapter enable the reader to understand quickly the classification of fixed or marginal costs.

Chapters 6, 7 and 8 are written by three well known personalities associated with the chemical industry, and they should be congratulated for the way they have given an account of their experiences of factory safety and the interpretation of the 'Alkali Acts' and other works regulations. Sir George Barnett's account of 'Factory legislation' is concise and is devoted to the safety aspects of the Factory Acts ranging from safeguarding machinery and plant to the precautions to be taken against toxic fumes and explosions of pressure vessels. Mr J. S. Carter's dissertation on the 'Alkali Acts' starts with the historical background and brings the reader up to date with recommendations for dealing with smoke and noxious fumes. Chapter 8 by Sir William Garrett on 'Industrial hazards' is well written and should be compulsory reading for all recruits to the chemical industry.

The final chapter is on 'Patents' and is most welcome because information on patentability and patent application procedure is to be found only in H.M.S.O. publications (which really are instruction sheets) or in the very large texts on patent law, etc., which are too time-consuming to read if one is not about to apply for a patent.

In conclusion it should be stated that the book is a most acceptable addition to the chemical engineering texts now available. The editing of the latter volumes of this series has improved, but there still remains a little overlapping, particularly in the later chapters on safety. However, as one cannot overemphasize safety in a chemical factory the overlapping is excusable.

G. V. Jeffreys

Letters to the Editors

Letters to the Editors on points of scientific interest related to combustion and flames are invited. The Editors do not hold themselves responsible for opinions expressed in correspondence. Anonymous contributions cannot be accepted.

Buoyant Diffusion Flames

IF gaseous fuel leaves a surface or emerges through an orifice into an unconfined atmosphere in which it burns as a flame, the rate of oxygen diffusion into the fuel stream determines the length of the flame, hence the name diffusion flame. If the fuel velocity at the orifice is high the momentum of the fuel largely determines the velocities of the unburnt fuel and the combustion products in the flame zone. For turbulent flow the flame length L may readily be shown to be independent of the volumetric flow of fuel Q and to be proportional to the orifice size D[1–3].

If, however, one considers a tank of liquid fuel or a pile of wood burning in air, the velocities of the gaseous fuel at the surface are usually relatively small—of the order 20 cm/s; this represents a velocity head much smaller than the buoyancy head associated with flames several metres in height. The turbulent flow pattern and hence the flame height L may be a function of buoyancy as well as of Q the total flow and the momentum arising from the orifice velocity V (i.e. $\sim Q/D^2$).

A simple dimensional analysis of the flow for any one fuel–air system, assuming that the mean flame temperatures and the gaseous composition at the flame tip do not vary for different values of Q and D, leads to a functional equation

$$\frac{L}{D} = \mathrm{f}_1\left(\frac{V^2}{gD}\right) = \mathrm{f}_2\left(\frac{Q^2}{gD^5}\right) \qquad \ldots . [1]$$

as a first approximation for any one fuel system where g is the acceleration due to gravity.

Q has a dual significance—it is a measure of the total quantity of fuel and hence of the air required for combustion and also Q/D^2 is a measure of the velocity and hence of the momentum. W. R. HAWTHORNE, D. S. WEDDEL and H. C. HOTTEL[2], in an analysis of a particular case, viz. a straight-sided conical flow from a small circular source, have previously shown the importance of the parameter V^2/gD. Their experimental work, however, was confined to flames where buoyancy played only a minor role.

If in equation 1 we now regard the effect of buoyancy as negligible, L/D cannot depend on any term containing g and L/D is therefore constant—the law for turbulent fuel jets. If one could decrease g and thereby decrease the velocity of the flame gases, the entrainment rate would decrease and the flames would be larger. Therefore L/D would be expected to be an increasing function of Q^2/gD^5.

In the course of investigations of the heat transfer from burning buildings, fabrics, etc., experiments have recently been conducted with cribs of wood (spruce) on a square base, the cribs having different heights thus giving different amounts of wood and hence different burning rates. From photographs of the flames, mean values of L were obtained for different values of Q for cribs of varying height and different values of D, the linear dimension of the base. In all cases the height of the crib was a small fraction only of L. On plotting L/D against $(\rho Q)^2/D^5$, where ρ is the density of the cold fuel vapour so that ρQ is the measured mean burning rate, it can be seen that the fifteen results obtained lie on one line which is straight within the range of these experiments (*Figure 1*). The Reynolds numbers of the 'cold' fuel assuming a viscosity of $\mu = 10^{-4}$ c.g.s. units had values in the range 2 000 to 14 000. These and experiments with two other types of fire conducted by C. T. Webster and M. M. Raftery will be reported later with a more extensive discussion of this problem.

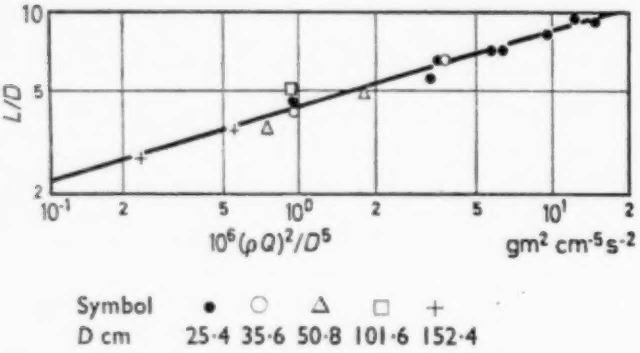

Figure 1. Flame heights for wood cribs on horizontal square base. L denotes mean flame height, D linear size of fire, and ρQ the measured mean rate of weight loss of wood crib (spruce)

W. A. KIRKBY[4] in his *Notes* in the March issue of this Journal referred to the work of V. I. BLINOV and G. N. KHUDIAKOV[5] and its review by H. C. HOTTEL[6]. In their experiments on the burning of liquid fuels in tanks of various sizes up to 23 metres, Blinov and Khudiakov reported that in two of the largest tanks 2·6 and 22·9 metres in diameter the ratios of flame height to tank diameter were the same (1·7) and stated that this was in accordance with expectation from the theory of turbulent fuel jets. Smaller tanks gave larger values of this ratio and these values were explained by stating that the Reynolds number was too low for fully turbulent conditions. There are difficulties associated with this view. The liquid burning rate was of the order 5 mm/min giving a velocity of the vapour at the liquid surface of about 10 to 20 cm/s. The velocity head is thus several orders less than the buoyancy head and the ratio 1·7 is very small compared with results for various fuels given by Hawthorne, Weddel and Hottel. In the light of the above arguments and experiments it is not self-evident that these two results can be interpreted as corresponding to fuel jets.

P. H. THOMAS

Fire Research Station,
Boreham Wood, Herts.

(*Received September 1960*)

References

[1] YAGI, S. *J. Soc. chem. Ind. (Japan)*, 1943, **46**, 608, 821, 873

[2] HAWTHORNE, W. R., WEDDEL, D. S. and HOTTEL, H. C. *Third Symposium (International) on Combustion*, p 266. Williams & Wilkins: Baltimore, 1949

[3] WOHL, K., GAZLEY, C. and KAPP, N. *Third Symposium (International) on Combustion*, p 288. Williams & Wilkins: Baltimore, 1949

[4] KIRKBY, W. A. *Combustion & Flame*, 1960, **4**, 84

[5] BLINOV, V. I. and KHUDIAKOV, G. N. *Dokl. Akad. Nauk S.S.S.R.* 1957, **113**, 1094

[6] HOTTEL, H. C. *Fire Abstracts & Reviews* (U.S. National Academy of Sciences), 1959, **1**, No. 2, 41; No. 3, Errata

---

Stability of Rich Hydrogen-Oxygen-Nitrogen Flames on a Flat Flame Burner

PREVIOUS work on hydrogen–oxygen flames has been confined to fast flames and to flames supported on cooled porous plate burners. G. N. BADAMI and A. C. EGERTON[1] were unable to study flat flames of hydrogen–air mixtures near the lower limit of inflammability on an Egerton–Powling type burner because there was too great a tendency to form cellular flames. Such cellular flame difficulties should be absent on the rich side of stoichiometric, but even here it has until recently been uncertain whether slow burning flames supported by the hydrogen–oxygen reaction could be obtained on this type of burner. Thus, the lowest burning velocities measured[2] using the bunsen burner method on hydrogen–oxygen–nitrogen mixtures on the rich side of stoichiometric is of the order of 80 to 90 cm/s, whilst more recently T. G. SCHOLTE and P. B. VAAGS[3], using a nozzle burner, have obtained a burning velocity of about 50 cm/s for a hydrogen–air mixture containing as much as 80 per cent hydrogen.

The object of this work has been a preliminary investigation of how far flames supported by rich hydrogen–oxygen mixtures can be brought within the range of the flat flame burner, and to measure their burning velocities. The method of achieving stability has been to lower the burning velocity by replacing some of the excess hydrogen by nitrogen. The burner used was of the Egerton–Powling type as modified by G. DIXON-LEWIS and G. L. ISLES[4] and it has been possible to study flames in this system with burning velocities between 7·3 cm/s and 12·5 cm/s. The burning velocities of the flat flames were measured by entraining fine magnesium oxide particles in the flame gases and photographing them under stroboscopic illumination. They were expressed in terms of linear flow velocity of gas at 18°C and 760 mm of mercury at the plane of the schlieren maximum. The burning velocities obtained ($\pm 0{\cdot}2$ cm/s), plotted against percentage of oxygen in the mixture, are shown in *Figure 1* for a number of hydrogen/nitrogen ratios and for an unburnt gas (matrix) temperature of 72°C.

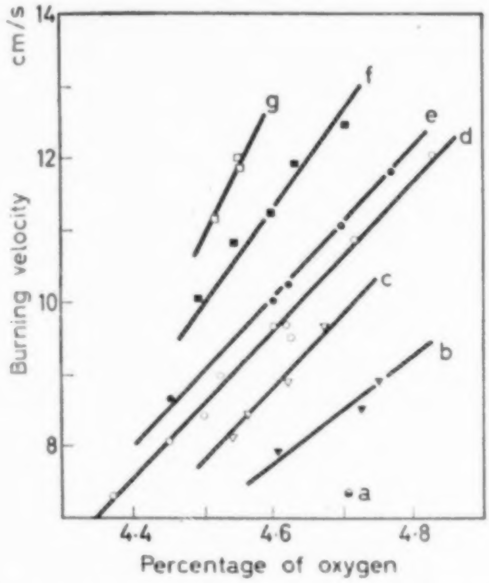

Figure 1. Burning velocities of hydrogen–oxygen mixtures against percentage oxygen content for various hydrogen–nitrogen ratios: (a) *0·121*, (b) *0·140*, (c) *0·175*, (d), *0·246*, (e) *0·315*, (f) *0·425*, (g) *0·562*

Corrections to the gas composition to allow for small variations from this average preheat temperature were made on the basis of the heat of combustion (cf. refs. 1, 5, 6). The flame temperatures of the mixtures varied between 790° and 880°C approximately.

For a given percentage of oxygen in the mixture the burning velocity increased on increasing the hydrogen/nitrogen ratio. For $(H_2)/(N_2) = 0{\cdot}565$ the only flames that could be stabilized were cusped flames near the matrix. On decreasing the oxygen supply flat flames could be obtained, but these oscillated badly. For $(H_2)/(N_2) > 0{\cdot}565$ no stable flames could be obtained under the conditions in the burner, and violent oscillations again occurred. At low $(H_2)/(N_2)$ ratios the limit is set essentially by the tendency of the flame to cusp if the $(H_2)/(O_2)$ falls below a limiting value. No flat flames were obtained with $(H_2)/(N_2) < 0{\cdot}12$.

These flames are of interest because for a fixed percentage of oxygen in the unburnt gas mixture the burning velocity may be altered by changing the $(H_2)/(N_2)$ ratio. To illustrate this, the burning velocities S_u of various mixtures preheated to 72°C, each containing 4·55 per cent of oxygen, are given in *Table 1*, together with the flame temperatures T_b and the thermal conductivities λ of the burnt gas at the flame temperature. The thermal conductivities were calculated by the method of A. L. LINDSAY and L. A. BROMLEY[7] from the conductivities of the separate gases. The sources of data for the latter are given elsewhere[8].

Table 1

H_2/N_2	0·140	0·175	0·246	0·315	0·425	0·562
S_u *cm/s*	7·47	8·36	9·16	9·63	10·77	12·00
T_b, °*K* (*calc.*)	1067	1070	1071·5	1073	1076	1079
$\lambda \times 10^5$ *cal cm*$^{-1}$ °*K*$^{-1}$ *S*$^{-1}$	17·75	18·50	20·50	22·54	26·05	30·83

Table 1 shows that on increasing the hydrogen content the burning velocity increases. There are three factors that may cause this: (*1*) the thermal properties of the mixture are changed, (*2*) the transport properties are changed, (*3*) the kinetics of the chemical reaction are affected.

It is seen that the replacement of nitrogen by hydrogen has little effect on the flame temperature. However, both the thermal conductivity of the burnt gaseous mixture and the densities ρ_b and ρ_u of the burnt and unburnt gases vary considerably with hydrogen content. As a basis for discussion the Semenov equation may be applied to the results. For second order reaction kinetics this equation is

$$S_u^2 = \frac{2\lambda\rho_b^2}{\rho_u^2} \cdot \frac{A a_u}{L\,(T_b - T_u)^2} \cdot \left(\frac{RT_b^2}{E}\right)^3 \exp(-E/RT_b)$$

Here L is the heat of combustion of unit volume of mixture at T_u; a_u is a concentration term and E and A are the overall activation energy and pre-exponential term respectively of the flame reaction. Under the conditions of constant oxygen only λ, ρ_u and ρ_b vary, since the flame temperature remains fairly constant. Thus, for second order kinetics, a plot of S_u^2 against $\lambda\rho_b^2\rho_u^{-3}$ should give a straight line through the origin. *Figure 2* shows that a curve is obtained, thus indicating a more complex situation.

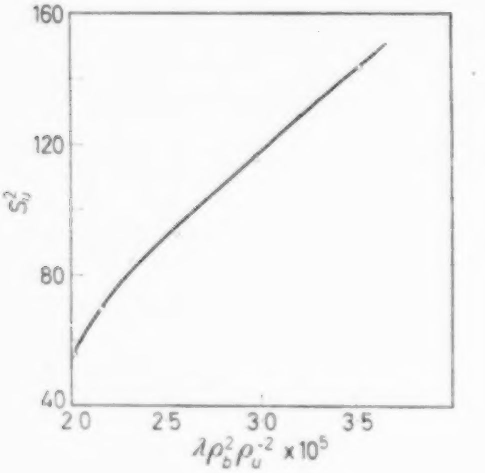

Figure 2. Plot of S_u^2 *against* $\lambda\rho_b^2\rho_u^{-2}$

The curvature is greatest at lower burning velocities where the flame is closest to the chimney top. Although pure kinetic factors may cause this, it is noteworthy that the curvature is in such a direction that it could be caused by a gradually increasing quenching by the top plate as the flame approaches it.

Finally it is interesting to note that a combination of the following three approximations: (*a*) that the flame is controlled by the four reactions

$$\mathrm{OH + H_2 = H_2O + H} \quad \ldots\ldots [1]$$
$$\mathrm{H + O_2 = OH + O} \quad \ldots\ldots [2]$$
$$\mathrm{O + H_2 = OH + H} \quad \ldots\ldots [3]$$
$$\mathrm{H + H + M = H_2 + M} \quad \ldots\ldots [4]$$

(*b*) that the pseudo-stationary state method may be applied to give radical concentrations in the reaction zone, and (*c*) that the reactions other than H atom recombination are thermoneutral, leads to an overall heat release rate which is second order in oxygen concentration. Since these flames are deficient in oxygen a rough basis for choosing the second order Semenov equation is provided.

G. Dixon-Lewis
A. Williams
Houldsworth School of Applied Science,
University of Leeds

(*Received September 1960*)

References

[1] Badami, G. N. and Egerton, A. C. *Proc. Roy. Soc. A*, 1955, **228,** 297
[2] Drell, I. L. and Belles, F. E. *N.A.S.A. Rep. No. 1383*, 1958
[3] Scholte, T. G. and Vaags, P. B. *Combustion & Flame*, 1959, **3,** 495
[4] Dixon-Lewis, G. and Isles, G. L. *Trans. Faraday Soc.* 1957, **53,** 193
[5] Egerton, A. C. and Thabet, S. K. *Proc. Roy. Soc. A*, 1952, **211,** 445
[6] Dixon-Lewis, G. and Isles, G. L. *Seventh Symposium (International) on Combustion*, p 475. Butterworths: London, 1958
[7] Lindsay, A. L. and Bromley, L. A. *Industr. Engng Chem.* (*Industr.*), 1950, **42,** 1508
[8] Dixon-Lewis, G. and Isles, G. L. *Eighth Symposium (International) on Combustion, 1960.* In press

Classified Contents

Activation energy and reaction order in methane–oxygen flames, **253**
Aliphatic amines, spontaneous ignition of, **265**
Anti-knock performance, interpretation of, of hydrocarbons in gasoline engines in terms of their combustion characteristics, **193**
Approximate solution of equation for self-ignition, **173**

Buoyant diffusion flames, **381**
Burning rates and ignition temperatures of hydrogen peroxide solutions, **99**

Carbon formation in premixed flames, **45**
Carbon monoxide flames, chlorine inhibition of, **213**
— influence of secondary atmospheric moisture on, **289**
Carbonaceous deposits, formation of polycyclic aromatic hydrocarbons and, from normal and reversed diffusion flames, **261**
— some properties of, accumulated in internal combustion engines, **107**
Cellulosic materials, ignition of, by radiation, **293**
Chlorine inhibition of carbon monoxide flames, **213**
Combustion, heterogeneous, of multicomponent fuels, **235**
Combustion processes, studies of, leading to ignition in hydrocarbons, **117**
Combustors, design of, for ramjet engines, **343**
Contribution to the theory of laminar flames with radial symmetry, **1**
Cool flames, effects of certain additives on two-stage, stabilized in a flat flame burner, **29**

Decomposition flame of solid ozone–oxygen mixtures, **284**
Design of combustors for ramjet engines, **343**
Detonation, theoretical calculations in gaseous, **137**
Development of detonation with pre-ignition, **335**
Diffusion flames, buoyant, **381**

Effects of certain additives on two-stage cool flames stabilized in a flat-flame burner, **29**
Effect of pressure on the mechanism and speed of the hydrazine decomposition flame, **9**
Emissivity of large hydrocarbon flames, prediction of, from the Mie theory, **191**
Ethyl nitrates, flame decomposition of some substituted, **201**
Extinction of a one-dimensional laminar flame between cooled porous plugs, **93**
Extinction of liquid fires, mechanisms of, with water sprays, **223**

Flame decomposition of some substituted ethyl nitrates, **201**
Flame extinction limits, a theory of, **325**
Flame propagation, theory of, in branched and unbranched chain systems, **357**
Flames, temperatures of, burning on porous burners, **285**
Formation of polycyclic aromatic hydrocarbons and carbon deposits from normal and reversed diffusion flames, **261**

Gaseous explosions in vented ducts, **301**

Heterogeneous combustion of multicomponent fuels, **235**
Hydrazine decomposition flame, effect of pressure on the mechanism and speed of, **9**
Hydrazine vapour, thermal conductivity of, **95**
Hydrogen and ethylene flames, kinetic parameters for, from flashback measurements, **243**
Hydrogen–oxygen–nitrogen flames, stability of rich, on a flat flame burner, **382**
Hydrogen peroxide solutions, burning rates and ignition temperatures of, **99**

Influence of secondary atmospheric moisture upon carbon monoxide flames, **289**
Ignition delay concept for recessed flameholders, **355**
Ignition of cellulosic materials by radiation, **293**
Interpretation of the anti-knock performance of hydrocarbons in gasoline engines in terms of their combustion characteristics, **193**

Kinetic parameters for the hydrogen and ethylene flames from flashback measurements, **243**

Laminar flames, contribution to the theory of, with radial symmetry, **1**
Laminar flame, extinction of a one-dimensional, between cooled porous plugs, **93**
Laminar flame propagation, one-dimensional, with an enthalpy gradient, **94**
Laminar flames, structure and propagation of, near a heat sink, **313**
Laminar flame, theory of a spherical premixed, **161**
Laminar spherical flame propagation, theory of steady: equations and numerical solution, **51**

Mechanisms of extinction of liquid fires with water sprays, **223**
Methane–oxygen flames, activation energy and reaction order in, **253**

Obituary: Sir Alfred Egerton, **97**
One-dimensional laminar flame propagation with an enthalpy gradient, **94**
Ozone–oxygen mixtures, decomposition flame of solid, **284**

Passage of explosions through narrow cylindrical channels, **149**
Prediction of the emissivity of large hydrocarbon flames from the Mie theory, **191**
Pre-ignition, development of detonation with, **335**
Premixed flames, carbon formation in, **45**
Production of acetylene and ethylene, use of reversed diffusion flames for, from paraffin hydrocarbons, **19**
Propellants, theory of burning of solid and liquid, **59**

Recent developments and notes, **77**, **181**, **270**, **368**

Self-ignition, approximate solution of equation for, **173**
Some properties of carbonaceous deposits accumulated in internal combustion engines, **107**
Spontaneous ignition of aliphatic amines, **265**
Stability of rich hydrogen–oxygen–nitrogen flames on a flat flame burner, **382**
Structure and propagation of laminar flames near a heat sink, **313**
Studies of combustion processes leading to ignition in hydrocarbons, **117**

Temperatures of flames burning on porous burners, **285**
Theoretical calculations in gaseous detonation, **137**
Theory of burning of solid and liquid propellants, **59**
Theory of flame extinction limits, **325**
Theory of flame propagation in branched and unbranched chain systems, **357**
Theory of a spherical premixed laminar flame, **161**
Theory of steady laminar spherical flame propagation: equations and numerical solution, **51**
Thermal conductivity of hydrazine vapour, **95**

Use of reversed diffusion flames for the production of acetylene and ethylene from paraffin hydrocarbons, **19**

Vented ducts, gaseous explosions in, **301**

Author Index

Adams, G. K. and Cook, G. B.: The effect of pressure on the mechanism and speed of the hydrazine decomposition flame, **9**
Adler, J.: *see* Spalding, D. B. and Adler, J.
Agnew, W. G.: The effects of certain additives on two-stage cool flames stabilized in a flat-flame burner, **29**
Akita, Kazuo: *see* Kazuo Akita
Arthur, J. R. and Napier, D. H.: The use of reversed diffusion flames for the production of acetylene and ethylene from paraffin hydrocarbons, **19**

Bagnall, E. C.: *see* Zelinski, J. J., Matthews III, L. J., Falk, F. and Bagnall, E. C.
Berlad, A. L. and Yang, C. H.: A theory of flame extinction limits, **325**
Bragg, S. L.: review of *Space Technology*, **281**
Bruszak, A. E.: *see* Wolfhard, H. G. and Bruszak, A. E.

Chen, Tze-Ning: *see* Tze-Ning Chen
Cook, G. B.: *see* Adams, G. K. and Cook, G. B.
Corbeels, R.: *see* Vandenabeele, H., Corbeels, R. and van Tiggelen, A.
Cullis, C. F. and Khokhar, B. A.: The spontaneous ignition of aliphatic amines, **265**

Daniels, P. H.: Carbon formation in premixed flames, **45**
Dixon-Lewis, G. and Williams, A.: Stability of rich hydrogen–oxygen–nitrogen flames on a flat flame burner, **382**

Eisen, C. L., Gross, R. A. and Rivlin, T. J.: Theoretical calculations in gaseous detonation, **137**

Falk, F.: *see* Zelinski, J. J., Matthews III, L. J., Falk, F. and Bagnall, E. C.
Favin, S.: *see* Westenberg, A. A. and Favin, S.
Fells, I.: review of *Annual Reports on the Progress of Chemistry, Volume 55, 1958*, **92**
Fine, B.: Kinetic parameters for the hydrogen and ethylene flames from flashback measurements, **243**
Foster, P. J. and McGrath, I. A.: Prediction of the emissivity of large hydrocarbon flames from the Mie theory, **191**
Friel, P. J.: *see* Lauer, J. L. and Friel, P. J.

Gray, P. and Wright, P. G.: The thermal conductivity of hydrazine vapour, **95**
Gross, R. A.: *see* Eisen, C. L., Gross, R. A. and Rivlin, T. J.

Inami, S. H.: *see* Wood, B. J., Wise, H. and Inami, S. H.

Jeffreys, G. V.: review of *Chemical Engineering Practice*, Vol. **11**, *Works Design, etc.*, **380**

Kaskan, W. E.: Temperatures of flames burning on porous burners, **285**
Kazuo Akita: *see* Tosiro Kinbara and Kazuo Akita
Kehat, E.: *see* Satterfield, C. N., Kehat, E. and Mendes, Maria A. T.
Khokhar, B. A.: *see* Cullis, C. F. and Khokhar, B. A.
Kinbara, Tosiro: *see* Tosiro Kinbara
Kirkby, W. A.: Recent developments and notes, **77**, **181**, **270**, **368**

Lauer, J. L. and Friel, P. J.: Some properties of carbonaceous deposits accumulated in internal combustion engines, **107**
Lindsey, A. J.: The formation of polycyclic aromatic hydrocarbons and carbon deposits from normal and reversed diffusion flames, **261**
Linnett, J. W.: Obituary: Sir Alfred Egerton, **97**
Lovachev, L. A.: The theory of flame propagation in branched and unbranched chain systems, **357**

McGrath, I. A.: *see* Foster, P. J. and McGrath, I. A.
Matthews III, L. J.: *see* Zelinski, J. J., Matthews III, L. J., Falk, F. and Bagnall, E. C.
Mendes, Maria A. T.: *see* Satterfield, C. N., Kehat, E. and Mendes, Maria A. T.
Menkes, J.: A contribution to the theory of laminar flames with radial symmetry, 1
Minkoff, G. J.: review of *Vistas in Free Radical Chemistry*, 91

Napier, D. H.: *see* Arthur, J. R. and Napier, D. H.
Nutt, C. W.: review of *Ionization Phenomena in Gases*, 282
Nutt, C. W.: review of *Frozen Free Radicals*, 379

Oppenheim, A. K., Stern, R. A. and Urtiew, P. A.: On the development of detonation with pre-ignition, 335

Palmer, H. B. and Seery, D. J.: Chlorine inhibition of carbon monoxide flames, 213
Palmer, H. B.: *see* Seery, D. J. and Palmer, H. B.
Parker, W. G.: review of *Rocket Propellants*, 91
—: review of *Rocket Propulsion*, 282
—: review of *Rocket Propellant Handbook*, 283
Povinelli, L. A.: The ignition delay concept for recessed flameholders, 355
Powling, J., Smith, W. A. W. and Thynne, J.: The flame decomposition of some substituted ethyl nitrates, 201

Rasbash, D. J. and Rogowski, Z. W.: Gaseous explosions in vented ducts, 301
Rasbash, D. J., Rogowski, Z. W. and Stark, G. W. V.: Mechanisms of extinction of liquid fires with water sprays, 223
—: review of *Explosions, Detonations, Flammability and Ignition*, 281
Rivlin, T. J.: *see* Eisen, C. L., Gross, R. A. and Rivlin, T. J.
Rogowski, Z. W.: *see* Rasbash, D. J. and Rogowski, Z. W.
—: *see* Rasbash, D. J., Rogowski, Z. W. and Stark, G. W. V.

Salooja, K. C.: Studies of combustion processes leading to ignition in hydrocarbons, 117
—: Interpretation of the anti-knock performance of hydrocarbons in gasoline engines in terms of their combustion characteristics, 193
Sandri, R.: On the decomposition flame of solid ozone–oxygen mixtures, 284
Satterfield, C. N., Kehat, E. and Mendes, Maria A. T.: Burning rates and ignition temperatures of hydrogen peroxide solutions, 99
Seery, D. J. and Palmer, H. B.: The influence of secondary atmospheric moisture upon carbon monoxide flames, 289
Seery, D. J.: *see* Palmer, H. B. and Seery, D. J.
Simms, D. L.: Ignition of cellulosic materials by radiation, 293
Smith, W. A. W.: *see* Powling, J., Smith, W. A. W. and Thynne, J.
Spalding, D. B.: The theory of steady laminar spherical flame propagation: equations and numerical solution, 51
—: The theory of burning of solid and liquid propellants, 59
—: Extinction of a one-dimensional laminar flame between cooled porous plugs, 93
— and Adler, J.: One-dimensional laminar flame propagation with an enthalpy gradient, 94
—: review of *Jets and Rockets*, 91
Stark, G. W. V.: *see* Rasbash, D. J., Rogowski, Z. W. and Stark, G. W. V.
Stern, R. A.: *see* Oppenheim, A. K., Stern, R. A. and Urtiew, P. A.

Tau-Yi Toong: *see* Tze-Ning Chen and Tau-Yi Toong
Thomas, P. H.: Buoyant diffusion flames, 381
Thring, M. W.: review of *Mathematical Aspects of Subsonic and Transonic Gas Dynamics*, 281
Thynne, J.: *see* Powling, J., Smith, W. A. W. and Thynne, J.
Toong, Tau-Yi: *see* Tau-Yi Toong
Tosiro Kinbara and Kazuo Akita: An approximate solution of the equation for self-ignition, 173
Tze-Ning Chen and Tau-Yi Toong: Structure and propagation of laminar flames near a heat sink, 313

Urtiew, P. A.: *see* Oppenheim, A. K., Stern, R. A. and Urtiew, P. A.

Vandenabeele, H., Corbeels, R. and van Tiggelen, A.: Activation energy and reaction order in methane–oxygen flames, 253
van Tiggelen, A.: *see* Vandenabeele, H., Corbeels, R. and van Tiggelen, A.

Westenberg, A. A. and Favin, S.: The theory of a spherical premixed laminar flame, 161
Williams, A.: *see* Dixon-Lewis, G. and Williams, A.
Wise, H.: *see* Wood, B. J., Wise, H. and Inami, S. H.
Wolfhard, H. G. and Bruszak, A. E.: The passage of explosions through narrow cylindrical channels, 149
Wood, B. J., Wise, H. and Inami, S. H.: Heterogeneous combustion of multicomponent fuels, 235
Wright, P. G.: *see* Gray, P. and Wright, P. G.

Yang, C. H.: *see* Berlad, A. L. and Yang, C. H.

Zelinski, J. J., Matthews III, L. J., Falk, F. and Bagnall, E. C.: The design of combustors for ramjet engines, 343

Name Index

Ablow, C. M. 242
Abrams, M. C. 190, 368
Adams, G. K. 9, 18, 59, 76, 105
Adler, J. 94, 95
Adrianov, V. N. 82, 276
Agnew, J. T. 44
Agnew, W. G. 29, 44
Agoston, G. A. 241, 242
Akimova, L. N. 273
Albright, L. F. 80
Anagnostou, E. 375
Anderson, W. H. 70, 76
Antal, P. 115
Antoine, A. C. 372
Arden, A. E. 211
Arthur, J. R. 19, 28, 49, 261, 264
Ashley, L. E. 89
Audrieth, L. F. 96
Austen, A. E. W. 182
Avery, W. H. 171, 331, 333
Azatyan, V. V. 367
Azoulay, A. 80

Badakhshan, A. 264
Badami, G. N. 382, 384
Badin, E. J. 44
Baer, P. G. 89
Bagnall, E. C. 343, 353
Bahn, G. S. 89, 90, 190
Baker, W. O. 112, 115
Baker, W. T. 353
Bamford, C. H. 300
Barbor, R. P. 187
Barenblatt, G. I. 5, 7
Barker, A. 91
Barnett, Sir George 380
Barrère, M. 282
Bartholomé, E. 363, 366, 367
Bartleson, J. D. 115
Battelle, G. 271
Baulknight, C. W. 89
Beatty, H. A. 121, 126, 132, 135
Bechert, K. 278
Beilby, Sir George 370
Bell, F. 279
Belles, F. E. 333, 384
Benedict, E. 192
Bennett, L. A. 96
Benson, S. W. 221
Berets, D. J. 147
Berl, W. G. 171
Berlad, A. H. 242
Berlad, A. L. 89, 244, 252, 325, 333
Bers, L. 281
Bills, K. W. 70, 76
Bird, R. 11, 18
Bird, R. B. 147, 162, 171
Birkel, G., Jr 90
Bishop, E. 188
Bjerklie, J. W. 190
Blackham, A. U. 126, 132, 135, 193, 199
Blackshear, P. L., Jr 90
Blanc, M. V. 159
Blinov, V. I. 84, 241, 279, 382
Blower, A. S. 184
Boerlin, H. 90
Bone, W. A. 335, 341
Bonilla, C. F. 83
Boone, T. H. 376
Botha, J. P. 170, 171, 288
Boudart, M. 260
Boyd, T. A. 44
Boynton, F. P. 190
Boys, S. F. 1, 7
Brabets, R. I. 284, 285
Bragg, S. L. 188, 281
Brandmaier, H. E. 90
Breazeale, J. D. 90
Brikowski, H. J. 242
Brinkley, S. R., Jr 89, 141, 147
Broida, A. 190
Brokaw, R. S. 245, 251, 252
Bromley, L. A. 383, 384
Bronowski, J. 184
Bruszak, A. E. 149, 159
Bulewicz, E. M. 219, 221
Burgess, M. J. 270
Burgoyne, J. H. 133, 136, 171, 241
Burke, E. 171
Burstein, S. Z. 90
Buss, J. H. 221
Butler, J. N. 375

Calcote, H. F. 190, 221, 369
Callear, A. B. 95, 96
Cambel, A. B. 355, 356
Campbell, E. S. 357, 367
Campbell, J. M. 44
Caplan, J. D. 44
Card, J. 312
Carhart, H. W. 135
Carpenter, N. 288
Carr, R. E. 242
Carslaw, H. S. 300
Carter, J. S. 380
Ceckler, W. 101, 102, 105
Chaiken, R. F. 89
Chamberlain, G. H. N. 40, 44, 199
Chambers, S. P. 78
Chambré, P. L. 173, 174, 180
Chandrasekhar, S. 173, 174, 180
Chen, Tze-Ning: *see* Tze-Ning Chen
Childs, J. H. 353
Choudhury, P. R. 356
Clamp, B. G. 186
Clemmow, D. M. 173, 180
Cobb, C. M. 89
Coble, R. L. 77
Cockcroft, Sir John 276
Cohen, E. C. 275
Cohen, P. M. 126, 129, 136
Collamer, D. O. 135
Combourieu, J. 274, 275
Commins, B. T. 49, 264
Cook, E. 90
Cook, G. B. 9, 180
Cooper, R. L. 264
Corbeels, R. 253
Cornelius, W. 44
Corner, J. 1, 7
Countryman, C. M. 190
Courant, R. 7
Coward, H. F. 80, 274, 333
Cramer, F. B. 89
Cramer, P. L. 44
Crank, J. 300
Crawford, B. L. 59, 76
Crellin, J. W. 135
Cremer, H. W. 380
Critchley, G. N. 368
Cubbage, P. A. 189, 301, 312
Cullis, C. F. 265, 269
Curtiss, C. F. 2, 7, 11, 18, 147, 162, 171, 278, 333
Cyphers, J. A. 171, 291, 292

Dalmai, G. 80
Danby, C. J. 43, 44
Daniels, F. 59, 76
Daniels, P. H. 45
Da Riva, I. 181
Davy, Sir Humphrey 97
Deckers, J. 260, 370
deJong, R. L. 323
Dekker, A. O. 70, 76
Delbourgo, R. 80
Dembrow, D. 171
Denniston, D. W., Jr 157, 159
Dery, R. J. 221, 292
de Soete, G. 372
DeZubay, E. A. 345, 353
Dickinson, R. 185
Ditchburn, R. W. 276
Dittrich, R. T. 353
Dixon-Lewis, G. 95, 330, 333, 382, 384
Donnell, Mrs A. R. 115
Donovan, R. E. 44
Dorsey, N. E. 96
Downs, D. 44
Drake, N. L. 211
Drell, I. L. 384
Drozdov, N. P. 216, 218–221
Dugger, G. L. 252, 319, 323, 355, 356

Dumont, L. F. 113, 115
Dunlap, F. 300
Dunn, R. 147
Durall, H. M. 211

Eckert, E. R. G. 183
Ede, A. J. 183
Edgar, G. 121, 135
Edse, R. 292
Effenberger, H. 379
Egbert, R. B. 191, 192
Egerton, Sir Alfred C. G. 92, 97, 98, 382, 384
Egloff, G. J. 44
Eisen, C. L. 137, 147
Elias, I. 89
Ellington, R. T. 252
El Wakil, M. M. 242
Emeleus, H. J. 265, 269
Emmons, H. 141
Erdelyi, A. 6, 7
Erhard, K. H. L. 40, 44
Essenhigh, R. H. 379
Evans, M. W. 188, 357, 367
Evered, D. S. 283
Everett, A. J. 260
Eyring, H. 273

Fabri, J. 1, 7
Falk, F. 343
Favin, S. 161
Fay, J. A. 187
Fehlner, F. P. 190
Fells, I. 92
Fenimore, C. P. 221, 288
Fenn, J. B. 221
Ferguson, R. E. 264
Fine, B. 243, 245, 246, 252
Finniecombe, J. R. 312
Fons, W. L. 190, 279
Foord, S. G. 259, 260
Forsyth, J. S. 245, 246, 252
Foster, P. J. 192
Foulatier, R. 275
Fox, M. D. 377
Fraeijs de Veubeke, B. F. 282
Francis, G. 282
Frank, C. E. 126, 132, 135, 193, 199
Frank-Kamenetzky, D. A. 173, 174, 180, 291
Fraser, R. P. 335, 341
Freeman, G. R. 43, 44
Friauf, J. 147
Friedman, R. 171, 213, 221, 291, 292, 332, 374
Friel, P. J. 107
Frier, J. L. 353
Fristrom, R. M. 161, 171
Frost, A. A. 221
Furno, A. L. 126, 132, 135
Fyodorov, G. G. 251, 252

Gál, D. 43, 44
Garden, R. 300
Garner, F. H. 121, 124, 135, 264
Garrett, Sir William 380
Garside, J. E. 245, 246, 252
Gatti, A. 77
Gaydon, A. G. 44, 221, 260, 264, 288
Gazley, C. 382
Geckler, R. D. 59, 76
Genensky, S. M. 173, 180
Gerrard, J. S. 186
Gerri, N. J. 221
Gerstein, M. 245, 251, 252, 374
Giddings, J. C. 14, 18, 357, 367
Gilbert, J. A. S. 49, 264
Gilbert, M. 17
Gilmore, F. R. 147
Ginell, R. 59, 76
Glover, D. 353
Godsave, G. A. E. 241
Goland, D. 90
Golovina, E. S. 251, 252
Gordon, A. S. 242
Gordon, J. S. 89, 90
Gordon, L. J. 90
Gordon, S. 147, 252
Gordon, W. E. 188
Goulard, M. 275
Goulard, R. 275
Grad, H. 76
Grard, F. 260
Graves, C. C. 353
Gray, P. 17, 18, 96, 104, 105, 211
Graziotti, R. 275
Green, L. 70, 76
Greene, E. F. 147
Greene, R. 89
Griffiths, J. V. 211
Grindell, D. H. 186
Grognard, M. 368
Gross, R. A. 86, 137, 147
Grosse, A. V. 284, 285
Grumer, J. 221, 292
Grunfelder, C. 171

Haar, L. 89
Halæs, J. S. 78
Hall, A. R. 17, 18, 96
Hall, J. G. 90
Hamburger, L. G. 183
Harnett, J. J. 90
Harris, M. E. 221, 292
Hart, A. B. 99, 105
Hartwell, F. J. 274
Hastie, R. D. 88
Hawksley, P. G. W. 191, 192
Hawthorne, W. R. 381, 382
Hazard, H. R. 271
Heimel, S. 375
Helmore, W. 193, 199
Henderson, C. B. 89
Herbert, M. V. 181
Hermach, F. L. 376
Heron, S. D. 121, 126, 132, 135
Hibbard, R. R. 242
Hicks, B. L. 180
Hicks, J. A. 211
Hilgers, G. 379
Hilsenrath, J. 147
Hinkley, P. L. 300
Hinshelwood, C. N. 43, 44
Hirschfelder, J. O. 2, 7, 11, 14, 18, 87, 147, 162, 168, 171, 221, 278, 333, 357, 367
Hiscock, D. 380
Hoare, D. E. 41, 44, 260
Hochstim, A. R. 89
Hooker, S. G. 273
Hornig, D. F. 221
Hottel, H. C. 84, 191, 192, 242, 275, 279, 372, 381, 382
Howe, E. L. 376
Huellmantel, L. W. 355, 356
Huff, V. N. 147, 252
Huffington, J. D. 173, 180
Hughes, E. C. 115
Hunstad, R. L. 374
Hunt, M. H. 89
Hunter, J. J. 277
Hunter, P. C. 44

Inami, S. H. 89, 235, 242
Isaac, I. 269
Isles, G. L. 95, 330, 333, 382, 384

Jackson, J. L. 124, 126, 132, 135
Jacobs, T. L. 211
Jaeger, J. C. 300
Jahn, G. 292, 366, 367
Jain, V. K. 58
Jaumotte, A. 282
Jeffreys, G. V. 380
Johnson, J. E. 135
Jolley, L. J. 265, 269
Jones, G. W. 126, 132, 135, 221, 333
Jones, H. 273
Jones, M. C. K. 195, 199
Jones, R. V. 83
Just, T. 81

Kapp, N. 382
Karlovitz, B. 157, 159
Kaskan, W. E. 221, 273, 288
Kauffman, F. 221
Kavanagh, G. M. 105
Kazuo Akita 173, 180
Kehat, E. 99
Kelly, A. 312
Kenny, W. F. 80
Kharasch, M. S. 91
Khokhar, B. A. 265, 269
Khudiakov, G. N. 84, 279, 382
Kimber, D. E. 185
Kirkby, W. A. 90, 190, 280, 379, 382
Kirkwood, J. G. 141, 147
Kistiakowsky, G. B. 147
Kit, B. 283
Klein, G. 2, 7, 11, 18, 316, 323
Knapschaefer, D. H. 157, 159
Knewstubb, P. F. 370
Knox, J. H. 83
Kogarko, S. M. 84, 374
Kolmogorov, A. N. 358, 367
Kompaneets, A. S. 335, 341
Kondratiev, V. N. 367
Koppang, R. R. 89, 90
Kozlov, G. I. 260

Kubert, B. R. 90
Küchler, E. 79
Kuethe, A. M. 5, 7

Laffitte, P. 80, 274
Lambert, J. D. 96
Lang, H. R. 277
Larkin, J. D. 187
Lauer, J. L. 107
Law, M. 300
Lawrence, E. K. 300
Lawrence, R. W. 59, 76
Lawson, D. I. 300
Leah, A. S. 288
Lee, J. C. 17, 18, 96, 104, 105
Lefebvre, A. H. 181
Le Grivès, E. 379
Leist, K. 280
Leslie, W. H. P. 277
Leveque, M. 191, 192
Levy, J. B. 213, 221, 374
Lewis, B. 44, 147, 221, 252, 259, 260, 292, 332
Lindsay, A. L. 383, 384
Lindsey, A. J. 49, 261, 264
Linnett, J. W. 98, 162, 171, 365, 367
Lister, D. 376
Litchfield, E. L. 159
Locklin, D. W. 184
Long, R. 124, 135, 264
Longwell, J. P. 252, 353
Lorell, J. 1, 7, 242
Lovachev, L. A. 357, 367
Lovell, W. G. 44, 272
Lyn, W. T. 182

McAdams, W. H. 287, 288, 332, 333
MacArthur, E. H. 376
McAuliff, Rita C. 376
McCone, A. 168, 171
McConnell, S. G. 186
McDonald, G. 290, 292
McGrath, I. A. 192
Maclean, J. D. 300
McMahon, D. G. 90
McMasters, A. W. 190
Makarov, I. V. 188
Malan, D. H. 300
Marble, F. E. 6, 353, 355, 356
Margerson, S. N. A. 312
Markstein, G. 1, 5, 7
Marrone, P. V. 85
Marshak, J. L. 183
Marshall, E. F. 115
Martin, F. J. 335, 341
Martin, G. F. 86
Martinengo, A. 81, 379
Matreyek, W. 112, 115
Matthews III, L. J. 343, 353
Mattocks, G. R. 186
May, E. R. W. 86
Mayer, E. 318, 323, 332
Mayorcas, R. 77
Melby, A. O. 44
Mellish, C. E. 365, 367
Mendes, Maria A. T. 99
Menkes, H. R. 5, 7
Menkes, J. 1, 5, 7, 162
Mentz, R. M. 90
Mickle, E. A. 288
Mie, G. 191, 192
Mikita, J. J. 113, 115
Millan, G. 1, 7, 10, 18, 181
Miller, D. G. 190, 368
Miller, J. 213, 221
Miller, J. E. 300
Millikan, R. C. 288
Minkopf, G. J. 91, 260, 379
Mishuck, E. 70, 76
Mitchell, W. 90
Moe, G. 70, 76
Moffat, W. C. 89
Mooradian, A. J. 188
Moore, G. E. 288
Morrell, V. E. 147, 252
Morrison, R. B. 147
Moyle, M. P. 147
Mrozowski, S. 115
Mueller, A. C. 78
Mueller, J. R. 6
Mukai, M. 264
Mullaney, G. J. 288
Mullins, B. P. 281
Murray, M. V. 78
Murray, R. C. 17, 18, 96
Myers, P. S. 242

Nalbandyan, A. B. 367
Naphtali, L. M. 90
Napier, D. H. 19, 28, 49, 261, 264
Needham, D. P. 211
Neu, J. T. 190
Neubert, U. 335, 341
Newitt, D. M. 133, 136
Nonhebel, G. 372
Nonweiler, T. R. F. 91
Norrish, R. G. W. 40, 44, 133, 136, 259, 260
Nugent, R. G. 171
Nutt, C. W. 283, 379

O'Brien, C. J. 89
Odell, T. 168, 171
Ogg, B. A. 96
Oppenheim, A. K. 335, 341
Orchin, M. 117, 121, 126, 135, 193, 199

Pahnke, A. J. 126, 129, 136
Palmer, H. B. 213, 221, 289, 292
Palmer, K. N. 301, 312
Pape, N. R. 112, 115
Parker, W. G. 91, 264, 282, 283
Parr, N. L. 86
Parr, R. G. 59, 76
Pascale, D. A. 221
Pastell, D. L. 44
Patrick, E. A. K. 88
Payman, W. 335, 341
Pearson, R. G. 221
Pease, R. N. 44, 218, 221
Penner, S. S. 2, 7, 59, 70, 76, 357, 367
Perez del Notario, P. 181
Perrin, J. R. 89
Perrine, J. 89
Perry, J. H. 242, 312
Petrovsky, I. G. 358, 367
Petty, D. S. 121, 135
Philpot, A. J. 276
Piskunov, N. S. 358, 367
Porter, G. 28
Potter, A. E. 333
Potter, A. E., Jr 244, 252, 333, 375
Poulson, B. V. 82
Povinelli, L. A. 355, 356
Powell, H. N. 288
Powell, R. 273
Powling, J. 201, 211
Prescott, R. 171
Pretty, W. E. 264
Priem, R. J. 242
Probert, R. P. 181
Putnam, A. A. 271

Rae, D. M. 86
Raftery, M. M. 381
Ramsay, Sir William 97
Rasbash, D. J. 223, 234, 282, 301, 312
Rassweiler, G. M. 41, 44
Ratcliffe, J. A. 277
Raymond, L. 182
Reed, L. E. 376
Renich, W. T. 171
Resnick, H. 105
Retailliau, E. R. 195, 199
Ricards, H. A., Jr 195, 199
Rice, O. K. 59, 76
Richardson, J. F. 241
Richardson, J. M. 141, 147
Rifkin, E. B. 41, 44, 198, 199
Rivlin, T. J. 137, 147
Roback, R. 90
Robb, J. C. 95, 96
Roberts, V. E. 300
Robinson, H. 312
Robinson, R. 89
Rogowski, Z. W. 223, 234, 301, 312
Rosen, G. 54, 58, 76, 333
Rosen, J. B. 333
Rosen, P. 353
Rosser, W. A. 213, 221
Rosser, W. A., Jr 44
Rossini, F. D. 147, 333
Rumbel, K. E. 374
Rummel, K. 48, 49
Russo, A. L. 85, 90
Rust, F. F. 135

Sadownikow, P. 269
Sagulin, A. B. 269
St Pierre, P. D. S. 77
Salooja, K. C. 117, 135, 193, 199
Sandri, R. 285
Sanz, I. 10, 18, 181
Satterfield, C. N. 99, 105
Sauer, F. H. 300
Saunders, O. A. 78, 183, 191, 192

Schalit, L. M. 357, 367
Scheffee, R. S. 89
Scheubel, F. N. 378
Schmidt, E. 335, 341
Scholte, T. G. 291, 292, 382, 384
Schultz, R. D. 70, 76
Schumb, W. C. 105
Schuster, F. 379
Scott, F. E. 126, 135
Scott, G. S. 126, 135
Seery, D. J. 213, 221, 289, 292
Seifert, H. S. 281
Semenov, N. N. 221, 252, 259, 260, 269, 291, 292
Senftleben, H. 192
Setchkin, N. P. 132, 135
Sherwood, C. M. 89
Shipman, C. W. 187
Shires, G. L. 77
Shorin, S. N. 82, 276
Shushpanov, P. I. 96
Signaigo, F. K. 44
Simkin, D. J. 89
Simmonds, W. A. 301, 312
Simmons, F. S. 190
Simms, D. L. 293, 300
Simon, D. M. 333
Simon, W. 90
Simpson, H. C. 242
Skinner, F. D. 89
Slootmaekers, P. J. 260
Smelt, R. 91
Smith, E. B. 272
Smith, E. C. W. 264
Smith, H. 89
Smith, L. S. A. 269
Smith, M. 135
Smith, P. B. 159
Smith, R. F. 83
Smith, R. W., Jr 90
Smith, S. R. 242
Smith, W. A. W. 201, 211
Smith, W. E. 85
Snyder, W. T. 356
Sondheim, D. W. 353
Sonnichsen, H. M. 211
Sortman, C. W. 121, 126, 132, 135
Spadaro, F. G. 190
Spakowski, A. E. 333
Spalding, D. B. 3, 7, 10, 18, 51, 58, 59, 76, 92, 94, 95, 168, 170, 171, 183, 234, 285, 288, 318, 322, 326, 332, 357, 367, 375, 377–379
Sparrow, E. M. 275
Speich, C. F. 184
Spindt, R. S. 112, 115
Stahl, R. W. 80
Staines, E. N. 96
Stark, G. W. V. 223, 234
Steele, Miss M. P. 58
Steinicke, H. 335, 341
Stent, F. S. 78
Stephanou, S. E. 90
Stern, R. A. 335, 341
Stesik, L. N. 273
Stevens, D. R. 112, 115
Stevenson, L. W. 78
Stocks, G. W. 18, 105
Stoltenberg, Maryanne P. 90
Stotter, A. 371
Stover, E. 77
Strauss, W. A. 292
Street, J. C. 44, 45, 49
Strehlow, R. A. 290, 292
Streng, A. G. 284, 285
Strong, R. L. 190
Sturgis, B. M. 44, 113, 115, 126, 129, 136
Sugden, T. M. 219, 221, 370
Suits, G. 77
Sullivan, M. V. 132, 136
Swarts, D. E. 117, 121, 126, 135, 193, 199
Szabó, Z. G. 43, 44

Tanford, C. 218, 221
Tang, T. L. 133, 136
Tarifa, C. S. 181
Tau-Yi Toong 313, 316, 323
Taylor, G. W. 133, 136
Taylor, J. 277
Taylor, W. 190
Taylor, W. H. 276
Tebbens, B. D. 264
Thabet, S. K. 384
Thomas, A. 45, 49, 82
Thomas, J. F. 264
Thomas, P. H. 173, 177, 180, 300, 382
Thomas, R. H. E. 78
Thompson, H. T. 211
Thompson, N. J. 132, 136
Thomson, Sir George 277
Thon, N. 180
Thorp, C. E. 284, 285
Thring, M. W. 186, 192, 281, 372
Thynne, J. 201
Titman, H. 159
Tollmien, W. 159
Toong, Tau-Yi: *see* Tau-Yi Toong
Topping, J. 276
Torry, R. 159
Tosiro Kinbara 173
Townend, D. T. A. 245, 246, 252
Trimble, M. H. 353
Trotman-Dickenson, A. F. 17, 18, 83, 92, 211, 221, 363, 367
Tze-Ning Chen 313, 316, 323

Uberoi, M. S. 5, 7
Underwood, G. 186
Unterberg, W. 190
Urtiew, P. A. 335
Usiskin, C. M. 275
Uyehara, O. A. 242

Vaags, P. B. 291, 292, 382, 384
Vandenabeele, H. 253
Vandenkerckhove, J. 282
Vanpee, M. 159, 260
van Rosenberg, H. E. 187
van Tiggelen, A. 253, 260, 368, 370, 372
van Wonterghem, J. 260
Vasiliu, J. 190
Veh, P. O. 48, 49
Vigers, B. E. A. 78
Villars, D. S. 90
Vines, R. G. 96
Viskanta, R. 82
Voevodsky, V. V. 367
von Elbe, G. 44, 221, 252, 259, 260, 292, 332
von Kármán, T. 1, 2, 7, 281, 357, 367
Vortmeyer, D. 379

Waddington, D. J. 269
Wagner, H. G. 81, 379
Walcutt, C. 198, 199
Walker, P. L., Jr 289, 292
Walker, R. E. 353
Wallin, S. C. 376
Walsh, A. D. 41, 44, 199, 259, 260
Ward, T. 87
Wares, G. W. 173, 180
Waring, G. J. 376
Wark, K., Jr 44
Warren, F. A. 91
Waterman, T. E. 284, 285
Watermeier, L. A. 290, 292
Waters, W. A. 91
Watkins, S. B. 380
Watson, D. 186
Watson, H. A. 80
Way, S. 374
Weatherston, R. C. 85
Webber, W. T. 89
Webster, C. T. 381
Webster, G. A. 124, 135
Weddel, D. S. 381, 382
Weeks, D. J. 191, 192
Weil, S. A. 252
Weinberg, F. J. 171, 255, 260, 271, 377
Weiss, K. 278
Weiss, M. A. 252, 353
Wellman, H. B. 190
Wells, F. E. 157, 159
Wentworth, R. L. 105
Westenberg, A. A. 161, 171
Wheeler, R. G. 44
Wheeler, R. V. 44, 270
Wheeler, W. H. 335, 341
Whitehouse, N. D. 371
Wilfong, R. E. 59, 76
Wilkins, R. L. 90
Wille, R. 379
Williams, A. 211, 384
Williams, F. A. 1, 7, 187
Williams, J. C. 242
Williams, J. D. 378
Willsher, J. P. 269
Winslow, F. H. 112, 115
Wires, R. A. 290, 292
Wise, H. 1, 7, 44, 89, 213, 221, 235, 241, 242
Wiseman, L. A. 59, 76

Withrow, L. L. 41, 44
Wohl, K. 382
Wolfe, C. L. 112, 115
Wolfe, J. K. 132, 136
Wolfhard, H. G. 18, 44, 149, 159, 260, 264
Wolfson, B. T. 147
Wood, B. J. 89, 235, 241, 242
Wood, W. W. 141, 147
Woods, S. D. 96
Wortman, J. 89
Wright, C. C. 289, 292
Wright, F. H. 6
Wright, P. G. 96
Wynne, C. G. 277

Yagi, S. 382
Yang, C. H. 89, 190, 325, 333, 369
Yumlu, V. S. 94, 95, 285, 288
Zabetakis, M. G. 80, 126, 1 135
Zaff, S. 89
Zaworski, R. J. 89
Zeldovich, Y. B. 5, 7, 216, 21 219, 221, 281, 291, 335, 341
Zelinski, J. J. 343, 353
Ziemer, R. W. 355, 356
Zisman, W. A. 132, 136
Zukoski, E. E. 353, 355, 356